Advanced Structured Materials

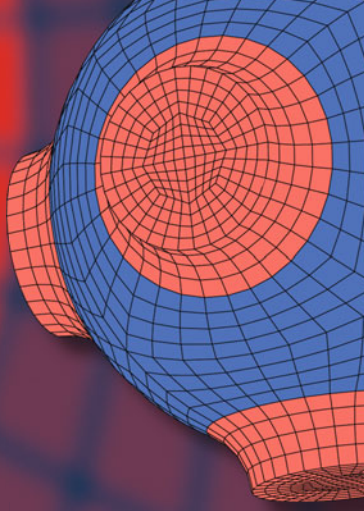

Anuj Tripathi
Jose Savio Melo *Editors*

Advances in Biomaterials for Biomedical Applications

Springer

Advanced Structured Materials

Volume 66

More information about this series at http://www.springer.com/series/8611

Anuj Tripathi · Jose Savio Melo
Editors

Advances in Biomaterials for Biomedical Applications

Springer

Editors
Anuj Tripathi
Nuclear Agriculture and Biotechnology Division
Bhabha Atomic Research Centre
Mumbai, Maharashtra
India

Jose Savio Melo
Nuclear Agriculture and Biotechnology Division
Bhabha Atomic Research Centre
Mumbai, Maharashtra
India

ISSN 1869-8433 ISSN 1869-8441 (electronic)
Advanced Structured Materials
ISBN 978-981-10-3327-8 ISBN 978-981-10-3328-5 (eBook)
DOI 10.1007/978-981-10-3328-5

Library of Congress Control Number: 2016960027

Printed on acid-free paper

This Springer imprint is published by Springer Nature
The registered company is Springer Nature Singapore Pte Ltd.
The registered company address is: 152 Beach Road, #22-06/08 Gateway East, Singapore 189721, Singapore

Preface

A meteoric scientific and technological revolution in biomedicine is underway and is ruling by advanced biomaterials. A number of factors involved in biomaterials' advancement complement each other. Science of materials, synthesis procedures, and analytical contrivance are some of the major factors that have transformed over a period of time, thus popularizing the biomaterials for their advanced biomedical applications. Much of revolution in biomaterials is fundamental in nature; however, advances are often based on the new and extended understanding of basic principles of biomaterials along with its applications.

Biomaterials are a class of materials that are intended for applications in the biomedical field without being biologically vulnerable. Among many, metallic and polymeric biomaterials have most widely been studied due to several advantages. The growing number of publications and technology patents in this field has encouraged us to provide a comprehensive outcome with future scope. We have selectively chosen topics based on the latest and demanding areas of research in biomedicine. Each chapter of this book has discussed distinct biomaterial types. Many chapters begin with the basics followed by advancement and then application of biomaterial. Overall, this book elaborates on the preparation process and modification of polymers, blends, composites, nanoclusters, and nanohybrids, including advanced approaches such as bioprinting and plasma processing. These biomaterials have further been discussed in terms of their application as a carrier for drug and gene delivery, imaging and sensing, and also as an adjuvant, which are especially elaborated in the field of cartilage regeneration therapy, cancer management, and for the induction and treatment of autoimmunity, respectively. The use of polymeric scaffolds for engineering tumor microenvironment and decellularized extracellular matrix as the scaffolds for various tissue recreations has also individually been discussed in separate chapters. The various nanohybrid systems such as gold nanoclusters, graphene nanoclusters, and magnetic nanoparticles and various nanoantimicrobial biomaterials have also been elaborated as advanced theranostics and developing antimicrobial biomaterials, respectively.

Arduous task of compiling recent 'Advances in Biomaterials for Biomedical Applications' and succinct pretension about their future requires greater leisure and

extensive reading. In this book, we have sought to bring together the expertise of scientists involved in the materials chemistry and theranostics, with the aim of providing overview on contemporary preparation and diversified applications of biomaterials. This book is appropriate to advanced graduate, introductory-level researchers, and also interdisciplinary and multidisciplinary scientists. It should also serve as a source book for statuary authorities and legislators charged with ethical monitoring and approving clinical applications.

We once again thank all the authors for the quality of their contributions that has enabled us to make possible this book beyond our own limited experience.

Mumbai, India

Anuj Tripathi
Jose Savio Melo

Contents

Editors and Contributors

About the Editors

Dr. Anuj Tripathi is a scientist at the Bhabha Atomic Research Centre, Mumbai, India. He is also an adjunct faculty at the Homi Bhabha National Institute, Mumbai, India. He is a recipient of the K.S. Krishnan research fellowship from the Board of Research in Nuclear Sciences, India. He has been a visiting researcher at Newcastle University, UK; Kyushu University, Japan; and Protista International AB and Lund University, Sweden. He has received several research fellowships from the Government of India funding organizations such as DBT, CSIR, DST, and HLL. He has several international research publications, book chapters, conference articles, and patents to his credit. He is an active participant in many scientific deeds in India for the promotion of biotechnology and materials science. He is an editorial board member of many journals and also a member of several international academic societies. He has received awards from various national and international organizations such as the Asian Polymer Association, Association of Separation Scientists and Technologists, and Indian Thermal Analysis Society. His major research interests are in the area of novel nano- and biomaterials development for tissue engineering, bioprocessing, and environmental biotechnology.

Dr. Jose Savio Melo is a senior scientist at the Bhabha Atomic Research Centre, India, where he heads the Enzyme and Microbial Technology Section of the Nuclear Agriculture and Biotechnology Division. His major research interest is in the field of applied enzymology with a special focus on designing heterogeneous biocatalysts for use in bioprocessing, biosensors, and bioremediation. He is also a professor at the Homi Bhabha National Institute (HBNI), Mumbai. He has several publications in international journals, books, and workshop proceedings to his credit and is a fellow of both the Maharashtra Academy of Sciences and the Society for Applied Biotechnology.

Contributors

Shekhar Agnihotri Department of Biotechnology, Thapar University, Patiala, Punjab, India

Neha Arya Department of Biochemistry, All India Institute of Medical Sciences Bhopal, Saket Nagar, Bhopal, Madhya Pradesh, India

RenuGeetha Bai Nanotechnology and Advanced Materials (NATAM), Faculty of Engineering, University of Nottingham Malaysia Campus (UNMC), Semenyih, Selangor, Malaysia

Yatendra Kumar Bhardwaj Radiation Technology Development Division, Bhabha Atomic Research Centre, Mumbai, India

Manisha Buriuli Department of Biotechnology and Medical Engineering, National Institute of Technology, Rourkela, Odisha, India

Chandrashekhar V. Chaudhari Radiation Technology Development Division, Bhabha Atomic Research Centre, Mumbai, India

Magali Cucchiarini Center of Experimental Orthopaedics, Saarland University Medical Center, Homburg/Saar, Germany

Xiaofeng Cui School of Chemistry, Chemical Engineering and Life Sciences, Wuhan University of Technology, Wuhan, Hubei, China; Stemorgan Therapeutics, Plano, TX, USA; Technical University of Munich, Munich, Germany

Rajendra R. Deshmukh Department of Physics, Institute of Chemical Technology, Mumbai, India

Navneet Kaur Dhiman Department of Biotechnology, Thapar University, Patiala, Punjab, India

Kumar Abhinav Dubey Radiation Technology Development Division, Bhabha Atomic Research Centre, Mumbai, India

Aurelien Forget University of South Australia, Future Industries Institute, Mawson Lakes, SA, Australia

Guifang Gao School of Chemistry, Chemical Engineering and Life Sciences, Wuhan University of Technology, Wuhan, Hubei, China; Stemorgan Therapeutics, Plano, TX, USA

Masanobu Horie Division of Biochemical Engineering, Radioisotope Research Centre, Kyoto University, Sakyo-Ku, Kyoto, Japan

Ying Huang School of Chemistry, Chemical Engineering and Life Sciences, Wuhan University of Technology, Wuhan, Hubei, China

Hiroyuki Ijima Department of Chemical Engineering, Faculty of Engineering, Kyushu University, Fukuoka, Japan

Akira Ito Department of Chemical Engineering, Faculty of Engineering, Kyushu University, Nishi-Ku, Fukuoka, Japan

Masamichi Kamihira Department of Chemical Engineering, Faculty of Engineering, Kyushu University, Nishi-Ku, Fukuoka, Japan

Yoshinori Kawabe Department of Chemical Engineering, Faculty of Engineering, Kyushu University, Nishi-Ku, Fukuoka, Japan

Sivakumar Manickam Nanotechnology and Advanced Materials (NATAM), Faculty of Engineering, University of Nottingham Malaysia Campus (UNMC), Semenyih, Selangor, Malaysia

Manu M. Joseph Laboratory of Biopharmaceuticals and Nanomedicine, Division of Cancer Research, Regional Cancer Centre, Trivandrum, Kerala, India

Jose Savio Melo Nuclear Agriculture and Biotechnology Division, Bhabha Atomic Research Centre, Mumbai, India

Kasturi Muthoosamy Nanotechnology and Advanced Materials (NATAM), Faculty of Engineering, University of Nottingham Malaysia Campus (UNMC), Semenyih, Selangor, Malaysia

Kutty Selva Nandakumar Medical Immunopharmacology Research, Southern Medical University, Guangzhou, China; Medical Inflammation Research, Medical Biochemistry and Biophysics, Karolinska Institute, Stockholm, Sweden

Krishnasamy N. Pandiyaraj Department of Physics, Sri Shakthi Institute of Engineering and Technology, Coimbatore, India

Preethi GU Laboratory of Biopharmaceuticals and Nanomedicine, Division of Cancer Research, Regional Cancer Centre, Trivandrum, Kerala, India

Ana Rey-Rico Center of Experimental Orthopaedics, Saarland University Medical Center, Homburg/Saar, Germany

Akhilesh Kumar Shakya Chemical Engineering Department, Texas Tech University, Lubbock, TX, USA

Shiji R Laboratory of Biopharmaceuticals and Nanomedicine, Division of Cancer Research, Regional Cancer Centre, Trivandrum, Kerala, India

Nana Shirakigawa Department of Chemical Engineering, Faculty of Engineering, Kyushu University, Fukuoka, Japan

Sreelekha TT Laboratory of Biopharmaceuticals and Nanomedicine, Division of Cancer Research, Regional Cancer Centre, Trivandrum, Kerala, India

Ajinkya M. Trimukhe Department of Physics, Institute of Chemical Technology, Mumbai, India

Anuj Tripathi Nuclear Agriculture and Biotechnology Division, Bhabha Atomic Research Centre, Mumbai, India

Unnikrishnan BS Laboratory of Biopharmaceuticals and Nanomedicine, Division of Cancer Research, Regional Cancer Centre, Trivandrum, Kerala, India

Lalit Varshney Radiation Technology Development Division, Bhabha Atomic Research Centre, Mumbai, India

Devendra Verma Department of Biotechnology and Medical Engineering, National Institute of Technology, Rourkela, Odisha, India

Xiao-Fei Zhang School of Chemistry, Chemical Engineering and Life Sciences, Wuhan University of Technology, Wuhan, Hubei, China

Polymers, Blends and Nanocomposites for Implants, Scaffolds and Controlled Drug Release Applications

Kumar Abhinav Dubey, Chandrashekhar V. Chaudhari, Yatendra Kumar Bhardwaj and Lalit Varshney

Abstract Polymer blends and nanocomposites are widely explored for different biomedical applications such as biodegradable scaffolds, biosensors, implants and controlled drug release. Both, synthetic and semi-synthetic polymers are used in medical applications and have their inherent advantages and disadvantages. Synthetic polymers offer flexibility of varying monomer unit, molecular weight, branching and thus offer a diverse set of physico-mechanical properties, whereas natural polymers offer superior biocompatibility and biodegradation profile. Availability of polymer blending techniques adds another dimension to the property set that polymers can offer, and therefore polymer blending is often used to tailor biodegradability and physico-mechanical properties. Polymers, in general, have poor mechanical properties when compared to metals and ceramics, putting a load bearing limit on polymer-based medical implants. The addition of reinforcing/functional filler is expected to overcome such disadvantages of polymers. Polymers composites are heterogeneous systems wherein polymers are compounded with micron or nano-size particles to render high strength, electrical conductivity or any other functional attribute. This chapter describes the technological aspects of polymer blends and nanocomposites with a specific reference to synthesis, characteristics and applications of multi-phasic polymer systems as implants, scaffolds, and controlled drug release matrices. A detailed account of synthetic and natural polymer nanocomposites along with a brief discussion on important nano-fillers used in medical applications and interface modification techniques is presented. Few examples of recently explored novel polymer blends and composites that displayed promising properties as implants, scaffolds, biosensors and control release matrices have also been discussed.

Keywords Polymers · Implants · Tissue engineering · Drug delivery

K.A. Dubey (✉) · C.V. Chaudhari · Y.K. Bhardwaj · L. Varshney
Radiation Technology Development Division, Bhabha Atomic Research Centre, Trombay, Mumbai 400085, India
e-mail: abhinav@barc.gov.in; abhinav.barc@gmail.com

A. Tripathi and J.S. Melo (eds.), *Advances in Biomaterials for Biomedical Applications*, Advanced Structured Materials 66,
DOI 10.1007/978-981-10-3328-5_1

Abbreviations

ABS	Acrylonitrile butadiene styrene
AFM	Atomic force microscopy
Bi_2O_3	Bismuth oxide
BN	Boron nitride
BNT	Born nitride tubes
DMF	Dimethyl formamide
CNTs	Carbon nanotubes
CTAB	Cetyl trimethylammonium bromide
CVD	Chemical vapour deposition
EG	Exfoliated graphene
EVA	Ethylene-vinyl acetate
EPDM	Ethylene propylene diene monomer
GIC	Graphene intercalated compound
GO	Graphene oxide
HDPE	High-density polyethylene
HEMA	2-Hydroxyethyl methacrylate
HUVEC	Human umbilical vein endothelial cells
LDPE	Low density polyethylene
LDS	Lauryl dodecyl sulfonate
MoS_2	Molybdenum disulfide
MWNT	Multi walled nanotube
NCB	Nano carbon black
NP	Nanoparticle
NCC	Nanocrystalline cellulose
NMP	N-Methylpyrrolidone
PC	Polycarbonates
PCL	Polycaprolactone
PDMS	Polydimethylsiloxane
PET	Polyethylene terephthalate
PEG	Polyethylene glycol
PEEK	Polyether ether ketone
PEI	Polyethylenimine
pHEMA	Polyhydroxyethylmethacrylate
PLA	Polylactic acid
PLGA	Poly(lactic-co-glycolic acid)
PMMA	Poly methylmethacrylate
PTFE	Polytetrafluoroethylene
PU	Polyurethane
PVA	Poly vinyl alcohol
PVC	Polyvinyl chloride
PVDF	Polyvinylidene fluoride
ROS	Reactive oxygen species
SC	Sodium cholate

SDBS	Sodium dodecylbenzenesulfonate
SDS	Sodium dodecyl sulphonate
SEM	Scanning electron microscopy
SPR	Surface plasmon resonance
STM	Scanning tunnelling microscopy
SWNT	Single walled nanotube
TDOC	Sodium taurodeoxycholate
TEOS	Tetraethoxysilane
THF	Tetrahydrofuran
TPU	Thermoplastic polyurethane
TTAB	Tetradecyltrimethylammonium bromide
UHMWPE	Ultra-high-molecular-weight polyethylene
VEGF	Vascular endothelial growth factor
WS2	Tungsten sulphide
XRD	X-ray diffraction
Nd:YAG	Neodymium-doped yttrium aluminium garnet

1 Introduction

Polymers are natural or synthetic macromolecules composed of many repeating units. They offer a variety of properties that make them amicable to different biomedical applications. The earliest use of polymers can be traced back to Mayan civilization though the modern era is believed to be heralded with the discovery of rubber vulcanization by Charles Goodyear in the nineteenth century (Bergström 2015). Today, polymers are among the most widely used materials, surpassing steel, aluminum and ceramics. In medicine, natural polymers are used since long time but synthetic polymers gained significance only in the last few decades. The application domain of polymers is as wide as the property set they offer, ranging from regenerative medicine to orthopedics (Aguilar 2013; Baran et al. 2014; Fabian and Wulff 2014; Hall 2015; Han 2015; Ivanova et al. 2014; Pruitt and Chakravartula 2011; Yang 2015).

Polymers are light, relatively inexpensive and closely mimic biological tissue. Indeed, macromolecules of biological origin were among the first explored for biological application such as sutures. Synthetic polymers though initially thought to have issues of biocompatibility and biodegradability, now play a major role in medicine, due to advancement in polymer synthesis, modification, blending and composite formation techniques. Synthetic biodegradable and biocompatible polymers are also now available and bio-functionalization techniques have been developed to improve interaction between polymers and cells or tissue, through surface modification. Such endeavor felicitates development of highly specialized polymers that serve the desired function, stay in the body only as long as they are

needed and then degrade, avoiding surgical intervention for the removal. Drug delivery systems, orthopedic fixation, ligament augmentation, vascular stents are among the most important medical functions of polymers.

Natural polymers are abundant in nature and are derived from plant or animal resources. Animal horn, a natural thermoplastic protein that is primarily composed of keratin, is reported to be used by medieval craftsmen to make lantern windows and moulded impressions. Cellulose, the most abundant natural polymer was isolated from plant cell wall and its chemical formula was determined in 1838. Cellulose, because of its high crystallinity and strength, can be converted into fiber and can be used for diverse set of applications. Oxidized cellulose suture was patented in 1951, to replace sheep intestines derived absorbable sutures and are still being explored for corporal body grafting and suture-less correction of severe penile chordee (El-Assmy et al. 2007). Chitosan, the second most abundant natural polymer has recently gained considerable attention due to its biodegradability, biocompatibility, antibacterial activity, haemostatic properties and ability to bind lipids. It is linear polysaccharide composed of randomly distributed β-(1-4)-linked D-glucosamine and N-acetyl-D-glucosamine, derived from shrimp and other crustacean shells. Alginate, carrageenan and pectin are other promising natural polymers for different biomedical applications. Natural rubber, vulcanization of which is considered an important step in the modern era, is also a plant based polymer, and is used for many surgical and medical applications (Feneley et al. 2015; Teo et al. 2016).

Synthetic and semi-synthetic polymers have their own advantages. They offer flexibility of varying monomer units, molecular weight, branching and thus offer a diverse set of physico-mechanical properties. The first semi-synthetic polymer synthesized was celluloid, a thermoplastic obtained by nitration of cellulose. World's first synthetic plastic claimed is Bakelite; today, a wide range of polymers with extremely high stretchability and strength are available. These polymers can be processed in different shapes, are light weight and meet structural and mechanical characteristics demanded by several medical applications. Polymers are also being extensively researched for the development of new applications, and many polymers are currently used in drug delivery devices, vascular stents, sutures, plastic surgery, orthopedics and orthodontic therapy.

Synthetic polymers can be broadly classified into biodegradable and non-biodegradable polymers, considering the application profile for biomedical applications. Non-biodegradable polymers are the one resistant to enzymatic, microbial or hydrolytic degradation during their application life. Accordingly such polymers are used as implants that are long lasting, in surgical applications or in conditions where in vivo application is desired. For ligament and tendon defects, polypropylene, ePTFE, PET/Dacron and nylon are preferred as they provide better mechanical stability than mammalian collagen scaffolds. Mammalian scaffolds contain type I collagen, type III collagen and elastin; though these biopolymers offers good interaction with the host tissue, their mechanical properties are very poor, leading to poor surgical outcome. Conversely, synthetic polymers mentioned above are durable though they have issues of biocompatibility. Implants, especially

orthopedic and regenerative surgery are increasing employing synthetic polymer based procedures. Biodegradable polymers, as the name suggests, degrade in the biological environment and are supposed to have good cyto-compatibility. Apart from naturally occurring biopolymers mentioned above, synthetically produced biodegradable polymers have also shown promising properties for medical applications. Poly lactic acid, polycaprolactone, poly (lactide-co-glycolide) and polyurethane-urea are widely researched for medical applications including implants and drug delivery (Teo et al. 2016; Ruys 2013).

Availability of polymer blending techniques provides another dimension to the property set that polymers can offer. Polymer blends can be a homogeneous or heterogeneous mixture of two or more polymers that can offer different combinatorial or novel properties (Dubey et al. 2012). One of the major objectives of polymer blending is overcoming the functional deficits of a polymer by adding another polymer. If a polymer is very brittle, it can be made tough by mixing it with a soft polymer; similarly, the biodegradability of polymer matrices can be tuned by making a blend of biodegradable and non-biodegradable polymers and varying the composition. pH stability, temperature stability and other properties can also be tuned by polymer blending. However, the thermodynamics of the polymer blends is generally unstable, leading to phase separation and poor physico-mechanical properties. Efforts are therefore needed to stabilize the morphology of polymer mixtures by tailoring the interface. A more recent development in the blending technology is the stimuli sensitive switching by making shape memory polymers, which are expected to be highly useful in medical applications. Examples of polymer blending include the blending of HDPE and LDPE to achieve intermediate flexibility, or nylon and urethane to achieve a balance of lubricity and elasticity. Additionally, polymers for medical use may be blended with specialized additives for enhancing properties to achieve specific functional requirements. Polymer blends of PC/ABS have been used for housing surgical instruments, PC/PET in surgical instruments and PVC/EVA bags and films for blood storage (Modjarrad 2014; McKeen 2014).

Polymers, in general, are insulators with mechanical properties poorer than metals and ceramics, putting a load bearing limit for polymer based medical implants. Polymers composites are heterogeneous systems wherein polymers are compounded with micron to nanosize particles with high strength, electrical conductivity or any other functional attribute. Nanosize particles have considerably higher surface area than their micro counterparts and have markedly different optical, magnetic and biological properties, allowing a profound increase in the polymer-nanoparticle interfacial area and associated interactions and development of formulations that are high strength, antibacterial or conducting can be realized. Silver nanoparticles based composites are the most notable example wherein antibacterial properties are imparted to the polymer matrices by nanofiller. Efficient interactions between filler and polymer matrix facilitate efficient load transfer and leads to high reinforcement at much lower filler loading. However, as the size of filler decreases, the dispersion and distribution of filler in the polymer matrix becomes difficult; moreover, intrinsic properties of polymer and of nanoparticle

play a crucial role in limiting the micromechanics of the nanocomposites for medical applications.

In following sections, properties of polymers, blends and fillers commonly used in medical applications are discussed with reference to reinforcement, conductivity, magnetic properties, biostability and other functional requirements. A brief introduction to the theoretical aspects of polymer blending, composites, conductivity and interface modification is also made. Finally, few recent examples of polymer blends and composites in regenerative medicine, dentistry and drug release are discussed.

2 Fillers for Reinforcement, Conduction, Antibacterial and Other Functionalities

2.1 Carbon Nanotubes

Carbon nanotubes (CNTs) are allotropes of carbon, having tubular structure with exceptional mechanical and electrical properties. High surface area of nanotubes, resistance to metabolism, aromatic structure, tubular geometry and nanosize diameter offers an opportunity of delivering therapeutic or diagnostic molecules drugs directly to targeted cells and tissues. CNTs diameters are of the order of few nanometer and length can be up to several millimeter, translating in extremely high aspect ratio. High intrinsic strength together with high aspect ratio makes CNTs as one of the most promising material for structural applications. CNTs can be visualized as seamlessly rolled graphene sheets. They are commonly categorized as single walled, double walled and multiwalled carbon nanotubes. The mechanical properties of CNTs are considerably higher than conventionally used structural materials. Several theoretical and indirect experimental estimates have been made for the mechanical characteristics of CNTs; however recently mechanical properties of MWNTs were measured directly through stress-strain measurements using an electron microscope. The elastic modulus was reported to be as 0.27–0.95 TPa, strength 10–52 GPa, elongation at break $\sim 5\%$ and toughness of ~ 770 J/g. Modulus of 1 TPa and strength of 100 GPa are now commonly accepted for MWNTs. SWNTs have higher strength than MWNTs due to the shear induced sliding of concentric cylinders present in the MWNTs. Though SWNTs have superior mechanical properties, but their dispersion in polymers is generally more difficult than the dispersion of MWNTs. Arc discharge, laser ablation and chemical vapour deposition are frequently used for the synthesis of nanotubes. The arc discharge procedure used for CNT synthesis is similar to the one used for fullerene synthesis. The procedure involves production of arc discharge between two high purity graphite electrodes in an inert atmosphere. After arc discharge for optimum time, nanotubes get deposited on the cathode. This process generally leads to formation of MWNTs but SWNT can also be produced if metal catalysts such as

Fe, Co, Ni, Y or Mo are used. The characteristics of nanotubes formed depend on various processing conditions such as the type of gas, catalyst used and system and plasma configurations. In the laser ablation technique, a high power laser is used to vaporize carbon from a graphite target at high temperature. Almost all lasers are used for the ablation though Nd:YAG (Neodymium-doped yttrium aluminium garnet) and CO_2 are most common. Both MWNTs and SWNTs can be produced by this technique. In order to generate SWNTs, metal particles as catalysts must be added to the graphite targets. Carbon nanotubes produced by laser ablation are purer, crystalline and have a narrow distribution of diameters. Chemical vapour deposition (CVD) is presently considered to be the most economically viable process for large scale synthesis of CNTs. In CVD, thermal decomposition of a hydrocarbon vapour is achieved in the presence of a metal catalyst. The process is easy to control and yields high purity nanotubes.

As CNTs can absorb or conjugate with variety of drugs, proteins and genes, they were investigated for drug delivery, gene therapy, immunotherapy, tissue regeneration and bio-sensing in several medical conditions (Gulati and Gupta 2012; Varkouhi et al. 2011; Foldvari and Bagonluri 2008). Functionalizing nanotube surface with polar groups increases the potency of CNTs to deliver therapeutic agents across the cytoplasmic membrane and nuclear membrane. The functionalization also improves CNTs chemical and biocompatibility with cellular components and facilitates cellular interaction. Figure 1 demonstrates the intensity of the free siRNA bands on the gel containing CNT-PEI reduced gradually with an increase of the CNT-polymer ratios (Varkouhi et al. 2011). CNT based drug delivery offers possibility of delivering drug directly inside the cells or tissue, via

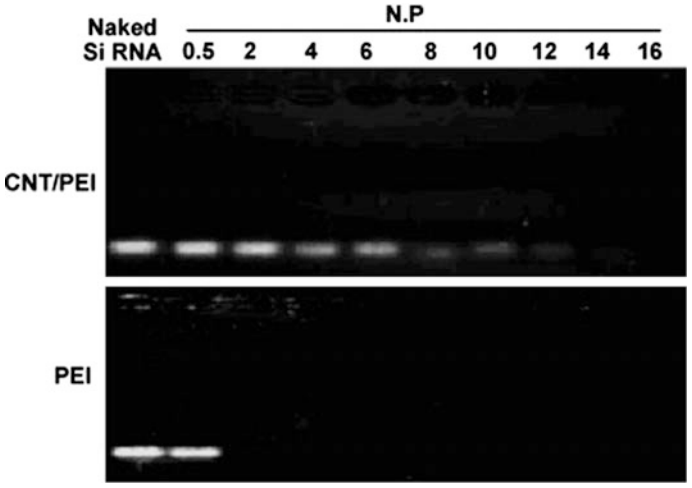

Fig. 1 Complex formation of CNT-PEI 25 kDa and PEI with siRNA as function of CNT/polymer ratio as studied by agarose gel electrophoresis (Varkouhi et al. 2011). Reproduced with the permission from Elsevier

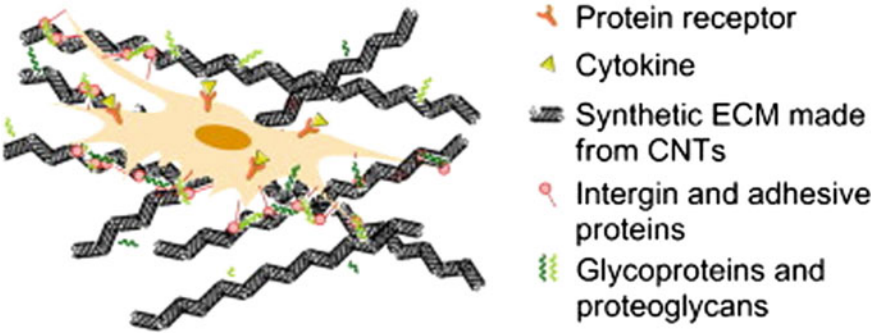

Fig. 2 Shows the adhesion of cells to CNTs. The adhesive properties of such substrates may have an indirect mechanism, where binding between CNTs first adhere to cell adhesion mediators which in turn adhere to cells (Newman et al. 2013). Reproduced with the permission from Elsevier

endocytosis pathway or via the insertion and diffusion pathway (Maruyama et al. 2015). CNTs have also been reported to enhance the bone tissue regenerations and neural differentiation in murine model (Newman et al. 2013; Park et al. 2013). It has been proposed that CNT first adhere to the cells via cell adhesion mediators (Fig. 2) (Newman et al. 2013). Notably, CNTs are also good free-radical scavengers and therefore are envisaged in alleviating chronic ailments (Nymark et al. 2014; Galano 2008).

2.2 Graphene

Graphene is a two dimensional one atom thick (<1 nm) sheet of carbon with a hexagonal conjugated structure. Due to presence of in plane δ-bonds and out of plane π-bonds, the graphene sheet has exceptionally high mechanical strength, making it strongest material ever discovered. Single-layered graphene exhibits Young's modulus of $\sim$1100 GPa and the tensile strength of 130 GPa. The presence of delocalized electrons in completely conjugated two dimensional network makes the thermal and electrical in-plane conductivity of graphene remarkable.

Graphene can be synthesized both by top-down and bottom up approaches. CVD and epitaxial growth have been extensively used to synthesize graphene; though up-scalability and cost effectiveness of these processes are lower in comparison to top down approach. The epitaxial growth of graphene has been used to grow graphene films on a single-crystal substrate under ultrahigh vacuum at high temperature. Unzipping of CNTs and arc discharge has also been explored extensively for production of graphene. In top down approach, graphene is generated from natural graphite through mechanical peeling, exfoliation or delamination. Graphene intercalated compounds (GIC) or expandable graphene (EG) are also available; in which graphite is intercalated using different reagents.

Graphene based biosensors for glucose, dopamine, DNA and proteins are reported recently. Drug delivery, medical imaging and photo thermal therapy in graphene based systems have also shown promising results. It was demonstrated that graphene oxide (GO) sheets that are soluble in buffers and serum without agglomeration. via π-stacking can be used for loading doxorubicin, a widely used cancer drug onto GO functionalized with antibody for selective killing of cancer cells in vitro (Fig. 3) (Sun et al. 2008). It was also established that dsDNA can bind to GO forming complexes (dsDNA/GO) in the presence of salts, which protects dsDNA from being enzymatically digested, by hindering the access of DNA enzymes (Liu et al. 2008). Graphene has shown increased therapeutic efficacy in phototherapy, as it has strong adsorption in the near-infrared region (Liu et al. 2015). It can be used not only for targeted delivery of molecules but also for ablation of malignant tumours, combining benefits of chemotherapy and phototherapy. The pH or other stimuli sensitive drug release behaviour has also been demonstrated by graphene polymer composites (Karimi et al. 2016). Biosensing applications of graphene and its polymer conjugates are enormous (Pumera 2011). GO has also exhibited high gene transfection efficiency and graphene/chitosan composites produced by solution casting method have also been investigated as scaffold materials in tissue engineering (Fan et al. 2010; Yang et al. 2010).

2.3 *Inorganic Fillers*

Inorganic nanoparticles possess unique electronic, optical, magnetic and mechanical properties and can be synthesized by physical or chemical methods. Physical methods involve vapour deposition and mechanical milling whereas chemical routes can be hydrothermal, sono-chemical, solvo-thermal, reverse-micelles, sol-gel, flame spray pyrolysis, organometallic synthesis, microwave method, thermal evaporation and mechano-chemical synthesis. In terms of mechanical reinforcement, silica, MoS_2, boron nitride and nanoclays are of special importance. Nanoclays are generally derived from naturally occurring clays such as montmorillonite, bentonite, kaolinite, hectorite, and halloysite. Among them, plate-like montmorillonite and tubular halloysite are the common nanoclays used for polymer nanocomposite synthesis. Like graphene, montmorillonite nanoclays are also nanosize sheets, having lateral dimensions varying from few nanometer to several microns. Though unlike graphene, interlayer interaction is electrostatic. Isomorphic substitution of an atom within the layer by other metal atom leads to generation of negative charge that is counter balanced by hydrated alkali or alkaline earth cations. Presence of week forces between clay layers makes their separation possible with action of suitable surfactant or polymer. Halloysite is also a naturally occurring aluminosilicate that is used for polymer nanocomposite synthesis. Boron nitride nanotubes (BNTs) are also promising filler for polymer reinforcement owing to their high elastic modulus that is comparable to CNT. BNTs are structural analogues of CNTs where C atoms are substituted by alternating B and N atoms.

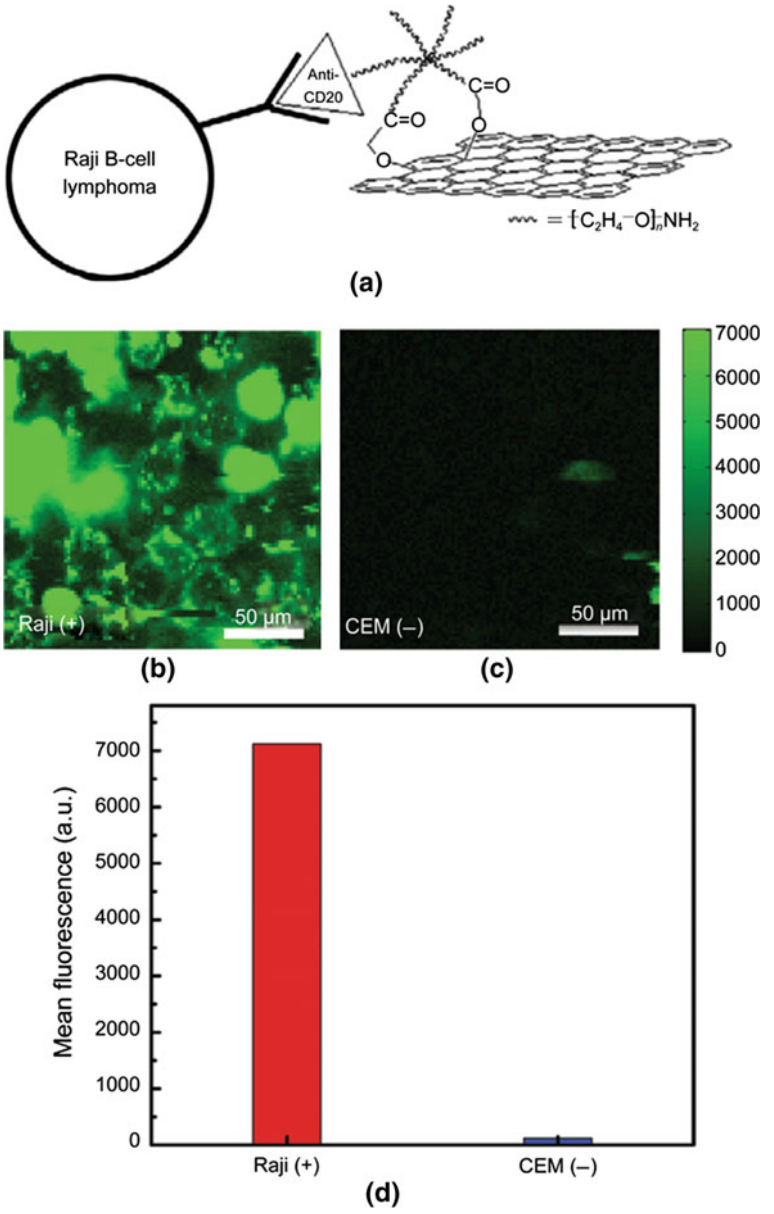

Fig. 3 Nano-graphene for targeted NIR imaging of live cells. **a** A schematic drawing illustrating the selective binding and cellular imaging of NGO–PEG conjugated with anti-CD20 antibody, Rituxan. **b** NIR fluorescence image of CD20 positive Raji B-cells treated with the NGO–PEG–Rituxan conjugate. The scale bar shows the intensity of total NIR emission (in the range 1100–2200 nm). Images are *false-colored green*. **c** NIR fluorescence image of CD20 negative CEM T-Cells treated with NGO–PEG-Rituxan conjugate. **d** Mean NIR fluorescence intensities in the image area for the both the positive (Raji) and negative (CEM) cells treated by NGO–PEG–Rituxan conjugate (Liu et al. 2008)

MoS_2 and the related WS_2 nanotubes have also been explored and they offer combination of strength and flexibility.

Metal oxides have been explored for diagnostic applications, and for imparting antibacterial, antifungal properties to polymer matrices (Bhattacharyya et al. 2011; McCarthy et al. 2007). Iron oxide nanoparticles show exceedingly good contrast in MRI; they have high sensitivity and follow metabolic pathways of cellular iron, making them very attractive for clinical applications (Liu et al. 2007). Gadolinium (Gd) is used due to their strong and stable photoluminescence properties (Maalej et al. 2015; McCarthy et al. 2007). Metal nanoparticle preparations have been developed for angiogenesis, cancer staging, tracking of immune cells and cellular targeting (Conniot et al. 2014; Sanna et al. 2014; Weissleder et al. 2014). Figure 4 presents organs and cell type distribution of injected nanomaterials (Weissleder et al. 2014; Keliher et al. 2011). Gold nanoparticles can bind to many different biological ligands as they have affinity for thiols, disulfides, phosphine, and amines (Giljohann et al. 2010). PEG conjugated gold nanoparticle was demonstrated to target the factor receptor (FR) on various cancer cells. The SPR band of the Au NPs can be used to generate heat at the tumour site (El-Sayed et al. 2006). Fe_3O_4, gamma phase nanoparticles can also used in hyperthermia treatment, due to their magnetic properties (Gupta et al. 2007). Under magnetic field such nanoparticles and their composites can produce, heat in a controlled fashion due to magnetic hysteresis loss. Au-based nanoparticles are also used as sensitizer in photo-thermal

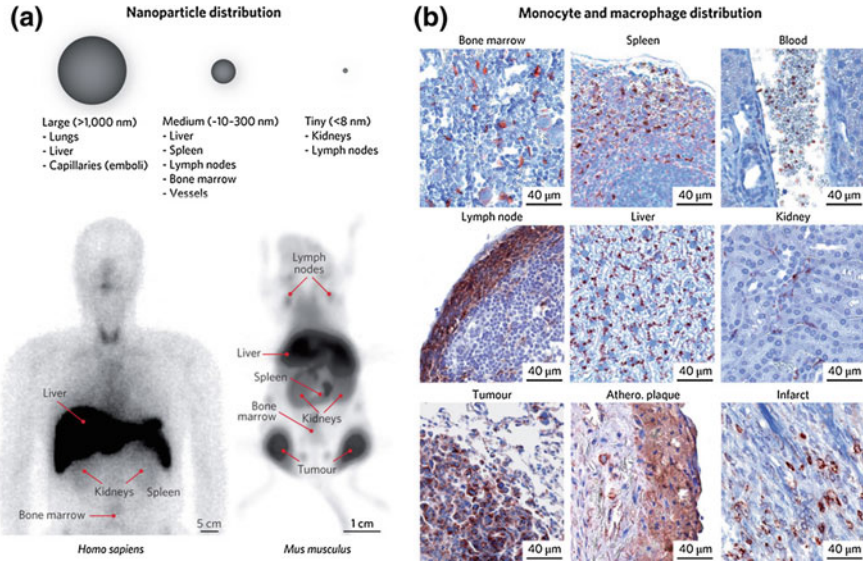

Fig. 4 Organ and cell type distribution of systemically injected nanomaterials. Most nanoparticles for in-vivo use fall into the intermediate category (10–300 nm), where distribution to liver, spleen, lymph nodes and bone marrow is common (Weissleder et al. 2014). Reproduced with the permission from Nature Publishing Group

therapies. Gd and CeO_2 nanoparticles are reported to quench ROS and reduce of mitochondrial damage (Yin et al. 2008). Antibacterial properties are reported in different types of metallic nanoparticles and their oxides. Silver nanoparticles have received highest attention as antimicrobial agent and their several commercial applications have emerged. Silver nanoparticle/polymer based composites are also extensively reported. Aluminium nanoparticles, Aluminium oxide NPs have wide-range of applications in industrial and personal care products. TiO_2 nanoparticles show accelerated antibacterial effect under UV light, via production of hydroxyl radicals. Zinc oxide nanoparticles have been found to exert selective toxicity to bacteria (Agren et al. 1991).

2.4 Natural Fillers

Flax, sisal, cotton, coir, ramie, jute and bamboo fibres are widely used in reinforcing polymer composites. Their availability, good mechanical properties, easy processability, low cost, low density, and biodegradability make them attractive choice. However, because of their natural origin their mechanical characteristics and density varies significantly with the source of origin. These fibres are generally of micro scale diameter, and therefore do not show high surface area effect on the polymer reinforcement, as shown by nanosize fillers. Nanocrystalline cellulose (NCC) is a recent development that possesses advantages because of nanoscale dimensions. NCC is generally synthesized by acid hydrolysis of native cellulose and the properties of final product markedly depend upon reaction time, temperature and acid concentration (George and Sabapathi 2015). NCCs are rigid rod-like crystals with diameter in the range of 10–20 nm and lengths of a few hundred nanometres. It has high specific strength and modulus making it a promising reinforcing agent for polymers. Furthermore, natural polymers are attractive for biomedical applications since they are of natural origin, they offer better biocompatibility than synthetic fillers.

3 Polymers for Biomedical Applications

Polymers are considered to be exciting matrices for structural applications, by virtue of their light weight, easy processability and long term stability. Large variety of polymers is used for medical applications and can be broadly classified as elastomers, thermoplastics and thermosets. An elastomeric polymer offers high toughness and excellent elongation at break along with good tensile strength. Such matrices are widely used in automobile, space, wire and cable, sports and nuclear industry. Elastomers have high molecular weight, amorphous structure and weak inter and intermolecular forces, translating in low elastic modulus but high elongation. Their glass transition temperature is considerably below room temperature;

therefore at room temperature segmental motions are possible, making them soft and flexible. However, reversibility of deformation demands covalent or ionic linkages between polymer chains. This can be achieved by using peroxides, metal oxides, sulphur, and ionic moieties or by radiation crosslinking. Elastomers are saturated or unsaturated and are used for variety of applications such as tyres, conveyor belts, vibration dampeners and insulating structures. Due to weak intermolecular bonding, elastomers need further reinforcement even after crosslinking to attain desired mechanical properties. Carbon black, fumed silica, clay, talc and mica are commonly used fillers for elastomer reinforcement. However conventional fillers demand high loading, increasing weight, hysteresis and processability. Therefore, there has been considerable interest in using nanofillers for their reinforcement. Elastomers and their composites are used for several biomedical applications. Natural rubber (poly isoprene), polyurethanes, silicones rubbers and thermoplastic elastomers are among the most commonly used elastomers for medical applications such as catheters, vascular access, prosthetic devices, transdermal drug delivery patches and urological aids (Yoda 1998).

Thermoplastics polymers have unique virtue of reprocess ability. These polymers become soft or melt over a specified temperature range and solidify again on cooling. Unlike elastomers, these polymers do not require crosslinking due to the presence of crystalline domain or polar intermolecular interactions. The presence of crystalline and amorphous domains allows a wide range of thermal and mechanical properties, opacity and permeability. The glass transition of thermoplastic can be above or below room temperature. These polymers can be extruded, injection moulded, compression moulded and transfer moulded reversibly. Nanoparticle additions have been reported to significantly improve properties like flame retardancy, durability and elastic modulus of thermoplastics such as acrylic ABS, nylon, polybenzimidazole, polyethylene, polystyrene, polyvinyl chloride and Teflon.

Thermosetting polymers, are highly crosslinked polymers and cannot be recycled or reprocessed. Prior to crosslinking they can be monomers/oligomer (liquid) or molten polymer filled in a mould of predefined shape and size, where in situ crosslinking takes place. Using suitable initiator, sensitizer or radiation, monomers/oligomer (liquid)/molten polymer transform into a highly rigid three dimensional structure. Epoxy, polyurethane and acrylate resins are widely used as thermosetting polymers. They contain un-saturation or highly strained groups that can be crosslinked at room temperature or at high temperature by aromatic/aliphatic amines or anhydrides or by high energy or UV radiation. Generally, high temperature cured thermosets have superior physico-mechanical properties than room temperature cured systems. A variety of fillers are used to improve modulus of thermosetting polymers. Glass fibre, carbon fibre, natural fibres are traditional choice and several commercial applications have been developed using them. Recently there has been a considerable interest in using nanofillers as reinforcing agents for thermosets. Due to their high strength and flexibility thin, yet strong structural objects can be made by using suitable thermosets-filler compositions. However, unlike thermoplastic nanocomposites, thermosets nanocomposites cannot be recycled, involves toxic solvents and are less chemical resistant. Corrosion

resistance, structural integrity, low cost, thermal insulation, and dielectric strength of thermosets make them useful for several medical applications such as medical instrumentation, tools and prosthetics.

4 Common Polymers for Biomedical Applications

4.1 Synthetic Biodegradable and Non Biodegradable Polymers

4.1.1 Polyolefins

Polyolefins are polymers made of repeating unit of olefin or alkenes. Polyethylene (HDPE, LDPE, and UHMWPE) and polypropylene are two most commonly used polyolefins. They are non biodegradable, hydrophobic, chemical and bacterial resistant thermoplastics. Polyolefins offer different crystallinity, branching and molecular weight options which in turns offers wide property domains to suit different applications. They are low cost, have good environmental stress-cracking resistance and are therefore used for wide range of medical applications including dilators, disposable hypodermic syringes, suture materials, meshes, packaging, medical vials, diagnostic devices, petridishes and surgical components. In cardiovascular applications, polyolefins are utilized as tubing and housings for blood supply. They are also utilized in production of blood bags to store blood. Metallocene PP is one of the polyolefins which has shown great potential in medical applications; UHMWPE is another highly used polyolefin. It has very high molecular weight ($\sim$2 M amu), abrasion resistance, impact strength and a low coefficient of friction and has been used as sliding surfaces of artificial joints in total joint arthroplasty. It is used as artificial hips, knees, as well as in shoulders, elbows, wrists, ankles and spinal disks. The alterative material for such applications is titanium, which offers disadvantages such as cytotoxicity, corrosion and release of metal ions over long term use. UHMWPE is therefore usually used for the replacement of total hip, knee, shoulder, ankle, elbows and spinal disk. It has good stability in radiation field, and is often crosslinked by high energy radiation to improve mechanical properties. UHMWPE based non absorbable sutures are also used for surgical applications as it offers good knot security and precise knot placement. Polyolefin elastomers are also gaining applications for medical applications. Propylene-based elastomers are reported to offer softness of elastomers and drape ability and abrasion resistance of propylene. For outdoor applications polyolefin-based elastomer showed better performance than thermoplastic polyurethane (TPU) material (Patel et al. 2009). In another interesting work, liquid blowout force results demonstrated that polyolefin elastomer offers better properties than silica filled PP (Brostow et al. 2007). In a recent review, titanized polypropylene meshes were compared with polypropylene, polyester and ePTFE

meshes for hernia surgery. For inguinal hernias, titanium-coated polypropylene mesh was associated with less post-operative pain in the short term, lower analgesic consumption and a quicker return to everyday activities (Kockerling and Schug-Pass 2014).

4.1.2 Fluropolymers

PTFE and PVDF are two most common synthetic fluorocarbon polymers used in medical applications. They are biocompatible, inert thermoplastic and have a low coefficient of friction. PTFE is used in vascular grafts and heart valves and PTFE sutures are used for repair of mitral valve for myxomatous implantable prosthetic heart valve rings. Elongated-PTFE (e-PTFE) is used in smaller arteries. Another type of PTFE, dense polytetrafluoroethylene (d-PTFE), results in lower levels of early infection following surgical procedures. d-PTFE has been identified as barrier membrane for guided tissue regeneration and guided bone regeneration around teeth and implants. PTFE is also used to deliver coronary stents and other devices as the guiding catheter. PTFE and PVDF membranes are used as filters for biological fluids. Both PTFE and PVDF can be made hydrophilic or oliophilic by surface modification. PTFE has been used in otorhinolaryngology, urology and in the treatment of vesicorneal reflux (Laustriat et al. 1990). ePTFE valve patches/conduits are recognized as excellent material for right ventricular outflow tract reconstruction due to biocompatibility and low antigenicity of ePTFE, and also due to the fluid dynamics of the valve. e-PTFE covered stents have significantly improved two-year transjugular intrahepatic portosystemic shunt patency (Saad 2014). Prosthetic graft PTFE has also been used in above-knee femoropopliteal arterial bypass.

4.1.3 Poly(Vinyl Chloride)

PVC is a polymer with an ethylene backbone with one covalently bound electronegative chlorine atom. It is among the most extensively used polymers for biomedical applications. However, for better stability and processability, PVC needs to be compounded with stabilizers and plasticizers, which raises medical concerns. Stabilizers are added to avoid autocatalytic dehydrochlorination and thermal degradation of the PVC chains during thermal processing. Plasticizers are used to enhance the flexibility of PVC, making it suitable for applications such as extracorporeal tubings, sheets and blood storage bags. It has shown direct cytotoxicity mainly due to the presence of stabilizers and plasticizers. Plasticizer di(2-ethylhexyl) phthalate (DEHP) was found to release from the PVC matrix and diffuse into the lipid bilayers of cells. Hormonal imbalance, birth defects and infertility have been reported for DEHP in rodent models. It is however important to note that these toxic effects are not reported upon parenteral administration. Blood storage bags are mostly made of PVC and therefore any leaching of plasticizers or of stabilizers, may

affect the blood component separation and storage. There are developments in the area of DEHP-free PVC bags for platelet storage and plasma storage. However there is no major breakthrough on the storage bags for RBC and still DEHP-plasticized PVC are in use (Prowse et al. 2014; Sampson and de Korte 2011).

4.1.4 Silicones

Unlike most of the polymers, which have carbon backbone, silicone based polymers consist of –Si–O– backbone. Silicone polymers are used as oils (oligomers) and elastomers (high molecular weight) in medical applications. The most common silicone polymer is PDMS which contains methyl as side group. Silicones are highly flexible biostable elastomers which present biocompatible, adhesion, hydrophobic, aesthetics, nonirritating and nonsensitizing behaviour. They are used in ophthalmology as tamponade, personal care, cosmetic surgery, topical/transdermal drug delivery and implants (Aliyar and Schalau 2015). PDMS has low surface energy and thus shows limited interfacial interactions with different substrates. Moreover, PDMS do not require stabilizers or plasticizers because of their intrinsic flexibility (low T_g) and stability, making them more hemo-compatibile and preferable over PVC. To make PDMS medical grade, impurities, such as catalysts, oligomers can be removed easily. Due to its low surface tension, minimal interfacial interaction, softness and elasticity, PDMS is expected to be associated with low risk of trauma if applied in biological applications. They are permeable to oxygen, carbon dioxide, water vapor and various small molecules, making transdermal drug delivery and wound management applications feasible. PDMS based subcutaneous contraceptive implant based drug delivery systems are used in vaginal ring for treatment of menopause associated urinary problems. PDMS based drug delivery systems are explored for angina pectoris, hormone replacement and pain management. PDMS is also very stable in terms of temperature and radiation sterilization.

4.1.5 Polyurethanes

Polyurethanes (PU) contain –NH–(C = O)–O– linkages and come in diverse variety including elastomers, thermoplastics and thermosets. The synthetic chemistry of PU allows offering variable hard and soft segments, aromatic or non aromatic or ester, ether or carbonate based. They are typically synthesized by reacting polyisocyanate with polyols (functionality greater or equal to 2). However non-isocynate based polyurethanes have also been developed (Usman et al. 2016). Aromatic and silicone based PUs shows better biostability, lower cost, high chemical resistance and more toughness, and are promising for long-term implants. In general PUs are biocompatible and hemocompatible, moreover, they do not need plasticizers and have low residual monomers impurities. Different extent of elasticities can be obtained by varying the hard and soft segments ratio in PU. Hard PUs have better biostability

while, soft polyether based polyurethanes, provide better patient comfort due to their soft feel. PUs are used in faecal incontinence as anal plugs (Deutekom and Dobben 2015). Collagen/PU bio-composites have also been used to explore biomedical applications (Zuber et al. 2015). PU is also used as biological adhesive and sealant (Scognamiglio et al. 2016). Elastomeric PU is also used in spinal surgery as disc replacement and stabilization of spinal movement to relieve nerve root compression. The main advantage of PU in such applications is its efficacy in closely matching the mechanical properties of spinal disk and maintaining motion between spinal segments (St John 2014). In a recent study, comparison was made between complications in silicone and polyurethane lines in peripherally inserted central catheters (PICC) in cancer and other patients. It was found that both lines have similar overall average post insertion complication rates; however polyurethane PICC lines were found to provide lower rates of infection, dislodgment, and thrombus and rupture complications (Seckold et al. 2015). Polyurethane coatings are also used in different medical applications, and can be used to impart variety of attributes such as hydrophilicity, non-thrombogenicity, drug release, or lubrication (Associates 2016). Polyurethanes are used in catheters; due to their excellent mechanical properties, very low thickness can be maintained allowing the maximum number of lumens at low outer diameter. PU building blocks can be tailored to offer different property combinations in PU (Aslam and Darouiche 2010); however, the design of polyurethanes for catheter relies on biocompatibility, toughness, good column strength and minimal kinking.

4.1.6 Poly Methylmethacrylate

PMMA is a hard polymer which is used in dentistry, ophthalmology, arthroplasty and other orthopedic applications. Its monomer rapidly polymerizes allowing onsite polymerization. It is biocompatible, tough and transparent. PMMA is harmless, however, since in situ polymerization is often used, exposure to methylmethacrylate (MMA) vapours puts a challenge to its use in medical applications (Leggat et al. 2009). In dental applications, use of PMMA is known since long time and was used for fabrication of denture bases. In orthopedics, it is used as bone cements, filler for bone cavities and defects, osteomyelitis and or vertebrae stabilization in osteoporosis (Frazer et al. 2005). Antibacterial agents are often added to MMA based formulations avoid implant related complications (Inzana et al. 2016). Figure 5 shows one interesting applications of PMMA for control drug release applications, wherein PMMA powder, carboxymethylcellulose hydrogel and PLGA microspheres composites were loaded with colistin and demonstrated to show continuous colistin release for 5 weeks (Shi et al. 2010). PMMA is used in non-metal clasp dentures; though other thermoplastics are increasingly explored to avoid the MMA associated complications, PMMA still offers better abrasion and functional properties (Fueki et al. 2014). PMMA is also used as cosmetic filling agent in dentistry and for orofacial medicine (Vargas et al. 2012). In orthopedics, PMMA can serve as a spacer and as a delivery vehicle for antibiotics (Jaeblon 2010; Cancienne et al. 2015).

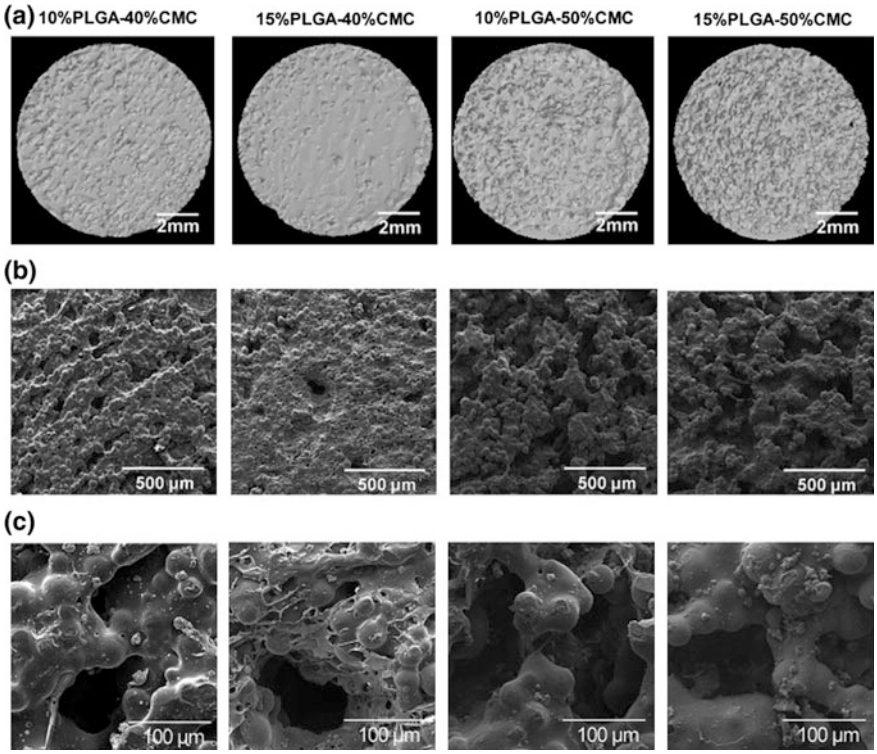

Fig. 5 Surface morphologies of PLGA microsphere-incorporating porous constructs characterized by **a** micro CT (size bars represent 2 mm); **b** SEM (lower magnification, size bars represent 500 µm); and **c** SEM (higher magnification, size bars represent 100 µm): surface porosity was created by incorporation of CMC hydrogel, and higher percentages of CMC incorporation led to greater surface roughness (Shi et al. 2010). Reproduced with the permission from Elsevier

Another common methacrylate in medical applications is poly-HEMA (pHEMA) made of 2-hydroxyethyl methacrylate monomer. Because of presence of one hydroxyl group per monomer unit, pHEMA is hydrophilic and shows good anti-fouling properties and thus used in hemocompatible coatings or to coat contact lenses (Kluin et al. 2013; Gautam et al. 2012).

4.1.7 Polyesters, Polycarbonates and Polyethers

Polyester as the name suggests contains ester linkage and can be of natural or of synthetic origin. Synthetic polyesters are generally non biodegradable and can be thermoplastic or thermosets. Aromatic polyesters are generally bio-stable and are used in membranes, filaments and meshes. Two main synthetic biodegradable polymers are poly (glycolic acid) and poly (lactic acid). The biodegradation of these

polyesters depends on the monomer, molecular weight and crystallinity. The main driving force of using these biodegradable polymers in medical applications is that their degradation involves natural metabolism. These polymers are thermoplastics and can be converted into different shapes to suit different applications ranging from coating to drug eluting stents. Modification of polyesters fibres have also been extensively investigated to make them suitable for different biomedical applications. Sericin-treated polyester fabrics was recently used as medical textile for potential applications in atopic dermatitis, pressure ulcers and rashes (Gupta et al. 2015). Polyesters contain ether linkages and polyacetal, polyether sulfone, polyethylene oxide (PEO) and polyether ether ketone (PEEK) are three major examples of such polymers. Polyether is used in orthopaedic bandages, plasters, in artificial tendon and other implant applications. PEEK is one of the most extensively studied polymer material for medical implants due to its superior biostability, creep resistance and also mechanical and wear properties Polycarbonates are highly rigid plastics; they have been explored for renal dialysis cartridge, heart-lung machine, trocars, tubing interconnector; however, the presence of hazardous ingredients puts a limit to the medical applications of polycarbonates.

4.1.8 Polyamides, PVA and EVOH

Polyamides are polymers that contain amide links therefore they represent a wide class of natural and synthetic polymers. Common naturally occurring polyamides are silk and wool whereas common synthetic amides are nylons, aramids, and sodium poly (aspartate). Nylon non-allergenic and resistant to chemicals is used for sutures in applications demanding high strength. Nylons are considered for balloon of catheters for angioplasty and transfusion lines and fittings, due to their excellent burst strength and flexibility.

PVA is derived from poly vinyl acetate by full hydroxylation. It has low protein adsorption, biocompatibility and bio-stability. It is used in soft contact lenses, tissue adhesion barriers, and as artificial cartilage (Baker et al. 2012). Ethylene vinyl alcohol is a copolymer of ethylene and vinyl alcohol. It has exceptional barrier properties making it highly suitable for stormy pouching system and dialysis bags. It has also gain prominence in drug delivery devices and implants.

5 Natural Polymers and Their Derivatives for Medical Use

The varieties of chemical structures existing in the natural polymers present precise molecular architecture and rationalize their numerous applications as biomaterials in high technological and biomedical fields. In general, biopolymers are the degradable class of polymers which are the part of or produced by living organisms. In principal, biopolymers are safe materials which can be obtained by processing of monomers or polymers found in nature following the good manufacturing practices

(GMP) and relevant regulations. Presently, biopolymers are used in food, pharmaceuticals, cosmetics, animal feed and other industrial applications. The inherited properties of biopolymers attract its applications as a biomimetic component for biomedical applications, however, some concerns are also associated like undesired active components within natural polymers may provoke immune responses. The most commonly used natural polymers in biomedical applications are described in this section.

5.1 Collagen

Collagen is the most abundant structural animal protein accounting for 25–35% of total body proteins in mammals. It is found in connective tissues, skin and in extracellular space and is synthesized mostly by fibroblast cells. It has good tensile strength, molecular weight ~3000 D and tissue dependent rigidity. It has been used in prosthetic heart valves and vascular prosthesis. Compared to the synthetic analogues discussed above; collagen has lesser rejection rate and higher biocompatibility. Collagen based drug delivery systems have been explored to treat infected corneal tissue or liver cancer and bone formation promotion, both as injectable and as oral drug carrier (Khan and Khan 2013). Collagen sponges are used in the severe burns and wound healing and collagen nanoparticles are also used as a sustained release formulation. Collagen based implants have been widely used as vehicles for transportation of cultured skin cells or drug carriers for skin replacement and burn wounds. Collagen has been used as bone substitute due to its osteoinductive activity. Collagen has been used as implantable carriers for bone inducing proteins, such as bone morphogenetic protein 2 (rhBMP-2) (Barboza et al. 2004). Collagen achieves rapid coagulation of blood through its interaction with the platelets providing temporary framework while the host cells regenerate their own fibrous stroma (Yadav et al. 2015). The use of collagen based haemostats has been proposed for reducing blood loss in generalized bleeding in a wide number of tissues and management of wounds to cellular organs such as liver or spleen (Lewis et al. 2016). The various types of collagen (so far 28 types are identified) are different in their structures (Sherman et al. 2015). Due to various types of collagens and their different immunological activity, its partial hydrolyzed form called 'Gelatin' has been extensively studied as a supportive biomaterial (Singh et al. 2011; Tripathi et al. 2009, 2013).

5.2 Cellulose, Hemicelluloses and Derivatives

Cellulose is the most abundant naturally occurring polymer. It is the main constituent of plants and natural fibbers. It is a polysaccharide having a linear chain of several hundred to over ten thousand β (1 → 4) linked D-glucose units. Cellulose and its

derivatives are extensively used for different medical applications since several decades. Cellulose ether is used in drug delivery formulations which allow swelling-driven release of drugs. The swelling behaviour can be designed to match the release requirement, as swelling proceeds from the surface to the glassy core of the tablet, the drug progressively dissolves in water and diffuses out from the polymer network. Due to the excellent biocompatibility of cellulose and its good mechanical properties the use of cellulose and its derivatives as biomaterials for the design of tissue engineering scaffolds has been increasing (Müller et al. 2006). Figure 6 represents different type of cellulose scaffolds seeded with primary bovine chondrocytes (Müller et al. 2006). Bacterial cellulose has been widely investigated for wound healing due to its purity and high water retention capacity. Hemicelluloses are the second most abundant polysaccharide after cellulose. Xylans are the main hemicelluloses in hardwood and they also predominate in annual plants and cereals making up to 30% of the cell wall material and one of the major constituents (25–35%) of lignocelluloses materials. Xylan has been considered as a suitable raw material to produce colonic drug delivery systems as it is biodegraded by enzymes produced by the colonic micro flora (Hamady 2013). It is known to induce faecal bulking effect and lowering of blood cholesterol and decrease of postprandial glucose and insulin responses. Some of xylans also show anti-phlogistic effect (Oliveira et al. 2010). Xylan rich hemi-celluloses have been reported to inhibit the growth rate of sarcoma 180 and other tumours, probably due to the indirect stimulation of the non-specific immunological host defence (Zhuang et al. 1993).

5.3 Chitin and Chitosan

Chitin is the second most abundant biopolymer in the world. It is the main component of the exoskeleton of crustaceans and insects, it also occurs, in nematodes and in the cell wall of yeast and fungi. However it is difficult to process as it is not soluble in most of the solvents under room conditions. Generally it is deacetylated to chitosan for practical applications. Chitosan has excellent biocompatibility, bioactivity and biodegradability. It has been known to have antibacterial and anti acid effect (Raafat and Sahl 2009). Chitosan shows antimicrobial action in against great variety of microorganisms, including algae, fungi and bacteria. It has also been found to be a preventive material for dental caries (Chen and Chung 2012). Chitosan has been explored as drug carrier for controlled release, bacterial plaque formation inhibition, decalcification of dental enamel promoting osteogenesis, fat absorbent action and the healing of ulcers and wounds. Chitosan has an in vivo stimulatory effect on both nitric oxide production and modulates peroxide production (Park and Kim 2010). Chitosan has potential to improve drug absorption and stabilization of drug components to increase drug targeting (Ahmed and Aljaeid 2016). In addition, chitosan can protect DNA and increase the expression period of genes (Bozkir and Saka 2004). Chitin or chitosan derivatives, which were conjugated with some kinds of anticancer agents, can execute better anticancer effects

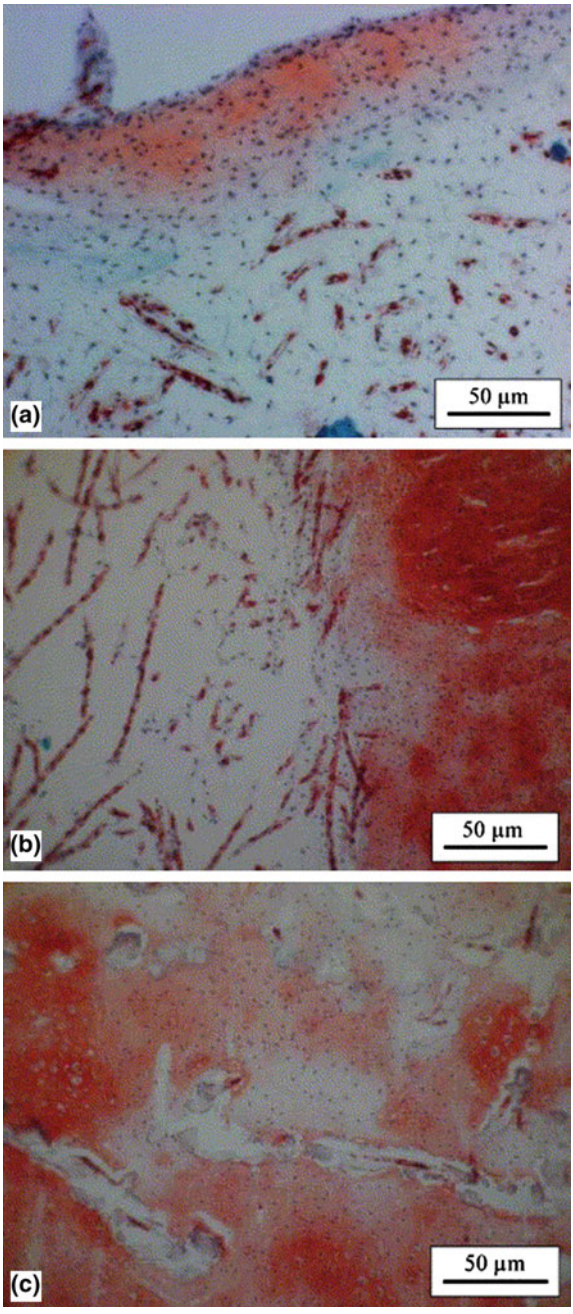

Fig. 6 Safranine-O staining of cellulose scaffolds seeded with primary bovine chondrocytes, in-vitro cultured for 6 weeks: **a** untreated, **b** $Ca(OH)_2$-treated and **c** CaP-coated samples (Müller et al. 2006). Reproduced with the permission from Elsevier

with gradual release of free drug in the cancer tissues. Chitosan is confirmed to partially inhibit the secretion of both interleukin-8 and tumornecrosis factor-α from mast cells, demonstrating that water-soluble chitosan has the potential to reduce the allergic inflammatory response (Kim et al. 2004). Chitosan promotes phagocytises and production of osteopontin and leukotriene by polymorphnuclear leukocytes, production of interleukin-1, transforming growth factor β1 and platelet-derived growth factor by macrophages, and production of interleukin-8 by fibroblasts, enhancing immune responses (Ueno et al. 2001). Chitosan and hydroxyapatite are among the highly researched bioactive biomaterials in cartilage and bone tissue engineering (Venkatesan and Kim 2010; Bhat et al. 2011; Kathuria et al. 2009).

5.4 Alginate and Carrageenan

Alginates are extracted from brown seaweed. Because of its biocompatibility, biodegradability, non-antigenicity and chelating ability (Tripathi et al. 2013), alginate is widely used in a variety of biomedical applications including tissue engineering, drug delivery and in some formulations preventing gastric reflux (Lee and Mooney 2012). Alginates are also widely used for impression making in the dental clinic because of its ease in handling. Carrageenan is a generic name for a family of gel-forming and viscosifying polysaccharides. Carrageenan is a sulphated polygalactan with 15–40% of ester-sulfate content. The anticoagulant activity of carrageenan makes it useful in anti-thrombic applications (Sokolova et al. 2014; Dore et al. 2013). The mechanism underlying the anticoagulant activity of carrageenan involves thrombin inhibition. Carrageenan is a selective inhibitor of several enveloped viruses, including such human pathogens as human immunodeficiency virus, herpes simplex virus (HSV), human cytomegalovirus, human rhinoviruses and others. Carrageenan acts primarily by preventing the binding or the entry of viruses into cells (Grassauer et al. 2008).

5.5 Silk

Silk is a natural protein fiber. Silk has been considered biocompatible and used for medical applications for centuries. It has been demonstrated that some of the wild silks have unique properties and are preferred for medical applications. For example spider silk has gained considerable attention in tissue engineering, regenerative medicine and other medical applications due to good elasticity and tensile strength. It showed good attachment and spreading of mouse fibroblast cells suggesting potential for medical applications (Reddy et al. 2013a, b). Recent studies with well-defined silkworm silk fibres and films suggest that the core silk fibroin fibre

exhibits biocompatibility under in vitro and in vivo conditions comparable with other commonly used biomaterials such as polylactic acid and collagen. The ability to genetically tailor the protein in silk provides additional advantages of silk based fibrous proteins. In scaffolds for tissue engineering of bone and ligaments, silk based scaffolds have shown encouraging results (Altman et al. 2003).

6 Polymer Blends and Composites for Medical Applications

6.1 Theory

6.1.1 Polymer Blending

Blending of two amorphous polymers can produce either a homogeneous mixture at the molecular level or a heterogeneous phase-separated blend. Separation of polymer chains produces two totally separated phases, and hence leads to macro-phase separation in polymer blends. The miscible polymer blend is a blend of two or more polymers that is homogeneous to the molecular level and fulfills the thermodynamic conditions for a miscible multicomponent system. Whereas, an immiscible polymer blend is the blend that does not comply with the thermodynamic conditions of phase stability. Equilibrium phase behavior of polymer blends complies with the general thermodynamic rules.

$$\Delta G_{mix} = \Delta H_{mix} - T\Delta S_{mix} < 0 \tag{1}$$

and

$$\mu_i^{'} = \mu_i^{''} \tag{2}$$

where ΔG_{mix}, ΔH_{mix}, and ΔS_{mix} are the Gibbs energy, enthalpy, and entropy of mixing of a system consisting of i components, respectively, μ'_i and μ''_i are the chemical potentials of the component i in the phase μ' and μ''. Whether polymers are miscible or not depends on a balance of interactions among all components in a system.

6.1.2 Micromechanics of Composites

Mechanical properties of polymer micro, meso or nano composites mainly depend on the polymer matrix, aspect ratio of filler, orientation and packaging density. Polymer-filler interface plays a critical role in determining mechanical properties of the composites. Due to the additive nature of the properties, several models have been proposed to predict mechanical properties of polymer composites. Most of the

work however is confined to fibre-reinforced composites, and the reinforcement theory for nanofillers is not yet fully established. Still, it is proposed that established micromechanical models can be applied to nanocomposites with a great deal of success. Among several models, rule of mixture, Halpin-Tsai and Neilsen's model are most frequently used.

Elastic modulus of the polymer composites in the simplest form can be described by following equation.

$$E_c = E_m V_m + E_f V_f \tag{3}$$

where E_m and E_f are the modulus of the matrix and filler respectively and V_m and V_f are their respective volume fractions. It is assumed that the filler distribution is isotropic and the filler covers full length of the matrix. It is also assumed that the bonding between filler and polymer matrix is strong and under applied stress, filler and polymer are equally strained. However, in practice, most of the composites depart from these ideal conditions and therefore different efficiency factors have been incorporated in the above equation. If reinforcement length and orientation efficiency factors are considered the Eq. (3) is modified as.

$$E_c = E_m V_m + E_f \eta_l \eta_o V_f \tag{4}$$

where η_l, η_o are length (for asymmetric fillers) and orientation efficiency factors. η_l can be defined using Cox's shear lag model as follows

$$\eta_l = 1 - \left[\frac{Tanh(\alpha \cdot l/d)}{\alpha \cdot l/d}\right] \tag{5}$$

where α is defined as

$$\alpha = \sqrt{-3E_m/2E_f \ln V_f} \tag{6}$$

Another important concept in determining length efficiency factor is the critical length of the filler which is essential for the stress transfer from the matrix to the filler. Stress transfer is expected to increase as the length to diameter ratio (l/d) of the filler increases, since the surface area is expected to increase with an increase in the length for a fixed diameter. It is therefore possible that at a particular length, transferred stress would be higher than the tensile strength of the filler and may lead to the breakage of the filler. This length is generally defined as a critical length (l_c) for a matrix-filler system. Subcritical length will lead to inefficient stress transfer and reinforcement and efficiency factor approaches to 1 as l/d increases. A porosity and filler area (dimension) correction factor can also be introduced in the above equation to take care of porosity generated during composite formation and to take in consideration the fact that dimension of all fillers are not equal. The modified equation can be presented as

$$E_c = [E_m V_m + E_f \eta_l \eta_o k V_f] \cdot (1 - V_p)^2 \tag{7}$$

where k and V_p are dimensional and porosity factors respectively.

Halpin-Tsai model predicts modulus of a polymer composite with oriented filler using following relation (Affdl and Kardos 1976)

$$E_c = E_m \frac{[1 + (2l/d)\eta V_f]}{1 - \eta V_f} \tag{8}$$

where η is defined as

$$\eta = \frac{E_f/E_m - 1}{E_f/E_m + 1} \tag{9}$$

For random orientation, the efficiency factors η_l and η_t are introduced. The model can be further refined as

$$E_c = E_m \left[\frac{3}{8} \cdot \frac{1 + (2l/d)\eta_l V_f}{1 - \eta_l V_f} + \frac{5}{8} \cdot \frac{1 + 2\eta_t V_f}{1 - \eta_t V_f}\right] \tag{10}$$

where

$$\eta_l = \frac{E_f/E_m - 1}{E_f/E_m + 2l/d} \tag{11}$$

and

$$\eta_t = \frac{E_f/E_m - 1}{E_f/E_m + 2} \tag{12}$$

These models consider aspect ratio as well as filler volume fractions and predict almost linear increase in the modulus whereas some models such as Guth have power functions. In case of symmetrical particles Nielsen's model is generally employed, which has been described as

$$\frac{E_c}{E_m} = \frac{1 + ABV_f}{1 - \psi BV_f} \tag{13}$$

$$A = k_E - 1 \tag{14}$$

$$B = \frac{\frac{E_f}{E_m} - 1}{\frac{E_f}{E_m} + A} \tag{15}$$

$$\psi \cong 1 + \frac{1 - \phi_m}{\phi_m^2} V_f \tag{16}$$

where E_f, E_C and E_m are the elastic modulus of the filler, polymer composite and polymer matrix respectively, k_E is the Einstein's coefficient. The constant A takes care of the aspect ratio and orientation of the filler and the factor B addresses relative difference in the modulus of the two components. ϕ_m is related to the packing density of the filler and ψ is associated with the filler volume fraction. In case of binary polymer blends, the elastic modulus varies substantially with the variation in the blend composition. Parallel and series model are often used to predict the elastic modulus data of blends. Parallel model which represents the upper bound of modulus values of a binary system can be described as

$$E = E_1\phi_1 + E_2\phi_2 \tag{17}$$

where E is the modulus of blend predicted by the model and E_1 and E_2 are the modulus of two polymers respectively and f_1 and f_2 are their respective volume fraction (Dubey et al. 2011). Series model, on the other hand predicts the lower boundary of modulus, as it assumes the components are arranged in series with the applied stress. It can be described as

$$\frac{1}{E} = \frac{\phi_1}{E_1} + \frac{\phi_2}{E_2} \tag{18}$$

6.1.3 Electrical Conductivity of Composites

The conductivity behavior of the composites is often governed by a power law:

$$\sigma = \sigma_t(V_f - V_c)^t \tag{19}$$

where V_f is the volume fraction of the filler, V_c is the percolation threshold, σ_f is the filler conductivity and t is the critical exponent. For different composites, t and V_c is expected to have different values. To get further insight into the conductivity behavior, additive model and modified Mamunya model can also be employed (Mamunya et al. 1996; Via et al. 2011; McLachlan 1986, 1987, 1988; Michels 1992). Additive model can be described as

$$\log(\sigma) = \log(\sigma_p) + H(V_f - V_C)^{\frac{G}{(V_f - V_C)^n}} + E \tag{20}$$

where σ is the conductivity of the composite, σ_p is the conductivity of the polymer and E, G, H and n are adjustable parameters related with the percolation, structure of the filler and surface energy.

7 Preparation of Polymer Nanocomposites and Interfacial Compatibility

Solvent mixing, melt mixing, shear mixing and in situ polymerization are some of the most common routes for nanocomposite synthesis. In solvent mixing, fillers are dispersed in a polymer solution and sonication assisted dispersion is generally used to disaggregate fillers. In melt mixing, the fillers are incorporated into molten polymer and distributive and dispersive mixing can be achieved. Another method of nanocomposite synthesis is dispersing nanofiller in monomer and polymerizing the dispersion. Polymer-filler interfacial interactions play an important role in mechanical and electrical properties. Stress transfer from the matrix to filler is necessary for reinforcement. A careful optimization of electrostatic interactions, hydrogen bonding, van der Waals interactions is needed to achieve good dispersion. Covalent or/and non covalent functionalization of the filler surface can be used to improve the interaction between the filler and the surface. In covalent approaches, a functional group or grafting of a suitable polymer is used; whereas, the non-covalent functionalization involves surfactants. Non-covalent modification is easier; though it leads to reduction in the yield strength. Physical modification involving plasma, heat or mechanical treatment can also be used. Chemical treatment using silanes and isocyanates is traditionally used to modify the filler surface.

8 Recent Research on Polymer Blends and Composites for Medical Applications

Polymer blending is extensively used to tailor biodegradability, hydrophilicity, mechanical properties, stimuli response, electrical and magnetic properties. Polylactic acid, a biodegradable aliphatic polyester, is among the most promising biomedical polymers; it has been blended with other polymers and reinforced with fillers for different medical applications. Bamboo charcoal particles have been recently used to reinforce PLA and reported 99% enhancement in the flexural strength (Fig. 7) (Ho et al. 2015). On the other hand, blending technology was used to develop PLA based shape polymer alloys which has potential of lifting 50 g of weight and thus claimed to have potential applications in the development of artificial muscles (Song et al. 2015). It has been recently reported that PLA/chitosan/keratin composites have better hardness than pristine PLA and

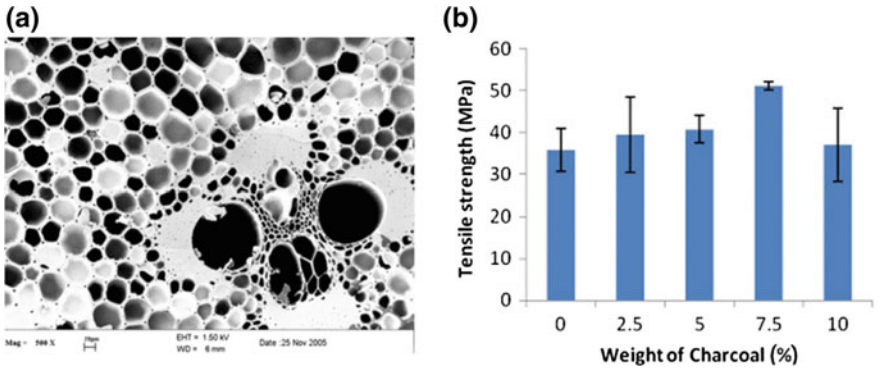

Fig. 7 **a** The porous structure of bamboo charcoal. **b** The tensile strength of pure PLA sample and BC/PLA composite with different BC contents (Ho et al. 2015). Reproduced with the permission from Elsevier

showed good viability/proliferation outcome in osteosarcoma cell line (Tanase and Spiridon 2014). Large porous PLA/calcium phosphate composite scaffolds were synthesized and cell seeding efficiencies of up to 50% have been reported (Koch et al. 2010; Charles-Harris et al. 2008). Combinatorial advantages of polymer composites were demonstrated in three dimensional porous composite of polylactide-co-glycoside and 45s5 bioactive glass; these composites offer significantly improved mechanical properties and osteointegrative potential than the matrix polymer (Lu et al. 2003). PLGA/alginate composite microspheres have been recently used for hydrophilic protein delivery (Zhai et al. 2015). Notably, cartilage-like tissue formation was reported in PLGA/alginate blends and in alginates, but not in PLGA, clearly indicating advantages of blending PLGA with alginate (Jin et al. 2007). Ulvan, a polysaccharide from green seaweeds (Lahaye and Robic 2007), was blended with polyethylene oxide and polycaprolactone; the blends were able to be electrospun and were proposed for applications in tissue engineering scaffolds, wound dressings, or drug delivery systems (Kikionis et al. 2015). Fucoidan/PCL composite mats were demonstrated to have more widely distributed osteoblast-like cells compared with pure PCL mats (Lee et al. 2012). Polymer blends are also used for the development of effective artificial nerve guide conduit to connect detached peripheral nerve ends (Chiono et al. 2009a, b). PCL guides have been shown to be successful in repairing small and medium size nerve defects by bio-mimetic coatings (Chiono et al. 2009a). Chitosan/gelatin natural blends combined the benefits of protein phase and polysaccharides phase; in in vitro neuroblast adhesion tests. Chitosan/gelatin films showed promising results as artificial nerve guides for peripheral nerve regeneration (Ciardelli and Chiono 2006). Chitosan/gelatin blends were found to show affinity towards neuroblastoma cells adhesion and proliferation at 80 wt% gelatin (Pulieri et al. 2008).

Dental implants are used to support dental crowns and bridges; a ring like implantable device was prepared from a composite of calcium-alginate

hydrogels/polycaprolactone for the localized delivery of metronidazole at the implant location to check bacterial growth (Lan et al. 2013). Hydrophilic polysaccharide and hydrophobic polycaprolactone have been blended for several applications (Garcia Cruz et al. 2008; Ciardelli et al. 2005). Composite polymeric scaffold with topographical cues and sustained biochemical release were also prepared and demonstrated to have synergistic effects on cell behaviour (Cutiongco et al. 2015). Polyvinyl alcohol/dextran blends were used in acute myocardial infarction model. These blends were used for the topical delivery of basic-fibroblast growth factor to promote angiogenesis in ischemic heart disease (Fathi et al. 2013). Polyurethane containing aniline pentamer (AP-PU) was blended with PCL to develop a platform substrate for investigating the effect of electrical signals on cell activities (Baheiraei et al. 2014). Poly(epsilon-caprolactone) scaffold modified by chitosan PCL scaffold were used to explore applications in heart valve and blood vessel tissue engineering (Mei et al. 2005). Figure 8 shows morphology of

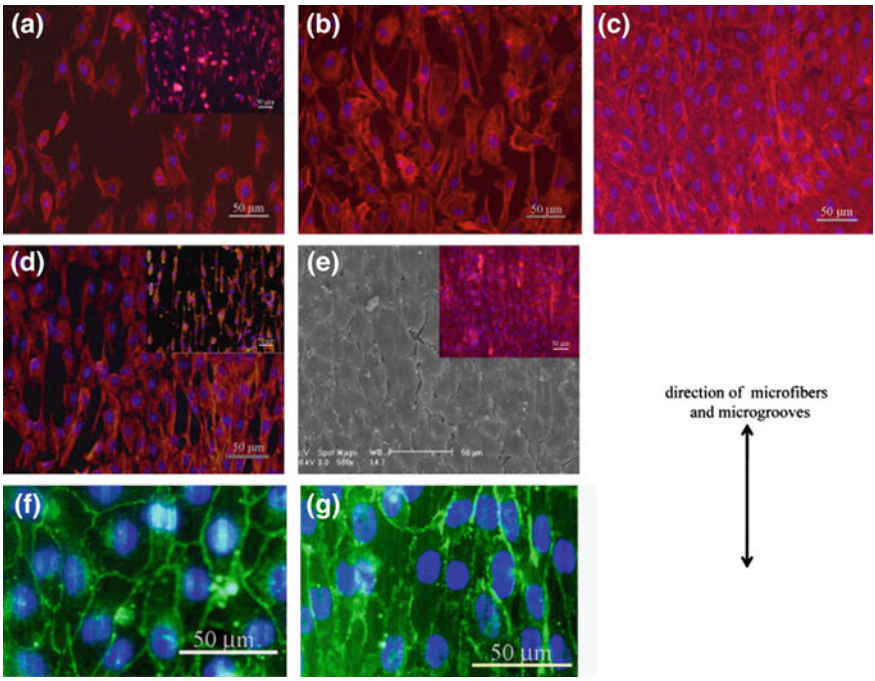

Fig. 8 Morphology of endothelial cells lining micropatterned grafts. **a–c** Cells cultured inside electrospun grafts patterned with microfibers. Overlays of fluorescently stained actin filaments (*red*) and cell nuclei (*blue*) of BAECs or EA.hy926 endothelial cells (*inset*) at **a** 2 h, **b** day 3 and **c** day 5 post-seeding. **d**, **e** Cells cultured inside hybrid grafts patterned with microgrooves. **d** Overlaid fluorescence image of BAECs or EA.hy926 endothelial cells (*inset*) at day 3 post-seeding. **e** SEM image of a BAEC monolayer at confluence and overlaid fluorescence image of a EA.hy926 endothelial cell monolayer (*inset*). **f**, **g** VE-cadherin staining (*green*) of (**f**) BAEC and (**g**) EA.hy926 monolayers on microgrooves at day 7 post-seeding. Double-headed arrows indicate the direction of microfibers and microgrooves (Uttayarat et al. 2010)

endothelial cells lining micro patterned grafts of three-dimensional electrospun polyurethane vascular grafts (Uttayarat et al. 2010).

Polymer blends and composites are extensively explored for bone repair and regeneration. Chitosan/calcium phosphate (CaP) composites were investigated as a potential implant candidate for bone defect repair. The composite containing the 5 mass/vol.% CaP lasted 40 min in vitro fatigue test until failure occurred (Ding 2006). Collagen/chitosan blend porous scaffolds were found to demonstrate improved biostability for skin tissue engineering. In vivo animal tests of these blend based scaffold revealed that they support and accelerate the fibroblasts infiltration from the surrounding tissue (Ma et al. 2003). Chitosan hydrogels/nano ZnO composite based bandages were prepared for wound dressing. These porous and flexible blends showed enhanced swelling, blood clotting, and antibacterial activity. In vivo evaluations of these bandages in Sprague–Dawley rats revealed faster reepithelialization and collagen deposition, suggesting the use of these bandages for burn wounds, chronic wounds, and diabetic foot ulcers (Sudheesh Kumar et al. 2012). Microspheres made of carboxymethyl chitosan, sodium alginate, and collagen blends showed platelet adherence, platelet aggregation, and platelet activation in vitro (Shi et al. 2016). Chitosan/gelatin blend based sponge has been show to work as an absorbable surgical haemostatic agent with good blood-clotting index at chitosan/gelatin sponge blend ratio of 5/5 (W/W). Blend based sponges showed haemostatic effect in rabbit artery bleeding and liver model tests compared to the two individual components (Fig. 9). No differences were observed in thrombin generation and cell toxicity tests with L929 cells were negative. Most importantly, on subcutaneous transplantation onto rabbits, a complete degradation of blends based sponges was observed along with vascular generation and proliferation (Lan et al. 2015). Chitosan-hyaluronic acid/VEGF loaded fibrin nanoparticles composite sponges were also reported to promote angiogenesis; 60% of the loaded VEGF was reported to be released in three days and Human umbilical vein endothelial cells (HUVECs) seeded on VEGF containing sponges showed tubule formation (Mohandas et al. 2015). Bioactive glass/chitosan/carboxymethyl cellulose blends were also showed potential for bone regeneration and hemostasis in critical-sized bone defects (Chen et al. 2015). Chitosan-hyaluronic acid/nano silver composite porous sponges were developed for drug resistant bacteria infected diabetic wounds and showed sliver nanoparticle dependent antibacterial activity against *Staphylococcus aureus* (Anisha et al. 2013a). Chitosan/PVA composite sponges showed higher haemostatic activity than pure chitosan sponges and erythrocytes cells were found to bind first to the surface of chitosan polymer in the sponges and then promote the binding with other cells in the solution (Chen et al. 2013). Chitosan-hyaluronan/nano chondroitin sulfate ternary composite sponges showed good cytocompatibility, proliferation and cell adhesion studies on human dermal fibroblast (Anisha et al. 2013b). Tranexamic acid-loaded chitosan/alginate composite microparticles were found to achieve hemostasis in 2.48 ± 0.88 min and stopped the bleeding in 1.90 ± 0.75 min in a liver transfection bleeding model (Li et al. 2012).

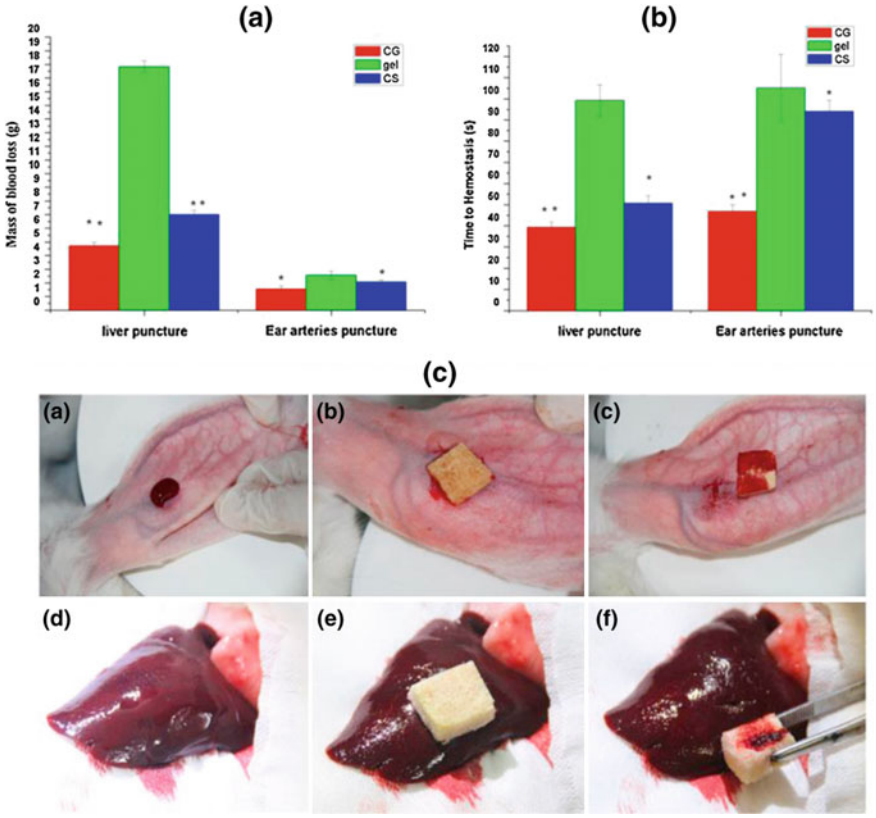

Fig. 9 **(a)** Blood loss in rabbit liver and ear artery injury; **(b)** Time to hemostasis in rabbit liver and ear artery injury; **(c)** hemostasis for CG composite hemostatic material in rabbit ear artery and liver hemostasis models. *a* Bleeding in freshly cut ear artery; *b* Using a CG composite hemostatic material on ear artery bleeding; *c* Ear artery bleeding stopped by the CG composite hemostatic material. *d* Bleeding when cutting the liver; *e* Using a CG composite hemostatic material on the liver; *f* Liver bleeding stopped by the CG composite hemostatic material. *P < 0.05, **P < 0.01 compared to the negative control analyzed by one way ANOVA with post hoc Scheffe test, N = 6 (Lan et al. 2015). Reproduced with the permission from Elsevier

Polymer/bioactive glass composite containing magnetic nanoparticles were develop for potential applications in the magnetic hyperthermia treatment and drug delivery (Jayalekshmi et al. 2013). Chitosan blended with heparin has shown lower platelet adhesion, significant thromboresistivity and lower haemolysis rate (Wang et al. 2012). Wet chemical synthesis of chitosan hydrogel-hydroxyapatite (HAp) composite membranes was done and biocompatibility studies and cytotoxicity studies on MG-63 osteosarcoma cells suggested that chitosan hydrogel-HAp composite membranes can be useful for tissue-engineering applications (Madhumathi et al. 2009). Chitosan dressings containing polyphosphate and silver nanoparticles were developed for the treatment of haemorrhage and infectious

complications. Procoagulant (polyphosphate) and an antimicrobial (silver) were loaded onto different amount in chitosan; these blends were found to accelerate blood clotting, increased platelet adhesion, generated thrombin faster, and absorbed more blood than chitosan. These composites also exhibited significantly greater bactericidal activity than chitosan (Ong et al. 2008).

Carbon nanotubes and graphene can be used to improve both, mechanical reinforcement and electrical conductivity of the polymers, therefore yielding biomaterials for a wide range of regenerative medicine applications. Dispersion of nanofillers in a polymer matrix is a challenge and as mentioned in the earlier sections, various approaches can be used to improve the filler dispersions. In a recent study, the dispersibility of MWCNTs in polyprolactone and polycarbonate polyurethane (PCU) with an incorporated polyhedral oligomeric silsesquioxane (POSS) was investigated and a computational model that can visualise MWCNTs and predict the chemical concentration for ideal nanocomposites was developed (Antoniadou et al. 2010). Nanocomposites based on poly L lactic acid (PLLA) and MWCNTs showed electrical percolation threshold within a range of 0.21–0.33 wt% MWCNTs and six orders of magnitude increase in conductivity of PLLA by optimal loading of MWNTs. It was found that PLLA/MWCNTS nanocomposites could be suitable substrates for primary stem cell culture (Lizundia et al. 2012). In an interesting work, PLGA/MWCNTs nanocomposites were synthesized via solvent casting technique and rat bone marrow-derived mesenchymal stem cells (MSCs) were employed to assess the biocompatibility of the nanocomposites in vitro. It was shown that the MWCNTs accelerated the hydrolytic degradation of PLGA and the cells could adhere to and spread on composite films via cytoplasmic processes. Furthermore, MSCs cultured onto PLGA/MWCNTS nanocomposites showed improved adhesion, viability and higher production of alkaline phosphates. The authors claimed that these results reflect the potential of thee composite matrices for the development of 3-D scaffolds for bone tissue engineering (Lin et al. 2011).

Designing biodegradable scaffolds with bone-compatible mechanical properties has been a significant challenge in the field of bone tissue engineering and regenerative engineering. PLGA/MWNT composites containing pristine and modified with hydroxyl (OH), carboxylic acid (COOH)) multi-walled carbon nanotubes (MWCNTs), were synthesized as three-dimensional porous scaffolds. It was shown that on adding just 3% MWCNTs, the compressive strength and modulus were significantly increased compared to pure PLGA scaffolds. These composites showed excellent cell adhesion, proliferation and mineralization. On implantation for 12 weeks, carbon nanotube functionalization indicated differences in inflammatory response, OH-modified MWCNTs showed the least response, and COOH-modified CNT showed the highest response (Mikael et al. 2014).

Conducting polymer composites have special significance in context of conducting tissues; however, the use of exogenous electrical stimulation to promote nerve regeneration has achieved only limited success. The design of biocompatible implants for neuron repair/regeneration ideally requires high cell adhesion as well as good electrical conductivity. Conditions impeding optimized outgrowth may arise from inadequate stimulus presentation due to differences in injury geometry or

signal attenuation. Implantation of an electrically-conductive biomaterial may mitigate this attenuation and provide a more reproducible signal. In a recent study, SWNT was selected as one possible material to impart electrical conductivity to a collagen type hydrogel. Neurite outgrowth within hydrogels increased 3.3 folds in 20-μg/mL SWCNT loaded biomaterials relative to the nanofiller-free control. Notably, electrical stimulation promoted greater outgrowth within SWCNT-free control; while combination of electrical stimulation and SWCNT-loading resulted in a markedly enhanced increase in outgrowth (Fig. 10) (Koppes et al. 2016). Recently, surface modified CNT and polymer composites have gained special attention. It was shown that plasma-treated chitin carbon nanotube composite scaffolds offers good neuron adhesion and supports of synaptic function and was claimed to have potential applications as an implantable electrode for stimulation and repair of neurons (Singh et al. 2016).

Magnetic field stimulation through polymer/magnetic filler composites can be useful in several therapeutic and diagnostic applications. Compounding of magnetic filler with a polymer matrix is a very common technique to achieve this. Core-shell particles can be made wherein, the polymer outer layer will stabilize the magnetic shell, that can add stimuli response or target the delivery and also tune the magnetic properties (Rodriguez-Arco et al. 2016). The development of a soft and multiple-environment-adaptive robotic platform with ferromagnetic particles impregnated in silicon-based polymer was recently reported; this flexible platform of human skin-like material was found to have controllability which can be operated like a human finger to manipulate biological objects (Gao et al. 2016). For molecular imaging novel core-shell magnetic microsphere for dual modal magnetic resonance imaging (MRI) and optical imaging was produced by one-pot emulsifier-free emulsion polymerization, which could provide high resolution rate of histologic structure information and realize high sensitive detection at the same time. The synthesized magnetic microspheres composed of cores containing oleic acid (OA) and sodium undecylenate (NaUA) modified Fe_3O_4 nanoparticles and styrene (St), Glycidyl methacrylate (GMA), and polymerizable lanthanide complexes (Gd(AA)3Phen and Eu(AA)3Phen) polymerized on the surface for outer shells. In vitro and in vivo MRI studies exhibited high signal enhancement on both T1- and T2-weighted MR images. These fascinating multifunctional properties suggest that the polymer microspheres have large clinical potential as multi-modal MRI/optical probes (Zhang et al. 2016). Chemically synthesized magnetic nanoparticles containing polyethyleneglycol-lactate polymer (PEG-LAC), chitosan, and polyethyleneimine were used as a gene delivery vehicle for enhanced siRNA delivery into cells has been explored (Arami et al. 2016). Notably, a series of pH and temperature-responsive polymer grafted iron oxide nanoparticles were prepared in a recent study, by simple coupling of aminated iron oxide nanoparticle with poly (N-isopropylacrylamide-ran-poly(ethylene glycol) methyl ether acryl ate)-block-poly(acrylic acid) (Dutta et al. 2016).

Nano-hydroxyapatite/gelatin nanocomposite scaffold were demonstrated to support cell adhesion and to heal the critical size bone defect created on rat calvarium (Samadikuchaksaraei et al. 2016). Polyvinyl alcohol and

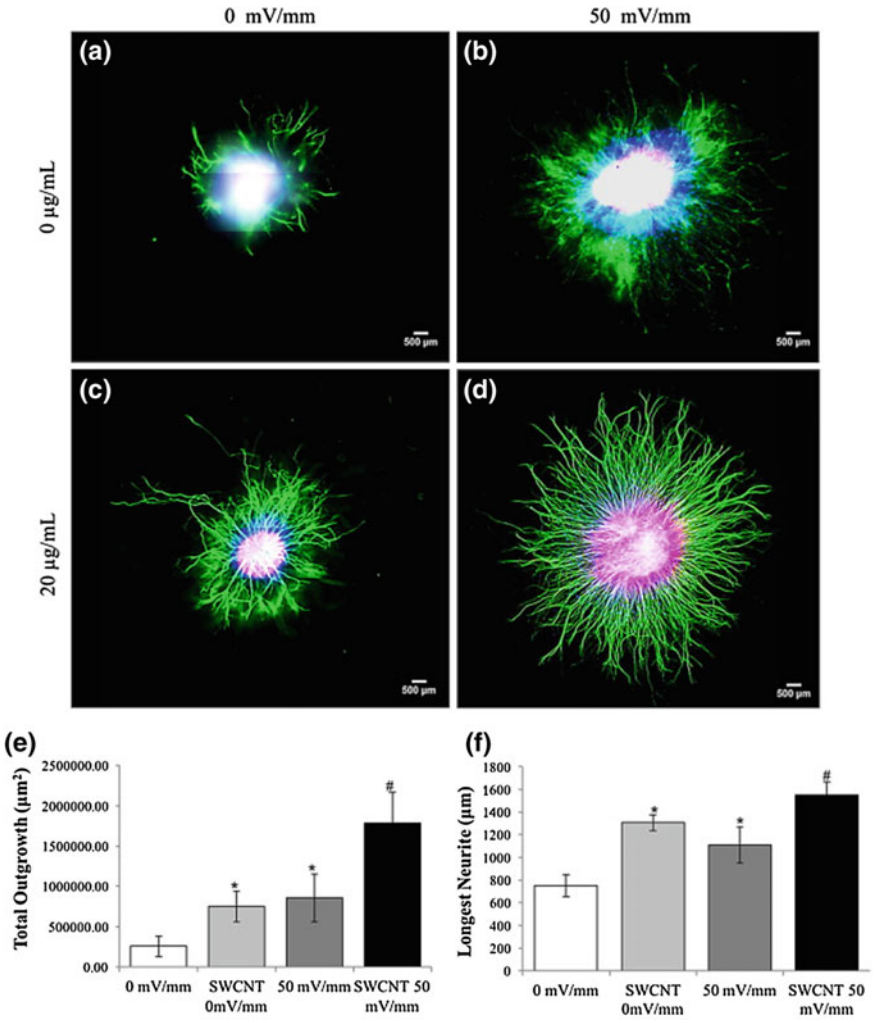

Fig. 10 Electrical stimulation enhances neurite outgrowth in SWCNT composite hydrogels. Neurite outgrowth is promoted by either electrical stimulation with 50 mV/mm (DC 8 h, 1 mA) (**b**) or inclusion of 20 µg/mL SWCNT within hydrogels (**c**) compared to control (0 µg/mL) hydrogels (**a**) with significant increases in outgrowth (**e**) and neurite length (**f**). When SWCNT are combined with 50 mV/mm, a robust increase of neurite outgrowth is observed compared to either singular cue alone (**d**) and significant increases are observed in both total neurite outgrowth (**e**) and neurite persistence length (**f**). *Green* = β-III-Tubulin neurites, *Red* = Phalloidin actin, *Blue* = DAPI nuclei, Bar = 500 µm, 20 ×. ∗ = $p < 0.05$ compared to all conditions, n = 3, standard error shown (Koppes et al. 2016). Reproduced with the permission from Elsevier

polyvinylpyrrolidone blend containing different concentrations of bioactive nanohydroxyapatite (nHAp) demonstrated higher effective conductivity and effective dielectric constant than those of PVA, PVP or nHAp. Enhancement of

electrical conductivity was reported to result in the increased biocompatibility of the fibrous scaffold (Chaudhuri et al. 2016). As stated above, the addition of graphene and graphene oxide nanosheets to bioactive polymers could enhance their electrical conductivity. Polyaniline and polyacrylonitrile composites with graphene and graphene oxide nanosheets were demonstrated to have a higher proliferation and differentiation of satellite cells (Mahmoudifard et al. 2016). Li et al. recently, reported three-dimensional nanocomposite scaffolds by mixing type I collagen extracted from porcine skin and polyvinyl pyrrolidone coated titanium dioxide (TiO_2) nanoparticles. These PVP-containing scaffolds have four times higher strength than that of scaffold without PVP, therefore degradation resistance was enhanced however, ultimate percentage of elongation decreased (Li et al. 2016). In general, for bionics and tissue engineering applications, the nano-composite films with highest electrical conductivity and moderate roughness showed highest cell attachment and proliferation (Gopinathan et al. 2016).

9 Future Scenario

Polymer nanocomposites and blends offer tremendous opportunity and their applications covers almost entire domain of medicine and surgery. Tissue culture, biosensing, surgical implants, drug delivery are among major areas wherein polymers are extensively used. Polymers can be biodegradable or non-biodegradable and hence can be used for diverse set of medical applications, depending on the functional requirement. With the advent of conducting fillers, a new era has emerged for the development of conducting scaffolds for applications such as nerve cell regeneration. Plastic and reconstructive surgery is increasingly using polymer nanocomposites and blends, for wound healing and regeneration. Many polymer based drug delivery systems have achieved commercial success and many are in developmental stage. However, the concerns related to toxicity of plasticizers and residual monomers in polymers used for medical use still needs to be further addressed. Efforts are needed to produce medical grade polymers with high reliability. In case of hybrid systems, especially for nanofiller based composites; a careful cytotoxicity analysis is needed to weigh all possible risks. Feasibility of sterilization of the polymer based formulations should also be kept in mind for the products to be used for medical applications.

References

Affdl JCH, Kardos JL (1976) The Halpin-Tsai equations: a review. Polym Eng Sci 16(5):344–352

Agren MS, Söderberg TA, Reuterving CO, Hallmans G, Tengrup I (1991) Effect of topical zinc oxide on bacterial growth and inflammation in full-thickness skin wounds in normal and diabetic rats. Eur J Surg 157(2):97–101

Aguilar Z (2013) Nanomaterials for medical applications, nanomaterials for medical applications
Ahmed TA, Aljaeid BM (2016) Preparation, characterization, and potential application of chitosan, chitosan derivatives, and chitosan metal nanoparticles in pharmaceutical drug delivery. Drug Design Dev Therapy 10:483–507
Aliyar H, Schalau G 2nd (2015) Recent developments in silicones for topical and transdermal drug delivery. Ther Deliv 6(7):827–839
Altman GH, Diaz F, Jakuba C, Calabro T, Horan RL, Chen J, Lu H, Richmond J, Kaplan DL (2003) Silk-based biomaterials. Biomaterials 24(3):401–416
Anisha BS, Biswas R, Chennazhi KP, Jayakumar R (2013a) Chitosan-hyaluronic acid/nano silver composite sponges for drug resistant bacteria infected diabetic wounds. Int J Biol Macromol 62:310–320
Anisha BS, Sankar D, Mohandas A, Chennazhi KP, Nair SV, Jayakumar R (2013b) Chitosan-hyaluronan/nano chondroitin sulfate ternary composite sponges for medical use. Carbohydr Polym 92(2):1470–1476
Antoniadou EV, Cousins BG, Seifalian AM (2010) Development of conductive polymer with carbon nanotubes for regenerative medicine applications. Conf Proc IEEE Eng Med Biol Soc 2010:815–818
Arami S, Rashidi MR, Mahdavi M, Fathi M, Entezami AA (2016) Synthesis and characterization of Fe3O4-PEG-LAC-chitosan-PEI nanoparticle as a survivin siRNA delivery system. Hum Exp Toxicol
Aslam S, Darouiche RO (2010) Mechanical integrity of hemodialysis catheters is maintained after exposure to a novel catheter lock solution. Infection Control Hospital Epidemiol: Off J Soc Hospital Epidemiol Am 31(11):1124–1129
Associates JIW (2016) http://www.mddionline.com/article/using-polyurethanes-medical-applications. Accessed June 2016
Baheiraei N, Yeganeh H, Ai J, Gharibi R, Azami M, Faghihi F (2014) Synthesis, characterization and antioxidant activity of a novel electroactive and biodegradable polyurethane for cardiac tissue engineering application. Mater Sci Eng C Mater Biol Appl 44:24–37
Baker MI, Walsh SP, Schwartz Z, Boyan BD (2012) A review of polyvinyl alcohol and its uses in cartilage and orthopedic applications. J Biomed Mater Res B Appl Biomater 100(5):1451–1457
Baran GR, Kiani MF, Samuel SP (2014) Healthcare and biomedical technology in the 21st century: an introduction for non-science majors. Healthcare Biomed Technol 21st Century: Introd Non-Sci Majors
Barboza EP, Caúla AL, Caúla FdO, de Souza RO, Geolás Neto L, Sorensen RG, Li XJ Wikesjö UME (2004) Effect of recombinant human bone morphogenetic protein-2 in an absorbable collagen sponge with space-providing biomaterials on the augmentation of chronic alveolar ridge defects. J Periodontol 75(5):702–708
Bergström J (2015) Mechanics of solid polymers: theory and computational modeling, mechanics of solid polymers: theory and computational modeling
Bhat S, Tripathi A, Kumar A (2011) Supermacroprous chitosan–agarose–gelatin cryogels: in vitro characterization and in vivo assessment for cartilage tissue engineering. J R Soc Interface 8(57):540–554
Bhattacharyya S, Kudgus RA, Bhattacharya R, Mukherjee P (2011) Inorganic nanoparticles in cancer therapy. Pharm Res 28(2):237–259
Bozkir A, Saka OM (2004) Chitosan-DNA nanoparticles: effect on DNA integrity, bacterial transformation and transfection efficiency. J Drug Target 12(5):281–288
Brostow W, Pietkiewicz D, Wisner SR (2007) Polymer tribology in safety medical devices: Retractable syringes. Adv Polym Technol 26(1):56–64
Cancienne JM, Burrus MT, Weiss DB, Yarboro SR (2015) Applications of local antibiotics in orthopedic trauma. Orthop Clin North Am 46(4):495–510
Charles-Harris M, Koch MA, Navarro M, Lacroix D, Engel E, Planell JA (2008) A PLA/calcium phosphate degradable composite material for bone tissue engineering: an in vitro study. J Mater Sci Mater Med 19(4):1503–1513

Chaudhuri B, Mondal B, Ray SK, Sarkar SC (2016) A novel biocompatible conducting polyvinyl alcohol (PVA)-polyvinylpyrrolidone (PVP)-hydroxyapatite (HAP) composite scaffolds for probable biological application. Colloids Surf B Biointerfaces 143:71–80

Chen C, Li H, Pan J, Yan Z, Yao Z, Fan W, Guo C (2015) Biodegradable composite scaffolds of bioactive glass/chitosan/carboxymethyl cellulose for hemostatic and bone regeneration. Biotechnol Lett 37(2):457–465

Chen C, Liu L, Huang T, Wang Q, Fang Y (2013) Bubble template fabrication of chitosan/poly (vinyl alcohol) sponges for wound dressing applications. Int J Biol Macromol 62:188–193

Chen CY, Chung YC (2012) Antibacterial effect of water-soluble chitosan on representative dental pathogens Streptococcus mutans and Lactobacilli brevis. J Appl Oral Sci 20(6):620–627

Chiono V, Tonda-Turo C, Ciardelli G (2009) Chapter 9: Artificial scaffolds for peripheral nerve reconstruction. Int Rev Neurobiol 87:173–198

Chiono V, Vozzi G, Vozzi F, Salvadori C, Dini F, Carlucci F, Arispici M, Burchielli S, Di Scipio F, Geuna S, Fornaro M, Tos P, Nicolino S, Audisio C, Perroteau I, Chiaravalloti A, Domenici C, Giusti P, Ciardelli G (2009b) Melt-extruded guides for peripheral nerve regeneration. Part I: poly(epsilon-caprolactone). Biomed Microdev 11(5):1037–1050

Ciardelli G, Chiono V (2006) Materials for peripheral nerve regeneration. Macromol Biosci 6(1):13–26

Ciardelli G, Chiono V, Vozzi G, Pracella M, Ahluwalia A, Barbani N, Cristallini C, Giusti P (2005) Blends of poly-(epsilon-caprolactone) and polysaccharides in tissue engineering applications. Biomacromolecules 6(4):1961–1976

Conniot J, Silva JM, Fernandes JG, Silva LC, Gaspar R, Brocchini S, Florindo HF, Barata TS (2014) Cancer immunotherapy: nanodelivery approaches for immune cell targeting and tracking. Front Chem 2:105

Cutiongco MF, Teo BK, Yim EK (2015) Composite scaffolds of interfacial polyelectrolyte fibers for temporally controlled release of biomolecules. J Vis Exp 102:e53079

Deutekom M, Dobben AC (2015) Plugs for containing faecal incontinence. Cochrane Database Syst Rev 7:CD005086

Ding S-J (2006) Preparation and properties of chitosan/calcium phosphate composites for bone repair. Dent Mater J 25(4):706–712

Dore CMPG, das C Faustino Alves MG, Will LSEP, Costa TG, Sabry DA, de Souza Rêgo LAR, Accardo CM, Rocha HAO, Filgueira LGA, Leite EL (2013) A sulfated polysaccharide, fucans, isolated from brown algae Sargassum vulgare with anticoagulant, antithrombotic, antioxidant and anti-inflammatory effects. Carbohydr Polym 91(1):467–475

Dubey KA, Bhardwaj YK, Chaudhari CV, Sarma KSS, Goel NK, Sabharwal S (2011) Electron beam processing of LDPE/EVA/PCR ternary blends: radiation sensitivity evaluation and physico-mechanical characterization. J Polym Res 18(1):95–103

Dubey KA, Chaudhari CV, Raje N, Panickar L, Bhardwaj YK, Sabharwal S (2012) Radiation-assisted morphology modification of LDPE/TPS blends: a study on starch degradation-processing-morphology correlation. J Appl Polym Sci 124(4):3501–3510

Dutta S, Parida S, Maiti C, Banerjee R, Mandal M, Dhara D (2016) Polymer grafted magnetic nanoparticles for delivery of anticancer drug at lower pH and elevated temperature. J Colloid Interface Sci 467:70–80

El-Assmy A, Eassa W, El-Hamid MA, Nour EM, Hafez AT (2007) Use of oxidized cellulose for corporal body grafting and suture-less correction of severe penile chordee: an experimental study in rabbits. BJU Int 99(5):1098–1102

El-Sayed IH, Huang X, El-Sayed MA (2006) Selective laser photo-thermal therapy of epithelial carcinoma using anti-EGFR antibody conjugated gold nanoparticles. Cancer Lett 239(1):129–135

Fabian TK, Wulff HCH (2014) Implant dentistry: theory and practice, implant dentistry: theory and practice

Fan H, Wang L, Zhao K, Li N, Shi Z, Ge Z, Jin Z (2010) Fabrication, mechanical properties, and biocompatibility of graphene-reinforced chitosan composites. Biomacromolecules 11(9):2345–2351

Fathi E, Nassiri SM, Atyabi N, Ahmadi SH, Imani M, Farahzadi R, Rabbani S, Akhlaghpour S, Sahebjam M, Taheri M (2013) Induction of angiogenesis via topical delivery of basic-fibroblast growth factor from polyvinyl alcohol-dextran blend hydrogel in an ovine model of acute myocardial infarction. J Tissue Eng Regen Med 7(9):697–707

Feneley RCL, Hopley IB, Wells PNT (2015) Urinary catheters: history, current status, adverse events and research agenda. J Med Eng Technol 39(8):459–470

Foldvari M, Bagonluri M (2008) 'Carbon nanotubes as functional excipients for nanomedicines: II drug delivery and biocompatibility issues. Nanomedicine 4(3):183–200

Frazer RQ, Byron RT, Osborne PB, West KP (2005) PMMA: an essential material in medicine and dentistry. J Long Term Eff Med Implants 15(6):629–639

Fueki K, Ohkubo C, Yatabe M, Arakawa I, Arita M, Ino S, Kanamori T, Kawai Y, Kawara M, Komiyama O, Suzuki T, Nagata K, Hosoki M, Masumi S, Yamauchi M, Aita H, Ono T, Kondo H, Tamaki K, Matsuka Y, Tsukasaki H, Fujisawa M, Baba K, Koyano K, Yatani H (2014) Clinical application of removable partial dentures using thermoplastic resin Part II: Material properties and clinical features of non-metal clasp dentures. J Prosthodont Res 58(2):71–84

Galano A (2008) Carbon nanotubes as free-radical scavengers. J Phys Chem C 112(24):8922–8927

Gao W, Wang L, Wang X, Liu H (2016) 'Magnetic driving flowerlike soft platform: biomimetic fabrication and external regulation'. ACS Appl Mater Interfaces

Garcia Cruz DM, Gomez Ribelles JL, Salmeron Sanchez M (2008) Blending polysaccharides with biodegradable polymers. I. Properties of chitosan/polycaprolactone blends. J Biomed Mater Res B Appl Biomater 85(2):303–313

Gautam R, Singh RD, Sharma VP, Siddhartha R, Chand P, Kumar R (2012) Biocompatibility of polymethylmethacrylate resins used in dentistry. J Biomed Mater Res B Appl Biomater 100(5):1444–1450

George J, Sabapathi SN (2015) Cellulose nanocrystals: synthesis, functional properties, and applications. Nanotechnol Sci Appl 8:45–54

Giljohann DA, Seferos DS, Daniel WL, Massich MD, Patel PC, Mirkin CA (2010) Gold nanoparticles for biology and medicine. Angew Chem Int Ed Engl 49(19):3280–3294

Gopinathan J, Quigley AF, Bhattacharyya A, Padhye R, Kapsa RMI, Nayak R, Shanks RA, Houshyar S (2016) Preparation, characterisation, and in vitro evaluation of electrically conducting poly(ε-caprolactone)-based nanocomposite scaffolds using PC12 cells. J Biomed Mater Res A 104(4):853–865

Grassauer A, Weinmuellner R, Meier C, Pretsch A, Prieschl-Grassauer E, Unger H (2008) Iota-Carrageenan is a potent inhibitor of rhinovirus infection. Virol J 5:107

Gulati N, Gupta H (2012) Two faces of carbon nanotube: toxicities and pharmaceutical applications. Crit Rev Ther Drug Carrier Syst 29(1):65–88

Gupta AK, Naregalkar RR, Vaidya VD, Gupta M (2007) Recent advances on surface engineering of magnetic iron oxide nanoparticles and their biomedical applications. Nanomedicine (Lond) 2(1):23–39

Gupta D, Chaudhary H, Gupta C (2015) Sericin-based polyester textile for medical applications. J Text Inst 106(4):366–376

Hall BK (2015) Bones and cartilage: developmental and evolutionary skeletal biology, 2nd edn. In: Bones and cartilage: developmental and evolutionary skeletal biology

Hamady ZZR (2013) Novel xylan-controlled delivery of therapeutic proteins to inflamed colon by the human anaerobic commensal bacterium. Ann R Coll Surg Engl 95(4):235–240

Han SK (2015) Innovations and advances in wound healing. Innov Adv Wound Healing

Ho M-P, Lau K-T, Wang H, Hui D (2015) Improvement on the properties of polylactic acid (PLA) using bamboo charcoal particles. Compos B Eng 81:14–25

Inzana JA, Schwarz EM, Kates SL, Awad HA (2016) Biomaterials approaches to treating implant-associated osteomyelitis. Biomaterials 81:58–71

Ivanova EP, Bazaka K, Crawford RJ (2014) New functional biomaterials for medicine and healthcare

Jaeblon T (2010) Polymethylmethacrylate: properties and contemporary uses in orthopaedics. J Am Acad Orthop Surg 18(5):297–305

Jayalekshmi AC, Victor SP, Sharma CP (2013) Magnetic and degradable polymer/bioactive glass composite nanoparticles for biomedical applications. Colloids Surf B Biointerfaces 101:196–204

Jin X, Sun Y, Zhang K, Wang J, Shi T, Ju X, Lou S (2007) Ectopic neocartilage formation from predifferentiated human adipose derived stem cells induced by adenoviral-mediated transfer of hTGF beta2. Biomaterials 28(19):2994–3003

Karimi M, Ghasemi A, Sahandi Zangabad P, Rahighi R, Moosavi Basri SM, Mirshekari H, Amiri M, Shafaei Pishabad Z, Aslani A, Bozorgomid M, Ghosh D, Beyzavi A, Vaseghi A, Aref AR, Haghani L, Bahrami S, Hamblin MR (2016) Smart micro/nanoparticles in stimulus-responsive drug/gene delivery systems. Chem Soc Rev 45(5):1457–1501

Kathuria N, Tripathi A, Kar KK, Kumar A (2009) Synthesis and characterization of elastic and macroporous chitosan-gelatin cryogels for tissue engineering. Acta Biomater 5(1):406–418

Keliher EJ, Yoo J, Nahrendorf M, Lewis JS, Marinelli B, Newton A, Pittet MJ, Weissleder R (2011) 89Zr-labeled dextran nanoparticles allow in vivo macrophage imaging. Bioconjug Chem 22(12):2383–2389

Khan R, Khan MH (2013) Use of collagen as a biomaterial: an update. J Indian Soc Periodontol 17(4):539–542

Kikionis S, Ioannou E, Toskas G, Roussis V (2015) Electrospun biocomposite nanofibers of ulvan/PCL and ulvan/PEO. J Appl Polymer Sci 132(26):n/a-n/a

Kim MS, You HJ, You MK, Kim NS, Shim BS, Kim HM (2004) Inhibitory effect of water-soluble Chitosan on TNF-α and IL-8 Secretion from HMC-1 Cells. Immunopharmacol Immunotoxicol 26(3):401–409

Kluin OS, van der Mei HC, Busscher HJ, Neut D (2013) Biodegradable vs non-biodegradable antibiotic delivery devices in the treatment of osteomyelitis. Expert Opin Drug Deliv 10(3):341–351

Koch MA, Vrij EJ, Engel E, Planell JA, Lacroix D (2010) Perfusion cell seeding on large porous PLA/calcium phosphate composite scaffolds in a perfusion bioreactor system under varying perfusion parameters. J Biomed Mater Res A 95(4):1011–1018

Kockerling F, Schug-Pass C (2014) What do we know about titanized polypropylene meshes? an evidence-based review of the literature. Hernia 18(4):445–457

Koppes AN, Keating KW, McGregor AL, Koppes RA, Kearns KR, Ziemba AM, McKay CA, Zuidema JM, Rivet CJ, Gilbert RJ, Thompson DM (2016) Robust neurite extension following exogenous electrical stimulation within single walled carbon nanotube-composite hydrogels. Acta Biomater

Lahaye M, Robic A (2007) Structure and functional properties of Ulvan, a polysaccharide from green seaweeds. Biomacromolecules 8(6):1765–1774

Lan G, Lu B, Wang T, Wang L, Chen J, Yu K, Liu J, Dai F, Wu D (2015) Chitosan/gelatin composite sponge is an absorbable surgical hemostatic agent. Colloids Surf B Biointerfaces 136:1026–1034

Lan S-F, Kehinde T, Zhang X, Khajotia S, Schmidtke DW, Starly B (2013) Controlled release of metronidazole from composite poly-ε-caprolactone/alginate (PCL/alginate) rings for dental implants. Dent Mater 29(6):656–665

Laustriat S, Geiss S, Becmeur F, Bientz J, Marcellin L, Sauvage P (1990) Medical history of teflon. Eur Urol 17(4):301–303

Lee JS, Jin GH, Yeo MG, Jang CH, Lee H, Kim GH (2012) Fabrication of electrospun biocomposites comprising polycaprolactone/fucoidan for tissue regeneration. Carbohydr Polym 90(1):181–188

Lee KY, Mooney DJ (2012) Alginate: properties and biomedical applications. Prog Polym Sci 37(1):106–126

Leggat PA, Smith DR, Kedjarune U (2009) Surgical applications of methyl methacrylate: a review of toxicity. Arch Environ Occup Health 64(3):207–212

Lewis KM, Kuntze CE, Gulle H (2016) Control of bleeding in surgical procedures: critical appraisal of HEMOPATCH (Sealing Hemostat). Med Dev (Auckland, N.Z.), 9:1–10

Li D, Li P, Zang J, Liu J (2012) Enhanced hemostatic performance of tranexamic acid-loaded chitosan/alginate composite microparticles. J Biomed Biotechnol 2012:981321

Li N, Fan X, Tang K, Zheng X, Liu J, Wang B (2016) Nanocomposite scaffold with enhanced stability by hydrogen bonds between collagen, polyvinyl pyrrolidone and titanium dioxide. Colloids Surf B Biointerfaces 140:287–296

Lin C, Wang Y, Lai Y, Yang W, Jiao F, Zhang H, Ye S, Zhang Q (2011) Incorporation of carboxylation multiwalled carbon nanotubes into biodegradable poly(lactic-co-glycolic acid) for bone tissue engineering. Colloids Surf B Biointerfaces 83(2):367–375

Liu G, Qin H, Amano T, Murakami T, Komatsu N (2015) Direct fabrication of the graphene-based composite for cancer phototherapy through graphite exfoliation with a photosensitizer. ACS Appl Mater Interfaces 7(42):23402–23406

Liu Y, Miyoshi H, Nakamura M (2007) Nanomedicine for drug delivery and imaging: a promising avenue for cancer therapy and diagnosis using targeted functional nanoparticles. Int J Cancer 120(12):2527–2537

Liu Z, Robinson JT, Sun X, Dai H (2008) PEGylated nanographene oxide for delivery of water-insoluble cancer drugs. J Am Chem Soc 130(33):10876–10877

Lizundia E, Sarasua JR, D'Angelo F, Orlacchio A, Martino S, Kenny JM, Armentano I (2012) Biocompatible poly(L-lactide)/MWCNT nanocomposites: morphological characterization, electrical properties, and stem cell interaction. Macromol Biosci 12(7):870–881

Lu HH, El-Amin SF, Scott KD, Laurencin CT (2003) Three-dimensional, bioactive, biodegradable, polymer-bioactive glass composite scaffolds with improved mechanical properties support collagen synthesis and mineralization of human osteoblast-like cells in vitro. J Biomed Mater Res A 64(3):465–474

Ma L, Gao C, Mao Z, Zhou J, Shen J, Hu X, Han C (2003) Collagen/chitosan porous scaffolds with improved biostability for skin tissue engineering. Biomaterials 24(26):4833–4841

Maalej NM, Qurashi A, Assadi AA, Maalej R, Shaikh MN, Ilyas M, Gondal MA (2015) Synthesis of Gd(2)O(3): Eu nanoplatelets for MRI and fluorescence imaging. Nanoscale Res Lett 10:215

Madhumathi K, Shalumon KT, Rani VV, Tamura H, Furuike T, Selvamurugan N, Nair SV, Jayakumar R (2009) Wet chemical synthesis of chitosan hydrogel-hydroxyapatite composite membranes for tissue engineering applications. Int J Biol Macromol 45(1):12–15

Mahmoudifard M, Soleimani M, Hatamie S, Zamanlui S, Ranjbarvan P, Vossoughi M, Hosseinzadeh S (2016) The different fate of satellite cells on conductive composite electrospun nanofibers with graphene and graphene oxide nanosheets. Biomed Mater 11(2):025006

Mamunya EP, Davidenko VV, Lebedev EV (1996) Effect of polymer-filler interface interactions on percolation conductivity of thermoplastics filled with carbon black. Compos Interfaces 4(4):169–176

Maruyama K, Haniu H, Saito N, Matsuda Y, Tsukahara T, Kobayashi S, Tanaka M, Aoki K, Takanashi S, Okamoto M, Kato H (2015) Endocytosis of multiwalled carbon nanotubes in bronchial epithelial and mesothelial cells. BioMed Res Int 2015:9

McCarthy JR, Kelly KA, Sun EY, Weissleder R (2007) Targeted delivery of multifunctional magnetic nanoparticles. Nanomedicine (Lond) 2(2):153–167

McKeen LW (2014) 3—plastics used in medical devices A2—Modjarrad, Kayvon. In: Ebnesajjad S (ed) Handbook of polymer applications in medicine and medical devices. William Andrew Publishing, Oxford, pp 21–53

McLachlan DS (1986) Equations for the conductivity of macroscopic mixtures. J Phys C: Solid State Phys 19(9):1339

McLachlan DS (1987) An equation for the conductivity of binary mixtures with anisotropic grain structures. J Phys C: Solid State Phys 20(7):865

McLachlan DS (1988) Measurement and analysis of a model dual-conductivity medium using a generalised effective-medium theory. J Phys C: Solid State Phys 21(8):1521

Mei N, Chen G, Zhou P, Chen X, Shao ZZ, Pan LF, Wu CG (2005) Biocompatibility of Poly (epsilon-caprolactone) scaffold modified by chitosan–the fibroblasts proliferation in vitro. J Biomater Appl 19(4):323–339

Michels MAJ (1992) Scaling relations and the general effective-medium equation for isolator-conductor mixtures. J Phys: Condens Matter 4(15):3961

Mikael PE, Amini AR, Basu J, Josefina Arellano-Jimenez M, Laurencin CT, Sanders MM, Barry Carter C, Nukavarapu SP (2014) Functionalized carbon nanotube reinforced scaffolds for bone regenerative engineering: fabrication, in vitro and in vivo evaluation. Biomed Mater 9(3):035001

Modjarrad K (2014) 1—Introduction in handbook of polymer applications in medicine and medical devices. William Andrew Publishing, Oxford, pp 1–7

Mohandas A, Anisha BS, Chennazhi KP, Jayakumar R (2015) Chitosan-hyaluronic acid/VEGF loaded fibrin nanoparticles composite sponges for enhancing angiogenesis in wounds. Colloids Surf B Biointerfaces 127:105–113

Müller FA, Müller L, Hofmann I, Greil P, Wenzel MM, Staudenmaier R (2006) Cellulose-based scaffold materials for cartilage tissue engineering. Biomaterials 27(21):3955–3963

Newman P, Minett A, Ellis-Behnke R, Zreiqat H (2013) Carbon nanotubes: their potential and pitfalls for bone tissue regeneration and engineering. Nanomed: Nanotechnol Biol Med 9 (8):1139–1158

Nymark P, Jensen KA, Suhonen S, Kembouche Y, Vippola M, Kleinjans J, Catalan J, Norppa H, van Delft J, Briede JJ (2014) Free radical scavenging and formation by multi-walled carbon nanotubes in cell free conditions and in human bronchial epithelial cells. Part Fibre Toxicol 11:4

Oliveira EE, Silva AE, Junior TN, Gomes MC, Aguiar LM, Marcelino HR, Araujo IB, Bayer MP, Ricardo NM, Oliveira AG, Egito ES (2010) Xylan from corn cobs, a promising polymer for drug delivery: production and characterization. Bioresour Technol 101(14):5402–5406

Ong SY, Wu J, Moochhala SM, Tan MH, Lu J (2008) Development of a chitosan-based wound dressing with improved hemostatic and antimicrobial properties. Biomaterials 29(32):4323–4332

Park BK, Kim M-M (2010) Applications of chitin and its derivatives in biological medicine. Int J Mol Sci 11(12):5152–5164

Park SY, Kang BS, Hong S (2013) Improved neural differentiation of human mesenchymal stem cells interfaced with carbon nanotube scaffolds. Nanomedicine (Lond) 8(5):715–723

Patel RM, Martin J, Claasen G, Allgeuer T (2009) Advances in polyolefin-based fibers for hygienic and medical applications. In: Polyolefin fibres: industrial and medical application, pp 154–182

Prowse CV, de Korte D, Hess JR, van der Meer PF (2014) Commercially available blood storage containers. Vox Sang 106(1):1–13

Pruitt LA, Chakravartula AM (2011) Mechanics of biomaterials: fundamental principles for implant design

Pulieri E, Chiono V, Ciardelli G, Vozzi G, Ahluwalia A, Domenici C, Vozzi F, Giusti P (2008) Chitosan/gelatin blends for biomedical applications. J Biomed Mater Res A 86(2):311–322

Pumera M (2011) Graphene in biosensing. Mater Today 14(7–8):308–315

Raafat D, Sahl H-G (2009) Chitosan and its antimicrobial potential—a critical literature survey. Microb Biotechnol 2(2):186–201

Reddy N, Jiang Q, Yang Y (2013a) Investigation of the properties and potential medical applications of natural silk fibers produced by Eupackardia calleta. J Biomater Sci Polym Ed 24(4):460–469

Reddy N, Jiang Q, Yang Y (2013b) Properties and potential medical applications of silk fibers produced by Rothischildia lebeau. J Biomater Sci Polym Ed 24(7):820–830

Rodriguez-Arco L, Rodriguez IA, Carriel V, Bonhome-Espinosa AB, Campos F, Kuzhir P, Duran JD, Lopez-Lopez MT (2016) Biocompatible magnetic core-shell nanocomposites for engineered magnetic tissues. Nanoscale 8(15):8138–8150

Ruys AJ (2013) Biomimetic biomaterials: structure and applications

Saad WE (2014) The history and future of transjugular intrahepatic portosystemic shunt: food for thought. Semin Intervent Radiol 31(3):258–261

Samadikuchaksaraei A, Gholipourmalekabadi M, Erfani Ezadyar E, Azami M, Mozafari M, Johari B, Kargozar S, Jameie SB, Korourian A, Seifalian AM (2016) Fabrication and in vivo

evaluation of an osteoblast-conditioned nano-hydroxyapatite/gelatin composite scaffold for bone tissue regeneratio. J Biomed Mater Res A
Sampson J, de Korte D (2011) DEHP-plasticised PVC: relevance to blood services. Transfus Med 21(2):73–83
Sanna V, Pala N, Sechi M (2014) Targeted therapy using nanotechnology: focus on cancer. Int J Nanomed 9:467–483
Scognamiglio F, Travan A, Rustighi I, Tarchi P, Palmisano S, Marsich E, Borgogna M, Donati I, de Manzini N, Paoletti S (2016) Adhesive and sealant interfaces for general surgery applications. J Biomed Mater Res B Appl Biomater 104(3):626–639
Seckold T, Walker S, Dwyer T (2015) A comparison of silicone and polyurethane PICC lines and postinsertion complication rates: a systematic review. J Vasc Access 16(3):167–177
Sherman VR, Yang W, Meyers MA (2015) The materials science of collagen. J Mech Behav Biomed Mater 52:22–50
Shi M, Kretlow JD, Nguyen A, Young S, Scott Baggett L, Wong ME, Kurtis Kasper F, Mikos AG (2010) Antibiotic-releasing porous polymethylmethacrylate constructs for osseous space maintenance and infection control. Biomaterials 31(14):4146–4156
Shi X, Fang Q, Ding M, Wu J, Ye F, Lv Z, Jin J (2016) Microspheres of carboxymethyl chitosan, sodium alginate and collagen for a novel hemostatic in vitro study. J Biomater Appl 30 (7):1092–1102
Singh D, Tripathi A, Nayak V, Kumar A (2011) Proliferation of chondrocytes on a 3-d modelled macroporous poly(hydroxyethyl methacrylate)-gelatin cryogel. J Biomater Sci Polym Ed 22 (13):1733–1751
Singh N, Chen J, Koziol KK, Hallam KR, Janas D, Patil AJ, Strachan AJGH, Rahatekar SS (2016) Chitin and carbon nanotube composites as biocompatible scaffolds for neuron growth. Nanoscale 8(15):8288–899
Sokolova EV, Byankina AO, Kalitnik AA, Kim YH, Bogdanovich LN, Solov'eva TF, Yermak IM (2014) Influence of red algal sulfated polysaccharides on blood coagulation and platelets activation in vitro. J Biomed Mater Res A 102(5):1431–1438
Song JJ, Chang HH, Naguib HE (2015) Biocompatible shape memory polymer actuators with high force capabilities. Eur Polymer J 67:186–198
St John KR (2014) The use of polyurethane materials in the surgery of the spine: a review. Spine J 14(12):3038–3047
Sudheesh Kumar PT, Lakshmanan V-K, Anilkumar TV, Ramya C, Reshmi P, Unnikrishnan AG, Nair SV, Jayakumar R (2012) Flexible and microporous chitosan hydrogel/nano zno composite bandages for wound dressing vitro and in vivo evaluation. ACS Appl Mater Interfaces 4(5):2618–2629
Sun X, Liu Z, Welsher K, Robinson JT, Goodwin A, Zaric S, Dai H (2008) Nano-graphene oxide for cellular imaging and drug delivery. Nano Res 1(3):203–212
Tanase CE, Spiridon I (2014) PLA/chitosan/keratin composites for biomedical applications. Mater Sci Eng C 40:242–247
Teo AJT, Mishra A, Park I, Kim YJ, Park WT, Yoon YJ (2016) Polymeric biomaterials for medical implants and devices. ACS Biomater Sci Eng 2(4):454–472
Tripathi A, Kathuria N, Kumar A (2009) Elastic and macroporous agarose-gelatin cryogels with isotropic and anisotropic porosity for tissue engineering. J Biomed Mater Res A 90(3):680–694
Tripathi A, Vishnoi T, Singh D, Kumar A (2013) Modulated crosslinking of macroporous polymeric cryogel affects in vitro cell adhesion and growth. Macromol Biosci 13(7):838–850
Ueno H, Mori T, Fujinaga T (2001) Topical formulations and wound healing applications of chitosan. Adv Drug Deliv Rev 52(2):105–115
Usman A, Zia KM, Zuber M, Tabasum S, Rehman S, Zia F (2016) Chitin and chitosan based polyurethanes: a review of recent advances and prospective biomedical applications. Int J Biol Macromol 86:630–645
Uttayarat P, Perets A, Li M, Pimton P, Stachelek SJ, Alferiev I, Composto RJ, Levy RJ, Lelkes PI (2010) Micropatterning of three-dimensional electrospun polyurethane vascular grafts. Acta Biomater 6(11):4229–4237

Vargas KF, Borghetti RL, Moure SP, Salum FG, Cherubini K, de Figueiredo MA (2012) Use of polymethylmethacrylate as permanent filling agent in the jaw, mouth and face regions–implications for dental practice. Gerodontology 29(2):e16–e22

Varkouhi AK, Foillard S, Lammers T, Schiffelers RM, Doris E, Hennink WE, Storm G (2011) SiRNA delivery with functionalized carbon nanotubes. Int J Pharm 416(2):419–425

Venkatesan J, Kim S-K (2010) Chitosan Composites for bone tissue engineering—an overview. Marine Drugs 8(8):2252–2266

Via MD, King JA, Keith JM, Bogucki GR (2011) Electrical conductivity modeling of carbon black/polycarbonate, carbon nanotube/polycarbonate, and exfoliated graphite nanoplatelet/polycarbonate composites. J Appl Polymer Sci

Wang X, Shi N, Chen Y, Li C, Du X, Jin W, Chang PR (2012) Improvement in hemocompatibility of chitosan/soy protein composite membranes by heparinization. Biomed Mater Eng 22(1–3):143–150

Weissleder R, Nahrendorf M, Pittet MJ (2014) Imaging macrophages with nanoparticles. Nat Mater 13(2):125–138

Yadav P, Yadav H, Shah VG, Shah G, Dhaka G (2015) Biomedical biopolymers, their origin and evolution in biomedical sciences: a systematic review. J Clin Diag Res: JCDR 9(9):ZE21–ZE25

Yang L (2015) Nanotechnology-enhanced orthopedic materials: fabrications, applications and future trends

Yang X, Tu Y, Li L, Shang S, Tao XM (2010) Well-dispersed chitosan/graphene oxide nanocomposites. ACS Appl Mater Interfaces 2(6):1707–1713

Yin J-J, Lao F, Meng J, Fu PP, Zhao Y, Xing G, Gao X, Sun B, Wang PC, Chen C, Liang X-J (2008) Inhibition of tumor growth by endohedral metallofullerenol nanoparticles optimized as reactive oxygen species scavenger. Mol Pharmacol 74(4):1132–1140

Yoda R (1998) Elastomers for biomedical applications. J Biomater Sci Polym Ed 9(6):561–626

Zhai P, Chen XB, Schreyer DJ (2015) PLGA/alginate composite microspheres for hydrophilic protein delivery. Mater Sci Eng C Mater Biol Appl 56:251–259

Zhang L, Liang S, Liu R, Yuan T, Zhang S, Xu Z, Xu H (2016) Facile preparation of multifunctional uniform magnetic microspheres for T1-T2 dual modal magnetic resonance and optical imaging. Colloids Surf B Biointerfaces 144:344–354

Zhuang C, Mizuno T, Shimada A, Ito H, Suzuki C, Mayuzumi Y, Okamoto H, Ma Y, Li J (1993) Antitumor protein-containing polysaccharides from a Chinese mushroom Fengweigu or Houbitake, Pleurotus sajor-caju (Fr.) Sings. Biosci Biotechnol Biochem 57(6):901–906

Zuber M, Zia F, Zia KM, Tabasum S, Salman M, Sultan N (2015) Collagen based polyurethanes-A review of recent advances and perspective. Int J Biol Macromol 80:366–374

Polyelectrolyte Complexes (PECs) for Biomedical Applications

Manisha Buriuli and Devendra Verma

Abstract Polyelectrolytes are a class of macromolecules which spontaneously acquire a net positive or negative charge when dissolved in an appropriate polar solvent such as water. Polyelectrolytes can co-react in aqueous solutions and form polyelectrolyte complexes (PECs) or polysalts, which resemble general self-assembly processes. It is believed that PECs are formed due to increase in entropy, caused by the liberation of low-molecular-weight counter ions. PECs can be classified into three types: soluble, colloidally stable, and coacervate complexes. Depending on the compatibility between the reacting polyelectrolytes, the electrostatic interaction between the anionic and cationic groups is stronger than most secondary interactions. Hence, this avoids the use of various chemical cross-linking agents, which reduces the possibilities of toxicity and other harmful effects that may be caused by the agents. PECs combine unique physicochemical properties, which are different from those of the individual components. These find a wide range of applications, such as membranes, as coatings on films and fibers, and as microcapsules for drug delivery, to name a few. PECs have immense potential uses in the field of ecology, biotechnology, medicine, and pharmaceutical technology.

Keywords Polyelectrolyte complexes · Wound healing · Drug delivery · Tissue engineering · Gene delivery · Bioadhesives

Abbreviations

2D	Two-dimensional
3D	Three-dimensional
ADA	Adenosine deaminase
AFM	Atomic force microscopy
AgSD	Silver sulfadiazine
APMA	N-(3-aminopropyl) methacrylamide hydrochloride

M. Buriuli · D. Verma (✉)
Department of Biotechnology and Medical Engineering,
National Institute of Technology, Rourkela 769008, Odisha, India
e-mail: vermad@nitrkl.ac.in

A. Tripathi and J.S. Melo (eds.), *Advances in Biomaterials for Biomedical Applications*, Advanced Structured Materials 66,
DOI 10.1007/978-981-10-3328-5_2

ASC	Adipose-derived stem cell
BMP	Bone morphogenetic protein
cCD	6-carboxymethylthio-β-cyclodextrin
cDNA	Complimentary deoxyribonucleic acid
CH	Chitosan
CLSM	Confocal laser scanning microscopy
CMC	Carboxymethyl cellulose
CPP	Chitosan-polyphosphate
CS	Chondroitin sulfate
CTPP	Chitosan-tripolyphosphate
DE	Degree of esterification
DEP	Dielectrophoresis
DHEA	Dehydroepiandrosterone
DOPA	3,4-dihydroxyphenylalanine
DNA	Deoxyribonucleic acid
DTT	1,4-dithiothreitol
ECM	Extracellular matrix
EDC	1-(3-dimethylaminopropyl)-3-ethyl-carbodiimide hydrochloride
EGFP	Enhanced green fluorescent protein
FE-SEM	Field-emission scanning electron microscopy
FGF	Fibroblast growth factor
FTIR	Fourier transform infrared spectroscopy
GAG	Glycosaminoglycan
GI	Gastrointestinal
HA	Hyaluronic acid or hyaluronan
HAp	Hydroxyapatite
HBPO	Hyper-branched polyether
HMC	Hydroxymethyl cellulose
HPMA	N-(2-hydroxypropyl) methacrylamide
HPMC	Hydroxypropyl methyl cellulose
HS	Heparan sulfate
iCMBA	Injectable citrate-based mussel-inspired bioadhesive
IPC	Interfacial polyelectrolyte complexation
LbL	Layer-by-layer
LPS	Lipopolysaccharide
MAP	Mussel adhesive protein
MSC	Mesenchymal stem cell
MTT	(3-(4,5-dimethylthiazol-2-yl)-2,5-diphenyltetrazolium bromide)
NiTi	Nickel-titanium
OREC	Organic rectorite
PAA	Poly(acrylic acid)

PAH	Poly(allylamine hydrochloride)
PAMAM	Poly(amidoamine)
PBS	Phosphate-buffered saline
PDL	Poly-D-lysine
pDNA	Plasmid deoxyribonucleic acid
PEC	Polyelectrolyte complex
PEG	Poly(ethylene glycol)
PEI	Polyethylenimine
PEMU	Polyelectrolyte multilayers
PGA	Poly(glutamic acid)
PgA	Poly(galacturonic acid)
PLGA	Poly-L-glutamic acid
PLL	Poly-L-lysine
PNiPAM	Poly-N-isopropylacrylamide
PP	Polyphosphate
PTA	Transactivator of transcription-based polypeptide
PU	Polyurethane
Px	Piroxicam
RGD	Arginylglycylaspartic acid
SCID	Severe combined immunodeficiency
SDS-PAGE	Sodium dodecyl sulfate poly-acrylamide gel electrophoresis
SEM	Scanning electron microscopy
TAT	Transactivator of transcription
TEM	Transmission electron microscopy
TNF	Tumor necrosis factor
TPP	Tripolyphosphate
UV-Vis	Ultraviolet-visible
VEGF	Vascular endothelial growth factor
XPS	X-ray photoelectron spectroscopy
XRD	X-ray diffraction

1 Introduction

Polyelectrolyte complexes (PECs) or polysalts are precipitates formed when two oppositely charged polyelectrolytes are allowed to co-react in aqueous solution. These PECs have been shown to display unique physical and chemical properties due to the considerably stronger electrostatic interactions compared to most other secondary binding interactions (Lee et al. 2002). The main driving force of PEC formation is the increase in entropy due to the release of the low molecular counter

ions. Hydrogen bonding and hydrophobic interaction are also known to play a part (Chelmecka 2004).

Interest in PECs was fueled after it was discovered that PECs are naturally produced by some marine organisms such as the sandcastle worm (*Phragmatopoma californica*) (Stewart et al. 2004). The PEC functions as a proteinaceous cement to join and construct their mineralized tubes. When removed about 1 cm from their tubes and placed on a bed of 0.5 mm diameter glass beads, the worms worked extensively to rebuild their tubes by cementing the available glass beads. The cement was found to consist of polyelectrolytes having net opposite charges at physiological pH. The robust nature of adhesive to prevail in underwater conditions and adhesion to various substrates suggest its many possible biomedical applications such as in bone cement and fixation.

1.1 Formation of PECs

The formation of a PEC takes place in three sequential steps (Fig. 1):
Step 1: *Primary complex formation*. There is random bond formation between the polyelectrolytes.
Step 2: *Secondary complex formation*. Here, intracomplex correction and rearrangement of the bonds take place which results in the formation of an orderly secondary complex.

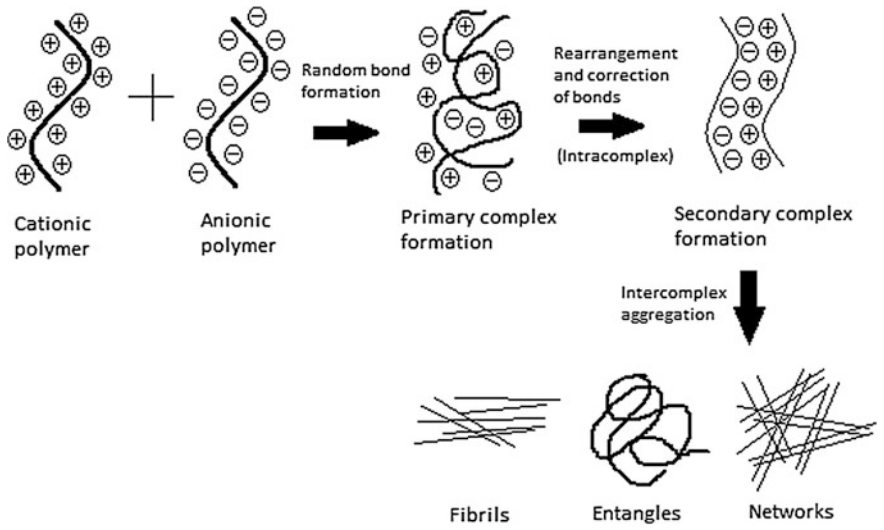

Fig. 1 Schematic representation of PEC formation

Step 3: *Intercomplex aggregation*. The hydrophobic interactions between the secondary complexes cause their aggregation. These complex aggregates may be in the form of large fibrils, entangles or networks.

1.2 Structure of PECs

PEC formation results in various structures, depending on the properties of individual polyelectrolytes and the external conditions provided during the reaction. As reported in the literature, the structure of any resultant PEC can be grouped into two models: ladder-like or scrambled egg (Michaels and Miekka 1961).

1.2.1 Ladder-like Structure

The ladder-like structure (Fig. 2a) is formed when a single-stranded hydrophilic segment interacts with a double-stranded hydrophobic segment. This phenomenon results from the intermixing of polyelectrolytes that have weak ionic entities and major differences in molecular dimensions (Hartig et al. 2007). The ladder-like structure is formed due to the "zippering action", as the ionic site which has reacted first will most likely result in the reaction of the ionic site immediately next to it, giving rise to the zippering effect.

1.2.2 Scrambled Egg Structure

The scrambled egg structure (Fig. 2b) is generally formed when a polymer contains a high number of chains. This model signifies complexes that arise due to intermixing of polyions with strong ionic entities and corresponding molar masses. These yield insoluble and extremely aggregated complexes under a stringent 1:1 stoichiometry.

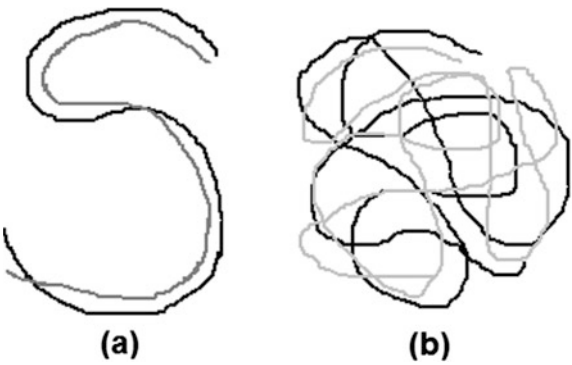

Fig. 2 Structural models of PEC: **a** Ladder-like, and **b** Scrambled egg

1.3 Types of PECs

PECs are generally classified based on their structure; the other classification being based on the main interaction forces acting during PEC formation (such as Coulomb's forces and van der Waal's forces).

Based on their structure, PECs are classified as, water-soluble, colloidally stable, and coacervate complexes.

1.3.1 Water-Soluble PECs

Intermixing of polyelectrolytes having large differences in molecular weights, containing weak ionic entities, and addition in non-stoichiometric proportions under certain salt conditions, results in water-soluble PECs. Water-soluble PECs have a long host chain with some small guest chains (Kabanov 2003). These PECs assume a conformation which is similar to that of the ladder-like structure.

1.3.2 Colloidally Stable PECs

PECs give rise to different types of colloidal systems depending on the compatibility between the polyelectrolytes. Polyelectrolytes with compatible charge densities give rise to very compact colloidal structures. On the other hand, polyelectrolytes with unsuitable charge densities result in colloidal particles with a high degree of swelling.

1.3.3 Coacervate PECs

A coacervate (spherical aggregate of colloidal droplets held together by hydrophobic forces) is formed when the interactive binding between the oppositely charged polyelectrolytes is mild due to low charge densities. They are known to exhibit viscoelastic nature (Spruijt et al. 2013).

1.4 Factors Influencing PEC Formation

There are numerous factors underlying PEC formation. Since the complexation results in a conformational loss, it has to be counter-balanced in order for the complexation to occur. The formation and stability of PECs depend on the following factors:

- Concentration of the polyelectrolytes
- Molecular weight of the polyelectrolytes

- pH of the medium
- Temperature of the medium
- Mixing order
- Mixing ratio
- Degree of ionization of each polyelectrolyte
- Charge density on the polyelectrolytes
- Position of ionic group on the polymeric chain.

1.5 Methods of Preparation of PECs

The simplest and the most widely used method of PEC formation is the polyelectrolyte titration, also called the drop-by-drop method. In this method, one polyelectrolyte is slowly added to a beaker containing the oppositely charged polyelectrolyte, under stirring conditions.

Though this method is the predominant method of PEC formation, it has certain disadvantages:

- The solvent which is present in the titrant dilutes the solution, and
- The polyelectrolyte (in the beaker) to which the titrant is added is continuously consumed in the complexation process.

As a result, the polyelectrolyte which is present in the beaker undergoes a gradual decrease in its concentration during the complexation process. To overcome this problem, many times the concentration of the polyelectrolyte in the beaker in taken 2–10 times higher than the other polyelectrolyte (Gärdlund et al. 2003).

The PEC solution can be easily cast into films by pouring in a container followed by air drying (Verma et al. 2012). Porous scaffolds can be fabricated using freeze drying and porogen leaching (Verma et al. 2009). PEC capsules are prepared by dropwise addition of one polyelectrolyte solution into another complementary charged polyelectrolyte solution (Amaike et al. 1998). This results in a core-shell structure where the first polyelectrolyte occupies the core. The shell consists of PEC of both the polyelectrolytes. The structure of these capsules depended on the order of addition of the polymer solutions. For example, spherical droplets were formed in the gellan solution when cationic chitosan solution was added to anionic gellan solution. The capsules had PEC as a shell with chitosan at the core. The capsules were found to be stable after washing with water and 80% ethanol. They were also strong enough for pinching and magnetic stirring in distilled water and resistant to acid, alkali, and boiling water. When gellan solution was added to chitosan solution, hemispherical droplets were formed at the air-chitosan solution interface (Wan et al. 2004).

For the preparation of PEC fibers, two methods have been described in the literature: (1) self-propelling by gravity in air, and (2) wet spinning technique (Amaike et al. 1998). The wet spinning technique with a roll-up apparatus is widely

preferred for formation of fibers, as it gives longer length fibers and ability to orient the fibers in a specific direction. The scaffolds generated by wet spinning technique followed by lyophilization do not cause any cytotoxicity and maintain cell growth (Shao and Hunter 2007).

As proposed by researchers, the fiber formation mechanism by interfacial polyelectrolyte complexation (IPC) includes four steps which are: (a) formation of PEC film (b) scattering of the complex (c) growth of nuclear fibers, and (d) coalescence of nuclear fibers (Wan et al. 2006). As the fiber is pulled off from the interface, the PEC at the interface is broken down into many individual domains. These domains act as nucleation sites for further complexation. As the nuclear fiber increases in size, the viscosity of the free excess components outside the fibers decreases, due to a decrease in concentration of the polyelectrolytes. Simultaneously, an increase in the ionic strength of the medium is observed, which results from the release of salt counter ions. The nuclear fiber eventually merges together. Regularly spaced gel droplets are observed along the fiber axis, which is formed by the excess polyelectrolytes. It was inferred that continuous fiber formation was related to the stability of the interface and the precipitation of a PEC in the solution. The dimensions of the fibers were found to be directly related to the area of contact between the two solutions. Also, it was seen that the draw rate affects the formation of fiber with beads. Lower the rate, lesser the beads in fiber. The bead formation is slow for viscous solutions. Lesser draw rates are required to form fibers at higher viscosities (Tuzlakoglu et al. 2004; Xu et al. 2015).

The layer-by-layer (LbL) self-assembly of polyelectrolytes has been widely used to prepare tailored ultrathin membranes with defined thickness, composition, and structure (Lvov et al. 1993; Shiratori and Rubner 2000). These membranes find their applications in bio-sensing, catalysis, filtration, and optics. For the preparation of membranes using LbL method, the substrate is alternatively dipped in complementarily charged polyelectrolytes. Strong electrostatic interaction at the interface of each layer stabilizes the structure. One advantage of the LbL method is that it allows nanometer-level control over the thickness and composition of the membranes. The thickness of the films can be controlled either through the number of layers that are deposited or by increasing the concentration of the polyelectrolyte in the solutions from which the films are formed.

A study reported the fabrication of PEC microfibers (Verma et al. 2011). The PEC microfibers were made from chitosan and alginate. PECs generally form nanoparticles when mixed at low concentrations ($\sim$0.1% w/v). The PEC microfibers were made at concentrations of about 1% w/v of each constituent. The fibers were around 1 μm in thickness. The homogeneous mixing of polyelectrolytes at this concentration was facilitated by sonication process. One of the important parameter, which affects final structure of the PECs is pH of the solutions. Sonication of polymer mixture at pH around 8 results in nanoparticles, whereas sonication at around pH 4 results in the formation of microfibers.

2 Applications of PECs

Morphologies of associated polyelectrolytes differ widely, depending on the balance of water, polymer, and salt ions within the complex (Porcel and Schlenoff 2009). The mixing of polycation and polyanion solutions results in dense precipitates. Once the bound water is removed (Porcel and Schlenoff 2009), the wet complexes are stiff or rubbery depending on their salt content (Michaels 1965). Most of the applications of PECs arise from their solid-like properties. Ionically bonded polymeric network structures, readily synthesized from linear polyelectrolytes, possess unusual physical and chemical properties not found in conventional polymers (Michaels 1965). PEC hydrogels, sponges, nanofibers, films, structure micro/nanoparticles, and coatings find various applications in biomedicine.

2.1 Wound Healing

2.1.1 Wound

Skin is the largest organ of the adult body which has a major role in protection from pathogens. A wound can be defined as an injury to the skin. This injury can be a cut, tear, puncture, burn, or even a bruise. The sources of the wound are many, but they relatively have the same effect. Injury to the skin can be fatal as it may act as an easy passage for the microorganisms which might be of pathogenic nature and can cause dreadful diseases. Wounds can be classified into various types. Depending on the source causing the wound, they can be of following types:

- Incision
- Lacerations
- Abrasions
- Avulsions
- Puncture wounds
- Penetration wounds
- Gun-shot wounds

Besides these, the wound can be *open* if cut by a sharp-edged object or *closed* if caused due to trauma by a blunt object. Wounds can have a profound effect on a specific region. Due to high regeneration capacity, skin wound heals quickly depending upon the degree of injury. However, sometimes it leads to serious consequences like infections, inflammations, scarring, and loss of function.

2.1.2 Phases of Wound Healing

Healing of wound is a spontaneous process which takes place by itself. Proper and faster wound healing is essential as it protects an individual from various kinds of pathogenic organisms and air-borne fungal infections. It is a complex and dynamic process in which the missing cells or tissue gets replaced by new cells. The healing process takes place in the following phases: hemostasis, inflammatory phase, proliferative or fibroblastic phase, and maturation or remodeling phase.

(i) *Hemostasis*

This is the first phase of wound healing which starts within few minutes from the time the person gets injured. After the injury, the sub-endothelium of the skin gets exposed, which is rich in collagen and certain tissue factors. Collagen and tissue factors are responsible for aggregation of platelets over the wounded area and form a plug to prevent further bleeding. The platelets get activated as soon as they get attached to the collagen of the exposed wound. The activated platelets start to degranulate, releasing many chemotactic factors which result in clot formation, leading to the conversion of soluble fibrinogen to insoluble fibrin and forms a mesh over the wound. Also, many growth factors (e.g. platelet derived growth factor) and vasoactive agents are also secreted at the wound site. These factors released by the platelets, result in attraction of inflammatory cells switching to next phase of wound healing.

(ii) *Inflammatory phase*

The cellular aspect of wound healing involves cells like neutrophils, macrophages, and lymphocytes which occurs within hours of injury. Neutrophils do not play a role in wound healing but are responsible for cleaning the wound site. They are responsible for engulfing bacteria and other infection-causing microorganisms. Macrophages are the most important cells responsible for wound healing. The major roles of macrophages in wound healing are:

- Phagocytose bacteria
- Secrete collagenases and elastases, which disintegrate the injured tissue and liberate cytokines
- Release cytokines that are responsible for growth and movement of fibroblasts and smooth muscle cells
- The release of compounds that attract endothelial cells to the wound site. This triggers their proliferation, which in turn promotes angiogenesis.

T-lymphocytes start to act within 72 h of injury. They release various lymphokines (e.g. basic fibroblast growth factor) which are responsible for promoting wound healing.

(iii) *Proliferative or fibroblastic phase*

In proliferative phase, the fibroblasts play a major role. Within 48–72 h of injury, the fibroblasts start to migrate towards the wound, marking the onset of proliferative phase and this migration may even start before the inflammatory phase ends. The proliferative phase consists of many steps which are not necessarily in a sequential manner: epithelialization, fibroplasia, angiogenesis, and contraction. A new network of blood vessels is built in the wound which comprises of collagen and extracellular matrix (ECM) (angiogenesis). The new granulation tissue formation is dependent upon fibroblasts. A healthy granulation tissue formation takes place when the fibroblasts have sufficient oxygen and nutrient supply from the blood vessels. There is a formation of an epithelial layer over the cut wound to protect it from the external environment (epithelialization).

(iv) *Maturation or remodeling phase*

This phase is initiated when collagen formation and degradation reaches an equilibrium state. In this phase, newly deposited type III collagen is converted to type I collagen. Rearrangement of collagen fibers takes place and lead to an increase in wound tensile strength. The actual tensile strength of the skin is not achieved. However, the newly replaced skin achieves a maximum of about 80% of its original tensile strength. Maturation phase can vary widely depending on the type of wound, from 3 days to 3 weeks, and in some cases even a year or longer.

2.1.3 Wound Dressings

Wound dressings are used beneath compression bandages in order to promote quick healing and to prevent the contact of the crude wound and the bandage. The range of dressings is becoming broader day by day. Modern dressings also have biological activities appended because microbial biofilm is believed to play a role in wound healing. There are four major functions a wound dressing should perform. They involve cleaning, absorbing, regulating, and adding medication. The choice of dressing mainly depends on the amount of wound exudate and the type of wound. The eight main categories of wound dressings are discussed below.

- *Gauze dressings*

These dressings are made of either woven or non-woven gauze. Gauze is non-occlusive and permeable and is the most readily available wound dressing. The drawback is that these types of dressings may promote desiccation in wounds with less exudate. Hence, under such conditions, they must be used along with a topical agent. They are inexpensive and are good for short term use. They come in different designs based on the comfort of the user.

- *Film dressings*

Film dressings, as the name suggests, are thin and flexible. They are made of clear polyurethane (PU) with an adhesive coating that adheres to the skin. The exudate and adhesive react and prevent the adhesion to wound bed while allowing the film to adhere to the dry skin around the wound. They can be used either as a primary or a secondary dressing. They are elastic in nature and adjust to body contours. Visualization of the wounds is possible with these types of transparent dressings.

- *Hydrogel dressings*

Hydrogels are gels that comprise of 80–90% water. Glycerin-based hydrogels are also available. Though they can absorb only less amount of fluid, they can keep the dry wounds moist because of the presence of ample amount of water in their structure. They cool the applied area and elevate pain. They are permeable to gas and water. Hence, they are not effective bacterial barriers. These are mostly non-adhesive and require a secondary dressing.

- *Foam dressings*

Foamed polymer solutions like PU contain small cells which can hold fluids and are used as dressings. They can be either layered in combination with other materials or they can be impregnated alone. They are non-adhesive to the wound and can easily be removed. They can be made with adhesive border and a transparent coating which can act as a bacterial barrier.

- *Alginate dressings*

Alginate is a polymer made from seaweeds. Alginate beads react with serum and wound exudate and convert it to a gel. The gel is moist and traps bacteria. The bacteria are washed off while changing the dressings. Alginate gels are non-occlusive and highly permeable. Hence, there must be a secondary dressing like gauze. Alginates are available as sheets, ropes, and alginate-tipped applicators. Hydrofiber dressings are prepared with carboxymethyl cellulose (CMC) sodium salt which is similar to alginates.

- *Composite dressings*

As the name suggests, composites are multilayer dressings. They are mostly made of three layers. The innermost layer is non-adherent and prevents trauma to the wound bed during a change of dressings. The middle layer prevents maceration by absorbing moisture and wicking it away from the wound bed. It also maintains a moist wound environment. The middle layer may be a hydrogel, foam, hydrocolloid or alginate. The outer layer acts as a bacterial barrier. It is made of a semipermeable film.

- *Hydrocolloid dressings*

Hydrocolloids contain hydrophilic colloidal compounds like gelatin, cellulose, and pectin. They have a strong film and foam adhesive back. They absorb surrounding exudate slowly and swell into a gel. Removal of hydrocolloid dressing may leave

some residue that gives foul odor. They insulate the wound thermally and have the least permeability to water, oxygen, and bacteria. These dressings have lower infection rates than other dressings.

- *Interactive dressings*

Wound dressings are classified as active, passive, and interactive. Passive dressings just have protective functions. Active dressings promote healing by creating a moist environment around the wound. Interactive wound dressings create a moist environment and also interact with the wound bed to enhance wound healing.

2.1.4 PEC-Based Wound Dressings

Alginate (or alginic acid) is an anionic biopolymer that is derived from acids obtained from brown seaweeds. Dressings made from alginate are not only biodegradable, they also have high absorbency rate (up to 20 times their weight). Depending on the type of seaweed species from which the alginate is made, the dressing may either gel or swell in the wound after absorption of wound fluid. To accelerate gel formation, an alginate dressing is incorporated with a mix of both sodium and calcium alginates. Calcium alginates tend to swell, whereas sodium alginates tend to dissolve or gel in the wound bed (Kent 2009). Alginate dressings promote new skin growth by keeping the wound moist, remove exudates, and promote hemostasis.

Chitosan and alginate dressings have been widely researched for wound healing applications. Chitosan, which is derived from deacetylation of chitin present in shrimps and other crustaceans, is extensively applied in biomedicine due to its low toxicity and high biocompatibility (Kathuria et al. 2009; Tripathi and Melo 2015). Alginates, when combined with a cationic biopolymer such as chitosan, can be made into a PEC-based wound dressing. PECs from alginate and chitosan can be prepared by adding chitosan solution dropwise to alginate solution. It can also be prepared by using a two-step process where calcium alginate beads are first formed, and then the gel beads are dropped into chitosan solution to form the PEC on the surface (Gåserød et al. 1998). Alginates have also been combined with silver, zinc, and CMC to improve the antimicrobial efficacy of the dressings.

Hydrogels are made up of three-dimensional hydrophilic material and contain about 90% water (Kumar and Tripathi 2012). Due to this, hydrogel dressings help control the exchange of fluids within the wound site. These dressings exhibit excellent biocompatibility because their surfaces produce low interfacial free energy when in contact with bodily fluids (Tsao et al. 2010, 2011). Hydrogels do not dissolve in water when crosslinkers are present, but these crosslinkers possess the significant risk of toxicity. Moreover, chemical crosslinkers form weak ionic interactions between various polymer chains. A PEC hydrogel can overcome these limitations.

A PEC membrane made from chitosan and γ-poly(glutamic acid) (γ-PGA), when tested for wound healing efficacy showed that the PEC provided an appropriate moisture content and exhibited good mechanical properties (Tsao et al. 2011). Since both these conditions were prevalent, the dressing could be easily removed from the wound without causing any damage to the newly regenerated tissue. The use of this dressing promoted more than 50% of re-epithelialization and regeneration of the wound, as revealed by histological examinations conducted on the newly regenerated tissue.

Chitosan and γ-PGA PEC matrices exhibit greater hydrophilicity, more favorable cytocompatibility, and a more extensive mechanical structure, compared with that of chitosan alone (Hsieh et al. 2005). Chitosan-γ-PGA hydrogel dressings have been reported to promote early new bone formation in the alveolar socket following tooth extraction (Chang et al. 2014). These dressings adhered better to wound surfaces than neat chitosan and were found to promote earlier as well as greater amounts of new bone formation than treatment with chitosan and gelatin sponge alone.

Chitosan-hyaluronic acid (HA) PEC hydrogel dressings were used to treat burn wounds (Vasile et al. 2012). HA is an anionic, non-sulphated glycosaminoglycan (GAG) found in the connective, neural, and epithelial tissues. It has very high molecular weight in the range of millions. It is known to have good biocompatibility, biodegradability, and gel-forming properties. Chitosan-HA PEC hydrogels are suitable for wounds healing applications as they combine and enhance the antimicrobial activity, prevent wound damage, and subsequently promote wound healing.

Chitosan and sodium alginate PEC sponge dressings impregnated with the drug, silver sulfadiazine (AgSD) as an antibacterial were used as a potential wound dressing material (Kim et al. 1999). The release of AgSD from the dressings was controlled by the number of repeated in situ PEC reactions between chitosan and sodium alginate. The dressing could protect the wound from bacterial invasion and the extent of cellular damage was found to reduce by the controlled release of AgSD from the sponge dressings. Granulation tissue formation and wound contraction were observed to be very fast in dressings containing AgSD and dehydroepiandrosterone (DHEA).

Chitosan-alginate PEC sponges have also been formed by incorporating curcumin (diferuloylmethane) found in turmeric to deter wound infection and accelerated healing (Dai et al. 2009). Curcumin is well known to have natural wound healing properties. In vivo animal testing revealed that adding curcumin into the sponge enhanced its therapeutic healing effect.

Wound dressings in the form of films were made from PECs of chitosan and alginate coacervates with calcium chloride (Wang et al. 2002). These dressings were found to increase incisional wound healing in model rats when compared to conventional gauze dressings. Post-operative observations showed the closing of the wound on day 14, extremely good remodeling on day 21 with thick collagen deposition and presence of mature fibroblast cells. Good biocompatibility and

wound-healing efficiency indicated that chitosan-alginate PEC film dressings have potential applications in wound healing.

Dressings were made by incorporating chitosan with polyphosphate (PP) to act as a procoagulant, and silver nanoparticles to act as an antimicrobial agent (Ong et al. 2008). Chitosan dressings were fabricated with different amounts and lengths of PP chains (45 or 65 phosphate units per chain). The PP-silver containing chitosan dressings were found to have superior hemostatic properties when compared to chitosan dressings. The PP present in the dressings was responsible for the accelerated production of sufficient amounts of thrombin to support earlier fibrin generation. Moreover, the presence of chitosan engaged RBCs to expand and solidify the growing thrombus, leading to the formation of a stable blood clot.

2.2 *Drug Delivery*

Drugs are constantly being developed to treat various diseases and abnormalities. In most cases, though the drugs perform very well in in vitro conditions, their performance in vivo is rather suppressed. This is due to deposition of the drug in non-specific locations in the system. Hence, drug delivery is considered to be one of the most challenging tasks in pharmacology. There are various methods that effectively deliver drugs in their respective locations, some of which include nano delivery vehicles like micelles and liposomes. One such delivery mechanism that has attracted recent interests involves encapsulation of the drug within PECs. These PECs act as reservoirs for drugs which are stored in the central region referred to as the core. The solid drug core is then surrounded by a capsule that consists of shells made of alternating anionic and cationic polyelectrolytes. The drug core can also be located in the shell region in some cases. The shells are designed such that they dissolve in specific locations in the system where the drug is deployed, depending on the local conditions prevailing there. Thus, multiple barriers that hinder drug delivery can be overcome by careful selection of layers that contribute to the shell.

Initially, studies were based on only strong polyelectrolytes in their fully charged states like polystyrene sulfonate, dextran sulfate, heparin, and polydimethyl diallyl ammonium chloride, with their pH maintained below 7. Later, the significance of weak polyelectrolytes such as poly(acrylic acid) (PAA), poly(galacturonic acid) (PgA), and alginate became known, since their charge densities can be controlled by adjusting the solution pH. The thickness of the layer in weak polyelectrolytes is the highest near the solution pK_a of the polyelectrolytes.

Two oppositely charged polyelectrolytes can be crosslinked (to form a PEC) through electrostatic interactions. Polyelectrolytes can also make a complex with surfactants and even biologically active micelles via electrostatic interactions. Hence, they find their use in various biomedical and pharmaceutical applications. PECs are ionic in nature with a hydrogel structure. They can also permeate body fluids. They possess many characteristics of proteins and this feature enables them to be less toxic. They are mostly hydrophilic with good mechanical strength and

have the ability to bind oppositely charged molecules. Thus, they are used for target specific applications.

PECs are formed by various techniques that involve mixing of solutions containing oppositely charged polymers. One such technique for preparing PECs is layer-by-layer (LbL) assembly technique. It involves the alternate deposition of ionic polyelectrolytes on a layer with opposite charge. The chemical composition and structure of the film are controlled to a better extent than other ultrathin film forming technologies and the polyelectrolyte is deposited in a predesigned layer-by-layer fashion. LbL is suitable for fabrication of films on flat surfaces with larger areas. Films with a thickness less than 100 nm are possible using LbL, and when many layers are formed to increase the thickness to micrometer levels, the loading capacity is increased to a greater extent. The increase in thickness also increases the mechanical robustness, which helps when nano-scaled hierarchical structures with integrated functions to be tailored. Various LbL assemblies like spin LbL, spray LbL, and exponential LbL has been developed to accelerate the LbL process. LbL methods offer flexibility and freedom to satisfy the needs of drug delivery systems with complex design considerations.

A study showed that crosslinking can be induced by varying the temperature to prepare non-detachable hydrogels (Khutoryanskaya et al. 2010). The hydrogels exhibited pH-dependent swelling properties. Another research prepared stable, single component multilayered PEC with cationic and anionic forms of the same polymer, chitosan (Bulwan et al. 2009). It exhibited good biocompatibility with bacteriostatic properties. The LbL technique can deposit polyelectrolytes on any substrate provided that the substrate does not dissolve in the coating solution, and the substrate has a charge in the coating solution.

2.2.1 Drug Loading

Loading and controlled release of small molecular weight drugs and small molecules are challenging goals that are required to be reached when it comes to drug delivery. LbL deposition of polyelectrolytes can elevate the efficiency of drug loading and targeting.

Ibuprofen, which is used for wound healing, incorporated in a PEC of poly (allylamine hydrochloride) (PAH) and dextran with hyaloplasm acid was formulated (Wang et al. 2009). This helped in the sustainable release of ibuprofen incorporated in surgical sutures. The quantity and release kinetics of the loaded drug can be adjusted by altering the parameters of LbL deposition without affecting the properties of the suture. Fibroblast growth factor (FGF) and heparin were loaded in aortic valves of porcine heart (De Cock et al. 2010). The growth factor activity was preserved and sustainable release of growth factor was also achieved. When prodrugs were loaded with thin LbL films, the desired anti-inflammatory effect was observed (Cao and He 2010).

Loading of hydrophobic drugs requires a hydrophobic core that can act as a reservoir for the drug to be loaded. A study synthesized a heparin-like sulfonated hyperbranched polyether (HBPO-SO_3) with an HBPO hydrophobic core and negatively charged sulfonic acid terminal groups (Hu and Ji 2010). This could self-assemble in aqueous media to form stable micelles with low cytotoxicity. These complexes with hydrophobic cores can be used as nano-reservoirs for hydrophobic guest molecules. The PEC could serve as a multifunctional coating that could help in anticoagulation and local drug delivery. The release rate of drugs depends on the size and solubility of the drug, the number of layers of polyelectrolyte deposition and thereby, the thickness of the shell and the types of polyions used for the LbL process. A study concluded that the shells act as a barrier between the core and the release conditions (Antipov and Sukhorukov 2004). When proper target conditions are achieved, the core dissolves and the shell becomes stable. A drug delivery assembly was described for dexamethasone in a reservoir-type control system with a semipermeable rate controlling membrane (Pargaonkar et al. 2005). The release profiles followed almost zero order kinetics. Hence, it the provided necessary proofs that drug release is a diffusion-controlled mechanism.

The release of drugs like dexamethasone involves two processes: initially, the bulk solution diffuses into the capsules to dissolve drug crystals and then the dissolved drug molecules diffuse out of the capsules. The dissolution of the crystal cores proceeds from the surface towards the crystal center. The smaller crystals dissolve faster than the larger crystals.

Drugs can also be loaded by the use of salts. Salts affect the polyelectrolyte multilayer assembly and also affect the preformed multilayers. Salt ions will screen electrostatic charges and induce swelling of the multilayers. This increases the permeability (Radtchenko et al. 2002). The permeation is blocked at low ionic strength and if the salt concentration is increased further, the drug is released.

2.2.2 Drug Release Triggers

The release of the drug normally takes place through diffusion, a non-specific process. Specific drug release is carried out with chemical and biological triggers. pH is one of the most common triggers for the release of drugs specific to organs. The pH gradient ranges from 1 in the stomach to 7.5 in the small intestine, when it comes to the gastrointestinal (GI) tract. Neutral and anionic polymers do not respond at low pH. However, cationic polymers like chitosan are responsive even at very low pH values. Polymers and polyelectrolytes are chosen according to their pI values. Swelling occurs due to charge imbalance inside the hydrogel structure, thereby decreasing the charge density to balance the surrounding pH. When the charge density becomes low such that the polyelectrolyte cannot hold the complex, swelling or dissolution occurs.

PECs like N-succinyl chitosan/alginate hydrogels and chitosan-acrylamide grafted hydroxymethyl cellulose (HMC) find potential drug release applications in the GI tract. PECs like poly (N-isopropylacrylamide) (PNiPAM)-chitosan show

thermo-responsive behavior and hence, the drug release is affected by temperature (Gandhi et al. 2015). In certain cases, drug release can be controlled by enzymes that are specific to a particular locus being targeted. For example, the bacteria in GI tract produce enzymes such as amylase, pectinase, xylanase, etc. The polysaccharides that could be substrates for these enzymes can be complexed with polyelectrolytes for drug release in these areas. Enzymes also cause local pH deviations in the hydrogel microenvironment that can affect drug release. A study described that HA and poly-L-lysine (PLL) planar films are invaded by living cells which gradually digest them with the release of enzymes (Picart et al. 2005). This can help in the intracellular release of encapsulated therapeutics. Drug release can also be initiated by applying external electric field when PECs are used. The field is removed when the required amount of drug is released. This type of release is suitable for drugs in the dermal, epidermal, and subcutanial regions.

Drug release can also be done by taking control of the swelling pressure. At elevated pH and temperature, the gels explode to release the drug. These are called self-exploding capsules (De Geest and De Smedt 2012). The microgels were synthesized with diameters larger than 100 μm to reduce the pressure required to overcome the capsule's tensile strength. Chitosan can form ionic complexes with multivalent counter ions like tripolyphosphate (TPP) and polyphosphate (PP), denoted as CTPP and CPP, respectively, that can be used to release acidic and water insoluble drugs. Drugs like 6-mercaptopurine were dispersed in a solution of chitosan in acetic acid and dropped into solutions of multivalent counter ions to obtain drug-loaded polyelectrolyte beads. The pH of the counter ion solutions was kept at extremes in order to prevent coacervation of the chitosan beads (Mi et al. 1999a, b). The pH of the medium was maintained below 6 so that the gelation was completely ionic. This increased the release rate of 6-mercaptopurine from CTPP and CPP gel beads in simulated intestinal fluid. Decreasing the pH increased the rate of release of drug from the complex. At simulated gastric fluid (pH 1.2), CTPP had slower release rates than CPP. Thus, by modifying the pH of the medium and the gelation, the release profiles of drugs from PECs can be controlled.

A study evaluated the drug release capabilities of matrix-based chitosan-alginate and chitosan-carrageenan systems (Tapia et al. 2004). The chitosan solution was prepared in 1% acetic acid solution, alginate in water, and carrageenan in 5.7% sodium chloride solution. The PEC was prepared by heating different ratios of the respective solutions at about 80 °C. It was then washed with distilled water and centrifuged at 10,000 rpm for 30 min. The PEC was then suspended in water at 9 °C, followed by vacuum drying, milling, and sieving. The PEC tablets were made by dry mixing the polymers with diltiazem hydrochloride, lactose, and magnesium stearate and were compressed by tableting machines to obtain 500 mg tablets. On testing the various ratios of polymers in PEC, it was found that the optimum ratio was the one in which the solution's viscosity and the supernatant's viscosity after centrifugation was the same. This was obtained with 30–40% chitosan in the mixture. The degree of swelling of the PEC made of chitosan-carrageenan was found to be higher than that of the normal polymer mixture in 0.1 N HCl, pH 1.2 (gastric pH) because of complete protonation of chitosan and electrostatic repulsions. However, the degree of swelling

of chitosan-alginate was very low, which is attributed to the presence of unionized alginate at a pH as low as 1.2. Thus, swelling in solution depended on the number of ionized groups present in the mixture of polymers. The drug release was characterized by dissolution studies. It showed that chitosan-carrageenan complexes had a low retardant capacity of drug release since carrageenan has the ability to promote entry of water into the tablet. When the concentration of carrageenan was increased to 70% v/v, the drug release was slowed down. Chitosan-alginate tablets had a high retardant capacity of drug release. This was due to the low degree of swelling of alginate gels. Thus, the swelling rate was found to affect the release of drugs in PECs. Thus, chitosan-alginate PECs were found to be better than chitosan-carrageenan PECs for drug release as lower concentrations of the former can result in a better-controlled drug release.

Nanoscale chitosan-carrageenan drug carriers were prepared by adding drops of diluted carrageenan into chitosan solution (Grenha et al. 2010). These nanocarriers had no cytotoxicity till 3 mg/mL of drug and had better resuspension in water. The electrical and mechanical properties of electrospun chitosan-carrageenan fibers were found to be enhanced by spinning them along with carbon nanotubes (Granero et al. 2010).

Hyaluronic acid (HA) is a high molecular weight GAG found throughout all tissues in living organisms. It is an ionic polysaccharide and can extensively form PECs with cationic biopolymers like chitosan. A study discussed the use of chitosan-HA PECs crosslinked with genipin for the controlled release of bone morphogenetic protein-2 (BMP-2) (Nath et al. 2015). BMP-2 along with BMP-7 has a strong capacity to induce bone formation. The chitosan-HA PECs were used to improve the half-life of BMP-2 and reduce the rapid clearance of BMP-2 from the body. Chitosan-HA PEC acted as a carrier by immobilizing BMP-2 for sustained and controlled drug delivery. Since chitosan-HA had both anionic and cationic biopolymers, they also provided better attachment and proliferation of pre-osteoblasts. The PEC solution was prepared by dissolving chitosan (1%) and HA (0.1–0.5%) in 1% acetic acid. To this solution, different amounts (1–4 mg per 50 mL chitosan-HA) of genipin (a gardenia fruit extract) was added. Genipin is a natural, non-toxic crosslinker, unlike glutaraldehyde which is toxic. The gelation was continued and the gel formed was freeze-dried to obtain porous PEC scaffolds. The degree of crosslinking increased with increasing genipin concentration, which in turn affected the in vitro swelling of the scaffold. In the absence of crosslinking, the degradation was high in the scaffolds. Scaffolds loaded with the highest amount of BMP-2 had the lowest initial burst release. BMP-2 release was gradual and sustained only after 3 days of drug loading. 1 μg of BMP-2 was released for 4 weeks by the scaffolds. Also, the protein absorption was found to be higher in the scaffolds, which was due to the cooperative nature of HA in chitosan-protein interactions.

Another study showed that the stability of chitosan/TPP nanoparticles can be increased markedly by coating them with HA (Almalik et al. 2013). It also reduced the toxicity of negatively charged chitosan/TPP nanoparticles. Chitosan/HA

delivery system was found to be useful in drug delivery to the corneal epithelium and the ocular surface (de la Fuente et al. 2008).

Pectin is a natural biopolymer and has a characteristic high stability in the GI tract, but easily degrades in the colon. Hence, pectin based systems are mostly used in colon drug delivery. A study briefly discussed chitosan-pectin PEC-based carrier systems for colon drug delivery (Pandey et al. 2013). Theophylline was studied as the drug. Chitosan was dissolved in 1% acetic acid and pectin was dissolved in water. They were then homogenized by mixing with gentle agitation, and dried under vacuum to yield a powder. The final composition of chitosan:pectin was 1:5. The tablet was made of 100 mg theophylline with 4% sodium starch glycolate, magnesium stearate, and lactose monohydrate. The tablet was then coated with a solution of Eudragit S100 in isopropyl alcohol. The ex vivo release studies were carried out by dissolution in solutions of pH 1.2–7.4. Chitosan-pectin tablets showed pH-dependent swelling behavior in all the solutions. The release profile of theophylline depended on factors like the type of anionic and cationic polymer, the percentage of coating, and swelling behavior. Drug release was not found below a pH of 4.6 due to the coating. However, at pH 6.8, there was a maximum of 90.9% drug release at the colon site. This was related to the reduction in the ionic interactions between chitosan and pectin at the colon site.

Water-insoluble coatings like hydroxypropyl methyl cellulose (HPMC) on chitosan-pectin PECs can reduce their swelling properties, thereby retarding the release of drugs (Macleod et al. 1999). Use of physical crosslinkers like calcium and covalent crosslinkers like EDC/NHS reduced the water uptake of the PECs and improved the tensile strength and degradation profile of the composites (Chen et al. 2010). Physical crosslinkers are more acceptable than covalent crosslinkers because of their biocompatibility.

A few other examples of drug delivery using PECs are tabulated in Table 1.

2.3 Gene Delivery

Gene delivery refers to the process of introducing a foreign gene into a host organism for the treatment of many genetic disorders such as sickle cell disease, severe combined immunodeficiency (SCID), and adenosine deaminase (ADA) deficiency. The ‘vehicles’ that carry the foreign genes are called vectors. The traditionally used vectors for gene delivery are viral or non-viral such as plasmids and liposomes. Viral vectors can carry only a limited amount of deoxyribonucleic acid (DNA) material and are known to cause immune reactions in patients. Though non-viral vectors do not trigger immune responses in the host, they have low-efficiency rates.

Researchers are looking for alternative methods of gene delivery to combine the carrying capacity and immune advantages of plasmids, and the efficiency rates of the viral vector. One such method is the use of ‘virosomes’. *Virosomes* are liposomes having an outer covering of viral surface proteins. The viral proteins interact

Table 1 Polyelectrolyte complexes (PECs) in drug delivery applications

Polymers employed in the PEC	Method	Drug employed	Target	Reference
Poly (vinyl pyrrolidone)–carboxyvinyl polymer	Mixing of polymer solutions	Chlorpheniramine maleate and indomethacin		Takayama and Nagai (1987)
Poly (acrylamido-2-methyl-1-propanesulfonate sodium -co- methyl methacrylate)	Free radical solution polymerization	Labetalol HCl, propranolol HCl, verapamil HCl, diltiazem HCl and oxprenolol HCl	Oral	Konar and Kim (1998)
Chitosan-tripolyphosphate and chitosan-phosphoric acid	Ionotropic gelation	6-mercaptopurine	Intestine	Mi et al. (1999a, b)
Chitosan-poly (acrylic acid)	Ionic crosslinking, freeze-drying	Amoxicillin	Stomach	de la Torre et al. (2003)
Phosphorylated chitosan-tripolyphosphate	Ionotropic gelation	Ibuprofen	Intestine	Win et al. (2003)
Poly (vinyl pyrrolidone)-poly (acrylic acid)	Template polymerization	Ketoprofen	Transmucosal	Chun et al. (2004)
Methylcellulose-carboxy vinyl polymer	Solid dispersion	Phenacetin		Ozeki et al. (2005)
Chitosan-polycarbophil	Freeze-drying			Lu et al. (2008)
Carbopol-chitosan	Freeze-drying	Theophylline		Lee et al. (2008)
Gum kondagogu-chitosan	Mixing of polymer solutions	Diclofenac		Naidu et al. (2009)
Gelatin-sodium carboxymethyl cellulose	Emulsification, phase separation	Isoniazid	Tuberculosis	Devi and Maji (2009)
Chitosan-carboxymethyl tamarind kernel powder	Drying	Budenoside	Colon	Kaur et al. (2010)

(continued)

Table 1 (continued)

Polymers employed in the PEC	Method	Drug employed	Target	Reference
Guar gum-xanthum gum	Drying	Domperidone		Singh et al. (2011)
Chitosan-pectin	Drying	Carvedilol		Kaur and Kaur (2012)
Xanthum gum-guar gum	Freeze-drying	Metoclopramide HCl	Nasal	Dehghan and Girase (2012)
Chitosan-sodium alginate copolymers	Free radical polymerization	5-fluorouracil		Li et al. (2013)
Random copolymers	Heating of polymer mixtures	Rhodamine B, bovine serum albumin		Wan et at. (2013)
Chitosan-pectin	Mixing of polymer solutions	Theophylline	Colon	Pandey et al. (2013)
Poly-L-lysine-cellulose sulfate	Mixing of polymer solutions	Rifampicin and risedronate	Bones	Vehlow et al. (2016)

with the surface proteins of the target cell and this leads to the release of foreign gene contents into the host.

In the recent years, polymer-based advancements in gene delivery have gained momentum. The goal is to deliver the desired gene into the target cell in such a manner that it results in successful expression of the protein encoded by the DNA. The desired gene must be combined with a 'transfection agent' such as a cationic polymer, to facilitate entry into the cell and overcome cell-based hindrances in the processing of DNA (Luo and Saltzman 2000; Pack et al. 2005) (Fig. 3). An ideal transfection agent should possess the following properties:

- The complex it forms with DNA should be small enough to be taken up by the cells
- It should facilitate internalization of DNA into the cells by active transport processes such as endocytosis
- It should protect the DNA from degradation by intracellular enzymes, and
- It should release the DNA payload at the right time and location so that it is accessible for subsequent processing.

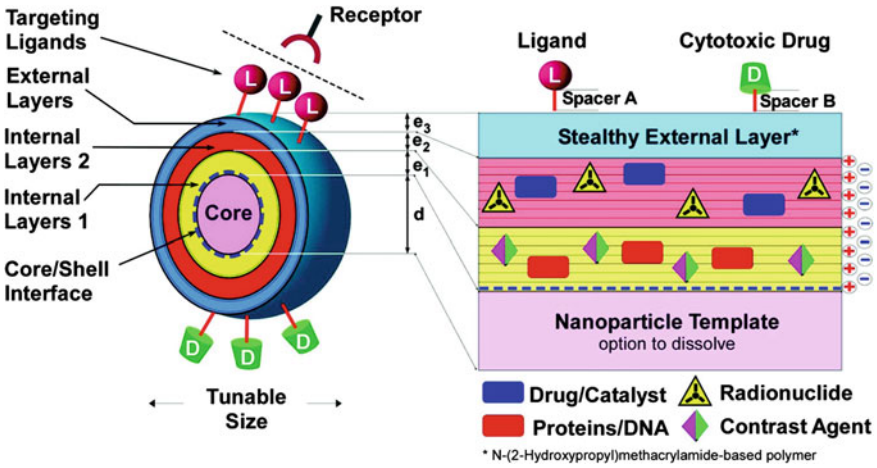

Fig. 3 A schematic depicting a new drug delivery system comprising of nanoparticles coated with multilayer shells. The shell is constructed in a stepwise manner using the layer-by-layer (LbL) polyelectrolyte multilayer (PEM) assembly method. The internal layers are divided into two compartments: Internal layer 1 (*yellow*) and *red* Internal layer 2 (*red*), indicating that different functionalities can be integrated into different layers. The Internal layer 1 is to serve as to compatible mediator between the core and the external layers. Both the internal layers can incorporate drugs, radionuclide for radiotherapy, proteins/nucleotides for bioactivity, or contrast agents for detection. The external layers carry functionalities such as enzymatically cleavable drugs or ligands for receptor mediated targeting, both of which must be accessible on the outside (Reprinted with permission from Schneider et al. (2009). Copyright 2009 American Chemical Society)

DNA itself is an anionic polyelectrolyte due to the presence of negatively charged sugar-phosphate backbone. Hence, the cationic polymers interact with negatively charged DNA readily and form PEC through electrostatic interactions. The formation of this PEC gives rise to complex coacervates nanoparticles in the order of 100–200 nm in size, which is ideal for size dependent internalization by cells. Also, if the proportions of cationic polymer and DNA are met aptly, they can form PECs with positive zeta potentials (Pack et al. 2005). Once it undergoes internalization through endocytosis, the PECs get packed inside tiny vesicles called *endosomes*. These endosomes are transported to other vesicles through lysosomes. Since the microenvironment inside endosomes and lysosomes are acidic, there are chances of DNA degradation. Moreover, lysosomes even contain enzymes that are capable of degrading DNA. In such cases, the success of an effective gene delivery depends on the ability of the polymer to deliver the DNA to the cytoplasm unharmed (Fig. 4).

Polyethylenimine (PEI) is a polymer having the highest cationic charge density potential. Once brought into the cytoplasm via endocytosis, protonation of PEI amines causes an influx of counter ions. This results in osmotic swelling, ultimately leading to polymer-DNA complex rupture and content release into the cytoplasm. A study successfully demonstrated that PEI caused luciferase gene transfection, indicating that its buffering capacity to pH changes inside endosomes and lysosomes (from pH 7–5) protected the DNA from nuclease degradation (Boussif et al. 1995). PEI was found to be highly efficient as a transfection agent.

Poly-L-lysine (PLL) was used for receptor-mediated gene transfer (Zauner et al. 1998). To promote internalization by receptor-mediated endocytosis, many cell

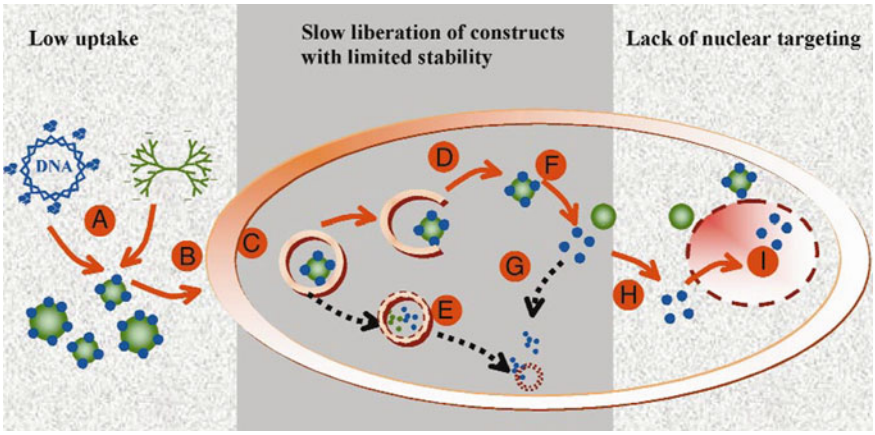

Fig. 4 Schematic drawing of DNA delivery pathways with three major barriers: low uptake across the plasma membrane, inadequate release of DNA molecules with limited stability, and lack of nuclear targeting: (*A*) DNA–complex formation (*B*) Uptake (*C*) Endocytosis (endosome) (*D*) Escape from endosome (*E*) Degradation (endosome) (*F*) Intracellular release (*G*) Degradation (cytosol) (*H*) Nuclear targeting (*I*) Nuclear entry and expression (Reprinted by permission from Macmillan Publishers Ltd: Nature Biotechnology, Luo and Saltzman, 18, 33–37, copyright 2000)

binding ligands for hepatocytes, T-cells, and transferrin were attached to PLL through covalent bonding. The addition of lysosomotropic agents (glycerol) and endosmolytic agents (membrane active peptides) to the transfection medium promoted the release of particles from internal vesicles. PLL-based gene transfer provided flexibility regarding the size of DNA and also facilitated receptor-ligand incorporation.

Nanospheres made from PECs of complimentary DNA (cDNA) and cationic biopolymers such as gelatin and chitosan were evaluated as non-viral gene delivery vehicles (Leong et al. 1998). Although these carriers showed lower transfection efficiency as compared to the two controls, lipofectamine and calcium phosphate, they showed increased expression of β-galactosidase. This gene delivery system possessed the following advantages: (1) conjugation of ligands to the nanosphere for receptor-mediated endocytosis was possible; (2) degradation of DNA in endosomes and lysosomes can be reduced by incorporating lysososmolytic agents; (3) nanospheres can encapsulate bioactive agents, apart from DNA (such as plasmids); (4) improved bioavailability of DNA due to shelter from degradation by serum nuclease; and (5) storage using lyophilization.

The layer-by-layer (LbL) assembly technique makes use of attractive electrostatic forces existing between oppositely charged polymers. When iterative dipping of a substance is carried alternately in cationic and anionic polymers, it gives rise to thin, multilayered polyelectrolyte films. This technique offers several advantages, such as control over film composition and thickness. Another practical advantage is the direct incorporation of DNA as an anionic layer, offering control over loading of DNA at the surface. Also, LbL allows incorporation of multiple layers of different types of DNA. This creates additional opportunities for internalization and uptake of the DNA by the cells.

The first report that applied multilayered polyelectrolyte thin films for gene delivery made use of alternate layers of anionic DNA and cationic poly(allylamine) (Lvov et al. 1993). Another study demonstrated that it is possible to develop DNA-containing multilayer polyelectrolyte films that offer controlled release of transcriptionally active DNA from surfaces (Zhang et al. 2004). Sustained release of functional plasmid (pDNA) under physiological conditions was promoted by deposition of alternating multilayers of anionic pDNA encoding for enhanced green fluorescent protein (EGFP) and a cationic synthetic degradable polyamine on planar silicon and quartz substrates using the LbL technique. The layers eroded gradually within 30 h when incubated in phosphate-buffered saline (PBS) at 37 °C. Characterization studies revealed that the DNA released had open circular topology and successfully promoted expression of EGFP.

A study described the erosion of multilayered films in a reducing environment (Blacklock et al. 2007). LbL films were made from DNA and transactivator of transcription (TAT)-based polypeptide (PTAT) having disulfide linkages in the backbone. Controlled disassembly of the multilayers was activated by 1,4-dithiothreitol (DTT) reduction of the disulfide bonds present in the PTAT backbone. When the study was carried out by replacing PTAT with PLL, the films

showed stability against DTT reduction. Hence, it was deduced that the presence of reducing condition is necessary to trigger DNA release from LbL films.

Ultrathin multilayered films with prolonged release of DNA were developed from pDNA and a cationic polymer having side chains capable of charge-shifting (Zhang and Lynn 2007). The erosion of pDNA-polymer films was due to the gradual hydrolysis of these side-chains. The assemblies were capable of releasing intact DNA up to a period of 3 months in PBS and promoted efficient transgene expression. This LbL assembly approach serves as an alternative to rapidly eroding thin films which incorporate polyamines that degrade hydrolytically or enzymatically.

Gene delivery systems have also been developed with ternary complexes. Initially, a binary complex of pDNA and protamine showed slight toxicity due to the presence of overall cationic charge (Kanda et al. 2013). A ternary complex of pDNA, protamine, and γ-poly(glutamic acid) (γ-PGA) when used as a transfection system not only showed no cytotoxicity, it also displayed a transfection efficiency as high as that of the binary pDNA-protamine system, although they possessed different zeta potentials. The endocytosis mechanism of both the complexes was also found to be different. The pDNA-protamine system was absorbed by caveolae-mediated endocytosis and the pDNA-protamine-γ-PGA system by clathrin-mediated endocytosis. Another ternary complex comprising of pDNA electrostatically assembled with a cationic polymer, polyamidoamine (PAMAM) dendrimers and an anionic polymer, chondroitin sulfate (CS) was developed for efficient gene delivery (Imamura et al. 2014). pDNA-PAMAM-CS ternary complex formed nanoparticles with negative zeta potential, expressed no cytotoxicity and agglutination, and showed high gene expression in the spleen of mice when injected intravenously.

2.4 Bioadhesives

A *bioadhesive* is a natural polymer that is produced or derived from living organisms and acts as an adhesive. Traditionally, starch and gelatin have been used as adhesives for general purposes, but these natural adhesives have well-known limitations such as low stability at higher temperatures. To overcome these disadvantages, natural adhesives were replaced with synthetic sealants like polyurethane (PU), epoxy, cyanoacrylate, and acrylic polymers. However, synthetic polymers pose biocompatibility issues. In the recent years, the bioadhesive market has expanded rapidly to the growing demands of bioadhesives in biomedical and other sectors. These bioadhesives are biocompatible, capable of retaining on the surface for a long period of time, and have fewer environmental concerns.

Bioadhesives are broadly classified into the following five categories:

(i) *Natural adhesives*

Natural adhesives are the oldest known adhesives to humankind. These adhesives are partially or fully synthesized from bio-based raw materials and are not substances used by biological systems as glues. Natural adhesives are easily available, cheap, easily degradable, non-toxic, and environmentally friendly. Examples of natural adhesives include rubber, gums, casein, bitumen, and animal-based adhesives such as collagen.

(ii) *Biological adhesives*

This type of bioadhesives are those which are naturally secreted by marine, water, and land organisms. Mollusks, worms, bacteria, fungi, spiders, insects, etc. are known to produce adhesives that adhere to various surfaces. One common example of biological adhesives is biofilm formation. *Biofilms* are groups of microorganisms that stick to each other and also adhere to a surface. The microorganisms attach via secretion of certain proteins and polysaccharides, and self-produce an extracellular matrix (ECM) within which the cells are embedded. Biofilm formation is the major cause of biofouling, which leads to corrosion of ship hulls and other major industrial systems.

(iii) *Biocompatible adhesives*

Biocompatible adhesives are specially designed for biomedical applications wherein interaction with living tissues takes place. This category can include both natural as well as synthetic adhesives. There is an increasing need of biocompatible adhesives for drug delivery and surgical (such as sutures) applications. Pectin, acacia gum, tragacanth, poly(vinyl alcohol) etc. are widely used biocompatible adhesives.

(iv) *Biomimetic adhesives*

Biomimetic adhesives are designed to closely resemble the biological structure and environment of a particular natural adhesive.

(v) *Bio-inspired adhesives*

These adhesives are designed by taking inspiration from nature's mechanisms and functions of adhesion.

This chapter will be focussing mainly only on the biocompatible, biomimetic, and bio-inspired adhesives used for biomedical applications.

2.4.1 Bioadhesives in Biomedical Applications

In the field of biomedicine, the most important application of bioadhesives is for the closure of surgical wounds. Among the various method applied for closing a wound, the most widely used ones are stitches (or sutures), surgical staples, and tapes.

In suturing, the doctor simply "sews" the ends of the skin for wound closure and secures a knot. The closure of wound promotes natural healing which may otherwise not happen. This method can be used for almost all types of internal and external wounds. The sutures used for this purpose may be absorbable or non-absorbable. The *absorbable* sutures are ones which start losing their strength as they are slowly broken down by the body with the passage of time and do not need a removal process afterward. *Non-absorbable* sutures require removal once the wound has healed. Sutures are often associated with wound infection and scar formation, not to mention the pain associated with it. Hence, the recent years have seen a rise in the use of bioadhesives for wound closure. These bioadhesives are biocompatible, low cost, easy to handle, firm, and avoid pain to the patient.

Tissue adhesives or *sealants* refer to a liquid or semi-liquid compounds which can be applied to tissue incisions to promote wound closure, hemostasis or adherence to soft tissues. An ideal tissue bioadhesive should possess the following properties:

- Non-toxic, sterilizable, easy to produce, affordable, cost-effective
- Possess flow properties for easy and precise application
- Exhibit rapid solidification under physiological conditions
- Should possess adhesiveness for sufficient period of time to allow tissue healing, and
- Possess mechanical properties throughout healing period.

The sandcastle worm, *Phragmatopoma californica*, is a marine polychaete worm which forms reefs. This worm forms a glue to build a protective tube by sticking bits of sand grains and broken seashells together underwater. The underwater glue is made up of different proteins having opposite charges, called as polyphenolic proteins (Stewart et al. 2004). This complex coacervate (or PEC) can be used to repair fractured bones instead of placing metal pins and screws. It can also be used as sealants for skin cuts and wound closure. The precursor proteins for the glue, Pc1, and Pc2, when isolated from the worm were found to contain repeated sequences of motifs which were rich in glycine, lysine, and 3,4-dihydroxyphenyl-L-alanine (L-DOPA) residues. The protein side chains possess phosphate and amine groups whose presence are known to promote adhesion under wet conditions.

Internal surgeries require strong wet tissue adhesion for sutureless closure. A study developed a citrate-based bioadhesive for sutureless wound closure, inspired from mussels (Mehdizadeh et al. 2012). The injectable citrate-based mussel-inspired bioadhesive (iCMBA) pre-polymer was developed using citric acid and polyethylene glycol (PEG), functionalized with catechol-containing compounds, dopamine, and L-DOPA through a polycondensation reaction. The developed PEC-based iCMBAs were found to be superior to the traditionally used tissue bioadhesive, fibrin glue. It possessed controlled biodegradability and good elastomeric mechanical properties that closely resembled that of tissues. More importantly, they did not elicit any inflammatory response and facilitated wound healing.

Another mussel-inspired PEC-based bioadhesive was developed using poly (acrylic acid) (PAA) and DOPA (Wang et al. 2015). The PAA-DOPA, when metal chelated with 'weak' crosslinker Zn^{2+} at pH 4, imparted superior adhesion as well as good mechanical properties to the bioadhesive under both dry and wet conditions. However, when chelated with 'strong' metal crosslinker Fe^{3+}, the results were poor. It was proposed that zinc chelated DOPA through electrostatic interactions with anionic carboxylic groups of PAA. This resulted in the spontaneous generation of PEC coacervate. Moreover, injection at low pH and then the presence of higher pH contributed to gelation of the bioadhesive. This system can prove to be an ideal material for tissue adhesion and other medical purposes.

A recombinant hybrid mussel adhesive was developed from mussel adhesive proteins (MAPs) and hyaluronic acid (HA) (Lim et al. 2010). Since pure natural MAPs are difficult to obtain, a recombinant hybrid of MAPs (fp-151 or fp-131) and HA was produced by mixing in the ratio of 8:2. PEC was formed between the cationic fp-151 or fp-131 and anionic HA. The resulting coacervation process increased the adhesive strength in both dry and wet environments and showed viscoelastic properties. Oil microencapsulation of the fp-151/HA and fp-131/HA coacervates further indicated superior adhesive properties. This demonstrated the possible uses of recombinant MAPs as bioadhesive and self-adhesive drug carriers in tissue engineering applications.

Barnacles are often found clinging to ship hulls, nuclear submarines and even other animals. Scientists studying barnacles' ability to stick to objects submerged in water found that in the final larval stage, the larvae (called *cyprids*) attach to different surfaces and undergo metamorphosis to become adult barnacles (Gohad et al. 2014). The adhesive plaques that are responsible for initial cyprid attachment contain proteins and peptides along with lipids. The adhesive system is essentially biphasic, having both a protein phase and a lipid phase. The presence of this biphasic system results in strong adhesion that can attach to virtually anything. This adhesive can be potentially used for various biomedical applications.

2.5 Tissue Engineering

A number of natural and synthetic polymers such as collagen, gelatin, fibrin, silk fibroin, alginate, chitosan, hyaluronic acid (HA), poly(glycolic acid), etc. are currently being employed for making scaffolds for tissue engineering applications (Kim and Lee 2016; Mousa et al. 2016; Yadav et al. 2015). Biological polymers contain functional groups which can be linked with cell adhesive proteins and growth factors, but they lack mechanical properties. On the other hand, synthetic polymers have superior mechanical properties and their structures can be controlled. However, it is a difficult task to link them with cell signaling molecules because of lack of functional groups. The binary blends of polymers have been explored for tissue engineering application because it is a cost-effective way of preparing new materials with the desired physicochemical and mechanical properties, as well as

coveted biological responses. Blends with synthetic and natural polymers can combine with the wide range of physicochemical properties of synthetic polymers as well as the biocompatibility and biological functionality of biopolymers (Costa and Mano 2014). Blends of complementary charged polymers, i.e., polyelectrolyte complexes (PECs) have also been investigated for tissue engineering application. Generally, PECs are prepared in combination with chitosan, a polycation. Poly-L-lysine (PLL) has also been explored as a polycationic polymer. As polyanionic polymers, various polymers have been explored such as gelatin, silk, poly(glutamic acid) (PGA), alginate, pectin, poly(galacturonic acid) (PgA), and hyaluronic acid (HA).

2.5.1 Alginate-Chitosan

Chitosan is the deacetylated derivative of chitin, composed of β-(1-4)-linked D-glucosamine units and a small amount of N-acetyl-D-glucosamine residues. Chitosan has been shown to exhibit excellent antimicrobial activity, biocompatibility, biodegradability, and accelerated wound healing property. Therefore, it is considered as a promising scaffold material in the regeneration of various tissues such as skin, bone, cartilage, liver, nerve, and cardiovascular tissue (Di Martino et al. 2005). The presence of amine groups imparts cationic nature to chitosan. Alginate is also a polysaccharide which has been extensively investigated for fabrication of scaffolds for tissue engineering. With its gelling property, biocompatibility, hydrophilicity and biodegradability under normal physiological conditions, it is an excellent polymer for tissue engineering. The carboxylate ions of alginate and amine groups of chitosan can bind together to form a PEC.

Both chitosan and alginate are highly hygroscopic and absorb the excess amount of fluid. This leads to a drastic decrease in mechanical properties of scaffolds made of only chitosan or alginate. A PEC of chitosan and alginate absorbs less amount of water as compared to the individual components and hence, shows the superior mechanical property. The fabrication of PEC scaffold is conducted at physiological conditions. Therefore, they can be easily incorporated with growth factors and cells. A porous scaffold made from chitosan and alginate polymers showed significantly better mechanical and biological properties compared to chitosan scaffolds (Li et al. 2005). Enhanced mechanical properties were attributed to the complex formation between chitosan and alginate. In vitro studies using osteoblasts showed that the scaffolds favored cell attachment, proliferation, and deposition of calcified matrix. In vivo study was conducted by implanting scaffolds in the muscles of rats. The results suggested that the alginate-chitosan scaffold does not cause a fibrotic response.

PEC can also be fabricated in fiber form. PEC fibers were prepared from alginate and chitosan by spinning highly concentrated alginate solution in diluted chitosan solution (Majima et al. 2005). Chitosan solution was used as a crosslinker. Mechanical tests showed that the prepared fibers displayed a good mechanical strength of above 200 MPa. Cell studies revealed superior adhesion of fibroblast cells and deposition of dense type I collagen on the fibers.

Mechanical properties and bioactivity of PEC scaffolds can be further enhanced by incorporation of hydroxyapatite (HAp) in the scaffolds. A study reported the fabrication of alginate-chitosan PEC scaffolds with and without the inclusion of HAp (Han et al. 2010). X-ray diffraction (XRD) and X-ray photoelectron spectroscopy (XPS) results revealed the formation of PEC scaffold by ionic interaction between NH_3^+ of chitosan and COO^- of alginate. Alginate-chitosan PEC scaffold exhibited significantly higher compressive strength compared to uncrosslinked alginate scaffold and Ca^{2+} crosslinked alginate scaffold. Considering the good biocompatibility of the PEC scaffold and better mechanical strength, alginate-chitosan scaffolds have the potential to be used for tissue engineering application.

To mimic ECM structure, PEC fibers have been synthesized and used for tissue engineering applications. PEC fiber formation was first reported in 1998 by Amaike and co-workers for the manufacturing of textile fibers (Amaike et al. 1998). In this fiber formation process, a fiber was drawn from the interface of two oppositely charged polymers. During this process, water-soluble polymers become insoluble in the form of PEC fibers at the interface. Another research further elucidated fiber formation mechanism. They found out that the PEC fibers coalescence in the 100 nm range and they combine to form a thicker fiber (Wan et al. 2006). This method of fiber formation has significant potential in tissue engineering because it is simple, toxic solvent-free, water-based method, and does not require high temperature. To avoid clumping of wet fibers, inorganic silica components were incorporated into the PEC fibers as crosslinkers.

In a study, a composite scaffold made of alginate, chitosan, collagen, and HAp was fabricated by electrospinning technique (Yu et al. 2013). In this method, alginate fibers were electrospun in a coagulation bath containing chitosan. These fibers were then dispersed in collagen and HAp solutions to coat fibers with the respective solutions. The distribution of each component was confirmed by confocal laser scanning microscope (CLSM) using fluorescent labeling of polymers. The distribution of different phases was also investigated using field-emission scanning electron microscopy (FE-SEM) and transmission electron microscopy (TEM). This new composite fiber showed better stability in collagenase solution in comparison to collagen films.

Since PEC preparation is done at room temperature and it does not require any toxic solvent, cells can be easily encapsulated within the PEC biomaterials. A PEC of alginate-chitosan with microencapsulated mouse osteoblast MC3T3-E1 cells combined with calcium phosphate cement was prepared (Qiao et al. 2013). The resultant construct was implanted subcutaneously in a nude mouse. The MC3T3-E1 cells were labeled with a fluorescent dye and traced in vivo. The encapsulated cells survived in the in vivo conditions for at least two weeks. Implanted construct promoted lamellar bone-like mineralization, deposition of new collagen, and showed angiogenesis after 4 weeks. At 8 weeks, the absorption of the bone cement and further deposition of collagen was observed.

Nano-ranged bioactive silica particles can form a tighter interface with the polymer matrix and enhance the mechanical strength of the composites.

Additionally, it can also improve biomineralization of the composite scaffolds. The synthesis and characterization of biocomposite scaffolds containing chitosan, alginate, and nano-silica for bone tissue engineering application was reported (Sowjanya et al. 2013). The scaffolds were fabricated using the freeze-drying (lyophilization) method. These nanocomposite scaffolds had a pore size of about 20–100 μm. The presence of nano SiO_2 in the scaffolds enhanced protein adsorption. The incorporation of nano silica did not affect biodegradability of the scaffolds but improved apatite deposition on these scaffolds. In vitro studies indicated no significant loss of cell viability of osteoprogenitor cells.

Chitosan/alginate-based PEC scaffolds were investigated for tissue regeneration after acute myocardial infarction (Deng et al. 2015). Scaffolds having different alginate to chitosan ratios were prepared by lyophilization. The prepared scaffolds showed high porosity and highly interconnected pores. In vitro evaluation using mesenchymal stem cells (MSCs) demonstrated biocompatibility, and ability to proliferate and maintain the paracrine activity of the MSCs. In vivo performance of seeded 3D PEC scaffolds with a polymeric ratio of 40/60 was evaluated in acute myocardial infarction model in rats. The results showed that the PEC scaffolds promoted a significant increase in the ejection fraction, improved neovascularization, attenuated fibrosis, and less left ventricular dilatation when compared to the control group.

Adhesions are abnormal fibrous connections between tissues and can occur following virtually any type of surgery. Adhesions develop after an injury to the normal peritoneal tissue. This injury can result from surgery, trauma, inflammation, infection, or foreign body placement in the peritoneal cavity. Post-operative adhesions develop due to inflammation, which is a part of body's normal healing process. Adhesions often require subsequent surgeries to remove them which is complicated process, not to mention time-consuming too. The most widely used method to prevent post-operative adhesions is to insert physical barriers. Most physical barriers have low success rates. A PEC membrane composed of chitosan and alginate was developed to prevent post-surgical adhesions in neurosurgery (Verma et al. 2012). The membranes were hygroscopic, possessed good mechanical properties, and controlled the release of the model drug, albumin. As fibroblast cells play an important role in adhesion formation, the adhesion and migration study using fibroblast and mixed neuronal cells were carried out. Keeping the concentration of alginate higher to impart the PEC an overall negative charge, the adhesion, and migration of fibroblasts and neuronal cells was stopped in vitro. Both fibroblasts cells and neuronal cells neither adhered nor migrated onto the PEC material after 5 days in vitro. Aqueous absorption study showed that PEC films were extremely hygroscopic and absorbed a significant amount of water. The amount of complex formed was dependent on the ratio of polyelectrolyte and it was found to be highest in films containing an equal amount of each polymer. Degradation study in lysozyme solution revealed that films were stable even after 1 month.

2.5.2 Silk-Chitosan

Silk is a natural polymeric biomaterial produced by silkworm. It has excellent mechanical properties, biocompatibility, and biodegradability. Silk consists of two protein layers: a hydrophobic fibroin inner layer and a hydrophilic sericin outer layer. Silk fibroin is known to be biocompatible and hence, it has been extensively investigated for many biomedical applications (Mandal et al. 2012; Mandal and Kundu 2008; Mobini et al. 2013). It is used in both native fiber form as well as in regenerated forms such as films, electrospun fibers, wet-spun fibers, hydrogels, and scaffolds.

The PEC formation between silk fibroin and chitosan is due to the ionic interactions between carboxylate moieties on silk fibroin and protonated amines on chitosan. In one study, researchers examined porous PEC scaffolds of silk fibroin and chitosan (Bhardwaj and Kundu 2011). The fabricated scaffolds showed pore sizes in the range of 100–160 μm, good interconnectivity, and high porosity. The scaffolds also exhibited reduced degradation rate in lysozyme when compared to pure chitosan scaffolds. Moreover, they also showed a higher compressive strength and modulus than scaffolds made from the individual components. Chitosan preserved its antibacterial effect when incorporated at the higher amounts in the blends. In vitro cytocompatibility tests demonstrated that the PEC scaffolds supported growth and adhesion of fibroblast cells.

In another study, silk fibroin-chitosan scaffolds were fabricated and investigated for cartilage tissue engineering (Bhardwaj et al. 2011). The researchers seeded bovine chondrocytes in the silk-chitosan scaffolds and cultured in vitro for 2 weeks. The constructs were analyzed for cell viability, histology, ECM components (GAG) and collagen types I and II, and biomechanical properties. The study demonstrated that silk fibroin-chitosan scaffolds support chondrocyte attachment and their growth. The chondrogenic phenotype was indicated by Alcian Blue histochemistry and showed relative expression of type II versus type I collagen. Fibroin-chitosan scaffolds with 1:1 ratio showed best results as they demonstrated the highest accumulation of GAG and collagen.

PEC-based scaffolds can also be loaded with growth factors for bone tissue engineering (Tong et al. 2016). In this study, vascular endothelial growth factor (VEGF) was directly added to silk fibroin-chitosan scaffolds. VEGF-containing scaffolds promoted significant human fetal osteoblast 1.19 cell growth and proliferation in the scaffolds.

Various studies have shown that mimicking nanofibrous structure of ECM has positive effects on cellular morphology and cellular activities including cell attachment, proliferation, and differentiation. Alignment of 3D nanofibrous silk fibroin-chitosan scaffolds was achieved using dielectrophoresis (DEP) (Dunne et al. 2014). DEP is a non-destructive electrokinetic mechanism which can be used to manipulate micro or nanoparticles such as DNA, proteins, nanotubes, and nanoparticles in aqueous solutions. The researchers studied effects of alternating current frequency, the presence of ions, silk fibroin to chitosan ratio, and post-DEP freezing temperature on fiber alignment. Highest alignment was achieved in silk fibroin-chitosan 50:50 samples prepared at 10 MHz with sodium chloride.

2.5.3 Pectin-Chitosan

Pectins are a family of polysaccharides rich in D-galacturonic acid, present in the primary cell walls of plants. Pectin is extracted mainly from apple pomace and peels of citrus fruits by means of an acidic aqueous extraction (Munarin et al. 2012). Commercial pectin consists predominantly of linear chains of α-(1-4)-D-galacturonic acid residues, partially methyl esterified. Pectin is classified depending on the degree of substitution of D-galacturonic carboxyl groups by methoxyl groups ($-OCH_3$), defined as the degree of esterification (DE). Pectins are either highly esterified (DE > 50%) or low-esterified (DE < 50%). Pectin has been investigated for colon-specific drug delivery systems because it can be degraded by enzymes produced by a large number of microorganisms present in the colon (Liu et al. 2003). Pectin has also been reported to exhibit anti-inflammatory and anti-carcinogenic properties (Tazawa et al. 1997).

A study reported the fabrication of pectin-chitosan porous scaffolds for bone tissue engineering (Coimbra et al. 2011). Elemental analysis showed that the final scaffolds were composed of approximately 30% w/w chitosan and 70% w/w pectin, irrespective of their initial proportions. Degradation studies conducted in PBS at pH 7.4 showed that the scaffolds lose approximately half of their weight after one month of study. SEM study revealed highly porous and irregular structure of the scaffolds. Assessment of its biocompatibility conducted on human osteoblast cells showed that the pectin-chitosan scaffolds supported cell adhesion and proliferation. MTT assay corroborated these findings.

Poly(galacturonic acid) (PgA), also known as pectic acid, is produced after degradation of pectin. PgA forms gels in the presence of calcium ions, similar to that of alginate. Porous, fiber-containing scaffolds comprising of PgA and chitosan were fabricated by optimizing freezing temperature and PEC concentration (Verma et al. 2009). At higher freezing temperature and concentration, scaffolds had sheet-like structure. It was inferred that the fiber formation occurred due to the assembly of PEC particles during the freezing process. The fiber formation occurred at 0.1 g/100 ml solution and −196 °C freezing temperature. PgA-chitosan containing HAp was also prepared. In vitro studies on human osteoblast cells showed that PgA-chitosan scaffolds did not support cell adhesion. However, the addition of HAp significantly improved cell adhesion.

In another study, nanocomposite scaffolds consisting of HAp, chitosan, and PgA was reported (Verma 2008; Verma et al. 2010). HAp was synthesized in the presence of PgA and chitosan in solution These biopolymers in solution acted as nucleating agents for crystallization of HAp. This method is similar to the way minerals deposit in living systems and hence, it is a biomimetic method of HAp synthesis. AFM images revealed the uniform distribution of HAp in the polymer matrix. There was nearly 100% improvement in elastic modulus of the chitosan-PgA-HAp nanocomposite in comparison to chitosan-HAp and PgA-HAP nanocomposite. Fourier transform analysis indicated that the increase in mechanical properties was attributed to the interfacial interactions between chitosan and PgA present in the nanocomposite. In vitro studies were conducted on human osteoblast

cells by culturing on both 2D and 3D structures of the nanocomposites. 2D structures were created simply coating on culture dishes and 3D scaffolds were prepared using lyophilization. The adhesion of osteoblast cells was found to be dependent on the amount of HAp present in the nanocomposite. Higher amounts of HAp favored better cell adhesion and proliferation. After few days of cell culture, osteoblast cells separated into colonies and subsequently into nodules. The formation of bone-like nodules was observed after 7 days of culture. The nodule size continued to increase with time and after 10 days of culture, nodules were in the range of 250–500 μm. Later, these nodules detached from the surface and coalesced together. SEM images showed the fibrous protein-like structure in the nodules.

A study reported nanocomposites made of chitosan, PgA, HAp, and sodium montmorillonite clay (Katti et al. 2010). The clay was first modified with three different unnatural amino acids before incorporating into the composite. XRD results showed an increase in the d-spacing as an indication of intercalation of amino acids into the d-spacing of the clay after being modified with the three unnatural amino acids. Cell culture experiments showed that the sodium montmorillonite clay modified with the three amino acids and the nanocomposite were biocompatible.

2.5.4 Gelatin-Chitosan

Porous scaffolds of chitosan and gelatin for dermal tissue engineering were fabricated by lyophilization (Tseng et al. 2013). These scaffolds were crosslinked using various crosslinking agents including glutaraldehyde, 1-(3-dimethylaminopropyl)-3-ethyl-carbodiimide hydrochloride (EDC), and genipin. Biocompatibility studies conducted on human fibroblast cells indicated that EDC-crosslinked scaffolds exhibited least cell toxicity as was evident from the highest number of cells that survived in the scaffold after four days of culture. EDC-crosslinked chitosan-gelatin scaffolds also showed superior mechanical properties in both dry and wet state. Moreover, the elastic modulus of EDC-crosslinked scaffolds was similar to that of commercial collagen wound dressings.

In another study, chitosan-gelatin porous scaffolds containing hyaluronic acid (HA) and heparan sulfate (HS) were fabricated using lyophilization technique. These scaffolds were prepared for neural tissue engineering (Guan et al. 2013). Electron microscopic images displayed that the chitosan-gelatin-HA-HS composite scaffolds had above 96% porosity and average pore size ranging from 90–140 μm. Cell viability assay and fluorescence microscopy observation revealed positive effects of HA and HS present in the scaffolds on adhesion and proliferation of neural stem and progenitor cells. Chitosan-gelatin-HA-HS composite scaffolds also promoted multilineage differentiation potentials of the cells with enhanced neuronal differentiation upon induction in comparison to chitosan-gelatin scaffolds without HA and HS.

One of the major challenges in tissue engineering is to mimic complex 3D structure of the native tissue. Bioprinting uses 3D printing technology that is used to

simultaneously deposit multiple types of cells and biomaterials to replicate complex tissue structures. Collagen has been primarily used for bioprinting purposes, but it suffers from poor printability and long crosslinking time. It becomes challenging to create a tissue construct with precise shape and configuration. To overcome this problem, chitosan/gelatin-based PEC was utilized for functional 3D bioprinting (Ng et al. 2016). Chitosan was complexed with the oppositely charged gelatin at a specific pH of 6.5 to form PECs. The fabricated polyelectrolyte blends were evaluated for their chemical interactions within the polymer blend, rheological properties, printing efficiency, and biocompatibility. The printed polyelectrolyte gels exhibited better shape fidelity and biocompatibility.

2.5.5 Poly(Glutamic Acid)-Chitosan

PEC of γ-poly(glutamic acid) (γ-PGA), a non-toxic, hydrophilic, and biodegradable polymer, with chitosan is widely used to enhance the hydrophilicity and cytocompatibility of chitosan-based biomaterials. γ-PGA contains carboxylate groups which form PEC with chitosan and has been successfully used in bio-glue and drug delivery systems (Hsieh et al. 2005). The authors used the powdered form of chitosan and added it to the γ-PGA solution to get a homogeneous solution, as mixing non-powdered chitosan and γ-PGA solution produced large aggregates at the interface. This study showed that the pores in the scaffolds were interconnected and the pore sizes were in the range of 30–100 μm. The addition of γ-PGA made the scaffolds more hydrophilic, cytocompatible and enhanced their load bearing capacity.

Porous poly-L-glutamic acid (PLGA)-chitosan PEC microspheres were developed through electrostatic interaction between the two polymers (Fang et al. 2014). Firstly, chitosan microspheres were prepared and then these microspheres were impregnated PLGA solution to form PEC microspheres at 37 °C. PEC microspheres showed better structural stability. The pore size of the microspheres was controlled by varying the solid content and freezing temperature. Chitosan microspheres with a concentration of 2% (w/v) and a freezing temperature of −20 °C exhibited an average pore size of 47.5 ± 5.4 μm. Due to strong electrostatic interaction, a large amount of PLGA (110.3 μg/mg) was homogeneously absorbed within the chitosan microspheres. These PEC microspheres retained their original size, pore diameter, and interconnected porous structure. They also promoted better chondrocyte attachment and proliferation when compared to chitosan microspheres. Chondrocytes containing PEC microspheres were injected into nude mice and found to produce significantly more cartilaginous matrix than on injection with chitosan microspheres.

Another study developed porous PEC-based scaffolds of PLGA and chitosan using lyophilization method (Yan et al. 2013). PLGA-chitosan scaffolds containing 2% polymer content and at a freezing temperature of −20 °C exhibited an interconnected porous structure with an average pore size of 150–200 μm. The scaffolds showed a swelling ratio of 700%. Resistance to degradation increased with increase

in chitosan concentration. The scaffolds exhibited gel-like behavior in both dry and wet state. In vitro culture conducted on rabbit adipose-derived stem cells (ASCs) indicated that the scaffolds supported cell attachment and growth. In vivo study was performed in rabbit articular cartilage repair model and indicated successful repair of articular cartilage defects after 12 weeks of implantation.

2.6 Cell-Based Therapy

Rejection of foreign cells by the immune system is a major hurdle in cell-based therapies and regenerative technologies. New technologies are emerging to prevent the rejection of transplanted cells by the immune system. These technologies involve placing the desired cells within a biocompatible material in an attempt to protect the cells from the host immune attack and prolong their function in vivo (Hennink and van Nostrum 2012; Nicodemus and Bryant 2008). Major functions of delivery materials are to provide structural support and proper environment for cells to function. Delivery of cells can be achieved using injectable matrices, soft scaffolds, membranes, and solid load-bearing scaffolds.

Articular cartilage has a limited regenerative capacity and this complicates the treatment of joint injuries and osteoarthritis. Newer strategies based on biomaterials and cells are being developed for the treatment of damaged cartilage. PECs-based on chondroitin sulfate (CS) and chitosan (CH) were used to encapsulate mesenchymal stem cells (MSCs) (Daley et al. 2015). MSCs were encapsulated in the PECs by the either of the following ways: using water-in-oil emulsification process, direct embedment of MSCs in PEC, or by co-embedding MSCs with PEC in agarose-based microbeads. Direct embedding of MSCs in PEC resulted in large particles. However, co-embedding of PEC particles with MSCs in agarose resulted in uniform microbeads of 80–90 μm in diameter. Cell viability was reported to be high irrespective of the embedding method. Both high and low CS:CH ratios resulted in more homogeneous microbeads than 1:1 formulation. Effect of PEC on chondrogenesis was evident from the higher expression of sulfated GAG and collagen type II in 10:1 CS:CH PEC-agarose microbeads compared to pure agarose beads.

In a recent study, series of polycations with different molecular weights of N-(3-aminopropyl) methacrylamide hydrochloride (APMA) and N-(2-hydroxypropyl) methacrylamide (HPMA) were prepared by reversible addition-fragmentation chain transfer (RAFT) copolymerization (Kleinberger et al. 2016). These polycations were complexed with alginate for cell encapsulation. Hydrogels with lower cationic charge density and lower molecular weight showed less cytotoxicity and cell adhesion. However, cells were found to be more mobile within alginate gels. This study suggests that cellular behavior also depends on the composition and molecular weights of the polyelectrolytes.

Cell-encapsulated spiral-shaped alginate fibers were produced through a combination of ionotropic gelation and a perfusion-based (LbL) technique (Sher et al. 2015). The spiral shape was achieved by reeling alginate fibers on cylindrical molds having different geometries and sizes. Chelation between alginate and chitosan altered the internal microenvironment of the 3D construct from solid to the liquefied state, while preserving the external geometry. Cell viability of encapsulated L929 cells by MTS cell proliferation and double-stranded DNA quantification assays suggested that liquefied 3D constructs favored survival of cells more than non-liquefied ones.

Besides mammalian cells, probiotic bacteria have also been encapsulated for biomedical applications. *Lactobacillus acidophilus* has beneficial effects on the health of the host. However, they must be protected from the acidic environment of the stomach and the bile in the small intestine. Microencapsulation of probiotics is a smart way to protect probiotic organisms against an unfavorable environment and maintain their metabolic active state. *L. acidophilus* was immobilized with xanthan-chitosan gel using extrusion method (Chen et al. 2015). The impact of various factors such as pH, concentration, and cell suspension-xanthan ratio on microencapsulation of *L. acidophilus* was investigated. Optimum pH and concentration of chitosan solution for *L. acidophilus* were 5.5 and 0.9%, respectively. Optimum xanthan concentration and cell suspension-xanthan ratio were 0.7% and 1:10, respectively. The optimum mixed bacteria glue liquid-chitosan ratio was 1:3.

In another study, hollow polymer microspheres were prepared to encapsulate *Escherichia coli* (Flemke et al. 2013). Hollow microspheres were based on porous calcium carbonate cores with an average size of 5 μm. The outer layer was prepared by LbL deposition of different polyelectrolytes and proteins onto the porous calcium carbonate cores. CLSM and microtiter plate fluorescence tests were used to investigate the effect of encapsulation process as well as polyelectrolytes on the survival rate of the cells. These studies indicated that approximately 40% of the cells survived the encapsulation process. The lag phase of cells treated with polyelectrolytes increased and the encapsulated *E. coli* cells were able to produce green fluorescent protein inside the microcapsules.

2.7 Coatings

Biomedical implants are coated with a variety of materials to improve their biocompatibility, tissue integration, and protection from body immune system. These coating can also be used as drug delivery systems.

Two types of multilayered coatings onto titanium were fabricated by electrostatic self-assembly (van den Beucken et al. 2006). In one of the coatings, DNA was used as the anionic polyelectrolyte and poly-D-lysine (PDL) was used as a polycationic polyelectrolyte. In the other coating, DNA was used as anionic polyelectrolyte and poly(allylamine hydrochloride) (PAH) was used as the cationic polyelectrolyte. The characterization of the coatings was done using ultraviolet-visible (UV-Vis)

spectrophotometry, AFM, XPS, contact angle measurement, and FTIR. Cell culture experiments were performed on titanium substrates with and without multilayered DNA-coatings to study cell proliferation, viability, and cell morphology. There was a progressive and uniform development of both the types of coatings on titanium, but the coating was more uniform on PDL/DNA when compared to PAH/DNA. The presence of DNA did not cause any mutagenic effect on cells and cell viability was not affected. However, an increase in proliferation of the cell was observed on both types of multilayered DNA-coatings compared to non-coated controls.

Preparation of biomaterial coatings based on polypeptides, poly-L-lysine and poly-L-glutamic acid multilayers possessing anti-inflammatory properties was reported (Benkirane-Jessel et al. 2004). In this study, piroxicam (Px), was incorporated into the coatings as an anti-inflammatory agent. In order to maximize the loading capacity, the drug was incorporated into the films in the form of complexes with a charged 6-carboxymethylthio-β-cyclodextrin (cCD). The anti-inflammatory properties of the multilayer construct with the drug were evaluated by determining the inhibition of tumor necrosis factor-α (TNF-α) production by human monocytic THP-1 cells. These cells were stimulated with lipopolysaccharide (LPS) bacterial endotoxin before the test. The results indicated that the drug maintained its anti-inflammatory property and its effect can be controlled by changing the film structure.

Highly uniform microporous thin films based on weak polyelectrolytes were assembled onto silicon substrates by sequential adsorption of an aqueous solution of poly(acrylic acid) and poly(allylamine) (Mendelsohn et al. 2000). These multilayers were then immersed briefly into acidic solution (pH $\approx$ 2.4), resulting in microporous structures. These porous structures were stable against further rearrangement under ambient conditions. The authors proposed that these transformations are based on interchain ionic bond breakage and reformation in the highly protonating environment, leading to an insoluble precipitate on the substrate. This mechanism of change in the structure of the film was studied by FTIR, AFM, in situ ellipsometry, and SEM for monitoring the morphological changes. These types of porous films have applications in biomedical areas such a peritoneal dialysis.

PEC coatings based on hyaluronic acid (HA) and a recombinant fusion protein consisting of mussel adhesive motifs and the arginylglycylaspartic acid (RGD) peptide (fp-151-RGD) were coated on titanium (Hwang et al. 2010). HA and fp-151-RGD were effectively distributed over the titanium surfaces. The coatings supported the proliferation of osteoblast cells (MC-3T3) on complex-coated titanium and exhibited over 5 times greater cell proliferation than titanium coated with only HA or fp-151-RGD.

HA and chitosan were deposited using LbL assembly process to engineer bioactive coatings for endovascular stent application (Thierry et al. 2003). Polyethyleneimine (PEI) primer layer was adsorbed on nickel-titanium (NiTi) disks to initiate the sequential adsorption of the HA and chitosan. Multilayer-coated NiTi disks exhibited enhanced antifouling properties compared to unmodified NiTi

disks, as demonstrated by a decrease of platelet adhesion by in vitro assay. However, ex vivo assay revealed that the coated disks failed to prevent fouling by neutrophils in a porcine model. Sodium nitroprusside-doped multilayers were shown to further reduce platelet adhesion compared to standard multilayers.

Bacterial fouling of implants is a major clinical issue. Innovative technologies are being developed to counter bacterial infection through surface modification and surface treatment (Campoccia et al. 2013). One of the strategies is to prevent protein adsorption. In a study, adsorption of proteins was investigated on polyelectrolyte multilayers (PEMUs) consisting of synthetic polyelectrolytes and proteins, including serum albumin, fibrinogen, and lysozyme (Salloum and Schlenoff 2004). Effects of surface and protein charge, polymer hydrophobicity, and hydrophilic repulsion on the mechanism of protein charge were investigated. It was found that electrostatic interaction was the dominant interaction in protein adsorption, as proteins having a complementary charge to the PEMUs were adsorbed. Adsorption of proteins having the same charge as PEMUs occurred to a much lower extent and driven by non-electrostatic forces. The introduction of a diblock copolymer containing poly(ethylene oxide) further minimized protein adsorption. However, none of the samples completely prevented protein adsorption.

2.8 Other Applications

It is necessary that the surface of contact lenses must be hydrophilic in order to be wet by tears to facilitate unblurred vision. Traditionally, contact lenses were prepared from neutral monomers and/or polymers. Soft and hard contact lenses having ionic charges on their surface were treated with lens solution consisting of a polymer having opposite charges (Ellis and Salamone 1979). This resulted in the formation of a hydrophilic PEC hydrogel at the lens surface, which cannot be dissolved easily by the fluids present in the eye. Both cationic and anionic surfaces can be developed on the lens surface by incorporation of respective cationic (dialkylaminoethyl acrylate or methacrylate, vinylpyridine, etc.) and anionic (acrylic and methacrylic acid, vinylsulfonic acid, etc.) monomer repeat units. Since the PEC hydrogel developed will be thin, lubricating, and oxygen-permeable, it provides a 'cushioning' effect between the eye and the lens. Also, it causes no irritation and avoids punctate staining. Therefore, the contact lens can be worn for up to 24 h.

PEC-based bandages have not only been developed for wound healing, but also for hemorrhage control. Uncontrolled hemorrhage is the leading cause of death in military combat and second leading cause of death of civilians. A study reported preparation of hemostatic bandage based on chitosan and organic rectorite (OREC)/sodium alginate (Zhang et al. 2015). The sponge was fabricated by solution intercalation and chemical crosslinking techniques. The structural and compositional analysis of the sponges showed uniform pore distribution and highly crosslinked sponges using both the methods, with and without the addition of OREC into them. They also exhibited biocompatibility and antibacterial properties.

The hemostatic performance of the sponges was evaluated in ear-artery, ear-vein, and liver injuries of rabbit model. Hemorrhage control study showed that addition of OREC into the chitosan-sodium alginate composite sponge significantly improved the hemostatic efficiency.

Electrospinning technique was employed to develop a pure chitosan nanofibrous mat to be used as a hemostatic material in combat settings (Gu et al. 2013). Since acidic chitosan is water-soluble, various alkaline solutions, namely Na_2CO_3, NH_3, and NaOH were used as neutralizing agents to avert their dissolution in aqueous conditions. The porosity of the nanofibrous mats was controlled by subjecting them to ultrasonication treatment for varying time duration. It was observed that the porosity of the chitosan mat increased with increase in ultrasonication time, and the water absorption time was found to reduce from 110 to 9 s. Various aspects of the chitosan mat such as hemoglobin binding efficiency, mechanical strength, contact angle measurement, and adsorption time of water droplets were also assessed. The nanofibrous chitosan mats thus developed proved to be an effective hemostatic wound dressing material for tissue engineering applications.

To develop biocompatible composite microspheres for novel hemostatic use, microspheres consisting of carboxymethyl chitosan, sodium alginate, and collagen were synthesized (Shi et al. 2016). In hemostatic function experiment, it was found that the composite could facilitate platelet adherence, platelet aggregation, and platelet activation in vitro. Moreover, the maximum swelling capacity of the composite submerged in PBS for 50 min was over 300% of that exhibited by commercial hemostatic compound microporous polysaccharide hemostatic powder. In addition, it also exhibited good biodegradability and non-cytotoxicity.

Hydraulic fracturing is a process used in gas wells to create fractures in the deep-rock formations to promote the easier flow of petroleum, natural gas, and brine. This is done by pumping millions of gallons of pressurised fluid underground to fragment the rocks and release the gas. The fracturing fluid is a slurry of water, proppant materials, and chemical additives. Their role is to increase the fracture and maintain the fracture after formation. Water-based polymer gels are usually employed in hydraulic fracturing to increase the viscosity of the fracturing fluid to maintain the fracture. However, after the fracturing process, the gel has to be degraded by various enzymes or gel breakers to a lower viscosity to facilitate its clean up. For this purpose, enzymes are either directly added to the hydraulic fluid or encapsulated in beads. It is necessary that the bursting and release of the enzymes is delayed enough to allow complete hydraulic fracturing. As PECs are widely used to delay drug release in pharmaceutics, a study made use of PEI-dextran sulfate PEC to encapsulate the degrading enzyme, pectinase (Barati et al. 2011). The nanoparticle-encapsulated pectinase enzyme was able to successfully degrade borate-crosslinked guar and hydroxypropyl guar gels with delayed breaking. Not only was the encapsulated gel-breaking enzyme uniformly distributed throughout the gel, the delayed breakage allowed sufficient time for gelation of the gels to occur. This was supported by comparing the results of SDS-PAGE and viscosity measurements of the gels degraded with unentrapped pectinase given sufficient time.

PECs have also been used as biocontrol agent carriers. In a study, *Trichoderma viride* spores were immobilized in a water-insoluble PEC of chitosan and poly (acrylic acid-*co*-maleic acid) as novel carriers of biocontrol agents (Gicheva et al. 2012). Three types of carriers were developed: PEC-coated chitosan beads, genipin-crosslinked chitosan beads, and PEC-coated crosslinked chitosan beads. *T. viride* spores were immobilized either in the bulk or on the surface of the beads. The spores were able to maintain their viability after immobilization and the microbiological tests showed that they successfully inhibited the growth of the plant pathogens *Alternaria* and *Fusarium*.

There is an increasing need to develop highly conducting fuel cells with reduced Ohmic losses and high efficiency. Proton exchange membranes were developed for direct methanol fuel cells from a nanostructured PEC hybrid of *N-p*-carboxy benzyl chitosan-silica-poly(vinyl alcohol) by sol-gel method (Tripathi and Shahi 2008). By crosslinking and the grafting of strong proton conducting $–SO_3H$ groups on inorganic segments and weak protonating –COOH groups on the organic segments, high proton conductivity and stability was achieved. The crosslinking density and the amount of *N-p*-carboxy benzyl chitosan-silica were varied. It was found that optimization *N-p*-carboxy benzyl chitosan-silica content is necessary to control the chemical and mechanical stabilities as well as proton and fuel transport properties. The developed membranes were tested under direct methanol fuel cell operating conditions and found to be stable, flexible, had good water retention capacities, and low methanol permeability. A great advantage of these membranes was their capacity to be functional under high-temperature conditions.

References

Almalik A, Donno R, Cadman CJ, Cellesi F, Day PJ, Tirelli N (2013) Hyaluronic acid-coated chitosan nanoparticles: molecular weight-dependent effects on morphology and hyaluronic acid presentation. J Controlled Release 172(3):1142–1150

Amaike M, Senoo Y, Yamamoto H (1998) Sphere, honeycomb, regularly spaced droplet and fiber structures of polyion complexes of chitosan and gellan. Macromol Rapid Commun 19:287–289

Antipov AA, Sukhorukov GB (2004) Polyelectrolyte multilayer capsules as vehicles with tunable permeability. Adv Colloid Interface Sci 111(1):49–61

Barati R, Johnson SJ, McCool S, Green DW, Willhite GP, Liang JT (2011) Fracturing fluid cleanup by controlled release of enzymes from polyelectrolyte complex nanoparticles. J Appl Polym Sci 121(3):1292–1298

Benkirane-Jessel N, Schwinté P, Falvey P, Darcy R, Haïkel Y, Schaaf P, Voegel JC, Ogier J (2004) Build-up of polypeptide multilayer coatings with anti-inflammatory properties based on the embedding of piroxicam–cyclodextrin complexes. Adv Funct Mater 14(2):174–182

Bhardwaj N, Kundu SC (2011) Silk fibroin protein and chitosan polyelectrolyte complex porous scaffolds for tissue engineering applications. Carbohydr Polym 85(2):325–333

Bhardwaj N, Nguyen QT, Chen AC, Kaplan DL, Sah RL, Kundu SC (2011) Potential of 3-D tissue constructs engineered from bovine chondrocytes/silk fibroin-chitosan for in vitro cartilage tissue engineering. Biomaterials 32(25):5773–5781

Blacklock J, Handa H, Manickam DS, Mao G, Mukhopadhyay A, Oupicky D (2007) Disassembly of layer-by-layer films of plasmid DNA and reducible TAT polypeptide. Biomaterials 28(1):117–124

Boussif O, Lezoualc'h F, Zanta MA, Mergny MD, Scherman D, Demeneix B, Behr JP (1995) A versatile vector for gene and oligonucleotide transfer into cells in culture and in vivo: polyethylenleeimine. Proc Natl Acad Sci 92(16):7297–7301

Bulwan M, Zapotoczny S, Nowakowska M (2009) Robust "one-component" chitosan-based ultrathin films fabricated using the layer-by-layer technique. Soft Matter 5(23):4726–4732

Campoccia D, Montanaro L, Arciola CR (2013) A review of the biomaterials technologies for infection-resistant surfaces. Biomaterials 34(34):8533–8554

Cao Y, He W (2010) Synthesis and characterization of glucocorticoid functionalized poly (N-vinyl pyrrolidone): a versatile prodrug for neural interface. Biomacromolecules 11(5):1298–1307

Chang HH, Wang YL, Chiang YC, Chen YL, Chuang YH, Tsai SJ, Heish KH, Lin FH, Lin CP (2014) A novel chitosan-γPGA polyelectrolyte complex hydrogel promotes early new bone formation in the alveolar socket following tooth extraction. PLoS ONE 9(3):1–11

Chelmecka M (2004) Complexes of polyelectrolytes with defined charge distance and different dendrimer counterions. Dissertation, Johannes Gutenberg University of Mainz

Chen PH, Kuo TY, Kuo JY, Tseng YP, Wang DM, Lai JY, Hsieh HJ (2010) Novel chitosan–pectin composite membranes with enhanced strength, hydrophilicity and controllable disintegration. Carbohydr Polym 82(4):1236–1242

Chen H, Song Y, Liu N, Wan H, Shu G, Liao N (2015) Effect of complexation conditions on microcapsulation of *Lactobacillus acidophilus* in xanthan-chitosan polyelectrolyte complex gels. Acta Sci Pol Technol Aliment 14(3):207–213

Chun MK, Cho CS, Choi HK (2004) Characteristics of poly (vinyl pyrrolidone)/poly (acrylic acid) interpolymer complex prepared by template polymerization of acrylic acid: effect of reaction solvent and molecular weight of template. J Appl Polym Sci 94(6):2390–2394

Coimbra P, Ferreira P, De Sousa HC, Batista P, Rodrigues MA, Correia IJ, Gil MH (2011) Preparation and chemical and biological characterization of a pectin/chitosan polyelectrolyte complex scaffold for possible bone tissue engineering applications. Int J Biol Macromol 48(1):112–118

Costa RR, Mano JF (2014) Polyelectrolyte multilayered assemblies in biomedical technologies. Chem Soc Rev 43(10):3453–3479

Dai M, Zheng X, Xu X, Kong X, Li X, Guo G, Luo F, Zhao X, Wei YQ, Qian Z (2009) Chitosan-alginate sponge: preparation and application in curcumin delivery for dermal wound healing in rat. BioMed Res Int 2009:1–8

Daley EL, Coleman RM, Stegemann JP (2015) Biomimetic microbeads containing a chondroitin sulfate/chitosan polyelectrolyte complex for cell-based cartilage therapy. J Mater Chem B 3 (40):7920–7929

De Cock LJ, De Koker S, De Vos F, Vervaet C, Remon JP, De Geest BG (2010) Layer-by-layer incorporation of growth factors in decellularized aortic heart valve leaflets. Biomacromlecules 11(4):1002–1008

De Geest BG, De Smedt SC (2012) Designing LbL capsules for drug loading and release. In: Decher G, Schlenoff (eds) Multilayer thin films: sequential assembly of nanocomposite materials, 2nd edn. Wiley-VCH Verlag GmbH, Weinheim, Germany, pp 749–763

de la Fuente M, Seijo B, Alonso MJ (2008) Novel hyaluronic acid-chitosan nanoparticles for ocular gene therapy. Invest Ophthalmol Vis Sci 49(5):2016–2024

de la Torre PM, Enobakhare Y, Torrado G, Torrado S (2003) Release of amoxicillin from polyionic complexes of chitosan and poly (acrylic acid). Study of polymer/polymer and polymer/drug interactions within the network structure. Biomaterials 24(8):1499–1506

Dehghan MH, Girase M (2012) Freeze-dried xanthan/guar gum nasal inserts for the delivery of metoclopramide hydrochloride. Iran J Pharm Res 11(2):513–521

Deng B, Shen L, Wu Y, Shen Y, Ding X, Lu S, Jia J, Qian J, Ge J (2015) Delivery of alginate-chitosan hydrogel promotes endogenous repair and preserves cardiac function in rats with myocardial infarction. J Biomed Mater Res, Part A 103:907–918

Devi N, Maji TK (2009) Preparation and evaluation of gelatin/sodium carboxymethyl cellulose polyelectrolyte complex microparticles for controlled delivery of isoniazid. AAPS PharmSciTech 10(4):1412–1419

Di Martino A, Sittinger M, Risbud MV (2005) Chitosan: a versatile biopolymer for orthopaedic tissue-engineering. Biomaterials 26(30):5983–5990

Dunne LW, Iyyanki T, Hubenak J, Mathur AB (2014) Characterization of dielectrophoresis-aligned nanofibrous silk fibroin-chitosan scaffold and its interactions with endothelial cells for tissue engineering applications. Acta Biomater 10(8):3630–3640

Ellis EJ, Salamone JC (1979) US Patent 4,168,112, 18 Sept 1979

Fang J, Zhang Y, Yan S, Liu Z, He S, Cui L, Yin J (2014) Poly (L-glutamic acid)/chitosan polyelectrolyte complex porous microspheres as cell microcarriers for cartilage regeneration. Acta Biomater 10(1):276–288

Flemke J, Maywald M, Sieber V (2013) Encapsulation of living *E. coli* cells in hollow polymer microspheres of highly defined size. Biomacromolecules 14(1):207–214

Gandhi A, Paul A, Sen SO, Sen KK (2015) Studies on thermoresponsive polymers: phase behaviour, drug delivery and biomedical applications. Asian J Pharm Sci 10(2):99–107

Gärdlund L, Wågberg L, Gernandt R (2003) Polyelectrolyte complexes for surface modification of wood fibres: II. Influence of complexes on wet and dry strength of paper. Colloids Surf, A 218 (1):137–149

Gåserød O, Smidsrød O, Skjåk-Bræk G (1998) Microcapsules of alginate-chitosan–I: a quantitative study of the interaction between alginate and chitosan. Biomaterials 19(20):1815–1825

Gicheva G, Paneva D, Manolova N, Naydenov M, Rashkov I (2012) New polyelectrolyte complex of chitosan: preparation, characterization, and application as a biocontrol agent carrier. J Bioact Compat Polym 27(2):148–160

Gohad NV, Aldred N, Hartshorn CM, Lee YJ, Cicerone MT, Orihuela B, Clare AS, Rittschof D, Mount AS (2014) Synergistic roles for lipids and proteins in the permanent adhesive of barnacle larvae. Nat Commun 5:1–9

Granero AJ, Razal JM, Wallace GG (2010) Conducting gel-fibres based on carrageenan, chitosan and carbon nanotubes. J Mater Chem 20(37):7953–7956

Grenha A, Gomes ME, Rodrigues M, Santo VE, Mano JF, Neves NM, Reis RL (2010) Development of new chitosan/carrageenan nanoparticles for drug delivery applications. J Biomed Mater Res, Part A 92(4):1265–1272

Gu BK, Park SJ, Kim MS, Kang CM, Kim JI, Kim CH (2013) Fabrication of sonicated chitosan nanofiber mat with enlarged porosity for use as hemostatic materials. Carbohydr Polym 97(1):65–73

Guan S, Zhang XL, Lin XM, Liu TQ, Ma XH, Cui ZF (2013) Chitosan/gelatin porous scaffolds containing hyaluronic acid and heparan sulfate for neural tissue engineering. J Biomater Sci Polym Ed 24(8):999–1014

Han J, Zhou Z, Yin R, Yang D, Nie J (2010) Alginate–chitosan/hydroxyapatite polyelectrolyte complex porous scaffolds: preparation and characterization. Int J Biol Macromol 46(2):199–205

Hartig SM, Greene RR, Dikov MM, Prokop A, Davidson JM (2007) Multifunctional nanoparticulate polyelectrolyte complexes. Pharm Res 24(12):2353–2369

Hennink WE, van Nostrum C (2012) Novel crosslinking methods to design hydrogels. Adv Drug Deliv Rev 64:223–236

Hsieh CY, Tsai SP, Wang DM, Chang YN, Hsieh HJ (2005) Preparation of γ-PGA/chitosan composite tissue engineering matrices. Biomaterials 26(28):5617–5623

Hu X, Ji J (2010) Construction of multifunctional coatings via layer-by-layer assembly of sulfonated hyperbranched polyether and chitosan. Langmuir 26(24):2624–2629

Hwang DS, Waite JH, Tirrell M (2010) Promotion of osteoblast proliferation on complex coacervation-based hyaluronic acid–recombinant mussel adhesive protein coatings on titanium. Biomaterials 31(6):1080–1084

Imamura M, Kodama Y, Higuchi N, Kanda K, Nakagawa H, Muro T, Nakamura T, Kitahara T, Sasaki H (2014) Ternary complex of plasmid DNA electrostatically assembled with

polyamidoamine dendrimer and chondroitin sulfate for effective and secure gene delivery. Biol Pharm Bull 37(4):552–559

Kabanov VA (2003) Fundamentals of polyelectrolyte complexes in solution and the bulk. In: Decher G, Schlenoff JB (eds) Multilayer thin films: sequential assembly of nanocomposite materials. Wiley-VCH Verlag GmbH, Weinheim, pp 47–86

Kanda K, Kodama Y, Kurosaki T, Imamura M, Nakagawa H, Muro T, Higuchi N, Nakamura T, Kitahara T, Honda M, Sasaki H (2013) Ternary complex of plasmid DNA with protamine and γ-polyglutamic acid for biocompatible gene delivery system. Biol Pharm Bull 36(11):1794–1799

Kathuria N, Tripathi A, Kar KK, Kumar A (2009) Synthesis and characterization of elastic and macroporous chitosan–gelatin cryogels for tissue engineering. Acta Biomater 5(1):406–418

Katti KS, Ambre AH, Peterka N, Katti DR (2010) Use of unnatural amino acids for design of novel organomodified clays as components of nanocomposite biomaterials. Philos Trans R Soc Lond A: Math Phys Eng Sci 368(1917):1963–1980

Kaur A, Kaur G (2012) Mucoadhesive buccal patches based on interpolymer complexes of chitosan–pectin for delivery of carvedilol. Saudi Pharm J 20(1):21–27

Kaur G, Jain S, Tiwary AK (2010) Chitosan-carboxymethyl tamarind kernel powder interpolymer complexation: investigations for colon drug delivery. Sci Pharm 78(1):57–78

Kent DJ (2009) Introducing… alginate dressings. Nursing Made Incredibly Easy 7(3):26–27

Khutoryanskaya OV, Potgieter M, Khutoryanskiy VV (2010) Multilayered hydrogel coatings covalently-linked to glass surfaces showing a potential to mimic mucosal tissues. Soft Matter 6(3):551–557

Kim H, Lee J (2016) Strategies to maximize the potential of marine biomaterials as a platform for cell therapy. Marine Drugs 14(2):1–37

Kim HJ, Lee HC, Oh JS, Shin BA, Oh CS, Park RD, Yang KS, Cho CS (1999) Polyelectrolyte complex composed of chitosan and sodium alginate for wound dressing application. J Biomater Sci Polym Ed 10(5):543–556

Kleinberger RM, Burke NA, Zhou C, Stöver HD (2016) Synthetic polycations with controlled charge density and molecular weight as building blocks for biomaterials. J Biomater Sci Polym Ed 12:1–9

Konar N, Kim CJ (1998) Drug release from drug-polyanion complex tablets: poly (acrylamido-2-methyl-1-propanesulfonate sodium-co-methyl methacrylate). J Controlled Release 57(2):141–150

Kumar A, Tripathi A (2012) Biopolymeric scaffolds for tissue engineering. In: Tiwari A, Shrivastava RB (eds) Biotechnology in biopolymers. Smithers Repra Publication Ltd., UK, pp 233–269

Lee SB, Lee YM, Song KW, Park MH (2002) Preparation and properties of polyelectrolyte complex sponges composed of hyaluronic acid and chitosan and their biological behaviors. J Appl Polym Sci 90(4):925–932

Lee MH, Chun MK, Choi HK (2008) Preparation of carbopol/chitosan interpolymer complex as a controlled release tablet matrix; effect of complex formation medium on drug release characteristics. Arch Pharmacal Res 31(7):932–937

Leong KW, Mao HQ, Truong-Le VL, Roy K, Walsh SM, August JT (1998) DNA-polycation nanospheres as non-viral gene delivery vehicles. J Controlled Release 53(1):183–193

Li Z, Ramay HR, Hauch KD, Xiao D, Zhang M (2005) Chitosan–alginate hybrid scaffolds for bone tissue engineering. Biomaterials 26(18):3919–3928

Li G, Song S, Zhang T, Qi M, Liu J (2013) pH-sensitive polyelectrolyte complex micelles assembled from CS-g-PNIPAM and ALG-g-P (NIPAM-co-NVP) for drug delivery. Int J Biol Macromol 62:203–210

Lim S, Choi YS, Kang DG, Song YH, Cha HJ (2010) The adhesive properties of coacervated recombinant hybrid mussel adhesive proteins. Biomaterials 31(13):3715–3722

Liu L, Fishman ML, Kost J, Hicks KB (2003) Pectin-based systems for colon-specific drug delivery via oral route. Biomaterials 24(19):3333–3343

Lu Z, Chen W, Hamman JH, Ni J, Zhai X (2008) Chitosan-polycarbophil interpolyelectrolyte complex as an excipient for bioadhesive matrix systems to control macromolecular drug delivery. Pharm Dev Technol 13(1):37–47

Luo D, Saltzman WM (2000) Synthetic DNA delivery systems. Nat Biotechnol 18(1):33–37

Lvov Y, Decher G, Sukhorukov G (1993) Assembly of thin films by means of successive deposition of alternate layers of DNA and poly (ally1amine). Macromolecules 26(20):5396–5399

Macleod GS, Collett JH, Fell JT (1999) The potential use of mixed films of pectin, chitosan and HPMC for bimodal drug release. J Controlled Release 58(3):303–310

Majima T, Funakosi T, Iwasaki N, Yamane ST, Harada K, Nonaka S, Minami A, Nishimura SI (2005) Alginate and chitosan polyion complex hybrid fibers for scaffolds in ligament and tendon tissue engineering. J Orthop Sci 10(3):302–307

Mandal BB, Kundu SC (2008) Non-bioengineered silk fibroin protein 3D scaffolds for potential biotechnological and tissue engineering applications. Macromol Biosci 8(9):807–818

Mandal BB, Grinberg A, Gil ES, Panilaitis B, Kaplan DL (2012) High-strength silk protein scaffolds for bone repair. Proc Natl Acad Sci 109(20):7699–7704

Mehdizadeh M, Weng H, Gyawali D, Tang L, Yang J (2012) Injectable citrate-based mussel-inspired tissue bioadhesives with high wet strength for sutureless wound closure. Biomaterials 33(32):7972–7983

Mendelsohn JD, Barrett CJ, Chan VV, Pal AJ, Mayes AM, Rubner MF (2000) Fabrication of microporous thin films from polyelectrolyte multilayers. Langmuir 16(11):5017–5023

Mi FL, Shyu SS, Kuan CY, Lee ST, Lu KT, Jang SF (1999a) Chitosan–polyelectrolyte complexation for the preparation of gel beads and controlled release of anticancer drug. I. Effect of phosphorous polyelectrolyte complex and enzymatic hydrolysis of polymer. J Appl Polym Sci 74(7):1868–1879

Mi FL, Shyu SS, Wong TB, Jang SF, Lee ST, Lu KT (1999b) Chitosan-polyelectrolyte complexation for the preparation of gel beads and controlled release of anticancer drug. II. Effect of pH-dependent ionic crosslinking or interpolymer complex using tripolyphosphate or polyphosphate as reagent. J Appl Polym Sci 74(5):1093–1107

Michaels AS (1965) Polyelectrolyte complexes. Ind Eng Chem 57(10):32–40

7Michaels AS, Miekka RG (1961) Polycation-polyanion complexes: preparation and properties of poly-(vinylbenzyltrimethylammonium) poly-(styrenesulfonate). J Phys Chem 65(10):1765–1773

Mobini S, Hoyer B, Solati-Hashjin M, Lode A, Nosoudi N, Samadikuchaksaraei A, Gelinsky M (2013) Fabrication and characterization of regenerated silk scaffolds reinforced with natural silk fibers for bone tissue engineering. J Biomed Mater Res, Part A 101(8):2392–2404

Mousa MH, Dong Y, Davies IJ (2016) Recent advances in bionanocomposites: preparation, properties, and applications. Int J Polym Mater Polym Biomater 65(5):225–254

Munarin F, Tanzi MC, Petrini P (2012) Advances in biomedical applications of pectin gels. Int J Biol Macromol 51(4):681–689

Naidu VG, Madhusudhana K, Sashidhar RB, Ramakrishna S, Khar RK, Ahmed FJ, Diwan PV (2009) Polyelectrolyte complexes of gum kondagogu and chitosan, as diclofenac carriers. Carbohydr Polym 76(3):464–471

Nath SD, Abueva C, Kim B, Lee BT (2015) Chitosan–hyaluronic acid polyelectrolyte complex scaffold crosslinked with genipin for immobilization and controlled release of BMP-2. Carbohydr Polym 115:160–169

Ng WL, Yeong WY, Naing MW (2016) Polyelectrolyte gelatin-chitosan hydrogel optimized for 3D bioprinting in skin tissue engineering. Int J Bioprinting 2(1):2–10

Nicodemus GD, Bryant SJ (2008) Cell encapsulation in biodegradable hydrogels for tissue engineering applications. Tissue Eng Part B: Rev 14(2):149–165

Ong SY, Wu J, Moochhala SM, Tan MH, Lu J (2008) Development of a chitosan-based wound dressing with improved hemostatic and antimicrobial properties. Biomaterials 29(32):4323–4332

Ozeki T, Yuasa H, Okada H (2005) Controlled release of drug via methylcellulose-carboxyvinylpolymer interpolymer complex solid dispersion. AAPS PharmSciTech 6(2):E231–E236

Pack DW, Hoffman AS, Pun S, Stayton PS (2005) Design and development of polymers for gene delivery. Nat Rev Drug Discovery 4(7):581–593

Pandey S, Mishra A, Raval P, Patel H, Gupta A, Shah D (2013) Chitosan–pectin polyelectrolyte complex as a carrier for colon targeted drug delivery. J Young Pharm 5(4):160–166

Pargaonkar N, Lvov YM, Li N, Steenekamp JH, de Villiers MM (2005) Controlled release of dexamethasone from microcapsules produced by polyelectrolyte layer-by-layer nanoassembly. Pharm Res 22(5):826–835

Picart C, Schneider A, Etienne O, Mutterer J, Schaaf P, Egles C, Jessel N, Voegel JC (2005) Controlled degradability of polysaccharide multilayer films in vitro and in vivo. Adv Funct Mater 15(11):1771–1780

Porcel CH, Schlenoff JB (2009) Compact polyelectrolyte complexes: "saloplastic" candidates for biomaterials. Biomacromolecules 10(11):2968–2975

Qiao P, Wang J, Xie Q, Li F, Dong L, Xu T (2013) Injectable calcium phosphate–alginate–chitosan microencapsulated MC3T3-E1 cell paste for bone tissue engineering in vivo. Mater Sci Eng, C 33(8):4633–4639

Radtchenko IL, Sukhorukov GB, Möhwald H (2002) Incorporation of macromolecules into polyelectrolyte micro- and nanocapsules via surface controlled precipitation on colloidal particles. Colloids Surf, A 202(2):127–133

Salloum DS, Schlenoff JB (2004) Protein adsorption modalities on polyelectrolyte multilayers. Biomacromolecules 5(3):1089–1096

Schneider GF, Subr V, Ulbrich K, Decher G (2009) Multifunctional cytotoxic stealth nanoparticles. A model approach with potential for cancer therapy. Nano Lett 9(2):636–642

Shao X, Hunter CJ (2007) Developing an alginate/chitosan hybrid fiber scaffold for annulus fibrosus cells. J Biomed Mater Res, Part A 82(3):701–710

Sher P, Oliveira SM, Borges J, Mano JF (2015) Assembly of cell-laden hydrogel fiber into non-liquefied and liquefied 3D spiral constructs by perfusion-based layer-by-layer technique. Biofabrication 7(1):1–7

Shi X, Fang Q, Ding M, Wu J, Ye F, Lv Z, Jin J (2016) Microspheres of carboxymethyl chitosan, sodium alginate and collagen for a novel hemostatic in vitro study. J Biomater Appl 30(7):1092–1102

Shiratori SS, Rubner MF (2000) pH-dependent thickness behavior of sequentially adsorbed layers of weak polyelectrolytes. Macromolecules 33(11):4213–4219

Singh M, Tiwary AK, Kaur G (2011) Investigations on interpolymer complexes of cationic guar gum and xanthan gum for formulation of bioadhesive films. Res pharm Sci 5(2):79–87

Sowjanya JA, Singh J, Mohita T, Sarvanan S, Moorthi A, Srinivasan N, Selvamurugan N (2013) Biocomposite scaffolds containing chitosan/alginate/nano-silica for bone tissue engineering. Colloids Surf, B 109:294–300

Spruijt E, Cohen Stuart MA, van der Gucht J (2013) Linear viscoelasticity of polyelectrolyte complex coacervates. Macromolecules 46(4):1633–1641

Stewart RJ, Weaver JC, Morse DE, Waite JH (2004) The tube cement of *Phragmatopoma californica*: a solid foam. J Exp Biol 207(26):472–4734

Takayama K, Nagai T (1987) Application of interpolymer complexation of polyvinylpyrrolidone/carboxyvinyl polymer to control of drug release. Chem Pharm Bull 35(12):4921–4927

Tapia C, Escobar Z, Costa E, Sapag-Hagar J, Valenzuela F, Basualto C, Gai MN, Yazdani-Pedram M (2004) Comparative studies on polyelectrolyte complexes and mixtures of chitosan–alginate and chitosan–carrageenan as prolonged diltiazem clorhydrate release systems. Eur J Pharm Biopharm 57(1):65–75

Tazawa K, Okami H, Yamashita I, Ohnishi Y, Kobashi K, Fujimaki M (1997) Anticarcinogenic action of apple pectin on fecal enzyme activities and mucosal or portal prostaglandin E2 levels in experimental rat colon carcinogenesis. J Exp Clin Cancer Res: CR 16(1):33–38

Thierry B, Winnik FM, Merhi Y, Silver J, Tabrizian M (2003) Bioactive coatings of endovascular stents based on polyelectrolyte multilayers. Biomacromolecules 4(6):1564–1571

Tong S, Xu DP, Liu ZM, Du Y, Wang XK (2016) Synthesis of the new-type vascular endothelial growth factor–silk fibroin–chitosan three-dimensional scaffolds for bone tissue engineering and in vitro evaluation. J Craniofac Surg 27(2):509–515

Tripathi A, Melo JS (2015) Preparation of a sponge-like biocomposite agarose–chitosan scaffold with primary hepatocytes for establishing an in vitro 3D liver tissue model. RSC Adv 5 (39):30701–30710

Tripathi BP, Shahi VK (2008) Functionalized organic—inorganic nanostructured N-p-carboxy benzyl chitosan—silica—PVA hybrid polyelectrolyte complex as proton exchange membrane for DMFC applications. J Phys Chem B 112(49):15678–15690

Tsao CT, Chang CH, Lin YY, Wu MF, Wang JL, Han JL, Hsieh KH (2010) Antibacterial activity and biocompatibility of a chitosan–γ-poly (glutamic acid) polyelectrolyte complex hydrogel. Carbohydr Res 345(12):1774–1780

Tsao CT, Chang CH, Lin YY, Wu MF, Wang JL, Young TH, Han JL, Hsieh KH (2011) Evaluation of chitosan/γ-poly (glutamic acid) polyelectrolyte complex for wound dressing materials. Carbohydr Polym 84(2):812–819

Tseng HJ, Tsou TL, Wang HJ, Hsu SH (2013) Characterization of chitosan–gelatin scaffolds for dermal tissue engineering. J Tissue Eng Regen Med 7(1):20–31

Tuzlakoglu K, Alves CM, Mano JF, Reis RL (2004) Production and characterization of chitosan fibers and 3-D fiber mesh scaffolds for tissue engineering applications. Macromol Biosci 4(8):811–819

van den Beucken JJ, Vos MR, Thüne PC, Hayakawa T, Fukushima T, Okahata Y, Walboomers XF, Sommerdijk NA, Nolte RJ, Jansen JA (2006) Fabrication, characterization, and biological assessment of multilayered DNA-coatings for biomaterial purposes. Biomaterials 27(5):691–701

Vasile C, Pieptu D, Dumitriu RP, Pânzariu A, Profire L (2012) Chitosan/hyaluronic acid polyelectrolyte complex hydrogels in the management of burn wounds. Revista medico-chirurgicalã a Societãţii de Medici şi Naturalişti din Iaşi 117(2):565–571

Vehlow D, Schmidt R, Gebert A, Siebert M, Lips KS, Müller M (2016) Polyelectrolyte complex based interfacial drug delivery system with controlled loading and improved release performance for bone therapeutics. Nanomaterials 6(3):53–74

Verma D (2008) Design of polymer-biopolymer-hydroxyapatite biomaterials for bone tissue engineering: through molecular control of interfaces. Dissertation, North Dakota State University of Agriculture and Applied Sciences

Verma D, Katti KS, Katti DR (2009) Polyelectrolyte-complex nanostructured fibrous scaffolds for tissue engineering. Mater Sci Eng, C 29(7):2079–2084

Verma D, Katti KS, Katti DR (2010) Osteoblast adhesion, proliferation and growth on polyelectrolyte complex–hydroxyapatite nanocomposites. Philos Trans R Soc Lond A: Math Phys Eng Sci 368(1917):2083–2097

Verma D, Desai MS, Kulkarni N, Langrana N (2011) Characterization of surface charge and mechanical properties of chitosan/alginate based biomaterials. Mater Sci Eng, C 31(8):1741–1747

Verma D, Previtera ML, Schloss R, Langrana N (2012) Polyelectrolyte complex membranes for prevention of post-surgical adhesions in neurosurgery. Ann Biomed Eng 40(9):1949–1960

Wan AC, Liao IC, Yim EK, Leong KW (2004) Mechanism of fiber formation by interfacial polyelectrolyte complexation. Macromolecules 37(18):7019–7025

Wan AC, Tai BC, Leck KJ, Ying JY (2006) Silica-incorporated polyelectrolyte-complex fibers as tissue-engineering scaffolds. Adv Mater 18(5):641–644

Wan X, Liu T, Hu J, Liu S (2013) Photo-degradable, protein–polyelectrolyte complex-coated, mesoporous silica nanoparticles for controlled co-release of protein and model drugs. Macromol Rapid Commun 34(4):341–347

Wang L, Khor E, Wee A, Lim LY (2002) Chitosan-alginate PEC membrane as a wound dressing: assessment of incisional wound healing. J Biomed Mater Res 63(5):610–618

Wang L, Chen D, Sun J (2009) Layer-by-Layer deposition of polymeric microgel films on surgical sutures for loading and release of ibuprofen. Langmuir 25(14):7990–7994

Wang W, Xu Y, Li A, Li T, Liu M, von Klitzing R, Ober CK, Kayitmazer AB, Li L, Guo X (2015) Zinc induced polyelectrolyte coacervate bioadhesive and its transition to a self-healing hydrogel. RSC Advances 5(82):66871–66878

Win PP, Shin-Ya Y, Hong KJ, Kajiuchi T (2003) Formulation and characterization of pH sensitive drug carrier based on phosphorylated chitosan (PCS). Carbohydr Polym 53(3):305–310

Xu B, Du L, Zhang J, Zhu M, Ji S, Zhang Y, Kong D, Ma X, Yang Q, Wang L (2015) Circumferentially oriented microfiber scaffold prepared by wet-spinning for tissue engineering of annulus fibrosus. RSC Adv 5(53):42705–42713

Yadav P, Yadav H, Shah VG, Shah G, Dhaka G (2015) Biomedical biopolymers, their origin and evolution in biomedical sciences: a systematic review. J Clin Diagn Res 9(9):ZE21-ZE25

Yan S, Zhang K, Liu Z, Zhang X, Gan L, Cao B, Chen X, Cui L, Yin J (2013) Fabrication of poly (L-glutamic acid)/chitosan polyelectrolyte complex porous scaffolds for tissue engineering. J Mater Chem B 1(11):1541–1551

Yu CC, Chang JJ, Lee YH, Lin YC, Wu MH, Yang MC, Chien CT (2013) Electrospun scaffolds composing of alginate, chitosan, collagen and hydroxyapatite for applying in bone tissue engineering. Mater Lett 93:133–136

Zauner W, Ogris M, Wagner E (1998) Polylysine-based transfection systems utilizing receptor-mediated delivery. Adv Drug Deliv Rev 30(1):97–113

Zhang J, Lynn DM (2007) Ultrathin multilayered films assembled from “charge-shifting” cationic polymers: extended, long-term release of plasmid DNA from surfaces. Adv Mater 19 (23):4218–4223

Zhang J, Chua LS, Lynn DM (2004) Multilayered thin films that sustain the release of functional DNA under physiological conditions. Langmuir 20(19):8015–8021

Zhang H, Lv X, Zhang X, Wang H, Deng H, Li Y, Xu X, Huang R, Li X (2015) Antibacterial and hemostatic performance of chitosan–organic rectorite/alginate composite sponge. RSC Adv 5 (62):50523–50531

Plasma Surface Modification of Biomaterials for Biomedical Applications

Ajinkya M. Trimukhe, Krishnasamy N. Pandiyaraj, Anuj Tripathi, Jose Savio Melo and Rajendra R. Deshmukh

Abstract Application oriented selection of a material depends on the bulk properties of that material. However, a first encountering feature of any material in an application is its surface and thus material's surface is one of the foremost parameter that decides the fate of material performance. Modulating the surface properties is considered as a potential approach to meet the application requirement. In past, various techniques (like, chemical, γ-irradiation, mechanical abrasion) have been developed for the surface modification of materials. These methods have certain disadvantages, like chemical treatment involve the disposal of polluted solvents/water in the environment, whereas other techniques may affect bulk properties of the material. Since three decades, plasma surface modification technique has attracted attention of scientists and technologists for creating new surfaces for various end-use applications such as textiles, food packaging, coatings, medical devices etc. Especially, low temperature plasma (low pressure and atmospheric pressure glow discharge) has attracted for its potential application in the new biomedical devices and biomaterials development. Plasma processing has proved itself a very promising and potent technology for modification of surface properties in an effective, environment friendly and

A.M. Trimukhe · R.R. Deshmukh (✉)
Department of Physics, Institute of Chemical Technology, Matunga,
Mumbai 400019, India
e-mail: rr.deshmukh@ictmumbai.edu.in

A.M. Trimukhe
e-mail: ajinkyatrimukhe@gmail.com

K.N. Pandiyaraj
Department of Physics, Sri Shakthi Institute of Engineering and Technology,
L&T by Pass, Chinniyam Palayam (Post), Coimbatore 641062, India
e-mail: dr.knpr@gmail.com

A. Tripathi · J.S. Melo
Nuclear Agriculture and Biotechnology Division, Bhabha Atomic Research Centre,
Mumbai 400094, India
e-mail: anujtri@barc.gov.in

J.S. Melo
e-mail: jsmelo@barc.gov.in

A. Tripathi and J.S. Melo (eds.), *Advances in Biomaterials for Biomedical Applications*, Advanced Structured Materials 66,
DOI 10.1007/978-981-10-3328-5_3

economical way for converting low cost materials into a value added materials. The surface properties and biocompatibility can be enhanced selectively and precisely without affecting material's bulk properties by the use of plasma surface modification technique. This chapter is providing a brief overview of low temperature plasma as a versatile technology for surface modification and its application pertaining to biomedical materials research. Various inferences are also drawn from the types of plasma used in the biomedical applications.

Keywords Plasma · Surface modification · Biomaterials · Antimicrobial · Sterilization · Tissue engineering

Abbreviations

3D	Three dimensional
AAc	Acrylic acid
AC	Alternate current
ACP	Amorphous calcium phosphate
APGD	Atmospheric pressure glow discharge
APPJ	Atmospheric pressure plasma jet
APPS	Atmospheric pressure plasma system
APTT	Activated partial thromboplastin time
Ar	Argon
BMA	Butyl methacrylate
BSA	Bovine serum albumin
CAP	Competitive ablation and polymerization
CG	Cationized gelatin
CHI	Chitosan
CN	Carbon nitride
DBD	Dielectric barrier discharge
DC	Direct current
DDSs	Drug delivery systems
DLC	Diamond like coating
EC	Endothelial cell
ECM	Extra cellular matrix
ePTFE	Expanded polytetrafluoroethylene
EtO	Ethylene oxide
EVA	Polyethylene-co-vinyl acetate
FAK	Focal adhesion kinase
FDA	Food and drug administration
FEP	Poly (tetrafluoroethylene-co-tetrafluoropropylene)
Fn	Fibronectin
FTIR	Fourier transform infrared
HA	Hydroxyapatite
HAEC	Human aortic endothelial cells
HMDSO	Hexamethyldisiloxane

HUVEC	Human vascular endothelial cell
IOLs	Intraocular lens
KDR	Kinase-insert domain-containing receptor
LDPE	Low density polyethylene
LPPS	Low pressure plasma system
LTE	Local thermodynamic equilibrium
LTP	Low temperature plasma
NF	Nanofibers
NVP	N-vinyl-2-pyrrolidone
PAECs	Pig aorta endothelial cells
PCL	Poly caprolactone
pdAA	Plasma deposited acrylic acid
PDC	Pulsed-DC
PE	Polyethylene
PECVD	Plasma enhanced chemical vapour deposition
PEEK	Polyether-ether-ketone
PEG	Poly (ethylene glycol)
PEN	Polyethylene naphthalate
PEO	Poly ethyleneoxide
PET	Polyethylene terephthalate
PIII	Plasma immersion ion implantation
PIIID	PIII-deposition
PLA	Poly (D,L-lactic acid)
PLGA	Poly (D,L-lactic acid-co-glycolic acid)
PLLA	Poly (L-Lactic acid)
PMMA	Poly methyl methacrylate
PP	Polypropylene
ppAA	Plasma polymerized acrylic acid
ppAAm	Plasma polymerized allylamine
pPEO	Plasma polyethyleneoxide
ppHMDS	Plasma polymerized hexamethyldisiloxane
ppPEO	Plasma polymerized polyethyleneoxide
ppTEOS	Plasma polymerized tetraethyl orthosilicate
pPTFE	Plasmapolytetrafluoroethylene
PS	Polystyrene
PSF	Polysulfone
PSP	Polystyrene plate
PTFE	Polytetrafluoroethylene
PU	Polyurethane
PVC	Poly vinyl chloride
RbMVEC	Rabbit microvascular endothelial cell
RER	Remote exposure reactor
RF	Radio frequency
RFGD	Radio frequency glow discharge

ROS	Reactive oxygen species
SBF	Simulated body fluid
SDBD	Surface-DBD
SE	Surface energy
SF_6	Sulphur hexafluoride
TCP	Tissue cultured plates
TE	Tissue engineering
TEM	Transmission electron microscope
TEOS	Tetra ethyl orthosilicate
TMOS	Tetra methyl orthosilicate
VDBD	Volume-DBD
VOC	Volatile organic compound
VSMC	Vascular smooth muscle cell
WBCT	Whole blood clotting time
XPS	X-ray photoelectron spectroscopy
XRD	X-ray diffraction

1 Introduction

Materials from synthetic, semi-synthetic or natural origin are in growing demand for various biomedical applications. However, a material gets devalued in its functionality in an intended application if it does not comply with the desired properties. Technological advancements provide flexibility to modulate the material properties as per the choice of application. Materials which are intended for use in biomedical applications should have suitable surface properties so that they are accepted by the human body. In this regard, surface hydrophilicity/wettability and surface energy play a vital role in addition to the surface morphology. Various surface modification techniques such as exposure to plasma, flame, chemicals, enzymes etc. have been used to enhance wettability and adhesion of polymers/films. Surface wettability can also be tailored by altering the chemical composition of the outermost layer of the material. In addition, surface roughness also has a significant role in enhancing the adhesion and wettability. A material's wettability is governed by molecular interaction of the angstrom size units present on their outermost surface layer (Deshmukh and Bhat 2011; Deshmukh and Shetty 2008). Therefore, the wettability of material surfaces does not originate from the organic molecule as a whole, but depends on the morphology and functional moieties present on the outermost surface. Further rearrangement of molecules takes place at the interface for minimization of surface energy and therefore only the low energy portions come in contact with surrounding phase. As a result, wettability is governed by the chemical nature of energetically preferred functional groups and the extent to which they are exposed to the surrounding. In the past few decades the downsides of the material have been overwhelmed by tailoring the surface properties of the materials

using various advanced surface modification techniques such as chemical etching, ozone treatment, laser treatment, UV radiation, electron beam, corona discharge, ion beam, and plasma based surface treatments (Sprang et al. 1995; Abenojar et al. 2009; Encinas et al. 2010; Gogolewski et al. 1996; Martin et al. 2007; Kaczmarek et al. 2002; Kim et al. 2004; Arenholz et al. 1991; Svorcík et al. 1997, 1998; Walachova et al. 2002). Moreover, differing on the relevance, the modification effect has to be cost effective and has to overcome the limitations due to uses of solvents, emission of volatile organic compounds (VOC), time consumption and lack of reproducibility. Various types of plasma surface modification technologies are being used to improve the surface energy, wettability, adhesion and other surface related properties of the material by incorporating variety of reactive functional moieties. The plasma processing pertains to various biomedical applications; for example, scaffolds for tissue engineering, artificial implants, cyto-compatibility, blood contacting devices, prostheses, ophthalmic devices, antimicrobial and anti-inflammatory surfaces, enteric coatings and functionalization of drugs for targeted drug delivery.

Plasma (ionized gas) the fourth state of matter consists of highly excited atoms, molecules, electrons, ions, UV-Vis radiations, radical species and neutrals. When a sufficient electric field is imposed, gaseous molecules are excited into energetic states and a glow discharge is generated. The high-density of energetically favoured reactive species in the plasma can alter the surface properties of any complex object. The tailoring/functionalization of the surfaces are limited to few tens of nanometers and hence bulk properties remain intact. Plasma surface modification is usually a reliable, reproducible and relatively inexpensive technique which is applicable to different sample structures and can be used practically for all types of materials like metals, polymers, textiles, ceramics, and composite (Sioshansi and Tobin 1996; Ratner 1993; Picraux and Pope 1984; Bhat et al. 2011; Deshmukh and Bhat 2011; Bhat and Deshmukh 2014; Mendhe et al. 2016). By controlling plasma parameters, a precise control and reproducibility in surface properties can be obtained. This can be achieved quite perfectly using in situ plasma diagnostic devices. By selecting suitable gases and/or monomer vapours, hydrophobic surfaces can be rendered to hydrophilic one and vice versa. One can adjust degree of hydrophilicity by selecting proper precursor gas and monomer. A change in surface energy is responsible for the change in wettability of the surfaces. Plasma deposition can result in uniform, conformal and pinhole free coatings with excellent adhesion to the substrate (Szycher and Sioshansi 1990; Arolkar et al. 2016). Plasma processing can provide sterile surfaces (Moreira et al. 2004; Mrad et al. 2013) and can be scaled up easily for industrial production. On the other hand, the applicability of non-plasma techniques for modifying surfaces of materials is limited (Ohl and Schroder 1999); as a result, plasma-surface modification technique is gaining importance in the biomedical field. It is therefore possible to change in continuum the chemical composition and properties such as surface energy, wettability, dyeability, adhesion, hardness, chemical inertness, lubricity, refractive index, and biocompatibility of materials surfaces. Importantly, the degree of modification of a surface by plasma treatment depends on several parameters such as reactor geometry, system pressure, power

applied, duty cycle, electrode geometry and the distance between them, time of treatment, type of gases/monomers and their flow rate, and also the type of polymer used. Regardless of the complexities of these factors, several effects can be broadly identified. Plasma cleaning or etching of substrate surface is one of them. This process involves removal of adsorbed species, contaminant, process aids etc. Hence cleaning of the surface is considered as the first step of plasma processing followed by actual etching/deposition of the material starts. This results in changes in chemical composition of outermost layer, surface morphology, surface properties and wetting behaviour. Surface engineering plays a vital role in biomedical applications. Biomedical material should possess both bio-compatibility and bioactive response. The interaction of surface of materials with living (blood, cells and bacteria) systems is a complex phenomenon and depends on numerous factors such as chemical composition of the surface, morphology and tribological properties etc. (Gupta and Gupta 2005; Jayagopal et al. 2008). This renders the pursuit of distinct material which meets the necessity of biocompatibility, cell adhesion, growth, proliferation and longlasting in vivo stability. To a great extent non-thermal (low temperature) plasma technology has proved that it can dramatically change the surface properties of the polymeric materials without altering their bulk properties (Dixon and Meenan 2012; Sanchis et al. 2006; Deynse et al. 2014; Noeske et al. 2004; Khorasani et al. 2008; Li and Chen 2006; Chen et al. 2008; Deshmukh and Shetty 2007a; Pandiyaraj et al. 2009; Bhowmik et al. 2004; Ou et al. 2010; Pappas et al. 2008; Sarani et al. 2011) and improve blood compatibility.

Plasma treatment of biomaterials requires less energy than equivalent conventional treatments. Chemical wet processing have drawbacks that thus require an additional step of effluent water treatment before it is discharged and the chemical treatment is non uniform. Secondly, remaining traces of used chemicals may be unsafe in respect of their application in bio-medical industry. Gaseous plasma treatment is highly surface specific and it does not affect the bulk properties of the material. Since no wet chemistry is involved, it is considered as an environment friendly approach that does not produce any waste/load on the environment. At present various types of biomaterials including metals, polymers, composites and ceramics are employed for biomedical engineering applications. In tissue engineering, biomaterials with suitable surface properties are required for better interaction of cells followed by tissue regeneration. The biological response of the living tissues towards biomaterials is governed by the surface properties like chemical composition, texture and surface energy. These materials entail unique methods of surface modification and impersonate tissue-microenvironment. Bio-integration is an ideal outcome expected from any artificial implant, scaffolds, and tissue culture surfaces. This implies the phenomena that occur at the interface between the implant and host tissues which do not generate harmful effects such as formation of unusual tissue, chronic inflammatory response and toxicity. Hence, it is very important to design and fabricate biomaterials used in implants with the specific surface properties. In addition, these biomaterials must possess suitable bulk properties in order to function properly in a bio-environment. A suitable approach is to fabricate biomaterials with desired bulk properties followed by a preferential treatment to

enhance the surface properties. In a way, we can create an ideal biomaterial with selective surface properties that are decoupled from the original/innate bulk properties. For instance, by modifying the surface functionality using thin film deposition, an optimal surface with physical, morphological and chemical properties can be attained. This technology is growing by leaps and bound to improve biocompatibility, multifunctionality and tribological properties of artificial devices. This averts the needs of high costs and long span to develop totally new material. In the biomedical context, 'good biocompatibility' refers to a prosthesis or biomaterial device that is non-inflammatory, non-toxic, does all the functions properly for which they have been made for, and should posses reasonable lifetime. For example, orthopaedic prostheses are made harder and more wear and tear resistant by exposing them to ion implantation. Orthodontic appliances, venous catheters and surgical instruments are treated to enhance friction and fretting resistance and also biocompatibility. To make wear-resistant biomedical components, they require coatings that should be exceptionally hard, which provide low friction and should be biocompatible. Diamond like carbon (DLC) coatings have improved these properties and prevent leaching of metallic ions into the body (Dearnaley and Arps 2005). There are several ways to offer such coatings from carbonaceous precursors, and also other elements such as titanium or silver nano-particles for imparting antimicrobial properties. Ion implantation of Ca^{+} on the Ti alloy surface for bone adhesion control is carried out on orthopaedic hip and dental implants. Also an artificial blood vessel requires ion implantation on polymeric surface for non-thrombogenicity of endothelial cell adhesion (Inoue et al. 1997). Plasma processing has also gained importance in sterilization of biomaterials as it operates near room temperature and comparatively faster than autoclaving and ethylene oxide based treatments. Plasma processing showed its potential application in enteric coating (Timmons et al. 2011), functionalization of drug for targeted delivery and controlled release (Kwok et al. 1999; Yoshida et al. 2013; Tanaka et al. 2006), fabrication of antimicrobial surfaces (Marciano et al. 2009; Matthes et al. 2013; Weltmann et al. 2008; Pankaj et al. 2014; Zhang et al. 2006a; Ehlbeck et al. 2011; Fricke et al. 2012), and in fabrication of functional polymeric substrate for tissue engineering (Schnabelrauch et al. 2014; Djordjevic et al. 2008; Chen and Su 2011). Some recent reports have described comprehensively the use of atmospheric pressure plasma processing (Park et al. 2012), gas discharge plasma (Bogaerts et al. 2002; Selwyn et al. 2001) and various other types of plasma based surface modification techniques for bio-medical applications (Chu et al. 2002; Geyter et al. 2014).

Low temperature plasma treatments are set to revolutionize biomedical materials industries. Currently low temperature plasma technology has found its way in biomedical field as a proven technique for surface modification of biomaterials. Gaseous plasma has been known for several decades, although, the commercial interest was begun only after the introduction of equipment's to produce plasmas on an industrial scale. This chapter deals with the potentiality and applicability of plasma assisted techniques to improve the bioactivity of polymeric surfaces by appropriate surface treatment using non-thermal plasma methods.

2 Classification of Plasma

Classification of plasma can be done on the basis of temperature, pressure and the source used. When the temperature of entire gas is high it is termed as "hot plasma". Due to incessant collisions, the temperature of electrons and ions/molecules gets raised and thus the whole system is in local thermodynamic equilibrium (LTE). Hot plasmas have thermal equilibrium with temperature in the order of 1000 K. Therefore, hot plasmas are not suitable for surface modification of biomaterials particularly, polymers. Such plasma is used for cutting, welding, fusion, etc. On the other hand, "cold plasma" is in non-equilibrium state and although the temperature of electrons is high, the system remains cold (Roth 2001a). The electrons in the cold plasma have energies in the range of 0.1–10 eV which is much higher than the energies of ions and molecules in their non-equilibrium state. The temperature of cold plasma is near room temperature, and hence it can be used for the surface modification of biomaterials. Low temperature plasma (LTP) has an advantage over thermal plasma as it can be applied to heat sensitive materials like polymers. Such cold plasma is commonly used in neon sign boards and fluorescent lamps. LTP can also be used in applications of textiles and plastic industries. Plasma can be induced by applying electric field of low frequency (50–500 kHz), radiofrequency (RF) (13.56 MHz) or microwave (915 MHz or 2450 MHz). Wherein, the electric field may be applied in the form of direct current (DC) or pulsed-DC (PDC). Plasma can also be classified on the basis of pressure of the system. When a system is evacuated the gaseous atoms at low pressure can be ionised easily and uniform glow discharge plasma can be created. However creating and maintaining vacuum conditions for large volumes become difficult. Working at atmospheric pressure is advantageous for continuous process at high speeds.

2.1 Atmospheric Pressure Plasmas

Atmospheric pressure plasmas can be classified into three categories: (a) Corona Discharge, (b) Dielectric Barrier Discharge (DBD) and (c) Atmospheric Pressure Glow Discharge (APGD).

(a) *Corona Discharge* It is the oldest type of plasma treatment employed in industries for the modification of polymeric surfaces. It consists of two parallel electrodes with narrow gap ($\sim$1 mm). One of the electrode is cylindrical in shape while other one is a knife shaped. The schematic diagram of a typical corona discharge system is shown in Fig. 1. In this system, a high voltage of 10–15kV is applied between the two electrodes. The intensity of corona discharges is weak which causes inhomogeneous plasma treatments of surface. Thus, it is not preferred for modification of polymer surfaces for biomedical applications. In this case, the density of the plasma species falls drastically from the point of

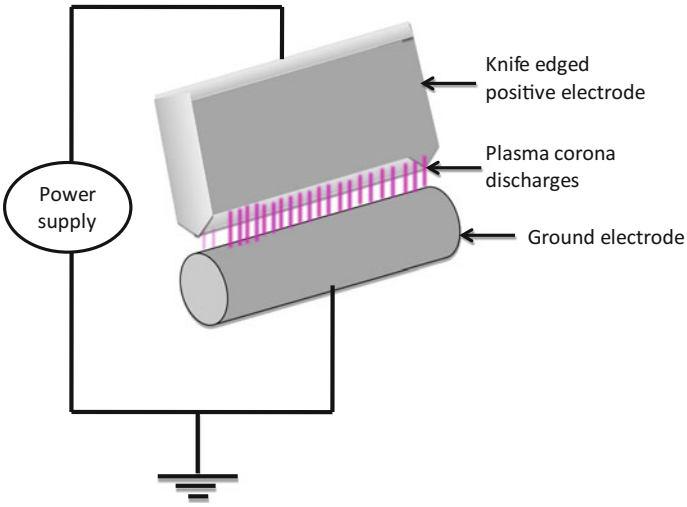

Fig. 1 Schematic representation of corona discharge system

generation to the targeted surface. Therefore, thicker samples cannot be processed by corona discharge.

(b) *Dielectric Barrier Discharge (DBD)* DBD is also known as silent discharge which is driven either via a high frequency alternate current (AC) or radio frequency (RF) source. The main advantage of DBD over other systems is that it can be operated at high pressure operating range (5–10^5 Pa) (Conrads and Schmidt 2000; Schutze et al. 1998). The first DBD system was used by Siemens in 1857 to generate ozone and till date it remains one of the significant industrial applications of DBD (Kogelschatz et al. 1999). In DBD systems, a high potential difference is applied between two parallel plate electrodes which are separated by a narrow gap. In DBD, a sufficiently high AC voltage is applied to the electrodes ($\sim$8 to 20 kV, 500 Hz–500 kHz). DBD cannot be generated by DC voltages due to the requirement of capacitive coupling which needs AC voltage. For preventing the short circuit and arcing between the oppositely charged electrodes, either one or both the electrodes are coated with appropriate dielectric material such as ceramic or glass. Due to this, it is called 'dielectric barrier discharge'. This dielectric layer also prevents electrodes from etching and corrosion. Additionally, the dielectric material also regulates the discharge current, thereby giving rise to a large number of short-lived (nanoseconds) micro-discharges that are dispersed uniformly throughout the electrode (Herbert 2009), thus attaining non-equilibrium plasma conditions. One can achieve a homogeneous treatment condition similar to a typical glow discharge regime by avoiding the streamers (Tendero et al. 2006). DBD is homogeneous as compared to the corona discharge. Depending upon the geometry, generation of DBD can be classified into volume-DBD (VDBD) and

surface-DBD (SDBD). In VDBD, the plasma is generated in volume between two parallel plate electrodes with a dielectric barrier. However, in SDBD, the microdischarge is generated on the surface of the dielectric. This causes more homogenous plasma in SDBD. Moreover, the microdischarge is higher on the surface in SDBD, therefore, the density of plasma is also higher as compared to VDBD. DBD system has one major advantage over other systems, which is the elimination of expensive vacuum systems, thus making it suitable for operation at higher pressure. This leads to lower operating cost and less time consumption, thus, allowing their execution in industrial surface modification process. The low heat generation at higher pressures concedes for a wide range of applications such as grafting, plasma polymerization, etching, cleaning etc. A typical dielectric barrier discharge (DBD) operating at atmospheric pressure reactor system is shown in Fig. 2.

In particular, DBDs have received more attention as compared to other cold atmospheric pressure plasma (CAP) systems, which is mainly due to easier ignition of stable plasmas and the ease of scaling up of the process (Kogelschatz 2003; Borcia and Brown 2007; Geyter et al. 2009). Considering the advantages of non-equilibrium plasma systems in atmospheric operational mode, DBD process is found to be suitable in biomedical research (Sarra-Bournet et al. 2006). It has been recently shown that it is possible to deposit a thin layer coating with embedded biomolecules using DBD plasma fed with aerosol of biomolecule solutions (Heyse et al. 2008; Ponte et al. 2011). Ponte et al. (2011) deposited organic films using DBD plasma for bio-medical applications. The degree of surface modification by plasma treatments are significantly influenced by the power fed, distance between electrodes and their geometry, working pressure, types of gas/monomer and their flow rate, process

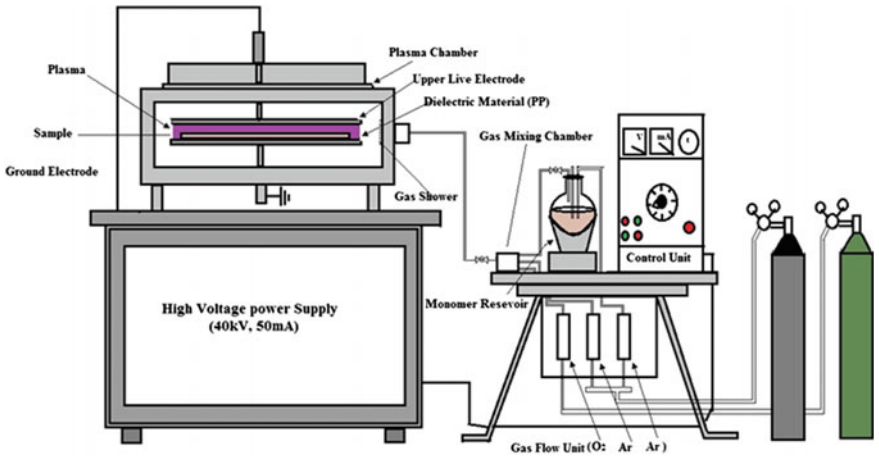

Fig. 2 Schematic of cold atmospheric plasma assisted dielectric barrier discharge (DBD) system. (Reproduce with permission from Pandiyaraj et al. 2016c)

time, and type of plasma. For example, the argon-plasma treatment shows effective etching than the air-plasma treatment.

(c) *Atmospheric Pressure Glow Discharge (APGD)* APGD is generated by applying relatively low voltages across symmetrical electrodes at high frequency (MHz) as compared with DBD. Electrodes are bare in APGD which gives higher electron densities ($\sim 10^{12}$). However, sometimes in APGD system, one of the electrodes is covered with a dielectric barrier to prevent arcing. Plasma is homogenous across the electrodes and gives one current pulse for every half cycle. Two parallel plate electrodes are connected with an RF power supply, separated by few millimetres. Hence, APGD is relatively uniform and stable as compared with DBD plasma. APGD has many advantages over DBD. Helium (He) is the preferred gas in APGD (Roth 2001b; Alexandrov 2009). Therefore, use of helium for commercial scale processing makes it costly, unless helium is significantly recovered. Roth et al. (2000) have developed a remote exposure reactor (RER) operating at atmospheric pressure using radio frequency source with electrode spacing of 2 mm. They have used He and air gases for sterilizing polypropylene (PP) fabric samples. Medical plastics treated with atmospheric-pressure plasma of He + O_2 showed increased surface oxygen moeties and hydrophilic polar groups onto the surface. This led to increased surface energy and improved bonding strength as a function of plasma treatment time (Guschl et al. 2008).

(d) *Atmospheric Pressure Plasma Jet (APPJ)* In general, plasma processing has advantages over other techniques to induce physico-chemical changes on the surface, however at times there are circumstances where it would be more appropriate if the plasma could be free of any restrictions. In this background, atmospheric pressure plasma jet (APPJ) is a very novel approach for surface modification, wherein plasma flux is expelled from the nozzle on to the substrate surface as shown in Fig. 3.

This technique provides flexibility of plasma modification to any object irrespective of its geometrical shape and size. In APPJ, the electron temperature is much higher than the gas temperature and therefore it has gained special interest in biomedical applications. The surface chemistry of a material is modified due to the electrons at high temperature, while the low gas temperature makes it suitable for thermally unstable materials. APPJ can produce uniform plasma plumes in the ambient air without the need of expensive vacuum system. APPJ can be operated with any of the sources like direct current (Zhu and Lopez 2012; Bussiahn et al. 2010), pulse excitation (Liu et al. 2011; Walsh and Kong 2007; Joh et al. 2012; Janda et al. 2011), radio frequency (Kim et al. 2007) and microwave (Arnoult et al. 2008). They could generate a desirable length of plasma plumes in the air. Unfortunately, the mainstream of APPJ is too narrow. The plasma produced using above sources has to deal with a common issue like, the transformation from glow to arc. This can be attained by using the resistive barrier discharge or by employing a hollow cathode discharge with sub-mm dimension in the case of DC sources. The dielectric barrier itself is the key in the DBD systems driven by higher frequency

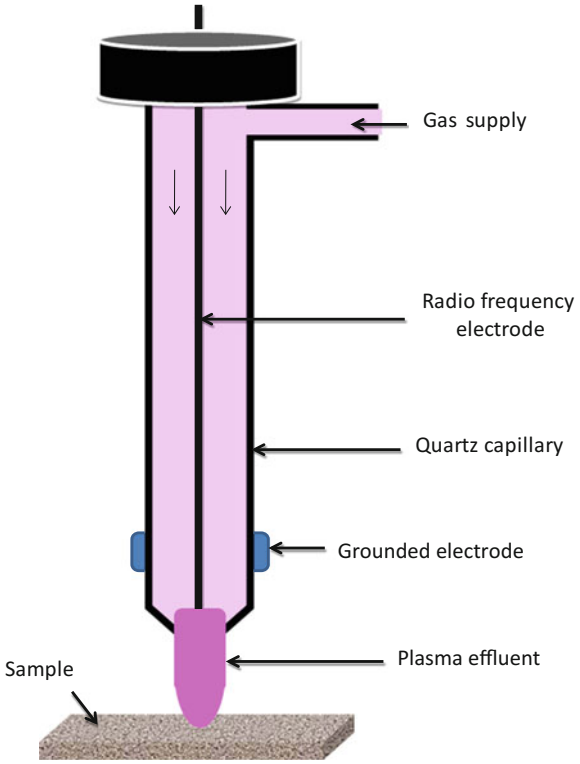

Fig. 3 Schematic of atmospheric pressure plasma jet (APPJ)

AC sources as it inhibits the discharge current to increase at the point of arcing. The DBDs can produce uniformly diffused plasma under specific circumstances which is filament free. For APPJ systems powered with RF, either metal electrodes are left bare or a set-up similar to the DBD can be used. In order to minimize the risk of arcing (due to thermionic emission), the cooling of electrode is necessary and the flow rate needs to be controlled too (Laroussi and Akan 2007). Conclusively, it is possible to produce plasma plumes using microwave which were constrained using a set of geometrical parameters and it has been explained by Park et al. (2003).

2.2 Low Pressure Plasma Processing

This method requires enclosed system connected to a suitable vacuum pump for creating low pressures in the system. Therefore, it can be used for batch processing. Low pressure plasma can be generated by applying A.C. or D.C. field. In A.C. high

frequency R.F. (13.56 MHz) is widely used. The inactivation of bacterial spores on stainless steel screws using low pressure plasma is given by Stapelmann et al. (2013).

(a) *Radio Frequency and Microwave Discharges* High frequency electromagnetic fields are used to produce radiofrequency (RF) and microwave discharges (Conrads and Schmidt 2000; Schutze et al. 1998; Hopwood 1992). RF discharges can be produced moderately in a wide range of frequencies between 1–100 MHz, but in most cases they are operated at a fixed frequency of 13.56 MHz. When compared to DC discharges, RF can be operated over a wide range of pressures (1–10^3 Pa). It is the most liable applied discharge systems that are commercially available and exclusively used for the surface modification of biomedical materials. Microwave discharges are operated at high frequency range, typically 2.45 GHz is fixed. When compared to RF and DC discharges, the pressure is more versatile with a range between 1 and 10^5 Pa. Since, it is operated at high pressure which leads to an increase in temperature of electrodes, the heat is inturn transferred to the substrate thus making it less viable for the treatment of thermally unstable materials such as polymers.

(b) *DC glow discharge* DC glow discharge is one of the most significant methods of producing low temperature (non-thermal) plasmas. In this type, DC discharge is formed between two electrodes at very low pressures (10^{-1}–10 Pa) (Conrads and Schmidt 2000; Schutze et al. 1998). Various types of discharges can be produced by suitable current amplification. When a proper glow discharge is generated, current starts flowing through the ionized gas which results in a voltage drop across the regime. Glow discharge is the preferred technique for surface modification, since it assures a homogeneous treatment all over the reactor. DC glow discharge is a well established technique with good control over different operating parameters and the process. In this process, the DC current can be applied either in a continuous or pulsed manner. Sometimes water cooled electrodes are also used for heat dissipation to avoid thermal damage of polymeric material during longer durations of plasma treatment. The other way of avoiding heating of electrodes is to operate DC glow discharge in pulsed mode. One of the major drawbacks of the DC driven systems is the etching and corrosion of electrode when it is directly exposed to certain reactive monomers under plasma environment. Figure 4 shows the schematic diagram of DC glow discharge plasma system.

Low pressure and atmospheric pressure plasma treatments have their merits and demerits. Therefore, final selection of the process is dictated by the extent of surface modification and the requirement of the process speed. Low pressure plasma system (LPPS) is equipped with a pumping unit, which consumes high electrical energy than atmospheric pressure plasma system (APPS). However, LPPS require less power to generate and sustain glow discharge in comparison to APPS. On the contrary, LPPS consumes fewer amounts of gases/monomer(s), which is important for the applications involving the use of expensive gases/monomers. The surface modifications achieved by LPPS are more uniform and have better control as

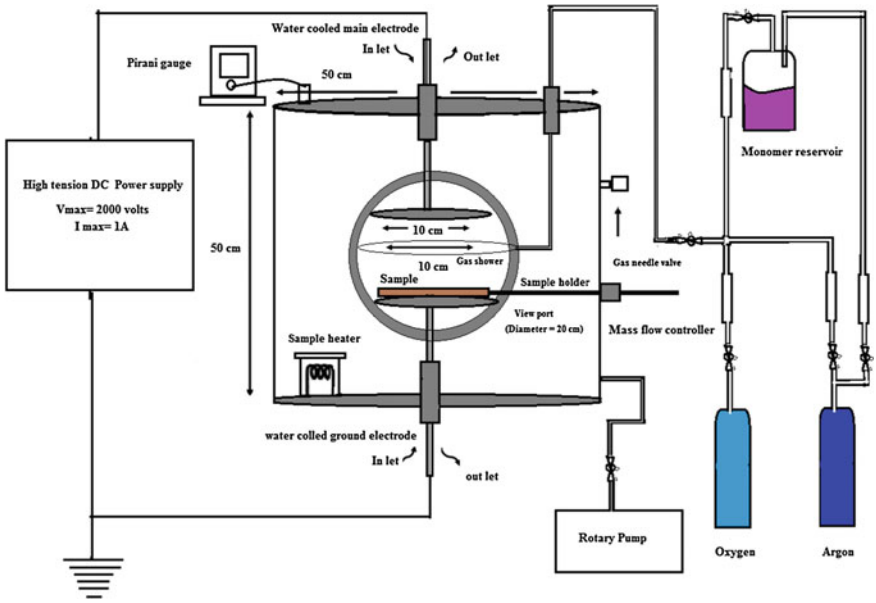

Fig. 4 Schematic experimental set up of DC glow discharge plasma system. (Reproduced with permission from Pandiyaraj et al. 2014b)

compared to APPS. The advantage of APPS is that it can be utilized as a part of continuous process (preferred in industry), whereas LPPS is restricted by batch to batch processing.

It has been found that the improvement in hydrophilicity/wettability obtained by gaseous plasma treatment changes with storage time. This phenomenon is referred as ageing, which takes place possibly due to surface contamination, blooming of additives, orientation of polar groups and absorption of ubiquitous contaminants (Deshmukh and Shetty 2007a). For various applications it is necessary to convert hydrophobic polymer into hydrophilic one by suitable surface modification technique and in ambient storage conditions, a driving force exists to restore the original structure or decrease the surface energy (SE) of the treated surface. This results in loss of high energy polar functional groups. It is has been shown that the hydrophobic recovery depends on treatment time and the type of polymer (Morra et al. 1989). Thus ageing can be considered as one of the steps of the treatment in the sense that it influences the outcome as determined by the properties imparted to the polymer surface. Though there is a decrease in surface energy because of ageing, it is clear from our previous studies that the surface energy value of aged samples is still adequately high as compared with the untreated one. Therefore such treated polymer surfaces can be considered suitable for further applications (Deshmukh and Shetty 2007a; Bhat et al. 2003). The optimum plasma parameters (treatment time and power) should be decided on the basis of hydrophobic recovery

(ageing) pattern of plasma processed material (Mendhe et al. 2016). In order to avoid the adverse effect of ageing, it is advisable to use freshly prepared (gaseous plasma processed) samples for better results. However, plasma surface grafted polymers and plasma polymerized films do not show much decrease in SE values and the modifications thus obtained are comparatively permanent. The processes of plasma grafting and plasma polymerization are discussed in detailed in the Sects. 3.4 and 3.5 of this chapter.

2.3 *Plasma Immersion Ion Implantation*

Plasma immersion ion implantation (PIII) process is useful and suitable for irregular shaped target materials irrespective of processing or implantation time, biasing, configurations and density of plasma. PIII system comprises of a vacuum chamber with a stage, source and high-voltage pulse modulator as shown in Fig. 5. In PIII processing, workpiece (sample) is kept in the plasma region. The sample is connected to a pulsed high negative voltage. The negative ions are repelled from the workpiece because the positive ions are directed towards it from plasma source that induces a sheath around the workpiece (Anders 2000). In PIII, ions are accelerated towards a target biomaterial surface using accelerating bias voltage in the range of 20–200 kV. The ion implantation creates significant changes on the surface,

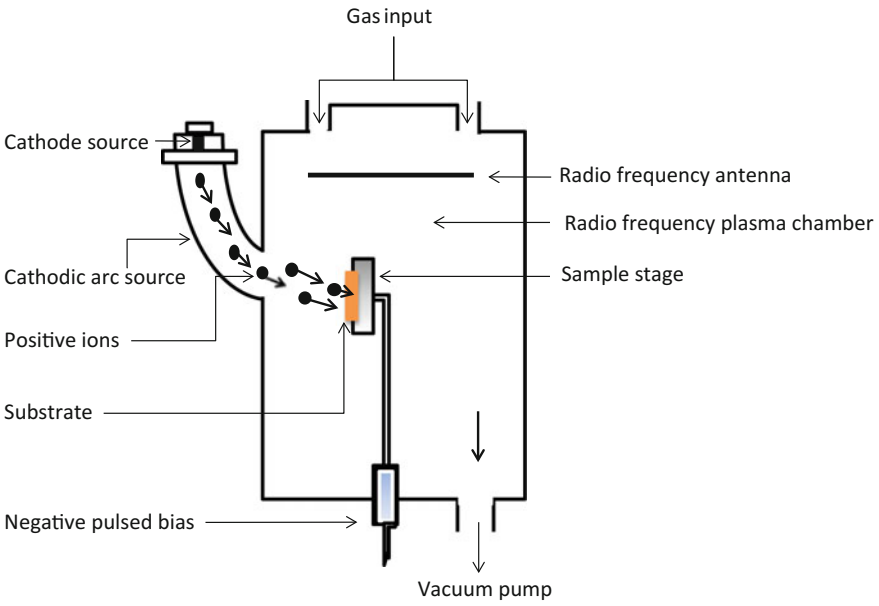

Fig. 5 Schematic representation of plasma immersion ion implantation system

although, modification is confined to the near-surface region due to limited penetration power of the ions ($\sim$1 μm), this results in only the surface properties getting modified.

The substrate biasing is done commonly on DC, Pulsing or RF modes. Thin film structuring and rates of deposition by reactants can be controlled by varying biasing and working pressure in the system (Harper et al. 1984; Bunshah 1994; Mattox 1989; Ensinger 1992). Ion implantation effect is different for different materials such as metals, ceramics, and polymers (Dearnaley and Hartley 1978; Venkatesan 1985). The physical changes in metal and ceramic biomaterials, arises due to atomic and nuclear collisions which often leads to the formation of highly disordered to more amorphous structures at the surface. The chemical and physical changes due to PIII process combine to create surfaces harder and more resistant to chemical attack and wear without compromising the material bulk properties. Several effects have been witnessed and in numerous ways they are analogous to those produced by collective ionizing radiation. The limited depth of penetration in PIII process due to large ion size results in pronounced effects confined to a very thin layer underneath the surface. In spite of many complex effects, in PIII two major competing processes occur: (1) chain scission, and (2) cross-linking. When the sample is exposed to ion implantation process, it interact with the substrate polymer atoms via electronic (ionization) and nuclear (recoil) interactions. Ionization leads to cross-linking in adjacent polymer chains, whereas recoil leads to chain scission (Lee et al. 1994). The cross-linking usually improves the polymer properties while chain scission may cause polymer degradation. By adjusting implantation parameters suitably, a three dimensional (3D) cross-linked surface layer can be created with hardness better that of steel along with improved wear resistance (Lee et al. 1993). Selective reduction or enhancement of chemical functional groups results in changing the chemical interactions on the polymer surface, which changes critical surface tension, degree of hydrophilicity/hydrophobicity.

Bioinertness in biomaterials such as titanium, silicons, etc. is another issue needed to address and solve by using this process in increasing their bioavailability by plasma ion implantation of elements like hydrogen, sodium, calcium, etc. Impinging hydrogen on the surface of silicon and nano-TiO_2 gives outstanding bioactivity through PIII process. Hydroxyl groups are produced on the surface that makes them more acceptable. The same can be done for excellent bioactivity of titanium through Ca/Na plasma immersion ion implantation deposition (PIIID). In PIII process energetic C, N, and O ions are embedded into the alloy surface to form a graded surface barrier layer of carbide, nitride, or oxide. In PIIID process the stable Ti–C, Ti–N, and Ti–O bonds are formed on alloy surface, which results in Ni depleted surface region. The depletion in nickel results in improved mechanical properties. Diamond like coating (DLC) and TiO_2 thin films can be made possible for blood compatible biomedical devices used in human body (Chen et al. 2002). PIIID process makes it possible by doping its surface with elements like Ca or P. Likewise antimicrobial properties can also be achieved through PIIID process by dual implantation method of reagent plasma of Cu/N_2 on polyethylene (PE) surfaces to yield excellent release rates and prolonged antibacterial properties. After thorough

understanding of PIIID process and applications, it has established it as a very promising and versatile technique in biomedical and biomaterials application. Micro/nano structuring of surfaces has enabled us to refine our view in bio responses to such surfaces.

3 Processes of Plasma Surface Modification

In order to use plasma for any applications, from surface engineering to biomedical, it is essential to understand the interactions of plasma with the substrate. Bombardment of ions, electrons and high energy neutrals take place on the surface and interactions are very complex. This results in the alteration of surface chemistry and topography, which provides various advantages in materials processing for their applications (Table 1). In the case of plasma processing using non-polymerising/polymerizing gases, mainly four types of phenomena takes place (a) surface cleaning (removal of contaminants), (b) etching or ablation of surface, (c) modification of surface chemical composition and (d) chemical functionalization (crosslinking) of the surface (Yasuda 1985; Clark et al. 1978).

Table 1 Advantages of plasma processes in biomaterials applications

Advantages of plasma surface modification
Easy sample preparation
Generate unique surface chemistry
Coating on various substrates with excellent adhesion
Conformal and pin-hole free films
Excellent barrier properties with low level of leaching
Sterilization and decontamination upon processing
Increase surface charge
Micro/nano patterning of scaffolds for tissue engineering
Improve cytocompatibility and bioavailability
Superior wear and tear properties
Increase surface energy
Offers surface cross-linking
Specific functional groups can be incorporated
Change in degree of hydrophilicity or hydrophobicity
Improved bio-sensing

3.1 Plasma Surface Cleaning

The first step of plasma processing is cleaning of surfaces. Interaction of energetic plasma species causes removal of low molecular weight contaminants such as oligomers, additives, loosely bound material, substrate residuals, ubiquitous contaminants, processing aids, adsorbed species, grease, and dirt which is also referred as "plasma cleaning" (Deshmukh and Shetty 2007a). Biomaterials are prone to attract various types of contaminants, solvents and volatile components during the process of manufacturing and storage. Adsorbed contaminants can may get accumulated on the material surfaces which resulting in altering the surface of the material and reducing the product performance. Low temperature plasma can remove any volatile surface contaminations in a few seconds when it is exposed to it (Cools et al. 2014). However, when the material is exposed to plasma for a very long time, plasma will not only remove the surface contaminants but also etches the top layer of the material (Fracassi et al. 1996; Lee et al. 1996).

3.2 Plasma Etching/Ablation

After plasma cleaning, ablation or etching of the surface begins. Ablation is the physical removal of material from the surface by the action of plasma. The surface of polymer/textile under plasma treatment of reactive or non-reactive gases literally etched or scraped out. Plasma etching comprises the interaction of high energetic plasma species with the material surface to produce volatile products and the etched material is then vapourized or pumped out of the plasma chamber as effluent gas. The second possibility is that the ablated material may be re-deposited as plasma polymer at different locations (Bhat and Wavhal 2000a). The etching can be improved by biasing the substrate stage that can cause precise targeting to bombard specific plasma species (ions/electrons) on the substrate surface. This is also useful for customized patterning. Plasma ablation of materials takes place through two principal processes i.e., physical sputtering and chemical etching. The removal of materials from the surface by chemically non-reactive gaseous plasma, such as argon (Ar) plasma, is a typical example of physical sputtering, which is essentially a momentum-exchange process. The energy of the impinging Ar+ is transferred to the colliding atom and the atom is knocked out from the structure and goes into the vapour phase. On the other hand, gaseous plasma produced using chemically reactive vapors/gases results in chemical etching. It involves chemical reaction of impinging species with the substrate such as oxidation by O_2 plasma. This type of plasma gas includes organic and inorganic molecular gases, such as O_2, N_2 and CF_4. When reactive but non-polymerizable gases (like O_2, N_2, NH_3, CF_4) are used to form plasma, functionalization of polymer surface takes place along with etching. Argon is a preferred inert gas for plasma surface cleaning and etching of materials because it is easily available, relatively low cost and gives a high etching yield.

Argon plasma may be generated by RF glow discharge (RFGD) or atmospheric pressure glow discharge (APGD). Applied electric field accelerates ions towards the substrate. However, the energy of Ar ions is not very high and hence they cannot go deep into the substrate. A major portion of their energy is transferred to the substrate atoms via elastic and inelastic collisions. In this process some surface atoms acquire sufficient energy to escape from the substrate into the vacuum chamber and subsequently pumped out. This is how gradual etching (ablation) occurs.

During etching weight loss of the material is observed which strongly depends upon the type of polymer and the plasma energy. Therefore, ablation can be monitored and reported in terms of weight loss of the material. Chain scission, rupturing of bonds, removal of loosely bound (mostly amorphous) material takes place during ablation. In general polymers are semicrystalline in nature where crystalline zones (regions) are more compact and tightly bound as compared to amorphous regions. Therefore, predominantly amorphous region gets degraded and etched away in the initial stage of etching (Bhat and Deshmukh 2002; Thomas et al. 1998; Yoon et al. 1996). This results in relative increase in surface crystallinity to some extent. This has been established by previous studies using Fourier transform infrared (FTIR) and X-ray diffraction (XRD) for silk biomaterial (Bhat and Nadiger 1978). Pandiyaraj and Selvarajan (2008) have also confirmed that the effect of plasma on the amorphous region is more as compared to the crystalline region of the cotton fabrics. In general, polymers having oxygen groups in backbone or side chains are more prone to etching than polyolefins. For example, under the same plasma conditions of plasma treatment, polyethylene terephthalate (PET) is more susceptible to etching than polypropylene (PP) (Radu et al. 2000).

Formation of free radicals and effective surface area increase during the ablation process. It enhances certain properties of the materials like, wettability, surface energy, surface roughness, biocompatibility and cytocompatibility (Deshmukh and Bhat 2003; Yoshida et al. 2013; Ohl and Schroder 1999; Wintermantel et al. 1996). Plasma etching can effectively increase the surface area for contact by roughening the surface. The modification in surface morphology can have a positive effect, as it can enhance the cell adhesion, growth and proliferation especially for in vitro and in vivo applications (Washburn et al. 2004; Khorasani et al. 2008). In most of the plasma surface modification techniques for bio-medical applications, argon plasma treatment is considered as a pre-treatment for subsequent reactive gaseous plasma treatment and deposition. Active species generated in the plasma cause etching to form volatile products which create the desirable micro and macro-features on the biomaterials surface to meet the desired biocompatibility in vivo.

3.3 Surface Functionalization Using Reactive Gases

After surface cleaning and limited etching by argon plasma treatment, a polymer is subjected to a reactive gaseous plasma treatment. At this stage, oxygen, air,

nitrogen, ammonia, or mixture of these gases with argon maybe used (Pandiyaraj et al. 2016a, b, 2015). The reactive gaseous plasma treatment allows incorporation of polar groups (e.g. oxygen containing moieties) onto the surface. These polar groups are responsible for the enhancement in surface energy. Gupta et al. have observed incorporation of oxygen containing polar functional groups on the surface of PET when exposed to argon plasma treatment at 80 W for different durations up to 100 s (Gupta et al. 2000). They have further showed that the post plasma exposure of the sample to the oxygen/atmospheric air incorporates oxygen containing functional groups. In this context, Pandiyaraj et al. have treated polypropylene (PP) in APGD argon plasma and have observed incorporation of polar functional groups on to the film surface (Pandiyaraj et al. 2016c). However, argon plasma treatment followed by oxygen plasma treatment is preferred to incorporate various functional groups such as OH, C=O, O–C=O, COOH etc., onto the substrate polymer. Further such functionalized surfaces form covalent bonding with the deposited layer (Pandiyaraj et al. 2015). These functional groups affect the surface properties of the material such as wettability, surface free energy and also the surface roughness (Cui and Brown 2002), and also enhance the material-material and material-cell interactions (Pandiyaraj et al. 2016a). The increase in hydrophilicity of the material can improve the performance. Besides, in specific applications of biomaterial like artificial stents or heart valves, adhesion of cells and proteins on the surface is very redundant, as it may lead to unwanted growth of tissue resulting in blockage and failure of the device. Commonly, fluorine containing monomers are used to make surface hydrophobic. Tanaka et al. (2006) have used CF_4 and C_3F_6 monomer precursors to make the surface of PLGA microcapsule super hydrophobic for controlled release of drug by APGD treatment.

3.4 Plasma Polymerization/Deposition

Plasma processing of polymeric materials may be classified in three groups (i) chemically non-reactive plasma, (ii) chemically reactive plasma and (iii) polymer forming plasma. The first two types are explained in the Sects. 3.2 and 3.3 as they are responsible for physical sputtering and chemical etching. The third type uses energetic plasma species (like, ions, electrons and radicals), which cause the transformation of monomers (low-molecular weight molecules) into polymers (high-molecular weight molecules) on the material surface. Interestingly, it has been found that most of the organic vapours, which do not polymerize by conventional polymerization technique, can be polymerized using plasma. Conventionally non polymerizable hydrocarbons such as benzene, acetylene, ethylene, ethane and methane can be polymerized using plasma for the synthesis of hydrogenated carbon films. In many cases, chemical and physical structures of plasma polymers are different than those of the conventional polymers, even if the same precursor monomers are used. Plasma can be generated using various organic or inorganic

monomer vapours capable of polymerization. Deposition occurs when the impinging species fails to bounce back from the colliding surface resulting in loss of kinetic energy and formation of chemical bond with the substrate. There are several factors affecting the deposition rate, for example, type of monomer, flow rate of monomers/gases, spacing between the electrodes and their geometry, power, working pressure and position of the substrate in the plasma chamber (Hollahan and Bell 1984). Unlike conventional polymers, plasma polymers do not contain repeating monomer units rather have complicated units that are highly cross-linked and fragmented units. Plasma polymers strongly adhere to the substrate polymer film due to covalent bonding and have higher elastic modulus. They do not show distinct glass transition temperature (T_g).

Plasma polymerization is a complex and wild reaction; hence it is not well understood. However, it is believed that the plasma polymerization involve two simultaneous processes i.e. (a) ablation which leads to the removal of material from the surface and (b) polymer formations due to the continuous deposition of monomers on surface of substrate. When monomer vapours (polymerizable gases) are passed into the plasma regime, competitive ablation and polymerization (CAP) take place. If the deposition is predominant over etching/ablation, a weight gain is observed (Bhat and Deshmukh 2014). The interaction of these two opposite processes and their co-existence in plasma is well known (Yasuda and Hsu 1978). Schematic representation of competitive ablation and polymerization, chain scission, free radical formation is shown in Fig. 6.

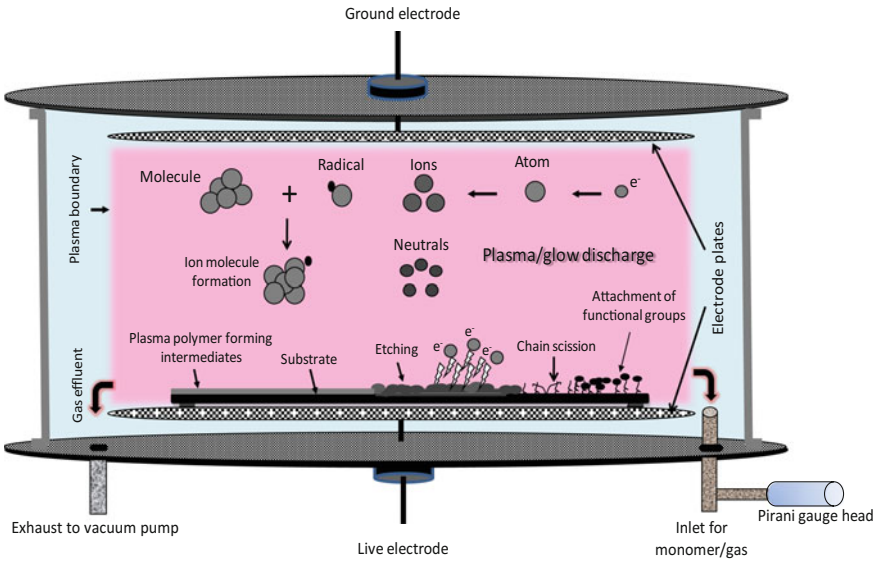

Fig. 6 Schematic representation of competitive ablation and polymerization (CAP) process in plasma state

Plasma induced polymerization and polymer-state polymerisation co-exists during the treatment. The formation of polymer mainly occurs under the influence of plasma i.e. via plasma-state polymerization. However, plasma-induced polymerization represents the polymerization of condensable monomer on the substrate. Plasma ablation competes with the polymer formation (deposition) in almost all the cases when plasma is used to treat the surfaces of solid materials (Shijian et al. 2002). Since etching and deposition occur simultaneously in plasma environment, it is very challenging to determine the absolute deposition rate on the substrate polymer. Deshmukh and Shetty (2007b) have studied the percentage weight gain of plasma polymerized hexamethyldisiloxane (PPHMDS) and plasma polymerized tetraethylorthosilicate (PPTEOS) deposited on PE films for various durations. They have observed increase in percentage weight of material by increasing the processing time, which suggested that the rate of deposition was higher than etching.

Several plasma polymers have been fabricated using organo-silicon monomers like, tetra ethyl orthosilicate (TEOS), tetra methyl orthosilicate (TMOS) and Hexamethyl disiloxane (HMDSO), which have shown excellent chemical and thermal resistance and outstanding optical, electrical and biomedical applicability (Boekema et al. 2013; Boekema et al. 2016; Hsu et al. 2012; Gubala et al. 2010; Deshmukh and Shetty 2007a; Arolkar et al. 2016). Timmons and Griggs (2004) have demonstrated that retention of specific functional groups from the monomer to a large extent is possible by controlling duty cycle in pulsed plasma polymerization. Bhattacharyya et al. (2010) and Xu et al. (2011) have demonstrated the applicability of pulsed plasma polymerization technique for controlling film chemistry and have found that it is very useful in biological applications. Dhayal et al. (2003) have carried out after glow plasma polymerization, to avoid simultaneous etching or ablation and fragmentation of monomer during polymerization. Ideally, modification of the outermost molecular layer should be enough to minimize the functional and mechanical properties of the materials and risks delamination. However, some coatings inherently have a specific thickness (Ratner et al. 1996), which ensures uniform coverage, protection against surface reversal and mechanical erosion. Plasma processing has advantages over other coating technologies as one can deposit a very thin (near to molecular level), uniform, conformal and pinhole free layer that can strongly adhered covalently to the variety of substrates like polymer, glass, ceramics, nanoparticles, alloys and metal surfaces (Arefi et al. 1992; Clark et al. 1978; Bhat and Wavhal 2000b). High cohesive and adhesive properties make them more resistant to leaching/delamination.

Dual plasma deposition is an extended approach that provides advantage of producing thin films consisting multi-elements with desirable functional properties (Chu et al. 2002). For example, nano composites of autocatalytic nature like titanium oxide (TiO_2), materials of optoelectronic nature like zinc oxide (ZnO), electronic applications like aluminium nitride (AlN), hard coating using titanium nitride (TiN) and metal doped with diamond like coating (DLC) have been synthesized. In this technique, metal and gas plasmas are simultaneously generated typically using a vacuum arc plasma source and a RF glow discharge source,

respectively. Since a metal vacuum arc plasma source is generally operated in a pulsing mode, the adatoms have sufficient time to diffuse and relax.

3.5 Plasma-Graft Polymerization

Tethering of functional moieties on to the material surface provide specific and selective functionality, which can be used to make material attractive or resistive for targeted application. In plasma-induced graft polymerisation, reactive and non-reactive gaseous plasma induces bond abstraction (breaking) and chain scissioning on the surface of material resulting in the formation of free radicals on the surface (Bhat et al. 2003; Pandiyaraj et al. 2009). These radicals initiate polymerization reactions when contacted with monomers in the liquid or vapour phase. As a result, a thin layer of grafted polymer is formed on the substrate polymer. Plasma induced graft polymerization is different from plasma polymerization; in the latter the plasma gas itself is a monomer (Gomathi et al. 2008). Plasma-graft polymerization is often used to alter the surface chemical composition by tethering the desired biomolecules for biomedical applications. Frankenberg-Schwager and Frankenberg (1990) have modified PET surface by plasma-induced graft polymerization of acrylic acid. The use of oxygen plasma leads to the formation of polar functionalities such as peroxide and hydroperoxide groups on PET surface and initiated grafting of acrylic acid by decomposition of hydroperoxides at elevated temperature. The result showed increase in grafting by increasing the concentration of acrylic acid, which reaches a maximum and then tends to decrease. It is possible that the higher exposure may lead to the loss of active centers that are otherwise responsible for the peroxidation during exposure to oxygen. Although, the magnitude of peroxidation would depend on the nature of the polymer, availability of adequate oxidative functional moieties for the initiation of the grafting of monomers onto the surface (Nunez et al. 1996; Taucher-Scholz et al. 1995; Müller and Streffer 1991). Grafting of PEO (a non-toxic water-soluble polymer) is extensively used for biomedical applications. PEO resists the adsorption of plasma proteins because of its strong hydrophilicity, chain mobility and lack of ionic charge (Natarajan 2001). The grafting of PEO on polymer surface would result in decreased protein adsorption and platelet adhesion. This versatile nature of PEO has led to many studies not only on the preparation of PEO derived surfaces but also on the subsequent uses of these surfaces as biomaterials (Ritter et al. 1996; Scholz et al. 1998; Durante et al. 1998; Nasonova et al. 2001). In situ and ex situ plasma grafting has been employed to render hydrophobic surfaces into hydrophilic and vice versa, depending upon the graft monomer. Song et al. (2000) used low-temperature plasma technique to graft poly (ethylene glycol) (PEG) onto the hydrophobic polysulfone (PSF) membrane surface to transform it into highly hydrophilic one. Further it was suggested that the plasma-induced surface alteration can alter the performance of a membrane by enhancing surface hydrophilicity and hemocompatibility.

4 Biomaterials and Surface Modification

4.1 Biomaterials

Biomaterial is defined as a natural or synthetic substance that includes part or a whole of living body or a biomedical unit that performs, augments or replaces natural functions of the body tissue. Ratner et al. (1996) defined biomaterial as a nonviable material used in a medical device, intended to interact with a biological system. Biomaterials is an exciting field covering various aspects of chemistry, materials science, biology and medicine that have been steadily and significantly developed over the last five decades. At present, biomaterials are clinically used to repair, reinforce or replace damaged functional parts of the human body, such as bone cement, bone plates, dental implants for tooth fixation, joint replacements, artificial ligaments and tendons, blood vessel prostheses, contact lenses, heart valves, skin adhesives, artificial tissue, breast implants and cardiovascular tubes (Nair and Laurencin 2006). As per the recent report of 'Markets and Markets' (Dec. 2015; report code: BT 1556), the biomaterials market is assumed to reach USD 130.57 Billion by 2020, which is increasing at a compound annual growth rate of 16% during the forecast period of 2015–2020. This report forcasting highest growth in the biomaterials market is expected in the Asia-Pacific region, majorly in India, China, and Japan. However, North America > Europe > Asia-Pacific > rest of the world, are sequenced in order to share the global biomaterials market in descending order. According to Hench (1998) and Leeuwenburgh et al. (2008) biomaterials are expected to improve the regeneration of natural tissues, thereby helping the restoration of functional, structural, metabolic and biomechanical performance as well as biochemical behaviour. It is important that the processes used for production of biomaterials should be simple to carry out, fast and affordable in view of the increasing number of patients who need various implants. Currently many types of biomaterials are used such as ceramics, metals, alloys, glasses, polymers and composites. The design of the above mentioned biomaterials has its own challenges based on their intended application at the biological site. Research in biomaterials is interdisciplinary in nature and therefore, there must be close collaborations among researchers from biochemistry, medicine, physics, materials science and other fields. In spite of promising results, there is an urgent need to develop new kinds of biomaterials with appropriate mechanical properties, durability and functionality (Ratner et al. 1996; Hill 1998; Enderle et al. 1999). For instance, an artificial heart-valve should flex for millions of cycles without failure and should have anti-thrombotic properties; a hemodialyzer must have the required permeability and a prosthetic hip joint should be able to with stand high stress (Enderle et al. 1999). Most of the materials do have suitable bulk properties. However, the biological responses are largely controlled by their surface properties such as surface chemistry, morphology and topography. Therefore we can say that the surface properties play a very important role in the functioning of a biomaterial. Hence, by carrying out suitable surface modification without affecting its mechanical properties and

functionality of the device, the tissue-interface related biocompatibility can be improved (Ratner et al. 1996).

4.2 Necessity of Surface Modification

The interactions of a biomaterial with biological components (like hard and soft tissues, blood and body-fluid) take place at the surface of material, and the biological stimuli triggers from living tissues to these extrinsic biomaterials, depends upon the surface attributes such as surface energy, chemical composition, surface morphology, the tendency to denaturalize neighbouring proteins and corrosion resistance (Pandiyaraj et al. 2016a; Pandiyaraj et al. 2014a; Liefeith et al. 1998; Chen et al. 2000; Zhao et al. 1999). The interactions between the implant and biological system at molecular level determine the biocompatibility of a material (Ohl and Schroder 1999). Besides, the general requirements of biomaterials are their stability, tissue compatibility, non-toxicity and reproducibility (Szycher and Sioshansi 1990). As usual, no single material can have all the required properties and therefore surface modification is usually carried out in order to improve the surface properties of biomaterials.

Durability and longevity are the important parameters for medical implants (Cui and Luo 1999). Metal implants are extensively used in bone replacements, especially for long bone and joint replacements. Metallic orthopaedic implants have desired bulk properties such as wear resistance, strength and elasticity, but relatively inferior poor surface properties. Therefore, it is limiting their application for compromising between the surface and bulk properties. Due to an increasing demand for biomaterials annually, many major medical device companies have recognized plasma technology as one of the principle approach for the surface engineering of biomaterials and the lucrative market (Table 2).

Table 2 General research areas and applications of plasma processing in biomaterials engineering (Chu et al. 2002)

Biomedical areas	Application of plasma processing
Blood-compatible surfaces	Stents, catheters, membranes (e.g. for hemodialysis), Vascular grafts, filters (e.g. for blood cell separation), heart-valves, biomolecules immobilized on surfaces
Non-fouling surfaces	Contact lenses, Intraocular lens (IOLs), catheters, wound healing, biosensors
Tissue engineering and cell culture	Cell growth, analytical assays, vascular grafts, implants, antibody production
Sterilization of devices and surgical tools	Tools of surgeon such as tweezers, scissors, gloves, syringes, various joints and implants
Biosensors	Immobilization of biomolecules on surfaces, protein adhesion
Barrier coatings	Gas-exchange membranes, time sustained release of drugs, pH sensitive drug release, reduction of leaches (e.g. plasticizers catalysts, additives, etc.) corrosion protection, device protection

Inventing totally new materials with desired properties is time consuming; whereas surface modification of existing biomaterials could be more viable and can be achieved in a much shorter time. For example, latest developments in biocompatible surface engineering for cell adhesion and growth are concentrating on tethering the extracellular matrix (ECM) proteins like fibronectin and laminin or amino acid sequences of these proteins on the surface (Ohl and Schroder 1999). Generally, these bioactive molecules are covalently bonded, and plasma treatment has a potential to create these covalent bonds (Moy et al. 1994; Okada and Yoshito 1992; Okada and Ikada 1995; Steele et al. 1994; Steele et al. 1995). In addition, plasma treatment can make highly inert hydrophobic surfaces using fluorine containing monomer/gas precursors. On such hydrophobic surfaces, the covalent bonds of bioactive molecules inhibit cell attachment, whereas the covalent bonds of hydrophilic surfaces can improve the biocompatibility (Beyer et al. 1997; Jansen and Kohnen 1995; Thelen et al. 1995; Favia et al. 1996; Seifert et al. 1997).

5 Effects of Plasma-Surface Modification on Biomaterials

5.1 Tailoring of Surface Morphology

Plasma-induced micro-patterning technique achieved through etching/ablation generates different patterns for different cell types. These microstructured biomaterials have the ability to control cell functions such as proliferation, differentiation and apoptosis (Ito 1999). Kapur et al. (1996) have also indicated that selectively patterned 3-D polymer substrates may be useful in the variety of biomaterial applications. Ha et al. (1997) have modified the surface of polyether-ether-ketone (PEEK) by oxygen plasma treatment or chemical etching. Results have shown that oxygen plasma treatment or chemical etching causes incorporation of polar functional groups (due to decreased contact angle) and increase in surface roughness due to the spherulitic structure of PEEK. They have concluded that surface activation of PEEK by oxygen plasma for biomedical applications has an edge over chemical etching. In other words, the biocompatibility of the PEEK surface is improved due to increase in surface energy by oxygen plasma treatment. Hence, it is suggested that inflammatory cell responses can be controlled to enhance the biocompatibility of medical devices (DeFife et al. 1999).

5.2 Plasma Sterilization

Any process that eliminates all forms of microbial life, including transmissible agents like viruses, bacteria, fungi, etc. from an object (biomaterial) is referred to as sterilization (Marlowe 1997). Materials or devices introduced in vivo and/or used

for in vitro experiments should be sterilized to avert subsequent infection that may lead to morbidity or mortality in vivo and could causes experimental failure in vitro (Andrews et al. 2007; Brígido-Diego et al. 2007). For safety, economical and practical reasons, biomedical devices and surgical instruments are sterilized before their clinical use. New approaches in low-temperature sterilization (especially for thermally instable materials and polymer based devices) and high level disinfection have emerged in the last two decades (Young 1997; Rutala et al. 1998). An overview of low temperature plasma based sterilization is given by Laroussi (2005). Plasma-based sterilization has a number of advantages over conventional sterilization processes. Plasma sterilization has advantages such as it is nontoxic, simple, cost-effective, fast procedure and suitable for online treatment of 3-D structures/workpieces/microstructures/medical instruments (Gadri et al. 2000; Adler et al. 1998). Plasma sterilization has an edge over other traditional sterilization techniques when dealing with thermolabile and thermostable microsurgical instruments, routine surgical instruments like, steel scissors, needles, microstripper, forceps, spatula and trephination devices. Low-pressure radio frequency glow discharge (RFGD) plasma operating normally below 1 Torr has been successfully used to sterilize surfaces. Usually, low temperature low-pressure glow discharge plasma is used in combination with working gas approved by healthcare and medical authority such as hydrogen peroxide, ethylene oxide or para-acetic acid vapour.

Points to be checked while plasma sterilization needs to be done;

1. The temperature of metallic (conducting) objects should not increase by electric field.
2. Avoid the shadowing effect while objects are being sterilized in stacking position (shadowing can reduce the intensity of field above the object closer to the ground plate) which could cause poor exposure of plasma and can lead to reduced or no sterilization of materials.
3. Since the penetration depth of UV radiation is very limited, UV biocide approach for stacked microorganisms is not suitable for thick biofilms results in plasma treatment is limited to surface sterilization.

US Food and Drug Administration (FDA) has approved plasma sterilization systems using two working gases and is commercially available since the early 1990s (Young 1997; Rutala et al. 1998; Vassal et al. 1998). It has been demonstrated that radio frequency and microwave plasmas can annihilate wide range of microorganisms, viruses, and bacteria (The et al. 1996; Gogolewski et al. 1996; Ayhan et al. 1998). It has been proved that plasma sterilization is a microbiologically safe procedure with adequate reduction factors of >6 log (Bialasiewicz et al. 1995). As compared to the other sterilization methods (which uses formaldehyde and ethylene oxide (EtO)), plasma sterilization not only kills the microorganisms, viruses and bacteria but also pumps out the dead organisms from the surface of the materials as this process is similar to plasma etching (Ayhan et al. 1998). Bathina et al. (1998) have demonstrated commercial viability of sterilizing non-lumen electrophysiology

catheters using hydrogen peroxide as a precursor gas for plasma sterilization without the residuals of harmful chemical after treatment.

Lerouge et al. (2000a) have observed high sporicidal efficacy with the higher concentration of reactive plasma species in microwave (MW) plasma sterilization. The surface and bulk properties of plasma sterilized catheters were evaluated and following observations were made: (i) limited oxidation at the surface due to plasma based sterilization (ii) no change in molecular weight due to plasma-based sterilization on surfaces, (iii) plasma-based sterilization slightly changes hydrolytic stability of catheters (iv) various plasma-based sterilization techniques induce different impacts on the catheters, such as a clear difference in coloration or the degradation of an additive (Lerouge et al. 2000b). In low-temperature gas-plasma sterilization, chemical modification (oxidation) is more responsible for sterilization, rather than physical modification (etching) (Lerouge et al. 2000c). Holy et al. (2001) compared three sterilization techniques ethylene oxide (EtO), RFGD plasma sterilization and gamma-irradiation in relation to their short and long-term effects on the molecular weight, morphology, degradation profile of the scaffolds and dimensions. They have shown that the RFGD plasma sterilization is the most suitable process for sterilizing polyester devices in tissue-engineering applications as this process does not affect the 3-D structure of the scaffolds.

Several case studies have been reported in the recent past showing the potential of plasma for biomaterials sterilization. For example, Miao and Yun (2011) have carried out sterilization of *Escherichia coli* using air DBD plasma at atmospheric pressure. They have observed that the germicidal efficiency depends on the time of plasma treatment, electrode gap, original cell density and surface characteristics of substrate material. The germicidal efficiency was found to be 99.999% under specific plasma treatment parameters. The alteration in cell structure and observation of protein leakage as observed by TEM indicated etching of cell membrane by active plasma species was the main reason of DBD air plasma sterilization. Korachi et al. (2010) have observed radical formation due to high voltage plasma, which results in physiological change in the microorganisms in water. Plasma creates radicals such as hydroxyl, ozone, oxygen and nitrogen oxide, and these radicals have direct impact on cell membrane. Changes in essential fatty acids disrupt or damage the cell membrane resulting in cell death. Plasma sterilization affects fatty acids in the cell membrane by producing radicals. However, another study suggests that the effect of plasma doesn't predominantly change pH and fatty acid profiles of *E. coli* and *S. aureus*. Artemenko et al. (2012) have evaluated the properties of selected plasma polymers that can be altered significantly by plasma parameters (power applied, pressure, electrode gap, working gas/monomer composition, use of pulsed or continuous plasma mode, etc.) used for a sterilization process. The authors in this work compared the effects of autoclaving, dry heat and UV treatment with plasma sterilization. The study effectively found physical changes by dry heating, the thickness of plasma polymerized poly(ethylene oxide) was reduced, but the highest reduction was found in sputtered nylon film by autoclaving and the thickness of polytetrafluoroethylene films were unchanged in any of the methods. Chemical changes exhibited chemical sensitivity in pPTFE and pSN films due to

hydrolysis whereas pPEO thermal degradation/oxidation due to dry heat treatment. Mrad et al. (2013) have found that the different duration of treatment of low pressure SF_6 plasma totally inactivate microorganism like, *E. coli* O157, *Klibsella pneumonia*, *Proteus spp*., *Enterobacter spp*., *Listeria monocytogene*, *S. aureus*, *Streptococcus spp.* and *Bacillus cereus*, on plasma treated PET, PVC and PE substrates. *Streptococcus spp.*, *Bacillus cereus* and *Proteus spp.* were completely killed in 30 s. However, *S. aureus*, *E. coli* O157 and *Enterobacter spp.* took 1 min, and *Listeria monocytogene* and *Klibsella pneumonia* took 3 min to become inactive. RF plasma treatment of fluorine functionalization decreases C and O atoms on the surface and develops non-polar sites (fluorine functionalities), which increases surface hydrophobicity. After a long storage period, the effect of SF_6 plasma treatment was found stable and permanent due to the fluorine atoms which retained on the surface and provide suitability for long term storage of material. Chau et al. (1996) have observed that microwave plasma removed outer bacteria layer partially. The bacterial cell bursts out due to osmotic pressure, or its internal structure was annihilated by the reactive oxygen species (ROS) and the UV radiation. Most of the time it has been observed that there are more than one layer of bacteria. The longer duration of plasma treatment will continue to attack the next layer of bacteria and the formation of carbon monoxide was detected which confirms the chemical reaction of reactive oxygen species with the hydrocarbons of microorganisms. The required duration for the complete annihilation of the spores of bacteria such as Bacillus was relatively more because the bacteria has a special protective core. Before reactive oxygen species (ROS) can strike and destroy the protective core of the bacterial spore, the plasma etching process has to go through three layers: the spore coat, the cortex and the germ cell wall. The outermost layer of the spore consists of high concentration of calcium ions. This layer reduces the chances of oxygen to react with the hydrocarbon bonds and thus etching rate is reduced. Therefore longer time is required for complete sterilization. However, with suitable gas composition, pressure and applied power, the etching rate can be enhanced to expedite the killing of the bacterial spores. Besides the etching mechanism, UV radiation present in the plasma has a lethal effect on bacteria. The UV radiation penetrated in the cell wall of bacteria causes breaking of unsaturated bonds, particularly the purine and pyrimidine components of nucleoproteins. The reactive oxygen species (ROS) and the UV radiation works as a powerful oxidizing agent. This accounts for the rapid and colossal destruction of *Escherichia coli* bacteria in the N_2O plasma. Brétagnol et al. (2008) have developed PEO-like coating using diethylene glycol dimethyl ether (DEGDME) having thickness of $\sim$20 nm and showed the effect of sterilization on bio adhesive properties of plasma polymerized polyethylene glycol (PEG) films. Autoclaving (121 °C for 12 min), ethylene oxide (EtO) exposure (typically between 37 and 63 °C for 3–4 h) and gamma rays treatment (up to 50 kGy) lead to a slight modification on the layer's surface chemistry, with reduction in oxygen content, PEO like character and some reticulation in comparison to plasma sterilization. The Ar/H_2 (90:10, 15 Pa, 100 sccm, 30 s) low pressure plasma treatments destroyed bacterial spores and inactivated bacterial endotoxins. Levif et al. (2011) have sterilized a non porous polyolefin

polymer packaging material (for example, BagLight™ PolySilk™ from Interscience™) to study the effect of inactivation, damage caused by plasma species and loosening of antimicrobial barrier. The packaging material neither interferes with the plasma sterilization process nor gets damaged by plasma species after exposure of N_2–O_2 flowing afterglow. They also showed non toxicity to human cells when the packaging was performed under sterile conditions. The same was done to evaluate and compare the characteristics towards the sterilization of *Bacillus atrophaeus* endospores cultured on a petri dish which showed less increase in surface energy as compared to the packaging material when exposed to N_2–O_2 afterglow. Along similar lines, Akitsu et al. (2005) examined the anti-bacterial effect using atmospheric pressure glow (APG) device. They have used O_2 and water vapour along with helium as a carrier gas. In this work, 10^6 log reduction of *Bacillus atrophaeus* and *G. stearothermophilus* was noticed. Important findings of this work are: (i) antibacterial effect of atmospheric pressure plasma (of nontoxic mixture of helium and water vapour or oxygen) generated using high power RF-APG device does not require vacuum chamber thus it allows continuous loading of objects. (ii) The oxygen/helium ratio is a decisive factor for relative amount of oxygen radicals and atomic oxygen. For maximum sterilization, the optimum ratio of oxygen/helium was found to be 0.06 and treatment time was 1 min. for *S. aureus*. (iii) Biological indicators were applied on to a non-woven sheet to measure the disinfection time. Complete disinfection was achieved in 20 min for spore-forming bacteria: *B. atrophaeus* and *G. stearothermophilus*, 5 min for *S. aureus*, and 1 min for *E. coli*, *S. enteritidis* and *C. albicans*.

5.3 Antimicrobial Coatings

Bacterial formation and adhesion on to a material surface results in the production of biofilm. Moreover, the reduced antibiotic susceptibility of a bacterial biofilm is a major concern to replace or remove the infected devices. Therefore, suitable pre-clinical processing of biomaterials is important for protection against microorganism. The mechanisms of bacterial adhesion (An and Friedman 1997; Hori and Matsumoto 2010) and biofilm formation can be avoided by coating the surface with suitable antibacterial agent. Plasma surface treatment inhibits the initial adhesion of bacteria to the material surface or destroys the bacteria when exposed to plasma treated surface. Cold atmospheric pressure plasmas have outstanding bactericidal properties and they are gentle to human skin. Since, silver nanoparticle is well known for anti-microbial property, it has been used as bactericidal surface coatings in various medical devices. Kumar et al. (2013) produced plasma polymerization of acrylic acid (PPAA) on the surface of PET mesh followed by immobilization of Ag nanoparticles to enhance the antibacterial property of the material. The results showed excellent antibacterial property of Ag containing PPAA-PET meshes with decrease in bacterial concentration >99.7% as comparison to untreated sample. Researchers have also used low temperature plasma for

enhancing the hydrophilicity and surface roughness of the polymeric films in order to increase the uptake of the Ag nanoparticles or a plasma polymer barrier coating for controlled release. Antibacterial tests comprising of microorganisms such as *Escherichi coli* and *Staphylococcus aureus* exhibit its efficiency more than 99.9%. Katsikogianni et al. (2008) have demonstrated one-step plasma treatment to PET films using Helium (He) and He/O_2 plasmas, which showed reduced adhesion of *S. epidermidis* in comparison with untreated PET film, even after 58 days of plasma treatment. Pandiyaraj et al. (2014a) have used tubular plasma reactor with radiofrequency glow discharge (RFGD) to modify the TiO_2/PET films. The surface of TiO_2/PET was modified using oxygen plasma generated by RF source of frequency 13.5 MHz at 0.15 mbar and varied time from 2 to 15 min. The adhesion of *Staphylococcus* was found to be highly suppressed when TiO_2/PET was exposed to oxygen plasma, which was predicted due to the physico-chemical changes induced by plasma treatment.

Some studies were also conducted on *Pseudomonas aeruginosa* clinical isolates, along with specific mutants, for adhesion on untreated and chemically modified poly (vinyl chloride) (PVC) surfaces of endotracheal intubation devices (Triandafillu et al. 2003; Balazs et al. 2003). The grafting of poly (ethylene glycol) has substantially reduced the adherence of *Staphylococcus aureus* (Harris et al. 2004). Oxygen plasma treatment make PVC surfaces hydrophilic surface which causes reduction in the number of adhering bacterias up to 70%. This is due to the introduction of oxygen containing functional groups onto the PVC substrate. In another study, plasma immersion ion implantation (PIII) technique was employed for modification of medical-grade PVC coated by triclosan or bronopol to improve the antibacterial properties (Zhang et al. 2006b). The surface was pretreated with O_2 plasma (30 min) to produce more wettable/hydrophilic surface so that antibacterial reagents triclosan or bronopol could be coated more efficiently. Subsequently, bombardment of argon (Ar) plasma ions was carried out to ensure the successful attachment of antibacterial moieties with the PVC surface. Experimental results showed that the plasma-modified PVC with bronopol exhibited good antibacterial properties against *S. aureus*. However, the plasma-modified PVC with triclosan showed better antibacterial performance against *E. coli*. But the antibacterial effect was found to be decreased with time. The blend of a plasma treatment followed by coating, deposition or grafting of a polymer or other molecules is quite familiar technique. Degoutin et al. (2012) have used low pressure RF argon plasma to graft acrylic acid on to a nonwoven Polypropylene, wherein the carboxyl moieties are used to immobilize gentamicin. The results confirmed 99% of bactericidal activity against *E.coli*. Plasma pre-treatment of poly (methyl methacrylate) (PMMA) followed by TiO_2 coating gives antibacterial properties due to the photocatalysis nature of TiO_2 (Su et al. 2010). Application of plasma treatment has also been demonstrated for developing antibacterial packaging films (Paisoonsin et al. 2013). A study showed the exposure of packaging grade polypropylene (PP) film to air DBD plasma for enhancing its hydrophilicity. Further, these films were dipped into the aqueous Zn $(NO_3)_2$ solution for the formation of ZnO nanoparticles using alkaline precipitation method. These ZnO-coated PP films showed better

antibacterial activities against both gram-negative *E. coli* and gram-positive *S. aureus* suggesting its potential application in antibacterial packing. Collectively, plasma assisted processes are suitable techniques for enhancing the material's antibacterial property.

5.4 Cell Interaction with Plasma Modified Surface

From last four decades, progress in tuning the surface properties of biomaterials for cell culture has given tremendous output in understanding the physical, chemical and biological cues that are involved in cell-material interaction. Plasma processing has proven itself as one of the promising techniques to design micro/nano structures, suitable film deposition and protein conjugation on the surface of biomaterials for effective cell culture. Positive charge, surface chemistry, wettability, surface morphology and topography are important physico-chemical parameters for understanding the adhesion and spreading of cells. Cell culture substrate surfaces are designed to mimic in vivo microenvironments of typical living tissues and organs. The desired grafting of hydrophobic or hydrophilic groups is a well-established method to tailor the surface energy (SE) and wettability for cellular and other biological interactions. Cell activation by interaction with biomaterial could lead cell spreading, migration and proliferation, which is variable depending upon cell types and surface composition. Since a cell interacts first with the material surface, major research was conducted on increasing the wettability of the substrates using plasma assisted techniques. Rearrangement of the grafted functional groups and change in surface morphology can occur during plasma surface treatment (Gupta et al. 2002). This reorganization is limited due to higher densities of grafted polymers. The relationship between the material properties like charge, composition, hydrophobicity, adhesion and growth of cells, micro/nano pattering of surface, surface geometries, surface area, cytoskeleton stretching, protrusions and migration of cells, will widen the understanding of researchers to design smart biomaterials with predetermined responses like, vascularization, gene expression and healing.

Plasma deposited acrylic acid (pdAA) and plasma deposited allylamine (pdAAm) functionalized coatings are widely used on different substrates for customized biomedical applications. Grafting of oxygen occurs during plasma deposition or after-plasma deposition in the presence of atmospheric oxygen. The pdAA functionalized surface has good wetting properties due to –COOH groups and have good stability in water. The water-contact angle decreases with the incorporation of oxygen groups onto the surface i.e. increase in wettability. The introduction of carboxylic group can be increased by generating high vapours from the feed of acrylic acid during plasma processing. Plasma polymerisation can be used to control oxygen and carbon content on the surface of biomaterials by controlling vapour flow rate of acrylic acid in plasma regime; however, it is impossible to prepare oxygen free plasma copolymer surfaces (Daw et al. 1998). The plasma

surface modification and plasma/protein combination increases oxygen content on the surface through new functional groups, namely carbonyl groups (–C=O) and carboxyl (–COOH), the oxygen is incorporated either in the form of alcohol or ether moities. Less fragmentation of acrylic acid monomer results in carbonyl groups to be attached on the surface. They are highly polar and resulting in increase of surface polarity. Buttiglione et al. (2007) have used vapours of acrylic acid and allylamine monomers along with Ar in the low pressure RF plasma system for the incorporation of –COOH groups onto the PET substrate. Their findings suggested that carboxylic groups can resist the neurite elongation and promote neuronal maturation of human nerve cells. Importantly, physical attributes on the surface can be introduced by creating a pattern on the surface of scaffold; where as chemical attributes on the surface can be obtained by introducing chemical groups (Karakecili et al. 2007). However, synergetic effects of physical and chemical attributes on various scaffolds increase differentiation and proliferation. Bretagnol et al. (2006) have shown selective proliferation of L929 mouse fibroblast cells after culture on a pulsed PEO-like/PAL micropatterned surface. Since the surface energy increases with increased functionalization of surfaces with carboxyls, the role of nitrogen functional groups becomes less important for cell viability and growth. Dhayal and Cho (2006) deposited acrylic acid films on the glass substrates by plasma polymerization and studied their interaction with leukemia cells in comparison to cell culture polystyrene. Results showed 60% reduction in cell growth on plasma polymerized acrylic acid films due to the presence of hydroxyl and carbonyl groups. Detomaso et al. (2005a) employed acrylic acid vapours as monomer precursor to deposit thin films using continuous and modulated glow discharges and found that carboxyl group present in the acrylic acid have ability to enhance fibroblasts adhesion. Vrekhem et al. (2015) developed two types of coatings to enhance the adhesion using dielectric barrier discharge; first between polymer and polymethylmethacrylate (PMMA) bone cement, and second between polymer and osteoblast cells. The cell adhesion and proliferation were tested by means of an MTS assay and live/dead staining after culturing osteoblast precursor cells (MC3T3) on the plasma treated materials. Both the methods considerably enhanced polymer adhesion to bone cement and plasma treated polymer surface to increase the cell adhesion and proliferation. Pandiayaraj et al. (2010) have used dip coating method to fabricate a thin layer of TiO_2 on the air plasma treated PET substrate and such TiO_2/PET films were modified using DC glow discharge air plasma as a function of was discharge potentials (350, 400 and 450 V). The biocompatibility of the TiO_2/PET films studied by measuring nucleation and growth of calcium and phosphorous on the TiO_2/PET film surfaces after immersion in simulated body fluids (SBF) for different days and examined by scanning electron microscopy (SEM). XPS results revealed that the air plasma treatment of TiO_2/PET film can enhance the proportion of Ti^{3+} in Ti2p and reduce carbaneous content on the surface. The changes in chemical and surface topography stimulate the growth rate of bone like apatite layers on the plasma modified TiO_2/PET film surface as shown in the Fig. 7.

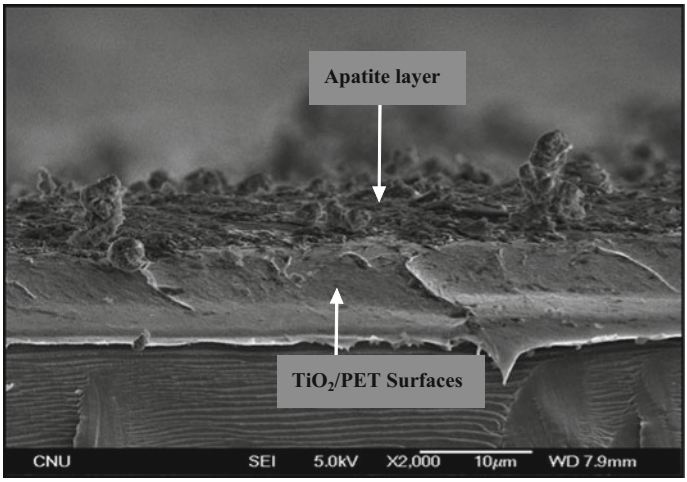

Fig. 7 The cross-section SEM image of plasma-treated TiO_2/PET exposed to SBF for 28 days. (Reproduced with permission from ref. Pandiyaraj et al. 2010)

A study demonstrated the correlation between plasma and protein based surface modification of polycaprolactone (PCL) scaffold using three approaches; (i) oxygen plasma treatment, (ii) protein coating, and (iii) oxygen plasma treatment followed by protein coating called as combined modification (for understanding the synergetic effect of surface modification by plasma and protein) and studied the effect on cell interactions (Yildirim et al. 2010). The significant increase in cells proliferation and differentiation result in mature osteogenic cells on combined modified scaffolds was achieved in comparison to other two types, which explained the combined effect of improved surface roughness, change in surface chemical functionality and increased protein adsorption on the surface of the scaffold. Increase in roughness enhanced adherence and endothelialisation during cell growth on patterned surfaces. Commonly, cells respond differently when they are cultured on any physically gradient surface in comparison to a chemically uniform surface. Another study demonstrates that plasma functionalized fluorocarbon based surfaces provide stimulus to coronary endothelial cells resulting in improved endothelialisation of vascular grafts (Pezzatini et al. 2008). It is attributed that fluorocarbon films enhance the adhesion and spreading of cells by creating a defined roughness (pattern) of the surface of substrate (Gristina et al. 2008). Authors have observed interaction of protruding filopodia from the cell membrane with individual structure of the material's surface resulting in more cell spreading, viability and attachment. Adhesion, growth and proliferation of endothelial cells as a function of duty cycles in plasma treatment were evaluated by calculating the percent carboxylic groups and thickness of coating on the material surface (Bhattacharyya et al. 2010; Xu et al. 2011). A study on plasma treated polystyrene showed that treatment times do not significantly affect the morphology of endothelial cell. However, the cell count was influenced by

treatment time in a continuous manner (Kooten et al. 2004). Unlike various cell lines, human mesenchymal cells are very sensitive to small change in surface chemistry that can ultimately affect the rate and quality of neo-tissue.

Nitrogen and ammonia plasmas can be used to functionalize surface of the biomaterial. Finke et al. (2011) employed microwave/RF plasma discharges of allylamine and ethylenediamine as monomer precursors, respectively, to coat nitrogen on titanium alloy substrate. The adhesion and spreading of MG-63 osteoblastic cells was found to be improved on these positively charged surfaces. However, authors' findings suggested no direct correlation between the densities of primary amino groups and an enhanced cell growth. In fact, other nitrogen-functional groups like, acid amides or imides play a vital role for initial cell behaviour. The amine functionalities present at the membrane surface can also be used for covalent binding of ligands such as heparin for blood compatibility applications. Nitrogen containing substrates improves cell adhesion, thus its surface patterning can be useful for implant coating, guided cell growth in tissue engineering, and also as cell capturing surfaces for biosensing and diagnostics. Zheng et al. (2015) used low temperature ammonia plasma to modify the surface of PET films, which showed improved cell affinity and it can be applicable in promoting cell adhesion and growth on the material surface. When cells interact and attract to the extracellular matrix (ECM) proteins, they are bound to retain their structure. For example, plasma polymerized poly-lysine surfaces are very promising for their properties such as attachment and growth of cells in nerve repair and also for other tissue engineered materials (Feng et al. 2003).

Several studies have been conducted to examine the potential of plasma surface modification in cell-culture for developing suitable tissue construct and devices. Chen et al. (2013) have successfully grafted N-vinyl-2-pyrrolidone (NVP) on the polystyrene films that was treated with gaseous (Ar, O_2 and Ar + O_2) plasma. Cell culture experiments on L929 cells suggested better cell growth and proliferation on the modified polystyrene surfaces. Additionally, Ar + O_2 plasma treated polystyrene film showed better cell distribution and growth rate in comparision to pure Ar or O_2 treated polystyrene films. Hsu and Chen (2000) have exposed polyurethane film to Ar plasma followed by L-lactide grafting and their cell compatibility against human umbilical vein endothelial cell lines and 3T3 fibroblast. The in vitro cell analysis revealed that the modified surface enhances the cellular adhesion and simultaneously decreases the activation of the platelet. Jiao et al. (2012) have treated poly (L-lactic acid) (PLLA) films using ammonia plasma as a function of power and treatment time and examined cytocompatibility using rat osteoblast-like cells. The density of amino functional group on the treated PLLA films increased initially and then decreased by increasing the power and treatment time. The promotion of cell adhesion and proliferation was considerably increased on the plasma treated PLLA film surfaces. Li and Huang (2007) used O_2 plasma to treat polyurethane (PU) films and also immobilized type I collagen on the PU surface. The results showed superior cell growth and adhesion of HeLa cells on collagen immobilized PU films and plasma treated PU films in comparision to the untreated PU. Some cell lines require a specific cell phenotype and that should remain throughout the culture for obtaining suitable

cell function. For example, hepatocytes function by maintaining round morphology, which could become fibroblastic in nature if these cells spread on the material surface. Ding et al. (2004) have reported that chitosan immobilization on PLLA by plasma coupling reaction showed that the morphology of hepatocyte cells tends to become round, however the rate of proliferation similar to cell culture plate. Along similar lines, Khorasani et al. (2008) reported the surface modification of poly (L-lactic acid) (PLLA) and poly (D, L-lactic acid-coglycolic acid) (PLGA) using O_2 plasma treatment. The cell affinity of O_2 plasma treated film was assessed by nervous tissue B65 cell culture. Results showed that the O_2 plasma treatment increased the hydrophilicity which thereby improved the cell adhesion in comparison to the pristine films. Lee et al. (2014) employed APPJ treatment for immobilization of L929 cell on polystyrene plate (PSP) without substantial change in surface roughness. This study also showed formation of actin filament and expression of vinculin (focal adhesion marker).

Pandiyaraj et al. (2016a) have used cold atmospheric pressure plasma technique to tailor the surface of low density polyethylene (LDPE) films to improve their adhesion and cytocompatibility at variable treatment parameters like, power, time and gas (Ar, O_2, air and Ar + O_2). Cold atmospheric pressure plasma unit used in this experiment is shown in Fig. 2. From XPS study it is clear that the incorporation of oxygen containing polar functional groups onto the surface of LDPE films is in the order of UT < Ar < O_2 < Air < Ar + O_2. LDPE films treated under higher discharge potential (14 kV) and treatment time 60 s showed improved surface roughness and functionalization. Plasma generated at 14 kV using Ar + O_2 gas incorporates polar functional groups such as C–O, C=O, –C=O, O–C=O etc. The gas flow rate was seen to affect the formation of polar functional groups proportional to the oxygen flow rate (0.2 < 0.4 > 0.6 liter per min (lpm)). The incorporation of polar functional groups with increase in surface roughness was found to be higher for sample treated at 0.2–0.4 lpm flow rate of O_2 gas in the Ar plasma regime. The plasma effect was not that significant when oxygen flow rate was increased to 0.6 lpm in Ar plasma regime which may be due to the decrease in electron density in the plasma at higher concentration of oxygen. The decrease in electron density is mainly due to smaller ionization cross section of oxygen, as compared to argon. Moreover, the addition of oxygen increased the resistance of plasma due to higher electron affinity of electronegative oxygen gas i.e. discharge in oxygen have negative ions that causes reduction in electron density (Rhee et al. 2007; Mansour et al. 2013; Rudd et al. 1983). This oxygen gas flow in Ar plasma regime thus affected NIH-3T3 (mouse embryonic fibroblast) cells adhesion and proliferation respective to the degree of surface modification of LDPE. Ar + O_2 treated LDPE films (treatment time of 30 s) showed increase in cell compatibility and also confirmed their non-toxicity to cells. Figure 8 shows the fluorescence microscopic images of NIH-3T3 cell adhesion and rate of proliferation on the surface of LDPE films with respect to time.

LDPE films treated with Ar + O_2 plasmashowed cell adhesion and proliferation equivalently well without introducing any discrepancy in cell physiology and morphology, in comparision to tissue culture plates (TCP). Hence, cold atmospheric

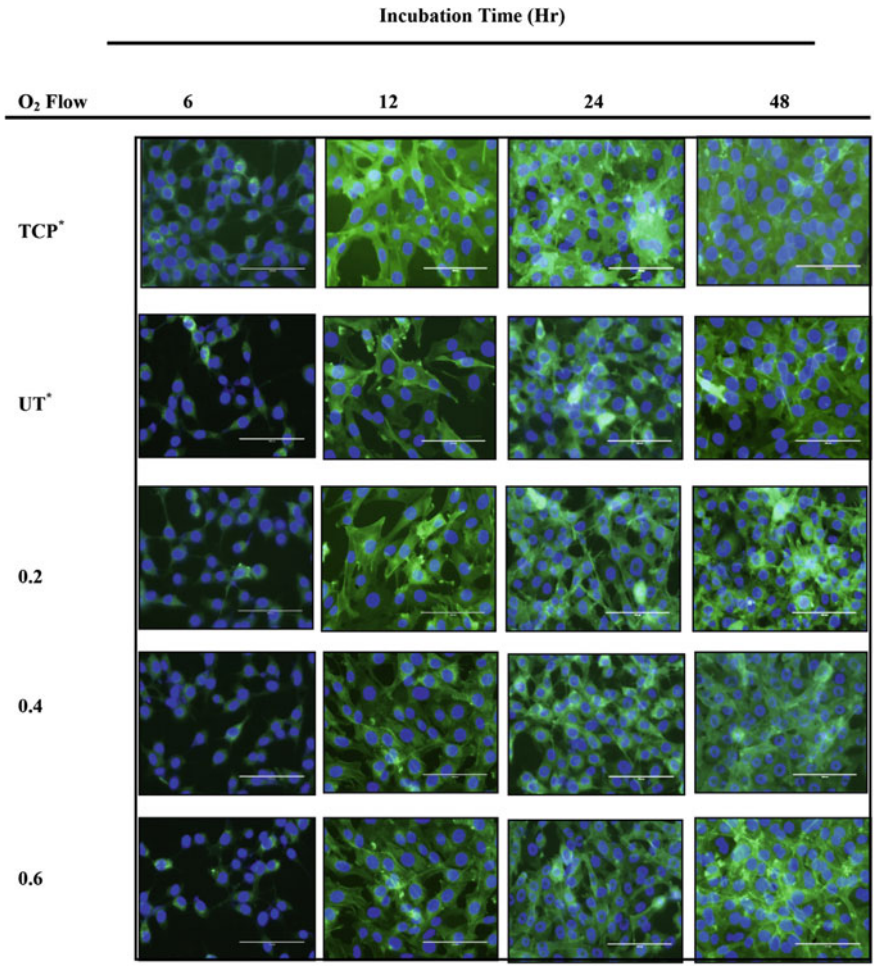

Fig. 8 Fluorescence microscopic images of NIH-3T3 cell adhesion on CAP plasma treated LDPE film surfaces as a function of O_2 gas flow rate in Ar plasma regime for different incubation times of 6, 12, 24 and 48 h (scale bar: 100 μm). (Reproduced with permission Ref. Pandiyaraj et al. 2016a)

pressure plasma treatment can be used to induce cyto-compatible properties on LDPE films. This study is clearly indicating the importance of plasma processing parameters and their optimum ratios for generating biocompatibility in the polymeric materials.

Polystyrene (PS) and poly(methyl methacrylate) (PMMA) films have also been treated with atmospheric pressure DBD plasma for increasing the cell-material interaction (Borges et al. 2013). The results indicated higher L929 cell proliferation in PMMA films in comparision to PS film, which was predicted as a function of higher surface roughness in PMMA films after plasma treatment. Rimpelov et al. (2014) have also shown the potential use of argon plasma for the modification of

PLLA surface for improving the adhesion and proliferation activity of HaCaT cells. Atmospheric pressure plasma was used to modify poly(D,L-lactic acid) (PLA) film surfaces by depositing 1,2-diaminopropane and acrylic acid as precursors to incorporate $–NH_2$ and –COOH groups respectively on PLA surface (Reno et al. 2012). The in vitro analysis states that the surface modification influences the cell adhesion and proliferation of 3T3 (mouse fibroblast), HaCaT cells (human keratinocytes) and MC-3T3 E1 (mouse pre-osteoblast). Moreover, cell proliferation assessed after 48 h by Tox-8 assay was found to be significantly higher for osteoblast cells and keratinocytes seeded onto both PLA–NH_2 and PLA–COOH films in comparison with untreated PLA films. Neděla et al. (2016) have studied the effect of argon plasma treatment on functionalized polyethylene naphthalate (PEN). The plasma modified PEN has a positive effect on adhesion and proliferation of vascular smooth muscle cell (VSMC).

Various biodegradable polymers such as poly(glycolic acid) (PGA), poly (L-lactic acid) (PLLA), and PGA coated with PLLA are used in cell transplantation and in vivo regeneration of vascular tissue. Chu et al. (1999) have employed RF glow discharge ammonia plasma for modification PLLA substrates. Their findings indicate that the modified PLLA and fibronectin (Fn)-coated modified PLLA exhibit substantial enhancement in rabbit microvascular endothelial cell (RbMVEC) and human vascular endothelial cell (HUVEC) as compared to PLLA and Fn-coated PLLA. Ammonia plasma treatment suitably modifies prosthetic biomaterials of various constructs with the subsequent transplantation of mammalian cells to be used in biological implants or tissue engineering. Bhattacharyya et al. (2010) have studied the effect of surface chemistry and plasma deposited film thickness effect on human aortic endothelial cells (HAEC) adhesion and proliferation. Adherence and growth rates of HAEC on pulsed plasma polymerized poly (vinyl acetic acid) films were measured as the function of surface density of –COOH groups. The duty cycle of the pulse was adjusted to produce films containing 3.6–9% –COOH groups. The percentage of –COOH groups was estimated from total carbon content as calculated from XPS data. HAEC exhibited enhanced cell adhesion and proliferation with increase in –COOH surface densities. The pulsed plasma polymerization time was varied to obtained films thickness varying from 25 to 200 nm. Further it was found that the growth was also dependent on the film thickness which was unexpected. Vascular grafts and stents made from biodegradable material with improved biocompatibility are in demand, particularly for pediatric patients. Poly(L-lactic acid) (PLLA) is a biodegradable polymer which is FDA-approved and is promising material for such applications. However, due to poor surface properties particularly hydrophobic nature of PLLA surface, tissue culture studies have shown that the attachment of endothelial cells (ECs) and their growth occurred relatively slow on PLLA surfaces. As a result, the slow EC recovery on the luminal side of PLLA stents provides an increased risk of induced thrombosis. In order to enhance surface properties of PLLA films, RF pulsed plasma polymerization was carried out and poly(vinyl acetic acid) monomer was used as a precursor (Xu et al. 2011). FTIR and XPS study revealed the incorporation of polar functional groups. Pulsed plasma polymerization was employed to

introduce –COOH surface groups onto the surface to further conjugate fibronectin (FN), followed by attachment of vascular endothelial growth factor to FN. Pig aorta ECs (PAE) and kinase-insert domain-containing receptor (KDR) transfected PAE showed increase in cell adhesion and proliferation, as well as significantly enhanced cell retention under fluidic shear stress on surface-modified PLLA in comparision to untreated PLLA. The results obtained clearly indicate that this combined surface modification technique using poly(vinyl acetic acid) deposition, FN conjugation, and vascular endothelial growth factor surface delivery can enhance endothelialization on PLLA, particularly when employed in conjunction with the growth of KDR-transfected ECs. The discussions in this section strongly support the idea that plasma-modified surfaces represent a very promising tool to modulate material surface and tune the complex cell behaviour for specific biomedical application. Table 3 has summarized some of the studies presenting the surface modification of materials using various plasmas and their effect on cell adhesion and growth.

5.5 Plasma-Surface Modification of Implants

The aging, genetic disorders and acute accidental skeletal injuries are prone to degenerate or destruct human skeletal system that result in pain, inflammation and joint stiffness. On an average, 90% of the population in their 40 s suffers from some degree of degenerative joint disease (Long and Rack 1998). When natural bone and joints no longer function adequately or the patient requires surgical support to relieve pain and increase the mobility, replacement of such defective bone and joint is required. Artificial materials such as metal, plastic or ceramic, are currently used as a gold standard clinical applications like hip and knee joint surgeries. The first knee replacement surgery was executed in 1968. Since then, advancements in surgical procedures and designing of implants have made this surgery one of the most successful clinical practices in biomedical field. Two decades back, more than a million total joint replacement surgeries were carried out across the globe to cure individuals suffering from severe arthritis and joint injury (Sioshansi and Tobin 1996). However, a recent report suggest that this number has increased worldwide, where only in US more than 7 million bone replacement surgeries (2.5 million hip replacement and 4.7 million knee replacement) were performed in 2010 (Kremers et al. 2015). Natural synovial joints like shoulder joints, hip, and knee are intricate and fragile structures that must function under stressed, adverse and complex conditions. The optimal performance of a human joint is governed by the desired combination of articular cartilage, a load-bearing connective tissue covering the bones in the joint and synovial fluid (Mow and Soslowsky 1991; Park and Lakes 1992).

A decisive factor for metallic implants is their rapid human body-cell acceptance and resistance to bacterial adhesion on their surfaces. Such anomalous events could be triggered by surface properties. Most artificial joints are made up of metallic component with a polymer. In order to improve the tribological properties as well as

Table 3 Types of plasma used for the modification and incorporation of functional moieties on materials surface for improving cell compatibility

S. No.	Plasma	Substrate/scaffold surface	Monomer/carrier gas	Functional groups	Cell lines	Observations	References
1	PECVD—RF (13.56 MHz)	PLA	Pretreatment with O_2 gas- SiOx Films	$–SiO_x$	MC3T3-E1 and L929	Wettability, protein adsorption, proliferation and attachment of cells	Sarapirom et al. (2013)
2	PECVD—RF (13.56 MHz)	Glass	Lysine	–C=O, –NH	Nerve cells	Enhanced growth and attachment	Feng et al. (2003)
3	RFGD—Variable Duty cycle	Si, PS, PET	Acrylic acid, NH_3	–COOH, –NH	hTERT-BJ1	Stable surface, sterilization, enhanced fibroblast adhesion	Detomaso et al. (2005a)
4	RFGD (13.56 MHz)	PET	H_2, Hyaluronan, NH_3	–NH	Chondrocytes	Differentiation, adhesion and proliferation	Barbucci et al. (2005)
5	PECVD—RF (13.56 MHz)	PET, TCPS	Acrylic acid	–COOH	3T3 murine	Wettability, stability	Detomaso et al. (2005b)
6	PECVD—RF (13.56 MHz)	PET	Acrylic acid	–COOH	Smooth muscle cells	Immobilization of proteins and cell growth	Gupta et al. (2002)
7	PECVD—RF (13.56 MHz)	Glass coverslips, PLGA	Acrylic acid	–COOH	$CaCO_2$	Novel mammalian cell sheet preparation	Majani et al. (2010)
8	RFGD (13.56 MHz)	PS	$Ar–O_2$	$–O_2$	Ki67	Adhesion and spreading	Kooten et al. (2004)
9	PECVD—RF (13.56 MHz)	PET	C_2F_4	–F	3T3 fibroblast	Adhesion, growth and proliferation	Senesi et al. (2007)
10	RFGD (13.56 MHz)	Biaxially oriented PP	$–NH_3$	–NH	MSC	Cells sensitive to surface	Mwale et al. (2006)
11	RFGD (13.56 MHz)	Glass coverslips	Octadecyltrichlorosilane	–SiO	EC	Adhesion, wettability, protein adsorption	Sanborn et al. (2002)

(continued)

Table 3 (continued)

S. No.	Plasma	Substrate/scaffold surface	Monomer/carrier gas	Functional groups	Cell lines	Observations	References
12	PECVD—RF (13.56 MHz)	PET	C_2F_4	–F	NCTC 2544, 3T3 fibroblast and MG-63	Satisfactory adhesion, good attachment and proliferation	Gristina et al. (2008)
13	PECVD—RF (13.56 MHz)	PCL	Protein coating (fibronectin)	–	7F2, CCRL-12557	Attachment, proliferation and osteoblastic differentiation	Yildirim et al. (2010)
14	PECVD—RF (13.56 MHz)	Glass coverslips	ppAAm and ppHex	–COOH	3T3 fibroblast	Proliferation and attachment of cells	Zelzer et al. (2008)
15	PECVD—RF (13.56 MHz)	PS	O_2	–COOH, –C=O, ether groups, –OH	1BR.3N	Attachment of cells	Mitchell et al. (2004)
16	PECVD—RF (13.56 MHz)	Glass	Acrylic acid	–COOH	Leukemia cells	Affects the growth f the cell	Dhayal and Cho, (2006)
17	PECVD—RF (13.56 MHz)	PS	CF_4	–F	MG63, SaOS2	Adhesive, non fouling and biomolecules immobilization	Mundo et al. (2010)
18	PECVD—RF (13.56 MHz)	PCL, PD, L, LA	O_2, C_2H_4/N_2 1:3	–NH	SaOS2, 3T3	Increases metabolic activity, cell colonization in core region of scaffold	Intranuovo et al. (2011)
19	RF Magnetron Sputtering	Titanium alloy substrates (Ti-6Al-4V-P)	Allyl amine and ethylene diamine, N_2: H_2 1:1	–N (amides and imides)	MG63	Cell adhesion, function and spreading	Finke et al. (2011)
20	PECVD—RF (13.56 MHz)	LUX tissue culture dishes	Acrylic acid	–COOH, –C=O	Osteosarcoma cell s	Adhesion	Daw et al. (1998)

(continued)

Table 3 (continued)

S. No.	Plasma	Substrate/scaffold surface	Monomer/carrier gas	Functional groups	Cell lines	Observations	References
21	PECVD—RF (13.56 MHz)	PLGA	$–O_2$, $–NH_3$	–O, –NH	NIH 3T3	Cell affinity and growth	Shen et al. (2007)
22	PECVD—RF (13.56 MHz)	PET	Acrylic acid and allylamine	–COOH, –NH	Human neuroblastoma SH-SY5Y cells	Adhesion, differentiation and maturation of neural cells	Buttiglione et al. (2007)
23	PECVD—RF (13.56 MHz), CO2 laser	PEEK	Acrylic acid	–COOH	MC3T3-E1	Adhesion, spreading and proliferation	Zheng et al. (2015)
24	PECVD—RF (13.56 MHz)	PET, Si	C_2F_4	–F	CVEC	Interaction with biological system, endothelialisation and angiogenesis, prosthesis integration, responsiveness to fluorocarbon	Pezzatini et al. (2008)
25	LPAPJ	PS, CNW Layers	Ar/NH_3 and Ar/N_2, Ar/H_2/C_2H_2:1050/25/1	–NH	L929	Adhesion, tissue repair or replacement, proliferation	Claudia et al. (2014)
26	PECVD—RF (13.56 MHz)	FEP	H_2/CH_3OH	–OH	Mouse neuroblastoma cells	adhesion	Vargo et al. (1992)
27	RFGD (13.56 MHz)	PS	O_2	–	PC12	Good protein adhesion	Lhoest et al. (1996)
28	Microwave plasma (2.45 GHz)	PS	N_2/O_2, H_2Ar	–	3T3	Good adhesion	Ohl and Schroder (1999)
29	RFGD (13.56 MHz)	Silicon wafer	O_2	–	Anti-mouse IgG (Biosensor)	Patterned immobilization	Flounders et al. (1997)

(continued)

Table 3 (continued)

S. No.	Plasma	Substrate/scaffold surface	Monomer/carrier gas	Functional groups	Cell lines	Observations	References
30	LPP	PCL, PLLA	O_2, Acrylic acid, allylamine	–O, –COO, –COOH, –NH	MC3T3-E1	Protein adsorption, cell attachment	Myung et al. (2014)
31	APP-DBD (22 kHz)	Cells cultured glass substrates, cells with gold np's, cells with focal adhesion kinase (FAK) and tooth	Ar, H_2O_2	–	G361 human melanoma	Cell death and bleaching	Lee et al. (2011)
32	AAPJ	Cells in H_2O_2 dispersion system	Ar, H_2O_2	–	HaCaT	Destruction of cells	Winter et al. (2014)
34	Microwave plasma (2.45 GHz)	Titanium surfaces	allylamine	–NH	MG63	Osteoblastic focal contact formation as vinculin, paxilin and p-FAK, cytoskeletal development and cell functions	Finke et al. (2007)
35	Microwave plasma (2.45 GHz)	PET	allylamine	–NH	Human skin fibroblast	Covalent binding of ligands, wettability, metabolic activity	Hamerli et al. (2003)

resistance to wear and tear of the metallic components in the artificial joints, various surface modification techniques have been suggested including plasma-grafting, plasma coating and ion implantation (Mckellop and Rostlund 1990; Rieu et al. 1991; Chengwei et al. 1995). As discussed in the earlier section, plasma surface treatment is one of the potential techniques to modify the materials surface for the improvement of cell compatibly. Moreover, latest developments of producing non-thermal or so-called cold atmospheric pressure plasmas pave the way for wide range of biomedical applications. Instead of understanding about fungicidal, bactericidal, and virucidal properties of cold atmospheric pressure plasmas, information about its effects on mammalian cells and tissues is still lacking. Functionlisation of large volume 3-D (both surface and bulk) scaffolds is highly desirable without any change in its structural properties. Chemical functionalisation of scaffolds can provide desired conditions for immobilisation of signalling biomolecules over the entire volume of the porous scaffolds.

Schröder et al. (2010) showed that antimicrobial properties can be imparted on titanium surface by plasma-based copper implantation, which allowed the release and generation of small concentrations of copper ions during contact with body fluids leads to an antimicrobial effect. This titanium surface was also functionalized with amino groups by the deposition of an ultra thin plasma polymer using a precursor monomer allylamine. This coating improved the adhesion and spreading of osteoblast cells without significantly reducing the generation of copper ions. Titanium samples coated with the cell-adhesive plasma polymer implanted in the intramuscular region in rats, showed a reduced inflammatory reaction as compared to uncoated titanium. In another study, microwave plasma of allylamine was used to coat a polymer film on titanium to boost the initial adhesion processes (Finke et al. 2009). The deposited layer of PPAAm was very thin (<50 nm), adherent, crosslinked, pinhole and additive free, and was found to be resistant to delamination and hydrolysis. The functionalization of titanium surface was found to be useful in osteoblastic focal adhesion formation and differentiated cell functions in vitro. Plasma surface modification of PPAAm could be an alternative approach to enhance the biocompatibility of titanium implants. Studies in cell culture investigations and implantation in rats revealed positive effects in in vitro and an in vivo performance compared to untreated samples. Titanium was also modified for functionalizing with –OH, –COOH, and $–NH_2$ using plasma polymerization of acrylic acid, allylamine and allyl alcohol, respectively (Ko et al. 2012). They further investigated the formation of bone like apatite on these functionalized titanium surfaces, wherein –OH, –COOH, and $–NH_2$ groups provided different behaviours to titanium surfaces in terms of bone-like apatite formation. COOH/Ti was favourable for bone-like apatite formation as compared to untreated Ti, OH/Ti and NH_2/Ti. Roy et al. (2011) reported synthesis of nano-hydroxyapatite (HA) coating on pure titanium using inductively coupled RF plasma spray (using normal and supersonic plasma nozzles) and their in vitro and in vivo biological response. The normal plasma nozzle based coating lead to improved phase decomposition, high amorphous calcium phosphate (ACP) phase formation, and substantial dehydroxylation of HA. On the other hand, coatings prepared by supersonic nozzle maintained the

crystallanity and phase purity of HA owing to relatively short exposure time of HA particles in the plasma. The microstructural analysis indicate that the coating is made of multigrain HA particles having ~200 nm, which consisted of recrystallized HA grains in the size range of 15–20 nm. The type of nozzle and working distance have a strong influence on HA coating properties while, plate power had little influence. The histological response of HA coatings prepared with supersonic nozzle were evaluated in vivo using the cortical defect model in rat femur. After 2 weeks of implantation in vivo, early implant-tissue integration was evident by the formation of osteoid on the HA coated implant surface.

Besides, several polymeric materials are also used as an implant in reconstructive surgery. Their surface modification in terms of better tissue-integrity is one of the important areas of research to improvise their performance. Considering these requirements, several studies have been conducted in the recent past. For example, Nandakumar et al. (2012) have used electro-spinning to fabricate fibrous 3-D scaffolds made of poly(ethylene oxide terephthalate)/poly (butylene terephthalate) copolymer to replicate the physical microenvironment of ECM. RF oxygen plasma exposure enhanced surface roughness of fibres at nano-scale with respect to plasma treatment time. Noticeable adsorption of bovine serum albumin (BSA) was found when scaffolds were subjected to plasma (for 15 and 30 min) in comparision with control fibres. Poly(L-lactic acid) (PLLA) nanofibers (NF) were produced using electrospinning technique and modified with cationized gelatin (CG) to enhance its compatibility with chondrocytes and to show in vivo and in vitro possible applications of CG-grafted PLLA nanofibrous membranes (CG-PLLA NFM) as a cartilage tissue engineering scaffold (Shen et al. 2007). In order to introduce –COOH groups on the surface of PLLA NF they were first exposed to oxygen plasma, followed by covalent grafting of CG molecules using water-soluble carbodiimide as the coupling agent. In vitro studies showed that CG-PLLA NFM could enhance viability, proliferation and differentiation of rabbit articular chondrocytes as compared to pristine PLLA NFM. The firm attachment of chondrocytes and in-growth of cells into the interior of CG-PLLA NF membrane was observed in SEM and also confirmed that cell morphology was unaltered. Enhanced cell differentiation in CG-PLLA NF membrane was affirmed by improved glycoaminoglycan and collagen secretion. The in-growth cells maintained the expression of characteristic markers like collagen II, aggregan and SOX 9 of chondrocytes. Further, cell–scaffold constructs were implanted subcutaneously using autologous chondrocytes. The histological examination and immunostaining confirmed the genesis of ectopic cartilage tissues. These results indicate the potential of plasma surface modification followed by grafting of CG molecules onto PLLA NF membrane to support chondrocyte proliferation, differentiation and cartilaginous matrix biosynthesis. Poly (L-lactide-co-D/L-lactide) based fiber meshes similar to structural features of the native extracellular matrix (ECM) were produced by electro-spinning (Schnabelrauch et al. 2014). Subsequently these fibres were coated with an ultrathin plasma polymerized allylamine (PPAAm) layer, to change its hydrophobic nature into a hydrophilic polymer network (as evident from contact angle measurements) and incorporated positively charged amino groups on the fiber surface so

as to interact with negatively charged pericellular matrix (PCM) components. Thus, the grafting of positively charged amino containing groups on PPAAm surfaces favoured an improved cell spreading on human gingiva epithelial cells (Ca9-22) and human uroepithelial cells (SV40-HUC-1). However in vivo study of a rat intramuscular implantation model indicated no change in local inflammatory tissue response in PPAAm-coated versus untreated polylactide meshes, which validated that the coating has no influence on the local inflammatory reaction. On the basis of these inferences, incorporation of positively charged amino groups onto biodegradable polymer mesh surfaces using plasma processing seems to be a promising approach to enhance the cellular acceptance of these materials. A study demonstrated the difference between wet chemical processing using ethylenediamine and a plasma glow discharge method using precursors heptylamine for the treatments of tissue engineering scaffold made of poly(lactide-co-glycolide) (PLGA). The plasma treatment incorporated amide and protonated amine (NH+) groups onto the surface and the bulk of the porous scaffold. Wet chemical processing also incorporated these (NH+) groups but the structural and chemical integrity were severely affected. Comparative examinations suggested that the RF glow discharge plasma treatment was more effective and appropriate. Thus plasma treatment was found to be useful in achieving functionalisation of 3-D objects without compromising on the structure and chemical integrity of scaffolds, hence maintaining their properties important for tissue engineering applications.

Welz et al. (2013) have focused on the interaction of cold atmospheric plasma with healthy head and neck mucosal cells at molecular level. The initial finding suggested no mutagenic effects after exposure to cold atmospheric plasma as confirmed by Comet assay. The results for pharyngeal and nasal tissue showed that cold atmospheric plasma treatment can reduce cell viability as a function of treatment time without significant damage to DNA. The results therefore show that the exposure of mucosal tissue cultures to cold atmospheric plasma does not have a significant mutagenic effect for treatment times of up to 120 s. Boxhammer et al. (2013) used the same plasma device (MiniFlatPlaSter), and found that the treatment times up to 240 s did not induce any mutations in V79 lung fibroblast hamster cells. On the other hand Arndt et al. (2013) showed that 120 s of cold atmospheric plasma treatment using the MiniFlatPlaSter device induced phosphorylation of H2AX in two melanoma cell lines. Nevertheless, a shorter duration of plasma treatment time of 60 s did not show any DNA-DSBs in the same experimental setup. Similarly, DNA damages were also reported as a function of plasma treatment time in different cold atmospheric plasma devices and cell lines (Vandamme et al. 2012; Sensenig et al. 2010; Kalghatgi et al. 2010). However, a comparison of various experimental findings obtained using different cold atmospheric plasma devices is difficult because of the variation in the production of their respective components. Kalghatgi et al. (2010) have explained dose-dependent DNA damage using cold atmospheric plasma by the formation of DNA crosslinks mediated by plasma induced intracellular reactive oxygen species (ROS), which is potentially harmful for the cellular metabolism. Cold atmospheric plasma induced intracellular ROS formation has been reported by several researchers (Vandamme et al. 2012; Sensenig et al. 2010;

Lupu and Georgescu 2010). It is well known that low doses of ROS have a positive effect on cell proliferation but induces mutagenesis, whereas high doses of ROS inhibit cell proliferation, induce cytotoxic effects which could lead to apoptosis of cells (Dreher and Junod,1996; Iyer and Lehnert 2002). Understanding of plasma treatments that directly affect cell behaviour are still in the initial stage and need more attention to validate their suitable use in the development of advanced biomedical devices and implants.

5.6 Plasma-Surface Modification for Blood Contacting Devices

Biocompatibility is not an intrinsic property of a material. It is one of the essential parameters of any material's selection and application in biomedicine, which entails it to have hydrophilicity and a low friction coefficient. The interactions between an implant and the surrounding tissues are very complicated. Most classes of polymeric materials have good mechanical strength and stability but they suffer due to the issues related to surface-induced thrombosis. When the device/implant comes in contact with blood, the deposition of plasma proteins (like fibrin) leads to the formation of thrombosis on the surface of implanted biomaterial followed by adhesion of platelets. The adhesion, activation and spreading of platelets and protein deposition are determined by the interaction between the plasma proteins and the surface of the implant. The main problem associated with blood contacting devices (like, artificial heart valves, catheters, various joints and implants) is that the surface of the artificial organ is not recognized by blood. In general, urgent replacement of artificial prostheses is indispensable for the patients who suffer with heart-valve disease and arteriosclerosis. Unfortunately, most of the products do not provide stable long term biofunctionality. Therefore, surface engineering is required in the biohybrid organ systems, which should posses a blood-contacting side that have an excellent hemocompatibility and a tissue-contacting side that should be cytocompatible. Materials used for such implants may have excellent resistance to wear, fatigue and degradation. However, the main problem of these materials is thrombogenicity (Goodman et al. 1996). For example, vascular prostheses used to replace large arteries works very well, but small-caliber artificial grafts having internal diameter of less than 5 mm do not work well. This may happen due to the localized constriction (stenosis) in the vascular graft, which eventually restricts the blood flow through the affected vessel (Mustard and Packham 1975). Therefore, in order to minimize the risk of thromboembolic complications in patients, anticoagulation therapy is necessary. Hence, it is necessary to either find new biomaterials with better blood compatibility or suitably modify the existing blood contacting materials.

Among the number of different surface treatment processes, plasma surface modification technique is preferred due to its various advantages as discussed in the Sect. 3. To make biomedical devices blood compatible, DLC and TiO thin films are deposited using plasma assisted techniques. PIIID process makes it possible by doping its surface with elements like calcium or phosphorous. The surface chemical composition, texture and morphology play a vital role in longevity and performance of such implants thus two major areas widely focused upon are; (1) basic problem governing the bioactivity and the compatibility of the biomaterials and medical implants with tissues, and (2) anticoagulation of blood on various artificial cardio-vascular materials. The general procedure to make surfaces anti-thrombogenic is grafting of specific functional groups using plasma/PECVD followed by immobilization (covalent, ionic, adsorption) of anti-thrombotic molecules on to the polymers. Polymeric materials have certain advantages such as light weight, easy processability and moldability, excellent resistance to corrosion, good mechanical properties etc. However, its poor surface properties particularly hydrophobicity and low surface energy causes undesired coagulation, thromboembolism and variable response to natural tissues. Immobilization of the protein is one of the ways of imparting anti-thrombogenic property in the blood-contacting materials, since polymeric material can be tailored easily to meet the requirements of tissue engineering. Previous study supports the use of synthetic polymers application as the implants and devices such as artificial heart-valves and artificial blood vessels (Favia and d'Agostino 1998). Application of plasma to improve the anti-thrombogenic property of the polymers is detailed discussed in this section.

For blood contacting devices, minimal interactions with the biological environment and non-fouling properties are important to obtain a good hemocompatibility and decrease the amount of thrombus formation. For example, blood bags used for hemodialysis are made of polyvinylchloride (PVC) with plasticizer membranes fabricated with polypropylene (PP). Polyethylene-therephtalate (PET) and Polytetrafluoroethylene (PTFE) are the materials of which modern vascular prostheses are made. Heart valves are made of PET or PTFE with metal leaflets that have pyrolytic carbon coating. These polymeric materials have some desirable bulk properties but have poor surface properties. For example, PTFE as a biomaterial has following suitable bulk properties: (i) high chemical inertness, (ii) low coefficient of friction and (iii) good thermal stability. However, due to low surface energy, thrombogenic reaction gets induced on the surface of PTFE when it comes in contact with blood resulting in poor performance as a small diameter, synthetic arterial substitute (Formichi et al. 1988). Therefore, immobilization of anti-thrombogenic molecules/moieties onto the polymeric surface provides means to alter the chemical, physical, biological and morphological attributes of the material's surface. Surface modification techniques that have been used to enhance cell seeding on blood contacting prostheses include immobilization of collagen, laminin, fibronectin, and similar like proteins and peptides. The removal of fluorine containing groups from the surface and introduction of desired functionality such as hydroxyl, carbonyl, carboxyl and amino groups also enhances material's compatibility (Sodhi 1996). Plasma surface modification technique is suggested as the best

choice for the modification of fluoropolymer surfaces. Clark and Hutton (1987) have demonstrated the use of hydrogen plasma for rapid defluorination of fluoropolymers up to a depth of 2 nm. Nitrogen plasma treatment to the surfaces of PTFE and ePTFE vascular graft also revealed the improved endothelial cell adhesion (Dekker et al. 1991; Griesser et al. 1994). PTFE and PET surface were modified using argon plasma followed by series of coatings/grafts using collagen and laminin, and subsequent immobilization of bioactive molecules like PEG, heparin or phosphatidyl choline via carbodiimide crosslinking. Plasma induced surface grafting and immobilization of biomolecules changes the surface conditions of vascular grafts. In vitro studies indicated significant reduction in fibrinogen adsorption and platelet adhesion on such modified surfaces which results in improving the biocompatibility (Chandy et al. 2000).

Pandiyaraj and his group have contributed extensively to understand the phenomena plasma surface modification of various polymeric materials and also develop novel surface treatments, polymerization and biomolecules immobilization approaches using various types of plasma for improving their biomedical applicability (Pandiyaraj et al. 2009, 2010, 2014b, 2015, 2016a, b, c, d, e). Various gaseous plasmas like, Ar, O_2, Air and Ar + O_2 have been used to modify the surface of LDPE films by low temperature DC excited glow discharge plasma and their in vitro blood compatibility has been studied (Pandiyaraj et al. 2014b). Ar + O_2 plasma treated LDPE film showed dramatic decrease in contact angle, which indicate that the surface has become more hydrophilic. Such hydrophilic surfaces cause the inhibition of platelet adhesion and protein adsorption. The whole blood clotting time (WBCT) for untreated LDPE film was 220 s, whereas plasma treated LDPE film exhibited improvement (i.e. WBCT was 475 s). Moreover, plasma treated films also showed reduction (up to 64%) in the formation of thrombus (Fig. 9).

Polyethylene glycol (PEG) is considered to be a suitable biocompatible polymer which has been examined for various biomedical applications. Similarly, its application for developing suitable biocompatible and hemocompatible surface

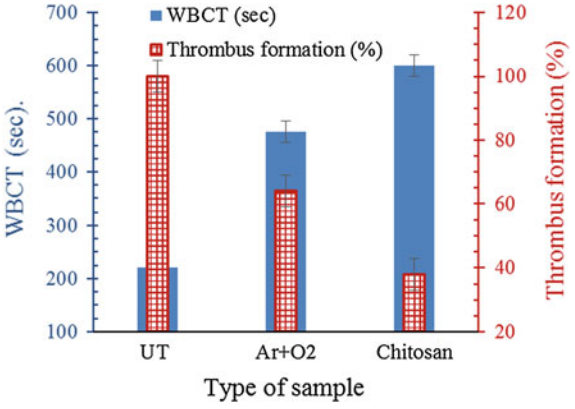

Fig. 9 Graph shows the amount of whole blood clotting time and formation of thrombus on the untreated (UT) and surface modified (Ar + O_2 and chitosan) LDPE films. (Adopted with permission from Pandiyaraj et al. 2014b)

preparation in combination with plasma processing have also been studied, some of them are discussed here. A study demonstrated PEG grafting on LDPE films by subjecting to DC glow discharge Ar plasma treatment (350 W, 5 min, 0.2 mbar) followed by O_2 purging in the absence of plasma for 20 min, which leads to the incorporation of oxygen moieties that are able to initiate plasma grafting of acrylic acid (AAc). Thereafter, plasma grafting of polyethylene glycol (PEG) was carried out for further enhancement of bioactivity. In adition to this PEG grafted surface acts as a spacer for immobilization of biomolecules like chitosan (CHI) (Pandiyaraj et al. 2015). These modified LDPE films inhibit the adhesion of platelets, adsorption of proteins and formation of thrombus in order of UT < Ar plasma < AAc < PEG < CHI. Finally, the CHI immobilized LDPE film showed improved biocompatibility measured in terms of WBCT (600 s), anti-thrombogenesis, low protein adsorption and reduced platelet adhesion. The chitosan modified LDPE film showed reduced thrombus formation up to 38% as shown in Fig. 9. The C1 s XPS of the acrylic acid grafted on LDPE film is fitted with three components centered at 285.0 (83%), 286.4 ± 0.1 (9%) and 288.7 ± 0.2 eV (9%) (Fig. 10a). The presence of ester and/or carboxylate group clearly confirms the successful grafting of AAc on the surface of LDPE films. However when PEG was grafted on such surface, it shows two predominant peaks at 285.0 and 286.8 eV which is assigned to C–C/C–H and C–O groups respectively. It also shows a very small peak at 288.5 eV corresponding to ester group (O–C=O) of AAc film, probably due to a very thin layer or partial covering of AAc grafted LDPE films by PEG. After CHI immobilization, the relative intensity of

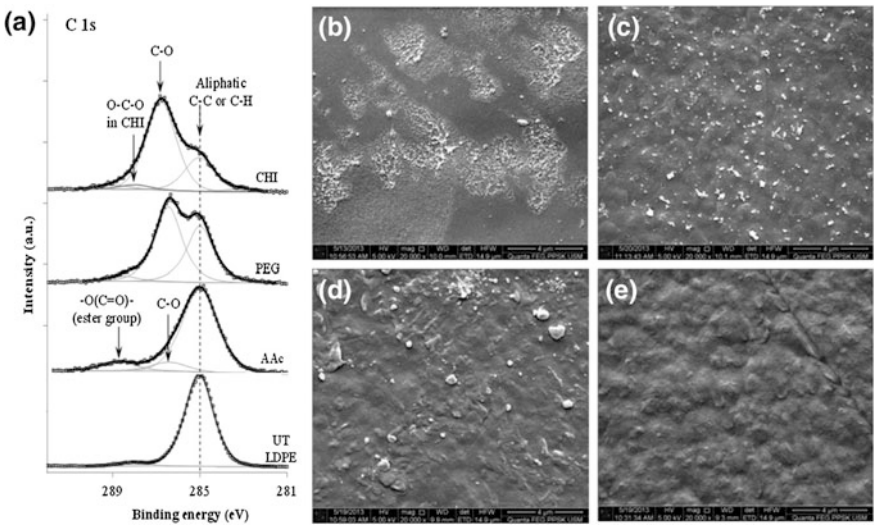

Fig. 10 C1S XPS spectra of untreated (UT), AAc, PEG and CHI immobilized LDPE films. SEM photograph of in vitro platelet adhesion tests: **a** untreated, **b** AAc grafted, **c** PEG immobilized and **d** CHI immobilized LDPE films and (**e**). (Reproduced with permission from Pandiyaraj et al. 2015)

peak at 285.0 eV decreased which corresponds to CH_3 in the acetylated chitosan moieties and also to aliphatic carbon from the underneath layer. The intensity of second peak at 286.8 eV corresponding to C–O in polysaccharides such as cellulose and chitosan is increased confirming the successful grafting of CHI molecules. Nevertheless there could be some contribution to this peak from the lower PEG layer. Understanding the effect of plasma surface modification, LDPE films were also analyzed by scanning electron microscope (SEM) for monitoring the in vitro platelet adhesion on the LDPE films (Fig. 10b–e). The untreated LDPE film shows highly dense platelet adhesion and accumulation on the surface. On the other hand, adhesion and accumulation of platelets was found to be further suppressed on AAc and PEG grafted LDPE films, which was almost absent on the chitosan (CHI) immobilized LDPE film surfaces. These results indicate that the surface modification of a material using plasma can make the material more biocompatible and provide flexibility to manufacture various biomedical devices.

A material's biocompatibility can also be affected by their molecular weight, which was demonstrated by Pandiyaraj et al. (2016e) by grafting of different molecular weight PEG (MW: 400, 4000 and 6000) on PET substrate. PET films were subjected to low pressure DC argon plasma followed by post plasma grafting of AAc. Grafting of PEG with different molecular weights was then carried out and their effect on in vitro hemocompatibility was studied. The in vitro analysis showed that PEG grafted PET film extends the formation of thrombus and lowers the adhesion of platelet. The molecular weight-4000 of PEG polymer was found to be optimum. In another experiment, PET films were modified using argon plasma for 10 min at discharge potential and working pressure of 400 V and 0.2 mbar, respectively, to create free radicals and to alter surface morphology so that the post plasma grafting of monomer would be successful (Pandiyaraj et al. 2009). Such argon plasma treated PET films were then dipped in acrylic acid solution followed by dipping in PEG solution. PEG provides reactive sites and acts as a spacer for immobilization of biomolecules (i.e. heparin or insulin) onto the PET surface. The result confirms that the platelet adhesion and protein-adsorptive resistance of Hep/Ins-PET were significantly improved. The WBCT of the untreated PET was 258 s and was found to have increased to 715 and 708 s on the heparin and insulin immobilized PET film, respectively. WBCT was seen to have increased approximately to 64% in surface modified PET film surfaces.

Cold atmospheric pressure (CAP) plasma assisted polymerization approach has been used to successfully enhance the anti-thrombogenic property of the polypropylene (PP) (Pandiyaraj et al. 2016c). In this study, PP films were first subjected to Ar plasma for 60 s followed by passage of oxygen gas in the plasma chamber in absence of plasma to incorporate oxygen moietes. Further, acrylic acid (AAc) and polyethylene glycol (PEG) in vapor phase were used as precursors for plasma grafting to develop biofunctional coatings on the surface of PP films. Immobilization of biomolecules (insulin, heparin and chitosan) was carried out on these functionalized PP films using wet chemistry. Incorporation of; (i) C–O, C=O and O–C=O groups confirmed successful grafting of AAc and PEG, (ii) C–N, C–O, C=O, O–C=O and C–Si groups confirmed immobilization of heparin and insulin,

(iii) C–N, C–O and C=O groups confirmed immobilization of chitosan as evident from XPS and FTIR. The contact angle of untreated PP film with respect to water was 92.2°, which reduces to less than 20° for biomolecules immobilized films indicating strong hydrophilic nature of the immobilized surface. The in vitro analysis indicates that the adhesion and activation of platelets reduced dramatically for AAc and PEG grafted PP films. Further, there is no evidence of adhesion and activation of platelets on the surface of biomolecules immobilized PP films. The quantitative reduction of platelets (90%) and their adhesion on the biomolecules immobilized surfaces was observed in comparision to untreated PP films.

The grafting of PEG on to the allylamine film deposited on silicon wafers using plasma polymerization prohibited the adsorption of horseradish peroxidase enzymes and collagen (Cole et al. 2007). A considerable reduction of γ-globulins adsorption was achieved by successful immobilization of PEG on to poly (vinylidene fluoride) membrane (Wang et al. 2002). Deposition of DLC coating using plasma polymerization of acetylene followed by ammonia plasma treatment and immobilization of heparin prolongs blood coagulation time by a factor of 10 (Steffen et al. 2000). Wang et al. (2006) have used acetylene plasma treatment on PET to increase clotting time and reduce the platelet adhesion and activation. The same author also reported the improvement of biocompatibility of PET by argon plasma discharge and grafted by different molecular weight water soluble polymer —PEG. In vitro studies showed that the PEG grafted PET films prolong the activated partial thromboplastin time (APTT) and reduce the platelet adhesion (Wang et al. 2005). Gomathi et al. (2012) have used nitrogen plasma to modify the surface of polypropylene and it was found that the modified PP exhibit reduced platelet adhesion when compared to the untreated one and increased partial thromboplastin time. Similarly, the effect of oxygen plasma treatment of PET was investigated. The plasma treated PET was grafted with acrylic acid and further coupled with polyethylene oxide, which finally reacted with insulin and/or heparin (Kim et al. 2000). The percentage platelet adhesion was increased slightly by grafting of AAc and decreased by coupling with PEO. However, further decrease was monitored in heparin immobilized PET substrate. The modification of poly(dimethyl siloxane) (PDMS) elastomer surface was achieved by Ar plasma treatment followed by deposition of pluronic F-68 or poly(ethylene glycol) methacrylate (PEGMA) grafting, the modified surface was found to be non-toxic and slightly hemolytic (Pinto et al. 2010).

Just like organic materials, inorganic materials are also used in biomedical field. Inorganic blood contacting materials/devices such as stents and artificial heart-valves are used in medical field due to their superior bulk properties. However, these have inferior surface properties resulting in poor blood compatibility. Therefore, surface modification of inorganic blood contacting devices/materials is a promising area of research. Decrease in thrombus formation was observed when ion implanted silicone rubber catheters were employed in the blood streams of test animals (Suzuki et al. 1990; Suzuki et al. 1988). Ion implanted hemodialysis catheters in over 150 patients showed significant decrease in thrombus formation (Uldall 1993). As a blood contacting material, DLC, carbon nitride

(CN), titanium-based films are widely used. Titanium oxide coatings are generally used in orthopaedic and dental prostheses. However, to enhance biocompatibility surface modification is required. For e.g. the blood compatibility can be improved significantly if a thin layer of rutile titanium oxide is formed on the surface of a matrix (Huang et al. 1998). In vitro blood compatibility analysis indicated that the TiO_2 film has less amounts of adherent platelets, longer clotting time, lower hemolytic rate, less aggregation and less pseudopodium of the adherent platelet (Leng et al. 2001a, b). It was observed that plasma surface treatment further improves these properties. Plasma processing seems to be a promising technology for developing better blood contacting materials that exhibit reduced platelet adhesion, decreased blood cell loss and enriched hemocompatibility.

5.7 *Plasma-Surface Modification for Reducing Bio-Fouling*

Silicone rubber is a well recognized material known for its biocompatibility and superior flexibility which is used to make catheters. However, silicone surface is susceptible to biofouling and thrombogenesis that may lead to catheter occlusion and demands replacement. Ion implantation on silicone rubber is found to efficiently reduce biofouling (Sioshansi and Tobin 1996). Silicone based gel implants commonly used in various surgical procedures for restoring the natural look (for example, breast reconstruction). The silicone rubber surface has very low surface energy (14 dynes cm^{-1}). If the critical surface tension is increased between 20 and 30 dyne cm^{-1}, it will restrict biodeposits when exposed to body fluids (Baier 1970). If the deposition rate of fibrinogen is equal to the removal rate, then no net thrombus formation on ion implanted catheter tips can be observed. In general, the biofouling is observed to reduce when the polymeric surfaces are transformed to a hydrophilic one i.e. by enhancing surface energy. This can be achieved by plasma assisted surface modification techniques. Plasma polymerization of acrylic acid (pp-AAc) was carried out on the polypropylene (PP) membranes. PEG chains of different lengths were covalently bonded onto the plasma modified PP surface and resulted in antifouling properties which were confirmed by BSA and fibrinogen filtration experiments. Such modified PP membranes lead to decreased protein adsorption due to electrostatic repulsion between negatively charged deposited layer and protein molecules (Zanini et al. 2007). In another study, microporous polypropylene membranes coated with acrylic acid and allylamine were found to reduce the fouling with bovine serum albumin (BSA) to less than 50%. The deposition of plasma polymer on the porous membrane surface was confirmed by ATR-FTIR spectra. The hydrophilicity of the surface played a role as important as that of the micropore size. The BSA solution flux through the plasma-treated membranes was found to be dependent on pH, whereas no significant effect of pH variation on the untreated membrane was found. Plasma polymerization creates surface charges which influences adsorption and removal of BSA (Kang et al. 2001).

5.8 *Plasma Polymer Modified Drug Delivery Systems*

Biomaterials have been used in drug delivery systems (DDSs). As a suitable drug carrier and its delivery, synthetic and natural polymers are emerged as potential materials. An ideal drug delivery system should be able to deliver biologically active molecule at the desired site with the proper delivery rate and duration, so as to maintain optimum therapeutic concentrations of the drug level in the body with minimum fluctuation (Nair and Laurencin 2006; Kumar et al. 2009). DDSs comprising of biodegradable polymers have received considerable attention, since they need not be removed after implantation. Drug release rate from polymeric matrices depends on various parameters such as the drug matrix interaction, drug properties, initial drug loading, nature of the polymer matrix and matrix geometry (Kumar et al. 2009). Biodegradable polymers such as PLA, PGA and their copolymer (PLGA) are studied extensively for drug delivery applications (Nair and Laurencin 2006). The drug release profile of matrix polymer depends on its surface properties and chain mobility of polymers. Crosslinking layer at the surface may strictly restrict chain mobility. The lower the molecular chain mobility, the lower is the drug release rate. Plasma processing can be used to crosslink surfaces of polymeric matrix so as to control the drug release rate. Plasma treatment has attracted attention of researchers as a potential polymer processing technique for applications in drug delivery systems. Kuzuya et al. (2008) have reported that argon plasma treatment of polymer encapsulated drug tablets suppress the rate of release of drug molecules due to the formation of crosslinking layer on the surface of the tablet. Various types of gaseous plasma treatments oxygen, nitrogen and argon have been successfully used to control drug release from poly(ethylene-co-vinyl acetate) (EVA). Plasma treatments are also effective to control the drug release rates from other types of polymers (Hagiwara et al. 2013). To avoid the initial burst effect and achieve sustained release from a drug-loaded polyurethane (PU), radio frequency (RF) glow discharge plasma polymerization technique was used to deposit a thin layer of butyl methacrylate (BMA) as the rate limiting coating (Kwok et al. 1999). The deposition time and applied power were optimised to obtain an appropriate crosslinked coating barrier for sustained release of drug ciprofloxacin. Tanaka et al. (2006) have used atmospheric pressure plasma of CF_4/He to offer hydrophobic coating on PLGA microcapsule surface and observed no initial burst and the slow release of drug.

6 Conclusions and Future Scopes

Among the emerging technologies for functional coatings, considerable progress in recent years is being witnessed in high-energy-content plasma processes, which involve the application of atmospheric pressure plasma deposition, plasma-assisted atomic layer deposition, pulsed plasma deposition and their hybrid systems. Considering the importance of plasma and its use for developing high-end

advanced biomaterials, this chapter has discussed the types of plasma used for the surface modification of materials in order to introduce functional moieties, micro/nano patterning, protective coatings and sterility for different biomedical applications. Optimal efficiency and longevity of such surfaces make wide applicability and acceptability of this process to create novel surfaces. Plasmas are promising because they are safe, environment friendly, sustain viability, shows precise control on the process and are commercially applicable. Understanding of every single stage of the plasma processing and nature of material to be processed is desirable for effective surface modification. Use of plasma surface modification provide possibility to tailor the structures at molecular level and to control the interfaces between layers and substrates for creating new films/membranes. Generally, on the basis of the nature of plasma used for biomedical applications, it is categorized as lethal-plasma and nonlethal-plasma. High intensities of lethal-plasma causes cell death. This is why, most of the plasma applications are based on lethal-plasma, for inactivation, bio-decontamination and sterilization of biomaterials. However, a paradigm shift is now observed towards the use of nonlethal-plasma based surface modification approach for controlling the responses of biological cells. The non-lethal plasma is often referred to as cold-plasma (low-temperature plasma). Due to the temperature susceptibility of many biological materials, low-temperature plasmas has developed great interest in the scientific community and presenting tremendous potential to be used in the modification of biomaterials. Microplasmas generated using plasma jets and plasma ejected from microdischarges finds applications in biomaterials as they contain high concentrations of excited species and radicals at the target site. This chapter has also summarised various operating parameters involved in plasma processing such as discharge power, exposure time, gas flow rate and type of plasma forming gases (air, argon, oxygen and mixed gases) which play a critical role for altering the surface's chemical functionality and physical morphology. Plasma treatment can significantly enhances hydrophilicity and biocompatibility of a material through the incorporation of polar functional groups and precised topographical changes. Furthermore, these modified surfaces are also suitable for graft polymerization to incorporate specific functional groups for the immobilization of biomolecules. Recent outcomes in regenerative medicine and tissue engineering have created a strong demand of biopolymeric materials those having specifically tailored surfaces to improve existing therapeutic strategies, implants and bio-devices. The plasma processing for modulating the surface chemical composition and morphology can have a direct effect on the behaviour of biomolecules (like, cells and proteins) that are intended to interact with it, which has been elaborated in the later sections of this chapter. Another notable processing is plasma assisted deposition and polymerization that facilitates enrichment of the blood compatibility and cytocompatibility. The research path of plasma science may be extended further into multidisciplinary areas, as we progress into the realm of nano and picometer-scale materials for miniaturizing the devices and their applications.

Besides several advantages of plasma processing, researchers are focusing on preventing the use of hazardous solvents in plasma-based strategies. The use of

such solvents may create problems with regard to cytocompatibility of a material. The use of cold-plasma for the surface modification is considered not to be an old technique which requires further exploration to increase the understanding of scientific community for developing novel biomaterials with desired properties. Until now, plasma processing of surface modification has been carried out extensively on two dimensional (2D) substrates (like, films or thin membranes). However, only few studies have demonstrated the applicability of plasma processing for surface modification of 3D porous scaffolds. Nevertheless, due to the customised needs of tissue engineering, surface modification of 3D porous scaffolds is becoming increasingly important and could be of future research interest in plasma science. A patient-specific (desired shape, size and immunocompatible), interconnected highly porous scaffold adapted with state-of-the-art plasma assisted surface modification technology can significantly improve the success of modern tissue engineering. Importantly, the limited gap between the electrodes in case of atmospheric pressure plasma is one of the major causes that restrict its applicability to modify large size 3D implants and scaffolds. To overcome the above mentioned limitations, development of non-thermal atmospheric pressure plasma torches may be the future to develop biocompatible polymeric and hybrid coatings on the surface of 3D substrates. Recent research findings suggest that plasma processing methods will increase in importance in the advancement of biomedicine. We believe that discoursing the technical aspects of various plasmas and their applications in biomedical fields can be helpful to the scientists and technologists, who are interested in developing this fascinating technology for the benefit of mankind.

References

Abenojar J, T-Coque R, Martínez MA, Martínez JMM (2009) Surface modifications of polycarbonate (PC) and acrylonitrile butadiene styrene (ABS) copolymer by treatment with atmospheric plasma. Surf Coat Technol 203(16):2173–2180

Adler S, Scherrer M, Daschner FD (1998) Costs of low-temperature plasma sterilization compared with other sterilization methods. J Hosp Infect 40(2):125–134

Akitsu T, Ohkawa H, Tsuji M, Kimura H, Kogoma M (2005) Plasma sterilization using glow discharge at atmospheric pressure. Surf Coat Technol 193(1–3):29–34

Alexandrov SE (2009) Chemical vapour deposition: precursors, processes and applications. In: Jones AC, Michel LH (eds), Royal society of chemistry print publication date: 22 Dec 2008 ISBN: 978-0-85404-465-8, doi:10.1039/9781847558794

An YH, Friedman RJ (1997) Laboratory methods for studies of bacterial adhesion. J Microbiol Methods 30(2):141–152

Anders A (2000) Handbook of plasma immersion ion implantation and deposition. Wiley, Hoboken, NJ 2

Andrews KD, Hunt JA, Black RA (2007) Effects of sterilisation method on surface topography and in-vitro cell behaviour of electrostatically spun scaffolds. Biomaterials 28:1014–1026

Arefi F, Andere V, Montazer-Rahmati P, Amouroux J (1992) Plasma polymerization and surface treatment of polymers. Pure Appl Chem 64(5):715–723

Arenholz E, Svorcík V, Kefer T, Heitz J, Bauerle D (1991) Structure formation in UV-laser ablated poly-ethylene-terephthalate (PET). Appl Phys A 53(4):330–331

Arndt S, Wacker E, Kaufmann S, Li YF, Shimizu T, Thomas HM, Morfill GE, Karrer S, Zimmermann JL, Bosserhoff AK (2013) Cold atmospheric plasma, a new strategy to induce senescence in melanoma cells. Exp Dermatol 22(4):284–289

Arnoult G, Cardoso RP, Belmonte T, Henrion G (2008) Flow transition in a small scale microwave plasma jet at atmospheric pressure. Appl Phys Lett (93)19:191507

Arolkar GA, Jacob SM, Pandiyaraj KN, Kelkar-ManeVR Deshmukh RR (2016) Effect of TEOS plasma polymerization on Corn Starch/Poly(ε-caprolactone) film: characterization, properties and biodegradation. RSC Adv 6:16779–16789

Artemenko A, Kylián O, Choukourov A, Gordeev I, Petr M, Vandrovcová M, Polonskyi O, Bačáková L, Slavinska D, Biederman H (2012) Effect of sterilization procedures on properties of plasma polymers relevant to biomedical applications. Thin Solid Films 520(24):7115–7124

Ayhan F, Ayhan H, Piskin E (1998) Sterilization of sutures by low temperature argon plasma. J Bioact Compatible Polym 13(1):65–72

Baier RE (1970) Surface properties influencing biological adhesion In: Mainly RS (ed) Adhesion in biological systems, Academic Press, New York. ISBN: 9780323156110

Balazs DJ, Triandafillu K, Chevolot Y, Aronsson B-O, Harms H, Descouts P, Mathieu HJ (2003) Surface modification of PVC endotracheal tubes by oxygen glow discharge to reduce bacterial adhesion. Surf Interface Anal 35:301–309

Barbucci R, Torricelli P, Fini M, Pasqui D, Favia P, Sardella E, d'Agostino R, Giardino R (2005) Proliferative and re-differentiative effects of photo-immobilized micro-patterned hyaluronan surfaces on chondrocyte cells. Biomaterials 26:7596–7605

Bathina MN, Mickelsen S, Brooks C, Jaramillo J, Hepton T, Kusumoto FM (1998) Safety and efficacy of hydrogen peroxide plasma sterilization for repeated use of electrophysiology catheters. J Am Coll Cardiol 32(5):1384–1388

Beyer D, Knoll W, Ringsdorf H, Wang JH, Timmons RB, Sluka P (1997) Reduced protein adsorption on plastics via direct plasma deposition of triethylene glycol monoallyl ether. J Biomed Mater Res 36(2):181–189

Bhat NV, Nadiger GS (1978) Effect of nitrogen plasma on the morphology and allied textile properties of tassar silk fibres and fabrics. Text Res J 48:685–691

Bhat NV, Wavhal DS (2000a) Preparation of cellulose triacetate pervaporation membrane by ammonia plasma treatment. J Appl Polym Sci 76:258–265

Bhat NV, Wavhal DS (2000b) Characterization of plasma polymerized thiophene onto cellulose acetate membrane and its application to pervaporation. Sep Sci Technol 35(2):227–242

Bhat NV, Deshmukh RR (2014) Plasma processing of textiles to enhance their dyeing and surface properties In: Nema SK, Jhala PB (eds) Plasma technologies for textile and apparel woodhead publishing India. ISBN: 978-938-030-855-5

Bhat NV, Deshmukh RR (2002) X-ray crystallographic studies of polymeric materials. Indian J Pure Appl Phys 40:361–366

Bhat NV, Netravali AN, Gore AV, Sathianarayanan MP, Arolkar GA, Deshmukh RR (2011) Surface modification of cotton fabrics using plasma technology. Text Res J 81(10):1014–1026

Bhat NV, Upadhyay DJ, Deshmukh RR, Gupta SK (2003) Investigation of plasma-induced photochemical reaction on a polypropylene surface. J Phys Chem B 107(19):4550–4559

Bhattacharyya D, Xu H, Deshmukh RR, Timmons RB Nguyen K (2010) Surface chemistry and polymer film thickness effects on endothelial cell adhesion and proliferation. J Biomed Mater Res 94(2):640–648

Bhowmik S, Chaki TK, Ray S, Hoffman F, Dorn L (2004) Effect of surface modification of high-density polyethylene by direct current and radio frequency glow discharge on wetting and adhesion characteristics. Metall Mater Trans A 35(3):865–877

Bialasiewicz AA, Fortsch M, Sammann A, Draeger J (1995) Plasma sterilization of selected ophthalmic instruments for combined intraocular surgery. Ophthalmic Res 27(1):124–127

Boekema BKHL, Hofmann S, van Ham BJT, Bruggeman PJ, Middelkoop E (2013) Antibacterial plasma at safe levels for skin cells. J Phys D: Appl Phys 46:422001 1–7

Boekema BKHL, Vlig M, Guijt D, Hijnen K, Hofmann S, Smits P, Sobota A, van Veldhuizen EM, BruggemanP Middelkoop E (2016) A new flexible DBD device for treating infected wounds:

in vitro and ex vivo evaluation and comparison with a RF argon plasma jet. J Phys D Appl Phys 49(044001):1–10

Bogaerts A, Neyts E, Gijbels R, Mullen J (2002) Gas discharge plasmas and their applications. Spectrochemica Acta Part B 57:609–658

Borcia G, Brown NMD (2007) Hydrophobic coatings on selected polymers in an atmospheric pressure dielectric barrier discharge. J Phys D Appl Phys 40:1927–1936

Borges AMG, Benetoli LO, Licínio MA, Zoldan VC, Santos-Silva MC, Assreuy J, Pasa AA, Debacher NA, Soldi V (2013) Polymer films with surfaces unmodified and modified by non-thermal plasma as new substrates for cell adhesion. Mater Sci Eng, C 33(3):1315–1324

Boxhammer V, Li YF, Köritzer J, Shimizu T, Maisch T, Thomas HM, Schlegel J, Morfill GE, Zimmermann JL (2013) Investigation of the mutagenic potential of cold atmospheric plasma at bactericidal dosages. Mutat Res Genet Toxicol Environ Mutagen 753(1):23–28

Bretagnol F, Ceriotti L, Lejeune M, Papadopoulou-Bouraoui A, Hasiwa M, Gilliland D, Ceccone G, Colpo P, Ross F (2006) Functional micropatterned surfaces by combination of plasma polymerization and lift-off processes. Plasma Processes Polym 3:30–38

Brétagnol F, Rauscher H, Hasiwa M, Kylián O, Ceccone G, Hazell L, Paul AJ, Lefranc O, Rossi F (2008) The effect of sterilization processes on the bioadhesive properties and surface chemistry of a plasma-polymerized polyethylene glycol film: XPS characterization and L929 cell. Acta Biomater 4(6):1745–1751

Brígido-Diego R, Sánchez MS, Ribelles JLG, Pradas MM (2007) Effect of γ-irradiation on the structure of poly(ethyl acrylate-co-hydroxyethyl methacrylate) copolymer networks for biomedical applications. J Mater Sci Mater Med 18(5):693–698

Bunshah RF (1994) Handbook of deposition technologies for films and coatings: Science, technology and applications. Noyes Publications, Park Ridge, NJ

Bussiahn R, Brandenburg R, Gerling T, Kindel E, Lange H, Lembke N, Weltmann KD, von Woedtke T, Kocher T (2010) The hairline plasma: An intermittent negative dc-corona discharge at atmospheric pressure for plasma medical applications. Appl Phys Lett 96 (14):143701

Buttiglione M, Vitiello F, Sardella E, Petrone L, Nardulli M, Favia P, d'Agostino R, Gristina R (2007) Behaviour of SH-SY5Y neuroblastoma cell line grown in different media and on different chemically modified substrates. Biomaterials 28:2932–2945

Chandy T, Das GS, Wilson RF, Rao GHR (2000) Use of plasma glow for surface-engineering biomolecules to enhance blood compatibility of Dacron and PTFE vascular prosthesis. Biomaterials 21(7):699–712

Chau TT, Kao KC, Blank G, Madrid F (1996) Microwave plasmas for low-temperature dry sterilization. Biomaterials 17(13):1273–1277

Chen JP, Su CH (2011) Surface modification of electrospun PLLA nanofibers by plasma treatment and cationized gelatin immobilization for cartilage tissue engineering. Acta Biomater 7(1):234–243

Chen JY, Wang LP, Fu KY, Huang N, Leng Y, Leng P, Yang YX, Wang J, Wan GJ, Sun H, Tian XB, Chu PK (2002) Blood compatibility and sp3/sp2 contents of diamond-like carbon (DLC) synthesized by plasma immersion ion implantation-deposition. (Special 6th Plasma-Based Ion Implantation workshop issue). Surf Coat Technol 156(1–3):289–294

Chen Y, Kang ET, Neoh KG, Wang P, Tan KL (2000) Surface modification of polyaniline film by grafting of poly(ethylene glycol) for reduction in protein adsorption and platelet adhesion. Synth Met 110(1):47–55

Chen Y, Gao Q, Wan H, Yi J, Wei Y, Liu P (2013) Surface modification and biocompatible improvement of polystyrene film by Ar, O_2 and Ar + O_2 plasma. Appl Surf Sci 265(15):452–457

Chen W, Ji-rong C, Li R (2008) Studies on surface modification of poly(tetrafluoroethylene) film by remote and direct Ar plasma. Appl Surf Sci 254(9):2882–2888

Chengwei C, Zhiming Z, Xitang T, Wang Y, Sun XT (1995) Influence of rapidly solidified structures on wear behavior of Ti-6AI-4V laser alloyed with TiC. Tribol Trans 38(4):875–878

Chu CFL, Lu A, Liszkowski M, Sipehia R (1999) Enhanced growth of animal and human endothelial cells on biodegradable polymers. Biochim Biophys Acta 1472(3):479–485
Chu PK, Chen JY, Wang LP, Huang N (2002) Plasma-surface modification of biomaterials. Mater Sci Eng R 36(5–6):143–206
Clark DT, Dilks A, Shuttleworth D (1978) Polymer surfaces. In: Clark DT, Feast WJ (eds) 1st edn. Wiley, New York, pp 185–210. ISBN-13: 978-0471996149
Clark DT, Hutton DR (1987) Surface modification by plasma techniques. I. The interactions of a hydrogen plasma with fluoropolymer surfaces. J Polym Sci, Part A: Polym Chem 25:2643
Claudia ES, Ana-Maria S, Sorin V, Catalin L, Lucia M, Amine A, Gheorghe D (2014) Plasma functionalization of carbon nanowalls and its effect on attachment of fibroblast-like cells. J Phys D Appl Phys 47:265203
Cole MA, Thissen H, Losic D, Voelcker NH (2007) A new approach to the immobilisation of poly (ethylene oxide) for the reduction of non-specific protein adsorption on conductive substrates. Surf Sci 601(7):1716–1725
Conrads H, Schmidt M (2000) Plasma generation and plasma sources. Plasma Sources Sci Technol 9(4):441–454
Cools P, Geyter N, Vanderleyden E, Dubruel P, Morent R (2014) Surface analysis of titanium cleaning and activation processes: non-thermal plasma versus other techniques. Plasma Chem Plasma Process 34(4):917–932
Cui FZ, Luo ZS (1999) Biomaterials modification by ion-beam processing. Surf Coat Technol 112(1–3):278–285
Cui NY, Brown NMD (2002) Modification of the surface properties of a polypropylene (PP) film using an air dielectric barrier discharge plasma. Appl Surf Sci 189(1–2):31–38
Daw R, Candan S, Beck AJ, Devlin AJ, Brook IM, MacNeil S, Dawson RA, Short RD (1998) Plasma copolymer surfaces of acrylic acid/1,7 octadiene: Surface characterisation and the attachment of ROS 17/2.8 osteoblast-like cells. Biomaterials 19:1717–1725
Dearnaley G, Arps JH (2005) Biomedical applications of diamond-like carbon (DLC) coatings: a review. Surf Coat Technol 200(7):2518–2524
Dearnaley G, Hartley NEW (1978) Ion implantation into metals and cabrides. Thin Solid Films 54(2):215–232
DeFife KM, Colton E, Nakayama Y, Matsuda T, Anderson JM (1999) Spatial regulation and surface chemistry control of monocyte/macrophage adhesion and foreign body giant cell formation by photochemically micropatterned surfaces. J Biomed Mater Res 45(2):148–154
Degoutin S, Jimenez M, Casetta M, Bellayer S, Chai F, Blanchemain N, Neut C, Kacem I, Traisnel M, Martel B (2012) Anticoagulant and antimicrobial finishing of non-woven polypropylene textiles. Biomed Mater 7(3):035001
Dekker A, Reitsma K, Beugeling T, Bantjes A, Feijien J, van Aken WG (1991) Adhesion of endothelial cells and adsorption of serum proteins on gas plasma-treated polytetrafluoroethylene. Biomaterials 12(2):130–138
Deshmukh RR, Shetty AR (2007a) Surface characterization of polyethylene films modified by gaseous plasma. J Appl Polym Sci 104(1):449–457
Deshmukh RR, Shetty AR (2008) Comparison of surface energies using various approaches and their suitability. J Appl Polym Sci 107:3707–3717
Deshmukh RR, Bhat NV (2011) Pre-treatments of textiles prior to dyeing: plasma processing. In: Hauser PJ (ed) Textile Dyeing In Tech Publisher, December, ISBN 978-953-307-565-5
Deshmukh RR, Shetty AR (2007b) Modification of polyethylene surface using plasma polymerization of silane. J Appl Polym Sci 106(6):4075–4082
Deshmukh RR, Bhat NV (2003) The mechanism of adhesion and printability of plasma processed PET films. Mater Res Innovations 7(5):283–290
Detomaso L, Gristina R, d'Agostino R, Senesi GS, Favia P (2005b) Plasma deposited acrylic acid coatings: Surface characterization and attachment of 3T3 murine fibroblast cell lines. Surf Coat Technol 200(1–4):1022–1025
Detomaso L, Gristina R, Senesi GS, d'Agostino R, Favia P (2005a) Stable plasma-deposited acrylic acid surfaces for cell culture applications. Biomaterials 26(18):3831–3841

Deynse AV, Cools P, Leys C, Morent R, Geyter ND (2014) Influence of ambient conditions on the aging behaviour of plasma-treated polyethylene surfaces. Surf Coat Technol 258:359–367

Djordjevic I, Britcher LG, Kumar S (2008) Morphological and surface compositional changes in poly(lactide-co-glycolide) tissue engineering scaffolds upon radio frequency glow discharge plasma treatment. Appl Surf Sci 254(7):1929–1935

Dhayal M, Cho SI (2006) Leukaemia cells interaction with plasma-polymerized acrylic acid coatings. Vacuum 80(6):636–642

Dhayal M, Forder D, Parry KL, Short RD, Bradley JW (2003) Using an afterglow plasma to modify polystyrene surfaces in pulsed radio frequency (RF) argon discharges. In: Proceedings of the eight international conference on plasma surface engineering, surface and coatings technology, pp 174–175:872–876

Ding Z, Chen J, Gao S, Chang J, Zhang J, Kang ET (2004) Immobilization of chitosan onto poly-l-lactic acid film surface by plasma graft polymerization to control the morphology of fibroblast and liver cells. Biomaterials 25(6):1059–1067

Dixon D, Meenan BJ (2012) Atmospheric dielectric barrier discharge treatments of polyethylene, polypropylene, polystyrene and poly(ethylene terephthalate) for enhanced adhesion. J Adhes Sci Technol 26(20–21):2325–2337

Dreher D, Junod AF (1996) Role of oxygen free radicals in cancer development. Eur J Cancer 32(1):30–38

Durante M, Furusawa Y, George K, Gialanella G, Greco O, Grossi G, Matsufuji N, Pugliese M, Yang TC (1998) Rejoining and misrejoining of radiation-induced chromatin breaks IV charged particles. Radiat Res 149(5):446–454

Ehlbeck J, Schnabel U, Polak M, Winter J, Woedtke Tvon, Brandenburg R, Hagen Tvondem, Weltmann KD (2011) Low temperature atmospheric pressure plasma sources for microbial decontamination. J Phys D Appl Phys 44(1):18 (013002)

Encinas N, Díaz-Benito B, Abenojar J, Martínez MA (2010) Extreme durability of wettability changes on polyolefin surfaces by atmospheric pressure plasma torch. Surf Coat Technol 205 (2):396–402

Enderle J, Blanchard S, Bronzino J (1999) Microbial Sensors In: Introduction to biomedical engineering, Elsevier Academic Press, New York, p 538. ISBN: 0-12-238660-0

Ensinger W (1992) Ion sources for ion beam assisted thin-film deposition. Rev Sci Instrum 63:5217–5233

Favia P, d'Agostino R (1998) Plasma treatments and plasma deposition of polymers for biomedical applications. In: Fifth international conference on plasma surface engineering and surface coatings technology, vol 98, issue 1–3, pp 1102–1106

Favia P, Perez-Luna VH, Boland T, Castner DG, Ratner BD (1996) Surface chemical composition and fibrinogen adsorption-retention of fluoropolymer films deposited from an RF glow discharge. Plasmas Polym 1(4):299–326

Feng X, Zhang J, Xie H, Hu Q, Huang Q, Liu W (2003) The RF plasma polymer of lysine and the growth of human nerve cells on its surface. In: Proceedings from the joint international symposia of the 6th APCPST, 15th SPSM, 4th international conference on open magnetic systems for plasma confinement and 11th KAPRA. Surf Coat Technol 171(1–3):96–100

Finke B, Schröder K, Ohl A (2009) Structure retention and water stability of microwave plasma polymerized films from allylamine and acrylic acid. Supplement: eleventh international conference on plasma surface engineering (PSE2008). Plasma Processes Polym (1):S70–S74

Finke B, Hempel F, Testrich H, Rebl H, Kylián O, Meichsner J, Biederman H, Nebe B, Weltmann KD, Schröder K (2011) Plasma processes for cell-adhesive titanium surfaces based on nitrogen-containing coatings. In: PSE 2010 special issue proceedings of the 12th international conference on plasma surface engineering. Surf Coat Technol 205(2):S520–S524

Finke B, Luethen F, Schroeder K, Mueller PD, Bergemann C, Frant M, Ohl A, Nebe B (2007) The effect of positively charged plasma polymerization on initial osteoblastic focal adhesion on titanium surfaces. Biomaterials 28(30):4521–4534

Flounders AW, Brandon DL, Bates AH (1997) Patterning of immobilized antibody layers via photolithography and oxygen plasma exposure. Biosens Bioelectron 12(6):447–456

Formichi MJ, Guidoin RG, Jausseran JM, Awad JA, Johnston KW, King MW, Courbier R, Marois M, Rouleau C, Batt M, Girard JF, Gosselin C (1988) Expanded PTFE prostheses as arterial substitutes in humans: late pathological findings in 73 excised grafts. Ann Vasc Surg 2(1):14–27

Fracassi F, d'Agostino R, Lamendola R, Filippo A, Rapisarda C, Vasquez P (1996) Plasma assisted dry etching of cobalt silicide for microelectronics applications. J Electrochem Soc 143 (2):701–707

Frankenberg-Schwager M, Frankenberg D (1990) DNA double-strand breaks: their repair and relationship to cell killing in yeast. Int J Radiat Biol 58(4):569–575

Fricke K, Koban I, Tresp H, Jablonowski L, Schröder K, Kramer A, Weltmann KD, Tvon Woedtke, Kocher T (2012) Atmospheric pressure plasma: a high-performance tool for the efficient removal of biofilms. PLoS ONE 7(8):e42539. doi:10.1371/journal.pone.0042539

Gadri RB, Roth JR, Montie TC, Kelly-Wintenberg K, Tsai PPY, Helfritch DJ, Feldman P, Sherman DM, Karakaya F, Chen Z (2000) Sterilization and plasma processing of room temperature surfaces with a one atmosphere uniform glow discharge plasma (OAUGDP). UTK plasma sterilization team. Surf Coat Technol 131(1–3):528–541

Geyter ND, Morent R, Van Vlierberghe S, Dubruel P, Leys C, Gengembre L, Schacht E, Payen E (2009) Deposition of polymethyl methacrylate on polypropylene substrates using an atmospheric pressure dielectric barrier discharge. In: Coatings Science International 2008. Prog Org Coat 64(2–3):230–237

Geyter N, Dubruel P, Morent R, Leys C (2014) Plasma assisted surface modification of polymeric biomaterials. In: Chu PK, Lu X (eds) Low temperature plasma technology: Methods and applications. CRC Press, Florida, pp 401–418. ISBN 13:978-1-4665-0991-7

Gogolewski S, Varlet PM, Dillon JG (1996) Sterility, mechanical properties, and molecular stability of polylactide internal-fixation devices treated with low-temperature plasmas. J Biomed Mater Res 32:227–235

Gomathi N, Sureshkumar A, Neogi S (2008) RF plasma-treated polymers for biomedical applications. Curr Sci 94(11):1478–1496

Gomathi N, Rajasekar R, Babu RR, Mishra D, Neogi S (2012) Development of bio/blood compatible polypropylene through low pressure nitrogen plasma surface modification. Mater Sci Eng, C 32(7):1767–1778

Goodman SL, Tweden KS, Albrecht RM (1996) Platelet interaction with pyrolytic carbon heart-valve leaflets. J Biomed Mater Res 32(2):249–258

Griesser HJ, Chatelier RC, Gengenbach TR, Johnson G, Steele JG (1994) Growth of human cells on plasma polymers: putative role of amine and amide groups. J Biomater Sci Polym Ed 5(6):531–554

Gristina R, D'Aloia E, Senesi GS, Milella A, Nardulli M, Sardella E, Favia P, d'Agostino R (2008) Increasing cell adhesion on plasma deposited fluorocarbon coatings by changing the surface topography. J Biomed Mater Res B: Appl Biomater 88B(1):139–149

Gubala V, Le NCH, Gandhiraman RP, Coyle C, Daniels S, Williams DE (2010) Functionalization of cyclo-olefin polymer substrates by plasma oxidation: Stable film containing carboxylic acid groups for capturing biorecognition elements. Colloids Surf, B 8:544–548

Gupta B, Hilborn J, Hollenstein C, Plummer CJG, Houriet R, Xanthopoulos N (2000) Surface modification of polyester films by RF plasma. J Appl Polym Sci 78(5):1083–1091

Gupta B, Plummer C, Bisson I, Frey P, Hilborn J (2002) Plasma-induced graft polymerization of acrylic acid onto poly(ethylene terephthalate) films: characterization and human smooth muscle cell growth on grafted films. Biomaterials 23:863–871

Gupta AK, Gupta M (2005) Synthesis and surface engineering of iron oxide nanoparticles for biomedical applications. Biomaterials 26(18):3995–4021

Guschl P, Hicks R, MacDavid S (2008) Atmospheric oxygen-helium plasma surface modification of medical plastics. In: Plasma Science, 2008. ICOPS 2008. IEEE 35th international conference on plasma science, Karlsruhe 2008, pp 1–1. doi:10.1109/PLASMA.2008.4590932

Ha SW, Hauert R, Ernst KH, Wintermantel E (1997) Surface analysis of chemically-etched and plasma-treated polyetheretherketone (PEEK) for biomedical applications. Surf Coat Technol 96(2–3):293–299

Hagiwara K, Hasebe T, Hotta A (2013) Effects of plasma treatments on the controlled drug release from poly(ethylene-co-vinyl acetate). Surf Coat Technol 216:318–323

Hamerli P, Weigel T, Groth T, Paul D (2003) Surface properties of and cell adhesion onto allylamine-plasma coated poly ethylene terephtalate membranes. Biomaterials 24:3989–3999

Harper JME, Cuomo JJ, Gambino RJ, Kaufman HR (1984) In Auciello O, Kelly R (eds) Ion bombardment modification of surfaces: fundamentals and applications. Elsevier, Amsterdam, pp 127–162

Harris LG, Tosatti S, Wieland M, Textor M, Richards RG (2004) Staphylococcus aureus adhesion to titanium oxide surfaces coated with non-functionalized and peptide-functionalized poly (l-lysine)-grafted-poly(ethylene glycol) copolymers. Biomaterials 25(18):4135–4148

Hench LL (1998) Biomaterials: a forecast for the future. Biomaterials 19(16):1419–1423

Herbert T (2009) In: Shishu R (ed) Plasma technologies for textiles. Cambridge, Woodhead publications, ISBN: 9781845690731

Heyse P, Roeffaers MBJ, Paulussen S, Hofkens J, Jacobs PA, Sels BF (2008) Protein immobilization using atmospheric-pressure dielectric-barrier discharges: a route to a straightforward manufacture of bioactive films. Plasma Processes Polym 5(2):186–191

Hill D (1998) Design engineering of biomaterials for medical devices. Wiley-VCHISBN 0-471-96708-4, p 480

Hollahan JR, Bell AT (1984) Techniques and applications of plasma chemistry. Wiley, New York

Holy CE, Cheng C, Davies JE, Shoichet MS (2001) Optimizing the sterilization of PLGA scaffolds for use in tissue engineering. Biomaterials 22(1):25–31

Hopwood J (1992) Review of inductively coupled plasmas for plasma processing. Plasma Sources Sci Technol 1(2):109–116

Hori K, Matsumoto S (2010) Bacterial adhesion: From mechanism to control. Biochem Eng J 48 (3):424–434

Hsu S, Lin CH, Tseng CS (2012) Air plasma treated chitosan fibers-stacked scaffolds. Biofabrication 4(015002):1–13. doi:10.1088/1758-5082/4/1/015002

Hsu S, Chen W (2000) Improved cell adhesion by plasma-induced grafting of l-lactide onto polyurethane surface. Biomaterials 21(4):359–367

Huang N, Yang P, Chen X, Leng YX, Zeng XL, Jun GJ, Zheng ZH, Zhang F, Chen YR, Liu XH (1998) Blood compatibility of amorphous titanium oxide films synthesized by ion beam enhanced deposition. Biomaterials 19(7–9):771–776

Inoue M, Suzuki Y, Takagi T (1997) Review of ion engineering center and related projects in ion engineering research institute. In: Materials synthesis and modification by ion and/or laser beams. Nucl Instr Meth Phys Res B 121(1–4):1–6

Intranuovo F, Sardella E, Gristina R, Nardulli M, White L, Howard D, Shakesheff KM, Alexander MR, Favia P (2011) PE-CVD processes improve cell affinity of polymer scaffolds for tissue engineering. Surf Coat Technol 205:S548–S551

Ito Y (1999) Surface micro patterning to regulate cell functions. Biomaterials 20(23–24):2333–2342

Iyer R, Lehnert BE (2002) Low dose, low-LET ionizing radiation-induced radio adaptation and associated early responses in unirradiated cells. Mutat Res Fundam Mol Mech Mutagen 503(1–2):1–9

Janda M, Martisovits V, Machala Z (2011) Transient spark: a dc-driven repetitively pulsed discharge and its control by electric circuit parameters. Plasma Sources Sci Technol 20:035015. doi:10.1088/0963-0252/20/3/035015

Jansen B, Kohnen W (1995) Prevention of biofilm formation by polymer modification. J Ind Microbiol 15(4):391–396

Jayagopal A, Stone GP, Haselton FR (2008) Light-guided surface engineering for biomedical applications. Bioconjugate Chemistry 19(3):792–796

Jiao Y, Xu J, Zhou C (2012) Effect of ammonia plasma treatment on the properties and cytocompatibility of a Poly (L-Lactic Acid) film surface. J Biomater Sci Polym Ed 23(6):763–777

Joh HM, Kim SJ, Chung TH, Leem SH (2012) Reactive oxygen species-related plasma effects on the apoptosis of human bladder cancer cells in atmospheric pressure pulsed plasma jets. Appl Phys Lett 101(5):053703

Kalghatgi S, Friedman G, Fridman A, Clyne AM (2010) Endothelial cell proliferation is enhanced by low dose non-thermal plasma through fibroblast growth factor-2 release. Ann Biomed Eng 38(3):748–757

Kaczmarek H, Kowalonek J, Szalla A, Sionkowska A (2002) Surface modification of thin polymeric films by air-plasma or UV-irradiation. Surf Sci 507–510:883–888

Kang MS, Chun B, Kim SS (2001) Surface modification of polypropylene membrane by low-temperature plasma treatment. J Appl Polym Sci 81(6):1555–1566

Kapur R, Spargo BJ, Chen MS, Calvert JM, Rudolph AS (1996) Fabrication and selective surface modification of 3-dimensionally textured biomedical polymers from etched silicon substrates. J Biomed Mater Res 33(4):205–216

Karakecili AG, Demirtas TT, Satriano C, Gümüsderelioglu M, Marletta G (2007) Evaluation of L929 fibroblast attachment and proliferation on Arg-Gly-Asp-Ser (RGDS)-immobilized chitosan in serum-containing/serum-free cultures. J Biosci Bioeng 104(1):69–77

Katsikogianni M, Amanatides E, Mataras D, Missirlis YF (2008) Staphylococcus epidermidis adhesion to He, He/O_2 plasma treated PET films and aged materials: Contributions of surface free energy and shear rate. Colloids Surf, B 65(2):257–268

Khorasani MT, Mirzadeh H, Irani S (2008) Plasma surface modification of poly (l-lactic acid) and poly (lactic-co-glycolic acid) films for improvement of nerve cells adhesion. Radiat Phys Chem 77(3):280–287

Kim DB, Rhee JK, Gweon B, Moon SY, Choe W (2007) Comparative study of atmospheric low pressure and radio frequency microjet plasmas produced in a single electrode configuration. Appl Phys Lett 91:151502

Kim JS, Kim YK, Lee KH (2004) Effects of atmospheric plasma treatment on the interfacial characteristics of ethylene-vinyl acetate/polyurethane composites. J Colloid Interface Sci 271 (1):187–191

Kim YJ, Kang IK, Huh MW, Yoon SC (2000) Surface characterization and in vitro blood compatibility of poly(ethylene terephthalate) immobilized with insulin and/or heparin using plasma glow discharge. Biomaterials 21(2):121–130

Kremers HM, Larson DR, Crowson CS, Kremers WK, Washington RE, Steiner CA, Jiranek WA, Berry DJ (2015) Prevalence of total hip and knee replacement in the United States. J Bone Joint Surg 97(17):1386–1397

Ko YM, Lee K, Kim BH (2012) Bone like apatite formation on modified Ti surfaces with COOH, NH_2, and OH functional groups by plasma polymerization. In: The 3rd international conference on microelectronics and plasma technology (ICMAP) 2011. Thin Solid Films 521:128–131

Kogelschatz U, Eliasson B, Egli W (1999) From ozone generators to flat television screens: history and future potential of dielectric-barrier discharges. Pure Appl Chem 71(10):1819–1828

Kogelschatz U (2003) Dielectric-barrier discharges: Their history, discharge physics and industrial applications. Plasma Chem Plasma Process 23(1):1–46

Korachi M, Gurol C, Aslan N (2010) Atmospheric plasma discharge sterilization effects on whole cell fatty acid profiles of Escherichia coli and Staphylococcus aureus. J Electrostat 68(6):508–512

Kumar DS, Banji D, Madhavi B, Bodanapu V, Dondapati S, Sri AP (2009) Nanostructured porous silicon—a novel biomaterials for drug delivery. Int J Pharm Pharm Sci 1(2):8–16

Kumar V, Jolivalt C, Pulpytel J, Jafari R, Arefi-Khonsari F (2013) Development of silver nanoparticle loaded antibacterial polymer mesh using plasma polymerization process. J Biomed Mater Res, Part A 101A(4):1121–1132

Kuzuya M, Sasai Y, Yamauchi Y, Kondo S (2008) Pharmaceutical and biomedical engineering by plasma techniques. J Photopolym Sci Technol 21(6):785–798

Kwok CS, Horbett TA, Ratner BD (1999) Design of infection—resistant antibiotic-releasing polymers II. Controlled release of antibiotics through a plasma deposited thin film barrier. J Controlled Release 62:301–311

Laroussi M (2005) Low temperature plasma based sterilization: overview and state-of-the-art. Plasma Processes Polym 2(5):391–400

Laroussi M, Akan T (2007) Arc-free atmospheric pressure cold plasma jets: a review. Plasma Processes Polym 4(9):777–788

Lee J, Hong J, Pearton S (1996) Etching of InP at ≳1 μm/min in Cl_2/Ar plasma chemistries. Appl Phys Lett 68(6):847–849

Lee EH, Rao GR, Lewis MB, Mansur LK (1994) Effects of electronic and recoil processes in polymers during ion implantation. J Mater Res 9(4):1043–1050

Lee JS, Kaibara M, Iwaki M, Sasabe I, Suzuki Y, Kusakabe M (1993) Selective adhesion and proliferation of cells on ion-implanted polymer domains. Biomaterials 14(12):958–960

Lee JH, Kwon JS, Om JY, Kim YH, Choi EH, Kim KM, Kim KN (2014) Cell immobilization on polymer by air atmospheric pressure plasma jet treatment. Jpn J Appl Phys 53:086202

Lee KJ, Kim SM, Ho BJ, Kim KT, Kim GC, Park GY (2011) biomedical applications of low temperature atmospheric pressure plasmas to cancerous cell treatment and tooth bleaching. Jpn J Appl Phys 50:08JF01

Leeuwenburgh SCG, Malda J, Rouwkema J, Kirkpatrick CJ (2008) Trends in biomaterials research: an analysis of the scientific programme of the World Biomaterials Congress 2008. Biomaterials 29:3047–3052

Leng YX, Yang P, Chen JY, Sun H, Wang J, Wang GJ, Huang N, Tian XB, Chu PK (2001a) Fabrication of Ti–O/Ti–N duplex coatings on biomedical titanium alloys by metal plasma immersion ion implantation and reactive plasma nitriding/oxidation. Surf Coat Technol 138(2–3):296–300

Leng WH, Zhang Z, Cheng SA, Zhang JQ, Nan C (2001b) Estimation of photoelectrocatalytic activity of titanium oxide film electrodes by AC impedance. Chin Chem Lett 12:1019

Lerouge S, Fozza AC, Wertheimer MR, Marchand R, Yahia LH (2000a) Sterilization by low-pressure plasma: the role of vacuum-ultraviolet radiation. Plasmas Polym 5(1):31–46

Lerouge S, Guignot C, Tabrizian M, Ferrier D, Yagoubi N, Yahia LH (2000b) Plasma-based sterilization: Effect on surface and bulk properties and hydrolytic stability of reprocessed polyurethane electrophysiology catheters. J Biomed Mater Res 52(4):774–782

Lerouge S, Wertheimer MR, Marchand R, Tabrizian M, Yahia LH (2000c) Effect of gas composition on spore mortality and etching during low-pressure plasma sterilization. J Biomed Mater Res 51(1):128–135

Levif P, Séguin J, Moisan M, Soum-Glaude A, Barbeau J (2011) Packaging materials for plasma sterilization with the flowing afterglow of an N_2–O_2 discharge: damage assessment and inactivation efficiency of enclosed bacterial spores. J Phys D: Appl Phys 44(40) 405201:13 pp

Lhoest JB, Detrait E, Dewez JL, den Bosch Van, de Aguilar P, Bertrand P (1996) A new plasma-based method to promote cell adhesion on micrometric tracks on polystyrene substrates. J Biomater Sci Polym Ed 7(12):1039–1054

Li R, Chen JR (2006) Studies on wettability of medical poly(vinyl chloride) by remote argon plasma. Appl Surf Sci 252(14):5076–5082

Li YH, Huang YD (2007) Engineering the study of collagen immobilization on polyurethane by oxygen plasma treatment to enhance cell adhesion and growth. In: Proceedings of the fifth Asian-European international conference on plasma surface engineering-AEPSE 2005 proceedings of the fifth asian-european international conference on plasma surface. Surf Coat Technol 201(9–11):5124–5127

Liefeith K, Sauberlich S, Frant M, Klee D, Richter EJ, Hocker H, Spiekermann H (1998) Characterization of the properties of differently modified titanium surfaces for dental implantology. 1: Methods for surface analysis. Biomedical technology. Biomed Eng 43(11):330–335

Liu JH, Liu XY, Hu K, Liu DW, Lu XP, Iza F, Kong MG (2011) Plasma plume propagation characteristics of pulsed radio frequency plasma. Appl Phys Lett 98(15):151502

Long M, Rack HJ (1998) Titanium alloys in total joint replacement—a materials science perspective. Biomaterials 19(18):1621–1639

Lupu AR, Georgescu N (2010) Cold atmospheric plasma jet effects on V79-4 cells. Roum Arch Microbiol Immunol 69(2):67–74

Majani R, Zelzer M, Gadegaard N, Rose FR, Alexander MR (2010) Preparation of Caco-2 cell sheets using plasma polymerised acrylic acid as a weak boundary layer. Biomaterials 31 (26):6764–6771

Mansour MM, E-Sayed NM, Farag OF, Elghazaly MH (2013) Effect of He and Ar addition on N_2 glow discharge characteristics and plasma diagnostics. Arab J Nucl Sci Appl 46(1):116–125

Marlowe DA (1997) Biocompatibility: assessment of medical devices and materials In: Braybrook JH (ed) Biomaterials sciences and engineering. Wiley, p 246

Marciano de Paul JA, Realino de Paul J, Pimenta FC, Rezende MH, Bara MTF (2009) Antimicrobial activity of the crude ethanol extract from Pimentapseudocaryophyllus. Pharm Biology 47(10):987–993

Markets and Markets (Dec. 2015; report code: BT 1556) http://www.marketsandmarkets.com/PressReleases/global-biomaterials.asp. Accessed 02 Sept 2016

Martin Y, Boutin D, Vermette P (2007) Study of the effect of process parameters for n-heptylamine plasma polymerization on final layer properties. Thin Solid Films 515 (17):6844–6852

Mattox DM (1989) Particle bombardment effects on thin-film deposition: A review. J Vac Sci Technol, A 7:1105–1114

Matthes R, Koban I, Bender C, Masur K, Kindel E, Weltmann KD, Kocher T, Kramer A, Hübner NO (2013) Antimicrobial efficacy of an atmospheric pressure plasma jet against biofilms of Pseudomonas Aeruginosa and Staphylococcus Epidermidis. Plasma Processes Polym 10(2):161–166

Mckellop HA, Rostlund TV (1990) The wear behavior of ion-implanted Ti-6Al-4V against UHMW polyethylene. J Biomed Mater Res 24(11):1413–1425

Mendhe P, Arolkar GA, Shukla SR, Deshmukh RR (2016) Low temperature plasma processing for the enhancement of surface properties and dyeability of wool fabric. J Appl Polym Sci 133(12):43097(1–8)

Miao H, Yun G (2011) The sterilization of Escherichia coli by dielectric-barrier discharge plasma at atmospheric pressure. Appl Surf Sci 257(16):7065–7070

Mitchell SA, Davidson MR, Emmison N, Bradley RH (2004) Isopropyl alcohol plasma modification of polystyrene surfaces to influence cell attachment behaviour. Surf Sci 561:110–120

Moreira AJ, Mansano RD, Pinto TA, Rua R, Zambon LD, Da Silva MV, Verdonck PB (2004) Sterilization by oxygen plasma. Appl Surf Sci 235:151–155

Morra M, Occhiello E, Garbassi F (1989) Contact angle hysteresis on oxygen plasma treated polypropylene surfaces. J Colloid Interface Sci 504:132

Mow VC, Soslowsky LJ (1991) Friction, lubrication, and wear- of diarthrodial joints. In: Mow VC, Hayes WC (eds) Basic orthopaedic biomechanics. Raven Press Ltd., New York, pp 245–292

Moy E, Lin FYH, Vogtle JW, Policova Z, Neumann AW (1994) Contact angle studies of the surface properties of covalently bonded poly-l-lysine to surfaces treated by glow-discharge. Colloid Polym Sci 272(10):1245–1251

Mrad O, Saloum S, Al-Mariri A (2013) Effect of a new low pressure SF_6 plasma sterilization system on polymeric devices. Vacuum 88:11–16

Müller WU, Streffer C (1991) biological indicators for radiation damage. Int J Radiat Biol 59(4):863–873

Mundo RD, Gristina R, Sardella E, Intranuovo F, Nardulli M, Milella A, Palumbo F, d'Agostino R, Favia P (2010) Micro/Nano scale structuring of cell-culture substrates with fluorocarbon plasmas. Plasma Processes Polym 7:212–223

Mustard JF, Packham MA (1975) The role of blood and platelets in atherosclerosis and the complications of atherosclerosis. Thrombosis et Diathesis Haemorrhagica 33(3):444–456

Mwale F, Wang HT, Nelea V, Luo L, Antoniou J, Wertheimer MR (2006) The effect of glow discharge plasma surface modification of polymers on the osteogenic differentiation of committed human mesenchymal stem cells. Biomaterials 27:2258–2264

Myung SW, Ko YM, Hoon KB (2014) Protein adsorption and cell adhesion on three-dimensional polycaprolactone scaffolds with respect to plasma modification by etching and deposition techniques. Jpn J Appl Phys 53:11RB01

Nair LS, Laurencin CT (2006) Polymers as biomaterials for tissue engineering and controlled drug delivery. Adv Biochem Eng Biotechnol 102:47–90

Nandakumar A, Tahmasebi Birgani Z, Santos D, Mentink A, Auffermann N, van der Werf K, Bennink M, Moroni L, van Blitterswijk C, Habibovic P (2012) Surface modification of electrospun fibre meshes by oxygen plasma for bone regeneration. Biofabrication 5(1):015006

Nasonova E, Gudowska-Nowak E, Ritter S, Kraft G (2001) Analysis of Ar-ion and X-ray-induced chromatin breakage and repair in V79 plateau-phase cells by the premature chromosome condensation technique. Int J Radiat Biol 77(1):59–70

Natarajan AT (2001) Fluorescence in situ hybridization (FISH) in genetic toxicology. J Environ Pathol Toxicol Oncol 20(4):293–299

Neděla O, Slepičk P, Kolská Z, Kasálková NS, Sajdl P, Veselý M, Švorčík V (2016) Functionalized polyethylene naphthalate for cytocompatibility improvement. React Funct Polym 100:44–52

Noeske M, Jost D, Silke S, Uwe L (2004) Plasma jet treatment of five polymers at atmospheric pressure: surface modifications and the relevance for adhesion. Int J Adhes Adhes 24:171–177

Nunez MI, McMillan TJ, Valenzuela MT, Ruiz de Almodovar JM, Pedraza V (1996) Relationship between DNA damage, rejoining and cell killing by radiation in mammalian cells. Radiother Oncol (1996) 39(2):155–165

Ohl A, Schroder K (1999) Plasma-induced chemical micro patterning for cell culturing applications: a brief review. Surf Coat Technol 116–119:820–830

Okada T, Ikada Y (1995) Surface modification of silicone for percutaneous implantation. J Biomater Sci Polym Ed 7(2):171–180

Okada T, Yoshito I (1992) In vitro and in vivo digestion of collagen covalently immobilized onto the silicone surface. J Biomed Mater Res 26(12):1569–1581

Ou J, Wang J, Zhang D, Zhang P, Liu S, Yan P, Liu B, Yang S (2010) Fabrication and biocompatibility investigation of TiO_2 films on the polymer substrates obtained via a novel and versatile route. Colloids Surf, B 76:123–127

Paisoonsin S, Pornsunthorntawee O, Rujiravanit R (2013) Preparation and characterization of ZnO-deposited DBD plasma-treated PP packaging film with antibacterial activities. Appl Surf Sci 273:824–835

Pandiayaraj KN, Selvarajan V, Rhee YH, Kim HW, Pavesec M (2010) Effect of dc glow discharge plasma treatment on PET/TiO_2 thin film surfaces for enhancement of bioactivity. Colloids Surf, B 79:53–60

Pandiyaraj KN, RamKumar MC, Kumar AA, Padmanabhan PVA, Deshmukh RR, Bendavid A, Su PG, Sachdev A, Gopinath P (2016a) Cold atmospheric pressure (CAP) plasma assisted tailoring of LDPE film surfaces for enhancement of adhesive and cytocompatible properties: Influence of operating parameters. Vacuum 130:34–47

Pandiyaraj KN, Ferraria AM, Bothelo de Regob AM, Deshmukh RR, Sud PG, Halleluyahe M, Ahmad SH (2015) Low-pressure enhancement immobilization of chitosan on low density polyethylene for bio-medical applications. Appl Surf Sci 328:1–12

Pandiyaraj KN, Selvarajan V, Rhee YH, Kim HW, Shah SI (2009) Glow discharge plasma-induced immobilization of heparin and insulin on polyethylene terephthalate film surfaces enhances anti-thrombogenic properties. Mater Sci Eng, C 29:796–805

Pandiyaraj KN, Selvarajan V, Rhee YH, Kim HW (2016e) Characterization and In Vitro Hemocompatibility of Polyethylene Terephthalate Film Surfaces Modified by DC Glow Discharge Plasma and Graft Polymerization. J Appl Polym Sci. doi:10.1002/app.29600 (in press)

Pandiyaraj KN, Deshmukh RR, Ruzybayev I, Shah SI, Su PG, Halleluyahe M Jr, Ahmad SH (2014a) Influence of non-thermal plasma forming gases on improvement of surface properties of low density polyethylene (LDPE). Appl Surf Sci 307:109–119

Pandiyaraj KN, RamKumar MC, Arun Kumar A, Padmanabhan PVA, Deshmukh RR, Bahd M, Shah SI, Su PG, Halleluyahe M Jr, Ahmad SH (2016c) Tailoring the surface properties of polypropylene films through cold atmospheric pressure plasma (CAPP) assisted polymerization and immobilization of biomolecules for enhancement of anti-coagulation activity. Appl Surf Sci 370:545–556

Pandiyaraj KN, Selvarajan V (2008) Non-thermal plasma treatment for hydrophilicity improvement of grey cotton fabrics. J Mater Process Technol 199(1–3):130–139

Pandiyaraj KN, Kumar AA, Ram Kumar MC, Deshmukh RR, Bendavid A, Su PG, Kumar SU, Gopinath P (2016a) Effect of cold atmospheric pressure plasma gas composition on the surface and cyto-compatible properties of low density polyethylene (LDPE) films. Curr Appl Phys 16:784e792

Pandiyaraj KN, Deshmukh RR, ShreeRam B, Mahendiran R (2014b) Improvement of surface and biocompatible properties of flexible transparent nano TiO_2 films using glow discharge plasma. J Nano Sci Nano Technol 2(4):436–441

Pandiyaraj KN, ArunKumar A, Ramkumar MC, Sachdev A, Gopinath P, Cools P, DeGeyter N, Morent R, Deshmukh RR, Hegde P, Han C, Nadagouda MN (2016d) Influence of non-thermal TiCl4/Ar + O_2 plasma-assisted TiOx based coatings on the surface of polypropylene (PP) films for the tailoring of surface properties and cytocompatibility. Mater Sci Eng C 62:908–918

Pankaj SK, Bueno-Ferrer C, Misra NN, O'Neill L, Jiménez A, Bourke P, Cullen PJ (2014) Surface, thermal and antimicrobial release properties of plasma-treated zein films. J Renew Mater 1(8):77–84

Pappas DD, Bujanda AA, Orlicki JA, Jensen RE (2008) Chemical and morphological modification of polymers under a helium-oxygen dielectric barrier discharge. In: Proceedings of the 35th international conference on metallurgical coatings and thin films. Surf Coat Technol 203(5–7):830–834

Park BJ, Lee D, Park JC, Lee IS, Lee KY, Hyun S, Chun MS, Chung KH (2003) Sterilization using a microwave-induced argon plasma system at atmospheric pressure. AIP. Phys Plasmas 10(11):4539–4544

Park JB, Lakes RS (1992) Biomaterials: An Introduction, 2nd edn. Plenum Press, New York. ISBN 978-0-387-37879-4

Park GY, Park SJ, Choi MY, Koo IG, Byun JH, Hong JW, Sim JY, Collins GJ, Lee JK (2012) Atmospheric-pressure plasma sources for biomedical applications. Plasma Sources Sci Technol 21(4):043001

Pezzatini S, Morbidelli Gristina R, Favia P, Ziche M (2008) A nanoscale fluorocarbon coating on PET surfaces improves the adhesion and growth of cultured coronary endothelial cells. Nanotechnology 19:275101

Picraux ST, Pope LE (1984) Tailored surface modification by ion implantation and laser treatment. Science 226(4675):615–622

Pinto S, Alves P, Matos CM, Santos AC, Rodrigues LR, Teixeira JA, Gil MH (2010) Poly (dimethyl siloxane) surface modification by low pressure plasma to improve its characteristics towards biomedical applications. Colloids Surf, B 8(1):20–26

Ponte GD, Sardella E, Fanelli F, Van Hoeck A, d'Agostino R, Paulussen S, Favia P (2011) Atmospheric pressure plasma deposition of organic films of biomedical interest. Surf Coat Technol 205:S525–S528

Radu CD, Kiekens P, Verschuren J (2000) Surface modification of textiles by plasma treatments. In: Pastore CM, Kiekens P (eds) Surface characteristics of fibres and textiles, surfactant series, vol 94, Marcel Dekker, NY, pp 203–218

Ratner BD, Hoffman AS, Schoen FJ, Lemons JE (1996) Biomaterials Science: An introduction to materials in medicine, vol. 2, Academic Press, New York, Elsevier Academic Press, pp 105–107, ISBN – 0-12-582463-7

Ratner BD (1993) Plasma deposition for biomedical applications: A brief review. J Biomater Sci Polym Ed 4(1):3–11

Renò F, D'Angelo D, Gottardi G, Rizzi M, Aragno D, Piacenza G, Cartasegna F, Biasizzo M, Trotta F, Cannas M (2012) Atmospheric pressure plasma surface modification of Poly(D,

L-lactic acid) increases fibroblast, osteoblast and keratinocyte adhesion and proliferation. Plasma Processes Polym 9(5):491–502
Rhee JK, Kim DB, Moon SY, Choe W (2007) Change of the argon-based atmospheric pressure large area plasma characteristics by the helium and oxygen gas mixing. The Third International Symposium on Dry Process (DPS 2005). Thin Solid Films 515(12):4909–4912
Rieu J, Pichat A, Rabbe LM, Rambert A, Chabrol C, Robelet M (1991) Ion implantation effects on friction and wear of joint prosthesis materials. Biomaterials 12(2):139–143
Rimpelov S, Peterková L, Kasálková NS, Slepička P, Švorčík V, Ruml T (2014) Surface modification of biodegradable Poly(L-Lactic Acid) by argon plasma: fibroblasts and keratinocytes in the spotlight. Plasma Processes Polym 11(11):1057–1067
Ritter S, Nasonova E, Scholz M, Kraft-Weyrather W, Kraft G (1996) Comparison of chromosomal damage induced by X-rays and Ar ions with an LET of 1840 keV/micrometer in G1 V79 cells. Int J Radiat Biol 69(2):155–166
Roth JR (2001a) 'Industrial plasma engineering' Vol. 1, January 1, 1995 by CRC Press, ISBN 9780750303170—CAT# IP376, IOP, Bristol
Roth JR (2001b) 'Industrial plasma engineering' Vol. 2, August 25, 2001 by CRC Press, ISBN 9780750305440—CAT# IP375, IOP, Bristol
Roth JR, Sherman DM, Gadri RB, Karakaya F, Chen Z, Montie TC, Winterberg KK (2000) A remote exposure for plasma processing and sterilization by plasma active species at one atmosphere. IEEE Trans Plasma Sci 28:56–63
Roy M, Bandyopadhyay A, Bose S (2011) Induction plasma sprayed nano hydroxyapatite coatings on titanium for orthopaedic and dental implants. Surf Coat Technol 205(8–9):2785–2792
Rudd ME, DuBois RD, Toburen LH, Ratcliffe CA, Goffe TV (1983) Cross sections for ionization of gases by 5-4000-keV protons and for electron capture by 5-150-keV protons. Phys Rev A 28:3244–3257
Rutala WA, Gergen MF, Weber DJ (1998) Comparative evaluation of the sporicidal activity of new low-temperature sterilization technologies: Ethylene oxide, 2 plasma sterilization systems, and liquid peracetic acid. Am J Infect Control 26(4):393–398
Sanborn SL, Murugesan G, Marchant RE, Kottke-Marchant K (2002) Endothelial cell formation of focal adhesions on hydrophilic plasma polymers. Biomaterials 23:1–8
Sanchis MR, Blanes V, Blanes M, Garcia D, Balart R (2006) Surface modification of low density polyethylene (LDPE) film by low pressure O_2 plasma treatment. Eur Polymer J 42:1558–1568
Sarani A, Nikiforov AY, Geyter ND, Morent R, Leys C (2011) Surface modification of polypropylene with an atmospheric pressure plasma jet sustained in argon and an argon/water vapour mixture. Appl Surf Sci 257(20):8737–8741
Sarapirom S, Lee JS, Jin SB, Song DH, Yu LD, Han JG, Chaiwong C (2013) Wettability effect of PECVD-SiOx films on Poly(lactic acid) induced by oxygen plasma on protein adsorption and cell attachment. J Phys: Conf Ser 423:012042
Sarra-Bournet C, Turgeon S, Mantovani D, Laroche G (2006) A study of atmospheric pressure plasma discharges for surface functionalization of PTFE used in biomedical applications. J Phys D Appl Phys 39(16):3461–3469
Scholz M, Ritter S, Kraft G (1998) Analysis of chromosome damage based on the time course of aberrations. Int J Radiat Biol 74(3):325–331
Schnabelrauch M, Wyrwa R, Reb H, Bergemann C, Finke B, Schlosser M, Walschus U, Lucke S, Weltmann KD, Nebe JB (2014) Surface-coated polylactide fiber meshes as tissue engineering matrices with enhanced cell integration properties. Int J Polymer Sci 439784:1–12
Schröder K, Finke B, Polak M, Lüthen F, Nebe B, Rychly J, Bader R, Lukowski G, Walschus U, Schlosser M, Ohl A, Weltmann KD (2010) Gas-discharge plasma-assisted functionalization of titanium implant surfaces. Mater Sci Forum 638–642:700–705
Schutze A, Jeong JY, Babayan SE, Park J, Selwyn GS, Hicks RF (1998) The atmospheric-pressure plasma jet: a review and comparison to other plasma sources. IEEE Trans Plasma Sci 26(6):1685–1694
Seifert B, Romaniuk P, Groth T (1997) Covalent immobilization of hirudin improves the haemocompatibility of polylactide—polyglycolide in vitro. Biomaterials 18(22):1495–1502

Selwyn GS, Herrmann HW, Park J, Henins I (2001) Materials processing using an atmospheric pressure, RF-generated plasma source. Contrib Plasma Phys 41(6):610–619

Senesi GS, D'Aloia E, Gristina R, Favia P, d'Agostino R (2007) Surface characterization of plasma deposited nano-structured fluorocarbon coatings for promoting in vitro cell growth. Surf Sci 601:019–1025

Sensenig R, Kalghatgi S, Cerchar E, Fridman G, Shereshevsky A, Torabi B, Arjunan KP, Podolsky E, Fridman A, Friedman G, Azizkhan-Clifford J, Brooks AD (2010) Non-thermal plasma induces apoptosis in melanoma cells via production of intracellular reactive oxygen species. Ann Biomed Eng 39(2):674–687

Shen H, Hu X, Yang F, Bei J, Wang S (2007) Combining oxygen plasma treatment with anchorage of cationized gelatin for enhancing cell affinity of poly(lactide-co-glycolide). Biomaterials 28:4219–4230

Shijian L, Van O, Wim J (2002) Surface modification of textile fibres for improvement of adhesion to polymeric matrices: a review. J Adhes Sci Technol 16(13):1715–1735

Sioshansi P, Tobin EJ (1996) Surface treatment of biomaterials by ion beam processes. Surf Coat Technol 83:175–182

Sodhi RNS (1996) Application of surface analytical and modification techniques to biomaterials research. J Electron Spectrosc Relat Phenom 81(3):269–284

Song YQ, Sheng J, Wei M, Yuan XB (2000) Surface modification of polysulfone membranes by low-temperature plasma–graft poly (ethylene glycol) onto polysulfone membranes. J Appl Polym Sci 78(5):979–985

Sprang N, Theirich D, Engemann (1995) Plasma and ion beam surface treatment of polyethylene. In: Fourth international conference on plasma surface engineering part 2. Surf Coat Technol 74–75(2):689–695

Stapelmann K, Fiebrandt M, Raguse M, Awakowicz P, Reitz G, Moeller R (2013) Utilization of low pressure plasma to inactivate bacterial spore on stainless steel screws. Astrobiology 13(7):597–606

Steele JG, Gengenbach TR, Johnson G, Mcfarland C, Dalton BA, Underwood PA, Chatelier RC, Griesser HJ (1995) In: Proceedings of the proteins at interfaces 2nd ACS symposium series 602, vol 436 American Chemical Society, Washington, DC

Steele JG, Johnson G, Mcfarland C, Dalton BA, Gengenbach TR, Chatelier RC, Underwood PA, Griesser HJ (1994) Roles of serum vitronectin and fibronectin in initial attachment of human vein endothelial cells and dermal fibroblasts on oxygen- and nitrogen-containing surfaces made by radiofrequency plasmas. J Biomater Sci Polymer Ed 6(6):511–532

Steffen HJ, Schmidt J, Gonzalez-ElipeA (2000) Biocompatible surfaces by immobilization of heparin on diamond-like carbon films deposited on various substrates. Surf Interface Anal 29:386–391

Su W, Wang S, Wang X, Fu X, Weng J (2010) Plasma pre-treatment and TiO_2 coating of PMMA for the improvement of antibacterial properties. Surf Coat Technol 205(2):465–469

Suzuki Y, Kusakabe M, Akiba H, Kusakabe K, Iwaki M (1990) In vivo evaluation of antithrombogenicity for ion implanted silicone rubber using indium-tropolone-platelets. Japan J Artif Organs 19:1092–1095

Suzuki Y, Kusakabe M, Iwaki M, Suzuki M (1988) Surface modification of silicone rubber by ion implantation. Nucl Instrum Methods Phys Res, Sect B 32(1–4):120–124

Svorcík V, Arenholz E, Rybka V, Ochsner R, Ryssel H (1998) AFM surface investigation of polyethylene modified by ion bombardment. Nucl Instrum Methods Phys Res, Sect B 142(3):349–354

Svorcík V, Rybka V, Hnatowicz V, Smetana K (1997) Structure and biocompatibility of ion beam modified polyethylene. J Mater Sci Mater Med 8(7):435–440

Szycher M, Sioshansi P (1990) Frisch EE (1990) Biomaterials for the 1990s: polyurethanes, silicones and ion beam modification techniques (Part II). Spire Corporation, Patriots Park, Bedford

Tanaka K, Kogoma M, Ogawa Y (2006) Fluorinated polymer coatings on PLGA microcapsules for drug delivery system using atmospheric pressure glow plasma. Thin Solid Films 506–507:159–162

Taucher-Scholz G, Heilmann J, Schneider M, Kraft G (1995) Detection of heavy-ion-induced DNA double-strand breaks using static-field gel electrophoresis. Radiat Environ Biophys 34 (2):101–106

Tendero C, Tixier C, Tristant P, Desmaison J, Leprince P (2006) The atmospheric-pressure plasma jet: a review and comparison to other plasma sources. Spectrochim Acta Part B 61(1):2–30

Thelen H, Kaufmann R, Klee D, Hoecker H, Fresenius J (1995) Development and characterization of a wettable surface modified aromatic polyethersulphone using glow discharge induced HEMA-graft polymerisation. Fresenius' J Anal Chem (3):290–296

Thomas H, Denda B, Hedler M, Kasermann M, Klein C, Merten TH (1998) Textile finishing with low temperature plasma. Melliand Textiliber 79:350–352

Timmons RB, Griggs (2004) Pulsed plasma polymerizations. In: Biederman H (ed) Plasma polymer films. Imperial College Press, London 217–246

Timmons RB, Owens DE, Iii, Windsor JB, Khorzad RK, Susut C, Less (2011) Encapsulated particles for enteric release. US Patent App. no. PCT/US2010/035872, Pub no. WO2011146078 A1

Triandafillu K, Balazs DJ, Aronsson BO, Descouts P, Tu QP, van Delden C, Mathieu HJ, Harms H (2003) Adhesion of Pseudomonas aeruginosa strains to untreated and oxygen-plasma treated poly(vinyl chloride) (PVC) from endotracheal intubation devices. Biomaterials 24:1507–1518

Uldall PR (1993) Surface treatment of biomaterials by ion beam processes. In: Nissenson AR, Fine RN (eds) Dialysis Therapy, 2nd edn. Hanley & Belfus, Philadelphia, PA, pp 5–10

van Kooten TG, Hetty ST, Busscher HJ (2004) Plasma-treated polystyrene surfaces: model surfaces for studying cell–biomaterial interactions. Biomaterials 25:1735–1747

Vandamme M, Robert E, Lerondel S, Sarron V, Ries D, Dozias S, Sobilo J, Gosset D, Kieda C, Legrain B, Pouvesle JM, Le Pape A (2012) ROS implication in a new antitumor strategy based on non-thermal plasma. Int J Cancer 130(9):2185–2194

Vargo TG, Thompson PM, Gerenser LJ, Valentini RF, Aebischer P, Hook DJ, Gardella JA Jr (1992) Monolayer chemical lithography and characterization of fluoropolymer films. Langmuir 8(1):130–134

Vassal PS, Favennec L, Ballet JJ, Brasseur P (1998) Hydrogen peroxide gas plasma sterilization is effective against *Cryptosporidium parvum* oocysts. Am J Infect Control 26(2):136–138

Venkatesan T (1985) High energy ion beam modification of polymeric films. Nucl Instrum Methods Phys Res, Sect B 7–8:461–467

Vrekhem S Van, Cools P, Declercq H, Van Tongel A, Vercruysse C, Cornelissen M, Geyter ND, Morent R (2015) Application of atmospheric pressure plasma on polyethylene for increased prosthesis adhesion. In: The 42nd international conference on metallurgical coatings and thin films. Thin Solid Films 596:256–263

Walachova K, Svorcík V, Bacakova L, Hnatowicz V (2002) Colonization of ion-modified polyethylene with vascular smooth muscle cells in vitro. Biomaterials 23(14):2989–2996

Walsh JL, Kong MG (2007) Room-temperature atmospheric argon plasma jet sustained with sub microsecond high-voltage pulses. Appl Phys Lett 91:221502

Wang J, Chen JY, Yang P, Leng YW, Wan GJ, Sun H, Zhao AS, Huang N, Chu PK (2006). In vitro platelet adhesion and activation of polyethylene terephthalate modified by acetylene plasma immersion ion implantation and deposition. In: Ion beam modification of materials—proceedings of the 14th international conference on ion beam modification of materials. Nucl Instr Meth Phys Res Sect B: Beam Interact Mater Atoms 242(1–2):12–14

Wang J, Pana CJ, Huang N, Sun H, Yang P, Leng YX, Chen JY, Wan GJ, Chu PK (2005) Surface characterization and blood compatibility of poly(ethylene terephthalate) modified by plasma

surface grafting. In: 13th international conference on surface modification of materials by ion beams. Surf Coat Technol 196(1–3):307–311
Wang P, Tan KL, Kang ET, Neoh KG (2002) Plasma-induced immobilization of poly (ethylene glycol) onto poly (vinylidene fluoride) microporous membrane. J Membr Sci 195(1):103–114
Washburn NR, Yamada KM, Simon CG Jr, Kennedy SB, Amis EJ (2004) High-throughput investigation of osteoblast response to polymer crystallinity: influence of nanometer-scale roughness on proliferation. Biomaterials 25(7–8):1215–1224
Weltmann KD, Brandenburg R, von Woedtke T, Ehlbeck J, Foest R, Stieber M, Kindel E (2008) Antimicrobial treatment of heat sensitive products by miniaturized atmospheric pressure plasma jets (APPJs). J Phys D Appl Phys 41(19):194008
Welz C, Becker S, Li YF, Shimizu T, Jeon J, Schwenk-Zieger S, Thomas HM, Isbary G, Morfill GE, Harreus U, Zimmermann JL (2013) Effects of cold atmospheric plasma on mucosal tissue culture. J Phys D Appl Phys 46:045401
Winter J, Tresp H, Hammer MU, Iseni S, Kupsch S, Schmidt-Bleker A, Wende K, D˙unnbier M, Masur K, Weltmann KD, Reuter S (2014) Tracking plasma generated H_2O_2 from gas into liquid phase and revealing its dominant impact on human skin cells. J Phys D: Appl Phys 47(28):285401
Wintermantel E, Mayer J, Blum J, Eckert KL, Luscher P, Mathey M (1996) Tissue engineering scaffolds using superstructures. Biomaterials: polymer scaffolding and hard. Tissue Eng 17(2):83–91
Xu H, Deshmukh RR, Timmons RB, Kytai TN (2011) Enhanced endothelialization on surface modified Poly(l-Lactic Acid) substrates. Tissue Eng Part A 17(5–6):865–876
Yasuda H, Hsu T (1978) Plasma polymerization investigated by the comparison of hydrocarbons and perfluorocarbons. Surf Sci 76:232–241
Yasuda H (1985) Plasma polymerization. Academic Press Inc, Orlando, New York, London
Yildirim ED, Besunder R, Pappas D, Allen F, Güçeri S, Sun W (2010) Accelerated differentiation of osteoblast cells on polycaprolactone scaffolds driven by a combined effect of protein coating and plasma modification. Biofabrication 2:014109
Yoon NS, Lim YJ, Tahara M, Takagishi T (1996) Mechanical and dyeing properties of wool and cotton fabrics treated with low temperature plasma and enzymes. Text Res J 66:329–336
Yoshida S, Hagiwara K, Hasebe T, Hotta A (2013) Surface modification of polymers by plasma treatments for the enhancement of biocompatibility and controlled drug release. Surf Coat Technol 233:99–107
Young JH (1997) New sterilization technologies In: Reichert M, Yung JH (Eds) Sterilization technology for the health care facility, Aspen Publishers, Gaithersburg, MD, pp 228–235. ISBN 0-8342-0838-5
Zanini S, Muller M, Riccardi C, Orlandi M (2007) Polyethylene Glycol grafting on polypropylene membranes for anti-fouling properties. Plasma Chem Plasma Process 27:446–457
Zelzer M, Majani R, Bradley James W, Rose J, Felicity RA, Davies MC, Alexander MR (2008) Investigation of cell–surface interactions using chemical gradients formed from plasma polymers. Biomaterials 29:172–184
Zhang W, Chu PK, Ji J, Zhang Y, Liu X, Fu RKY, Ha PCT, Yan Q (2006a) Plasma surface modification of poly vinyl chloride for improvement of antibacterial properties. Biomaterials 27:44–51
Zhang W, Chu PK, Ji J, Zhang Y, Fu RKY, Yan Q (2006b) Antibacterial properties of plasma-modified and triclosan or bronopol coated polyethylene. Polymer 47:931–936
Zhao Q, Zhai GJ, Ng DHL, Zhang XZ, Chen ZQ (1999) Surface modification of Al_2O_3 bioceramic by NH^{+2} ion implantation. Biomaterials 20(6):595–599

Zheng Y, Xiong C, Wang Z, Li X, Zhang L (2015) A combination of CO_2 laser and plasma surface modification of poly(ether ether ketone) to enhance osteoblast response. Appl Surf Sci 344:79–88

Zhu W, Lopez JL (2012) A DC non-thermal atmospheric-pressure plasma micro jet. Plasma Sources Sci Technol 21:034018

Biomaterials for Induction and Treatment of Autoimmunity

Akhilesh Kumar Shakya and Kutty Selva Nandakumar

Abstract Use of biomaterials in autoimmunity research is widely explored, as an adjuvant to induce antigen specific immune responses, for facilitating induction of experimental models to study disease pathogenesis and for designing novel therapeutic targets. Similarly, polymeric biomaterials are explored as a delivery vehicle for sustained and specific release of auto-antigens/drugs to treat autoimmune disorders. Although considered as biocompatible, implantation/injection of polymers like silica and metallic implants are associated with development of chronic inflammation and autoimmunity. Despite these compatibility concerns, biomaterials are still considered as favorable materials for several applications in the autoimmunity field.

Keywords Autoimmunity · Biomaterials · Polymer · Auto-antigen specific immunotherapy · Poly-*N*-isopropylacrylamide · Arthritis

Abbreviations

APCs	Antigen presenting cells
ASIA	Adjuvant induced autoimmune syndrome
bFGF	Basic fibroblast growth factor
CFA	Complete Freund's adjuvant
CIA	Collagen induced arthritis
CII	Collagen type II

A.K. Shakya (✉)
Chemical Engineering Department, Texas Tech University,
Lubbock, TX 79409-3121, USA
e-mail: akhilesh.shakya@ttu.edu

K.S. Nandakumar
Medical Immunopharmacology Research, Southern Medical University,
Guangzhou, China
e-mail: Nandakumar.kutty-Selva@ki.se

K.S. Nandakumar
Medical Inflammation Research, Medical Biochemistry and Biophysics,
Karolinska Institute, Stockholm, Sweden

A. Tripathi and J.S. Melo (eds.), *Advances in Biomaterials for Biomedical Applications*, Advanced Structured Materials 66,
DOI 10.1007/978-981-10-3328-5_4

CS	Chitosan
DCs	Dendritic cells
EAE	Experimental autoimmune encephalomyelitis
EAU	Experimental autoimmune uveoretinitis
HA	Hyaluronic acid
LSECs	Liver sinusoidal endothelial cells
MS	Multiple sclerosis
NGF	Nerve growth factor
NPs	Nanoparticles
PHCCC	*N*-Phenyl-7-(hydroxyimino)cyclopropa[*b*]chromen-1a-carboxamide
PLGA	Poly(lactic-*co*-glycolic acid)
PNiPAAm	Poly-*N*-isopropylacrylamide
Treqs	T regulatory cells
TCR	T cell receptor
VUR	Vesicoureteral reflux

1 Introduction

Autoimmunity is a sign of imbalance between the regulatory and effector immune responses, which mainly emerge as a result of either defective elimination or improper control of self-reactive lymphocytes. This imbalance causes breakdown of immunological tolerance against self-molecules or tissues resulting in autoimmune disorders. In most of these clinical manifestations, the initiating events are unknown. However, genetics, epigenetics and environmental factors are identified as decisive factors in the establishment of autoimmunity. Prevalence of autoimmune disorders (multiple sclerosis, rheumatoid arthritis and type 1 diabetes) is approximately 1% in the worldwide population (Cooper and Stroehla 2003). In addition, inflammatory conditions like atherosclerosis (hardening and narrowing of the arteries) (Hansson and Hermansson 2011; Ketelhuth and Hansson 2015) and inflammatory bowel disease (inflammation in colon and small intestine) (Colia et al. 2016) may have autoimmune components (Ross 1990; Galperin and Gershwin 1997). Female preponderance in the development of chronic autoimmune diseases is well documented with more than 75% autoimmune cases are reported in females. Especially, young females at the age of or after puberty are ten times more susceptible for developing autoimmune diseases (Beeson 1994; Smith and Germolec 1999). Generally, these autoimmune disorders are characterized by systemic or localized (tissue-specific) chronic inflammation, which leads to progressive destruction of target tissues.

Autoimmune diseases are a major concern worldwide due to high economic burden to the society and because of poor understanding of disease initiation and pathogenic events. Patients usually visit the clinics at a later stage of the disease

development, making it difficult to intervene at the disease initiation stage. However, disease specific clinical manifestations start long time before the clinical symptoms appear. For example, presence of anti-citrullinated protein/peptide specific antibodies (ACPAs) is observed several years before the onset of Rheumatoid arthritis (Rantapaa-Dahlqvist et al. 2003). To understand the pathogenic pathways in autoimmune diseases, several animal models are used that can either be induced or spontaneously developed (Kannan et al. 2005; Asquith et al. 2009). Conventional therapies for autoimmune disorders are based on immuno-suppressive, antiviral or antibacterial treatments. Currently, patients are treated with biologicals or drugs that can block the pro-inflammatory cytokines, B and/or T cells. Moreover, oral medications like angiotensin and statins are also being used in the clinics. Despite the effectiveness of these medications, specificity of the treatments and side effects of the drugs are major concerns that should be taken into consideration while developing future novel immunotherapies (Fairweather 2007).

Biomaterials have been well explored in immunology for the development of new vaccines, therapeutics, tissue regeneration and in the induction of diseases in animal models to study the inflammatory pathogenic pathways. Biomaterials can be used in different ways: as suppressors to inhibit the immune response against therapeutics, as an adjuvant for sustained release and enhancing immunogenicity of an antigen or as attenuators to modulate the immune responses. As an immune system attenuator, they can reduce the immune responses against the delivered drugs or therapeutic protein(s). For example, in blood transfusion studies, polymers can minimize the chances of rejection. Covalent conjugation of monomethoxy polyethylene glycol (mPEG) to the cells or tissues significantly reduced the possibility of rejection by inducing a state of tolerance (Scott et al. 1997; Scott and Murad 1998). Moreover, attachment of PEG to the egg white lysozyme antigen also reported to diminish T cell responses (So et al. 1996). As the immune system suppressor, they can be an alternate to conventional immunosuppressive drugs like cyclosporine, which is associated with undesirable side effects (Descotes 2004). Similarly, multiwall carbon nanotubes (CNTs) suppressed the systemic immune responses in mice (Mitchell et al. 2009). Inhibitory effect of polyhydroxy C60 (fullerene) was also reported on type 1 hypersensitive reactions (Ryan et al. 2007). Others biomaterials like chitosan, PLGA particles and dendrosomes have also been shown to have suppressive role in type I and III hypersensitive reactions (Balenga et al. 2006; Gomez et al. 2008). Biomaterial polymers are well explored as a delivery system and/or as an adjuvant in designing several methods of delivery system for slow release of the antigen and for the induction of antigen-specific immune responses. In this context, apart from sustained release, polymers can also stabilize the antigen for eliciting an effective immune resonse. For example, polymeric system based on 1,6-bis(pcarboxyphenoxy) hexane and 1, 8-bis (p-carboxyphenoxy)- 3,6-dioxaoctane significantly stabilized the *Bacillus anthracis* antigen (Petersen et al. 2012). Adjuvant property of polymers depends on the charge, format, chemistry and the balance between their hydrophobicity and hydrophilicity properties (Shakya and Nandakumar 2012a). Apart from being used

for antigen delivery, during last decade, biomaterials are also tested in the autoimmunity field as an adjuvant for induction of autoimmune responses and as therapeutics for treatment of autoimmune diseases.

Failure of tolerance towards self-antigens is a crucial component in the induction of autoimmunity. Both central and peripheral tolerance mechanisms that are essential to control self-reactive immune cells are compromised. In healthy individuals, these tolerance mechanisms inhibit induction of autoimmune responses. However, when tolerance is breached, immune cells become hyperactive towards self-proteins leading to destruction of tissue organization and organ structure. Hence, to design and develop protective strategies against development of autoimmunity, to explore disease mechanisms and treat them successfully, biomaterials have been widely explored. This chapter updates use of such biomaterials in autoimmunity research.

2 Biomaterials for the Induction of Experimental Autoimmunity

For dissecting the complexity of autoimmune diseases, validation of existing therapies and identifying novel therapeutic targets, animal models (also called as disease models) are a pre-requisite (Kannan et al. 2005; Asquith et al. 2009). These disease models can be induced with a self-antigen and an appropriate adjuvant. However, these models may reflect either part of the clinical disease or represent the clinical spectrum of a sub-population of the patients. Hence, the induced models are often chosen based on the scientific question and therapeutic targets. Nevertheless, very few studies reported the use of biomaterials with an auto-antigen for induction of autoimmunity.

2.1 Experimental Arthritis

Rheumatoid arthritis (RA) is an autoimmune disorder, characterized by chronic inflammation of articular joints and associated with progressive depletion of extracellular matrices, cartilage and bone. Various chronic and acute models have been developed by immunization with joint-specific as well as ubiquitously expressed antigens with an adjuvant. For example, collagen type II (CII) is a major protein present in the articular cartilage, target for autoimmune attack in arthritis. When CII is mixed with an adjuvant and immunized to susceptible animals having a permissible genetic background, it induces polyarthritis so called collagen induced arthritis (CIA), a classical model for arthritis. Commonly used adjuvants in the induction of autoimmunity are Freund's adjuvants, which are oil based with or without mycobacterial derivatives. However, use of these type of adjuvants tend to induce a

biased immune response, especially by inducing a particular T helper (Th) cell signaling pathways and thereby masking the actual response towards a particular antigen (Petrovsky and Aguilar 2004; Shakya and Nandakumar et al. 2012b). Moreover, they are also associated with localized and systemic toxicities. Therefore, there is a need for biocompatible and immunologically inert adjuvant for the development of an animal model to study the development of autoimmune diseases in detail. Very recently, our group demonstrated the adjuvant potential of temperature responsive poly-*N*-isopropylacrylamide (PNiPAAm) based polymers for the development of collagen induced arthritis (CIA) in mice (Shakya et al. 2011; Shakya and Nandakumar 2015). PNiPAAm in solution phase can easily be mixed with CII at room temperature (25 °C) but above its lower critical solution temperature (LCST) at 32 °C, PNiPAAm precipitates along with CII and act as a depot for slow release of CII (Fig. 1). Thus, CII mixed with PNiPAAm induced arthritis that is independent of any particular Th-type immune response. After mixing with PNiPAAm, CII retained its native epitopes, an essential factor in arthritis development (Shakya et al. 2011) because denatured CII did not induce disease development. Autoimmune responses induced by PNiPAAm-CII mixture were found to be toll like receptors (TLRs) independent. Presence of CII specific T cell receptor (TCR) or mutation in *Ncf1* subunit of mitochondrial NADPH complex induced severe arthritis after PNiPAAm-CII immunization (Shakya et al. 2011). Interestingly, hydrophilic-hydrophobic balance of a polymer was found to be an important factor in determining its adjuvant property (Shakya et al. 2016). Similar to this homopolymer PNiPAAm, adjuvant property of copolymers poly-*N*-

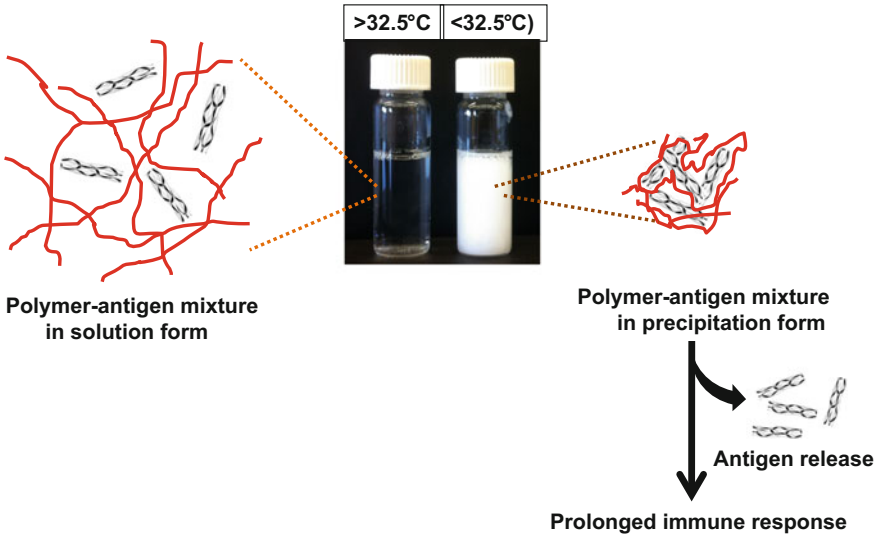

Fig. 1 Schematic representation of temperature dependent phase transition of stimuli-responsive polymer, PNiPAAm with collagen type II (CII) molecules. Below the cloud point (~32.5 °C), polymer and CII are in solution form however they precipitate at body temperature. Polymer generates a depot effect and release CII slowly to get a prolonged immune response

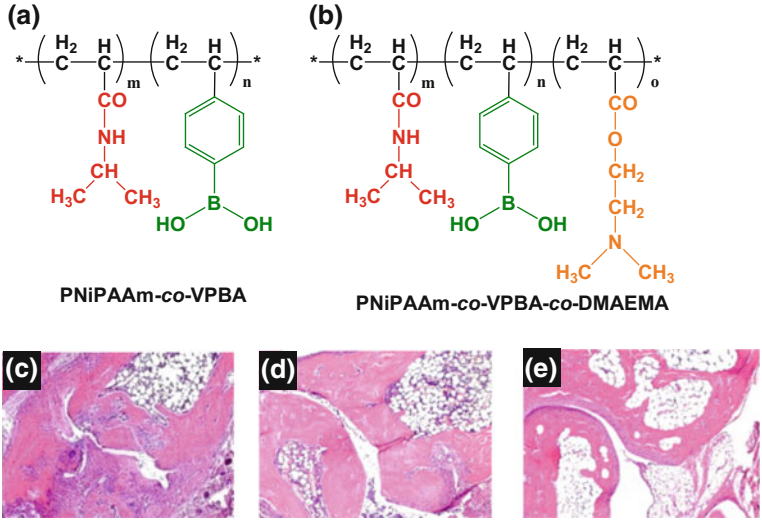

Fig. 2 Chemical structure of copolymers poly-*N*-isopropylacrylamide-*co*-vinylphenylboronic acid (PNiPAAm-*co*-VPBA) (**a**) and poly-N-isopropylacrylamide-*co*-vinylphenylboronic acid-*co*-dimethylaminoethylmethacrylate (PNiPAAm-*co*-VPBA-*co*-DMAEMA) (**b**). Histology analysis of paws of arthritis mice received which injection of CII protein with CFA (**c**), PNiPAAm-*co*-VPBA-*co*-DMAEMA–CII (**d**) and phosphate buffer saline alone (**e**). All the images were captured at 20 × magnification (Reproduced from permission Shakya et al. 2013; Vaccine 31(35):3519–3527)

isopropylacrylamide-*co*-vinylphenylboronic acid (PNiPAAm-*co*-VPBA) and poly-N-isopropylacrylamide-*co*-vinylphenylboronic acid-*co*-dimethylaminoethylmethacrylate (PNiPAAm-*co*-VPBA-*co*-DMAEMA) were also demonstrated with CII antigen. These copolymers were synthesized through free radical polymerization process and characterized by gel permeation chromatography to determine their molecular weights. These polymers were found to be biocompatible under in vitro conditions and did not show any detectable systemic and localized toxicity in vivo. Mice injected with these copolymers and CII developed significant level of CII specific antibody response, which mainly consists of all IgG subtypes (Shakya et al. 2013) (Fig. 2). Macrophages are the major infiltrating cells found at the injection site of PNiAAm-CII mixture. Exacerbation of arthritis in the absence of reactive oxygen species (ROS) in rodents was reported earlier (Holmdahl et al. 2016). In this context, it is of interest to note that ROS produced by macrophages attenuated the autoimmune response and development of arthritis (Gelderman et al. 2007; Pizzolla et al. 2011; Shakya et al. 2016).

2.2 *Experimental Autoimmune Encephalomyelitis*

Multiple sclerosis (MS) is a well known chronic autoimmune neurological disorder, associated with multiple patches of inflammation and demyelination of the central

nervous system. To understand the pathogenesis of MS, experimental autoimmune encephalomyelitis (EAE) is the most commonly used animal model. EAE is T cell driven autoimmune disorder, with a characteristic infiltration of mononuclear cells like macrophages and B cells into the inflammatory site. EAE mimics several clinical features of MS patients like demyelinating lesions of central nervous system (CNS) white matter and foam like myelin debris in active lesions (Getts et al. 2012). In mice, EAE can be induced either by immunization with myelin antigens or by adoptive transfer of myelin specific T cells. Immunization with myelin antigens in genetically susceptible rodents involves use of an adjuvant and characterized by demyelination primarily in the spinal cord mediated by the immune system. Immunization with myelin proteins breaks down the peripheral tolerance mechanisms leading to activation and differentiation of myelin specific T cells in the secondary lymphoid organs (Yednock et al. 1992). Then the activated T cells cross the blood brain barrier where they get reactivated by CNS antigens presented by tissue resident antigen presenting cells (Kawakami et al. 2004). This reactivation of T cells induces expression of pro-inflammatory cytokines (TNF-α, IL-17 and GM-CSF), which may cause nervous tissue injury either directly or by activating immune cells present in the vicinity. Moreover, adjuvants used for such disease development are also associated with toxicity problems. As an alternate, recently organotypic slice culture based model was developed. For example, to understand the role of pro-inflammatory cytokines in MS, a non viral polymer poly (2-dimethylaminoethylmethacrylate) based gene delivery approach and an ex vivo organotypic slice cultures were developed to transduce the cells with genes encoding the pro-inflammatory cytokines. Polymer based biocompatible system has efficiently transduced different cell types in organotypic brain slice system through delivery of TNF and IFN-γ genes. Expression and release of TNF and IFN-γ cytokines induced inflammation-mediated myelin loss in cerebellar slices, which represents an ex vivo system for studying the pathogenesis of MS (Mathew et al. 2013).

3 Adjuvant Induced Autoimmune Syndrome

The concept of adjuvant induced autoimmune syndrome (ASIA) was first recognized in 2011, although patients having diverse symptoms after treatment with silicone or paraffin fillers were reported by Miyoshi in 1964 (Alijotas-Reig 2015). According to ASIA concept, chronic systemic inflammation and autoimmune disorders can develop by repeated exposure to biomaterials especially to the materials used in plastic surgeries such as silicone implant used for breast augmentation (Hajdu et al. 2011). Silicone is a polymer of dimethylsiloxane that has been extensively explored in biomedical applications due to its variable degree of viscosity, which depends on the length of polymer used. Silicone mainly gained its popularity in breast implants despite its wide usage in other implantable products like ventriculo-peritoneal and heart valves (Hajdu et al. 2011). Today breast, buttock and face augmentation by the use of liquid silicone is most commonly adopted

plastic surgery method in USA and other countries. However, capsular fibrosis and contracture, scleroderma, local adverse reactions and other autoimmune disorders are associated with silicone implants despite its acceptable biocompatibility nature (Gabriel et al. 1994; Sanchez-Guerrero et al. 1995; Hajdu et al. 2011; Franca et al. 2013). Association of silicone with autoimmune disorders was first reported in 1984, when a spectrum of autoimmune diseases like rheumatoid arthritis, systemic lupus erythematosus (SLE), polymyositis and sclerosis were reported in 24 patients who had received silicone injection (Kumagai et al. 1984). In another study, one out of three silicone implanted patients developed RA symptoms, second patient developed symptoms like SLE, and third one developed connective tissues abnormality (van Nunen et al. 1982). During last few years many cases of connective tissue disorders have been documented with silicone implants (Spiera et al. 1994; Holmich et al. 2007; Nesher et al. 2015; Singh et al. 2016). Besides silicone, other biomaterials like alum and hyaluronic acid may also be responsible for ASIA (Alijotas-Reig et al. 2012) (Alijotas-Reig 2015). Causative factors and symptoms identified for ASIA syndrome include repeated biomaterials injection, development of local chronic inflammation, systemic symptoms such as joint pain, fever, fatigue and vasculitis. Risk factors for the development of ASIA include family history of autoimmunity, autoimmune reaction against implants and allergic reaction against the injected materials (Goren et al. 2015). Very recently a case of adjuvant induced autoimmune syndrome was reported when dextranomer/hyaluronic acid copolymer (Deflux) was used for the injection to treat vesicoureteral reflux (VUR). Deflux injections cure about 85% primary VUR abnormalities in females however 0.6–0.7% of patients are refractory to the treatment. Suda et al., from Japan reported occurrence of autoimmune disease in a female patient having ureteral obstruction, who has received repeated injections of Deflux (Suda et al. 2016). Besides the polymeric biomaterials, ASIA has also been reported with metallic implants. Most common type of metals reported for induction of autoimmunity is nickel and titanium. In a case study, 23 year old female had nickel titanium chain implant for cosmetic purpose. After 1 year post implantation she developed autoimmune symptoms like thrombocytopenia, anemia and neutropenia (Loyo et al. 2013).

4 Biomaterials for Delivery of Drug/Antigen(S) for Treatment of Autoimmune Diseases

Generally treatments are often initiated either before or around the onset of disease to block its development as well as revert an established disease by intervention therapy. However, in many common autoimmune diseases in fact the disease starts many years, maybe decades, before the clinical diagnosis. Hence, establishing tolerance towards self-antigens by vaccination is needed and efforts are being made to develop such vaccines for autoimmune diseases (Correale et al. 2008; Nicholas et al. 2011; Lernmark and Larsson 2013; Rosenthal et al. 2015). In this context, use of

well-defined, biodegradable materials as delivery vehicles for drugs and vaccines are highly useful for optimized target delivery (Hunter et al. 2014).

4.1 Rheumatoid Arthritis

Administration of autoantigen through oral route is a well-known strategy to achieve peripheral immune tolerance against autoimmune diseases like rheumatoid arthritis, diabetes and experimental uveitis. Effectiveness of oral tolerance depends on several factors such as the nature, dose, frequency of the administered antigen, genetic background of the recipient and the degree of antigen uptake by antigen presenting cells of gastrointestinal tract (GI). In the harsh environment of GI tract, the amount of antigen delivered to the mucosa is extremely small. Therefore, efficient antigen delivery systems are justified with a controlled release of antigens at mucosal sites, while providing protection to the antigen against GI environment. In this context, particulate systems in nano and micron size ranges have been explored to achieve optimal level of peripheral immune tolerance. For example, poly(lactide-*co*-glycolide) (PLGA) nanoparticles encapsulated with CII were synthesized by water in oil in water emulsion (w/o/w) by a solvent evaporation method. Mice fed with single dose of CII encapsulated PLGA particles, which contained 40 μg of CII, noticeably had reduced clinical symptoms of arthritis with low level of anti-CII antibodies in the serum (Kim et al. 2002).

For RA, a delivery system that can deliver the drug at the effector site (articular cartilage) is more beneficial than the systemic delivery. Most of the developed systems do not have specificity to deliver the drug at the site of interest, therefore significantly large amount of drugs are required, which cause severe toxicity problems. Therefore to balance between effectiveness and minimizing the side effects, several systems like liposome, soft gels, micro-emulsion, topical formulations, nano-dispersions and pellets have been developed (Fig. 3). Among them, liposome based delivery system is widely explored for targeted delivery of anti-rheumatic drugs. These delivery systems are biocompatible, degradable, immunologically inert and can encapsulate significant amount of drugs (Kapoor et al. 2014).

Another strategy to enhance the bioavailability of drug/protein is PEGylation, which is the covalent attachment of polyethylene glycol polymer to the drug/antigen. This strategy has been successfully explored for increasing the therapeutic potential of anti-rheumatic drugs like TNF-related apoptosis inducing ligand (TRAIL). In a study, site specific *N*-terminal PEGylation of TRAIL induced 13-fold higher stability, however, this procedure has slightly reduced TRAIL functionality. Therefore to improve the bioactivity of TRAIL in other study, nano-sized complexes of PEGylated TRAIL protein were synthesized by using negatively charged hyaluronic acid (HA). These nanocomplexes were shown promising therapeutic potential to treat arthritis in mice, possibly due to sustained release of TRAIL or good stability of proteins under in vivo system (Kim et al.

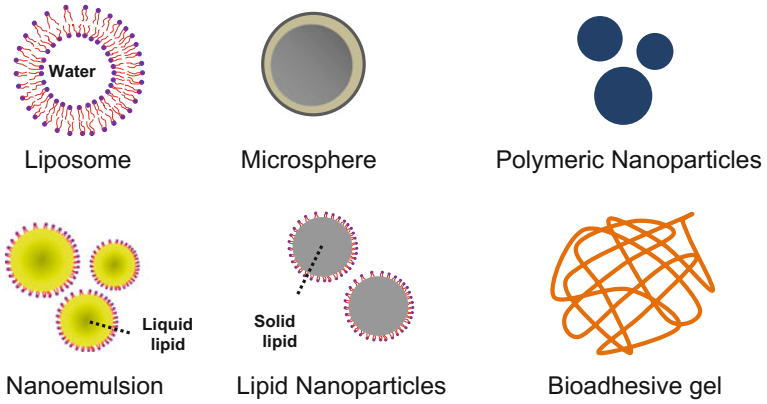

Fig. 3 Different vehicle systems used for delivery of antigens or drugs used in immunotherapy

2010). Furthermore, PEGylation enhances in vivo shelf life of the proteins by reducing their renal clearance. PEG also improves drug solubility, stability and minimizes immune reaction against the therapeutic proteins by shielding proteins from water molecules (Fig. 4).

4.2 Multiple Sclerosis

Transplantation of cells is an attractive therapeutic approach to treat demyelinating diseases like MS. Neuronal precursor cells have shown promising results in remyelination due to their differentiation ability into neural cells. Various delivery systems have been demonstrated for effective delivery of these precursor cells into the central nervous system. For example, three dimensional nano-fiber based poly (glycolic-*co*-lactide)/chitosan (PLGA/CS) scaffold was able to induce the precursor cells (PC12) into neural cell differentiation in the presence of nerve growth factor (NGF) and basic fibroblast growth factor (bFGF). Enhanced expression of nestin, β-tubulin and microtubule associated protein were observed in PC12 cells seeded on PLGA/CS scaffold. Moreover, PC12 seeded scaffolds transplanted into lateral ventricles of EAE affected mice reduced the clinical signs of the disease significantly (Hoveizi et al. 2015). Another vaccine controlled release system based on colloidal gel containing the immunomodulating peptide was also demonstrated for the treatment of EAE. Colloidal gel from alginate-chitosan and PLGA polymers was able to deliver the Ac-PLP-BPI-NH_2-2 peptide in a controlled manner. This peptide was designed to bind the MHCII and intracellular adhesion molecule (ICAM)-I simultaneously. Colloidal gel based vaccine, when administrated subcutaneously into mice having encephalomyelitis, suppressed and delayed the severity of EAE symptoms compared to the control group. Expression of IL-6 and IL-17 was found to be lower in vaccinated mice than in control mice, which

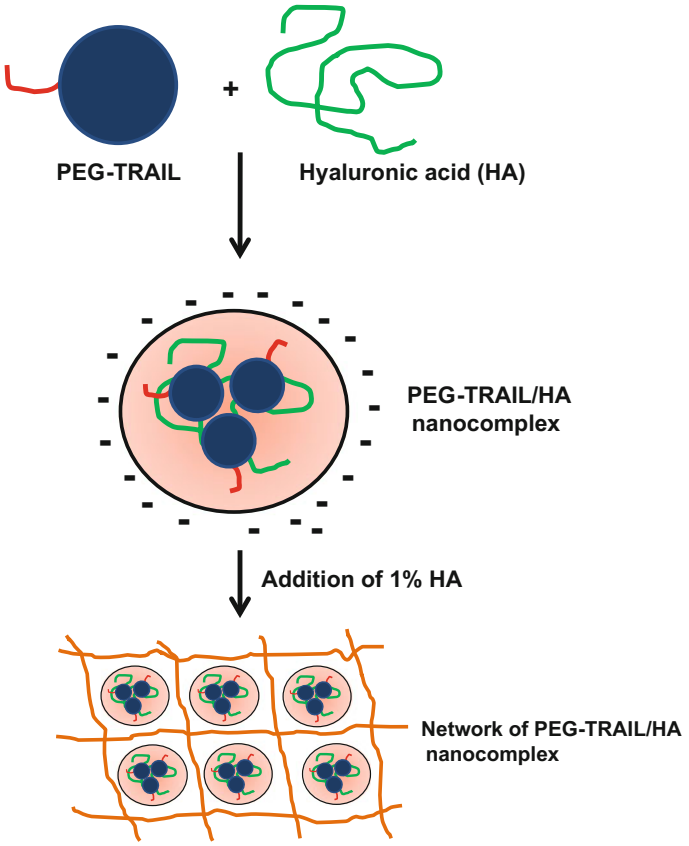

Fig. 4 Schematic representation of nanocomplex release system formation through ionic interaction between PEG-TRAIL molecules and hyaluronic acid (HA). HA exist in anionic form in biological fluids which formed the complex with cationic charged PEG-TRAIL molecules (Reproduced from permission Kim et al. 2010 Biomaterials 31(34):9057–9064)

demonstrates long term suppression of the disease (Buyuktimkin et al. 2012). In another study, antigen loaded micron-sized PLGA particles were demonstrated to deliver the encephalitogenic peptides through intravenous infusion to prevent the onset of disease, thereby ameliorating the clinical symptoms of EAE. Peptide loaded micron size particles (MPs) were taken up by marginal zone macrophages expressing the MARCO receptors that modulate the activity of T regulatory cells (T_{regs}) (Getts et al. 2012). In a different study, capability of PLGA nanoparticles has been demonstrated to treat EAE in mice. Myelin antigen coupled nanoparticles were able to prevent and treat the established experimental encephalomyelitis (Hunter et al. 2014).

Table 1 Delivery systems and administrative routes of anti-rheumatic drugs/biomolecules

Anti-rheumatic drug/molecule	Delivery systems		References
Ketoprofen	Bioadhesive gels	Transdermal delivery	(Singh et al. 2009)
	Eudragit based microparticles	Oral delivery	(El-Kamel et al. 2001)
Methotraxate	Polylactic acid based microspheres	Intra-articular delivery	(Liang et al. 2004)
	Solid in oil nano-carrier	Transdermal delivery	(Yang et al. 2012)
Prednisolone	Cyclodextrins	Intravenous	(Hwang et al. 2008)
Diclofenac	Solid lipid nanoparticles	Transdermal delivery	(Liu et al. 2010)
Indomethacin	Liposomes	Oral delivery	(Soehngen et al. 1988)
Prostaglandin E1	Lipid microspheres	Intravenous delivery	(Moriuchi-Murakami et al. 2000)
Collagen type II	PLGA nanoparticles	Oral delivery	(Kim et al. 2002)

Immune tolerance capacity of liver has also been utilized for the treatment of autoimmune disorders. A recent study has shown that liver sinusoidal endothelial cells (LSECs) can induce T_{regs} to achieve hepatic tolerance. Polymeric nanoparticles encapsulated with auto-antigenic peptide can selectively deliver the peptide to LSECs for the induction of T_{regs}. Thus, NPs based on auto-antigen peptide delivery can effectively prevent the onset of clinical symptoms of EAE in mice. Interestingly, a single dose of NP significantly improved the established EAE due to the activation of T_{regs} (Carambia et al. 2015). Other than the vaccine approaches, drugs encapsulated in polymeric NPs were tried to treat EAE. For example, *N*-Phenyl-7-(hydroxyimino)cyclopropa[*b*]chromen-1a-carboxamide (PHCCC) molecule encapsulated PLGA NPs target the DCs to skew the inflammatory Th17 response towards protective T_{reg} response. PHCCC molecules can easily be encapsulated into NPs and 89% of the drug was found to be released within 3 days. Moreover, DHCCC encapsulated NPs were 36 fold less cytotoxic compared to the soluble drug. Treatment of EAE mice with DHCCC encapsulated NPs administrated at 3 days interval significantly delayed the onset of disease and improved the clinical score compared to the soluble drug of same dose and frequency (Gammon et al. 2015) (Table 1).

4.3 Type1 Diabetes

Type1 diabetes (T1D) is a chronic autoimmune disorder characterized by devastation of insulin secreting beta cells by autoreactive T cells. Lack of insulin secretion from beta cells leads to hyperglycemia and abnormal glucose metabolism (Nicholas et al. 2011) (Fig. 5). Similar to most of the autoimmune diseases, both genetic and environmental factors contribute to the development of type 1 diabetes. Especially, contribution of autoreactive T lymphocytes is well recognized in the

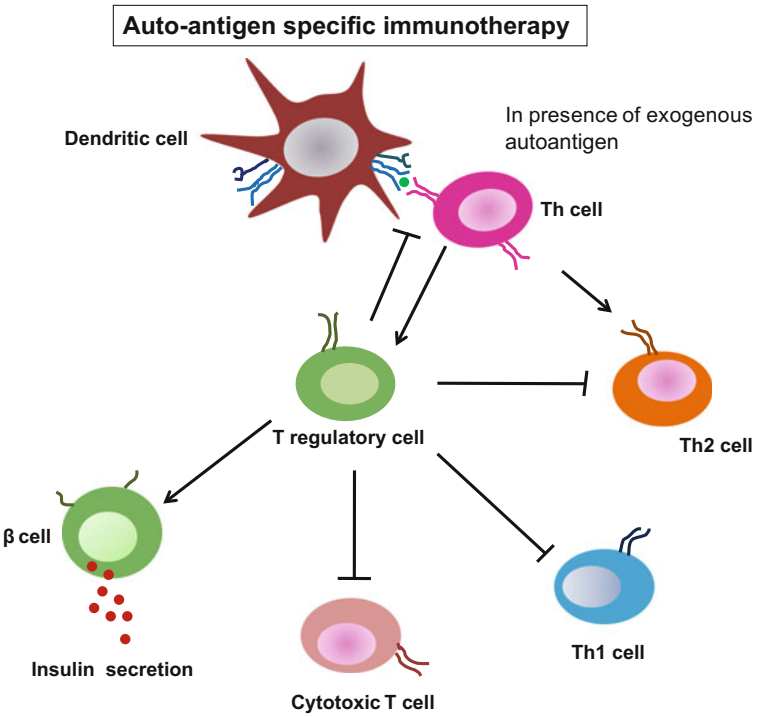

Fig. 5 Mechanism of auto-antigen specific immunotherapy. During antigen specific immunotherapy DCs process the antigen and present to naïve Th cells through secretion of IL-10 cytokine. In this context, activated Th cells activate the T_{regs} and Th2 cells, which block the proliferation of auto-reactive Th1 and CTL cells through secretion of IL-10. Activation of T_{regs} leads to the prevention of beta cell death and this way immuno-tolerance is achieved against the auto-antigen (Nicholas et al. 2011)

establishment of T1D (van Belle et al. 2011). Therefore immunomodulation of autoreactive T cell response is one of the major strategies to treat the disease. For a successful immunotherapy, selection of suitable vaccine and its efficient delivery are major concerns. Various biomaterials are explored for design and effective delivery of drug/vaccine against T1D. For example, PLGA polymeric nanoparticles (NPs) were used to encapsulate insulin as an autoantigen and CpG oligodeoxynucleotides as an adjuvant. The antigen loaded NPs were embedded in PuraMatrix peptide hydrogel for sustained release of the antigen. PuraMatrix is biodegradable, biocompatible and self-assembling peptides based material, which can form 3-D matrix in the presence of physiologic medium with 5–200 nm pore size. Antigen loaded PuraMatrix based hydrogel was injected subcutaneously in non-obese diabetic (NOD) mice in order to evaluate the vaccine efficacy. Although, this vaccine has induced formation of temporary granuloma, which had huge filtration of lymphocytes and macrophages, overall, this approach represents promising immuno tolerance model for the treatment of T1D (Yoon et al. 2015).

Another strategy to control the development of autoimmune diabetes is by minimizing the autoimmune reactions by induction of immunological tolerance. In steady state, beta cells, which undergoes apoptosis is recognized by antigen presenting cells (efferocytosis) for the induction of immunological tolerance. However at the time of abnormal efferocytosis, APCs are unable to recognize apoptotic beta cells, which result in the induction of autoimmune T1D or other disorders. Therefore to help APCs for better recognition, researchers have synthesized and used micron-sized particles containing beta-cell antigens as an alternate source of apoptotic beta cells. For example, phosphatidylserine-liposomes encapsulated with insulin peptides when administrated into NOD mice induced tolerogenic dendritic cells and attenuated the autoreactive immune responses. Liposomal-based immunotherapy minimized the development of autoimmunity and thereby reduced the symptoms of diabetes. Using liposomes for immunotherapy has several advantages in terms of easy preparation methods and administering protocols compared to the existing immunotherapy regimen. Liposomes are also able to protect the antigen from degradation under in vivo conditions (Pujol-Autonell et al. 2015).

4.4 Autoimmune Uveitis

Uveitis is the most common autoimmune ocular disorder, which is one of the major causes for blindness in developing countries. Currently, uveitis is treated by repeated intraocular injection of corticosteroids, which are associated with side effects and patient inconvenience. Alternatively immunosuppressive therapies are also in use to treat chronic autoimmune uveoretinitis, which make patients more susceptible for infections. Therefore, biodegradable polymers based delivery systems in the form of implants have been studied for effective and localized delivery of the drugs (Gammon et al. 2015). For example, ability of polymeric nanoparticles for slow release of drugs to treat autoimmune uveoretinitis has been demonstrated. A single dose of poly(lactic) acid NPs encapsulated with betamethasone phosphate drug administrated intravenously into Lewis rats was able to improve the clinical score of EAU with significantly reduced infiltration of macrophages, auto-reactive T cells and hypertrophic morphology of muller cells (Sakai et al. 2006).

5 Conclusion

In conclusion, biomaterials in autoimmunity are attractive resources for induction and treatment of autoimmune disorders. However, their biocompatibility properties should be studied in detail before their long-term use.

References

Alijotas-Reig J (2015) Human adjuvant-related syndrome or autoimmune/inflammatory syndrome induced by adjuvants. Where have we come from? Where are we going? A proposal for new diagnostic criteria. Lupus 24(10):1012–1018

Alijotas-Reig J, Garcia-Gimenez V, Llurba E et al (2012) Autoimmune/inflammatory syndrome (ASIA) induced by biomaterials injection other than silicone medical grade. Lupus 21 (12):1326–1334

Asquith DL, Miller AM, McInnes IB et al (2009) Animal models of rheumatoid arthritis. Eur J Immunol 39(8):2040–2044

Balenga NA, Zahedifard F, Weiss R et al (2006) Protective efficiency of dendrosomes as novel nano-sized adjuvants for DNA vaccination against birch pollen allergy. J Biotechnol 124 (3):602–614

Beeson PB (1994) Age and sex associations of 40 autoimmune diseases. Am J Med 96(5):457–462

Buyuktimkin B, Wang Q, Kiptoo P et al (2012) Vaccine-like controlled-release delivery of an immunomodulating peptide to treat experimental autoimmune encephalomyelitis. Mol Pharm 9 (4):979–985

Carambia A, Freund B, Schwinge D et al (2015) Nanoparticle-based autoantigen delivery to Treg-inducing liver sinusoidal endothelial cells enables control of autoimmunity in mice. J Hepatol 62(6):1349–1356

Colia R, Corrado A, Cantatore FP (2016) Rheumatologic and extraintestinal manifestations of inflammatory bowel diseases. Ann Med:1–9

Cooper GS, Stroehla BC (2003) The epidemiology of autoimmune diseases. Autoimmun Rev 2 (3):119–125

Correale J, Farez M, Gilmore W (2008) Vaccines for multiple sclerosis: progress to date. CNS Drugs 22(3):175–198

Descotes J (2004) Immunotoxicology of drugs and chemicals: an experimental and clinical approach. Elsevier, Amsterdam

El-Kamel AH, Sokar MS, Al Gamal SS et al (2001) Preparation and evaluation of ketoprofen floating oral delivery system. Int J Pharm 220(1–2):13–21

Fairweather D (2007) Autoimmune disease: mechanisms. Encyclopedia of Life ScienceS, p 1–6

Franca DC, de Castro AL, Soubhia AM et al (2013) Evaluation of the biocompatibility of silicone gel implants—histomorphometric study. Acta Inform Med 21(2):93–97

Gabriel SE, O'Fallon WM, Kurland LT et al (1994) Risk of connective-tissue diseases and other disorders after breast implantation. N Engl J Med 330(24):1697–1702

Galperin C, Gershwin ME (1997) Immunopathogenesis of gastrointestinal and hepatobiliary diseases. JAMA 278(22):1946–1955

Gammon JM, Tostanoski LH, Adapa AR et al (2015) Controlled delivery of a metabolic modulator promotes regulatory T cells and restrains autoimmunity. J Control Release 210:169–178

Gelderman KA, Hultqvist M, Pizzolla A et al (2007) Macrophages suppress T cell responses and arthritis development in mice by producing reactive oxygen species. J Clin Invest 117 (10):3020–3028

Getts DR, Martin AJ, McCarthy DP et al (2012) Microparticles bearing encephalitogenic peptides induce T-cell tolerance and ameliorate experimental autoimmune encephalomyelitis. Nat Biotechnol 30(12):1217–1224

Gomez S, Gamazo C, San Roman B et al (2008) Allergen immunotherapy with nanoparticles containing lipopolysaccharide from Brucella ovis. Eur J Pharm Biopharm 70(3):711–717

Goren I, Segal G, Shoenfeld Y (2015) Autoimmune/inflammatory syndrome induced by adjuvant (ASIA) evolution after silicone implants. Who is at risk? Clin Rheumatol 34(10):1661–1666

Hajdu SD, Agmon-Levin N, Shoenfeld Y (2011) Silicone and autoimmunity. Eur J Clin Invest 41 (2):203–211

Hansson GK, Hermansson A (2011) The immune system in atherosclerosis. Nat Immunol 12 (3):204–212
Holmdahl R, Sareila O, Olsson LM et al (2016) Ncf1 polymorphism reveals oxidative regulation of autoimmune chronic inflammation. Immunol Rev 269(1):228–247
Holmich LR, Lipworth L, McLaughlin JK et al (2007) Breast implant rupture and connective tissue disease: a review of the literature. Plast Reconstr Surg 120(7 Suppl 1):62S–69S
Hoveizi E, Tavakol S, Ebrahimi-Barough S (2015) Neuroprotective effect of transplanted neural precursors embedded on PLA/CS scaffold in an animal model of multiple sclerosis. Mol Neurobiol 51(3):1334–1342
Hunter Z, McCarthy DP, Yap WT et al (2014) A biodegradable nanoparticle platform for the induction of antigen-specific immune tolerance for treatment of autoimmune disease. ACS Nano 8(3):2148–2160
Hwang J, Rodgers K, Oliver JC et al (2008) Alpha-methylprednisolone conjugated cyclodextrin polymer-based nanoparticles for rheumatoid arthritis therapy. Int J Nanomed 3(3):359–371
Kannan K, Ortmann RA, Kimpel D (2005) Animal models of rheumatoid arthritis and their relevance to human disease. Pathophysiol 12(3):167–181
Kapoor B, Singh SK, Gulati M et al (2014) Application of liposomes in treatment of rheumatoid arthritis: quo vadis. Sci World J 2014:978351
Kawakami N, Lassmann S, Li Z et al (2004) The activation status of neuroantigen-specific T cells in the target organ determines the clinical outcome of autoimmune encephalomyelitis. J Exp Med 199(2):185–197
Ketelhuth DF, Hansson GK (2015) Modulation of autoimmunity and atherosclerosis—common targets and promising translational approaches against disease. Circ J 79(5):924–933
Kim WU, Lee WK, Ryoo JW et al (2002) Suppression of collagen-induced arthritis by single administration of poly(lactic-co-glycolic acid) nanoparticles entrapping type II collagen: a novel treatment strategy for induction of oral tolerance. Arthritis Rheum 46(4):1109–1120
Kim YJ, Chae SY, Jin CH et al (2010) Ionic complex systems based on hyaluronic acid and PEGylated TNF-related apoptosis-inducing ligand for treatment of rheumatoid arthritis. Biomater 31(34):9057–9064
Kumagai Y, Shiokawa Y, Medsger TA Jr et al (1984) Clinical spectrum of connective tissue disease after cosmetic surgery. Observations on eighteen patients and a review of the Japanese literature. Arthritis Rheum 27(1):1–12
Lernmark A, Larsson HE (2013) Immune therapy in type 1 diabetes mellitus. Nat Rev Endocrinol 9(2):92–103
Liang LS, Jackson J, Min W et al (2004) Methotrexate loaded poly(L-lactic acid) microspheres for intra-articular delivery of methotrexate to the joint. J Pharm Sci 93(4):943–956
Liu D, Ge Y, Tang Y et al (2010) Solid lipid nanoparticles for transdermal delivery of diclofenac sodium: preparation, characterization and in vitro studies. J Microencapsul 27(8):726–734
Loyo E, Jara LJ, Lopez PD et al (2013) Autoimmunity in connection with a metal implant: a case of autoimmune/autoinflammatory syndrome induced by adjuvants. Auto Immun Highlights 4 (1):33–38
Mathew A, Pakan JM, Collin EC et al (2013) An ex-vivo multiple sclerosis model of inflammatory demyelination using hyperbranched polymer. Biomater 34(23):5872–5882
Mitchell LA, Lauer FT, Burchiel SW et al (2009) Mechanisms for how inhaled multiwalled carbon nanotubes suppress systemic immune function in mice. Nat Nanotechnol 4(7):451–456
Moriuchi-Murakami E, Yamada H, Ishii O et al (2000) Treatment of established collagen induced arthritis with prostaglandin E1 incorporated in lipid microspheres. J Rheumatol 27(10): 2389–2396
Nesher G, Soriano A, Shlomai G et al (2015) Severe ASIA syndrome associated with lymph node, thoracic, and pulmonary silicone infiltration following breast implant rupture: experience with four cases. Lupus 24(4–5):463–468
Nicholas D, Odumosu O, Langridge WH (2011) Autoantigen based vaccines for type 1 diabetes. Discov Med 11(59):293–301

Petersen LK, Phanse Y, Ramer-Tait AE et al (2012) Amphiphilic polyanhydride nanoparticles stabilize Bacillus anthracis protective antigen. Mol Pharm 9(4):874–882

Petrovsky N, Aguilar JC (2004) Vaccine adjuvants: current state and future trends. Immunol Cell Biol 82(5):488–496

Pizzolla A, Gelderman KA, Hultqvist M et al (2011) CD68-expressing cells can prime T cells and initiate autoimmune arthritis in the absence of reactive oxygen species. Eur J Immunol 41 (2):403–412

Pujol-Autonell I, Serracant-Prat A, Cano-Sarabia M et al (2015) Use of autoantigen-loaded phosphatidylserine-liposomes to arrest autoimmunity in type 1 diabetes. PLoS ONE 10(6): e0127057

Rantapaa-Dahlqvist S, de Jong BA, Berglin E et al (2003) Antibodies against cyclic citrullinated peptide and IgA rheumatoid factor predict the development of rheumatoid arthritis. Arthritis Rheum 48(10):2741–2749

Rosenthal KS, Mikecz K, Steiner HL 3rd et al (2015) Rheumatoid arthritis vaccine therapies: perspectives and lessons from therapeutic ligand epitope antigen presentation system vaccines for models of rheumatoid arthritis. Expert Rev Vaccines 14(6):891–908

Ross R (1990) Mechanisms of atherosclerosis–a review. Adv Nephrol Necker Hosp 19:79–86

Ryan JJ, Bateman HR, Stover A et al (2007) Fullerene nanomaterials inhibit the allergic response. J Immunol 179(1):665–672

Sakai T, Kohno H, Ishihara T et al (2006) Treatment of experimental autoimmune uveoretinitis with poly(lactic acid) nanoparticles encapsulating betamethasone phosphate. Exp Eye Res 82 (4):657–663

Sanchez-Guerrero J, Colditz GA, Karlson EW et al (1995) Silicone breast implants and the risk of connective-tissue diseases and symptoms. N Engl J Med 332(25):1666–1670

Scott MD, Murad KL (1998) Cellular camouflage: fooling the immune system with polymers. Curr Pharm Des 4(6):423–438

Scott MD, Murad KL, Koumpouras F et al (1997) Chemical camouflage of antigenic determinants: stealth erythrocytes. Proc Natl Acad Sci U S A 94(14):7566–7571

Shakya AK, Holmdahl R, Nandakumar KS et al (2013) Characterization of chemically defined poly-N-isopropylacrylamide based copolymeric adjuvants. Vaccine 31(35):3519–3527

Shakya AK, Kumar A, Holmdahl R et al (2016) Macrophage-derived reactive oxygen species protects against autoimmune priming with a defined polymeric adjuvant. Immunol 147(1):125–132

Shakya AK, Kumar A, Klaczkowska D et al (2011) Collagen type II and a thermo-responsive polymer of N-isopropylacrylamide induce arthritis independent of Toll-like receptors: a strong influence by major histocompatibility complex class II and Ncf1 genes. Am J Pathol 179 (5):2490–2500

Shakya AK, Nandakumar KS (2012a) Applications of polymeric adjuvants in studying autoimmune responses and vaccination against infectious diseases. J R Soc Interface 10 (79):20120536

Shakya AK, Nandakumar KS (2012b) Polymers as immunological adjuvants: an update on recent developments. J BioSci Biotech 3:199–210

Shakya AK, Nandakumar KS (2015) Synthetic polymer as an adjuvant in collagen-induced arthritis. Curr Protoc Mouse Biol 4(1):11–24

Singh M, Solomon IH, Calderwood MS et al (2016) Silicone-induced Granuloma After Buttock Augmentation. Plast Reconstr Surg Glob Open 4(2):e624

Singh S, Gajra B, Rawat M et al (2009) Enhanced transdermal delivery of ketoprofen from bioadhesive gels. Pak J Pharm Sci 22(2):193–198

Smith DA, Germolec DR (1999) Introduction to immunology and autoimmunity. Environ Health Perspect 107(Suppl 5):661–665

So T, Ito HO, Koga T et al (1996) Reduced immunogenicity of monomethoxypolyethylene glycol-modified lysozyme for activation of T cells. Immunol Lett 49(1–2):91–97

Soehngen EC, Godin-Ostro E, Fielder FG et al (1988) Encapsulation of indomethacin in liposomes provides protection against both gastric and intestinal ulceration when orally administered to rats. Arthritis Rheum 31(3):414–422

Spiera RF, Gibofsky A, Spiera H (1994) Silicone gel filled breast implants and connective tissue disease: an overview. J Rheumatol 21(2):239–245

Suda K, Yanai T, Kawakami H et al (2016) Deterioration of autoimmune condition associated with repeated injection of dextranomer/hyaluronic acid copolymer: a case report. J Ped Surg Case Reports 4:10–12

van Belle TL, Coppieters KT, von Herrath MG (2011) Type 1 diabetes: etiology, immunology, and therapeutic strategies. Physiol Rev 91(1):79–118

van Nunen SA, Gatenby PA, Basten A (1982) Post-mammoplasty connective tissue disease. Arthritis Rheum 25(6):694–697

Yang F, Kamiya N, Goto M (2012) Transdermal delivery of the anti-rheumatic agent methotrexate using a solid-in-oil nanocarrier. Eur J Pharm Biopharm 82(1):158–163

Yednock TA, Cannon C, Fritz LC et al (1992) Prevention of experimental autoimmune encephalomyelitis by antibodies against alpha 4 beta 1 integrin. Nat 356(6364):63–66

Yoon YM, Lewis JS, Carstens MR et al (2015) A combination hydrogel microparticle-based vaccine prevents type 1 diabetes in non-obese diabetic mice. Sci Rep 5:13155

Decellularized Tissue Engineering

Nana Shirakigawa and Hiroyuki Ijima

Abstract Tissue Engineering consists of cells, a scaffold and cytokines. Decellularization represents the removal of cells from tissues or organs. Recently, decellularized tissue has been investigated as a scaffold for tissue engineering, termed decellularized tissue engineering. Importantly, the decellularized organ retains its original structure, which is then used as a template for organ construction. The decellularized organ also retains the tissue-specific extracellular matrix. Therefore, decellularized tissue can be used as a matrix to provide a suitable microenvironment for inoculated cells. Based on these concepts, the reconstruction of tissues/organs with decellularized tissue/organ has been attempted using decellularized tissue engineering. In this chapter, we introduce the typical methods used, history and attainment level for the reconstruction of specific tissues/organs. First, the different decellularized techniques and characteristics are introduced. Then, the commonly used analysis methods and cautionary points during decellularization and reconstruction with decellularized tissues/organs are explained. Next, the specific methods and characteristics of decellularized tissue engineering for specific tissues/organs are introduced. In these sections, the current conditions, problems and future work are explained. Finally, we conclude with a summary of this chapter.

Keywords Tissue engineering · Decellularization · Decellularized organ · Extracellular matrix · Blood vessel · Heart · Cartilage · Liver · Lung · Adipose · Skin · Kidney · Tendon · Nerve · Pancreas · Solubilized decellularized tissue

Abbreviations

CKD	Chronic kidney disease
CYP	Cytochrome P450
DC	Decellularized
DNA	Deoxyribonucleic acid

N. Shirakigawa · H. Ijima (✉)
Department of Chemical Engineering, Faculty of Engineering, Kyushu University, Fukuoka, Japan
e-mail: ijima@chem-eng.kyushu-u.ac.jp

A. Tripathi and J.S. Melo (eds.), *Advances in Biomaterials for Biomedical Applications*, Advanced Structured Materials 66,
DOI 10.1007/978-981-10-3328-5_5

ECM	Extracellular matrix
ESRD	End-stage renal disease
GA	Glutaraldehyde
HCl	Hydrochloric acid
MSCs	Mesenchymal stem cells
PTFE	Polytetrafluoroethylene
SDS	Sodium dodecyl sulfate

1 Introduction

Tissue engineering was propounded by Langer and Vacanti (1993) about two decades ago. The concept was to construct tissues by combining cells, scaffolds, and cytokines. Recently, the use of decellularized (DC) tissues as a scaffold for culturing cells or as a template for organs has been the focus of research. DC-tissues are obtained by removing cells from tissues that consist of an organ-specific extracellular matrix (ECM). Therefore, DC-tissues are expected to be an effective scaffold that has suitable components for the construction of tissues. In addition, DC-organs are also expected to be effective templates for the construction of organs because they retain their original three-dimensional structure. The seeding of cells to DC-tissues or DC-organs is termed "recellularization". Currently, the reconstruction of various tissues or organs by the recellularization of DC-tissues or DC-organs is being investigated.

Decellularization techniques can be divided into two categories: chemical agents and physical treatments. Table 1 shows the major agents/treatments of each decellularization mechanism and their characteristics (derived from Crapo et al. (2011) and summary of this chapter). Decellularization of tissues or organs is performed by using one agent/treatment or combining agents/treatments. In addition, the procedures for using chemical agents follow a pattern, for example, perfusion via blood vessels, or soaking on orbital shaker. The procedure depends on the structure or characteristics of each tissue/organ (Shirakigawa et al. 2012). The important characteristics and behaviors that should remain after decellularization depend on the target tissue/organ. Therefore, different methods of decellularization are used for different tissues/organs.

To date, DC-blood vessels, heart (containing heart valves), cartilage, liver, lung, adipose, dermal, kidney, tendon, nerve, and pancreas have been reported. The search results with "PubMed" are shown in Fig. 1. "Decellularized" and each organ/tissue name (such as "decellularized vascular/vessel" or "decellularized heart") were used as keywords for the search. Studies reporting decellularization are shown in this distribution. Although decellularization can be performed in any tissue/organ, the tissues/organs usually require reconstruction as a scaffold.

Table 1 Variation of decellularization agents

Agent	Mechanism	Characteristics
Chemical agents		
Acid and bases	Denature proteins	Used for solubilization of DC-tissue
Detergents	Forms micelle with phospholipid "cell membrane"	Difficult to remove from the tissue
Ionic detergents e.g. sodium dodecyl sulfate (SDS)		Widely used for decellularization Most powerful detergent for decellularization Associated with ECM, difficult to remove
Non-ionic detergent e.g. Triton X-100		Widely used for decellularization, but weaker than ionic detergents Perfect decellularization by Triton X-100 is difficult
Zwitterionic detergent e.g. CHAPS		Not commonly used Low power detergent for decellularization compared with Triton X-100 or SDS
Organic solvents e.g. Acetone e.g. Alcohols (ethanol)	Affinity for lipids	Usually used for adipose decellularization Sometimes used for sterilization
Enzymes e.g. Nuclease (DNase, RNase) e.g. Trypsin	Catalyzes the hydrolysis of ribonucleotide and deoxyribonucleotide chains Severs peptide bonds	Nuclease is a poor decellularization agent Usually used with other detergents Trypsin is a poor decellularization agent Damages the ECM
Physical treatments		
Freezing and thawing	Ice crystals disrupt cell membranes	Ice crystal formation may disrupt ECM structure
High pressure	Bursts cells and removes the cells	Can disrupt ECM structure

Derived from Crapo et al. (2011) and a summary of this chapter

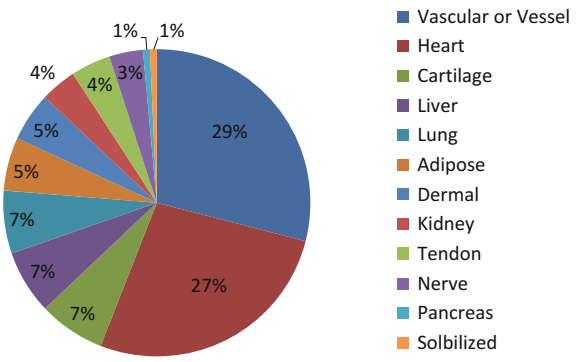

Fig. 1 Distribution of papers studying DC-tissues or organs (based on a PubMed search; date of search: 23 August 2016). The key words were "decellularized" and each organ/tissue name. The total number of papers was 1657

Each organ has a unique structure that performs a specific function, and this is important when evaluating which methods should be used for each tissue/organ. However, some basic methods of decellularization are common. First, this review will describe the common analysis methods and important points of decellularization and recellularization. Then, we focus on each tissue and organ in order and important points regarding each tissue/organ will be explained.

2 Common Analysis Methods and Cautionary Points During Decellularization and Recellularization

The method of decellularization depends on the target tissue/organ characteristics. However, some basic methods are common to all tissue/organ decellularization. These methods can be divided into three categories.

- Perfect cell removal
- Remaining tissue/organ-specific three-dimensional structure
- Remaining tissue/organ-specific ECM components.

Here, we introduce the widely used methods. First, histological evaluation, especially hematoxylin and eosin staining, is usually performed in most studies of DC-tissue/organs. Hematoxylin and eosin stains cell nuclei and other cell components purple and pink, respectively. Therefore, the above three points can be evaluated qualitatively by comparing the staining tissue/organ before and after decellularization.

Second, DNA content as an index of cell removal is widely used for quantitative analysis. The ideal value of DNA content of DC tissue was reported to be <50 ng dsDNA per mg ECM dry weight (Crapo et al. 2011), although, evidence for this was not shown. However, another study reported that DNA content should be evaluated based on wet weight (Mazza et al. 2015). If the dry weight is used, the value will be affected by the weight of cells because the tissue/organ weight is changed by cell removal during decellularization. We have measured the wet and dry weight of rat native/DC-liver right lobe and evaluated the water content ratios from these values. The water content of native liver was about 70%. However, the water content of DC-liver was greater than 99%. These results suggested that the dry cell weight was about 30% of the wet weight and the dry ECM weight was less than 1% of the wet weight. Therefore, the weight of cells can affect the dry weight of the target tissue/organ. Therefore, the wet weight should be used for quantitative analysis. By contrast, Lee et al. (2014) reported the ratio of remaining DNA in DC-liver versus that of native liver. They suggested that the remaining 3–4% DNA in the DC-tissue/organ was not a problem. Although the standard for analysis of DNA content is yet to be determined, the quantitative analysis of decellularization is important.

Once cells have been removed by decellularization, it is important that the ECM should remain. The ECM mainly consists of collagen fibers and proteoglycan complexes. Therefore, collagen and glycosaminoglycan are often evaluated as typical components of collagen fibers and proteoglycan complexes, respectively. These are sometimes evaluated quantitatively using an evaluation kit (Methe et al. 2014), or using qualitative immunostaining methods (Uygan et al. 2010). The ideal values of collagen and glycosaminoglycan have not been reported. Even if the value decreases by decellularization, if it will not affect the organ function or construction; therefore, the values are not critical. Furthermore, the specific components of each tissue/organ are evaluated. For example, collagen IV and laminin in the kidney (Peloso et al. 2015). In addition, each organ-specific structure is evaluated, such as the blood vessel network in the liver and alveolar size in the lung.

Recellularization of DC-tissues/organs will be performed if necessary. The cell adhesion and histological analysis of recellularized tissue are commonly evaluated. Then, further evaluations of functions are performed depending on the specific organ function such as the pumping movement in the heart and gas exchange in the lung. In summary, following the common analyses of DC-tissues/organs, further analyses are required for each tissue/organ. Next, we discuss some cautionary points during DC and recellularization.

First is the time from harvest of the tissue/organ to the finish of decellularization and sterilization. When reconstruction of the tissue/organ is performed using DC-tissue/organ, the length of time from harvest of the tissue/organ to the finish of decellularization and sterilization directly affects the time until the constructed tissue/organ can be administered to the patient. Long-term decellularization can denature or reduce the resolution of the ECM of the DC-tissue/organ. Furthermore, if the time is prolonged, a risk of contamination is increased and the cost for construction of the tissue/organ is increased.

Second, the washing process is important because the chemical agents used for decellularization are cytotoxic. The DC-tissue/organ should be washed before use as a scaffold for cell culture or transplantation. The washing process is usually performed for a few hours or days, which is the same or longer than that of incubation with the decellularization agent.

Third, the circulation system is important. During decellularization and recellularization, some solutions should be used sequentially. The circulation system is built by combining pumps and tubes, and is usually developed by each researcher based on their specific requirements and therefore, they are not standardized. In some organs, air bubbles in the flow solution can disrupt organ structures such as the vascular network in liver. Therefore, the flow solution should be continuous, and air vents should be contained in the circulation system when sensitive organs are used.

Fourth, stability of the flow solution speed or flow pressure in the tissue/organ is very important to maintain the structure of the DC-tissue/organ. Circulation of a solution at a high speed may cause the collapse of internal structures of the DC-tissue/organ. In addition, control of the speed of circulating culture medium is important especially during cell seeding because it affects cell adhesion.

Furthermore, the seeding process and conditions should be optimized, e.g. the type and number of seeded cells, the seeding method such as via the artery, and the period until restart of the culture medium circulation after cell seeding.

Finally, the sterilization of DC-tissues/organs is important for cell culture or construction of the tissue/organ for transplantation. Bacterial growth in DC-tissues/organs should be avoided during decellularization and recellularization. Therefore, antibacterial agents are often added to the circulating solution such as washing solution. In addition, the sterilization procedure is sometimes performed before transplantation or cell seeding. However, sterilization can damage the ECM of DC-tissues/organs. For example, gamma irradiation and peracetic acid can denature proteins. Therefore, the sterilization procedure should be selected depending on the organ characteristics. Based on the above points, the decellularization and recellularization procedure should be performed under mild conditions. In the Sect. 3 (3.1–3.12), we focus on specific tissues/organs and explain their background, structure, decellularization, and recellularization processes. In addition, some recent studies are introduced. The strain, decellularization method, tissue/organ specific evaluation except common analysis and future works are shown and summarized in each table.

3 Decellularization of Various Organs

3.1 Blood Vessels

Background

Injury of blood vessels due to accident or illness requires reparative surgery. Autografts are sometimes used, but these processes also cause the injury to the normal tissues and the limited with the range of uses. Thus, it is not considered a suitable treatment approach. Injured blood vessels are sometimes reinforced by stents. However, stents treatment has a limited range of application. Therefore, artificial blood vessels are required for clinical treatment. Each year, 1.4 million patients in the USA need arterial prostheses (Hasan et al. 2014).

Artificial blood vessels are the oldest artificial organ. Large artificial blood vessels (inner diameter (ID) $\geq$ 6 mm) were developed using synthetic polymers such as Dacron and polytetrafluoroethylene (PTFE). These Artificial blood vessels are good and have long-term patency for clinical treatment (Conte 1998). However, small (narrow) artificial blood vessels (internal diameter; ID < 6 mm) with suitable function have not been developed. Retaining patency in these vessels is difficult. Furthermore, artificial blood vessels consisting of synthetic polymers cannot replace native tissue. The ID of blood vessels in children should increase with growth, but this does not occur with synthetic artificial blood vessels. Conte (1998) reported "The 'ideal' vascular graft would be characterized both by its mechanical attributes and post implantation healing responses". Given the economic considerations, low cost and long-term durability are also important issues. Therefore, the development of

tissue-engineered artificial blood vessels to replace native tissues is required. Currently, materials such as cell-seeded synthetic materials, biodegradable polymers, cell sheets, and biopolymer are being studied. An example of biopolymer based artificial blood vessels that is close to clinical application is discussed. Sugiura et al. (2016) reported that 50:50 Poly (1-lactide-co-Ɛ-caprolactone) is allowed to flow into a glass tube and lyophilized. Then, the tube was coated with polylactic acid by electrospinning. The obtained tube was 3 mm in length and transplanted into mice for 8 weeks by infrarenal aortic interposition with microsurgery. Endothelialization and cell invasion were observed, but how to replace the native tissue in long term is being evaluated. However, products with sufficient function have not been developed. Another issue is that mechanical strength decreases with time by biodegradation. Therefore, the balance between biodegradation and maturation of blood vessels is a problem. However, when a DC-blood vessel is used, biodegradation is not necessary because it is an original basic structure.

Structure of blood vessels

The structure of blood vessels is shown in Fig. 2. The internal surface is covered with endothelial cells that provide antithrombogenicity. The medium layer consists of smooth muscle cells and controls the expansion and shrinkage of blood vessels. The ECM fixes the layers between the internal surface and medium layer. Mechanical strength is an important characteristic of blood vessels. It is determined in two directions, circumferential and longitudinal tensile strength. However, the values are dependent between studies.

Decellularized blood vessels

It is important to develop small artificial blood vessels. When scaled up from animals to humans, the size of vessels should be carefully considered because although the diameter is similar between species the length is different in humans. There have been many reports about DC-blood vessels (Moroni and Mirabella 2014; Mahara et al. 2015; Umashanakar et al. 2016). The mechanical strength of DC-blood vessels is important when used as a scaffold for the construction of blood vessels. However, the structure is a simple straight tube. Therefore, the decellularization methods used are common and include the use of flowing detergent and physical treatments such as high hydrostatic pressure. After decellularization, recellularization is usually performed using DC tissue engineering. Since, cells flow in the blood, so flowing cells can attach to the surface of DC-blood vessels indicating recellularization may not be necessary. The products made from synthetic polymers such as Dacron and PTFE are not recellularized. Therefore, recellularization might not be necessary for small artificial blood vessels. A trend of recent studies is non-seeding, which provides

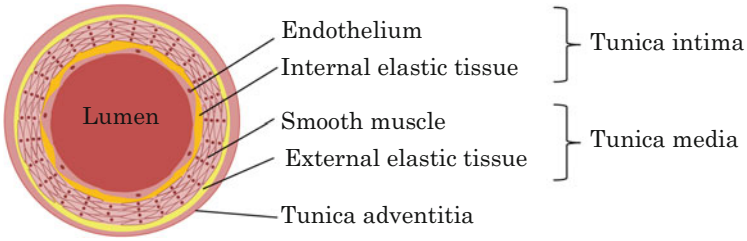

Fig. 2 The structure of blood vessels

Table 2 Recent studies of DC-blood vessels

Strain (reference)	Decellularization method	Artifice	Specific points	Future work
Ostrich carotid artery (Mahara et al. 2015)	Ultrahigh hydrostatic pressure (980 MPa, 10 min) → 40 U/ml DNase and 20 mM $MgCl_2$ for 3 days	10 M peptide solution at 60 °C to improve cell adherence	Samples were transplanted in pigs for 20 days as bypass graft between left and right femoral artery Small-diameter (ID: 2–4 mm) long-bypass (80–90 cm) Branchless	Long-term patency and immunogenicity under log-term transplantation model should be researched
Bovine pericardium patch (Umashanakar et al. 2016)	Nondetergent method (proprietary process) → 0.2% Glutaraldehyde for 10 min → 8% glutamic acid for 24 h → 70% ethanol	Mildly cross-linked	Samples were transplanted in pig ascending aorta for 1 year Patch Long-term transplantation	Complete structural regeneration (collagen, elastin formation)
Rat thoracic aorta (Gong et al. 2016)	0.5% SDS, 0.5% Triton X-100 and 0.5% sodium deoxycholate → 0.2 mg/ml DNase and 20 mg/ml RNase	100 μm thick nanofibrous PCL layer outside the decellularized vessel	Transplanted to infrarenal aorta Coating with nanofibrous material outside the decellularized vessel	Incorporating anticoagulant or antiplatelet drug delivery and nanotechnology to enhance biocompatibility and hemocompatibility

anti-thrombogenicity and improvement of cell adhesion. Table 2 summarizes the findings of three studies.

These studies used interesting techniques. Mahara et al. (2015) reported the decellularization of ostrich carotid artery using a non-detergent method. This material is very interesting because the ostrich carotid artery is narrow, long and straight without branching. Blood vessels usually have many branches. If the branches are tied to form a straight scaffold, the knot will prevent the smooth flow of blood and coagulation may occur. Therefore, the use of a straight blood vessel without unexpected branches is important for obtaining an ideal scaffold. They showed the long-term patency of the transplanted DC-artery using a porcine experiment. The advancement of this research for clinical use is expected. Umashanakar et al. (2016) proposed the use of DC-blood vessels as a patch for treatment of a blood vessel hole. This method is expected to be used for a wide variety of areas including accidents during surgery. The development of this patch is expected. Gong et al. (2016) suggested that mechanical strength was decreased during decellularization treatment. Therefore, they coated DC-blood vessels with a nanofibrous material using electrospinning to improve its strength. Using suitable material for specific role in association with other materials is a good idea. In these studies, recellularization was not performed.

Future work

Tissue-engineered artificial blood vessels should have anti-blood clotting property and mechanical strength. To achieve these objectives, artificial blood vessel should be sufficiently endothelialized and have an elastic force similar to the native tissue. The perfect replacement of ECM of DC-vessels by native cells and tissue will hopefully achieve these objectives. Collagen is the main constituent of ECM and is a trigger for coagulation. Therefore, the use of pre-endothelialization or anti-blood clotting coating for complete endothelialization is necessary for clinical use. Furthermore, the long-term stability of endothelialization is needed. The mechanical strength of DC-blood vessels is expected to be close to the strength of the original, so the hope for its use as a scaffold for the construction of blood vessels is high.

3.2 Heart Valves

Background

In Germany, 29,672 heart valve surgeries were performed in 2013, and the patient number is increasing globally (Theodoridis et al. 2016). Currently there are two basic types of artificial heart valve products: mechanical heart valves and bioprosthetic heart valves. Both have advantages and disadvantages. Mechanical heart valves are made of artificial biomaterials (mainly pyrolytic carbon) that allow them to be used for a lifetime, but patients are treated daily with Warfarin, an anticoagulation medicine. In addition, the level of the medicine is checked more than once per month. Bioprosthetic heart valves are made of porcine aortic valves or bovine

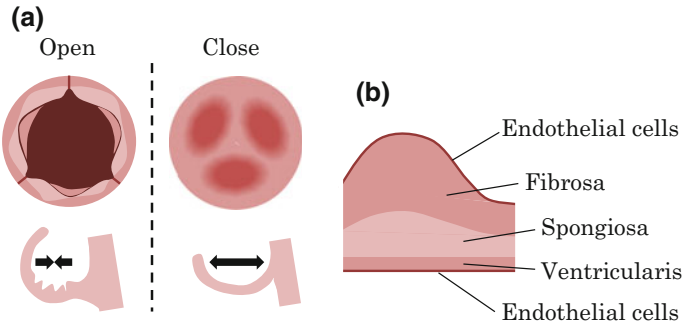

Fig. 3 The structure and characteristics of heart valves. **a** Images of the aortic valve in open and closed position (from the aorta). **b** Aortic valve histology emphasizing trilaminar structure

pericardial xenografts. These are treated with glutaraldehyde (GA). The GA treatment devitalizes and sterilizes tissues and also reduces tissue immunogenicity (Roosens et al. 2016). Patients receiving transplanted bioprosthetic heart valves have to take Warfarin for the first few months, but the valves suffer from calcification and have to be transplanted again 10–20 years later. Therefore, the development of a novel heart valve that can be used for a lifetime without Warfarin is desired.

Structure of heart valves

The structure and characteristics of heart valves are shown in Fig. 3. As shown in Fig. 3b, the surface of the heart valve consists of endothelial cells. The internal middle layer consists of interstitial cells. The heart valves perform repetitive opening and closing movements many times during lifetime (Fig. 3a). Therefore, durability is important.

Decellularization of heart valves

Mechanical grafts require mechanical strength and biocompatibility when used for heart valves. However, the endothelialization of the surface is needed for anti-coagulation. Recent studies are shown in Table 3.

The commonly used detergents are not powerful for decellularization. Although the decellularization of heart valves is thought to be difficult because of its internal vascular network, but reports suggest all cells can be removed. However, bioprosthetic heart valves, which retain some cells, are widely used. Therefore, the complete removal of cells may not be important. The disadvantages of mechanical valves are anti-coagulation and for bioprosthetic valves it is prolonging the effective application period by anti-calcification. DC-heart valves are expected to resolve these problems. Therefore, characteristic analysis of DC-heart valves should include anti-coagulation and anti-calcification. Some studies have reported the clinical use of DC-heart valves. In these studies, recellularization was not performed. The endothelialization of DC-heart valves is thought to occur after transplantation in vivo. Mechanical valves and bioprosthetic valves were not endothelialized but have been used in clinical treatment. Therefore, endothelialization before transplantation may not be important.

Table 3 Recent studies on DC-heart valves

Strain (reference)	Decellularization	Sterilization	Recellularization	Specific evaluation
Porcine (Ota et al. 2007)	80% PEG for 68 h → 100 kGy gamma irradiation → 70 U/mK DNase for 48 h	(100 kGy gamma irradiation)	PERV and a1, 3-Gal were analyzed by PCR Transplanted in rats and dogs calcification was determined	Hyperacute rejection evaluation Hemodynamic functional evaluation Effect of gamma irradiation to collagen
Human (Cebotari et al. 2011; Sarikouch et al. 2016)	0.5% SDC, 0.5% SDS for 36 h	Not shown	Transplanted to patients Analysis of peak gradient by MRI size growth with child growth	Provide further data and follow-up of transplanted patients
Porcine (Theodoridis et al. 2016)	0.5% Triton X-100 for 24 h → 0.5% SDS for 24 h	7.5% iodine solution for 5 min	SDS quantification by uniaxial tensile test porcine aorta-derived endothelial cells were seeded onto cusps and biocompatibility was analyzed	In vivo testing in large animals
Porcine (Zhou et al. 2015)	1% Triton X-100 and 0.05% trypsin → 0.2 mg/ml DNase and 20 mg/ml RNase for 1 h	Not shown	Coated with 10 mg/ml 20 kDa PEG, 1 mg/ml RGD peptide and 1000 pg/ml VEGF Endothelial progenitor cells were seeded and adhesion/growth were analyzed	Evaluation of endothelialization in vivo, differentiation under shear stress

RGD Arg-Gly-Asp, *VEGF* vascular endothelial growth factor, *PERV* vascular endothelial growth factor, *PEG* polyethylene glycol

Future work

The structure of heart valves is simple, therefore, the clinical application of artificial heart valves is hoped for in the near future. To improve the current treatment, the long-term (more than 20 years) stability of endothelialization and mechanical strength should be evaluated. To achieve this, both the endothelialization of the surface but the replacement of native tissues in the middle layer of heart valves may be necessary to construct a complete heart valve. If this can be achieved, the heart valves will grow in conjunction with the growth of a child to adulthood.

3.3 Heart

Background

Heart disease is the leading cause of death in the USA and throughout many advanced countries (Sánchez et al. 2015). Although the gold standard treatment for end-stage heart failure is still heart transplantation through surgery, the shortage of donor organs is a severe problem. Even if a matching donor is found, there are risks of postsurgical complications (Zia et al. 2016). As with any other organ transplantation, patients are treated with long-term immune-suppressants that cause a variety of side effects including immunodeficiency, hypertension, diabetes and renal insufficiency. Therefore, 24% patients die within 5 years after transplantation. To solve these problems, the development of tissue-engineered hearts is required.

Structure of the heart

The heart mainly consists of muscle and blood vessels as shown in Fig. 4. Its function is to pump blood throughout the whole body and its internal surface is composed of endothelial cells that allow blood cells to adhere. The internal middle layer consists of high-density muscle except in the heart valves.

Decellularization of the heart

To construct an artificial heart, DC-tissues should retain the original three-dimensional structure as a scaffold for cell adhesion. Endothelial cells should attach and cover the internal surface. Muscle cells should invade into the middle layer and grow. To perform its functions, the muscle cells have to beat strongly and steadily. A summary of recent studies is shown in Table 4.

SDS and Triton X-100 are usually used for decellularization of the heart. These solutions enter the heart via the ascending aorta. The heart muscle contains a very narrow vascular network; therefore, detergents cannot be used with this network

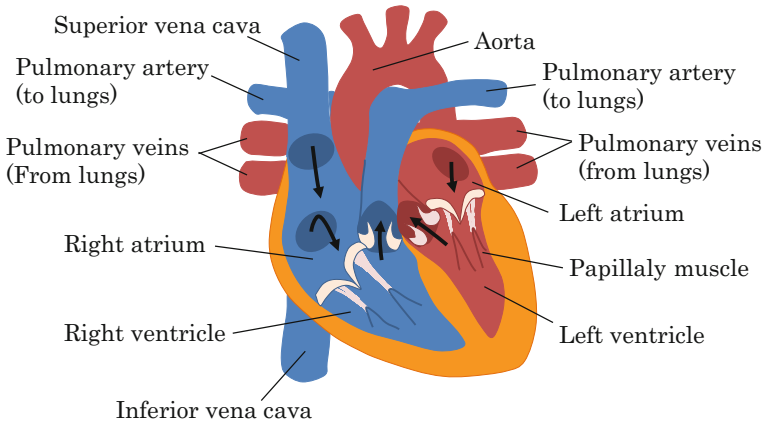

Fig. 4 Structure of the heart. *Arrow* shows the flow of blood

Table 4 Recent studies of decellularized hearts

Strain (reference)	Decellularization	Sterilization	Recellularization	Specific evaluation	Future works
Rat (Ott et al. 2008)	1% SDS → 1% Triton X-100	Perfuse with antibiotics—containing PBS for 124 h	5–7.5 × 10^7 rat neonatal-cardiomyocyte cells/one DC-heart injected in the anterior left ventricle and 2 × 10^7 rVECs were perfused through the aorta	Functional assessment of contractile force analysis of movement, heterotopic transplantation	Improve the contractile force (currently 2% of adult rat) Optimization of seeded cells
Rat (Yasui et al. 2014)	0.5% SDS → 1% Triton X-100	Perfuse antibiotic-containing PBS for 30 min	1 × 10^8 rat neonatal-cardiomyocyte cells/one DC-heart perfused through the aorta	Electrocardiograms ventricular pressure Live tissue imaging of calcium transient responses	Improve conduction velocity placement of cells
Pigs (Methe et al. Methe et al. 2014)	−80 °C → room temperature → 4% SDC → 1% SDC → 1% Triton X-100	0.1% peracetic acid for 3 h	None	Assessment of DC-heart matrix in detail	Potential immunogenic reactions Infectious risks through porcine retrovirus or α-Gal epitopes
Pigs (Kitahara et al. 2016)	−80 °C → 4 °C → 1% SDS → 1% Triton X-100	Gamma irradiation	1.5 × 10^7 pMSCs/one DC-heart compared seeding methods (coronary perfusion vs. injection)	Heterotopic transplantation Coronary angiography histological analysis	Optimization of seeding cells and re-endothelialization method
Human (Sánchez et al 2015, 2016)	1% SDS	Not shown	hMSCs or HUVECs seeded on sliced DC-human heart	Cell differentiation Electrical activity	Optimization of cell type for recellularization

rVEC rat vascular endothelial cell, *hMSC* human mesenchymal stem cell, *HUVEC* human umbilical vein endothelial cell, *SDC* Sodium deoxycholate

because detergents attack the middle layer cells of the heart wall by diffusion from an internal surface. Thus, a powerful detergent for decellularization is required. Furthermore, Triton X-100 is used to remove remaining SDS or cell debris inside the DC-matrix.

Recellularization of DC-heart

The heartbeat is maintained by heart muscles. Therefore, recellularization with cardiomyocytes is necessary for reconstruction of the heart. To develop sufficient muscle strength, a high cell density and culture of muscle inside the DC-heart are important. Furthermore, electrical activation is required during recellularized DC-heart culture to improve the strength of seeded cardiomyocytes. Although Ott et al. (2007) have performed electrical activation of heart cells during a medium circulation culture. Kitahara et al. (2016) suggested that differentiation of mesenchymal stem cells (MSCs) to heart muscle or endothelial cells was not sufficient without electrical activation. Although circulation culture systems containing an electrical activation system are complicated, this is required for the construction of functional muscle. Furthermore, the placement of each suitable cell to a suitable place is difficult. Kitahara et al. (2016) also suggested that the transmission of electric signals will not be successful if certain cells such as immature cells (e.g. myoblasts) are seeded and differentiated inside the DC-heart. Recent studies reported the use of heterotopic transplantation. However, coagulation occurred after the transplantation because complete endothelialization was not performed, and long-term transplantation with blood flow was not achieved.

Future work

The improvement of muscle strength of recellularized DC-heart is necessary to construct an alternative organ for the heart. To date, only a few of the adult heart functions gave been reported (Ott et al. 2008). To improve the muscle strength of recellularized DC-heart, high-density placement of muscle cells is important. In addition, electric activation is also important for training the constructed muscle. A pacemaker might be required to maintain a steady heartbeat. During the recellularization of DC-heart, uniform recellularization is required in each heart atrium and cardiac chamber. Furthermore, the complete endothelialization of internal surfaces is important for anti-coagulation in the heart. These studies can be performed with animal models, but when the scale-up will be performed for humans, much higher cell numbers will be needed. The adult human heart contains 2×10^9 cardiomyocytes (Smit and Dohmen 2014). The growth and maturation of seeded cells inside the DC-heart during organ culture will be important. However, the construction of a bioreactor system to train muscle to achieve the required blood pressure and flow is important for recellularized DC-heart cultures. In addition, a reinforcement product such as a heart cell sheet or reinforcement patch with DC-heart powder may be useful alternatives to whole heart products.

3.4 Liver

Background

There are about 27,000 deaths annually in the USA due to liver disease (Yagi et al. 2013). End stage liver diseases including cirrhosis, chronic viral hepatitis, hepatocellular carcinoma, injuries from alcohol abuse, or even inborn metabolic disorders, often lead to demands for organ transplantation (Sabetkish et al. 2015). However, 20% of patients die on the waiting list due to a shortage of organ donors (Mazza et al. 2015). The liver is a regenerative organ and even if 70% of the liver is harvested, the donor can survive (Shirakigawa et al. 2013). Often, a living liver transplantation is performed in the clinic because of a cadaveric donor shortage. However, this treatment has a potential risk of death for the donor, and therefore, alternative treatments should be developed such as tissue-engineered liver construction.

Structure of liver

The structure of the liver is shown in Fig. 5. The liver consists of millions hepatic lobules, which are the minimum functional unit of the liver. Hepatocytes are the main cell type involved in liver functions. The liver has a fine blood vessel network, and hepatocytes require oxygen for their survival and function.

Decellularization of liver

Liver, composed of hepatocytes, has many functions and is the central organ of metabolism. Because hepatocytes require oxygen, recellularization of hepatocytes and construction of blood vessel networks are important for the construction of a functional liver. A summary of recent studies is shown in Table 5.

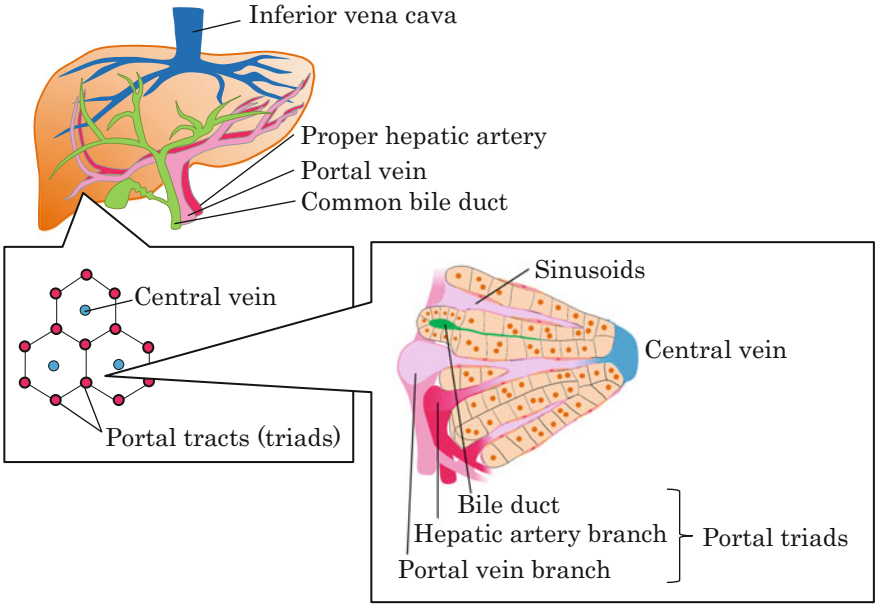

Fig. 5 Structure of the liver

Table 5 Recent studies of decellularized liver

Strain (reference)	Decellularization	Sterilization	Recellularization	Specific evaluation	Future works
Rat (Uygan et al. 2010)	Frozen → 4 °C → 0.01%–1% SDS for 72 h → 1% Triton X-100 for 30 min	0.1% peracetic acid for 3 h	2×10^8 primary rat hepatocytes seeded via portal vein divided in four steps	Vascular structure albumin synthesis Urea secretion heterotopic transplantation	High density cell seeding (20% of native liver) endothelialization Biliary tract reconstruction
Rat (Shirakigawa et al. 2013)	Rat right lobe 4% Triton X-100 3 h→0.5 mg/ml DNase, RNase 6 h	5% GA → 70% ethanol	1×10^6 HepG2 cells in collagen from surroundings 2–3.6 × 10^6 HUVECs via portal vein	Vascular structure albumin synthesis	High density cell seeding
Pigs (Yagi et al. 2013)	−80 °C → 4 °C → 0.01%–1% SDS for 72 h→ 1% Triton X-100 for 30 min	0.1% peracetic acid for 3 h → ultraviolet irradiation for 1 h	1×10^9 primary pig hepatocytes seeded via portal vein divided in four steps	Vascular structure Bile duct structure albumin synthesis urea secretion	Application for acute hepatic failure Endothelialization
Rat, sheep (Sabetkish et al. 2015)	Rat: 1% Triton X-100 for 1 h→ 0.05% SDS Sheep: 1% SDS and 5% Triton X-100	Not shown	Rat: 1.8 × 10^7 new born rat cells seeded via portal vein	Hepatic enzyme level	Adhesion, migration Differentiation Proliferation and survival of seeded cells Immunogenic effects of xenogeneic scaffold
Piglet (Ko et al. 2015)	1% Triton X-100, 0.1% ammonium hydroxide for 2–3 days	1.2 MRad gamma irradiation	5×10^7 vascular endothelial cells seeded via portal vein	Heterotopic transplantation and fluoroscopic angiography	Immobilization anti-thrombotic agents, recellularization with hepatocytes

(continued)

Table 5 (continued)

Strain (reference)	Decellularization	Sterilization	Recellularization	Specific evaluation	Future works
Human (Mazza et al. 2015)	Human left lobe -80 °C→ 4 °C → 0.025% Trypsin-EDTA → 0.01% SDS → 3% Triton X-100 → 1% SDS (for 2 weeks)	0.1% peracetic acid/4% ethanol	5 × 5 × 5 mm sized DC-liver and 2 × 10^6 LX2, HepG2, SK-Hep1 cells were seeded respectively	Transplanted subcutaneously in mice and biocompatibility was analyzed	Endothelialization, placement to suitable place Proteomic studies of ECM Liver functional analysis

EDTA ethylenediaminetetraacetate

To construct a fine vascular network, the original three-dimensional structure of the liver should be used as a scaffold. Therefore, chemical agents are used for the decellularization of liver via the portal vein, the major blood vessel in the liver. The vascular network structure was evaluated by forming a template of it with resin. Previous reports observed an intact vascular-tree network. However, the quality of the remaining structure is different between studies. At the macroscopic levels, they show similarities to the original structure. However, the liver requires oxygen, so the thickness of the hepatocytes aggregate that can survive is a maximum of 50 μm. The remaining vascular network structure should contain small diameter vessels for use as a template in DC-liver. Thus, the ideal distance between blood vessels is less than 100 μm. Even if the cell growth (regeneration of liver) occurs during the culturing of recellularized DC-liver or transplantation in vivo, the length between blood vessel structures in the template (i.e. DC-liver) should be less than 1 mm (Shirakigawa et al. 2013).

Recellularization is necessary for functional liver construction because hepatocytes perform the main functions of the liver. For recellularization, various liver cells were used (Table 5). After recellularization of DC-liver with hepatocytes, liver specific functions were determined as follows: albumin synthesis as an index of protein synthesis ability, cytochrome P450 (CYP) activity as an index of drug metabolism ability and urea secretion. Albumin synthesis or urea secretion was reported in recellularized DC-liver cultures. Therefore, drug metabolism functions such as CYP activity should also be analyzed in recellularized DC-liver. Currently, the function of recellularized DC-liver is reduced compared with native liver. An improvement in seeded cell density is expected. It is assumed that the minimum liver weight required to support a patient with acute liver failure is approximately 5–10% of total liver weight. Therefore, about 10 billion human cells, or 50–100 million rat cells must survive and function in the reconstructed liver (Caralt et al. 2014).

Heterotopic transplantations of porcine and rat DC-liver were reported. However, coagulation occurred inside the transplanted graft in the liver. In addition, long-term transplantation with blood flow was not achieved. Therefore, the perfect endothelialization is needed.

Future work

Hepatocytes require an oxygen supply for survival and function indicating a functional vascular network is necessary. Therefore, endothelialization is required in DC-liver. The inoculation of a high cell density should improve liver specific functions of DC-liver. However, to achieve a high cell density similar to native numbers in vivo is difficult. Cells need to be seeded at a low density of about 1/10 that in vivo. Then, reconstruction to the in vivo cell density should be occur following cell growth and neo-vascularization during recellularized DC-liver culture or transplantation in vivo. Additionally, it would be useful to have bile secretion in DC-liver. In the future, it is hoped reconstructed liver grafts are used for orthotopic transplantation. The ECM containing ratio of the liver is very low compared with other organs and the mechanical strength of DC-liver is weak; thus,

it might be difficult to maintain abdominal pressure. Reinforcement of the constructed graft may be needed.

3.5 *Lung*

Background

In the USA, nearly 30 million patients currently suffer from end-stage lung disease, with 12.1 million adults affected by chronic obstructive pulmonary disease, the fourth leading cause of death (Song et al. 2011). Lung transplantation remains the only definitive treatment, but donor shortage is a severe problem. Therefore, the construction of an alternative donor lung is required.

Structure of lung

The lung function is to exchange gas. Oxygen is supplied from the atmosphere to blood, and carbon dioxide is released from the blood to the atmosphere. To achieve this, the lung has fine vascular networks and many alveoli as shown in Fig. 6. The surface of an alveolus consists of epidermal cells and the lung can shrink and expand with the movement of the diaphragm.

Decellularization of lung and recellularization

The lung is a special organ because it has three phases: gas, liquid, and solids that exchange gas between the blood and atmosphere. Cells are usually cultured in liquid culture medium, but epidermal cells on the surface of alveolus have to be exposed to the atmosphere. The three-dimensional structure of the airways should be retained before and after decellularization of the lung. Therefore, the solution circulation system for decellularization has to contain a channel for retaining the airway structure including fine structures such as alveoli and the vascular network. Therefore, the detergent method is usually used for decellularization. The solutions usually enter the lung via the lung artery, but the airways can also be used. A summary of four recent reports are shown in Table 6.

As mentioned above, because oxygen should be supplied from the atmosphere to blood in the lung, the construction of blood vessels and alveolar surfaces is important. Therefore, the seeding and culture of epidermal cells and endothelial

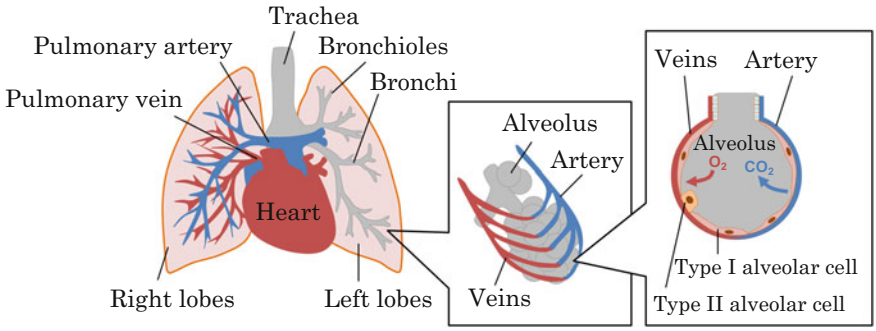

Fig. 6 Structure of the lung

Table 6 Recent reports of decellularization of the lung

Strain (reference)	Decellularization	Sterilization	Recellularization	Specific evaluation	Future works
Rat (Ott et al. 2010)	0.1% SDS for 120 min → for 10 min 1% Triton X-100	Not shown	6×10^7 HUVECs via pulmonary artery and veins respectively at 4:1, 3×10^8 rat fetal lung cells via airways	Orthotopic transplantation (6 h), O_2 and CO_2 exchange Alveolar size, number and volume	Maturation of recellularized DC-lung by optimization of pre-culture conditions
Rat (Song et al. 2011)	0.1% SDS for 120 min → 1% Triton X-100 for 10 min	Not shown	Same as above Dry ventilation 5 days before transplantation	Orthotopic transplantation of left lung (14 days) gas exchange Alveolar size and number	Epidermal cellularization of airways Regeneration of a functional mucociliary apparatus
Human (Nichols et al. 2016)	−80 °C → 45 °C → 1% SDS for 2 days → 0.1% SDS for 1 day	3% H_2O_2	3.5×10^7 cells: 13LU cells via airways or HUVECs via pulmonary artery	Heavy smoker versus non-smoker Observation by PET-CT, static compliance	Construction of alveolar-capillary junction Evaluation of gas exchange through blood
Rat, human (Ren et al. 2016)	Rat: 0.1% SDS for 120 min → 1% Triton X-100 for 10 min Human: 0.5% SDS for 4–7 days → 1% Triton X-100 for 1 day	Rat: not shown Human: 200 Gy gamma irradiation	Rat: hiPSC-ECs 4×10^7 cells and hiPSC-PCs 2×10^7 cells were seeded via PA and PV Human: hiPSC-ECs 2.8×10^8 cells and hiPSC-PCs 1.25×10^8 cells were seeded via PA and PV	Seeded rat lung: endothelial coverage and wet/dry ratio Seeded rat left lung: orthotopic transplantation for 3 days	Complete endothelial coverage and mature vascular function

PET-CT positron emission tomography/computed tomography, *PA* pulmonary artery, *PV* pulmonary vein

cells is necessary. After recellularization of DC-lung, specific analyses are performed: comparison of alveolar size and number before and after decellularization, and evaluation of gas exchange of oxygen and carbon dioxide. In addition, the fetal cells or cell lines were seeded on airways instead of primary lung cells. The growth ability of primary lung cells might be poor. Orthotopic transplantation for a few days was reported, but the size of the transplanted recellularized DC-lung was reduced by macroscopic observation (Song et al. 2011). The engraftment of recellularized DC-lung is still difficult.

Future work
Functional lungs should perform gas exchange with breathing. To achieve this, there are three important points: (1) no leakage of air from airways by epidermal cellularization of the airways; (2) the constructed organ should have sufficient mechanical strength for breath; and (3) blood can flow in the vascular network without clotting. These points should be achieved before its clinical use. In addition, the long-term stability and the homogeneity of constructed lung should be determined.

3.6 Kidney

Background
Chronic kidney disease (CKD) is a global public health issue with an estimated prevalence of 8–16% worldwide. End-stage renal disease (ESRD) eventually develops in 0.15–2% of patients with overt CKD annually, and renal replacement therapy with dialysis or transplantation is required (Figliuzzi et al. 2014). Nearly 1 million patients in the USA live with ESRD, with over 100,000 new diagnoses every year. Although hemodialysis has increased the survival of patients with ESRD, transplantation remains the only available curative treatment. However, donors are lacking. In addition, even patients that receive a transplanted kidney from a donor, 20% of recipients experience an episode of acute rejection within 5 years of transplantation, and approximately 40% of recipients lose graft function within 10 years after transplantation (Song et al. 2013). The development of tissue-engineered kidney is required as a solution to these problems.

Structure of the kidney
The kidney filters the blood and creates urine to control fluid balance, and regulate the balance of electrolytes. All the blood in our bodies passes through the kidneys several times a day. The structure of the kidney is shown in Fig. 7.

Decellularization of kidney and recellularization
Kidney filters the blood plasma to form urine. Then, reabsorption is performed via renal tubules. The kidney consists of two systems: blood vessels and urinary ducts. A summary of recent studies is shown in Table 7.

Decellularization of the kidney is usually performed by passing the detergent solution through the artery because the kidney structure is important for reconstruction using the kidney as a scaffold. As a detergent, SDS is widely used for

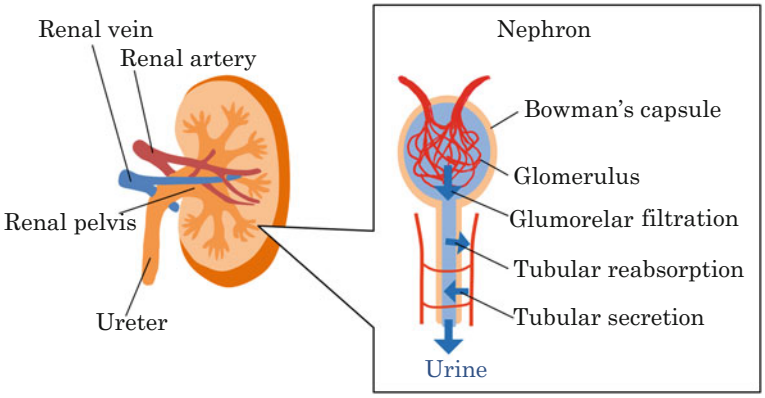

Fig. 7 Structure of the kidney

kidney decellularization indicating removing cells in the kidney is difficult. Reconstruction of the kidney requires the construction of a blood vessel system and urinary duct system. To achieve this, endothelial cells were seeded via the artery and kidney cells were seeded via the urethra (Song et al. 2013). Another study used stem cells seeded via the artery to allow the cells to differentiate in DC-kidney (Guan et al. 2015). Currently, the construction of a blood vessel system and urinary duct system is difficult. During orthotopic transplantation, coagulation occurred in DC-kidney when the endothelial cells were seeded suggesting that the complete construction of a vascular network system is required for the construction of a kidney. When the recellularization of DC-kidney was performed with kidney cells, creatinine or urea syntheses as kidney functions were evaluated. However, these functions should be improved as an alternative to hemodialysis or kidney donors.

Future work

The complete construction of a vascular network is necessary because of the high blood flow through kidneys. Kidney cells should be inoculated at a suitable area and the construction of the urethra is required. The performance of kidney function should be improved; however, functions such as filtration by the glomerulus or reabsorption via the renal tubules will be difficult to achieve.

3.7 Adipose

Background

In plastic surgery, the construction of adipose tissue is valuable for reconstruction and cosmetics. After resection for breast cancer, breast reconstruction requires adipose construction of cm in size. Reconstruction can be achieved by allografts; however, the allograft has to move with blood vessels. Therefore, the dermis or muscle must be cut open. High biocompatibility synthetic materials such as clinical silicon have been developed. However, atrophy occurs in 10% of transplanted

Table 7 Recent studies of decellularized kidney

Strain (reference)	Decellularization	Sterilization	Recellularization	Specific evaluation	Future works
Rat (Song et al. 2013)	1% SDS for 12 h → 1% Triton X-100 for 30 min	Not shown	5×10^7 HUVECs were seeded via artery and 6×10^7 rat neonatal kidney cells were seeded via urethra	Orthotopic transplantation was performed and urine flow and creatinine clearance were determined	Evaluate bleeding or graft thrombosis during transplantation Demonstrate physiologic graft size and anatomic features
Rat (Peloso et al. 2015)	Left kidney: 1% Triton X-100 for 85 min → 1% SDS for 85 min	Not shown	4×10^6 human pancreatic carcinoma cells (MIA-PaCa2) were seeded via artery	Glomerular volume and glomerular hilum vascular diameters Orthotopic transplantation	Optimization of decellularized protocol Endothelialization
Rat (Guan et al. 2015)	0.5% SDS for 4 h	Not shown	1×10^8 mouse ES cells via artery and urethra	Vascular tree observation Orthotopic transplantation Creatinine, urea	Scale up Seeded cell maturation Improve recellularization
Rat (Mei et al. 2016)	0.1% Triton X-100 for 3 h → 0.8% SDS for 3 h	Not shown	No	Partial transplanted into lower 1/3 of left kidney	Continual angiogenesis
Rat (Zhan et al. 2015)	0.1% Triton X-100 for 125 min → 0.8% SDS for 250 min	2KC Gray X-Gray for 4 min	No	Orthotopic transplantation Vascular casting	Regeneration of glomeruli and tubules

patients and the shape of the transplanted material can change. In addition, although the adipose tissue loses elasticity with age, artificial materials remain unchanged. Therefore, the balance of the body changes with time. Recently, studies have reported the injection of autograft adipose, obtained from the abdomen or thigh by absorption of adipose. However, survival and shape control of injected adipose is difficult. Thus, the development of tissue-engineered adipose is required.

Structure of adipose
Adipose consists of adipose cells, ECM, and a fine vascular network, which is simple in structure. Adipose cells contain a fat reservoir, so the size of the cell depends on the amount of fat.

Decellularization of adipose
A summary of recent reports of decellularization of adipose is shown in Table 8. Adipose does not contain large blood vessels. Therefore, it cannot be perfused with chemical agents via blood vessels. Thus, DC-adipose was obtained by repeated freeze-thaw cycles and soaking in decellularized agent solution. The differentiated ratio of adipose was increased when adipose-derived stem cells were seeded onto decellularized adipose. The mixture of cells and DC-adipose is usually transplanted subcutaneously, and the engraftment of the transplanted tissue is examined for functional analysis. In addition, the density of the vascular network required for engraftment of transplanted tissue is often performed. Oil red O staining of the adipose is used for analysis of transplanted tissues.

Future work
Adipose tissue injection is performed in plastic surgery, but the survivability of transplanted adipose obtained from the abdomen or thigh by absorption of adipose is less than 50%. The survivability can be improved to 85–90% by injection of a mixture consisting of adipose tissue and adipose-derived stem cells selected by centrifugation. However, the reconstruction of a sufficient volume adipose is difficult using these methods alone. These problems might be resolved by combining a scaffold such DC-adipose tissue with adipose-derived stem cells. As a scaffold, it should be effective for adipose construction because it will promote adipose-derived stem cell differentiation. In addition, the formation of a vascular network using DC-adipose as a scaffold will allow the survival of transplanted adipose. The improvement of survival rate of the transplanted tissue or the acceleration of adipose tissue formation should be examined in the future. However, the control of its three-dimensional shape may be difficult. Combining other materials such as synthetic biodegradable polymers that become a gel in situ might allow its flexible formation.

3.8 Dermis

Background
The skin is our first line of defense against the outside world and provides a barrier against physical and biological attack, moisture retention, thermoregulation or

Table 8 Recent studies of decellularized adipose

Strain (reference)	Decellularization	Sterilization	Recellularization	Specific evaluation	Future works
Rat groin skin/adipose tissue flaps (2×4 cm^2) (Zhang et al. 2016a)	(−80 °C→ R.T.) × 3 cycles → 0.25% trypsin/EDTA for 2 h → 1% Triton X-100 for 2 days	70% ethanol	2×10^5 HUVECs via artery and vein 1×10^6 hASCs and 2×10^5 HUVECs injected at 10 sites	Implanted with microsurgery Oil red O staining Vessel density	Increasing the patency of the vascular plexus
Human ($4 \times 2 \times 1$ cm) (Wang et al. 2013)	(−80 °C → R.T.) × 3 cycles → 0.25% trypsin/EDTA for 2 h → 1% Triton X-100 for 3 days	Not shown	Freeze-dried and crushed by mill. Then, mixed with saline. 2×10^5 live cells from 0.5 ml of fresh graft (containing 4×10^4 hASCs) were suspended	Subcutaneously injected into the back of nude rats Vessel density	Research on sterilization and immune responses in large animal models Cell plus multiple growth factor injection, revealing the role of each cell type in fat
Mice (Lu et al. 2014)	(−80 °C → 37 °C) × 3 cycles → 0.05% trypsin/EDTA for 16 h → 99.9% isopropanol for 2 days → 0.05% trypsin/EDTA for 4 h → 99.9% isopropanol for 8 h	Rinsing 3 times in 70% ethanol	No cell, heparin cross-linked by using EDC/NHS, then bFGF binding was performed	Subcutaneously transplanted Oil red O staining Vessel density	Optimization of heparin cross-linking and bFGF binding Long-term stability Large volume engineering
Mice (Zhang et al. 2016b)	(−80 °C → 37 °C) × 3 cycles → 0.05% trypsin/EDTA for 16 h → 99.9% isopropanol for 2 days → 100 U/ml Benzonase for 16 h → 99.9% isopropanol for 8 h	Rinsing in 70% ethanol	No cell, heparin cross-linked by EDC/NHS, then bFGF binding was performed and mincing	Subcutaneous injection Oil red O staining Vessel density	Dynamics analysis of ECM during the course of adipose neo tissue development Large tissue construction

(continued)

Table 8 (continued)

Strain (reference)	Decellularization	Sterilization	Recellularization	Specific evaluation	Future works
Human (Han et al. 2015)	(−80 °C → 37°C) × 3 cycles → 0.25% trypsin/EDTA for 16 h → 99.9% isopropanol for 2 days → 0.25% trypsin/EDTA for 6–16 h→DNase/RNase/Lipase for 16 h	3 times rinsing in 70% ethanol	1×10^6 rASCs were seeded on 150 mg samples	Subcutaneously transplanted in rats Blood vessel diameter and density	Revealing the role and characterization of the host cell population in the observed fat formation

R.T. room temperature, *rASC* rat adipose derived stromal cells, *EDC* ethylenedichloride, *NHS* N-Hydroxysuccinimide, *bFGF* basic fibroblast growth factor

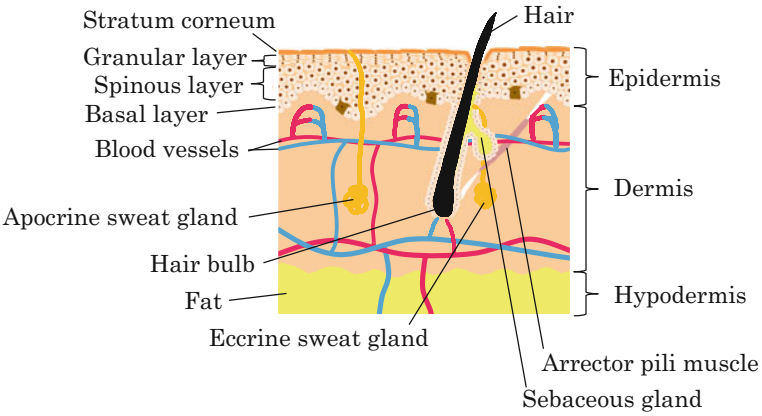

Fig. 8 Structure of the skin

excretion of waste products by sweating, as well as transmitting touch sensations. The skin heals itself by natural reconstruction when lightly injured. However, larger wounds may result in prolonged healing time complicated by infection or which might not heal (Nyame et al. 2015). When the skin is destroyed over a large area, it might be life threatening. Autografts remain the gold standard for the management of large wounds. However, injuries such as large area burns cannot be treated with autografting. In addition, when autograft treatment is performed, the surrounding skin is injured forming a new wound. To resolve these problems, many bioproducts have been developed to promote the healing of skin functions.

Structure of the skin

The skin consists of a subcutaneous bilayer formed by the epidermis and dermis as shown in Fig. 8. The epidermis is 0.1–0.3 mm thick and mostly consists of keratinocytes (about 95%). The dermis is tightly connected to the epidermis by a basement membrane. The dermis consists of ECM and fibroblasts, and has a fine vascular network connected to the subcutaneous tissue. The dermis contains nerves, hair roots, sebaceous glands, and sweat glands.

Bioproducts and decellularized skin

In the tissue engineering field, Rheinwold and Green (1975) reported a method of expanding keratinocytes in vitro and keratinocyte cell sheets are sold as a tissue-engineered bioproducts (Epicel®, Genzyme Biosurgery, Corp., Cambridge, MA, and Jace®, Japan Tissue Engineering Co. Ltd., Aichi, Japan). The protocol uses a skin sample larger than 1 cm^2 isolated from the patient. Then, the keratinocytes are isolated and cultured. After 2–3 weeks, a sheet of cultured epidermis measuring 1000 cm^2 is produced. However, this product only consists of the epidermis. In a deep wound, the dermis is also injured and because the keratinocyte cell sheet preparation requires the long-term culture of a patient's cells with high cost, this treatment is not suitable for acute injury.

Allograft is another treatment after autograft. Allografts need to be sterilized to avoid disease transmission. During sterilization, graft proteins are denatured killing the graft cells. Therefore, this product consists of denatured human ECM and another person's dead cells. It can be used as a temporary alternative skin that functions as a barrier. After transplantation, the allograft is slowly replaced by the regenerating host tissue. Although it does not have a special function, low cost production may be achieved because it is produced by the sterilization of human skin. Another product, GammaGraft® (Promethean LifeSciences, Inc., Pittsburgh, PA) is a ready-to-use, gamma-irradiated allograft.

Decellularized allograft products are also available. Allograft products contain dead cells, which have no healing effect. Therefore, its function is similar to the allograft product. Decellularization allows a space for the patient's cells to invade, and it can perform as a scaffold for the reconstruction of skin. AlloDerm® (LifeCell Corporation, Branchburg, NJ) or Graftjacket® (Wright Medical Technology, Inc., Memphis, TN) are already available. Recently, MatrACELL® (LifeNet Health, Inc., Virginia Beach, VA) is a human DC-dermis product that uses a non-denaturing anionic detergent (N-lauroyl sarcosinate) (Moore et al. 2015). Gentler decellularization procedures should be developed. In addition, allogenic skin has been developed, consisting of human cells and biomaterials such as collagen. For example, Apligraf® (Organogenesis, Canton, MA) has a bilayer structure. The upper epidermal layer is formed by promoting human keratinocytes (epidermal cells). The lower dermal layer combines bovine collagen I and human fibroblasts (dermal cells), which produce additional matrix proteins. However, these products do not contain a vascular network, hair roots or sweat glands, and therefore can be improved.

Other products use xenografts or DC-xenografts. The most important benefit of these products is that the material can be obtained in large quantities and with a large size. Porcine xenografts are the most commonly used xenograft (Nyame et al. 2015). Xenografts act as a temporary barrier and decrease the healing time. DC-xenografts might act as a template for the reconstruction of skin and may have a function similar to DC-allografts if a suitable treatment is developed and performed.

Future work

Although many bioproducts have been developed for skin treatment, and clinical studies have been reported for these products, the optimal procedure for each product or treatment method has not been developed, and should be investigated in the future. However, the high cost of these techniques is a disadvantage. Because these products will be used to treat large areas, the cost should be reduced. New products of DC-skin should follow one of two paths: (i) perfect skin that is identical to native skin that functions immediately after transplantation, and does not require replacement by the patient's own skin; and (ii) a low cost skin with wide versatility that can be stored at room temperature, and used as a template for the reconstruction of skin. This would be invaded by the patient's cells and help skin cell growth and neo-vascularization.

Currently, a recellularized DC-dermis is not available. The recellularization of DC-dermis has advantages and disadvantages. An advantage is that seeded cells may promote replacement with the patient's cells or produce ECM if human

fibroblast cells are also seeded. If a patient's cells are seeded, the time to replacement may be decreased. A disadvantage is the high cost of cell seeding, culture processes for recellularization, and transportation or storage. After recellularization and culture, the products should be used within a few days and transported at 37 °C, or otherwise stored in a freezer to keep the seeded cells alive. However, it may become a perfect skin immediately. Furthermore, the cell source is a problem. For cells that are ready-to-use, identification of the patient immune type or a highly efficient method for cell growth will be needed. To develop low cost skin, DC-skin using xenografts may be useful compared with allografts. To improve the function of DC-skin as a scaffold, some additional functions are required such as promoting cell growth or neo-vascularization, and antibacterial activity to decrease the risk of infections.

Finally, no products or studies have reported the reconstruction of nerves, hair roots, sebaceous glands, and sweat glands, and this should be addressed in future studies. In addition, the visual appearance of the reconstructed skin should be as natural as possible to enhance the quality of life of the patients. Even if this raises the costs, some patients will hope for a natural visual reconstruction.

3.9 Cartilage

Background

Aging population has increased the number of patients suffering from cartilage disorders such as osteoarthritis, the most common joint disease in the USA, affecting an estimated 27 million Americans (Bautista et al. 2016). Additionally, if the cartilage is injured, self-repair is limited because it consists of dense ECM without a vascular network. When the injury is small, treatments such as bone drilling or autograft transplantation can be used. Bone drilling describes the drilling of the subchondral bone to induce blood flow. The blood coagulates at the injured cartilage area and becomes cartilage. However, the reconstructed cartilage is fiber cartilage not hyaline cartilage. Autograft transplantation describes the harvesting of a small rod of cartilage from an area that is not subject to strain from body weight and that is then transplanted to the injured area. Using this method, the transplanted cartilage is similar to the original cartilage, but its usable range is limited. However, these methods cannot be performed in patients with a large injury. When the healing of cartilage injury is difficult, an artificial joint might be transplanted. However, the durability of artificial joints is limited to 10–20 years. Therefore, this treatment is not suitable for young patients.

In the tissue-engineering field, tissue-engineered cartilage is available as Jack™ (Japan Tissue Engineering Co.). This method harvest a small cartilage sample from the patient, then the chondrocytes are isolated and cultured in Atelocollagen gel for four weeks. Furthermore, the proliferating chondrocytes with gel are transplanted to the injured site. This method is a novel treatment. However, the healing time is long, about 6–12 months is needed until the patient can walk. Thus, the development of a new treatment method for the reconstruction of hyaline cartilage in a short-term is required.

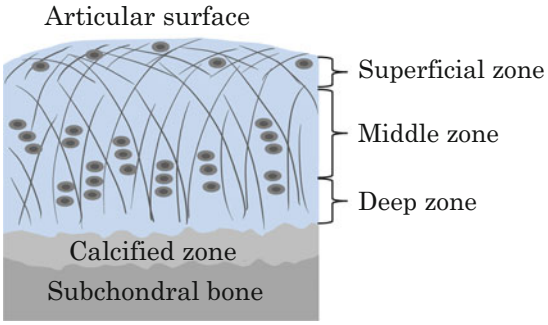

Fig. 9 The structure of cartilage

Structure
Cartilage overlaid on the subchondral bone consists of dense ECM (Fig. 9). The superficial zone consists of collagen II fibers aligned in parallel to the articular surface to resist shear stress, and the deep zone consists of the same fibers aligned perpendicularly to the bone interface to absorb compressive loads. There is no vascular network in cartilage.

Decellularized cartilage
A summary of recent studies about DC-cartilage are shown in Table 9.

Because there is no vascular network in cartilage, decellularization of cartilage is usually performed by freeze-thawing or diffusion of detergents from the surface. Some studies have used cartilage directly without chopping. Decellularization of cartilage is often performed after chopping. The reason is that cartilage consists of dense ECM and the diffusion of a detergent may be difficult. In addition, when it is transplanted to the injured site, its shape may be controlled better when added as a chopped sample. For recellularization, MSCs are widely used. The necessity of recellularization is unclear, but the cartilage cells are needed to maintain the cartilage for a long time. However, the seeding density and method must be optimized.

Future work
When DC-cartilage is used without chopping, it might be used as a template for the reconstruction of cartilage. If the original ECM exists, then reconstruction may be achieved in a short time. However, the control of its shape to match the injured site and the method of seeding cells inside the dense ECM will be difficult. The decellularized chopped cartilage or solubilized DC-cartilage may be better for shape control, but the construction of a three-dimensional structure will also be difficult. Evidence for the promotion of reconstructed cartilage using DC-cartilage is needed.

3.10 Tendon

Background
Tendons connect bone and muscle. The most commonly affected tendons are the finger and hand flexors and extensors, the rotator cuff, and the Achilles tendon. In

Table 9 Recent studies of decellularized cartilage

Strain (reference)	Decellularization	Evaluation	Future work
Pig tibiofemoral joints (Bautista et al. 2016)	Freeze-thaw four cycles → 0.125 U/ml chondroitinase for 24 h → 0.1% SDS for 24 h → 100 U/ml DNase and 1 U/ml RNase → 0.1% peracetic acid	3×10^7 MSCs/ml-sample were seeded and centrifuged at 400 × g for 5 min, then cultured and analyzed	In vivo implantation
Human nasoseptal cartilage (Graham et al. 2016	Triton X-100 for 12 h → 90 U/ml DNase and 85 mg/ml RNase for 5 h	Mechanical and biocompatibility testing	Long-term stability and structural/mechanical characteristics Repopulated with appropriate host cells In vivo preclinical animal model experiments
Pig femoral condyles cartilage (Rowland et al. 2016)	−80 °C and lyophilized for 24 h → freezer/mill → 2.5mM $MgCl_2$, 0.5 mM $CaCl_2$ and 50 U/ml DNase → homogenize	Flow in silicone molds and lyophilized, crosslinked and sterilized via dehydrothermal treatment Sterilized in 70% ethanol for 15 min 8×10^6 MSCs/ml were seeded	Hierarchical organization of the newly synthesized tissue

particular, acute Achilles tendon ruptures have an increasing incidence of 18 per 100,000 (Lovati et al. 2016). When injured seriously, movement of the connected part is difficult, and self-repair is difficult. Large tendon damage needs to be repaired using any tissue substitutes. Allograft transplantation is usually performed, but there are disadvantages, such as slow incorporation into host tissues, potential disease transmission, danger of infection, tunnel widening caused by immune responses, delayed tendon-bone healing, and lower mechanical character (Dong et al. 2015). In addition, both synthetic and biological scaffolds have been used in studies, but a viable tendon substitute is not yet widely available for clinical applications. Therefore, a tissue-engineered tendon should be developed.

Structure

Tendons consist of a low cell density (5%) of collagen fibers containing collagen I (more than 90%) (Lovati et al. 2016).

Decellularized tendon

There are many reports about DC-tendons (Lovati et al. 2016). A summary of recent reports is shown in Table 10.

The diffusion of detergent for the decellularization of tendons is difficult because of the presence of dense collagen fibers. Therefore, freeze/thaw cycles are widely used for the decellularization of tendons, and sliced tendons are sometimes used. The sliced tendon is used to form a rod by "rolling up" the tissue. However, slicing can

Table 10 Recent studies on decellularized tendons

Strain (reference)	Decellularization	Sterilization	Recellularization	Specific evaluation	Future work
Porcine (Yin et al. 2013)	10 × 10 mm × 80 m sliced tendon → 200 U/ml DNase for 14 h	Not shown	5×10^5 human tendon stem/progenitor cells per scaffold	Rolled decellularized tendons were transplanted into rat Achilles tendon for 2 weeks mechanical properties compared with non-seeding group	A longer period of in vivo study
Rats (Farnebo et al. 2014)	−70 °C → 2% SDS in 1% ethylenediaminetetraacetic acid	5% peracetic acid	No	Biomechanical testing Transplanted into rats	Reseeding with pluripotent cells Potential risk of graft burst
Beagle dogs (Pan et al. 2015)	Achilles tendons freeze/thaw → 300 μm slice → nuclease treatment → freeze-dried	Ethylene oxide gas	No	Transplanted into rabbits Biomechanical testing	Long-term study Comparison of natural graft Scale-up
Human digitorum tendons (Schmitt et al. 2013)	−70 °C → 0.1% SDS in 0.1% ethylenediaminetetraacetic acid for 24 h	Not shown	ASCs were seeded at 1–2×10^6 cells/ml/cm-tendon	Subcutaneous implantation in nude rats	Analysis of seeded cell necrosis Long-term study Transplantation to a large animals for orthotopic graft repair
Rabbit semitendinosus tendon (Dong et al. 2015)	Frozen → 0.05% Trypsin-EDTA for 1 h → 1.5% peracetic acid mixed with 2% Triton X-100 for 4 h → neutralization with 5% $NaHCO_3$	Not shown	Not performed	Transplanted to rabbit anterior cruciate ligament biomechanical test	Compare with autograft Analysis of pH effect Long-term study Analysis of immunologic rejection

ASC adipose derived stromal cells

change its mechanical strength. A rabbit model is often used for the analysis of tendon repair (Lovati et al. 2016). After transplantation, histological analyses and biomechanical tests are performed (Pan et al. 2015). Results suggest that the DC-tendon will be useful for tendon repair. However, it is not currently ready for clinical use. Previous analyses were performed in animal models. For human clinical use, the mechanical strength will be different. Therefore, an index of its strength for clinical use should be developed. In addition, long-term stability analysis is required and the role of DC-tendons should be determined during healing.

Future work

The promotion of tendon reconstruction of tendon is expected by the use of DC-tendon as a template. However, the necessity of recellularization of DC-tendon is still unclear. In addition, its mechanical strength and durability should be studied further. Although tendon injury is not life threatening, it can reduce the quality of life for patients. Its structure is very simple, so the quick development of reconstruction techniques is desired.

3.11 Pancreas

Background

According to the World Health Organization, at least 285 million people worldwide suffer from diabetes. While pharmaceutical interventions and insulin supplementation are the most common treatment of diabetes, these do not represent a cure and can potentially lead to long term complications (Goh et al. 2013). β-cell replacement through islet or pancreas transplantation is the only therapy that can reliably re-establish a stable euglycemic state (Peloso et al. 2016). However, transplantations have a disadvantage of a severe donor shortage. To solve this problem, studies have attempted to develop artificial pancreas using a machine to control blood glucose levels in an ideal range by the injection of insulin based on monitoring of the blood glucose level. Recently, the downsizing of machines and the stabile control of blood glucose levels have been reported (Haidar et al. 2015). However, long-term stability is still a problem. Therefore, a tissue-engineered pancreas might resolve these problems.

Structure

The pancreas contains endocrine and exocrine tissues. Endocrine islets contain α-cells and β-cells, which produce glucagon and insulin, respectively that control the blood glucose level. Although the pancreas consists of exocrine islets (more than 90%), it is abnormalities of the endocrine islets that affect the patient's life. Therefore, reconstruction of the endocrine system should be developed.

Decellularization and recellularization

DC-pancreas might be used as a scaffold for the transplantation of islets that can survive in vivo. A summary of recent studies of DC-pancreas are shown in Table 11.

Table 11 Recent studies of decellularized pancreas

Strain (reference)	Decellularization	Sterilization	Recellularization	Specific evaluation	Future work
Mice (Goh et al. 2013)	0.5% SDS for 5.4 h → 1% Triton X-100 for 15 min	Not shown	3×10^7 MIN-6 cells via portal vein and 3×10^7 AR42J cells via pancreatic duct	Vascular structure AFM Insulin gene expression	Optimization of recellularization procedure
Human (Peloso et al. 2016)	1% Triton X-100 and 0.1% ammonium hydroxide solution for 48 h → DNase and 0.0025% magnesium chloride	12 kGy gamma irradiation	2×10^6 human primary pancreatic endothelial cells	Vascular structure double line perfusion system	Understanding the mechanisms of interactions between the matrix and cells Using optimal cell for regeneration of the endothelium and islets

AFM atomic force microscope

The pancreas is a soft organ with a vascular network. Therefore, decellularization of the pancreas is usually performed by detergents without physical treatment. After decellularization, recellularization is required for full functionality. Either pancreas cells or endothelial cells are seeded and cultured and then the vascular density or insulin secretion is evaluated. However, the seeding of each cell type at a suitable location will be difficult.

Future work

Previous studies have not reported an improvement of the mass transfer between islets and blood because of the difficulty of constructing a vascular network. In addition, the stabilization of transplanted islets in vivo is also a problem that needs to be solved. Therefore, for transplanted islets to survive, the construction of a vascular network is needed. DC-pancreas may be a suitable ECM for islets, but it is very soft. A previous study reported that the kidney was used as a scaffold to construct pancreas (Willenberg et al. 2015). Furthermore, the reconstructed pancreas should be strengthened to endure abdominal pressure. DC-pancreas might be achieved if a fine vascular network can be achieved in the scaffold. Finally, by seeding each cell type at each suitable location, the DC-pancreas function might be improved.

3.12 Others

Tissues and organs consist of cells and ECM. Therefore, the decellularization of any tissue and organ can be performed in theory. However, the difficulty of decellularization depends on the specific structure of each tissue and organ. A summary of studies on the decellularization of other tissues and organs is shown in Table 12.

Table 12 Studies on the decellularization of other tissues and organs

Organ/strain (reference)	Decellularization	Sterilization	Recellularization	Specific evaluation	Future work
Native bovine bone (Bhumiratana et al. 2016)	High velocity stream of water to remove the marrow for 1 h → 0.5% SDS for 24 h → 50 U/ml DNase and 1 U/ml RNase for 3–6 h	70% ethanol for 1 h	About 10^7 pASCs/ml-decellularized bone	Transplantation to pig mandible Observation by CT/CT with time	Vascularization of implanted tissues
Rats sciatic nerves (Wakimura et al. 2015)	1% SDS for 24 h → 1% Triton X-100 for 1 h	7 days rinsed in antibiotic-antimycotic-containing PBS	No	15 mm in length implanted at the center of rat thigh by end-to-end suturing	Application to a big animal for clinical treatment

CT computerized tomography

As shown in Table 12, decellularization has been applied to bone and nerves. In these tissues, the promotion of reconstruction might be achieved by decellularized tissues containing the original ECM components and structure for use as a template. If the efficiency of DC-tissues for reconstruction is shown, then other DC-tissues may be studied further.

4 Solubilized Decellularized Tissues/Organs

Background
The survival, original function, and growth of isolated cells or transplanted cells from tissues or organs can be difficult. The construction of an in vivo-like microenvironment is required for such cells. The solubilization of DC-tissues/organs will allow the collection of material for tissue culture or construction. However, it is still unclear what factors affect cell differentiation, for example, physical specifications such as hydrophobic character, or ECM content.

Efficient cell differentiation is a problem in the tissue engineering field. It was reported that differentiation can be promoted by culturing cells on specific ECM (Nakamura and Ijima 2013). Solubilized DC-tissues/organs might be used as a potential scaffold for differentiation. In addition, for solubilized DC-tissues/organs, the shape of the material may be controlled by coating or gelation of the three-dimensional structure, which might be useful for cell culture material and construction of the tissue/organ. A summary of recent studies of solubilized decellularized tissues/organs is shown in Table 13.

For the solubilization of DC-tissues/organs, there are two methods: (i) the tissue/organ is chopped *before* decellularization; and (ii) the tissue/organ is chopped *after* decellularization. When a tree-like vascular network is present, the perfusion of a chemical agent via the network will achieve efficient decellularization. Therefore, after decellularization, DC-tissues/organs might be easier to dissociate. However, if the chopping is performed before decellularization, a greater decrease in ECM might occur during decellularization because of the increased surface area. When there are many fine vascular structures, the severed ends of the vascular structures will be present at the chopped surface allowing the detergent to diffuse more efficiently. When few vascular structures are present, it is better to perform decellularization after chopping because the diffusion of the detergent depends on the surface area. Retention of the three-dimensional native structure is not required because the DC-tissue/organ will be solubilized. Physical treatments such as freeze/thaw cycles are often combined. For the solubilization of DC-tissues/organs, 0.1 N HCl and pepsin are often used. Collagen, which is the main component of ECM, is usually derived with HCl; however, pepsin is also used because HCl alone cannot solubilize DC-tissue/organ efficiently. However, acid or enzymes can damage the ECM. Therefore, the amount used or length of incubation should be reduced.

Table 13 Recent studies of solubilized decellularized tissues/organs

Species (reference)	Decellularization	Solubilization	Application for experiment	Specific evaluation	Future work
Porcine nerve, spinal cord, brain (Crapo et al. 2012)	Freeze-dried → 0.02% trypsin/0.05% EDTA for 1 h → 3% Triton X-100 for 1 h → 1 M sucrose → 4% deoxycholate for 1 h → 0.1% peracetic acid in 4% ethanol for 2 h → freeze-dried	Comminuted into particles (<1 mm) → solubilized with 1 mg/ml pepsin in 0.01N HCl → neutralized with 0.1 N NaOH and isotonically balanced with 10 × PBS	Addition to medium	PC12 cells were seeded on a PLL-coated plate at 1500 cells/cm^2. Then, ECM was added 50:50 to medium and cultured for 2 days. Cell differentiation was analyzed. PC12 had greater differentiation in presence of 100 μg/ml ECM compared with PBS controls	Application for regenerative medicine
Rat livers (Nakamura and Ijima 2013)	4% Triton X-100 in CMF-PBS was perfused for 6 h 0.2 mg/ml DNase and 0.2 mg/ml RNase in CMF-PBS was circulated for 12 h	The obtained decellularized liver (L-ECM) was cut into small pieces and solubilized in 6N HCl for 3 days	L-ECM film 0.03 mg/ml L-ECM solution was prepared and added in culture plate at 200 μl/1.1 cm^2. Then, it was air-dried for 2 days. The film was cross-linked with 1% glutaraldehyde for 3 h Specific analysis	The immobilization and release of growth factor was analyzed by L-ECM film and Collagen I film. L-ECM film immobilized HGF more than Collagen I. Primary rat hepatocytes were cultured on HGF immobilized L-ECM film	To form a gel
Rat livers (Lee et al. 2014)	1% Triton X-100 and 0.1% NH_4OH in distilled water was perfused for 4 h Then, distilled water was perfused to wash out the decellularizing solution in the matrix. After that, the matrix	Then, the LEM was solubilized with 10% pepsin in 0.1 M HCl for 48 h at room temperature. The final concentration of LEM was adjusted to 40 mg/ml by 0.1 M HCl	LEM Hydrogel Formation LEM was mixed with 10% 10 × PBS and the pH of the solution was adjusted to 7.4 with 0.5 N NaOH. Then, it was incubated for 30 min at 37 °C. The final	Primary rat hepatocytes (7.5 × 10^5 cells/100 μl) in LEM hydrogels were cultured and compared with Collagen I. Albumin secretion and urea synthesis in LEM were higher than with	To examine inflammatory responses of LEM hydrogel Long-term maintenance of LEM hydrogel in vivo

(continued)

Table 13 (continued)

Species (reference)	Decellularization	Solubilization	Application for experiment	Specific evaluation	Future work
	(LEM) was freeze-dried and chopped		concentration of LEM in the hydrogel was adjusted 10 or 20 mg/ml They also prepared a coating solution of LEM and a 2D culture was performed	Collagen I. These were transplanted subcutaneously in mice for 7 days. The availability of albumin positive cells in LEM was higher than for Collagen I	Biocompatibility of LEM hydrogel (e.g., inflammatory responses) should be checked Other organs
Porcine brain (DeQuach et al. 2011)	Brains ware cut into halves → 0.1% SDS for 3–4 days → frozen	1 mg/ml pepsin in 0.1 M hydrochloric acid → final concentration was 20 mg/ml	Matrix coating Brain matrix coating 1 mg/ml brain matrix added to 0.1 M acetic acid for 1 h Matrix gel Matrix solution was neutralized with NaOH and 10 × PBS. Diluted to 16 and 12 mg/ml with PBS and injected into mouse back subcutaneously to form a gel	iPSC-derived neurons were cultured on a brain matrix	Long-term studies to assess in vivo biocompatibility, degradation time, and cell infiltration and survival
Porcine and human pericardia (Self-Naraghi et al. 2010)	Porcine pericardium: 1% SDS for 24 h, Human pericardia: 1% SDS for 60 h → freeze-dry → milled to powder	10 mg/ml ECM and 0.1 M HCl and 1 mg/ml pepsin	Neutralized to pH 7.4 by adding 1 M NaOH and 10 × PBS	90 µl samples were injected into rat left ventricular-free wall. Then neovascularization was observed	Produce the material using patient's own tissues Human trial

PLL poly-L-lysine, *HGF* hepatocyte growth factor, *iPSC* induced pluripotent stem cell

Future works
Solubilized DC-tissue/organ can be used as an ECM matrix for culture dish coating or as a three-dimensional culture material by gelation. The concentration of the matrix or gel strength should be optimized. Furthermore, the construction of an organ might require a combination of three-dimensional printing technology or decellularized organs. In addition, its application by injection-like spray, as a patch of tissue or to reinforce tissues will be useful.

5 Conclusions

Dermis and heart valve bioproducts from bovine or porcine have already been developed and decellularized human dermis is already available. These tissues are easy to use clinically because their function is simple or it is used at a denuded area. However, the knowledge gained using these materials can be applied to other tissues/organs. The use of other tissues/organs with xenografts is also expected to be developed in the near future. Of course, DC-tissue/organ allografts can be used, but these treatments can be expanded by using xenografts. Organs such as the heart or liver from cadaveric donors are not usually used for transplantation. However, DC-organs can be obtained from cadaveric donors. We have discussed the various studies on the reconstruction of tissues/organs based on DC-tissue/organ in Sect. 3. However, the most common problem for the reconstruction of a functional organ is the endothelialization or construction of a vascular network in the DC-organ. By developing efficient vascularization methods, these studies will be improved. Another common problem is the seeding method used to inoculate cells to a suitable location. Mature cells could be used or immature cells could be seeded first and mature cells seeded second. The latter method is expected to be more successful, but there is a risk of cancer from the immature cells. Therefore, differentiation methods should be improved. The DC-tissue/organ can be used to construct a suitable microenvironment for cells. The reconstruction of various tissues/organs is expected based on the use of decellularized tissues/organs.

References

Bautista CA, Park HJ, Mazur CM et al (2016) Effects of chondroitinase ABC-mediated proteoglycan digestion on decellularization and recellularization of articular cartilage. PLoS ONE 11:e0158976

Bhumiratana S, Bernhard JC, Alfi DM et al (2016) Tissue-engineered autologous grafts for facial bone reconstruction. Sci Transl Med 8:343ra83

Caralt M, Velasco E, Lanas A et al (2014) Liver bioengineering: from the stage of liver decellularized matrix to the multiple cellular actors and bioreactor special effects. Organogenesis 10:250–259

Cebotari S, Tudorache I, Ciubutaru A et al (2011) Use of fresh decellularized allografts for pulmonary valve replacement may reduce the reoperation rate in children and young adults early report. Circulation 124(Suppl 1):S115–S123
Conte MS (1998) The ideal small arterial substitute: a search for the Holy Grail? FESEB J 12:43–45
Crapo PM, Gilbert TW, Badylak SF (2011) An overview of tissue and whole organ decellularization processes. Biomaterial 32:3233–3243
Crapo PM, Medberry CJ, Reing JE et al (2012) Biologic scaffolds composed of central nervous system extracellular matrix. Biomaterials 33:3539–3547
DeQuach JA, Yuan SH, Goldstein LS et al (2011) Decellularized porcine brain matrix for cell culture and tissue engineering scaffolds. Tissue Eng Part A 17:2583–2592
Dong S, Huangfu X, Xie G et al (2015) Decellularized versus fresh-frozen allografts in anterior cruciate ligament reconstruction: an in vitro study in a rabbit model. Am J Sports Med 43:1924–1934
Farnebo S, Woon CY, Bronstein JA et al (2014) Decellularized tendon-bone composite grafts for extremity reconstruction: an experimental study. Plast Reconstr Surg 133:79–89
Figliuzzi M, Remuzzi G, Remuzzi A (2014) Renal bioengineering with scaffolds generated from rat and pig kidneys. Nephron Exp Nephrol 126:113–118
Goh SK, Bertera S, Olsen P et al (2013) Perfusion-decellularized pancreas as a natural 3D scaffold for pancreatic tissue and whole organ engineering. Biomaterials 34:6760–6772
Gong W, Lei D, Li S et al (2016) Hybrid small-diameter vascular grafts: anti-expansion effect of electrospun poly □-caprolactone on heparin-coated decellularized matrices. Biomaterials 76:359–370
Graham ME, Gratzer PF, Bezuhly M et al (2016) Development and characterization of decellularized human nasoseptal cartilage matrix for use in tissue engineering. Laryngoscope. doi:10.1002/lary.25884
Guan Y, Liu S, Sun C et al (2015) The effective bioengineering method of implantation decellularized renal extracellular matrix scaffolds. Oncotarget 6:36126–36138
Haidar A, Legault L, Messier V et al (2015) Comparison of dual-hormone artificial pancreas, single-hormone artificial pancreas, and conventional insulin pump therapy for glycaemic control in patients with type 1 diabetes: an open-label randomised controlled crossover trial. Lancet Diabetes Endocrinol 3:17–26
Han TT, Toutounji S, Amsden BG et al (2015) Adipose-derived stromal cells mediate in vivo adipogenesis, angiogenesis and inflammation in decellularized adipose tissue bioscaffolds. Biomaterials 72:125–137
Hasan A, Memic A, Annabi N et al (2014) Electrospun scaffolds for tissue engineering of vascular grafts. Acta Biomater 10:11–25
Kitahara H, Yagi H, Tajima K et al (2016) Heterotopic transplantation of a decellularized and recellularized whole porcine heart. Interact CardioVasc Thorac Surg 22:571–579
Ko IK, Peng L, Peloso A et al (2015) Bioengineered transplantable porcine livers with re-endothelialized vasculature. Biomaterials 40:72–79
Langer R, Vacanti JP (1993) Tissue engineering. Science 260:920–926
Lee JS, Shin J, Park HM et al (2014) Liver extracellular matrix providing dual functions of two-dimensional substrate coating and three-dimensional injectable hydrogel platform for liver tissue engineering. Biomacromolecules 15:206–218
Lovati AB, Bottagisio M, Moretti M (2016) Decellularized and engineered tendons as biological substitutes: a critical review. Stem Cells Int 2016:7276150
Lu Q, Li M, Zou Y et al (2014) Delivery of basic fibroblast growth factors from heparinized decellularized adipose tissue stimulates potent de novo adipogenesis. J Control Release 174:43–50
Mahara A, Somekawa S, Kobayashi N et al (2015) Tissue-engineered acellular small diameter long-bypass grafts with neointima-inducing activity. Biomaterials 58:54–62
Mazza G, Rombouts K, Hall AR et al (2015) Decellularized human liver as a natural 3D-scaffold for liver bioengineering and transplantation. Sci Rep 5:13079

Mei J, Yu Y, Li M et al (2016) The angiogenesis in decellularized scaffolt-mediated the renal regeneration. Oncotarget 7:27085–27093
Methe K, Bächdahl H, Johansson BR et al (2014) An alternative approach to decellularize whole porcine heart. BioRes Open Access 3:327–338
Moore MA, Samsell B, Wallis G et al (2015) Decellularization of human dermis using non-denaturing anionic detergent and endonuclease: a review. Cell Tissue Bank 16:249–259
Moroni F, Mirabella T (2014) Decellularized matrices for cardiovascular tissue engineering. Am J Stem Cells 3:1–20
Nakamura S, Ijima H (2013) Solubilized matrix derived from decellularized liver as a growth factor-immobilizable scaffold for hepatocyte culture. J Biosci Bioeng 116:746–753
Nichols JE, Francesca SL, Vega SP et al (2016) Giving new life to old lungs: methods to produce and assess whole human paediatric bioengineered lungs. J Tissue Eng Regen Med. doi:10.1002/term.2113
Nyame TT, Chiang HA, Leavitt T et al (2015) Tissue-engineered skin substitutes. Plast Reconstr Surg 136:1379–1388
Ota T, Taketani S, Iwas S et al (2007) Novel method of decellularization of porcine valves using polyethylene glycol and gamma irradiation. Ann Thorac Surg 83:1501–1507
Ott HC, Matthiesen TS, Goh SK et al (2008) Perfusion-decellularized matrix: using nature's platform to engineer a bioartificial heart. Nat Med 14:213–221
Ott HC, Clippinger B, Conrad C et al (2010) Regeneration and orthotopic transplantation of a bioartificial lung. Nat Med 16:927–933
Pan J, Liu GM, Ning LJ et al (2015) Rotator cuff repair using a decellularized tendon slices graft: an in vivo study in a rabbit model. Knee Surg Sports Traumatol Arthrosc 23:1524–1535
Peloso A, Ferrario J, Maiga B et al (2015) Creation and implantation of acellular rat renal ECM-based scaffolds. Organogenesis 11:58–74
Peloso A, Urbani L, Cravedi P et al (2016) The human pancreas as a source of protolerogenic extracellular matrix scaffold for a new-generation bioartificial endocrine pancreas. Ann Surg 264:169–179
Ren X, Moser PT, Gilpin SE et al (2016) Engineering pulmonary vasculature in decellularized rat and human lungs. Nat Biotechnol 33:1097–1102
Rheinwald JG, Green H (1975) Serial cultivation of strains of human epidermal keratinocytes: the formation of keratinizing colonies from single cells. Cell 6:331–343
Roosens A, Somers P, Somer FD et al (2016) Impact of detergent-based decellulairization method on porcine tissues for heart balve engieering. Ann Biomed Eng 44:2827–2839
Rowland CR, Colucci LA, Guilak F (2016) Fabrication of anatomically-shaped cartilage constructs using decellularized cartilage-derived matrix scaffolds. Biomaterials 91:57–72
Sabetkish S, Kajbafzadeh AM, Sabetkish N et al (2015) Whole-organ tissue engineering: decellullarization and recellularization of three-demensional matrix liver scaholds. J Biomed Mater Res A 103A:1498–1508
Sánchez PL, Fernández-Santos ME, Costanza S et al (2015) Acellular human matrix: a critical step toward whole heart grafts. Biomaterials 61:279–289
Sánchez PL, Fernández-Santos ME, Espinosa MA et al (2016) Data from acellular human heart matrix. Data Brief 8:211–219
Sarikouch S, Horke A, Tudorache I et al (2016) Decellularized fresh homografts for pulomonary valve replacement: a decade of clinical experience. Eur J Cardiothorac Surg 50:281–290
Schmitt T, Fox PM, Woon CY et al (2013) Human flexor tendon tissue engineering: in vivo effects of stem cell reseeding. Plast Reconstr Surg 132:567e–576e
Seif-Naraghi SB, Salvatore MA, Schup-Magoffin PJ et al (2010) Design and characterization of an injectable pericardial matrix gel: a potentially autologous scaffold for cardiac tissue engineering. Tissue Eng Part A 16:2017–2027
Shirakigawa N, Ijima H, Takei T (2012) Decellularized liver as a practical scaffold with a vascular network template for liver tissue engineering. J Biosci Bioeng 114:546–551

Shirakigawa N, Takei T, Ijima H (2013) Base structure consisting of an endothelialized vascular-tree network and hepatocytes for whole liver engineerig. J Biosci Bioeng 116:740–745

Smit FE, Dohmen PM (2014) Bio-artificial heart as ultimate treatment of end-stage heart failure. Med Sci Monit Basic Res 20:161–163

Song JJ, Kim SS, Liu Z et al (2011) Enhanced in vivo function of bioartificial lungs in rats. Ann Thorac Surg 92:998–1006

Song JJ, Guyette JP, Gilpin SE et al (2013) Regeneration and experimental orthotopic transplantation of a bioengineered kidney. Nat Med 19:646–651

Sugiura T, Tara S, Nakayama H et al (2016) Novel bioresorbable vascular graft with sponge-type scaffold as a small-diameter arterial graft. Ann Thorac Surg (in press)

Theodoridis K, Müller J, Ramm R et al (2016) Effects of combined cryopreservation and decellularization on the biomechanical, structural and biochemical properties of porcine pulmonary heart valves. Acta Biomater (in press)

Umashankar PR, Sabareeswaran A, Sachin JS (2016) Long-term healing of mildly cross-linked decellularized bovine pericardial aortic patch. J Biomed Mater Res B (in press)

Uygan BE, Sato-Gutierrez A, Yagi H et al (2010) Organ reengineering through development of a transplantable recellularized liver graft using decellularized liver matrix. Nat Med 16:814–820

Wakimura Y, Wang W, Itoh S et al (2015) An experimental study to bridge a nerve gap with a decellularized allogeneic nerve. Plast Reconstr Surg 136:319e–327e

Wang L, Johnson JA, Zhang Q et al (2013) Combining decellularized human adipose tissue extracellular matrix and adipose-derived stem cells for adipose tissue engineering. Acta Biomater 9:8921–8931

Willenberg BJ, Oca-Cossio J, Cai Y et al (2015) Repurposed biological scaffolds: kidney to pancreas. Organogenesis 11:47–57

Yagi H, Fukumitsu K, Fukuda K et al (2013) Human-scale whole-organ bioengineering for liver transplantation: a regenerative medicine approach. Cell Transplant 22:231–242

Yasui H, Lee JK, Yoshida A et al (2014) Excitation propagation in three-dimensional engineered hearts using decellularized extracellular matrix. Biomaterials 35:7839–7850

Yin Z, Chen X, Zhu T et al (2013) The effect of decellularized matrices on human tendon stem/progenitor cell differentiation and tendon repair. Acta Biomater 9:9317–9329

Zhan JS, Wang ZB, Lin KZ et al (2015) In vivo regeneration of renal vessels post whole decellularized kidneys transplantation. Oncotarget 6:40433–40442

Zhang Q, Johnson JA, Dunne LW et al (2016a) Decellularized skin/adipose tissue flap matrix for engineering vascularized composite soft tissue flaps. Acta Biomater 35:166–184

Zhang S, Lu Q, Cao T et al (2016b) Adipose tissue and extracellular matrix development by injectable decellularized adipose matrix loaded with basic fibroblast growth factor. Plast Reconstr Surg 137:1171–1180

Zhou J, Ding J, Nie B et al (2015) Promotion of adhesion and proliferation of endothelial progenitor cells on decellularized valves by covalent incorporation of RGD peptide and VEGF. J Mster Sci: Mater Med 27:142

Zia S, Mozafari M, Natasha G et al (2016) Hearts beating through decellularized scaffolds: whole-organ engineering for cardiac regeneration and transplantation. Crit Rev Biotechnol 36:705–715

Current Progress in Bioprinting

Xiao-Fei Zhang, Ying Huang, Guifang Gao and Xiaofeng Cui

Abstract With the advances of stem cell research, development of intelligent biomaterials and three-dimensional biofabrication strategies, highly mimicked tissue or organs can be engineered. Among all the biofabrication approaches, bioprinting based on inkjet printing technology has the promises to deliver and create biomimicked tissue with high throughput, digital control, and the capacity of single cell manipulation. Therefore, this enabling technology has great potential in regenerative medicine and translational applications. The most current advances in organ and tissue bioprinting based on the thermal inkjet printing technology are described in this chapter, including vasculature, muscle, cartilage, and bone. In addition, the benign side effect of bioprinting to the printed mammalian cells can be utilized for gene or drug delivery, which can be achieved conveniently during precise cell placement for tissue construction. With layer-by-layer assembly, three-dimensional tissues with complex structures can be printed using converted medical images. Therefore, bioprinting based on thermal inkjet is so far the most optimal solution to engineer vascular system to the thick and complex tissues. Collectively, bioprinting has great potential and broad applications in tissue engineering and regenerative medicine. The future advances of bioprinting include the integration of different printing mechanisms to engineer biphasic or triphasic tissues with optimized scaffolds and further understanding of stem cell biology.

X.-F. Zhang and Y. Huang contributed equally to this work.

X.-F. Zhang · Y. Huang · G. Gao · X. Cui
School of Chemistry, Chemical Engineering and Life Sciences,
Wuhan University of Technology, 122 Luoshi Rd, Wuhan, Hubei, China

G. Gao · X. Cui
Stemorgan Therapeutics, Plano, TX, USA

X. Cui (✉)
Technical University of Munich, Munich, Germany
e-mail: xfc.cui@gmail.com

A. Tripathi and J.S. Melo (eds.), *Advances in Biomaterials for Biomedical Applications*, Advanced Structured Materials 66,
DOI 10.1007/978-981-10-3328-5_6

Abbreviations

3D	Three dimensional
AFS	Amniotic fluid-derived stem cells
BCP	Biphasic calcium phosphate
BG	Bioactive glass
BMPs	Bone morphogenic proteins
CAD	Computer aided design
CAM	Computer aided manufacturing
CaP	Calcium phosphate
CIJ	Continuous inkjet
CT	Computed tomography
DOD	Drop on demand
ECM	Extracellular matrix
EIJ	Electrostatic inkjet
FGFs	Fibroblast growth factors
GDNF	Glial cell line-derived neurotrophic factor
GelMA	Gelatin methacrylate
HA	Hyaluronic acid
hASCs	Human adipose-derived stem cells
HMVECs	Human microvascular endothelial cells
hTMSCs	Human nasal inferior turbinate tissue-derived mesenchymal stromal cells
IGF-1	Insulin-like growth factor 1
LaBP	Laser-assisted bioprinting
MRI	Magnetic resonance imaging
MSCs	Mesenchymal stem cells
MTU	Muscle-tendon unit
NGF	Nerve growth factor
NHDF	Normal human dermal fibroblasts
ODP	Omnidirectional printing
PAVICs	Porcine aortic valve interstitial cells
PCL	Poly-caprolactone
PDGF	Platelet-derived growth factor
PEG	Poly (ethylene) glycol
PEGDA	Poly (ethylene) glycol diacrylate
PEGDMA	Poly (ethylene) glycol dimethacrylate
PF127	Pluronic F127
PGA	Poly-glycolic acid
PLA	Poly-lactic acid
PLGA	Poly (lactic-co-glycolic acid)
pNIPAAM	Poly (*N*-isopropylacrylamide)
PTH	Parathyroid hormone
PU	Polyurethane
RFP	Rifampicin

RGD	Arg-Gly-Asp
sECMs	Synthetic extracellular matrices
SMC	Smooth muscle cells
TCP	Tri-calcium phosphate
TGF-β	Transforming growth factor-β
VEGF	Vascular endothelial growth factor
VIC	Valve leaflet interstitial cells

1 Introduction

Three dimensional (3D) printing, as one of the 3D fabrication technologies, has been introduced more than 30 years since Charles Hull first invented a 3D lithography in 1986 (Shafiee and Atala 2016). During early 1990s, Sachs et al. developed a powder-based free form fabrication method contributing a significant development for 3D printing. A regular ink-jet print-head is used in this approach and binders are applied to the powder bed to cement the loose powders together. Hence, in the early stage, 3D printing technology was mainly used on rapid tooling using metals and ceramics (Bose et al. 2013). Nowadays, with the dramatic development of 3D printing technology, it has massive applications in automotive industry, military services, archaeology, electrical device engineering and recently in biofabrication (Radenkovic et al. 2016).

Biofabrication is a process by arranging cellular and non-cellular component in space to mimic the composition and functionality of the human tissue (Arealis and Nikolaou 2015). Bioprinting as a 3D biofabrication technology can precisely allocate cell-laden biomaterials to construct complex 3D functional living tissues or artificial organs (Mandrycky et al. 2016). Bioprinting is also referred as an additive biomanufacturing process by depositing materials such as living cells, nucleic acids, drug particles, proteins, extracellular matrix (ECM) components, growth factors and other biochemical factors in a layer by layer fashion. Bioprinted subjects usually demonstrate appropriate resolution and mechanical properties (Ozbolat et al. 2016).

The high printing resolution of bioprinting allows cells/matrix/biomolecules and biomaterials to be precisely dispensed to mimic the native tissue structure (Jana and Lerman 2015). Unlike conventional tissue engineering methods such as chemical/gas foaming, solvent casting, fiber bonding, particle/porogen leaching, freeze-drying, thermally induced phase separation, membrane lamination, foam-gel and electrospinning, only bulk properties can be controlled, but the pore size, shape, network, internal architecture and topology cannot be decided. Additionally, the specific requirement of the porosity is not able to be achieved using traditional tissue engineering approaches as well (An et al. 2015; Zhu et al. 2016; Bose et al. 2013). Assisted with computer aided design (CAD) technologies, bioprinting can produce complex 3D structures from nanoscale to microscale with low cost and

high efficiency. The three major techniques used in bioprinting are inkjet printing, extrusion printing and light-assisted printing (Zhu et al. 2016). The printed structures with specific requirements of pore size, structure, gerometries, porosity and pore interconnectivity can be realized using different 3D printing technologies with various biomaterials as bioink (Jana and Lerman 2015).

Nowadays, with the increasing number of ageing population and the threat of trauma or diseases leading to the loss in the tissue architecture and its functions, autograft and allograft transplantation of tissues are usually used to recover the acute injury or chronic disease (Xiong et al. 2015). However, donor shortage is always a serious challenge and many people die while waiting for a suitable organ transplantation. Moreover, high cost and allogeneic transplant may cause immune rejection which would be huge hurdles for the recipient. Since the late 1980s, the first hybrid artificial organ was produced. Tissue engineering has been considered a promising technique that can alleviate the crisis of organ shortage. Due to the complex architecture of the tissue, it requires to combine multiple cell types and different components precisely in order to form a three dimensional structure. An appropriate technology should generate a tissue not only combining multiple cells with suitable biochemical factors, but also mimicking the microarchitecture of the tissue as well as the in vivo microenvironment for the cells (Guillemot et al. 2010b). Organ printing has the promises to achieve these goals. Organ printing or 3D bioprinting is the combination of computer aided design and tissue engineering, which uses patient's autologous cells based on the computer aided model to produce personalized artificial organ (Xiong et al. 2015; Radenkovic et al. 2016). Bioprinting is still in its immature stage and there are many challenges that need to be solved such as high resolution cell deposition, controlled cell distributions, vascularization, and innervation within the 3D tissues. However, with the high demand of organ transplantation, bioprinting could be an effective way to relieve the stress of the organ shortage (Mandrycky et al. 2016). Nowadays, organ printing research is focusing on many areas such as skin, cartilage, bone, aortic valve, vascular trees, kidney and is gradually moving towards other tissues (Jana and Lerman 2015). With the development of organ printing technology, the ultimate goal is to achieve the organs and tissues functionalization, overcome the limitation of organ shortage and achieve life-long immunosuppression (Radenkovic et al. 2016).

In this chapter, the most current bioprinting techniques and bio-ink materials are introduced and summarized, followed by the examples of tissue and organ printing applications as well as the discussion of existing challenges.

2 Bioprinting Techniques

With the robust advancement of printing technology, there are more than 40 different 3D printing techniques that are currently being used in research or commercial applications. Among these, inkjet printing, extrusion printing, laser assisted

printing and stereolithography are the most widely used technologies. A brief overview of these 3D bioprinting techniques are presented here.

2.1 Inkjet Printing

Inkjet printers were initially developed in 1970s. At that time, inkjet printing was just a 2D printing technique due to the limitation of the technique. In 1992, inkjet printers were modified with a chamber with an elevator stage controlling the z-axis of the printer. Thus 3D printing based on this technique was achieved. Inkjet printing was introduced as one of the first approaches for additive manufacturing process (Jana and Lerman 2015; Derby 2015). With the digital control of a computer, inkjet printing can precisely control the size of the printed pattern and the deposition of generated droplets (Xu et al. 2013b). There are four approaches existing for inkjet droplet squeezing, which are thermal, piezoelectric, acoustic and electrostatic inkjet printing. Among these, thermal and piezoelectric are the most widely utilized for structure fabrication (Ihalainen et al. 2015). When working as a bioprinting process in tissue engineering, the bioinks are always hydrogels or pre-polymer solutions with or without cells encapsulated and deposited on the surface as demanded. For the reasons of fast fabrication and low-cost properties, inkjet printing technique has been utilized in wide variety of areas and has been highly successful commercially (Derby 2015).

As mentioned above, thermal and piezoelectric inkjet printing approaches are two main processes applied in bioprinting technology. With thermal, the ink drops are ejected from the nozzles due to the high pressure of air bubbles generated by the localized high speed heating up to 300 °C (Jana and Lerman 2015). According to the previous research, thermal inkjet printer is able to construct 3D cell-laden constructs. This printing technique has the advantages of high throughput and low cost. Therefore, it has been used in numerous biofabrication and biomedical applications. A research group simultaneously printed human mesenchymal stem cells (MSCs) with bioactive glass (BG) and hydroxyapatite polymerized in a poly (ethylene) glycol dimethacrylate (PEGDMA) scaffold. Compared to the conventional scaffold generation process, the cells were distributed uniformly in the printed scaffold and completely avoided the cell accumulation caused by the gravity (Gao et al. 2014). Thermal inkjet printing is an efficient and economic printing approach, however, it still has many challenges. The droplet directionality is fairly low, and the geometrical shapes are usually irregular due to the weakness of hydrogels. In addition, the nozzle clogging can always threaten the smooth printing process. Different from the thermal inkjet printing which uses heat change to create pressure, the piezoelectric system changes the voltage to generate the pressure and finally lead ink to be extruded out of the nozzle. Compared to the thermal inkjet printer, inks in the piezoelectric system are not exposed to the heat. However, the thermal inkjet printing head design is simpler and more robust. Hence, thermal inkjet

printing can be more suitable for bioprinting than piezoelectric printing system (Jana and Lerman 2015; Ihalainen et al. 2015).

Inkjet printing mechanisms can be classified into three categories according to the difference of droplet generators, which are continuous inkjet printing (CIJ), drop on demand (DOD) inkjet printing, and electrostatic inkjet printing (EIJ). For CIJ, due to its high printing speed and the capacity to finish large scale printing, it is always used in commercial production. Although it is a scale-up fast printing technique, the continuous fluid jetting and the material recirculation can lead to the wastage and contamination of ink materials (Derby 2015). Considering the resolution and the cost of the printing, DOD inkjet printers are more recommended. For this printing mechanism, thermal and piezoelectric are the most widely used techniques. For thermal drop on demand inkjet printers, it can eject inks from reservoir as needed. And the piezoelectric drop on demand printers can utilize different range of voltage to adjust the shape and the size of the droplet (Shafiee and Atala 2016). EIJ printing utilizes applied electrostatic repulsion to eject the individual drops (Umezu et al. 2005). In the past 40 years, CIJ and DOD these two techniques have been widely used for commercial applications. However, EIJ is just recently available in market and its development is still ongoing.

2.2 *Extrusion Printing*

Extrusion printing is actually a modified version from inkjet printing. Inkjet printing requires bioink with low viscosity in order to form the droplets. Materials with high viscosity usually cannot be printed using this method. Extrusion printing utilizes pneumatic and mechanical screw plunger dispensing system to allocate bioinks. Instead of depositing droplets, unremitted cylindrical lines are generated by the applied continuous force. Bioinks such as cells, cell-laden hydrogels with high cell density, as well as biomaterials with various viscosities can be loaded into the cartridge and printed with extrusion printing system. The extrusion speed, procedure, the deposit location on 3D stage can be adjusted by the computer aided operator. Currently, the extrusion dispensers can be divided into pneumatic micro nozzles and screw-based nozzles. The first type uses compressed gases to extrude the bioink out of the nozzle. Hence, it is able to extrude materials with different viscosities. The limitation of this system is that it cannot conduct mass control during the process. The later type is able to print without inlet air to reduce the cost. However, the screw-based nozzles may have difficulties when printing highly viscous materials (Mandrycky et al. 2016; Shafiee and Atala 2016).

Based on the concept of extrusion printing, bioplotting technique was developed in 2000. Since this technology can inject the materials out of the container as continuous filaments, it is also called direct writing system. The mechanisms of bioplotting are mechanical and pneumatic and it is able to operate bioink in ambient or physiological temperature (Jana and Lerman 2015; Kumar et al. 2016). A wide variety of materials can be used in bioplotting, such as cells, polymers and cell

encapsulated matrics. However, the printing flexibility of bioplotting still requires improvement (Chia and Wu 2015; Buyukhatipoglu et al. 2010). When printing materials with encapsulated cells, the rapid printing speed can provide high shear stress and finally result in decrease of the cell viability. In order to print cells, the nozzle diameter is limited by the size of the cells while this requirement conversely limited the printing resolution (Zhu et al. 2016; Munaz et al. 2016).

The extrusion printer has acceptable compatibility with different types of materials, and can also print materials with wide range of viscosities. What needs to be taken into consideration is the reasonable cost. As a typical extrusion printer, it always has multiple printer heads which allow different type of bioinks to be printed at the same time. Besides, it can also well control the shapes, pores, porosity, and cell distribution of the printed scaffolds or prosthetics for tissue engineering. All these benefits contribute in making extrusion printing technique to be the most widely used commercial 3D printing technology in recent years (Mandrycky et al. 2016; Jana and Lerman 2015).

2.3 Laser Assisted Printing

The origin of laser assisted printer is based on modified laser direct write and laser induced forward transfer techniques. Laser assisted printing of biomaterial is mainly treated by photo-polymerization method. Wide range of cells can be printed in this process and the cell viability can also be retained (Zhu et al. 2016). A laser assisted printing system usually consists of four parts, which are pulsed laser source, a laser focusing tool, a laser energy absorbing metallic ribbon film and a receiving substrate (Koch et al. 2013). The printing mechanism is similar to conventional typewriters. In laser assisted printing techniques, the ribbon structure contains two layers. The top layer of the ribbon is an energy absorbing layer, which is usually a glass coated with a nano-thickness gold and titanium film. And liquid biological materials are suspended on the bottom of the layer. During the printing process, laser pulse focuses on the upper layer in designed area, with the evaporation of the film, the interface produces a high pressure bubble (Ferris et al. 2013; Mandrycky et al. 2016). The suspended bioink liquid will be further ejected onto the receiving substrate in droplet form. The z-axis movement can be controlled according to an elevator system. Laser assisted printing does not have nozzles in the system. Hence, the nozzle clogging problem won't happen and wide variety materials can be applied with this printing technology (Jana and Lerman 2015; Shafiee and Atala 2016).

Many materials such as hydrogels, ceramic materials, epoxy-based photoresist SU-8, as well as cells and cell-encapsulate material can be used in laser based printing. During the printing process, by optimizing the materials printing condition it can improve the dimensional accuracy and surface property of the printed object (Xiong et al. 2015). Compared to inkjet printing, laser assisted printer is able to print structure from pico to micro scale. Besides, laser based technique doesn't use nozzles, so the clogging problems can be effectively avoided and broader

biomaterials can be used. However, laser assisted printing technology still has drawbacks. Before processing, materials used in printing should be combined with material-coated metallic film separately. This procedure is time consuming and costly. Furthermore, the throughput of laser assisted printer is quite slow comparing to other printing techniques, which limits its commercial applications (Mandrycky et al. 2016; Radenkovic et al. 2016).

2.4 Stereolithography

In early 1980s, stereolithography was developed as a solid freeform technique. Similar to laser assisted printing techniques, stereolithography printing uses ultraviolet rays to selectively solidify the liquid photo-sensitive polymer layer by layer and finally forms a complex structure (Brunello et al. 2016). For stereolithography printing, there are two important factors which can affect the printing results. The first is the computer design of the structure. The printed structure is formatted in stereolithography file by using computer aided techniques such as magnetic resonance imaging (MRI) and computed tomography (CT). After the CAD design, the structure is sliced into uniform thin layers and can be cured layer by layer. The second factor is the curing kinetics. Stereolithography is a bottom-up printing process. The light solidifies the layer and then layers overlapped to generate the structure (Mandrycky et al. 2016; Brunello et al. 2016).

Due to the high resolution and accuracy of stereolithography, wide range of materials such as curable acrylics and epoxies can be used to fabricate engineering constructs (Chia and Wu 2015). Some medical implant and even engineered tissue constructs can also be formed using this technology. Previously, polypropylene fumarate based materials, gelatin based materials, and trimethylene carbonate based materials were utilized to fabricate bone implants. These biomaterials were capable for photo-polymerization and were used in stereolithography printing (Lee et al. 2010a). In tissue engineering application, some high molecular weight polymers, such as D, L-lactide and poly (propylene) fumarate, have been used in tissue engineering scaffold fabrication. These materials have ester group and are able to hydrolyze in vitro and in vivo. Poly (ethylene) glycol diacrylate (PEGDA) and PEGDMA hydrogel with cell-laden constructs can also be printed using stereolithography (Jana and Lerman 2015).

The schematic drawing of these four different widely used 3D printing techniques introduced above is shown in Fig. 1. Table 1 is the comparison of each technique. All these printing technologies can be used in biomedical and tissue engineering. Different printing techniques have their advantages and limitations. When printing cell laded biomaterials, cell viability should be considered at highest priority. The printing resolution, accuracy, amount of printed layers, the structure dimension of the printed subject and the overall printing time should also be taken into consideration before printing (Munaz et al. 2016).

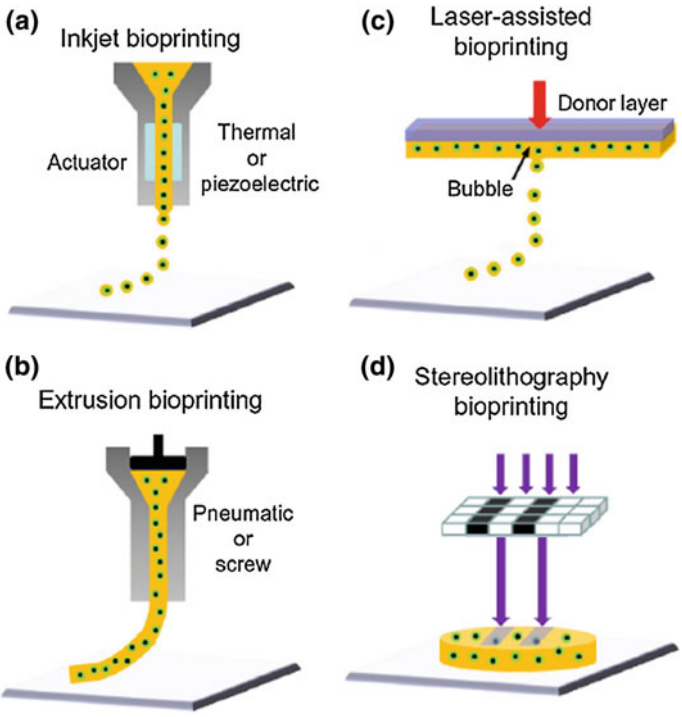

Fig. 1 Schematic drawing representing the different printing techniques. **a** Inkjet printing; **b** extrusion printing; **c** laser-assisted printing; **d** stereolithography (Mandrycky et al. 2016)

3 Bioprinting Process

A typical bioprinting process is generally divided into three phases, which are the pre-processing, processing, and post processing. For pre-processing, it involves digital design and material selection. After the first stage, the designed images are sent to the bioprinting system and the bioinks are loaded for processing. Finally, in the post pros-processing phase, the printed constructs are transferred into a bioreactor for tissue maturation. Details of these three steps are described below.

3.1 Pre-Processing

A blueprint of the tissue or organ should be formed by computer aided design in pre-processing stage. In the design, precise information of the printed structure and the cells location should be decided. Nowadays, there are many approaches to obtain different information like anatomy, histological structure, composition and human organ topology for the computer design (Rezende et al. 2015).

Table 1 Comparison of four types of printing techniques

Foci	Inkjet printing	Extrusion printing	Laser-assisted printing	Stereolithography	References
Printing process	Serial (drop by drop)	Serial (line by line)	Serial (dot by dot)	Continuous (projection based)	(Zhu et al. 2016)
Cost	Low	Moderate	High	Low	(Mandrycky et al. 2016)
Printing speed	Medium (<10,000 droplets/s)	Slow (10–50 μm/s)	Medium high (∼100droplets/s)	Fast (<40.000 mm/s)	(Zhu et al. 2016; Jana and Lerman 2015)
Printing resolution	High (10–150 pL)	Moderate (5 μm)	High (<500 nm)	High (∼1.2 μm)	(Mandrycky et al. 2016; Zhu et al. 2016; Jana and Lerman 2015)
Mechanical integrity	Poor	Poor	Poor	Fair	(Zhu et al. 2016)
Viscosity	3.5–12 mPa/s	30 mPa/s to above 6×10^7 mPa/s	1–300 mPa/s	Without limitation	(Mandrycky et al. 2016)
Quality of the structure	Poor	Good	Fair	Good	(Mandrycky et al. 2016)
Cell density	Low (<10^6 cells/mL)	High (cell spheroids)	Medium (<10^8 cells/mL)	Medium (<10^8 cells/mL)	(Mandrycky et al. 2016; Jana and Lerman 2015)
Cell viability	>85%	40–80%	>95%	>85%	(Mandrycky et al. 2016; Zhu et al. 2016; Jana and Lerman 2015)

(continued)

Table 1 (continued)

Foci	Inkjet printing	Extrusion printing	Laser-assisted printing	Stereolithography	References
Feature	Thermo/pH/photo-sensitive, low viscosity	Thermo/photo-sensitive, low to high viscosity	Photo-sensitive, varying viscosity	Photo-sensitive, viscosities depending on the concentrations of ingredients	(Zhu et al. 2016; Jana and Lerman 2015)
Materials used in printing	Alginate, PEGDMA, collagen hydrogel, media, cells and proteins	Alginate, GelMA, collagen hydrogel, melt, cells, proteins and ceramics	Collagen hydrogel, media, cells, proteins and ceramics	GelMA, GelMA-PEGDA hybrid hydrogel, curable acrylics and epoxies	(Mandrycky et al. 2016; Jana and Lerman 2015)

The first approach is 3D computer models. For bioprinting model, it always contains information such as complex 3D geometries surface information. This kind of model can be created using MRI and CT. CT is the most frequently used technique to obtain medical images. Compared with the conventional image technologies, CT is non-destructive and reproducible. It also allows the users to measure the relevant biological parameters in a quantitative manner (Kumar et al. 2016). The advantage of using computational models is it can help to define the rules, predict the properties of printed tissues, and also improve the design of the implant (Fedorovich et al. 2011).

The second approach is to use computer aided techniques. Computer aided designing (CAD) and computer aided manufacturing (CAM) are used not only in pre-processing, but are also critical during print process and post-processing stage. For Bio-CAD system, it can mimic the 3D anatomic structures, differentiates heterogeneous tissue types, and produce desired computational tissue model (Munaz et al. 2016). The relevant tissue models can be simulated on computers to predict the fabrication process feasibility by Bio-CAM. Furthermore, this technique is able to enhance the understanding of the physical and chemical mechanisms during the printing. The combined use of Bio-CAD and Bio-CAM can accelerate the printing speed and improve the quality of the printed tissue (Mandrycky et al. 2016).

In addition, the biomaterial parameters should also be confirmed during this stage. All factors should be optimized to confirm the high quality of the printed tissues (Bose et al. 2013).

3.2 Processing

During the processing stage, suitable bioprinter (detail discussed in the previous section of the chapter) is used to print bioinks into desired structures. Optimal bioink is important to guarantee the smooth printing process by homogeneously packing inside the cartridge. The printing ability is determined by the bioink flowability. Hence, the properties of bioink are crucial on the results of bioprinting (Bose et al. 2013).

3.3 Post Processing

Post processing stage is essential for 3D printing tissues. In bioprinting post processing, a bioreactor is an important tool for tissue engineering. Bioreactor is able to provide dynamic environment for tissue maturation and it also plays a pivotal role in scaling up bioprinting. In order to enhance the tissue fusion, maturation and remodeling more effectively, a novel conceptual design of the bioreactor is presented. The bioreactor has three perfusions and each of them has their respective

functions. The first one is to provide dynamic environment for printed tissues and the second one is to enhance media perfusion through an intra-organ branched vascular tree. There are many strong, porous, non-biodegradable, removable minitubes existing in the third perfusion. These minitubes serve as temporal support and artificial microchannels. This bioreactor is aimed to provide enough time and support to fulfill the intravascular perfusion initiation in the intra-organ branched vascular system. However, the porosity level and the distance between minitubes should be well defined by systematic mathematical modeling and computer simulation. In addition, finding the suitable fabrication and coating materials for minitubes and how to avoid tissue damage are still the challenges for this novel bioreactor invention (Mironov et al. 2009; Mironov et al. 2011).

4 Materials Used in Bioprinting

Considering bioprinting applications in tissue engineering, some materials such as synthetic polymers, cells and growth factors are used to fabricate bone or orthopedic implantation. Biomaterial used should be printable, and also non-cytotoxic and biodegradable in vivo. It should be able to enhance surrounding host tissue formation and to avoid second surgery removal of the implant. The mechanical strength of the initial materials should be relatively high to provide sufficient support for seeded cells. And it should be stiff enough for handling and implantation. The printed biomaterials utilized in tissue engineering should also possess properties to promote cells adhesion, maturation, proliferation and differentiation (Fedorovich et al. 2011; Arealis and Nikolaou 2015). In this part, various materials for bioprinting are discussed comprehensively.

4.1 Bioinks

Properties of hydrogel pre-polymers such as printability and crosslinkability, mechanical properties, biocompatibility and by-products as well as degradation controllability are critical for printing. The classification of bioinks are mainly divided into natural polymers and synthetic polymers (Mandrycky et al. 2016).

4.1.1 Natural Polymers

Bioinks using natural polymers without encapsulated cells usually work as the mechanical support during cell culture and growth. Typically used biological materials include gelatin, collagen, alginate, chitosan, hyaluronic acid (HA) and agarose (Mandrycky et al. 2016; Radenkovic et al. 2016). Collagen is the most abundant natural derived ECM material from tissues. Its low melting point allows it

to be printable at low temperature but forming gels at body temperature (Choi et al. 2011; Cui and Boland 2009). Agarose is in the gel form at room temperature, but it can revert into solution when temperature is above 37 °C. Alginate is a naturally derived linear copolymer from the wall of brown algae. Cell viability can be retained when printing with algiante. However, the mechanical strength of the printed gel constructs and the sustainability could be relatively low. Some crosslinkers such as $CaCl_2$ can harden the alginate structure at high concentration and low temperature, which rapidly enhances the mechanical strength of the structure (Guillemot et al. 2010a; Guillemot et al. 2010b). Chitosan is a polysaccharide with linear structure. Using NaOH as cross-linker can form gel matrix rapidly (Munaz et al. 2016). Gelatin is a material biocompatible to cells. In tissue engineering, it is also used to improve the strength of bones and joints in the defect regeneration (Pulieri et al. 2008). Hyaluronan is an anionic polysaccharide promoting cartilage regeneration. It is a weak material even after crosslinking. Hence, certain modification such as UV-curable methacrylate can be used to form a 3D scaffold (Hung et al. 2016). Nature materials mentioned above can also be combined for bioprinting, which can improve the viscosity, mechanical strength and biocompatibility for the bioink with improved efficiency for printing (Tirella et al. 2009).

Alginate and gelatin composite encapsulated cardiomyocyte with calcium chloride solution as the crosslinker has been used to fabricate a cardiac tissue construct by inkjet printing. The structure of the resulting tissue successfully demonstrated the electrical stimulation and excitation coupling with connected ventricles (Xu et al. 2009). An alginate and gelatin composite hydrogel was also used to form the heart valve by extrusion printing. The printed heart valve with porcine aortic valve interstitial cells and smooth muscle cells were encapsulated and incubated for 10 min in calcium chloride for cross-linking. The resulted scaffold maintained the cell viability up to 82% (Duan et al. 2013). Other natural materials mixed with alginate were also used in bone regeneration. Previous research showed outstanding shear thinning properties in bioprinting and anatomically correct meniscus constructs using the combination of alginate with nanocellulose (Markstedt et al. 2015). More combination such as alginate and collagen hydrogel forming vascularized bone tissues (Xu et al. 2013b), and alginate with chitosan to print vassal like cellular microfluidic (Zhu et al. 2016) were reported previously.

4.1.2 Synthetic Polymers

One of the major advantages of synthetic polymers is their chemical and mechanical properties can be well controlled. The limitation of mechanical properties and biodegradability existing in nature polymers can be solved by using synthetic polymers. Various types of synthetic polymers have been applied in various applications owning to their excellent properties. Poly (ethylene) glycol (PEG) hydrogel can be attached by proteins, cells, antibodies due to its brilliant biocompatibility. Most commonly used PEG hydrogels are PEGDA and PEGDMA. These hydrogels can represent different characteristics under different conditions

(Munaz et al. 2016). Increasing focus is moving onto utilizing the combination of synthetic polymers to print mechanically stable constructs. These combinations are usually used in hard tissue fabrication (Radenkovic et al. 2016).

Some materials such as calcium phosphate (CaP), tri-calcium phosphate (TCP), HA, poly-lactic acid (PLA), poly-glycolic acid (PGA), poly (lactic-co-glycolic acid) (PLGA) as well as poly-caprolactone (PCL) are usually applied to print hard materials (Mota et al. 2015; Detsch et al. 2011). PLA, PGA and PCL possess excellent biocompatibilities, biodegradabilities and mechanical strength. These synthetic polymers can not only accelerate the process of bone repair, but also inhibit inflammation and foreign body reactions (Lopes et al. 2012). CaP demonstrates excellent bioactivity and osteoconductivity. It is widely used in bone construction and repair (Bose et al. 2013). Some other composites such as CaP/PCL, CaP/PLA and CaP/PEGDA have been investigated in bone regeneration as well (Bergemann et al. 2016). TCP is one of the major components found in bone mineral with alpha and beta isotypes. When using TCP to fabricate hard tissue, it is able to enhance the structure compressive strength and provide excellent osteoconductivity (Munaz et al. 2016). However, scaffold fabricated using pure TCP is too brittle to handle. The compressive strength can be improved by adding PLA. The printed hybrid TCP/PLA scaffolds demonstrated improved stability and also activated osteoblasts migration (Bergemann et al. 2016). HA is the most widely used calcium phosphate both in research and clinically. HA is resorbable in vivo but this property is uncontrollable and unpredictable (Mohamed et al. 2011). HA/PCL and PLGA/TCP/HA composites have been used in bioprinting to fabricate hard tissues (Yao et al. 2015; Kim et al. 2012).

4.2 Cells and Tissues

Simultaneously printing cells and other biomaterials in a defined and organized manner is able to produce biological substitutes with enhanced efficiency in tissue regeneration and function restoration. The utilization of tissue and cell printing approach can finally eliminate the need for tissue grafts and mechanical devices (Pati et al. 2015a). Some cells such as cardiac cells, osteoblasts, pluripotent cells, endothelial cells, fibrosarcoma as well as osteosarcoma cells have been successfully printed into engineered tissues by various research groups (Jana and Lerman 2015). In order to fabricate the highly mimetic tissue, several factors need to be considered in cell selection and processing for bioprinting. The physiological properties of cells in printed structure should mimic the cells in vivo. Under optimized microenvironment, the printed cells can maintain or develop their in vivo functions. The artificial tissues always encapsulate multiple types of cells, which play different roles in tissues. Cells providing function are called primary cells and the others are named supporting cells. When printing multiple types of cells, these cells can be seeded in the same or different hydrogels and printed simultaneously (Mandrycky et al. 2016).

Tissue fusion is a key process for cell construction in artificial tissue. This process relies on the cell self-organizing properties. When printing multiple cells or tissues, different tissues can merge together due to the surface tension forces and intergrowth of cells. This process can stimulate cell proliferation. When merging similar cell types, it can be called homotypic cell fusion. When fusion of bone marrow derived dendritic cells with neuron cells from brains or with myocyte cells from heart, different cell types like these merged together can be called heterotypic fusion. Due to the affect of the fusion phenomena, shrinkage of the printed cell structure and decrease of the mechanical strength may happen. Using appropriate scaffold support can prevent the undesired deformation to some extent (Munaz et al. 2016). To obtain artificial tissues, the interaction between cells and the scaffold determines the quality of the printed objects. Therefore, seeking a suitable scaffold is as important as finding a corresponding cell source (Radenkovic et al. 2016). The materials of the scaffold used in tissue fabrication should have good biocompatibility. Also the printed scaffold should support cell attachment and promote cell differentiation. The scaffold should be non-toxic and have suitable degradation rate as required. Additionally, the printed constructs should have the ability to promote mineralization and vascularization. Finally, the mechanical strength of the cell-laden scaffolds should be strong enough for handling and implantation (Arealis and Nikolaou 2015).

4.3 Additives

Some smaller biomolecules such as growth factors, enzymes, polynucleotides, polypeptides, proteins as well as other biomacromolecules (polysaccharides and DNA) have been utilized in many applications. These various biomolecules are widely used in biosensors, chromatography, diagnostic immunoassays, cell culture, DNA microarrays, analytical procedures, and even in bioprinting (Ihalainen et al. 2015). In bioprinting, these biomolecules are usually printed with cells during tissue fabrication to increase or decrease the levels of cells proliferation, differentiation and migration in the printed subjects (Jana and Lerman 2015).

Biomaterials used can provide relatively mild conditions in water-based 3D printing process. Therefore, growth factors and other bioactive components can be incorporated into the bioinks to improve the functionality of the printed tissues. The most frequent used growth factor is transforming growth factor-β (TGF-β). TGF-β is able to stimulate chondrogenic differentiation. But high content of this growth factor can lead to the hypertrophy (Hung et al. 2016). Bone morphogenic proteins (BMPs) are very important for bone tissue engineering. They can promote osteoprogenitors and MSC differentiation by inducing the osteogenesis process in vivo. Vascular endothelial growth factor (VEGF) is an angiogenic protein and it relates to the proliferation of endothelial cells. Fibroblast growth factors (FGFs) are also the type of proteins which induce angiogenesis. Along with other growth factors, such as insulin-like growth factor 1 (IGF-1), platelet-derived growth factor (PDGF) and

parathyroid hormone (PTH), all these growth factors play pivotal roles in tissue engineering (Bose et al. 2013; Fedorovich et al. 2011). By printing growth factors and cells to produce tissue constructs is an effective approach to evaluate the cell behavior and interactions between cells and growth factors in the structure (Jana and Lerman 2015).

Some small molecules can also be added into the printing materials. Previous research combined the use of growth factors and small molecules to enhance the bone formation (Sivolella et al. 2013). Another study used inkjet-printing technology to print rifampicin (RFP) and biphasic calcium phosphate (BCP) nanoparticles with PLGA to form a micropattern. This micropattern was able to consistently release the antibody for several months to prevent bacterial infection in an implant for wound healing. The use of BCP also accelerated the differentiation of osteoblasts (Lee et al. 2012).

Material selection and bioink formation are major hurdles for bioprinting. The most challenging issue is the printed tissues demonstrating limited survivability of the cells and the lack of therapeutic efficiency. To print functional tissue, appropriate printing techniques and suitable biomaterials properties should be well considered. There is still a long way to go in bioprinting (Bose et al. 2013).

5 Applications of Bioprinting

Challenges such as vascular network construction, incorporation of various cell types and appropriate mechanical integration of biomaterials and growth factors still exist in biopirnting. However, much progress has been made in organ bioprinting. Several tissues, including bone, cartilage, skin, vasculature, heart and neuronal tissues, have already been generated by printing. Smaller functional tissue components fabricated through 3D bioprinting can be used in drug screening and toxicity testing. If assembled rationally, one can form larger constructs in a "bottom-to-up" manner. In the following section, the most current advances in organ and tissue bioprinting based on 3D bioprinting, especially the thermal inkjet printing technology, are described.

5.1 Vasculature

The ultimate goal of tissue engineering is to build a functional, physiologically relevant organ which can be used for medical research or clinical transplantation. A functional vascular system is vital for organ survival. Without blood circulation, the tissues will lack oxygen and nutrients and the wastes accumulate. Under such circumstance, the cells rapidly enter programmed cell death and necrosis. Thus, printing organs with branched microvascular tree is the most critical and challenging task.

A vascular system consists of a complex network of blood vessels with various diameters ranging from 20 μm to 2.5 cm, from extremely fine capillaries to the aorta of the body. Researchers have explored various approaches to print vasculatures. Given the potentially adverse effect of scaffolds, scaffold-free small diameter vasculature was constructed using a rapid prototyping bioprinting. Smooth muscle cells and fibroblasts were aggregated into multicellular spheroids or cylinders and then were printed layer-by-layer, ultimately formed single- and double-layered small diameter vascular tubes (OD ranging from 0.9 to 2.5 mm). However, vascular patterning remains a major challenge for small-diameter blood vessel tissue engineering (Norotte et al. 2009). A study printed living alginate gelatin hydrogel valve conduits with the incorporation of dual cell types, including aortic root sinus smooth muscle cells (SMC) and aortic valve leaflet interstitial cells (VIC), in a regionally constrained manner (Duan et al. 2013). The printed aortic valve conduits were viable over 7 days in culture. The authors successfully fabricated aortic valve hydrogel conduits using 3D bioprinting, but the temperature around hydrogel need to be well controlled during printing in order to avoid premature gelation, and printing time was also difficult to control.

Crosslinking strategies may offer better control of tissue mechanic properties and reduce printing time. Biomolecules or appropriate hydrogels would likely improve cell viability, spreading, and proliferation. For example, tetraPEG-acrylate derivatives were crosslinked with synthetic extracellular matrices (sECMs), such as HA and gelatin derivatives, into extrudable hydrogels for printing tissue constructs. These stiffer hydrogels have rheological properties more suitable for bioprinting high-density cell suspensions. Through layer-by-layer deposition of hydrogel with NIH 3T3 cells, tubular tissue constructs were formed (Skardal et al. 2010).

Thermal inkjet bioprinting have shown great potential in building vascular tree. In an elegant study of vascular fabrication, human microvascular endothelial cells (HMVECs) and fibrin scaffold were utilized as bioink for microvasculature construction (Cui and Boland 2009). The authors precisely fabricated micronized fibrin channels using a drop-on-demand polymerization. In this study, thermal inkjet bioprinting technique showed minor damage to cells. After three weeks in culture, the printed HMVECs aligned themselves inside the fibrin channels and proliferated to form a vessel-like structure.

In the vascular system, changes that are part of aging are most apparent in the arteries. Arterial elasticity at age seventy is only about half of what it was at age twenty. Veins, in general, do not change as much with age as arteries. A novel simultaneous 3D printing/photocrosslinking technique for rapidly engineering aortic valve scaffolds had been developed by using PEGDA hydrogels (700 or 8000 MW) supplemented with alginate (Hockaday et al. 2012). The printed valve conduit scaffolds spanned a range of clinically relevant sizes as small as 12 mm ID, which is approximately the size of a 6 month infant aortic valve, and up to 22 mm ID valve, which is an adult size. The scaffolds were able to support cell adhesion and migration of porcine aortic valve interstitial cells (PAVICs). The relatively rapid printing time (14–45 min), with no requirement for further processing

post-fabrication (e.g. joining components), support that this technique is an efficient process for engineering anatomically precise soft tissue scaffolds.

In the approach to fabricate a reduced-sized 3D vascular channel networks and directly incorporate into hydrogels, sacrificial filament, such as Pluronic F127® (PF127, 20–25% w/w), was used in bioprinting. PF127 is an interesting material for its specific properties, i.e., it is liquid at 4 °C and solidifies when warmed. PF127 is approved for clinical applications by the American Food and Drug Association FDA. Vascular networks were constructed through the omnidirectional printing (ODP) by using a fugitive ink within a photopolymerized Pluronic F127-diacrylate matrix (Wu et al. 2011). However, cell adhesion and proliferation were not considered in the previous study. Another study developed an aqueous fugitive ink composed of Pluronic F127 and gelatin methacrylate (GelMA) to fabricate embedded vasculature (Kolesky et al. 2014). The authors investigated viability of normal human dermal fibroblasts (NHDF) cells and 10T1/2 fibroblast cells in the hydrogel and observed the proliferation of printed cells over time. Heated gelatin solution served as a sacrificial element. A group used a 3D direct printing technique to construct hydrogel scaffolds containing fluidic channels (Lee et al. 2010b). In that study, layer-by-layer printing was performed to build a 3D hydrogel block. A hollow channel within the collagen scaffold formed in heating processes. The authors also demonstrated that the dermal fibroblasts grew well in a scaffold containing fluidic channels. These approaches allow one to fabricate engineered tissue constructs in which vasculature and multiple cell types are programmably placed within extracellular matrices. Collectively, the sacrificial 3D bioprinting technique is an exciting advance that may simplify the patterning of vascular features and reduce printing time.

5.2 Muscle

Injuries to the musculoskeletal system are common, debilitating and expensive. Most fractures of long bones, for example, heal by them-selves, whereas large segmental defects do not. In many cases, inflammation and the degree of damage to surrounding tissues directly affect the regeneration ability of a tissue. The severe injuries of muscle result in the formation of a dense scar. Furthermore, imperfect healing always leads to chronic impairment (Evans and Huard 2015). The musculoskeletal system functions to transfer the force generated in muscle through tendon onto bone to produce movement. Thus, developing methods by which to fabricate composite structures is an important step in the engineering of increasingly complex tissue constructs (Lu et al. 2010; Yang and Temenoff 2009).

Bioprinting as an enabling technology possesses the advantages of high throughput, digital control, and highly accurate delivery of various biological factors to the desired locations for numerous applications such as 3D tissue fabrication. A single integrated muscle–tendon unit (MTU) construct was fabricated by printing four different components, including thermoplastic polyurethane (PU) and

C2C12 cell-laden hydrogel-based bioink for muscle development, and poly (ε-caprolactone) co-printed with NIH/3T3 cell-laden hydrogel-based bioink for tendon development (Merceron et al. 2015). The mechanically heterogeneous polymeric scaffold was elastic on the muscle side and relatively stiff on the tendon side, in addition to having a tissue-specific distribution of cells with myoblasts on the muscle side and fibroblasts on the tendon side. Furthermore, the final construct exhibited good cell compatibility (>80% cell viability at 1 and 7 day after printing).

Patterned growth factors also can be used in bioprinting to derive subpopulations of multiple lineages (e.g., bone and muscle-like cells). Inkjet bioprinting method was utilized to create spatial differentiation of adult stem cells in direct register to printed patterns of BMP-2 immobilized to fibrin (Phillippi et al. 2008). The results provide proof-of-concept for engineering spatial control of stem cell fates.

C2C12 skeletal muscle cells have been widely used to create muscle tissue because of their capacity of infinite proliferation and differentiation into multinucleated myotubes. C2C12 can align on materials after printing. Inkjet bioprinting was used to print and align C2C12 cells onto the micro-sized cantilevers (Cui et al. 2013). The results showed that printed cells aligned evenly with each other and formed mature myotubes after only 4 days. Furthermore, the printed myotubes were functional and responded to the electrical stimulation synchronously. The bioprinted myotubes can also be used for muscle exercise studies with electric stimulations at various frequencies.

Other bioprinting approaches have also been used to develop skeletal muscle myofibers. Microcontact printing technique, a soft lithographic technique based on the transfer of a "molecular ink" from an elastomeric stamp to a surface has been used to print fibronectin stripes (10, 25, 50 μm in width) onto biodegradable L-lactide/trimethylene carbonate copolymer films (Altomare et al. 2010). A well alignment of C2C12 cells were observed along the pattern 24 h after seeding, especially on fibronectin stripes 10 and 25 μm in width. In addition, layer-by-layer stereolithography technique was successfully employed to develop the antagonistic actuator pairs that mimic the function of musculature hydrostats such as octopus tentacles (Peele et al. 2015). 3D bioprinting seems to be useful approach to induce cell alignment and to improve myotube formation. However, the future work should be focused mainly on the bioink preparation, such as combination of ECM and growth factors, to fabricate healthy myotubes and to induce myofiber development.

5.3 Cartilage

Cartilage defects resulting from osteoarthritis, aging, and joint injury are the major cause of joint pain and chronic disability. Articular cartilage is aneural and avascular and nourished only by synovial fluid, therefore mature cartilage cannot heal spontaneously (Minas 2012). The most common treatments for cartilage repair include microfracture, osteochondral transfer, and autologous chondrocytes implantation; however, these treatments cannot restore hyaline cartilage (McCormick et al. 2014).

In addition, the current cartilage tissue engineering strategies still cannot fabricate new tissue that is indistinguishable from native cartilage with respect to the zonal organization, ECM composition, and mechanical properties (Hunziker 2002).

Inkjet bioprinting is able to directly repair cartilage tissue with closely mimicked native cartilage anatomy to the lesion site without additional damage. PEG macromers have been widely used in cartilage tissue engineering because of its biocompatibility and the similar compressive modulus of native human cartilage after polymerization (Fig. 2). In addition, PEG is water soluble with low viscosity and can be modified to be photocrosslinkable, which makes it attractive for 3D bioprinting. One of the major challenges in articular cartilage tissue engineering is the stabilization of the implanted biomaterial scaffold in the joint as well as the integration between the implant and surrounding native tissue. A thermal inkjet printer was modified to precisely deposit human articular chondrocytes and PEGDMA into repair cartilage defects of osteochondral plugs (served as 3D biopaper) (Cui et al. 2012b). Printed human chondrocytes were evenly distributed in the 3D PEGDMA hydrogel with simultaneous polymerization during printing (Fig. 3). Chondrocytes encapsulated in PEGDMA hydrogel proliferated and differentiated more effectively into cartilage. Furthermore, the printed cartilage implant attached firmly with surrounding tissue and the more extensive ECM production was observed at the interface between the hydrogel scaffold and the host cartilage tissue. This study indicates the importance of direct cartilage repair and promising anatomic cartilage engineering using 3D bioprinting technology.

Initial cell seeding density induces ECM production and is crucial for cell based cartilage tissue engineering. In order to overcome this restricted cell density in inkjet bioprinting, the influence of cell density, growth, and differentiation factors on cartilage tissue engineering was evaluated (Cui et al. 2012c). Results showed that FGF2/TGFβ1 cocktail combination synergistically promoted neocartilage formation. ECM production per chondrocyte at low cell density was much higher

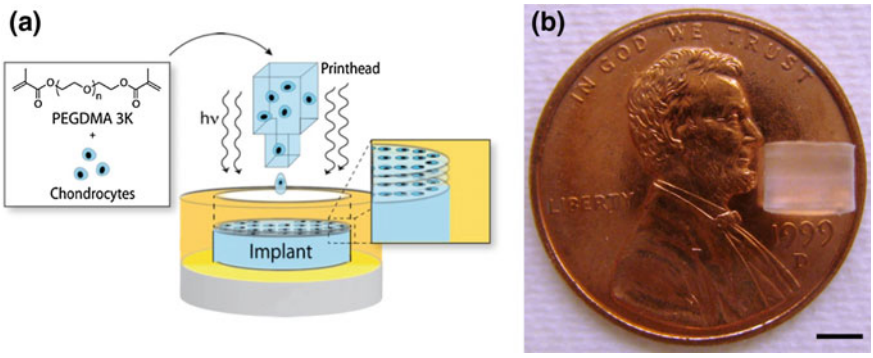

Fig. 2 Printed neocartilage tissue. **a** Schematic of cartilage bioprinting with simultaneous photopolymerization and layer-by-layer assembly. **b** A printed neocartilage tissue with 4 mm in diameter and 4 mm in height. Scale bar, 2 mm. (Cui et al. 2012c)

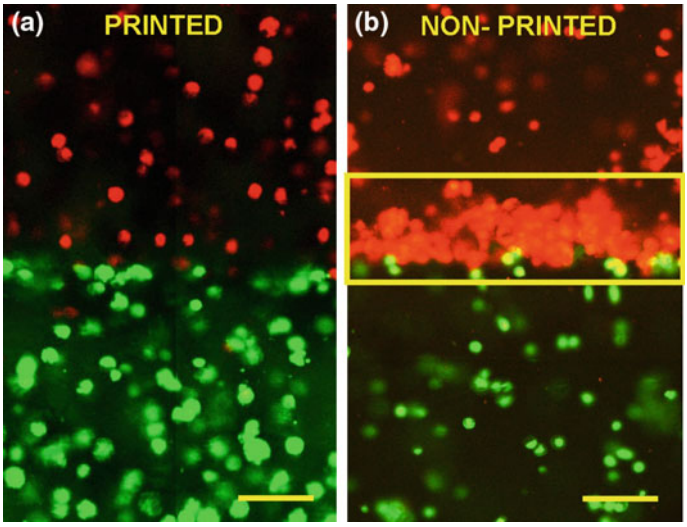

Fig. 3 Cells labeled with green and orange fluorescent dyes demonstrate the zonal cartilage bioprinting feasibility. **a** Printed cells maintained their initially deposited positions in the 3D hydrogel. The printing and photopolymerization process was completed in 4 min with cell viability of 90% ($n = 3$). **b** Cells accumulated to the bottom or interface due to gravity without simultaneous photopolymerization. It took 10 min of UV exposure to gel the construct with the same size as in A, resulting cell viability was 63% ($n = 3$). Scale bars, 100 μm (Cui et al. 2012b)

than that at high cell seeding density. This above studies implicated the importance and feasibility of direct cartilage repair with the bioprinting successfully controlling placement of individual cells, preserving cell viability, maintaining chondrogenic phenotype, and demonstrating integration with host tissue (Di Bella et al. 2015).

Researchers also have utilized other scaffold for cartilage regeneration. PCL and chondrocyte cell-encapsulated alginate hydrogel were printed using layer-by-layer deposition (Kundu et al. 2015). The group investigated the scaffolds and implants in vitro and in vivo. The PCL-alginate hydrogels showed negligible effects on the viability of the chondrocytes and the cell-printed PCL–alginate scaffolds (chondrocytes + TGF-β) showed higher ECM and GAG content in the engineered cartilage. Electrospinning system also was used in conjugation with 3D bioprinting method to promote chondrogenesis. A hybrid inkjet printing/electrospinning system had been utilized to fabricate cartilage tissues (Xu et al. 2013a). Electrospinning of PCL fibers was alternated with inkjet printing of rabbit elastic chondrocytes suspended in a fibrin-collagen hydrogel in order to fabricate a five-layer tissue construct of 1 mm thickness. The chondrocytes proliferated and maintained their basic biological properties within the printed constructs. Electrospinning system significantly enhanced biological and mechanical properties of the cartilage constructs. In addition, several groups printed with PCL and cell-laden hydrogel to fabricate ear-shaped constructs. In addition, PEG was deposited as a sacrificial layer to

support the main structure (Lee et al. 2014a). Mixing alginate with nanocellulose can also be used to build ear and meniscus constructs (Markstedt et al. 2015).

In order to create functional cartilage, further studies should focus on the improvement of the zonal architecture of articular cartilage scaffolds and the capability to recapitulate native cartilage extracellular matrix and growth factor signaling.

5.4 Bone

Bone has the unique internal self-healing abilities; however, large-scale bone defects cannot be healed completely without interpretation (Mourino and Boccaccini 2010; Seitz et al. 2005). Bone defects can be resulted from trauma, infection, neoplasm and failed arthroplasty. With the acceleration of the aging population, the clinical need to effectively treat bone defects is increasing (Reichert et al. 2009). Allograft or xenograft graftings are optional approaches, but these processes have constraints including limited tissues, requirement of secondary surgery, the possibility of immunologic rejection and risk of infection (Mourino and Boccaccini 2010). Tissue engineered approaches, particularly 3D bone printing, are effective to overcome these problems. Bone printing is the combined deposition of osteogenic cells and hydrogels to yield porous constructs (Fedorovich et al. 2011). The 3D printing technique can overcome most of the shortcomings of bone grafts and traditional bone tissue engineering.

Scaffolds and cells are crucial for all 3D printing approaches. In bone bioprinting, hydrogels are popular materials to be used. Progenitor cells such as the mesenchymal stem cells have been widely investigated with respect to efficacy to form bone. However, the survival and osteogenic differentiation of MSCs in hydrogels is limited. The modification of hydrogels can partially solve the problems. Hydrogels modified with adhesive sequences such as the Arg-Gly-Asp (RGD) motif, ubiquitously presented in many extracellular matrix proteins, can promote cell adhesion, survival and differentiation. Other sequences like MMP target sequence and heparin-binding domains also can be used to enhance osteogenesis. Bone constructs was fabricated by thermal inkjet printing of PEGDMA hydrogel and human MSCs (Gao et al. 2015b). In that study, acrylated RGD and MMP peptides were co-printed with PEGDMA hydrogel with simultaneous photopolymerization. The printed peptides conjugated PEG scaffold demonstrated the excellent biocompatibility with a cell viability of 87.9 $\pm$ 5.3%. Peptides conjugation significantly promoted MSC osteogenic differentiation, as well as mechanical properties of scaffolds. The same group also compared the osteogenic differentiation of human MSCs in PEGDMA-bioactive glass and HA. A thermal inkjet bioprinter was used to fabricate these cell-laden scaffolds. MSCs interacted with PEG-HA showed the highest cell viability, increased compressive modulus, collagen production and alkaline phosphate activity after 21-day culture in vitro (Gao et al. 2014).

Combination of hydrogel modification and inkjet printing are very promising in bone printing. Several studies have attempted to mimic the ECM microenvironment by integrating one or more ECM proteins on supportive synthetic biomaterials. In a recent study, bone tissues were printed using PEGDMA, gelatin methacrylate, and human MSCs (Gao et al. 2015a). The combination of natural and synthetic materials advanced scaffold biocompatibility with >80% of the cells survival during the printing process and enhanced MSC osteogenic and chondrogenic differentiation. 3D printed scaffolds were made from a composite of PCL, PLGA, and b-TCP and mineralized ECM was laid by human nasal inferior turbinate tissue-derived mesenchymal stromal cells (hTMSCs) (Pati et al. 2015b). After culturing in a bioreactor system, the scaffolds were decellularized and seeded with cells. The scaffolds demonstrated an obviously osteogenic stimulation in vitro and in vivo.

As discussed above, one challenge in the engineering of bone grafts is vascularization. An insufficient supply of oxygen and nutrients throughout the grafts would induce the loss of cellular function and eventually lead to cell death. Incorporation of microchannels into a construct is promising for induction of in vivo vascularization and host tissue ingrowth. Incorporation of growth factors into printed bone tissues is effective in cell proliferation, differentiation and eventually resulting in tissue formation and integrity. For example, gene delivery using PDGF has been applied to enhance vascularization (Storrie and Mooney 2006). In addition, BMPs or VEGF were printed into construct without losing their functionality and promoted osteogenesis and vascularization of bone grafts (Arealis and Nikolaou 2015).

The printed bone equivalents can be used to study homo- and heterotypic cell-cell interactions under physiological conditions, and to investigate drug responses, which would be a powerful tool between animal experiments and clinical trials. Pre-vascularization still remains challenging at clinically relevant dimensions. In the future, it is needed to print implants that can initiate vascularization and bone formation in orthotropic environments.

5.5 *Skin Tissue*

Skin is the largest organ of the human body, and it plays a vital role in maintaining homeostasis as well as in providing protection from the external environment. Major burn injuries are difficult to repair in clinic due to the structure complexity, the high risk of infection and the potential destruction of deeper skin layers including the dermis (Michael et al. 2013). The traditional skin tissue engineering developed several skin substitutes like Integra® and Matriderm® that are already applied in the clinical application, being complemented by the use of autologous split-thickness skin grafts. However, the fixed dimensions of skin equivalents could not satisfy personalized treatment and commercial skin products must be changed many times during treatment which may increase the cost of wound care and management.

By precise depositing multiple types of matrix materials and cells in a layer-by-layer manner, 3D bioprinting technology has been adopted for skin tissue fabrication in recent times. Fibroblasts and keratinocytes are major cells used in skin tissue engineering for construction of dermis and epidermis, respectively. Collagen, the main component of skin ECM, is the most commonly used material in skin tissue engineering. Several studies have shown that laser-assisted bioprinting (LaBP) is an outstanding tool for the generation of multicellular 3D constructs mimicking tissue structures. Collagen embedded with fibroblasts and keratinocytes were used as bioink to print skin tissue (Koch et al. 2012). The 3D skin constructs were used to investigate cell functions and tissue formation process. Adhesion and gap junctions are fundamental for tissue morphogenesis and cohesion is formed in the skin constructs. Another group printed human adipose-derived stem cells (hASCs) in a free-scalable 3D grid pattern by means of LaBP (Gruene et al. 2011). They observed that LaBP process showed no side effect on stem cell proliferation and differentiation. Even pre-differentiated hASCs could be utilized for the generation of 3D tissue grafts.

In addition to LaBP, droplet-based bioprinting has also been used for skin tissue fabrication. A flexible automated on-demand platform was developed for the free-form fabrication of living human skin by printing keratinocytes and fibroblasts on or into collagen scaffolds (Lee et al. 2014b). The platform consists of eight independently controlled cell-dispensing channels that can precisely place cells, ECM, scaffold materials, and growth factors in any user-defined 3D pattern. The final printed 3D constructs were morphologically and biologically representative of in vivo human skin tissue.

For successful skin grafting, vasculature is necessary to keep cells alive. Cells such as endothelial cells, keratinocytes and fibroblasts can be printed using inkjet devices onto gels with high cell viability over 90% (Cui et al. 2012a). These cells were co-printed to promote vascularization in skin implants. In another study, three cell types and two materials were deposited through inkjet printing to build skin graft, in which the top and bottom layers were made of collagen with dispersed keratinocytes (top) and fibroblasts (bottom), with the middle layer made of fibrin gel embedded with endothelial cells (Yanez et al. 2015). The cellular behavior of fibroblasts and keratinocytes was studied in vitro and in vivo. The wound healing accelerated in newly printed skin graft when it was compared to a commercially available skin wound dressing (Apligraf) or without any type of dressing. Wound contraction was improved by up to 17% when compared with the control groups. This study established that the presence of endothelial cell network throughout the skin graft maintained the graft's long-term life and induced the integration of grafts to the host. Stem cells have been used in skin printing to enhance angiogenesis. A group prepared bioink using fibrin-collagen gel embedded with amniotic fluid-derived stem cells (AFSCs). They directly printed over full-thickness skin wounds in nu/nu mice (Skardal et al. 2012). An increased microvessel density in AFS-treated wounds was observed. AFS cell-conditioned media induced endothelial cell migration in vitro through paracrine action of AFS cells.

The induction of de novo hair follicle or sweat gland growth in skin grafts is critical challenges in skin tissue engineering. So far, no successful strategies of generating human hair follicles from adult cells have yet been reported. The ability to closely emulate this functional niche would initiate hair neogenesis between the dermal papillae and epidermal cells (Ng et al. 2016). The advanced 3D printing techniques could be feasible to fabricate skin equivalents which virtually mimic native skin with vasculature, nerve, sweat glands and hair follicles.

5.6 Neuronal Tissue

Neuronal cells are surrounded by glial cells in the peripheral nervous system and the interactions between them and their surrounding environment are essential for nerve function. A current challenge in repairing the aged or injured peripheral neural system is to find an alternative to autologous nerve grafting (Tse et al. 2016). A recent study developed a piezoelectric inkjet printer with a nozzle diameter of 60 μm to print porcine Schwann cells and neuronal analogue NG108-15 cells (Tse et al. 2016). Even over a high voltage (230 V), the cells maintained a fairly good viability (fibroblasts had a viability of 89%, neuronal cells 96% and Schwann cells 90%). Schwann cells maintained their phenotype through the process of inkjet printing and a slight increase in viability was observed in seven days after printing.

For the treatment of short nerve injury gaps, the direct suturing of the two nerve ends is quite common. Nerve guidance conduit is an alternative approach for peripheral nerve repair, in which an implantable entubulation device is used. Micro-stereolithography was used to print nerve guidance conduits (Pateman et al. 2015). In the above mentioned study, the authors printed PEG-based nerve guidance conduits. The printed 3D constructs had relatively high resolution (50 μm). The dimensions of 1 mm in internal diameter, 5 mm in length and a 250 μm in wall thickness provided support for re-innervation of Schwann and dorsal root ganglion cells. This study highlights the promising potential of stereolithography for the rapid production of precise and intricate nerve guide structures, which might permit individual customization as well.

Customized medical treatments could convey significant advantages by targeting treatment directly to a specific injury or disease profile of a patient. Recently, Johnson et al. demonstrated a customized nerve repair technology based on microextrusion printing (Johnson et al. 2015). Alginate, calcium chloride, PLGA, PCL, silicone, and gelatin hydrogel served as the printed materials. GelMA hydrogel containing either nerve growth factor (NGF) or glial cell line-derived neurotrophic factor (GDNF) served as the printed luminal supplement. In vitro studies revealed that 3D printed physical and biochemical cues provided axonal guidance and chemoattractant/chemokinetic functionality for superior cervical ganglia, dorsal root ganglia and Schwann cells. In vivo studies of the regeneration of bifurcated injuries across a 10 mm complex nerve gap in rats showed that the 3D printed scaffolds achieved successful regeneration of complex nerve injuries,

resulting in enhanced functional return of the regenerated nerve. This technology enables the simultaneous incorporation of anatomical geometries, biomimetic physical cues, and spatially controlled biochemical gradients in a one-pot 3D manufacturing approach. This platform is promising in fundamental understanding of neuroregeneration and clinical treatment of complex nerve injuries.

Development of an accurate *in vitro* model of the brain remains a significant obstacle at the tissue or organ level. Peptide modified gellan gum substrates were used to build layered brain-like structures (Lozano et al. 2015). In that report, gellan gum was incorporated with RGD and then combined with primary cortical neurons to form bioink. The gellan gum-RGD hydrogel had a profound positive effect on primary cell proliferation and network formation. The viability of encapsulated cells after the printing process remained stable for 5 days. The printed cells were also evenly dispensed in the hydrogel. The authors established a low-cost, simple extrusion printing technique and bioink (RGD-GG) which could be used to create contained, layered and viable 3D cell structures.

Another group employed bioprinting to fabricate the fully biocompatible conduit using mouse bone marrow derived stem cells, Schwann cells and agarose (Owens et al. 2013). MSCs were chosen to promote cell-cell interactions and to differentiate into Schwann cells. The printed graft was made using 0.5 mm diameter multicellular cylinders, and reinforced with a surrounding collagen tube. The grafts were further implanted into mice and the histology results after 40 weeks indicated that axon regrowth was evident in regions surrounding the agarose rods. It was the first attempt to biofabricate a fully cellular bioprinted nerve graft and there are many adjustments still needed to improve and eventually optimize the performance of such a graft.

6 Challenges and Potentials

Even with the progresses made, bioprinting still faces challenges. The key elements of realizing functional bioprinting include the capacity of stable and precise positioning, the availability of printable biomaterials, and optimal cell sources. In addition, vascularization, innervation, and maturation are also crucial to engineer functional tissues.

In order to facilitate cell seeding and maturation, materials with cell compatibility and ideal mechanical properties are selected. Materials have an important influence on cell behavior, including cell attachment, cell motility, surface antigen display and regulation of gene expression (Stevens and George 2005). However, many published studies used a limited range of materials (Murphy and Atala 2014). Components of cellular extracellular matrix, including collagen, fibrin and HA, were used either alone or in combination with others reported previously. PEG-GelMA integrated by photoinitiation not only improves mechanical properties of GelMA, but also promotes stem cell survival and differentiation (Gao et al. 2015a; Gao et al. 2015b). Nemeth group developed nanopatterned PEG-GelMA-HA hydrogels which

could promote chondrogenic differentiation of stem cells (Nemeth et al. 2014). Thermoresponsive polymer poly (*N*-isopropylacrylamide) grafted hyaluronan (HA-pNIPAAM) was used to support extrusion of a range of biopolymers which underwent tandem gelation, ensured long-term mechanical stability and maintained chondrocyte viability (Kesti et al. 2015). These studies indicate that use of biomaterials in combination could enhance cell function. In future work, the multiple materials might be printed to construct a complex solid organ.

In reality, the ECM components are complex and demonstrating gradients of various components. Single material can only provide limited functions. Recently, tissue decellularization approach is developed which is facilitating researchers to analyze exact ECM compositions, localizations and biological functions (Baptista et al. 2009). Decellularized tissue specific ECM Scaffolds may serve as the useful biomaterials for bioprinting. In addition to the functional group, the structure of ECM components could be modified to improve mechanical properties or degradation kinetics.

The various approaches of 3D bioprinting have their respective advantages and disadvantages. In order to overcome the various challenges in bioprinting, it is necessary to combine different bioprinting approaches with different mechanisms.

Tissue or organs comprise multiple cell types with specific biological and chemical functions. Therefore, the choice of cells for tissue or organ printing are essential to deliver the correct functioning of the fabricated construct by providing physical function and supportive properties for vascularization or stem cell maintenance and differentiation (Murphy and Atala 2014). In tissue engineering, one fundamental problem is to isolate primary cells from tissues. As above mentioned, stem cells are promising for tissue-engineering applications and a large number of studies proved their suitability for bioprinting. However, some aspects must be considered in future applications. First, the control of cell proliferation and differentiation has not been fully understood. The timing of cellular proliferation is important for cell expansion to sufficient numbers. High cell density leads to quick tissue assembly and cell maturation. For example, 3D aggregates increase cell-cell interaction and produce more extracellular matrix, which helps to form the microtissues or even whole organs. Cell differentiation is crucial for long term cellular function. Researchers have developed several approaches involving appropriate scaffold, gene delivery or use of small molecules to promote cell survival and eliminated the side effect of bioprinting. Second, how to incorporate different cell types at an appropriate composition ratio and position. Although 3D bioprinting can precisely place cells or growth factors to the desired positions, the various culture conditions and cell sensitivity are vital for printing functional tissues. Most importantly, the safety of these printed cells and tissues requires further verification for clinical transplantation to patients. With the advances of cell conservation, bioreactors, cell reprogramming and gene editing technology, cell proliferation and differentiation could be controllable and the transformed non-immunogenic stem cells would be suitable for clinical applications.

7 The Future

Although 3D printing technology has been an active topic for decades, investigations in bioprinting are much more recent and this field is developing rapidly. 3D printing demonstrates the feasibility of constructing living systems and the flexibility of printing various subjects from soft to hard tissues with minimal side effects. In fact, the benign effects to the printed cells can be used for many other attractive applications, such as gene transfection and targeted drug delivery. The bioprinting system is versatile for 2D and 3D tissue application in both avascular and vascular tissue construction. Currently, the printed tissues can be used for drug discovery and preclinical testing. The behavior and metabolism of cells and microtissues could be analyzed systematically on a 'organs-on-chip' platform connected by a microfluidic network (Marx 2015). One promising clinical application for bioprinting is to develop the 'in vivo bioprinting', with the aid of a hand-held printer or printhead to directly and precisely deposit cells and materials on or in a patient to repair the lesion with various shapes and thickness with digital control. It is very promising in individual therapy and eliminates the requirement of secondary surgical intervention.

8 Conclusions

Although the current stage of bioprinting is still experimental, 3D bioprinting has shown great potential in tissue engineering applications. In order to overcome the remaining challenges in technology and biology, it is necessary to recruit experts in various fields, such as engineering, biology, chemistry, computer and medicine. 3D bioprinting has advanced dramatically enhanced regenerative approach for constructing living organs with vascular and nerve systems, which are promising to fabricate complex organs and ultimately achieve successes in organ transplantation.

References

Altomare L, Riehle M, Gadegaard N et al (2010) Microcontact printing of fibronectin on a biodegradable polymeric surface for skeletal muscle cell orientation. Int J Artif Organs 33 (8):535–543

An J, Teoh JEM, Suntornnond R et al (2015) Design and 3D printing of scaffolds and tissues. Engineering 1(2):261–268

Arealis G, Nikolaou VS (2015) Bone printing: new frontiers in the treatment of bone defects. Injury 46:S20–S22

Baptista PM, Orlando G, Mirmalek-Sani SH et al (2009) Whole organ decellularization—a tool for bioscaffold fabrication and organ bioengineering. Conf Proc IEEE Eng Med Biol Soc 2009:6526–6529

Bergemann C, Cornelsen M, Quade A et al (2016) Continuous cellularization of calcium phosphate hybrid scaffolds induced by plasma polymer activation. Mater Sci Eng C Mater Biol Appl 59:514–523
Bose S, Vahabzadeh S, Bandyopadhyay A (2013) Bone tissue engineering using 3D printing. Mater Today 16(12):496–504
Brunello G, Sivolella S, Meneghello R et al (2016) Powder-based 3D printing for bone tissue engineering. Biotechnol Adv
Buyukhatipoglu K, Chang R, Sun W et al (2010) Bioprinted nanoparticles for tissue engineering applications. Tissue Eng. Part C Methods 16:631–642
Chia HN, Wu BM (2015) Recent advances in 3D printing of biomaterials. J. Biol. Eng. 9:4
Choi WS, Ha D, Park S et al (2011) Synthetic multicellular cell-to-cell communication in inkjet printed bacterial cell systems. Biomaterials 32:2500–2507
Cui X, Boland T (2009) Human microvasculature fabrication using thermal inkjet printing technology. Biomaterials 30:6221–6227
Cui X, Boland T, D'Lima DD et al (2012a) Thermal inkjet printing in tissue engineering and regenerative medicine. Recent Pat Drug Deliv Formul 6(2):149–155
Cui X, Breitenkamp K, Finn MG et al (2012b) Direct human cartilage repair using three-dimensional bioprinting technology. Tissue Eng Part A 18(11–12):1304–1312
Cui X, Breitenkamp K, Lotz M et al (2012c) Synergistic action of fibroblast growth factor-2 and transforming growth factor-beta1 enhances bioprinted human neocartilage formation. Biotechnol Bioeng 109(9):2357–2368
Cui X, Gao G, Qiu Y (2013) Accelerated myotube formation using bioprinting technology for biosensor applications. Biotechnol Lett 35(3):315–321
Derby B (2015) Additive manufacture of ceramics components by inkjet printing. Engineering 1 (1):113–123
Detsch R, Schaefer S, Deisinger U et al (2011) In vitro: osteoclastic activity studies on surfaces of 3d printed calcium phosphate scaffolds. J Biomater Appl 26(3):359–380
Di Bella C, Fosang A, Donati DM et al (2015) 3D bioprinting of cartilage for orthopedic surgeons: reading between the lines. Front Surg 2:39
Duan B, Hockaday LA, Kang KH et al (2013) 3D bioprinting of heterogeneous aortic valve conduits with alginate/gelatin hydrogels. Biomed. Mater. Res. 101:1255–1264
Evans CH, Huard J (2015) Gene therapy approaches to regenerating the musculoskeletal system. Nat Rev Rheumatol 11(4):234–242
Fedorovich NE, Alblas J, Hennink WE et al (2011) Organ printing: the future of bone regeneration? Trends Biotechnol 29(12):601–606
Ferris CJ, Gilmore KG, Wallace GG et al (2013) Biofabrication: an overview of the approaches used for printing of living cells. Appl Microbiol Biotechnol 97(10):4243–4258
Gao G, Schilling AF, Hubbell K et al (2015a) Improved properties of bone and cartilage tissue from 3D inkjet-bioprinted human mesenchymal stem cells by simultaneous deposition and photocrosslinking in PEG-GelMA. Biotechnol Lett 37(11):2349–2355
Gao G, Schilling AF, Yonezawa T et al (2014) Bioactive nanoparticles stimulate bone tissue formation in bioprinted three-dimensional scaffold and human mesenchymal stem cells. Biotechnol J 9(10):1304–1311
Gao G, Yonezawa T, Hubbell K et al (2015b) Inkjet-bioprinted acrylated peptides and PEG hydrogel with human mesenchymal stem cells promote robust bone and cartilage formation with minimal printhead clogging. Biotechnol J 10(10):1568–1577
Gruene M, Pflaum M, Deiwick A et al (2011) Adipogenic differentiation of laser-printed 3D tissue grafts consisting of human adipose-derived stem cells. Biofabrication 3(1):015005
Guillemot F, Souquet A, Catros S et al (2010a) Laser-assisted cell printing: principle, physical parameters versus cell fate and perspectives in tissue engineering. Nanomedicine (Lond.) 5:507–515
Guillemot F, Souquet A, Catros S et al (2010b) High-throughput laser printing of cells and biomaterials for tissue engineering. Acta Biomater 6(7):2494–2500

Hockaday LA, Kang KH, Colangelo NW et al (2012) Rapid 3D printing of anatomically accurate and mechanically heterogeneous aortic valve hydrogel scaffolds. Biofabrication 4(3):035005
Hung KC, Tseng CS, Dai LG et al (2016) Water-based polyurethane 3D printed scaffolds with controlled release function for customized cartilage tissue engineering. Biomaterials 83:156–168
Hunziker EB (2002) Articular cartilage repair: basic science and clinical progress. A review of the current status and prospects. Osteoarthr Cartil 10(6):432–463
Ihalainen P, Maattanen A, Sandler N (2015) Printing technologies for biomolecule and cell-based applications. Int J Pharm 494(2):585–592
Jana S, Lerman A (2015) Bioprinting a cardiac valve. Biotechnol Adv 33(8):1503–1521
Johnson BN, Lancaster KZ, Zhen G et al (2015) 3D printed anatomical nerve regeneration pathways. Adv Funct Mater 25(39):6205–6217
Kesti M, Muller M, Becher J et al (2015) A versatile bioink for three-dimensional printing of cellular scaffolds based on thermally and photo-triggered tandem gelation. Acta Biomater 11:162–172
Kim J, Mcbride S, Tellis B et al (2012) Rapid-prototyped plga/β-tcp/hydroxyapatite nanocomposite scaffolds in a rabbit femoral defect model. Biofabrication 4(2):25003–25013(25011)
Koch L, Deiwick A, Schlie S et al (2012) Skin tissue generation by laser cell printing. Biotechnol Bioeng 109(7):1855–1863
Koch L, Gruene M, Unger C et al (2013) Laser assisted cell printing. Curr Pharm Biotechnol 14:91–97
Kolesky DB, Truby RL, Gladman AS et al (2014) 3D bioprinting of vascularized, heterogeneous cell-laden tissue constructs. Adv Mater 26(19):3124–3130
Kumar A, Mandal S, Barui S et al (2016) Low temperature additive manufacturing of three dimensional scaffolds for bone-tissue engineering applications: Processing related challenges and property assessment. Mater Sci Eng: R: Rep 103:1–39
Kundu J, Shim JH, Jang J et al (2015) An additive manufacturing-based PCL-alginate-chondrocyte bioprinted scaffold for cartilage tissue engineering. J Tissue Eng Regen Med 9(11):1286–1297
Lee JH, Gu Y, Wang H et al (2012) Microfluidic 3D bone tissue model for high-throughput evaluation of wound-healing and infection-preventing biomaterials. Biomaterials 33(4):999–1006
Lee JS, Hong JM, Jung JW et al (2014a) 3D printing of composite tissue with complex shape applied to ear regeneration. Biofabrication 6(2):024103
Lee JW, Kim JY, Cho DW (2010a) Solid free-form fabrication technology and its application to bone tissue engineering. Int J Stem Cells 3:85–95
Lee V, Singh G, Trasatti JP et al (2014b) Design and fabrication of human skin by three-dimensional bioprinting. Tissue Eng Part C Methods 20(6):473–484
Lee W, Lee V, Polio S et al (2010b) On-demand three-dimensional freeform fabrication of multi-layered hydrogel scaffold with fluidic channels. Biotechnol Bioeng 105(6):1178–1186
Lopes MS, Jardini AL, Filho RM (2012) Poly (lactic acid) production for tissue engineering applications. Procedia Eng 42(4):1402–1413
Lozano R, Stevens L, Thompson BC et al (2015) 3D printing of layered brain-like structures using peptide modified gellan gum substrates. Biomaterials 67:264–273
Lu HH, Subramony SD, Boushell MK et al (2010) Tissue engineering strategies for the regeneration of orthopedic interfaces. Ann Biomed Eng 38(6):2142–2154
Mandrycky C, Wang Z, Kim K et al (2016) 3D bioprinting for engineering complex tissues. Biotechnol Adv 34(4):422–434
Markstedt K, Mantas A, Tournier I et al (2015) 3d bioprinting human chondrocytes with nanocellulose–alginate bioink for cartilage tissue engineering applications. Biomacromolecules 16(5):1489–1496
Marx V (2015) Tissue engineering: organs from the lab. Nature 522(7556):373–377
McCormick F, Harris JD, Abrams GD et al (2014) Trends in the surgical treatment of articular cartilage lesions in the United States: an analysis of a large private-payer database over a period of 8 years. Arthroscopy 30(2):222–226

Merceron TK, Burt M, Seol YJ et al (2015) A 3D bioprinted complex structure for engineering the muscle-tendon unit. Biofabrication 7(3):035003
Michael S, Sorg H, Peck CT et al (2013) Tissue engineered skin substitutes created by laser-assisted bioprinting form skin-like structures in the dorsal skin fold chamber in mice. PLoS ONE 8(3):e57741
Minas T (2012) A primer in cartilage repair. J Bone Joint Surg Br 94 (11 Suppl A):141–146
Mironov V, Kasyanov V, Markwald RR (2011) Organ printing: from bioprinter to organ biofabrication line. Curr Opin Biotechnol 22(5):667–673
Mironov V, Visconti RP, Kasyanov V et al (2009) Organ printing: tissue spheroids as building blocks. Biomaterials 30:2164–2174
Mohamed KR, El-Rashidy ZM, Salama (2011) In vitro properties of nano-hydroxyapatite/chitosan biocomposites. Ceram Int 37 (8):3265–3271
Mota C, Puppi D, Chiellini F et al (2015) Additive manufacturing techniques for the production of tissue engineering constructs. J Tissue Eng Regen Med 9(3):174–190
Mourino V, Boccaccini AR (2010) Bone tissue engineering therapeutics: controlled drug delivery in three-dimensional scaffolds. J R Soc Interface 7(43):209–227
Munaz A, Vadivelu RK, St. John J et al (2016) Three-dimensional printing of biological matters. J Sci: Adv Mater Devices 1(1):1–17
Murphy SV, Atala A (2014) 3D bioprinting of tissues and organs. Nat Biotechnol 32(8):773–785
Nemeth CL, Janebodin K, Yuan AE et al (2014) Enhanced chondrogenic differentiation of dental pulp stem cells using nanopatterned PEG-GelMA-HA hydrogels. Tissue Eng Part A 20(21–22):2817–2829
Ng WL, Wang S, Yeong WY et al (2016) Skin bioprinting: impending reality or fantasy? Trends Biotechnol
Norotte C, Marga FS, Niklason LE et al (2009) Scaffold-free vascular tissue engineering using bioprinting. Biomaterials 30(30):5910–5917
Owens CM, Marga F, Forgacs G et al (2013) Biofabrication and testing of a fully cellular nerve graft. Biofabrication 5(4):045007
Ozbolat IT, Peng W, Ozbolat V (2016) Application areas of 3D bioprinting. Drug Discov Today
Pateman CJ, Harding AJ, Glen A et al (2015) Nerve guides manufactured from photocurable polymers to aid peripheral nerve repair. Biomaterials 49:77–89
Pati F, Ha DH, Jang J et al (2015a) Biomimetic 3D tissue printing for soft tissue regeneration. Biomaterials 62:164–175
Pati F, Song TH, Rijal G et al (2015b) Ornamenting 3D printed scaffolds with cell-laid extracellular matrix for bone tissue regeneration. Biomaterials 37:230–241
Peele BN, Wallin TJ, Zhao H et al (2015) 3D printing antagonistic systems of artificial muscle using projection stereolithography. Bioinspir Biomim 10(5):055003
Phillippi JA, Miller E, Weiss L et al (2008) Microenvironments engineered by inkjet bioprinting spatially direct adult stem cells toward muscle- and bone-like subpopulations. Stem Cells 26 (1):127–134
Pulieri E, Chiono V, Ciardelli G (2008) Chitosan/gelatin blends for biomedical applications. J Biomed Mater Res, Part A 86A(2):311–322
Radenkovic D, Solouk A, Seifalian A (2016) Personalized development of human organs using 3D printing technology. Med Hypotheses 87:30–33
Reichert JC, Saifzadeh S, Wullschleger ME et al (2009) The challenge of establishing preclinical models for segmental bone defect research. Biomaterials 30(12):2149–2163
Rezende RA, Kasyanov V, Mironov V et al (2015) Organ Printing as an Information Technology. Procedia Eng 110:151–158
Seitz H, Rieder W, Irsen S et al (2005) Three-dimensional printing of porous ceramic scaffolds for bone tissue engineering. J Biomed Mater Res B Appl Biomater 74(2):782–788
Shafiee A, Atala A (2016) Printing Technologies for Medical Applications. Trends Mol Med 22 (3):254–265
Sivolella S, Biagi MD, Brunello G et al (2013) Delivery systems and role of growth factors for alveolar bone regeneration in dentistry. J Phys Chem 83(7):869–873

Skardal A, Mack D, Kapetanovic E et al (2012) Bioprinted amniotic fluid-derived stem cells accelerate healing of large skin wounds. Stem Cells Transl Med 1(11):792–802

Skardal A, Zhang J, Prestwich GD (2010) Bioprinting vessel-like constructs using hyaluronan hydrogels crosslinked with tetrahedral polyethylene glycol tetracrylates. Biomaterials 31 (24):6173–6181

Stevens MM, George JH (2005) Exploring and engineering the cell surface interface. Science 310 (5751):1135–1138

Storrie H, Mooney DJ (2006) Sustained delivery of plasmid DNA from polymeric scaffolds for tissue engineering. Adv Drug Deliv Rev 58(4):500–514

Tirella A, Orsini A, Vozzi G et al (2009) A phase diagram for microfabrication of geometrically controlled hydrogel scaffolds. Biofabrication 1(4):251–260

Tse C, Whiteley R, Yu T et al (2016) Inkjet printing Schwann cells and neuronal analogue NG108-15 cells. Biofabrication 8(1):015017

Umezu S, Suzuki H, Kawamoto H (2005) Droplet formation and dropping position control in electrostatic inkjet phenomena. NIP & Digital Fabrication conference:283–286

Wu W, DeConinck A, Lewis JA (2011) Omnidirectional printing of 3D microvascular networks. Adv Mater 23(24):H178–183

Xiong R, Zhang Z, Huang Y (2015) Identification of optimal printing conditions for laser printing of alginate tubular constructs. J Manuf Process 20:450–455

Xu T, Baicu C, Aho M et al (2009) Fabrication and characterization of bio-engineered cardiac pseudo tissues. Cancer Res 74(2):1–10

Xu T, Binder KW, Albanna MZ et al (2013a) Hybrid printing of mechanically and biologically improved constructs for cartilage tissue engineering applications. Biofabrication 5(1):015001

Xu T, Zhao W, Zhu JM et al (2013b) Complex heterogeneous tissue constructs containing multiple cell types prepared by inkjet printing technology. Biomaterials 34(1):130–139

Yanez M, Rincon J, Dones A et al (2015) In vivo assessment of printed microvasculature in a bilayer skin graft to treat full-thickness wounds. Tissue Eng Part A 21(1–2):224–233

Yang PJ, Temenoff JS (2009) Engineering orthopedic tissue interfaces. Tissue Eng Part B Rev 15 (2):127–141

Yao Q, Wei B, Guo Y et al (2015) Design, construction and mechanical testing of digital 3d anatomical data-based PCL- HA bone tissue engineering scaffold. J Mater Sci Mater Med 26 (1):1–9

Zhu W, Ma X, Gou M et al (2016) 3D printing of functional biomaterials for tissue engineering. Curr Opin Biotechnol 40:103–112

Controlled Gene Delivery Systems for Articular Cartilage Repair

Magali Cucchiarini and Ana Rey-Rico

Abstract Delivery of efficient and safe gene transfer vectors capable of achieving appropriate levels of therapeutic gene expression into the target place is a very valuable strategy for articular cartilage repair. Diverse nonviral and viral gene vehicles have been studied to modify relevant cell populations involved in cartilage regenerative processes, among which the nonpathogenic, effective, and relatively safe recombinant adeno-associated viral (rAAV) that have emerged as the preferred gene delivery system to treat human disorders. The clinical adaptation of these systems is still limited by several hurdles including the presence of immune and toxic responses in the host organism, the ubiquity of rate-limiting steps associated with physiological barriers, and the possibility of dissemination to nontarget sites that may impair their therapeutic action. The use of controlled release strategies to deliver gene transfer vectors such as rAAV may provide powerful tools to enhance the temporal and spatial presentation of therapeutic agents into a defined target and overcome such obstacles in vivo. The goal of the present work is to provide an overview of the most recent advances in gene therapy approaches for cartilage repair based on the use of adapted biomaterials as controlled delivery platforms of gene transfer vectors to improve the efficiency of the therapeutical transgene.

Keywords rAAV vectors · Controlled release · Cartilage repair

Abbreviations

3D	Three-dimensional
AlgPH155	Alginate
BMP	Bone morphogenetic protein
CDMP	Cartilage-derived morphogenetic protein
ECM	Extracellular cartilage matrix
ELP	Elastin-like polypeptides

M. Cucchiarini (✉) · A. Rey-Rico
Center of Experimental Orthopaedics, Saarland University Medical Center, Kirrbergerstr. Bldg 37, D-66421 Homburg/Saar, Germany
e-mail: mmcucchiarini@hotmail.com

A. Tripathi and J.S. Melo (eds.), *Advances in Biomaterials for Biomedical Applications*, Advanced Structured Materials 66,
DOI 10.1007/978-981-10-3328-5_7

FG	Fibrin glue
FGF-2	Basic fibroblast growth factor
GAMs	Gene-activated matrices
HpNPs	Heparin/superparamagnetic iron oxide
HSV	Herpes simplex viral vector
IGF-I	Insulin-like growth factor I
IL-1	Interleukin-1
IL-1Ra	IL-1 receptor antagonist
i.m.	Intramuscular
i.p.	Intraperitoneal
ITRs	Inverted terminal repeats
MMPs	Matrix metalloproteinases
MSCs	Mesenchymal stem cells
nHA	Nanohydroxyapatite nanoparticles
nHA-pDNA	nHA-plasmid DNA
OPF	Oligo(poly(ethylene glycol) fumarate)
p	Plasmid
PCL	Poly-ε-caprolactone
PDGF-B	Platelet-derived growth factor subunit B
PEG	Polyethylene glycol
PELA	Polyethylene glycol-poly(D,L-lactide)
PEO	Poly(ethylene oxide)
PLG	Poly(lactide-co-glycolide)
PLGA	Poly(lactide-co-glycolide)
pNIPAAm	Poly(N-isopropylacrilamide)
pNIPAAm-co-AAc	Poly(N-isopropylacrylamide-co-acrylic acid)
polyA	Polyadenylation signal
PPO	Poly(propylene oxide)
PTHrP	Parathyroid hormone-related protein
PU	Polyurethane
rAAV	Recombinant adeno-associated viral vector
RAD16-I	Self-assembling peptides with (RADA)4 sequence
RUNX2	Runt-related transcription factor 2
SAMs	Self-assembled monolayers
s.c.	Subcutaneous
scAAV	Self-complementary AAV
SF	Silk fibroin
SOX	Sex determining region Y-box
TGF-β	Transforming growth factor beta
TNF	Tumor necrosis factor
TNFR:Fc	TNF-immunoglobulin Fc fusion protein

1 Cartilage Damage: Current Outcomes

Articular cartilage is the multiphasic tissue that lines the weight-bearing surface of joints consisting of chondrocytes cells (<5%), interstitial fluid (60–85%) and an extracellular cartilage matrix (ECM) composed of type-II collagen (15–22%), proteoglycans (4–7%), and other biomacromolecules (Ma and Langer 1999; Mow et al. 1992; Spiller et al. 2011). Due to its avascular nature, cartilage has a limited ability to self-healing and full repair of cartilage defects is thus a major clinical challenge that may progress to osteoarthritis (Goldring and Goldring 2007; Sandell 2012; Johnstone et al. 2013), a critical disorder affecting a large number of patients (Mankin 1974a, b). In addition, precluding the formation of a blood clot and other self-healing processes in cartilage tissue is mostly due to the lack of vascularization. The exclusive presence of highly differentiated chondrocytes with basal synthetic and mitotic activities and the absence of chondrogenically competent progenitor cells in the adult cartilage tissue may compensate for the decline in cell potency during ageing which limit the response of cartilage to injury.

Lesions of the cartilaginous tissue may have a limited extension in focal cartilage defects or generalized during osteoarthritis. Structural integrity from focal defects is disrupted in delimited areas affecting only to the cartilaginous zone if the defect is chondral or involving also the subchondral bone if it is osteochondral (Orth et al. 2014). Thus, a differential pattern of healing is observed for both types of focal defects. Hence, chondral defects are partially repopulated by cells migrating from synovial fluid resulting in a insufficient filling that usually led to degeneration in the term of weeks to months. Although, the poor integration in these type of defects are often results in focal discontinuity with regions of hypocellularity and cluster formation into the adjacent tissue (Madry et al. 2011). Conversely, osteochondral defects ($\sim$5% of articular cartilage defects) are filled with a blood clot if the bone marrow comes across the defect. Existence of pluripotential mesenchymal stem cells in the blood clot can differentiate into chondrocytes and osteoblasts which can ultimately form the cartilage repair tissue and reconstituted chondral bone, respectively. Eventually, chondrogenesis process was completed after some months by the appearance of round cells and new cartilaginous matrix. However, the resulting repair tissue did not integrate with the existing nearby matrix and chondrocytes. It was monitored that the adjacent cartilage tissue does not participate in the filling of the defect that could be apoptotic over-time resulting in an acellular region (Orth et al. 2014). Current therapeutic options to repair injured cartilage include marrow stimulation techniques (Johnson 2001; Steadman et al. 2003; Steinwachs et al. 2008; Kim et al. 1991), transplantation of tissue or cells as autologous chondrocytes or mesenchymal stem cells (MSCs) and replacement surgery (Brittberg et al. 1994; Horas et al. 2003; Bentley et al. 2003; Knutsen et al. 2004). Yet, none of them are capable of reproducing the natural functions of the native, hyaline cartilage, rather leading to the formation of a poorly mechanically functional fibrocartilaginous surface (type-I collagen). Hence, extensive efforts are ongoing to improve these procedures and a substantial progress has been achieved

in the last few years by identifying novel methods and factors that may stimulate the reparative processes in sites of cartilage injury. So far, regenerating the desirable phenotypic response from host and/or co-delivered progenitor cells remains a major issue in orthopaedics.

2 Principles of Gene Transfer for Cartilage Repair

The development of gene delivery vehicles have emerged as a promising technology to treat cartilage disorders by directly transferring of genes encoding for therapeutic factors into the places of injury that result in a temporarily and spatially defined delivery of a candidate agent (Rey-Rico and Cucchiarini 2016a). Of note, the administration of candidate genes instead of short-life molecules (recombinant factors) may allow to prolong the therapeutic effects and eventually slowing down or stopping the over time progression of the cartilage disorder.

2.1 Target Cells

Gene therapy strategies aiming at the repair of damaged articular cartilage surface might target joint cells relevant to the clinical problem, i.e. chondrocytes of the adjacent (uninjured) tissue to afford protection against further degradation, synoviocytes to control inflammatory events potentially activated or to replace the chondrocytes by differentiation, cells of surrounding tissues involved in pathological processes (subchondral bone, meniscus, tendons), and progenitor cells that may arise from the bone marrow to fill the lesions or for transplantation and regenerative purposes (Cucchiarini and Madry 2010; Madry et al. 2011).

Genetic modification of chondrocytes, synovial lining cells and surrounding tissues has been widely documented in different gene transfer approaches for cartilage regeneration (Trippel et al. 2004; Madry and Cucchiarini 2013, 2014; Elmallah et al. 2015). So far, progenitor cells especially MSCs constitute also potential targets for gene transfer as they can be isolated in a relative non-invasive and abundant way from different sources as bone marrow (Prockop 1998), bone (Noth et al. 2002), adipose tissue (Zuk et al. 2001), muscle (Peng and Huard 2004), synovium (De Bari et al. 2001), periosteum (Zarnett and Salter 1989), and perichondrium (Dounchis et al. 1997).

More recent approaches describe the use of autologous compounds capable of improving the effectiveness of microfracture technique and avoiding the more laborious steps of preparation and expansion associated to the use of cells (Rey-Rico and Cucchiarini 2016b). By this method a marrow aspirate is collected from the patients, genetically modified ex vivo (Pascher et al. 2004; Rey-Rico et al. 2015a; Frisch et al. 2014a, 2015, 2016a, b), and implanted into cartilage defects (Pascher et al. 2004).

2.2 Candidate Factors

A potential advantage of gene transfer is the establishment of a variety of sequences encoding for therapeutic factors with a known ability to promote cartilage reparative processes. Hence, current gene transfer strategies for repairing articular cartilage defects focus on increasing chondrogenic differentiation of MSCs into chondrocytes for cartilage regeneration and into osteoblasts to promote the repair of the subchondral bone. So far, the production and maintenance of a new cartilaginous matrix rich in type-II collagen and proteoglycans, the increase of the cellularity of the repair tissue to prevent the hypertrophic differentiation of chondrocytes and the inhibition of articular cartilage degeneration are also other potential targets (Cucchiarini and Madry 2010; Orth et al. 2014; Madry et al. 2011).

Among the growth factors candidates to support chondrogenesis are members of the transforming growth factor beta (TGF-β) superfamily such as TGF-β1 and TGF-β2 (Hanada et al. 2001; Lee et al. 2001; Joyce et al. 1990), bone morphogenetic protein 2 (BMP-2) (Sellers et al. 1997; Hanada et al. 2001), BMP-7 (Asahina et al. 1996; Klein-Nulend et al. 1998), members of the fibroblast growth factor family such as the basic fibroblast growth factor (FGF-2) (Jentzsch et al. 1980) and parathyroid hormone-related protein (PTHrP) (Vortkamp et al. 1996). Growth factors increasing cell proliferation include FGF-2 (Trippel et al. 1993), and the insulin-like growth factor I (IGF-I) (Trippel 1995). Potential candidate for enhancing matrix synthesis are IGF-I (Nixon et al. 1999), BMP-2, BMP-7 and the cartilage-derived morphogenetic proteins (CDMP) (Erlacher et al. 1998; Katayama et al. 2004). Transcription factors such as the sex determining region Y-box (SOX) 5, 6, and 9 (SOX trio, i.e. SOX5, SOX6, SOX9) (Lefebvre et al. 2001) Cbfa-1/runt-related transcription factor 2 (RUNX2) (Inada et al. 1999), Cart-1 (Zhao et al. 1994), and the Ets family members (Sumarsono et al. 1996) are also potential candidates as they directly modulate the expression of genes involved in chondrogenesis as type-II collagen or aggrecan (Madry et al. 2011). Another potential gene transfer approach for cartilage regeneration focus on the inhibition of degenerative pathways within the repair tissue. Potential targets for this strategy include cytokines mediating catabolic events as members of the interleukin-1 (IL-1) (Goldring et al. 1994) and tumor necrosis factor (TNF) (Pelletier and Martel-Pelletier 1994) families to suppress the production of matrix-degrading enzymes such as the matrix metalloproteinases (MMPs) (Pelletier and Martel-Pelletier 1994).

2.3 Gene Transfer Vectors

Gene transfer focuses on the introduction of foreign genes or gene sequences in a target cell population to treat a particular disorder in affected individuals by gene therapy and/or regenerative medicine, based on the sustained expression of the transgene cassette, compared with the direct application of the therapeutic product

itself that exhibits a short pharmacological half-life (Rey-Rico and Cucchiarini 2016a). Once the foreign genetic material enters into the cell, it may be transferred towards the nucleus where it either integrates into the host genome or remains extrachromosomal under an episomal form for subsequent expression of the transgenes being delivered. However, the susceptibility of naked DNA to degradation by nucleases present in the biological medium, the hydrophilic polyanionic nature of the DNA macromolecule and its large size prevents passive penetration of DNA through the cell membrane (Nam et al. 2009; Ibraheem et al. 2014). Hence, the DNA must be associated with vectors able to carry the therapeutic molecule into the target cell (Ibraheem et al. 2014).

Gene transfer vectors currently involved in cartilage repair include nonviral (Goomer et al. 2000; Gelse et al. 2008; Morrey et al. 2008; Pi et al. 2011; Cucchiarini et al. 2015) and viral vehicles such as adenoviral (Gelse et al. 2003; Imperiale and Kochanek 2004; Pohle et al. 2012; Zhang et al. 2015a; b; Garza-Veloz et al. 2013; Wang et al. 2014), retro-/lentiviral (Hardingham et al. 2006; Yamada et al. 1991; Mbita et al. 2014; Shields et al. 2015; Shi et al. 2015), herpes simplex viral vectors (HSV) (Jenkins and Turner 1996; Lachmann 2004; Wu et al. 2013), and recombinant adeno-associated viral (rAAV) vectors (Wang et al. 2011; Bao et al. 2012; Mason et al. 2012; Cucchiarini et al. 2013; Glass et al. 2014; Cucchiarini and Madry 2014; Frisch et al. 2014a, b; Rey-Rico et al. 2015a).

2.3.1 Nonviral Vectors

Gene transfer via nonviral vectors (transfection) consist the incorporation of DNA, either naked or complexed with cationic polymers (polyplexes) or with cationic lipids (lipoplexes), into the target population. It is considered as a safe method which avoids the risk of acquiring replication competence and of insertional mutagenesis without inducing immune responses in the host, however, its use is limited due to the low transfection efficiencies (40–50% maximum) and short-term transgene expression levels (Goomer et al. 2000; Madry et al. 2005; Saraf and Mikos 2006).

2.3.2 Viral Vectors

Gene transfer using viral vectors (transduction) is based on the natural cellular entry pathways of viruses from which they are derived. The most common viruses that have been manipulated thus far for gene transfer purposes are adenoviruses, HSV, retro- and lentiviruses, and AAV (Robbins and Ghivizzani 1998). Modification of these viruses can be achieved by replacing, at least to a certain extent, the viral coding sequences by a therapeutic transgene cassette. In general, viral vectors have

showed better clinical potential compared with nonviral vehicles due to their higher efficiency to deliver gene sequences and achieving a long-term transgene expression in vivo (Loser et al. 2002).

Adenoviruses are one of the most exploited viral based vectors for cartilage repair (Gelse et al. 2003; Imperiale and Kochanek 2004; Pohle et al. 2012; Zhang et al. 2015a, b; Garza-Veloz et al. 2013; Wang et al. 2014) as they allow for high transduction efficiencies and transgene expression in the variety of cells, enabling direct approaches in vivo. However, their use is limited by their immunogenicity and reduced transgene expression over time (1–2 weeks) as the transgenes are kept as episomal elements (Cucchiarini and Madry 2010).

Retrovirus and lentiviral vectors instead can integrate inside the host genome of the target, allowing for the replication and maintenance of the transgene over extended period of time. Yet, the main concern regarding their use is that this might lead to insertional mutagenesis with the potential to activate tumorigenic genes (Chang and Gay 2001; Yi et al. 2005; Knight et al. 2013). So far, retroviral vectors have a restricted host range and can not transduce nondividing cells, making them rather suitable for ex vivo approaches requiring the extraction of the target cells from the host before modification and reimplantation (Evans et al. 1996; Mason et al. 2000; Grande et al. 2003; Murphy et al. 2003). Additionally, in vivo administration of retroviruses in human subjects may be inhibited by the complement depending on the producer line employed to generate them (Spitzer et al. 1999). Lentiviral vectors may provide alternatives to retroviral gene vehicles as they can integrate in the genome of nondividing cells, allowing for long-term transgene expression (Gouze et al. 2003; Glass et al. 2014) but it is also exhibiting a risk for insertional mutagenesis and the issue of safety regarding their typical origin.

The main advantages of using HSV vectors include their ability to infect nondividing cells, to establish latency in some cell types, and to carry large gene sequences (Robbins and Ghivizzani 1998; Lachmann 2004). Still, the use of HSV-based vectors has been limited due to their toxicity in many cell types. In this sense, although the first generation vectors have induced high levels of cytoxicity, recent work has demonstrated that second generation HSV were less deleterious, in particular for cartilage repair (Oligino et al. 1999; Lachmann 2004; Wu et al. 2013). Nevertheless a remaining issue with this type of vectors is the transient nature of transgene expression that can be afforded via HSV (Oligino et al. 1999).

Active investigation is currently ongoing based on the application of the most advanced rAAV gene transfer vehicles that have emerged as the vectors of choice to treat human disorders (Evans and Huard 2015; Rey-Rico and Cucchiarini 2016a, b).

2.3.3 rAAV Vectors: Emerging Gene Transfer Tools for Cartilage Regeneration

rAAV vectors are derived from a non-pathogenic, replication-defective human parvovirus (Rose et al. 1969) that can be manipulated to produce recombinant viral

constructs by removing all AAV coding sequences and replacing them by a transgene cassette (Berns and Giraud 1995; Daya and Berns 2008) making them less immunogenic than adenoviral vectors and less toxic than HSV (Smith-Arica and Bartlett 2001; Grieger and Samulski 2012; Kotterman and Schaffer 2014). rAAV are small (~20 nm) vectors (Fig. 1), capable of transducing both dividing and nondividing cells at relatively high gene transfer efficiencies (up to 100%) (Arai et al. 2000; Venkatesan et al. 2013; Rey-Rico et al. 2015b, c; Rey-Rico and Cucchiarini 2016a; Diaz-Rodriguez et al. 2015; Tao et al. 2016a, b) allowing for direct gene transfer approaches in vivo through the dense ECM of targeted tissues as cartilage (Venkatesan et al. 2013). These potential advantages from rAAV over the other type of viral vectors make them as preferred gene delivery system to treat human disorders (Cucchiarini and Madry 2005, 2010; Madry et al. 2006, 2007; van der Laan et al. 2011; Zhang et al. 2011a; Jacobs and Wang 2011; Cucchiarini et al. 2012; Evans et al. 2013; Madry and Cucchiarini 2013; Nieto and Salvetti 2014; Evans and Huard 2015; Rey-Rico and Cucchiarini 2016a, b). So far, the therapeutic success of rAAV vectors has been supported by an increasing number of phase I-III clinical gene therapy trials including rheumatoid arthritis (Mease et al. 2009, 2010; Evans et al. 2013) and osteoarthritis (Evans et al. 2013).

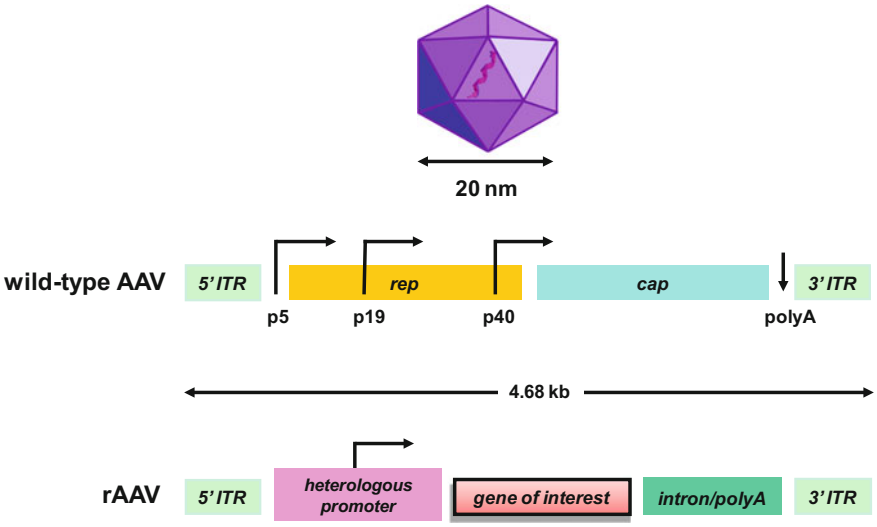

Fig. 1 Genomic organization of wild-type AAV and rAAV vectors. The wild-type AAV genome with *rep* (replication) and *cap* (capsid) genes along with a polyadenylation signal (polyA) is flanked by two inverted terminal repeats (ITRs) (~4.68 kb). The *arrows* indicate the viral transcription promoters (p5, p19, and p40). A classical rAAV vector with the ITRs at either end of a transgene cassette (heterelogous promoter, gene of interest, intron/polyA signal), is depicted below

3 Application of Controlled Delivery Strategies for Effective Gene Transfer to Articular Cartilage

A main issue to achieve an effective gene transfer directly targeted to the sites of cartilage injury is due to the limited accessibility of the lesions for the treatment. Delivery of candidate gene sequences into the sites of cartilage injury can be performed indirectly by collection, modification and re-implantation of the patient's cells into the sites of injury (*ex vivo* approach) or by direct administration of therapeutic composition via open joint surgery (arthrotomy) (direct delivery) (Cucchiarini and Madry 2010; Evans and Huard 2015) (Fig. 2). Current clinical trials using *ex vivo* approaches for cartilage repair involve the injection of cells genetically modified with retroviral vectors to overexpress IL-1 receptor antagonist (IL-1Ra) for the treatment of patients with rheumatoid arthritis (Evans et al. 2005; Wehling et al. 2009) or TGF-β1 for osteoarthritis (Bendele et al. 1999). While

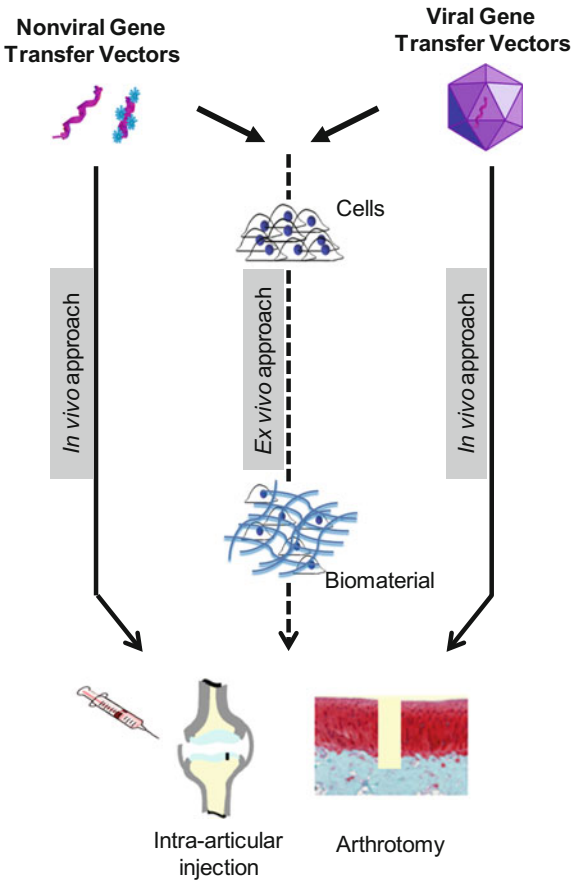

Fig. 2 Strategies for gene delivery to the articular cartilage. Delivery of candidate gene sequences into the sites of cartilage injury can be performed indirectly by collection, modification, and reimplantation of the patient's cells in sites of injury (*ex vivo* approach) or by direct administration of the therapeutic composition (*in vivo* delivery) via open joint surgery (arthrotomy) or intra-articularly inside the joint space

ex vivo delivery may constitute a safer approach compared with the direct delivery in the sense as cells instead of gene transfers vector are introduced in the sites of injury. Although, its use still remains a costly procedure, requiring complex and laborious steps of cell harvesting and expansion. Besides, direct administration of gene transfer vectors constitutes a simple and cost-effective approach compared with the *ex vivo* delivery. Direct delivery of rAAV vectors has been conducted to overexpress a transgene encoding for human tumor necrosis factor receptor-immunoglobulin Fc fusion protein (TNFR:Fc) which is equivalent to etanercept (an anti-TNF drug) for the treatment of rheumatoid arthritis (Frank et al. 2009; Mease et al. 2010).

3.1 Controlled Release of Gene Transfer Vectors: Principles

Despite of clear advantages from direct administration of gene transfer vectors for cartilage regeneration in terms of cost-effectiveness, their adapted use in patients may still be precluded by some hurdles associated to the carrier vector itself. For example, despite nonviral gene transfer is considered a safe method as it avoids the risk of acquiring replication competence and of insertional mutagenesis without inducing immune responses in the host, its use is limited by the low transfection efficiencies (40–50% maximum) and short-term transgene expression levels achieved (Goomer et al. 2000; Madry et al. 2005; Saraf and Mikos 2006). On the other hand viral gene transfer may be limited by a high immunogenicity of the viral vector (adenovirus) (Berns and Giraud 1995; Breyer et al. 2001) and the existence of patient-associated factors and of physiological barriers (pre-existence of neutralizing antibodies in the host against the viral capsid proteins, inhibition of transduction by particular anticoagulants) that may interfere in the achievement of an effective vector delivery, processing and expression of the transgene in the target cells (Summerford and Samulski 1998; Calcedo and Wilson 2013; Rey-Rico and Cucchiarini 2016a).

Administration of gene transfer vectors based on technologies exploited so far for the controlled delivery of pharmaceutical drugs and other recombinant molecules (Tiwari et al. 2012; Santo et al. 2013; Lam et al. 2015; Lorden et al. 2015) may be a powerful tool to address the issues associated to the use of these vectors in clinical settings. Considering this, controlled delivery systems based on the use of polymeric biomaterials have been conceived to improve the temporal and spatial presentation of therapeutic agents in a defined target as a mean to protect the cargo from physiological degradation improving patient compliance and enhancing quality control in the manufacturing products (Ekenseair et al. 2013; Lam et al. 2015). An effective controlled gene delivery system should enable to maintain

elevated concentrations of foreign sequences in the cellular microenvironment in order to achieve a durable expression of transgene with prolonged therapeutics effects of the transgene product while overcoming pre-exisiting barriers that may preclude its successful uptake and intracellular processing including the existence of neutralizing host immune responses (Han et al. 2000; Wang and Pham 2008; Gower and Shea 2013; Lee and Kim 2014; Chen et al. 2014; Lorden et al. 2015).

3.2 Biomaterials as Controlled Delivery Systems of Gene Transfer Vectors

Biomaterials play a pivotal role in tissue regeneration and medicine-assisted regenerative approaches. They can implement a space for tissue ingrowth, capable of mimicking the natural environment by providing a substrate for cell attachment, and also presents chemical, biological, and/or mechanical cues that can facilitate its integration with the host (De Laporte and Shea 2007; Gower and Shea 2013). Besides other applications, biomaterials have also been exploited as controlled release vehicles that can maintain therapeutic concentrations of diffusible tissue-inductive factors and eventually able to promote tissue regeneration.

Biomaterials may be engineered to control the release of gene transfer vectors either via encapsulation (vector loading during the fabrication of the scaffold) or immobilization (incorporation of the vector in a preformed scaffold) So far, these systems may led to a polymeric release (slow, gradient release of the vector both at immediate and distant vicinity of the system via degradation of the polymeric matrix where the vector was encapsulated) or a substrate-mediated delivery (delivery of the vector immobilized at the surface of the biomaterial being its release restricted to the immediate proximity of the system) (Fig. 3). Different polymeric systems have been exploited because they are exhibiting specific features for controlled delivery of gene transfer vector. Alongside hydrogel-based biomaterials show release patterns via diffusion and might be modulated to reduce vector spreading to nontarget places. Moreover, solid matrices provide a substrate-mediated delivery to circumvent mass transfer limitations. On the other hand use of microspheres for vector inclusion may afford shielding that reduces vector-directed immune responses. Another important parameter is origin of the polymer that involved in the delivery system. For example, natural polymers that have a high biocompatibility and biodegradability, while synthetic polymers exhibit a higher reproducibility (Han et al. 2000; Segura et al. 2003; Pannier and Shea 2004; Dang and Leong 2006; De Laporte and Shea 2007; Wang and Pham 2008; Gower and Shea 2013).

In the following sections the most advances strategies employed to exploit the use of biomaterials as controlled delivery systems for the different classes of gene transfer vectors in cartilage regeneration approaches are discussed.

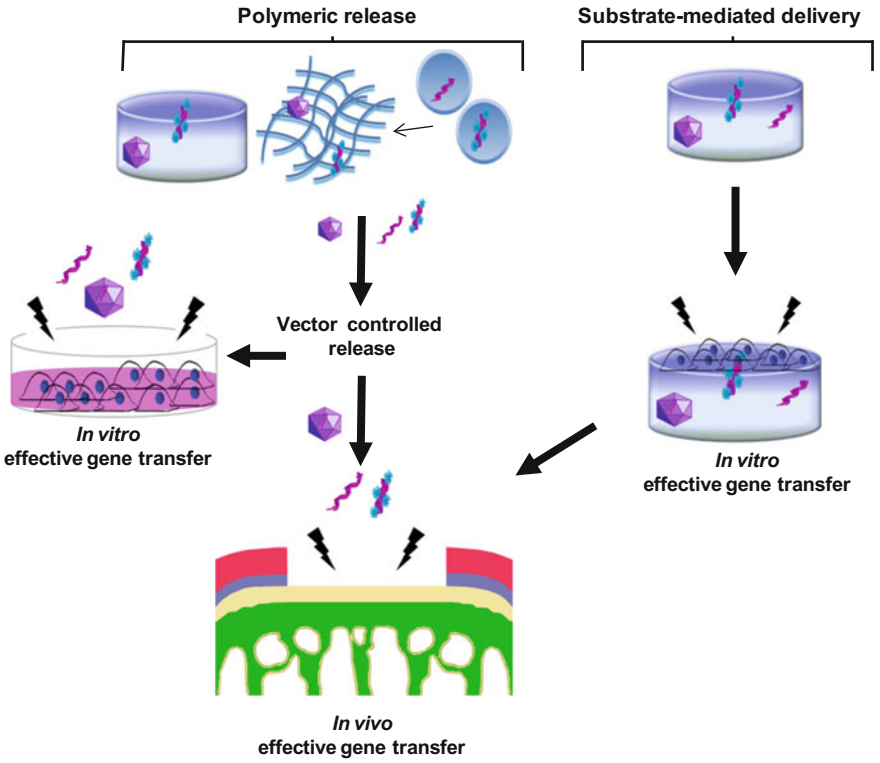

Fig. 3 Current strategies for the controlled delivery of gene transfer vectors in cartilage regeneration. Controlled release may be performed either by polymeric release or substrate-mediated delivery. Polymeric release is based on the incorporation of a vector in a biomaterial (hydrogel, solid matrix, microspheres), with controlled release profile generated by degradation of the polymer allowing for a prolonged expression of the therapeutic gene product in the target cell at the immediate and more distant vicinity of the system. Substrate-mediated delivery implicates the immobilization of the gene transfer vector on a surface that supports cell adhesion. As the vector can only infect cells from the material surface, gene transfer and expression of the therapeutic product is restricted to the immediate proximity of the substrate. Both approaches focus on the consecution of an effective gene transfer into the cartilage lesions

3.3 Controlled Release of Nonviral Vectors

Localized delivery of nonviral vectors has been performed using naked DNA (Walter et al. 2001; Eliaz and Szoka 2002; Diez and Tros de Ilarduya 2006; Rives et al. 2009; Aviles et al. 2010; Park et al. 2013) and DNA complexed in lipoplexes (Ramgopal et al. 2009; Kulkarni et al. 2011; Shepard et al. 2011) or polyplexes (Ramgopal et al. 2009; Lei et al. 2010; Gojgini et al. 2011; Tierney et al. 2012; Li et al. 2012; Tokatlian et al. 2012; Keeney et al. 2013; Needham et al. 2014; Zhang et al. 2014; Siegman et al. 2015) as a means to overcome the barriers of systemic

delivery (serum aggregation, clearance by the reticuloendothelial system) or to avoid vector degradation, facilitating its entrance in the cell (Pannier and Shea 2004). Controlled nonviral gene delivery has been studied using hydrogels (Eliaz and Szoka 2002; Lei et al. 2010, 2011; Kulkarni et al. 2011; Shepard et al. 2011; Gojgini et al. 2011; Li et al. 2012; Tokatlian et al. 2012; Park et al. 2013; Keeney et al. 2013; Needham et al. 2014; Zhang et al. 2014; Siegman et al. 2015), solid matrices (Ramgopal et al. 2009; Aviles et al. 2010; Tierney et al. 2012; He et al. 2012), and microspheres (Diez and Tros de Ilarduya 2006; Lei et al. 2011; Xu et al. 2016).

Local gene delivery via hydrogel scaffolds has been studied through the encapsulation of naked DNA during hydrogel formation (Eliaz and Szoka 2002; Park et al. 2013) using synthetic polymers such as poly(lactide-co-glycolide) (PLGA) (Eliaz and Szoka 2002) or poly(N-isopropylacrilamide) (pNIPAAm) (Park et al. 2013). Although naked DNA lead to the achievement of gene expression and guided repair *in vivo* (Bonadio et al. 1999), but its low gene transfer efficiency and rapid diffusion of the DNA from the hydrogel network urged to search for alternative gene delivery systems like those based on the controlled release of DNA complexed in lipoplexes or polyplexes (Tokatlian et al. 2012). Gene delivery via polyplexes (Lei et al. 2010; Gojgini et al. 2011; Li et al. 2012; Tokatlian et al. 2012; Siegman et al. 2015) or lipoplexes (Kulkarni et al. 2011; Shepard et al. 2011) has been studied by using different hydrogel systems including fibrin (Lei et al. 2010, 2011), hyaluronic acid (Lei et al. 2010; Gojgini et al. 2011; Tokatlian et al. 2012; Siegman et al. 2015), and polyethylene glycol (PEG) (Lei et al. 2010; Shepard et al. 2011; Li et al. 2012; Needham et al. 2014) to target different cell populations among which MSCs (Gojgini et al. 2011; Li et al. 2012; Tokatlian et al. 2012) in a variety of tissue engineering approaches (Tables 1 and 2).

Use of hydrogels as controlled gene delivery systems focused on cartilage repair is a very valuable but still a developing strategy. Osteochondral and chondral units are especially promising tissues for polymeric gene delivery approaches because of the limited blood flow to these regions which could cause problems in the delivery of DNA-polymer complex, and eventually it can affect the potential of the delivered genes to induce differentiation of infiltrated MSCs (Needham et al. 2014). Needham et al. (2014) recently described an innovative approach for delivering of DNA polyplexes using an oligo(poly(ethylene glycol) fumarate) (OPF) hydrogel scaffold to repair osteochondral injury. For that an OPF layered scaffold mimicking the native osteochondral tissue organization was simultaneously loaded with DNA polyplexes encoding for the RUNX2 and/or for the SOX trio to generate bone and cartilage tissues, respectively, in a rat osteochondral defect model. At 6 weeks of post-implantation, combination of RUNX2 and SOX trio DNA showed a significantly improved healing ability compared with empty hydrogels or each factor alone (Needham et al. 2014). Another interesting approach has recently been described by Gonzalez-Fernández et al. (2016). These authors produced gene-activated constructs by encapsulating MSCs and nanohydroxyapatite nanoparticles (nHA) complexed with plasmid (p) DNA (pDNA) encoding for transforming growth factor-beta 3 (pTGF-β3), bone morphogenetic protein 2

Table 1 Controlled release of nonviral vectors: part I: hydrogels and microspheres

Vector	Biomaterial	Subtype	System	Release profile	Efficacy	Targets	References
Naked DNA	Hydrogel	PLGA	Injectable implant	Sustained release for 2 months	Sustained expression, tolerance *in vivo*	CV1 cells, s.c. injection (mouse)	Eliaz and Szoka (2002)
		pNIPAAm	pNIPAAm-co-AAc nanogel	Not reported	Effective internalization	hMSCs, s.c. injection (mouse)	Park et al. (2013)
Lipoplexes		PEG	Hydrogel modified with affinity peptides	~59, 75, and 80% in K8, K4, and RDG hydrogels for 6 days	5–15-fold increased transfection with K8 and K4 hydrogels	HT1080 cells	Shepard et al. (2011)
		Fibrin	Microspheres in fibrin gel	100% release by 24 h from fibrin gels, slower release with microspheres	Enhanced angiogenesis	Ear ulcer model (rabbit)	Kulkarni et al. (2011)
Polyplexes		Alginate	nHA-pDNA	Not reported	Complexion of pDNA with hyaluronic acid led to nuclear transport	Higher chondrogenesis and reduced hypertrophy by co-delivery of pTGF-β3/pBMP2	Gonzalez-Fernandez et al. (2016)
		PEG	OPF porous scaffold	Not reported	Combination of RUNX2 and SOX trio DNA improved healing relative to empty hydrogels	Osteochondral defect (rat)	Needham et al. (2014)
				Not free diffusion of polyplexe in hydrogel	Reduced polyplexes aggregation, effective gene transfer	NIH 3T3 cells, chorionic chick embryo	Lei et al. (2010)
			Hydrogel with nanosized micelles	Not reported	Higher transfection efficiency in the presence of micelles	hMSCs	Li et al. (2012)
		Fibrin		<1% released at 3 days	Effective gene transfer	Chorionic chick embryo	Lei et al. (2011)

(continued)

Table 1 (continued)

Vector	Biomaterial	Subtype	System	Release profile	Efficacy	Targets	References
				Not free diffusion of polyplexes in hydrogel	Reduced polyplexes aggregation, effective gene transfer	NIH 3T3 cells, chorionic chick embryo	Lei et al. (2010)
		Hyaluronic acid	Porous hydrogel	Sustained release for 14 days in the presence of collagenase I treatment (<25% release)	Reduced aggregation of polyplexes	HEK293T cell	Siegman et al. (2015)
			Fibrin hydrogel	<1% released at 3 days	Effective gene transfer	Chorionic chick embryo	Lei et al. (2011)
			Microporous hydrogel	Controlled release for 10 days	Sustained transgene expression for up to 10 days	mMSCs	Tokatlian et al. (2012)
			MMP- degradable hydrogel	Stiffer hydrogels resulted in lower release rates in buffer, collagenase I and hyaluronidase	Higher N/P ratios lead to higher gene transfer efficiency but also higher toxicity	mMSCs	Gojgini et al. (2011)
				Not free diffusion of polyplexes in hydrogel	Reduced polyplexes aggregation, effective gene transfer	NIH 3T3 cells, chorionic chick embryo	Lei et al. (2010)
Naked DNA	Microspheres		PLGA	Faster release with low molecular weight or hydrophilic polymers	Transfection efficiency similar to control plasmid	HepG2	Diez and Tros de Ilarduya (2006)
Polyplexes			PELA	Controlled release for 42 days	Peak of BMP-2 secretion at day 2	MC3T3-E1	Xu et al. (2016)

PLGA poly(lactic/glycolic acid); *pNIPAAm* poly(N-isopropylacrylamide); *pNIPAAm-co-AAc* poly(N-isopropylacrylamide-co-acrylic acid); *PEG* polyethylene glycol; *nHA-pDNA* nanohydroxyapatite-plasmid DNA; *OPF* oligo(poly(ethylene glycol) fumarate); *MMP* matrix metalloproteinase; *PELA* polyethylene glycol-poly(D, L-lactide); *hMSCs* human mesenchymal stem cells; *mMSCs* mouse MSCs; *s.c.* subcutaneous

Table 2 Controlled release of nonviral vectors: part II: solid scaffolds

Vector	Subtype	System	Release profile	Efficacy	Targets	References
Naked DNA	PLG	Porous scaffold	High initial burst during the first 3 days, sustained release for 2 weeks	Peak of expression on the first days, decline at 1–2 weeks	i.p. injection (mouse)	Rives et al. (2009)
		Layered scaffolds from microsphere modified with cationic polymers	Low burst effect and sustained release for 2 weeks with polydopamine	Similar expression with or without polydopamine	HEK293T cells, i. p. injection (mouse)	Aviles et al. (2010)
Lipoplexes	PCL	Film	Slow release, increased with gelatin depending on its MW	Expression for 9 days at low MW, for 18 days at high MW	COS7 cells	Ramgopal et al. (2009)
Polyplexes			Burst at day 5 then lack of release	Not reported	COS7 cells	Ramgopal et al. (2009)
	PEG	Electrospun fibers	Sustained release for 4 weeks	Acceleration of healing	Skin wound (rat)	Yang et al. (2012)
				Peak of transfection at 7 days then decrease	HUVECs, s.c. injection (rat)	He et al. (2012)
	Collagen	Collagen-GAG, collagen-hydroxyapatite	Sustained release for 2 weeks	Prolonged expression with collagen-hydroxyapatite	MSCs	Tierney et al. (2012)
		Microspheres loaded in scaffold	Sustained release for 2 weeks (50% from microspheres, 65% from scaffolds)	Peak of expression at day 7	HUVECs, hMSCs	Alexander et al. (2013)

PLG poly(lactic/glycolic); *PCL* poly-ε-caprolactone; *PEG* polyethylene glycol; *MSCs* mesenchymal stem cells; *hMSCs* human MSCs; *i.p.* intraperitoneal; *s.c.* subcutaneous

(pBMP2), or a combination of both (pTGF-β3-pBMP2) into alginate hydrogels. Gene delivery of TGF-β3 and BMP2 and subsequent cell-mediated expression of these therapeutic genes resulted in a significant increase in sulfated glycosaminoglycan and collagen production, particularly in the pTGF-β3-pBMP2 co-delivery group in comparison to the delivery of either pTGF-β3 or pBMP2. In contrast, greater levels of calcium deposition were observed in pTGF-β3- and pBMP2-only groups compared with co-delivery group, with a high deposition and expression of type-X collagen, which is suggesting that these constructs were supporting MSC hypertrophy and progression along the endochondral pathway (Gonzalez-Fernandez et al. 2016).

Incorporation of DNA loaded microspheres into hydrogels is a valuable strategy to increase DNA loading capability of the hydrogel network while providing a controlled gene delivery. Kulkarni et al. loaded DNA polyplexes into fibrin microspheres and subsequently included them into fibrin hydrogels (Kulkarni et al. 2011). Their results showed differential degradation and DNA release profiles when polyplexes were encapsulated into microspheres compared with the direct loading into fibrin scaffolds.

Different biomaterials have been used for fabricating solid matrices as the delivery systems of nonviral gene transfer vectors, which are natural polymers like collagen (Tierney et al. 2012; Alexander et al. 2013), synthetic polyester copolymers like poly(lactide-co-glycolide) (PLG) (Rives et al. 2009; Aviles et al. 2010) and poly-ε-caprolactone (PCL) (Ramgopal et al. 2009), and also non-biodegradable polymers such as PEG (Yang et al. 2012).

Production of gene-activated matrices (GAMs) for tissue regeneration has been investigated by incorporation of DNA polyplexes into collagen, collagen-glycosaminoglycan and collagen-nHA scaffolds (Tierney et al. 2012). Transient expression profiles showed that the GAMs act as a polyplex depot system permitting the infiltration of MSCs throughout the scaffold and become transfected over a period of time. It was noticed that the levels of gene transfer reduced over a period of time (from days 3 to 14) for all types of scaffolds. However, collagen-nHA GAMs exhibited the highest and most sustained levels of transgene expression (Tierney et al. 2012).

3.4 Controlled Release of Classical Viral Vectors

While less explored, the controlled delivery of viral vectors has raised particular attention in the past years as a possible means to overcome the hurdles associated with their use in the *in vivo* conditions for immunogenic and toxic responses specially associated to the use of adenoviral vectors (Beer et al. 1998; Sailaja et al. 2002) and to afford protection against clearance by the host in different tissue engineering approaches (Beer et al. 1998; Matthews et al. 1999; Sailaja et al. 2002; Garcia del Barrio et al. 2004; Turner et al. 2007; Mok et al. 2007) (Tables 3 and 4).

Table 3 Controlled release of adenoviral vectors

Biomaterial	Subtype	System	Release profile	Efficacy	Targets	References
Hydrogel	Poloxamer 407	Thermosensitive hydrogel	Not reported	Increased transduction	Vascular smooth muscle cells, balloon-injured carotid arteries (rat), percutaneous injection in iliac arteries (rabbit), intratumoral injection (mouse)	Levy et al. (2001)
	Alginate	Hydrogel spheres	Sustained release for 7 days	High efficiency for 7 days	U343 cells	Park et al. (2012)
	Fibrin	Hydrogel	Slow release	Half-maximal activity at 45 h Bone formation at 4 weeks	Fibroblasts, i.m. injection (mouse)	Schek et al. (2004)
			Sustained release for 192 h	Enhanced bioactivity	Fibroblasts	Breen et al. (2006)
	Collagen	Ig G complexation in collagen gel	Controlled release	70% transduction at day 1 and further decrease	Rat aortic smooth muscle cells	Levy et al. (2001)
		Hydrogel			Fibroblasts	

(continued)

Table 3 (continued)

Biomaterial	Subtype	System	Release profile	Efficacy	Targets	References
			Slow release	Bioactivity decreased		Schek et al. (2004)
Microspheres/microparticles	PLGA	Microencapsulation of Ads	Release over 100 h	Increased transduction in the presence of Nabs	HeLa cells, s.c. injection (mouse)	Beer et al. (1998)
			Release for 8 days	Higher efficiency with PLL	9L, HeLa cells	Matthews et al. (1999)
			~100% at 10 days	Higher expression	HeLa, Raw 264.1 cells	Mok et al. (2007)
		Encapsulation in microparticles	Controlled release for 5 days	Expression for 7 weeks	Injection (mouse)	Garcia del Barrio et al. (2004)
	PLG	Microspheres	Peak of release at 2 days then decrease	Enhanced expression	HEK293T, A549 cells	Turner et al. (2007)
	Alginate	Microspheres	Not reported		Inoculation in immunized mouse	

(continued)

Table 3 (continued)

Biomaterial	Subtype	System	Release profile	Efficacy	Targets	References
				Reduced immune responses		Sailaja et al. (2002)
Solid scaffolds	PU	Collagen-coated scaffold	Controlled release	Efficient gene delivery *versus* free vector	Arterial smooth muscle cells	Mei et al. (2006)
	HA	Disks	70% released after 16 h	Bioactivity for 6 months	Fibroblasts	Hu et al. (2007)
	PCL	Electrospun fibrous scaffold	40% released at 14 days	High transduction	HEK293T cells	Liao et al. (2009)
	SF	Solid scaffolds	Controlled release for 21 days	Effective transduction, enhanced osteogenesis	MSCs, calvarial defects (mouse)	Zhang et al. (2011b)
	Bioglass-SF	Mesoporous scaffolds	Controlled release for 21 days	Increased MSC recruitment	MSCs, s.c. injection (mouse)	Zhang et al. (2013)
			Not reported	Enhanced osteogenesis	Periodontal cells	Zhang et al. (2015c)

PLGA poly(lactic/glycolic acid); *PLG* poly(lactic/glycolic); *PU* polyurethane; *PCL* poly-ε-caprolactone; *SF* silk fibroin; *MSCs* mesenchymal stem cells; *i.m* intramuscular; *s.c.* subcutaneous

Table 4 Controlled release of lenti-/retroviral vectors

Vector	Biomaterial	Subtype	System	Release profile	Efficacy	Targets	References
Retroviral	Solid scaffolds	SAMs	Substrate-mediated gene delivery	~85% transduction efficiency after 4 h	>90% on NH(2)-terminated surfaces	NIH3T3 cells	Gersbach et al. (2007)
Lentiviral	Hydrogel	Fibrin/HA	Hydrogel complexed with hydroxyapatite nanoparticles	Initial burst of release (40% at 4 h), controlled released for 6 days (75%)	Expression reduced in the presence of HA, decline between days 9 and 35	HEK293T cells, s.c. injection (mouse)	Kidd et al. (2012)
	Solid scaffold	PCL	3D woven scaffolds	Not reported	Decreased inflammation via IL-1Ra expression	MSCs	Glass et al. (2014)

SAMs self-assembled monolayers; *PCL* poly-ε-caprolactone; *3D* three-dimensional; *IL-1Ra* interleukin 1 receptor antagonist; *s.c.* subcutaneous; *MSCs* mesenchymal stem cells

Encapsulation of viral vectors into the microparticles has yielded effective and localized gene expression while preventing systemic vector spread compared with the free vector supply (Rejman et al. 2004; Jang et al. 2011). The encapsulation of viral vectors in microparticles provides a shielding to the viral vectors and thus reducing the immune responses directed against them (Beer et al. 1998; Sailaja et al. 2002). Use of synthetic biodegradable polymers such as PLG (Turner et al. 2007) and PLGA (Beer et al. 1998; Matthews et al. 1999; Mok et al. 2007) has increased the attention in the last years in order to produce microspheres for encapsulation of adenoviral vectors (Beer et al. 1998; Matthews et al. 1999; Sailaja et al. 2002; Garcia del Barrio et al. 2004; Turner et al. 2007; Mok et al. 2007). The release of the viral vector from these particles is governed by a combination of polymer degradation and subsequent diffusion from the particle. By tuning the polymer formulation, a modulation in the rate of hydrolysis may be achieved which resulting in a controlled degradation and release kinetics (Jang et al. 2011). Instead, this approach is still limited by the low efficiency of virus loading into the final particles (<25%), a broad distribution of the particle size, and a burst release of the adenoviral vectors at an initial stage (Sailaja et al. 2002; Turner et al. 2007; Wang et al. 2007). In order to overcome these limitations Park et al. encapsulated adenoviral vectors into alginate beads by using electrospraying technique for designing injectable systems to be delivered into the target sites (Sailaja et al. 2002). Their results showed that release of adenoviral vector containing the reporter gene encoding for green fluorescent protein (AdGFP) from alginate beads formed at 0.5 wt% alginate concentration exhibited a superior GFP activity of U343 glioma cells over 7 days compared with beads formed at other alginate concentrations, although this efficiency was lower than that achieved by free adenoviral vector (Sailaja et al. 2002).

Entrapment of viral vectors into hydrogels is an advantageous approach to reduce the spread of the recombinant material in nontarget places and provide a contained and sustained supply of the therapeutic gene only where it required (Rey-Rico et al. 2015c). The release profile of the vector from the hydrogel will be mainly conditioned by the porosity of hydrogel and interactions of viral vector to the hydrophylic polymer network (Gower and Shea 2013). Different hydrogel systems from both natural (Levy et al. 2001; Schek et al. 2004; Breen et al. 2006; Kidd et al. 2012; Park et al. 2012) or synthetic origin (Levy et al. 2001) has been exploited for controlled release of adenoviral or lentiviral vectors (Kidd et al. 2012).

Scaffold-mediated delivery of viral vectors have also been reported using different porous 3D matrices to genetically modify different cell types seeded on these materials (Mei et al. 2006; Hu et al. 2007; Gersbach et al. 2007; Liao et al. 2009; Zhang et al. 2012, 2015c; Glass et al. 2014). The supply of vector-presenting substrates to the cells or tissues can place the cells and vector in close proximity during delivery and may thereby function to overcome mass transfer limitations and thus enhance the delivery efficiency (Jang et al. 2011). Glass et al. immobilized lentiviral vectors onto PCL woven scaffolds to induce the over expression of IL-1Ra in MSCs for developing engineered cartilage constructs with immunomodulatory properties (Glass et al. 2014). In the presence of IL-1, IL-1Ra-expressing engineered cartilage

produced cartilage-specific ECM while resisting IL-1-induced upregulation of MMPs and maintained mechanical properties similar to native articular cartilage.

An advanced approach to retain viral gene transfer vectors into scaffold for a long period of time is the lyophilization (Croyle et al. 2001). Hu et al. lyophilized adenovirus expressing a β-galactosidase reporter gene (AdLacZ) on hydroxyapatite disks and observed a maintenance of their bioactivity for 6 months when stored at −80 °C (Hu et al. 2007). Instead, a high burst effect in the release of adenovirus from hydroxyapatite disks was observed during the first hour with ∼60% of virus released after this time. In the same study the authors lyophilized an adenovirus encoding BMP-2 (AdBMP-2) in gelatin sponges and placed them into rat critical-size calvarial defects for 5 weeks. Their results showed that while the free-form delivery of AdBMP-2 had only modest effects on bone formation, AdBMP-2 lyophilized in gelatin sponges led to more than 80% regeneration of critical-size calvarial defects (Hu et al. 2007).

Zhang et al. (2013) loaded adenoviruses coding for the platelet-derived growth factor subunit B (PDGF-B) (AdPDGF-B) into bioglass-silk fibrin scaffolds for evaluating their ability to restore damaged tissue through the recruitment of MSCs. A controlled release profile of PDGF-B was observed up to 3 weeks with an increased MSCs recruitment in the in vitro conditions and also in the in vivo conditions by subcutaneous implantation in mice model. In another study, the same authors tested the ability of AdBMP-7 and/or AdPDGF-B incorporated in similar scaffolds for promoting the regeneration of periodontal defects in dogs (Zhang et al. 2015c). The data showed that scaffolds loaded with AdPDGF-B were capable of partially regenerating the periodontal ligament while AdBMP7 scaffolds primarily improved new bone formation. Thus, the combination of both AdPDGF-B and AdBMP-7 synergistically promoted periodontal regeneration (Zhang et al. 2015c).

3.5 Controlled Release of rAAV Vectors

Despite of increasing number of studies reporting the efficiency of rAAV vector as one of the most adapted gene transfer systems in musculoskeletal translational research (Hu et al. 2007; Rey-Rico and Cucchiarini 2016a, b), these vectors are also capable of targeting most of the relevant cells like hMSCs (Pagnotto et al. 2007; Stender et al. 2007; Cucchiarini et al. 2011; Venkatesan et al. 2012), chondrocytes (Madry et al. 2003; Ulrich-Vinther et al. 2004, 2005; Watson et al. 2013; Venkatesan et al. 2013; Cucchiarini and Madry 2014), and osteoblasts (Yang et al. 2005; Dey et al. 2014). However, there are still some limitations that may preclude their adapted in vivo use. For instance, a rapid dispersion of viral particles from the joint space may prevent effective transduction of repair cells that are recruited to the defect site over time (Lee et al. 2011a). Additionally, a nonspecific transduction adjacent to the target place may also occur (Jang et al. 2004). On the other hand, an effective rAAV transduction might be affected by the presence of neutralizing antibodies directed against the viral capsid proteins which commonly present for

instance in the synovial fluid of the patients having joint diseases (considerably a large part of the human population affected) (Chirmule et al. 1999; Cottard et al. 2004; Calcedo and Wilson 2013). The other possible inhibition of viral uptake could be mediated by clinical compounds such as heparin (Summerford and Samulski 1998). In order to overcome these issues, different scaffolds have been tested in diverse *in vitro* studies to develop rAAV controlled delivery systems which are able to target and efficiently transduce key cell populations involved in cartilage regeneration, such as hMSCs (Lee et al. 2011a; Dupont et al. 2012; Schmidt et al. 2014; Rey-Rico et al. 2015b, c; Diaz-Rodriguez et al. 2015) (Table 5). Lee et al. reported the use of fibrin glue (FG) hydrogels to release rAAV vectors encoding for TGF-β1 (rAAV-TGF-β1) to target hMSCs (Lee et al. 2011a). They observed the release of rAAV-TGF-β1 from diluted FG hydrogels was higher in concentration resulted in greater upregulation of cartilage-specific gene expression in hMSCs in comparison to the release behavior of undiluted FG hydrogel. This was attributing due to the presence of more open network structure in diluted FG hydrogels in comparison with undiluted hydrogels suggesting that the open polymeric structures plays a vital role for efficient release of rAAV TGF-β vectors. In a recent study, FG-polyurethane (PU) hybrid scaffolds were prepared by polymerization of FG (containing rAAV-encoding for β-galactosidase) in porous PU discs which were further implanted subcutaneously in rats (Schmidt et al. 2014). In contrast to the study performed by Lee et al, these authors of this study observed significantly higher levels of β-galactosidase activity after the release of rAAV-*lacZ* from hydrogels that contains higher concentrations of FG.

Self-assembling peptides RAD16-I containing the arginine-alanine-aspartic acid (RAD) motif in a pure form or combined with hyaluronic acid have also been examined for the release of rAAV vectors to genetically modify hMSCs (Rey-Rico et al. 2015c). These peptides can form stable hydrogels and encapsulate viable cells upon exposure to physiological pH and ionic strength (Zhang et al. 1993; Capito et al. 2008; Semino 2008). Their ideal biocompatibility like lack of immunogenicity, thrombogenicity, inflammatory responses and production under mild conditions make them promising candidates for various tissue engineering approaches (Johnstone et al. 2013). Such systems showed high efficiency of encapsulating and releasing of rAAV in a sustained and controlled manner for effective transduction (up to 80%) without deleterious effects on cell viability (up to 100%) or on their potential for chondrogenic differentiation monitored over the period of 21 days (Rey-Rico et al. 2015c).

Poly(ethylene oxide) (PEO)- and poly(propylene oxide) (PPO)-based "smart" or "intelligent" self-assembling, temperature-sensitive copolymers have also been utilized as efficient rAAV-mediated delivery systems due to their capacity to form polymeric micelles and to undergo sol-to-gel transition upon heating (Alvarez-Lorenzo et al. 2010, 2011). Specifically, encapsulation of rAAV vectors in poloxamer PF68 and poloxamine T908 polymeric micelles allowed for an effective, durable, and safe modification of hMSCs via rAAV to levels similar or even higher than the approach of direct vector application (up to 95% of gene transfer efficiency) (Rey-Rico et al. 2015b) (Fig. 4). Of further note, these copolymers were

Table 5 Controlled release of rAAV vectors

Biomaterial	Subtype	System	Release profile	Efficacy	Targets	References
Hydrogel	Alginate	Alginate/poloxamer composite systems crosslinked at room temperature (AlgPH155 + PF127 [C]) or high temperature (AlgPH155 + PF127 [H])	AlgPH155 + PF127 [C]) leaded to a most controlled release profile	Higher transduction efficiency with AlgPH155 + PF127 [H]	hMSCs	Diaz-Rodriguez et al. (2015)
	FG	Hydrogel	Biphasic, higher release at low fibrin concentration, (100% released at 2 weeks)	High efficiency at low FG concentration, decline after 8 days	hMSCs	Lee et al. (2011a)
		Fibrin/PU hybrid scaffold	High initial burst, maximal vector retention at high FG (37% *versus* 68% released with 50 and 25 mg/ml fibrin after 4 days)	High transduction at high fibrin concentration	s.c. injection (rat)	Schmidt et al. (2014)
	RAD16-I	Self-assembling peptide hydrogel pure or combined with HA	Faster release at high peptide concentration (0.4%), complete release at 6–10 days except for spheres at 0.4% with 90% of release only after 21 days	80% transduction efficiency with spheres at 0.4%, time-course decline of expression	hMSCs	(Rey-Rico et al. 2015c)
Micro-/ nanoparticles	Polystyrene, magnetite	Microspheres	Not reported	Transduction efficiency similar to free virus injection	C12S cells, systemic injection (mouse)	Mah et al. (2002)
	HpNPs	Nanoparticles	Magnetically-guided delivery	Short (3 h) magnetic field exposure leading to transduction similar to free vector application at 24 h	HEK293T, PC12 cells	Hwang et al. (2011)

(continued)

Table 5 (continued)

Biomaterial	Subtype	System	Release profile	Efficacy	Targets	References
Micelles	Poloxamer F68, poloxamine 908	Micellar systems	Not reported	Enhanced expression, restoration in conditions of gene transfer inhibition	hMSCs	Rey-Rico et al. (2015b)
Solid scaffolds	PCL	Porous scaffold	Not reported	Peak of BMP-2 expression after 1 week in hMSCs, at 7 weeks in human amniotic fluid-derived stem cells	hMSCs, human amniotic fluid-derived stem cells, femoral defects (rat)	Dupont et al. (2012)
		Electrospun scaffolds of ELP-PCL	60% released by day 2 and sustained release for 1 week	>80% transduction efficiency	NIH-3T3 fibroblasts	Lee et al. (2011b)
	PLGA, gelatin	Scaffold/sponge	Not reported	Enhanced expression	HeLa cells s.c. injection (mice)	Li et al. (2015)

FG fibrin glue; *PU* polyurethane; *RAD-16-I*: self-assembling peptide with (RADA)4 sequence; *HpNPs* heparin/superparamagnetic iron oxide; *PCL* poly-ε-caprolactone; *ELP* elastin-like polypeptides; *PLGA* poly(lactic/glycolic acid); *hMSCs* human mesenchymal stem cells; *s.c.* subcutaneous

capable of restoring gene transfer in hMSCs when applying rAAV-specific inhibitors like heparin or rAAV capsid antibody, allowing for instance to deliver a chondrogenic *sox9* sequence for enhanced chondrogenic differentiation. Furthermore, various hydrogel composite structures based on alginate (AlgPH155) and poloxamer PF127 have also been prepared by crosslinking at either high temperature (50 °C; AlgPH155 + PF127 [H]) or room temperature (23 °C) (AlgPH155 + PF127 [C]) for successive encapsulation and release of rAAV vectors (Diaz-Rodriguez et al. 2015). Strikingly, hydrogels based on AlgPH155 alone showed high initial burst release of rAAV while it crosslinked form i.e. AlgPH155 + PF127 [C] showed sustained release pattern of rAAV, which leads to high transduction efficiencies in hMSCs (∼80%) over an extended period of evaluation (up to 21 days).

Scaffold-mediated delivery of rAAV vectors has been tested using PCL-based scaffolds for evaluating the ability of the constructs to transduce fibroblasts seeded on the top of them in the *in vitro* condition (Lee et al. 2011b) and to promote endogenous bone reparation of femoral defects in rats in the *in vivo* condition using self-complementary AAV scAAV2.5-BMP2-coated scaffolds preseeded with MSCs (Dupont et al. 2012). Interestingly, Dupont et al. observed a higher bone ingrowth and enhanced mechanical properties of defects treated with acellular scAAV2.5-BMP2-coated scaffolds relative to defects treated with scAAV2.5-BMP2 scaffolds preseeded with MSCs that failed to display significant differences relative to control conditions (Dupont et al. 2012).

4 Conclusions

Adapting controlled delivery strategies for the delivery of therapeutic genes is an attractive approach to bypass the natural obstacles for an efficient and stable gene expression in an individual host. A multiplicity of systems (hydrogels, solid matrices, microspheres…) of both natural and synthetic origin have been exploited to control the delivery of gene transfer vectors in different regenerative medicine approaches, with a more limited number of studies focused on cartilage regeneration.

When designing a gene delivery system for cartilage regeneration, it is very is important to consider that a favourable system in vitro may not generate similar/sufficient or adapted effects in a native in vivo environment. It will thus be fundamental to test the adaptability of the systems in sites of tissue damage using clinically relevant, complex orthotopic animal models of cartilage defect as a means to enhance the natural repair processes. Another important parameter to keep in mind in manufacturing the system itself is the pharmacokinetic release profile of the vector from the biomaterial, as the initial rate of vector delivery may significantly impact the extent of transgene expression. The strength of the interaction between the biomaterial and the gene transfer vector should also be optimized to adjust the rate of vector retention without preventing its release while allowing for an effective vector internalization in its target (Seidlits et al. 2013; Gower and Shea 2013;

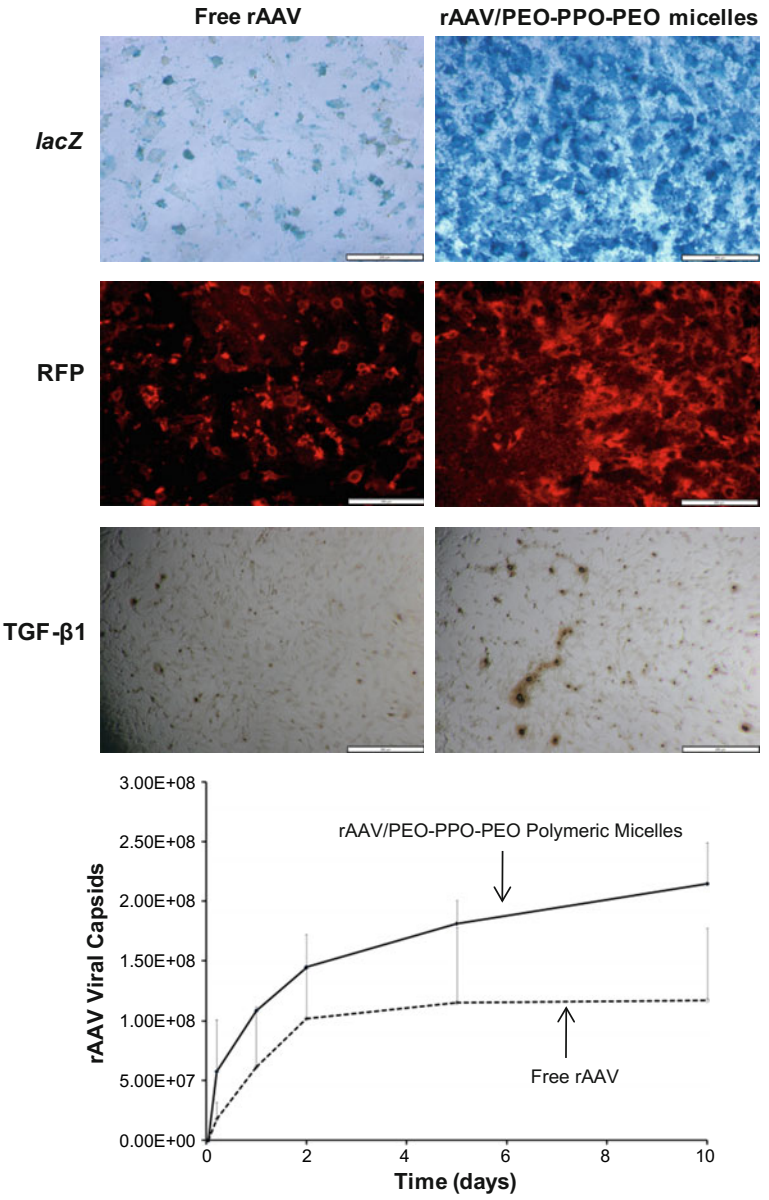

Fig. 4 rAAV-mediated transduction of MSC (*lacZ* and RFP) and chondrocytes (hTGF-β1) via PEO-PPO-PEO polymeric micelles. Detection of the transgenes was performed by X-Gal staining *(LacZ)*, live fluorescence (RFP) and immunohistochemistry (TGF-β) (all representative data at day 3 post-transduction; magnification 10x; scale bar: 200 μm). Higher levels of transgene expression (lacZ, RFP, TGF-β) were noted when rAAV was delivered via polymeric micelles as compared with free vector treatment. Amounts of rAAV-*lacZ* diffused into the culture medium were quantified by AAV Titration ELISA. Delivery of rAAV via polymeric micelles increased the number of rAAV viral capsids detected in culture media over-time when compared with free vector condition

Rey-Rico and Cucchiarini 2016a). Also, the duration of therapeutic gene expression needs to comply with the specific requirements of the cartilage tissue and adapted to the evolution of disorder to be treated (focal cartilage defect *versus* generalized osteoarthritis). Hence, a counterbalance between the rate of vector delivered and the profiles/course of transgene expression will have to be accomplished, as a short-term expression may be ineffective while a very prolonged expression may inhibit further needed steps for regeneration (Gower and Shea 2013). So far, the nature of the biomaterial involved as gene delivery system will also be conditioned by the characteristics and spread from the barriers (pharmacological, physiological, immune, toxic) directed against each particular class gene vector (nonviral *versus* viral vehicle). Lastly, even though by optimization of a new or an already clinically tested material for cartilage regeneration (Andereya et al. 2006; Kon et al. 2014), the identification and production of a new functional gene delivery system derived from it will have to receive approbation from regulatory agencies to satisfy additional important specifications (ease of fabrication, scalability, sterilization, long-term storage, cost-effectiveness), a long and laborious procedure (Cucchiarini et al. 2014).

Yet, despite these remaining challenges, recent advances in the use of biomaterials as controlled gene delivery systems of cartilage reparative factors is a promising, new avenue of research that may clearly improve cartilage repair in patients in a close future.

Acknowledgements This work was supported by a grant from *Deutsche Forschungsgemeinschaft* (DFG RE 328/2-1 to ARR and MC).

References

Alexander JC, Browne S, Pandit A, Rochev Y (2013) Biomaterial constructs for delivery of multiple therapeutic genes: a spatiotemporal evaluation of efficacy using molecular beacons. PLoS ONE 8(6):e65749–e65758

Alvarez-Lorenzo C, Rey-Rico A, Sosnik A, Taboada P, Concheiro A (2010) Poloxamine-based nanomaterials for drug delivery. Front Biosci (Elite Ed) 2:424–440

Alvarez-Lorenzo C, Sosnik A, Concheiro A (2011) PEO-PPO block copolymers for passive micellar targeting and overcoming multidrug resistance in cancer therapy. Curr Drug Targets 12(8):1112–1130

Andereya S, Maus U, Gavenis K, Muller-Rath R, Miltner O, Mumme T, Schneider U (2006) First clinical experiences with a novel 3D-collagen gel (CaReS) for the treatment of focal cartilage defects in the knee. Z Orthop Ihre Grenzgeb 144(3):272–280

Arai Y, Kubo T, Fushiki S, Mazda O, Nakai H, Iwaki Y, Imanishi J, Hirasawa Y (2000) Gene delivery to human chondrocytes by an adeno-associated virus vector. J Rheumatol 27(4): 979–982

Asahina I, Sampath TK, Hauschka PV (1996) Human osteogenic protein-1 induces chondroblastic, osteoblastic, and/or adipocytic differentiation of clonal murine target cells. Exp Cell Res 222(1):38–47

Aviles MO, Lin CH, Zelivyanskaya M, Graham JG, Boehler RM, Messersmith PB, Shea LD (2010) The contribution of plasmid design and release to in vivo gene expression following delivery from cationic polymer modified scaffolds. Biomaterials 31(6):1140–1147

Bao L, Zhu T, Zhao D, Han X, Guan J, Shi Z, Zhang L (2012) Adeno-associated virus-mediated osteoprotegerin gene transfer protects against joint destruction in a collagen-induced arthritis rat model. Joint Bone Spine 79(5):482–487

Beer SJ, Matthews CB, Stein CS, Ross BD, Hilfinger JM, Davidson BL (1998) Poly (lactic-glycolic) acid copolymer encapsulation of recombinant adenovirus reduces immunogenicity in vivo. Gene Ther 5(6):740–746

Bendele A, McAbee T, Sennello G, Frazier J, Chlipala E, McCabe D (1999) Efficacy of sustained blood levels of interleukin-1 receptor antagonist in animal models of arthritis: comparison of efficacy in animal models with human clinical data. Arthritis Rheum 42(3):498–506

Bentley G, Biant LC, Carrington RW, Akmal M, Goldberg A, Williams AM, Skinner JA, Pringle J (2003) A prospective, randomised comparison of autologous chondrocyte implantation versus mosaicplasty for osteochondral defects in the knee. J Bone Joint Surg Br 85(2):223–230

Berns KI, Giraud C (1995) Adenovirus and adeno-associated virus as vectors for gene therapy. Ann N Y Acad Sci 772:95–104

Bonadio J, Smiley E, Patil P, Goldstein S (1999) Localized, direct plasmid gene delivery in vivo: prolonged therapy results in reproducible tissue regeneration. Nat Med 5(7):753–759

Breen A, Strappe P, Kumar A, O'Brien T, Pandit A (2006) Optimization of a fibrin scaffold for sustained release of an adenoviral gene vector. J Biomed Mater Res A 78(4):702–708

Breyer B, Jiang W, Cheng H, Zhou L, Paul R, Feng T, He TC (2001) Adenoviral vector-mediated gene transfer for human gene therapy. Curr Gene Ther 1(2):149–162

Brittberg M, Lindahl A, Nilsson A, Ohlsson C, Isaksson O, Peterson L (1994) Treatment of deep cartilage defects in the knee with autologous chondrocyte transplantation. N Engl J Med 331(14):889–895

Calcedo R, Wilson JM (2013) Humoral immune response to AAV. Front Immunol 4:341–347

Capito RM, Azevedo HS, Velichko YS, Mata A, Stupp SI (2008) Self-assembly of large and small molecules into hierarchically ordered sacs and membranes. Science 319(5871):1812–1816

Cottard V, Valvason C, Falgarone G, Lutomski D, Boissier MC, Bessis N (2004) Immune response against gene therapy vectors: influence of synovial fluid on adeno-associated virus mediated gene transfer to chondrocytes. J Clin Immunol 24(2):162–169

Croyle MA, Cheng X, Wilson JM (2001) Development of formulations that enhance physical stability of viral vectors for gene therapy. Gene Ther 8(17):1281–1290

Cucchiarini M, Madry H (2005) Gene therapy for cartilage defects. J Gene Med 7(12):1495–1509

Cucchiarini M, Madry H (2010) Genetic modification of mesenchymal stem cells for cartilage repair. Biomed Mater Eng 20(3):135–143

Cucchiarini M, Madry H (2014) Overexpression of human IGF-I via direct rAAV-mediated gene transfer improves the early repair of articular cartilage defects in vivo. Gene Ther 21(9):811–819

Cucchiarini M, Ekici M, Schetting S, Kohn D, Madry H (2011) Metabolic activities and chondrogenic differentiation of human mesenchymal stem cells following recombinant adeno-associated virus-mediated gene transfer and overexpression of fibroblast growth factor 2. Tissue Eng Part A 17(15–16):1921–1933

Cucchiarini M, Venkatesan JK, Ekici M, Schmitt G, Madry H (2012) Human mesenchymal stem cells overexpressing therapeutic genes: from basic science to clinical applications for articular cartilage repair. Biomed Mater Eng 22(4):197–208

Cucchiarini M, Orth P, Madry H (2013) Direct rAAV SOX9 administration for durable articular cartilage repair with delayed terminal differentiation and hypertrophy in vivo. J Mol Med (Berl) 91(5):625–636

Cucchiarini M, Madry H, Guilak F, Saris DB, Stoddart MJ, Koon Wong M, Roughley P (2014) A vision on the future of articular cartilage repair. Eur Cell Mater 27:12–16

Cucchiarini M, Henrionnet C, Mainard D, Pinzano A, Madry H (2015) New trends in articular cartilage repair. J Exp Orthop 2(1):8–15

Chang LJ, Gay EE (2001) The molecular genetics of lentiviral vectors–current and future perspectives. Curr Gene Ther 1(3):237–251

Chen W, Meng F, Cheng R, Deng C, Feijen J, Zhong Z (2014) Advanced drug and gene delivery systems based on functional biodegradable polycarbonates and copolymers. J Control Release 190:398–414

Chirmule N, Propert K, Magosin S, Qian Y, Qian R, Wilson J (1999) Immune responses to adenovirus and adeno-associated virus in humans. Gene Ther 6(9):1574–1583

Dang JM, Leong KW (2006) Natural polymers for gene delivery and tissue engineering. Adv Drug Deliv Rev 58(4):487–499

Daya S, Berns KI (2008) Gene therapy using adeno-associated virus vectors. Clin Microbiol Rev 21(4):583–593

De Bari C, Dell'Accio F, Tylzanowski P, Luyten FP (2001) Multipotent mesenchymal stem cells from adult human synovial membrane. Arthritis Rheum 44(8):1928–1942

De Laporte L, Shea LD (2007) Matrices and scaffolds for DNA delivery in tissue engineering. Adv Drug Deliv Rev 59(4–5):292–307

Dey S, Laredj L, Damjanovic K, Muller M, Beard P (2014) Growth of osteosarcoma cells in a three-dimensional bone-like matrix alters their susceptibility to adeno-associated virus. J Gen Virol 95(Pt 7):1539–1543

Diaz-Rodriguez P, Rey-Rico A, Madry H, Landin M, Cucchiarini M (2015) Effective genetic modification and differentiation of hMSCs upon controlled release of rAAV vectors using alginate/poloxamer composite systems. Int J Pharm 496(2):614–626

Diez S, Tros de Ilarduya C (2006) Versatility of biodegradable poly(D, L-lactic-co-glycolic acid) microspheres for plasmid DNA delivery. Eur J Pharm Biopharm 63(2):188–197

Dounchis JS, Goomer RS, Harwood FL, Khatod M, Coutts RD, Amiel D (1997) Chondrogenic phenotype of perichondrium-derived chondroprogenitor cells is influenced by transforming growth factor-beta 1. J Orthop Res 15(6):803–807

Dupont KM, Boerckel JD, Stevens HY, Diab T, Kolambkar YM, Takahata M, Schwarz EM, Guldberg RE (2012) Synthetic scaffold coating with adeno-associated virus encoding BMP2 to promote endogenous bone repair. Cell Tissue Res 347(3):575–588

Ekenseair AK, Kasper FK, Mikos AG (2013) Perspectives on the interface of drug delivery and tissue engineering. Adv Drug Deliv Rev 65(1):89–92

Eliaz RE, Szoka FC Jr (2002) Robust and prolonged gene expression from injectable polymeric implants. Gene Ther 9(18):1230–1237

Elmallah RK, Cherian JJ, Jauregui JJ, Pierce TP, Beaver WB, Mont MA (2015) Genetically modified chondrocytes expressing TGF-beta1: a revolutionary treatment for articular cartilage damage? Expert Opin Biol Ther 15(3):455–464

Erlacher L, Ng CK, Ullrich R, Krieger S, Luyten FP (1998) Presence of cartilage-derived morphogenetic proteins in articular cartilage and enhancement of matrix replacement in vitro. Arthritis Rheum 41(2):263–273

Evans CH, Huard J (2015) Gene therapy approaches to regenerating the musculoskeletal system. Nat Rev Rheumatol 11(4):234–242

Evans CH, Robbins PD, Ghivizzani SC, Herndon JH, Kang R, Bahnson AB, Barranger JA, Elders EM, Gay S, Tomaino MM, Wasko MC, Watkins SC, Whiteside TL, Glorioso JC, Lotze MT, Wright TM (1996) Clinical trial to assess the safety, feasibility, and efficacy of transferring a potentially anti-arthritic cytokine gene to human joints with rheumatoid arthritis. Hum Gene Ther 7(10):1261–1280

Evans CH, Robbins PD, Ghivizzani SC, Wasko MC, Tomaino MM, Kang R, Muzzonigro TA, Vogt M, Elder EM, Whiteside TL, Watkins SC, Herndon JH (2005) Gene transfer to human joints: progress toward a gene therapy of arthritis. Proc Natl Acad Sci U S A 102(24): 8698–8703

Evans CH, Ghivizzani SC, Robbins PD (2013) Arthritis gene therapy and its tortuous path into the clinic. Transl Res 161(4):205–216

Frank KM, Hogarth DK, Miller JL, Mandal S, Mease PJ, Samulski RJ, Weisgerber GA, Hart J (2009) Investigation of the cause of death in a gene-therapy trial. N Engl J Med 361(2): 161–169

Frisch J, Venkatesan JK, Rey-Rico A, Schmitt G, Madry H, Cucchiarini M (2014a) Determination of the chondrogenic differentiation processes in human bone marrow-derived mesenchymal stem cells genetically modified to overexpress transforming growth factor-beta via recombinant adeno-associated viral vectors. Hum Gene Ther 25(12):1050–1060

Frisch J, Venkatesan JK, Rey-Rico A, Schmitt G, Madry H, Cucchiarini M (2014b) Influence of insulin-like growth factor I overexpression via recombinant adeno-associated vector gene transfer upon the biological activities and differentiation potential of human bone marrow-derived mesenchymal stem cells. Stem Cell Res Ther 5(4):103–114

Frisch J, Rey-Rico A, Venkatesan JK, Schmitt G, Madry H, Cucchiarini M (2015) Chondrogenic differentiation processes in human bone marrow aspirates upon rAAV-mediated gene transfer and overexpression of the insulin-like growth factor I. Tissue Eng Part A 21(17–18): 2460–2471

Frisch J, Rey-Rico A, Venkatesan JK, Schmitt G, Madry H, Cucchiarini M (2016a) rAAV-mediated overexpression of sox9, TGF-beta and IGF-I in minipig bone marrow aspirates to enhance the chondrogenic processes for cartilage repair. Gene Ther 23(3):247–255

Frisch J, Rey-Rico A, Venkatesan JK, Schmitt G, Madry H, Cucchiarini M (2016b) TGF-beta gene transfer and overexpression via rAAV vectors stimulates chondrogenic events in human bone marrow aspirates. J Cell Mol Med 20(3):430–440

Garcia del Barrio G, Hendry J, Renedo MJ, Irache JM, Novo FJ (2004) In vivo sustained release of adenoviral vectors from poly(D, L-lactic-co-glycolic) acid microparticles prepared by TROMS. J Control Release 94(1):229–235

Garza-Veloz I, Romero-Diaz VJ, Martinez-Fierro ML, Marino-Martinez IA, Gonzalez-Rodriguez M, Martinez-Rodriguez HG, Espinoza-Juarez MA, Bernal-Garza DA, Ortiz-Lopez R, Rojas-Martinez A (2013) Analyses of chondrogenic induction of adipose mesenchymal stem cells by combined co-stimulation mediated by adenoviral gene transfer. Arthritis Res Ther 15(4):R80–R92

Gelse K, Muhle C, Knaup K, Swoboda B, Wiesener M, Hennig F, Olk A, Schneider H (2008) Chondrogenic differentiation of growth factor-stimulated precursor cells in cartilage repair tissue is associated with increased HIF-1alpha activity. Osteoarthritis Cartilage 16(12):1457–1465

Gelse K, von der Mark K, Aigner T, Park J, Schneider H (2003) Articular cartilage repair by gene therapy using growth factor-producing mesenchymal cells. Arthritis Rheum 48(2):430–441

Gersbach CA, Coyer SR, Le Doux JM, Garcia AJ (2007) Biomaterial-mediated retroviral gene transfer using self-assembled monolayers. Biomaterials 28(34):5121–5127

Glass KA, Link JM, Brunger JM, Moutos FT, Gersbach CA, Guilak F (2014) Tissue-engineered cartilage with inducible and tunable immunomodulatory properties. Biomaterials 35(22):5921–5931

Gojgini S, Tokatlian T, Segura T (2011) Utilizing cell-matrix interactions to modulate gene transfer to stem cells inside hyaluronic acid hydrogels. Mol Pharm 8(5):1582–1591

Goldring MB, Fukuo K, Birkhead JR, Dudek E, Sandell LJ (1994) Transcriptional suppression by interleukin-1 and interferon-gamma of type II collagen gene expression in human chondrocytes. J Cell Biochem 54(1):85–99

Goldring MB, Goldring SR (2007) Osteoarthritis. J Cell Physiol 213(3):626–634

Gonzalez-Fernandez T, Tierney EG, Cunniffe GM, O'Brien FJ, Kelly DJ (2016) Gene delivery of TGF-beta3 and BMP2 in an MSC-laden alginate hydrogel for articular cartilage and endochondral bone tissue engineering. Tissue Eng Part A 22(9–10):776–787

Goomer RS, Maris TM, Gelberman R, Boyer M, Silva M, Amiel D (2000) Nonviral in vivo gene therapy for tissue engineering of articular cartilage and tendon repair. Clin Orthop Relat Res (379 Suppl):S189–S200

Gouze E, Pawliuk R, Gouze JN, Pilapil C, Fleet C, Palmer GD, Evans CH, Leboulch P, Ghivizzani SC (2003) Lentiviral-mediated gene delivery to synovium: potent intra-articular expression with amplification by inflammation. Mol Ther 7(4):460–466

Gower RM, Shea LD (2013) Biomaterial scaffolds for controlled, localized gene delivery of regenerative factors. Adv Wound Care (New Rochelle) 2(3):100–106

Grande DA, Mason J, Light E, Dines D (2003) Stem cells as platforms for delivery of genes to enhance cartilage repair. J Bone Joint Surg Am 85-A Suppl 2:111–116

Grieger JC, Samulski RJ (2012) Adeno-associated virus vectorology, manufacturing, and clinical applications. Methods Enzymol 507:229–254

Han S, Mahato RI, Sung YK, Kim SW (2000) Development of biomaterials for gene therapy. Mol Ther 2(4):302–317

Hanada K, Solchaga LA, Caplan AI, Hering TM, Goldberg VM, Yoo JU, Johnstone B (2001) BMP-2 induction and TGF-beta 1 modulation of rat periosteal cell chondrogenesis. J Cell Biochem 81(2):284–294

Hardingham TE, Oldershaw RA, Tew SR (2006) Cartilage, SOX9 and Notch signals in chondrogenesis. J Anat 209(4):469–480

He S, Xia T, Wang H, Wei L, Luo X, Li X (2012) Multiple release of polyplexes of plasmids VEGF and bFGF from electrospun fibrous scaffolds towards regeneration of mature blood vessels. Acta Biomater 8(7):2659–2669

Horas U, Pelinkovic D, Herr G, Aigner T, Schnettler R (2003) Autologous chondrocyte implantation and osteochondral cylinder transplantation in cartilage repair of the knee joint. A prospective, comparative trial. J Bone Joint Surg Am 85-A (2):185–192

Hu WW, Wang Z, Hollister SJ, Krebsbach PH (2007) Localized viral vector delivery to enhance in situ regenerative gene therapy. Gene Ther 14(11):891–901

Hwang JH, Lee S, Kim E, Kim JS, Lee CH, Ahn IS, Jang JH (2011) Heparin-coated superparamagnetic nanoparticle-mediated adeno-associated virus delivery for enhancing cellular transduction. Int J Pharm 421(2):397–404

Ibraheem D, Elaissari A, Fessi H (2014) Gene therapy and DNA delivery systems. Int J Pharm 459(1–2):70–83

Imperiale MJ, Kochanek S (2004) Adenovirus vectors: biology, design, and production. Curr Top Microbiol Immunol 273:335–357

Inada M, Yasui T, Nomura S, Miyake S, Deguchi K, Himeno M, Sato M, Yamagiwa H, Kimura T, Yasui N, Ochi T, Endo N, Kitamura Y, Kishimoto T, Komori T (1999) Maturational disturbance of chondrocytes in Cbfa1-deficient mice. Dev Dyn 214(4):279–290

Jacobs F, Wang L (2011) Adeno-associated viral vectors for correction of inborn errors of metabolism: progressing towards clinical application. Curr Pharm Des 17(24):2500–2515

Jang JH, Houchin TL, Shea LD (2004) Gene delivery from polymer scaffolds for tissue engineering. Expert Rev Med Devices 1(1):127–138

Jang JH, Schaffer DV, Shea LD (2011) Engineering biomaterial systems to enhance viral vector gene delivery. Mol Ther 19(8):1407–1415

Jenkins FJ, Turner SL (1996) Herpes simplex virus: a tool for neuroscientists. Front Biosci 1: d241–d247

Jentzsch KD, Wellmitz G, Heder G, Petzold E, Buntrock P, Oehme P (1980) A bovine brain fraction with fibroblast growth factor activity inducing articular cartilage regeneration in vivo. Acta Biol Med Ger 39(8–9):967–971

Johnson LL (2001) Arthroscopic abrasion arthroplasty: a review. Clin Orthop Relat Res (391 Suppl):S306–S317

Johnstone B, Alini M, Cucchiarini M, Dodge GR, Eglin D, Guilak F, Madry H, Mata A, Mauck RL, Semino CE, Stoddart MJ (2013) Tissue engineering for articular cartilage repair–the state of the art. Eur Cell Mater 25:248–267

Joyce ME, Roberts AB, Sporn MB, Bolander ME (1990) Transforming growth factor-beta and the initiation of chondrogenesis and osteogenesis in the rat femur. J Cell Biol 110(6):2195–2207

Katayama R, Wakitani S, Tsumaki N, Morita Y, Matsushita I, Gejo R, Kimura T (2004) Repair of articular cartilage defects in rabbits using CDMP1 gene-transfected autologous mesenchymal cells derived from bone marrow. Rheumatology (Oxford) 43(8):980–985

Keeney M, Onyiah S, Zhang Z, Tong X, Han LH, Yang F (2013) Modulating polymer chemistry to enhance non-viral gene delivery inside hydrogels with tunable matrix stiffness. Biomaterials 34(37):9657–9665

Kidd ME, Shin S, Shea LD (2012) Fibrin hydrogels for lentiviral gene delivery in vitro and in vivo. J Control Release 157(1):80–85

Kim HK, Moran ME, Salter RB (1991) The potential for regeneration of articular cartilage in defects created by chondral shaving and subchondral abrasion. An experimental investigation in rabbits. J Bone Joint Surg Am 73(9):1301–1315

Klein-Nulend J, Louwerse RT, Heyligers IC, Wuisman PI, Semeins CM, Goei SW, Burger EH (1998) Osteogenic protein (OP-1, BMP-7) stimulates cartilage differentiation of human and goat perichondrium tissue in vitro. J Biomed Mater Res 40(4):614–620

Knight S, Collins M, Takeuchi Y (2013) Insertional mutagenesis by retroviral vectors: current concepts and methods of analysis. Curr Gene Ther 13(3):211–227

Knutsen G, Engebretsen L, Ludvigsen TC, Drogset JO, Grontvedt T, Solheim E, Strand T, Roberts S, Isaksen V, Johansen O (2004) Autologous chondrocyte implantation compared with microfracture in the knee. A randomized trial. J Bone Joint Surg Am 86-A (3):455–464

Kon E, Filardo G, Perdisa F, Di Martino A, Busacca M, Balboni F, Sessa A, Marcacci M (2014) A one-step treatment for chondral and osteochondral knee defects: clinical results of a biomimetic scaffold implantation at 2 years of follow-up. J Mater Sci Mater Med 25(10):2437–2444

Kotterman MA, Schaffer DV (2014) Engineering adeno-associated viruses for clinical gene therapy. Nat Rev Genet 15(7):445–451

Kulkarni MM, Greiser U, O'Brien T, Pandit A (2011) A temporal gene delivery system based on fibrin microspheres. Mol Pharm 8(2):439–446

Lachmann R (2004) Herpes simplex virus-based vectors. Int J Exp Pathol 85(4):177–190

Lam J, Lu S, Kasper FK, Mikos AG (2015) Strategies for controlled delivery of biologics for cartilage repair. Adv Drug Deliv Rev 84:123–134

Lee HH, Haleem AM, Yao V, Li J, Xiao X, Chu CR (2011a) Release of bioactive adeno-associated virus from fibrin scaffolds: effects of fibrin glue concentrations. Tissue Eng Part A 17(15–16):1969–1978

Lee KH, Song SU, Hwang TS, Yi Y, Oh IS, Lee JY, Choi KB, Choi MS, Kim SJ (2001) Regeneration of hyaline cartilage by cell-mediated gene therapy using transforming growth factor beta 1-producing fibroblasts. Hum Gene Ther 12(14):1805–1813

Lee S, Kim JS, Chu HS, Kim GW, Won JI, Jang JH (2011b) Electrospun nanofibrous scaffolds for controlled release of adeno-associated viral vectors. Acta Biomater 7(11):3868–3876

Lee YS, Kim SW (2014) Bioreducible polymers for therapeutic gene delivery. J Control Release 190:424–439

Lefebvre V, Behringer RR, de Crombrugghe B (2001) L-Sox5, Sox6 and Sox9 control essential steps of the chondrocyte differentiation pathway. Osteoarthritis Cartilage 9 Suppl A:S69–S75

Lei Y, Huang S, Sharif-Kashani P, Chen Y, Kavehpour P, Segura T (2010) Incorporation of active DNA/cationic polymer polyplexes into hydrogel scaffolds. Biomaterials 31(34):9106–9116

Lei Y, Rahim M, Ng Q, Segura T (2011) Hyaluronic acid and fibrin hydrogels with concentrated DNA/PEI polyplexes for local gene delivery. J Control Release 153(3):255–261

Levy RJ, Song C, Tallapragada S, DeFelice S, Hinson JT, Vyavahare N, Connolly J, Ryan K, Li Q (2001) Localized adenovirus gene delivery using antiviral IgG complexation. Gene Ther 8 (9):659–667

Li H, Zhang FL, Shi WJ, Bai XJ, Jia SQ, Zhang CG, Ding W (2015) Immobilization of FLAG-tagged recombinant adeno-associated virus 2 onto tissue engineering scaffolds for the improvement of transgene delivery in cell transplants. PLoS ONE 10 (6):e0129013–e0129027

Li Y, Yang C, Khan M, Liu S, Hedrick JL, Yang YY, Ee PL (2012) Nanostructured PEG-based hydrogels with tunable physical properties for gene delivery to human mesenchymal stem cells. Biomaterials 33(27):6533–6541

Liao IC, Chen S, Liu JB, Leong KW (2009) Sustained viral gene delivery through core-shell fibers. J Control Release 139(1):48–55

Lorden ER, Levinson HM, Leong KW (2015) Integration of drug, protein, and gene delivery systems with regenerative medicine. Drug Deliv Transl Res 5(2):168–186

Loser P, Huser A, Hillgenberg M, Kumin D, Both GW, Hofmann C (2002) Advances in the development of non-human viral DNA-vectors for gene delivery. Curr Gene Ther 2(2): 161–171

Ma PX, Langer R (1999) Morphology and mechanical function of long-term in vitro engineered cartilage. J Biomed Mater Res 44(2):217–221

Madry H, Cucchiarini M (2013) Advances and challenges in gene-based approaches for osteoarthritis. J Gene Med 15(10):343–355

Madry H, Cucchiarini M (2014) Tissue-engineering strategies to repair joint tissue in osteoarthritis: nonviral gene-transfer approaches. Curr Rheumatol Rep 16(10):450–460

Madry H, Cucchiarini M, Terwilliger EF, Trippel SB (2003) Recombinant adeno-associated virus vectors efficiently and persistently transduce chondrocytes in normal and osteoarthritic human articular cartilage. Hum Gene Ther 14(4):393–402

Madry H, Kaul G, Cucchiarini M, Stein U, Zurakowski D, Remberger K, Menger MD, Kohn D, Trippel SB (2005) Enhanced repair of articular cartilage defects in vivo by transplanted chondrocytes overexpressing insulin-like growth factor I (IGF-I). Gene Ther 12(15):1171–1179

Madry H, Kohn D, Cucchiarini M (2006) Gene therapy in orthopaedic surgery. Orthopade 35(11):1193–1202

Madry H, Weimer A, Kohn D, Cucchiarini M (2007) Tissue engineering for articular cartilage repair improved by gene transfer. Current concepts. Orthopade 36(3):236–247

Madry H, Orth P, Cucchiarini M (2011) Gene therapy for cartilage repair. Cartilage 2(3):201–225

Mah C, Fraites TJ Jr, Zolotukhin I, Song S, Flotte TR, Dobson J, Batich C, Byrne BJ (2002) Improved method of recombinant AAV2 delivery for systemic targeted gene therapy. Mol Ther 6(1):106–112

Mankin HJ (1974a) The reaction of articular cartilage to injury and osteoarthritis (first of two parts). N Engl J Med 291(24):1285–1292

Mankin HJ (1974b) The reaction of articular cartilage to injury and osteoarthritis (second of two parts). N Engl J Med 291(25):1335–1340

Mason JB, Vandenberghe LH, Xiao R, Wilson JM, Richardson DW (2012) Influence of serotype, cell type, tissue composition, and time after inoculation on gene expression in recombinant adeno-associated viral vector-transduced equine joint tissues. Am J Vet Res 73(8):1178–1185

Mason JM, Breitbart AS, Barcia M, Porti D, Pergolizzi RG, Grande DA (2000) Cartilage and bone regeneration using gene-enhanced tissue engineering. Clin Orthop Relat Res (379 Suppl): S171–S178

Matthews C, Jenkins G, Hilfinger J, Davidson B (1999) Poly-L-lysine improves gene transfer with adenovirus formulated in PLGA microspheres. Gene Ther 6(9):1558–1564

Mbita Z, Hull R, Dlamini Z (2014) Human immunodeficiency virus-1 (HIV-1)-mediated apoptosis: new therapeutic targets. Viruses 6(8):3181–3227

Mease PJ, Hobbs K, Chalmers A, El-Gabalawy H, Bookman A, Keystone E, Furst DE, Anklesaria P, Heald AE (2009) Local delivery of a recombinant adenoassociated vector containing a tumour necrosis factor alpha antagonist gene in inflammatory arthritis: a phase 1 dose-escalation safety and tolerability study. Ann Rheum Dis 68(8):1247–1254

Mease PJ, Wei N, Fudman EJ, Kivitz AJ, Schechtman J, Trapp RG, Hobbs KF, Greenwald M, Hou A, Bookbinder SA, Graham GE, Wiesenhutter CW, Willis L, Ruderman EM, Forstot JZ, Maricic MJ, Dao KH, Pritchard CH, Fiske DN, Burch FX, Prupas HM, Anklesaria P, Heald AE (2010) Safety, tolerability, and clinical outcomes after intraarticular injection of a recombinant adeno-associated vector containing a tumor necrosis factor antagonist gene: results of a phase 1/2 Study. J Rheumatol 37(4):692–703

Mei L, Jin X, Song C, Wang M, Levy RJ (2006) Immobilization of gene vectors on polyurethane surfaces using a monoclonal antibody for localized gene delivery. J Gene Med 8(6):690–698

Mok H, Park JW, Park TG (2007) Microencapsulation of PEGylated adenovirus within PLGA microspheres for enhanced stability and gene transfection efficiency. Pharm Res 24(12): 2263–2269

Morrey ME, Anderson PA, Chambers G, Paul R (2008) Optimizing nonviral-mediated transfection of human intervertebral disc chondrocytes. Spine J 8(5):796–803

Mow VC, Ratcliffe A, Poole AR (1992) Cartilage and diarthrodial joints as paradigms for hierarchical materials and structures. Biomaterials 13(2):67–97

Murphy JM, Fink DJ, Hunziker EB, Barry FP (2003) Stem cell therapy in a caprine model of osteoarthritis. Arthritis Rheum 48(12):3464–3474

Nam HY, Park JH, Kim K, Kwon IC, Jeong SY (2009) Lipid-based emulsion system as non-viral gene carriers. Arch Pharm Res 32(5):639–646

Needham CJ, Shah SR, Dahlin RL, Kinard LA, Lam J, Watson BM, Lu S, Kasper FK, Mikos AG (2014) Osteochondral tissue regeneration through polymeric delivery of DNA encoding for the SOX trio and RUNX2. Acta Biomater 10(10):4103–4112

Nieto K, Salvetti A (2014) AAV vectors vaccines against infectious diseases. Front Immunol 5:5–13

Nixon AJ, Fortier LA, Williams J, Mohammed H (1999) Enhanced repair of extensive articular defects by insulin-like growth factor-I-laden fibrin composites. J Orthop Res 17(4):475–487

Noth U, Osyczka AM, Tuli R, Hickok NJ, Danielson KG, Tuan RS (2002) Multilineage mesenchymal differentiation potential of human trabecular bone-derived cells. J Orthop Res 20 (5):1060–1069

Oligino T, Ghivizzani S, Wolfe D, Lechman E, Krisky D, Mi Z, Evans C, Robbins P, Glorioso J (1999) Intra-articular delivery of a herpes simplex virus IL-1Ra gene vector reduces inflammation in a rabbit model of arthritis. Gene Ther 6(10):1713–1720

Orth P, Rey-Rico A, Venkatesan JK, Madry H, Cucchiarini M (2014) Current perspectives in stem cell research for knee cartilage repair. Stem Cells Cloning 7:1–17

Pagnotto MR, Wang Z, Karpie JC, Ferretti M, Xiao X, Chu CR (2007) Adeno-associated viral gene transfer of transforming growth factor-beta1 to human mesenchymal stem cells improves cartilage repair. Gene Ther 14(10):804–813

Pannier AK, Shea LD (2004) Controlled release systems for DNA delivery. Mol Ther 10(1):19–26

Park H, Kim PH, Hwang T, Kwon OJ, Park TJ, Choi SW, Yun CO, Kim JH (2012) Fabrication of cross-linked alginate beads using electrospraying for adenovirus delivery. Int J Pharm 427 (2):417–425

Park JS, Yang HN, Woo DG, Jeon SY, Park KH (2013) Poly(N-isopropylacrylamide-co-acrylic acid) nanogels for tracing and delivering genes to human mesenchymal stem cells. Biomaterials 34(34):8819–8834

Pascher A, Palmer GD, Steinert A, Oligino T, Gouze E, Gouze JN, Betz O, Spector M, Robbins PD, Evans CH, Ghivizzani SC (2004) Gene delivery to cartilage defects using coagulated bone marrow aspirate. Gene Ther 11(2):133–141

Pelletier JP, Martel-Pelletier J (1994) Role of synovial inflammation, cytokines and IGF-1 in the physiopathology of osteoarthritis. Rev Rhum Ed Fr 61(9 Pt 2):103S–108S

Peng H, Huard J (2004) Muscle-derived stem cells for musculoskeletal tissue regeneration and repair. Transpl Immunol 12(3–4):311–319

Pi Y, Zhang X, Shi J, Zhu J, Chen W, Zhang C, Gao W, Zhou C, Ao Y (2011) Targeted delivery of non-viral vectors to cartilage in vivo using a chondrocyte-homing peptide identified by phage display. Biomaterials 32(26):6324–6332

Pohle D, Kasch R, Herlyn P, Bader R, Mittlmeier T, Putzer BM, Muller-Hilke B (2012) Adenoviral transduction supports matrix expression of alginate cultured articular chondrocytes. Biotechnol Bioeng 109(9):2402–2408

Prockop DJ (1998) Marrow stromal cells as stem cells for continual renewal of nonhematopoietic tissues and as potential vectors for gene therapy. J Cell Biochem Suppl 30–31:284–285

Ramgopal Y, Mondal D, Venkatraman SS, Godbey WT, Yuen GY (2009) Controlled release of complexed DNA from polycaprolactone film: comparison of lipoplex and polyplex release. J Biomed Mater Res B Appl Biomater 89(2):439–447

Rejman J, Oberle V, Zuhorn IS, Hoekstra D (2004) Size-dependent internalization of particles via the pathways of clathrin- and caveolae-mediated endocytosis. Biochem J 377(Pt 1):159–169

Rey-Rico A, Frisch J, Venkatesan JK, Schmitt G, Madry H, Cucchiarini M (2015a) Determination of effective rAAV-mediated gene transfer conditions to support chondrogenic differentiation processes in human primary bone marrow aspirates. Gene Ther 22(1):50–57

Rey-Rico A, Venkatesan JK, Frisch J, Rial-Hermida I, Schmitt G, Concheiro A, Madry H, Alvarez-Lorenzo C, Cucchiarini M (2015b) PEO-PPO-PEO micelles as effective rAAV-mediated gene delivery systems to target human mesenchymal stem cells without altering their differentiation potency. Acta Biomater 27:42–52

Rey-Rico A, Venkatesan JK, Frisch J, Schmitt G, Monge-Marcet A, Lopez-Chicon P, Mata A, Semino C, Madry H, Cucchiarini M (2015c) Effective and durable genetic modification of human mesenchymal stem cells via controlled release of rAAV vectors from self-assembling peptide hydrogels with a maintained differentiation potency. Acta Biomater 18:118–127

Rey-Rico A, Cucchiarini M (2016a) Controlled release strategies for rAAV-mediated gene delivery. Acta Biomater 29:1–10

Rey-Rico A, Cucchiarini M (2016b) Recent tissue engineering-based advances for effective rAAV-mediated gene transfer in the musculoskeletal system. Bioengineered. doi:10.1080/21655979.2016.1187347

Rives CB, des Rieux A, Zelivyanskaya M, Stock SR, Lowe WL, Jr. Shea LD (2009) Layered PLG scaffolds for in vivo plasmid delivery. Biomaterials 30 (3):394–401

Robbins PD, Ghivizzani SC (1998) Viral vectors for gene therapy. Pharmacol Ther 80(1):35–47

Rose JA, Berns KI, Hoggan MD, Koczot FJ (1969) Evidence for a single-stranded adenovirus-associated virus genome: formation of a DNA density hybrid on release of viral DNA. Proc Natl Acad Sci U S A 64(3):863–869

Sailaja G, HogenEsch H, North A, Hays J, Mittal SK (2002) Encapsulation of recombinant adenovirus into alginate microspheres circumvents vector-specific immune response. Gene Ther 9(24):1722–1729

Sandell LJ (2012) Etiology of osteoarthritis: genetics and synovial joint development. Nat Rev Rheumatol 8(2):77–89

Santo VE, Gomes ME, Mano JF, Reis RL (2013) Controlled release strategies for bone, cartilage, and osteochondral engineering–part I: recapitulation of native tissue healing and variables for the design of delivery systems. Tissue Eng Part B 19(4):308–326

Saraf A, Mikos AG (2006) Gene delivery strategies for cartilage tissue engineering. Adv Drug Deliv Rev 58(4):592–603

Schek RM, Hollister SJ, Krebsbach PH (2004) Delivery and protection of adenoviruses using biocompatible hydrogels for localized gene therapy. Mol Ther 9(1):130–138

Schmidt C, Bezuidenhout D, Zilla P, Davies NH (2014) A slow-release fibrin matrix increases adeno-associated virus transduction of wound repair cells in vivo. J Biomater Appl 28(9):1408–1418

Segura T, Volk MJ, Shea LD (2003) Substrate-mediated DNA delivery: role of the cationic polymer structure and extent of modification. J Control Release 93(1):69–84

Seidlits SK, Gower RM, Shepard JA, Shea LD (2013) Hydrogels for lentiviral gene delivery. Expert Opin Drug Deliv 10(4):499–509

Sellers RS, Peluso D, Morris EA (1997) The effect of recombinant human bone morphogenetic protein-2 (rhBMP-2) on the healing of full-thickness defects of articular cartilage. J Bone Joint Surg Am 79(10):1452–1463

Semino CE (2008) Self-assembling peptides: from bio-inspired materials to bone regeneration. J Dent Res 87(7):606–616

Shepard JA, Wesson PJ, Wang CE, Stevans AC, Holland SJ, Shikanov A, Grzybowski BA, Shea LD (2011) Gene therapy vectors with enhanced transfection based on hydrogels modified with affinity peptides. Biomaterials 32(22):5092–5099

Shi CH, Wang WS, Zhang ZD, Li CJ, Guo FJ, Li F, Chen AM (2015) Effect of lentivirus-mediated uPA silencing on the proliferation and apoptosis of chondrocytes and the expression of MMPs. J Huazhong Univ Sci Technolog Med Sci 35(1):111–116

Shields AM, Klavinskis LS, Antoniou M, Wooley PH, Collins HL, Panayi GS, Thompson SJ, Corrigall VM (2015) Systemic gene transfer of binding immunoglobulin protein (BiP) prevents disease progression in murine collagen-induced arthritis. Clin Exp Immunol 179(2):210–219
Siegman S, Truong NF, Segura T (2015) Encapsulation of PEGylated low-molecular-weight PEI polyplexes in hyaluronic acid hydrogels reduces aggregation. Acta Biomater 28:45–54
Smith-Arica JR, Bartlett JS (2001) Gene therapy: recombinant adeno-associated virus vectors. Curr Cardiol Rep 3(1):43–49
Spiller KL, Maher SA, Lowman AM (2011) Hydrogels for the repair of articular cartilage defects. Tissue Eng Part B 17(4):281–299
Spitzer D, Hauser H, Wirth D (1999) Complement-protected amphotropic retroviruses from murine packaging cells. Hum Gene Ther 10(11):1893–1902
Steadman JR, Briggs KK, Rodrigo JJ, Kocher MS, Gill TJ, Rodkey WG (2003) Outcomes of microfracture for traumatic chondral defects of the knee: average 11-year follow-up. Arthroscopy 19(5):477–484
Steinwachs MR, Guggi T, Kreuz PC (2008) Marrow stimulation techniques. Injury 39(Suppl 1): S26–S31
Stender S, Murphy M, O'Brien T, Stengaard C, Ulrich-Vinther M, Soballe K, Barry F (2007) Adeno-associated viral vector transduction of human mesenchymal stem cells. Eur Cell Mater 13:93–99
Sumarsono SH, Wilson TJ, Tymms MJ, Venter DJ, Corrick CM, Kola R, Lahoud MH, Papas TS, Seth A, Kola I (1996) Down's syndrome-like skeletal abnormalities in Ets2 transgenic mice. Nature 379(6565):534–537
Summerford C, Samulski RJ (1998) Membrane-associated heparan sulfate proteoglycan is a receptor for adeno-associated virus type 2 virions. J Virol 72(2):1438–1445
Tao K, Frisch J, Rey-Rico A, Venkatesan JK, Schmitt G, Madry H, Lin J, Cucchiarini M (2016a) Co-overexpression of TGF-beta and SOX9 via rAAV gene transfer modulates the metabolic and chondrogenic activities of human bone marrow-derived mesenchymal stem cells. Stem Cell Res Ther 7:20–31
Tao K, Rey-Rico A, Frisch J, Venkatesan JK, Schmitt G, Madry H, Lin J, Cucchiarini M (2016b) rAAV-mediated combined gene transfer and overexpression of TGF-beta and SOX9 remodels human osteoarthritic articular cartilage. J Orthop Res. doi:10.1002/jor.23228
Tierney EG, Duffy GP, Hibbitts AJ, Cryan SA, O'Brien FJ (2012) The development of non-viral gene-activated matrices for bone regeneration using polyethyleneimine (PEI) and collagen-based scaffolds. J Control Release 158(2):304–311
Tiwari G, Tiwari R, Sriwastawa B, Bhati L, Pandey S, Pandey P, Bannerjee SK (2012) Drug delivery systems: an updated review. Int J Pharm Investig 2(1):2–11
Tokatlian T, Cam C, Siegman SN, Lei Y, Segura T (2012) Design and characterization of microporous hyaluronic acid hydrogels for in vitro gene transfer to mMSCs. Acta Biomater 8(11):3921–3931
Trippel SB (1995) Growth factor actions on articular cartilage. J Rheumatol Suppl 43:129–132
Trippel SB, Wroblewski J, Makower AM, Whelan MC, Schoenfeld D, Doctrow SR (1993) Regulation of growth-plate chondrocytes by insulin-like growth-factor I and basic fibroblast growth factor. J Bone Joint Surg Am 75(2):177–189
Trippel SB, Ghivizzani SC, Nixon AJ (2004) Gene-based approaches for the repair of articular cartilage. Gene Ther 11(4):351–359
Turner P, Petch A, Al-Rubeai M (2007) Encapsulation of viral vectors for gene therapy applications. Biotechnol Prog 23(2):423–429
Ulrich-Vinther M, Duch MR, Soballe K, O'Keefe RJ, Schwarz EM, Pedersen FS (2004) In vivo gene delivery to articular chondrocytes mediated by an adeno-associated virus vector. J Orthop Res 22(4):726–734
Ulrich-Vinther M, Stengaard C, Schwarz EM, Goldring MB, Soballe K (2005) Adeno-associated vector mediated gene transfer of transforming growth factor-beta1 to normal and osteoarthritic human chondrocytes stimulates cartilage anabolism. Eur Cell Mater 10:40–50

van der Laan LJ, Wang Y, Tilanus HW, Janssen HL, Pan Q (2011) AAV-mediated gene therapy for liver diseases: the prime candidate for clinical application? Expert Opin Biol Ther 11 (3):315–327

Venkatesan JK, Ekici M, Madry H, Schmitt G, Kohn D, Cucchiarini M (2012) SOX9 gene transfer via safe, stable, replication-defective recombinant adeno-associated virus vectors as a novel, powerful tool to enhance the chondrogenic potential of human mesenchymal stem cells. Stem Cell Res Ther 3(3):22–36

Venkatesan JK, Rey-Rico A, Schmitt G, Wezel A, Madry H, Cucchiarini M (2013) rAAV-mediated overexpression of TGF-beta stably restructures human osteoarthritic articular cartilage in situ. J Transl Med 11:211–224

Vortkamp A, Lee K, Lanske B, Segre GV, Kronenberg HM, Tabin CJ (1996) Regulation of rate of cartilage differentiation by Indian hedgehog and PTH-related protein. Science 273(5275):613–622

Walter E, Dreher D, Kok M, Thiele L, Kiama SG, Gehr P, Merkle HP (2001) Hydrophilic poly (DL-lactide-co-glycolide) microspheres for the delivery of DNA to human-derived macrophages and dendritic cells. J Control Release 76(1–2):149–168

Wang C, Pham PT (2008) Polymers for viral gene delivery. Expert Opin Drug Deliv 5(4):385–401

Wang C, Ruan DK, Zhang C, Wang DL, Xin H, Zhang Y (2011) Effects of adeno-associated virus-2-mediated human BMP-7 gene transfection on the phenotype of nucleus pulposus cells. J Orthop Res 29(6):838–845

Wang D, Molavi O, Lutsiak ME, Elamanchili P, Kwon GS, Samuel J (2007) Poly(D, L-lactic-co-glycolic acid) microsphere delivery of adenovirus for vaccination. J Pharm Sci 10(2):217–230

Wang H, Li Y, Chen J, Wang X, Zhao F, Cao S (2014) Chondrogenesis of bone marrow mesenchymal stem cells induced by transforming growth factor beta3 gene in Diannan small-ear pigs. Zhongguo Xiu Fu Chong Jian Wai Ke Za Zhi 28(2):149–154

Watson RS, Broome TA, Levings PP, Rice BL, Kay JD, Smith AD, Gouze E, Gouze JN, Dacanay EA, Hauswirth WW, Nickerson DM, Dark MJ, Colahan PT, Ghivizzani SC (2013) scAAV-mediated gene transfer of interleukin-1-receptor antagonist to synovium and articular cartilage in large mammalian joints. Gene Ther 20(6):670–677

Wehling P, Reinecke J, Baltzer AW, Granrath M, Schulitz KP, Schultz C, Krauspe R, Whiteside TW, Elder E, Ghivizzani SC, Robbins PD, Evans CH (2009) Clinical responses to gene therapy in joints of two subjects with rheumatoid arthritis. Hum Gene Ther 20(2):97–101

Wu Y, Li J, Kong Y, Chen D, Liu B, Wang W (2013) HSV-1 based vector mediated IL-1Ralpha gene for knee osteoarthritis in rabbits. Zhong Nan Da Xue Bao Yi Xue Ban 38(6):590–596

Xu X, Qiu S, Zhang Y, Yin J, Min S (2016) PELA microspheres with encapsulated arginine-chitosan/pBMP-2 nanoparticles induce pBMP-2 controlled-release, transfected osteoblastic progenitor cells, and promoted osteogenic differentiation. Artif Cells Nanomed Biotechnol 1–10

Yamada Y, Horton W, Miyashita T, Savagner P, Hassell J, Doege K (1991) Expression and structure of cartilage proteins. J Craniofac Genet Dev Biol 11(4):350–356

Yang M, Ma QJ, Dang GT, Ma KT, Chen P, Zhou CY (2005) Adeno-associated virus-mediated bone morphogenetic protein-7 gene transfer induces C2C12 cell differentiation into osteoblast lineage cells. Acta Pharmacol Sin 26(8):963–968

Yang Y, Xia T, Chen F, Wei W, Liu C, He S, Li X (2012) Electrospun fibers with plasmid bFGF polyplex loadings promote skin wound healing in diabetic rats. Mol Pharm 9(1):48–58

Yi Y, Hahm SH, Lee KH (2005) Retroviral gene therapy: safety issues and possible solutions. Curr Gene Ther 5(1):25–35

Zarnett R, Salter RB (1989) Periosteal neochondrogenesis for biologically resurfacing joints: its cellular origin. Can J Surg 32(3):171–174

Zhang F, Su K, Fang Y, Sandhya S, Wang DA (2015a) A mixed co-culture of mesenchymal stem cells and transgenic chondrocytes in alginate hydrogel for cartilage tissue engineering. J Tissue Eng Regen Med 9(1):77–84

Zhang F, Yao Y, Su K, Fang Y, Citra F, Wang DA (2015b) Co-transduction of lentiviral and adenoviral vectors for co-delivery of growth factor and shRNA genes in mesenchymal stem cells-based chondrogenic system. J Tissue Eng Regen Med 9(9):1036–1045

Zhang J, Sen A, Cho E, Lee JS, Webb K (2014) Poloxamine/fibrin hybrid hydrogels for non-viral gene delivery. J Tissue Eng Regen Med. doi:10.1002/term.1906

Zhang M, Yuan H, Huang Z, Hu F (2011a) Recombinant-adeno-associated viral vector-mediated gene therapy for cardiovascular diseases. Zhong Nan Da Xue Xue Bao Yi Xue Ban 36(2): 178–184

Zhang S, Holmes T, Lockshin C, Rich A (1993) Spontaneous assembly of a self-complementary oligopeptide to form a stable macroscopic membrane. Proc Natl Acad Sci U S A 90(8): 3334–3338

Zhang Y, Fan W, Nothdurft L, Wu C, Zhou Y, Crawford R, Xiao Y (2011b) In vitro and in vivo evaluation of adenovirus combined silk fibroin scaffolds for bone morphogenetic protein-7 gene delivery. Tissue Eng Part C 17(8):789–797

Zhang Y, Wu C, Luo T, Li S, Cheng X, Miron RJ (2012) Synthesis and inflammatory response of a novel silk fibroin scaffold containing BMP7 adenovirus for bone regeneration. Bone 51(4):704–713

Zhang Y, Ma Y, Wu C, Miron RJ, Cheng X (2013) Platelet-derived growth factor BB gene-released scaffolds: biosynthesis and characterization. J Tissue Eng Regen Med. doi:10.1002/term.1825

Zhang Y, Miron RJ, Li S, Shi B, Sculean A, Cheng X (2015c) Novel MesoPorous BioGlass/silk scaffold containing adPDGF-B and adBMP7 for the repair of periodontal defects in beagle dogs. J Clin Periodontol 42(3):262–271

Zhao GQ, Eberspaecher H, Seldin MF, de Crombrugghe B (1994) The gene for the homeodomain-containing protein Cart-1 is expressed in cells that have a chondrogenic potential during embryonic development. Mech Dev 48(3):245–254

Zuk PA, Zhu M, Mizuno H, Huang J, Futrell JW, Katz AJ, Benhaim P, Lorenz HP, Hedrick MH (2001) Multilineage cells from human adipose tissue: implications for cell-based therapies. Tissue Eng 7(2):211–228

Biomaterials Based Strategies for Engineering Tumor Microenvironment

Neha Arya and Aurelien Forget

Abstract Tissue engineering aims to gain mechanistic insights into human diseases and to develop new treatment protocols. Although 2-dimensional (2-D) flat petri dish culture and in vivo disease-based models are the industrial gold standards for understanding the underlying disease pathophysiology and for drug screening/testing, they are associated with certain limitations. While the 2-D cell culture systems fail to mimic in vivo signaling, animal-based disease models are associated with long incubation period, high cost, ethical constraints as well as depiction of human pathology in different species. Therefore, there has been a paradigm shift towards the development of 3-dimensional (3-D) based in vitro disease models. These models act as bridging gaps between the aforementioned conventional strategies thereby fastening clinical translation. In this regard, biomedical engineering plays a key role towards the development of tissue engineering based 3-D disease models. These models have demonstrated success in recapitulating human diseases in terms of in vivo morphology and signaling. This chapter will present examples of biomaterials-based 3-D engineered disease models with a focus on cancer.

Keywords Tissue engineering · In vitro disease models · 3-dimensional · Spheroids · Scaffolds

Abbreviations

2-D	Two-dimensional
3-D	Three-dimensional
α-SMA	α-smooth muscle actin

N. Arya (✉)
Department of Biochemistry, All India Institute of Medical Sciences Bhopal, Saket Nagar, Bhopal 462020, Madhya Pradesh, India
e-mail: neha.biochemistry@aiimsbhopal.edu.in

A. Forget
University of South Australia, Future Industries Institute, University Blv, Mawson Lakes, SA 5095, Australia

A. Tripathi and J.S. Melo (eds.), *Advances in Biomaterials for Biomedical Applications*, Advanced Structured Materials 66,
DOI 10.1007/978-981-10-3328-5_8

ABC	ATP-binding cassette
bFGF	Basic fibroblast growth factor
CAFs	Cancer-associated fibroblasts
CAM-DR	Cell-adhesion mediated drug resistance
CCL2	Chemokine CC-motive ligand 2
CNS	Central nervous system
CSCs	Cancer stem cells
CSFs	Colony stimulating factors
CSF1	Colony stimulating factor 1
DCIS	Ductal carcinoma in situ
DEAE	Diethylaminoethyl
E-cad	Epithelial-cadherin
ECM	Extracellular matrix
EGF	Epidermal growth factor
EGFR	Epidermal growth factor receptor
EMT	Epithelial to mesenchymal transition
EPC	Endothelial progenitor cell
FAP	Fibroblast activation protein
Fe_3O_4	Iron oxide
GA	Glutaraldehyde
GAG	Glycosaminoglycan
G-CSF	Granulocyte colony stimulating factor
GEMs	Global eukaryotic microcarriers
GM-CSF	Granulocyte macrophage colony stimulating factor
HA	Hyaluronic acid
HCC	Hepatocellular carcinoma cells
HGF	Hepatocyte growth factor
HIF-1	Hypoxia-inducible transcription factor 1
HMF	Human mammary fibroblasts
HPV 16	Human papilloma virus 16
HTS	High throughput screening
IGF1	Insulin-like growth factor 1
IL-6	Interleukin-6
IL-8	Interleukin-8
MFs	Myofibroblasts
MMPs	Matrix metalloproteases
MP	Microparticles
N-cad	Neural-cadherin
NO	Nitric oxide
NSCLS	Non-small cell lung cancer
PCL	Poly(ε-caprolactone)
PDGF	Platelet-derived growth factor
PDT	Photodyanmic therapy
PEG	Polyethylene glycol

PHEMA	Polyhydroxyethylmethacrylate
PLA	Polylactide
PLG	Poly(lactide-co-glycolide)
PLGA	Polylactic-co-glycolide
PLLA-*b*-PEG-folate	Polyl-lactic acid-*b*-polyethylene glycol-folate
PVA	Polyvinyl alcohol
RCCS	Rotary cell culture system/bioreactor
RGD	Arginine-glycine-aspartic acid
RTK	Receptor tyrosine kinase
SCLC	Small cell lung cancer
SDF1	Stromal-cell derived factor 1
sECM	Synthetic ECM
SV-40	Simian virus 40
TAMs	Tumor associated macrophages
TCPS	Tissue culture polystyrene
TE	Tissue engineering
TGFβ	Transforming growth factor β
TNF-α	Tumor necrosis factor α
VEGF	Vascular endothelial growth factor
VPF	Vascular permeability factor
$ZnPcS_{mix}$	Zinc sulfophthalocyanine

1 Introduction

Cancer is a disease of grave importance and is the second most leading cause of deaths in United States. In the next few years, it is expected to bypass heart diseases as the lead cause of deaths (Siegel et al. 2015). High incidents of death rates associated with cancer have resulted in extensive research that aim towards the development of high-end treatment protocols. However, the research so far has not contributed to a promising decline in mortality rates associated with cancer. As a result, high incidence of death rates combined with slow progress in treatment protocols has generated demands to revise our research strategies, particularly in the area of tumor biology as well as drug screening in order to develop a strong co-relation between benchside to bedside.

Cancer treatment is usually performed either by surgery, radiotherapy or chemotherapy or a combination of these strategies. However, systemic side effects of chemotherapy and radiotherapy drastically affect the healthy tissues. Further, a tumor is a complex tissue in which cancer cells utilize the supporting information from the underlying stromal cells in order to develop into a malignant phenotype. Therefore, there is a strong need to characterize tumor heterogeneity as well as cross-talk between malignant cells and underlying support cells in order to generate

cancer cell specific chemotherapeutics and devise more effective treatment protocols. As a result of exploring better treatment protocols, tremendous research is going on at the interface of cancer cell-tumor microenvironment. In this, extracellular matrix (ECM) in the tumor microenvironment plays a pivotal role in supplying a dense network of structural as well instructional entities thereby regulating the function and fate of cancer cells.

During cancer development and progression, ECM undergoes continuous remodeling in terms of its composition and organization. Therefore, in order to generate critical and deep understanding of tumor biology and metastasis, it is indeed important to understand the influence of individual micro-environmental parameters on the aforementioned process. Although challenging, this further suggests that understanding tumor microenvironment may allow development of new paradigms in therapeutics. Gold standard techniques utilized till date are associated with two-dimensional (2-D) culture methods or in vivo tumor models. Although well established and thoroughly utilized, these techniques are associated with certain disadvantages thereby promoting the development of improved in vitro tumor models that along with simple in vitro culturing practice, recapitulates in vivo like characteristics. Although there are a number of techniques used for the development of three-dimensional (3-D) in vitro tumor models, tissue engineering has showed promising results as a new player in the field of in vitro tumor models (Hutmacher 2010; Hutmacher et al. 2010).

This chapter would begin with a brief overview of tumor microenvironment and its associated cells which would be followed by the significance and limitations of tumor models reported in the literature used for drug testing or studying tumor biology. Eventually, recent developments in the area of 3-D tumor models, with an emphasis on biomaterial-based ECM platforms developed using tissue engineering (TE) would be discussed.

2 Recapitulating the in Vivo Tumor Microenvironment

Stephen Paget proposed the “seed and soil” hypothesis that introduced the landmark role of tumor microenvironment in promoting tumor metastasis (Paget 1989). Certain organs are more susceptible to metastasis compared to others, which was hypothesised to be related to the fact that the ‘soil’ or local tumor microenvironment of the susceptible tissues promote conditions that allow tumor cells (seed) to grow in these organs than in others. It is the crosstalk between the ‘soil’ and the ‘seed’ that supports a subpopulation of cancer cells against chemotherapy, thereby contributing to drug resistance and hence treatment failure.

The tumor counterpart is defined by the genetically abnormal cells while the connective tissue framework of the tumor tissue is defined by the epithelial parenchyma of carcinoma, the surrounding and interwoven stroma (Mueller and Fusenig 2004). Tumor microenvironment or the framework in vivo comprises of

the ECM, which is the tumor matrix as well as the cellular components like the vasculature and supporting stromal cells; the microenvironment greatly influences tumor growth and invasive properties (Bissell and Radisky 2001) (Fig. 1). The non-neoplastic microenvironment (accessory cells) of a tumor consists of cancer-associated fibroblasts (CAFs), immune cells and endothelial cells (Mueller and Fusenig 2004) (Fig. 1). As mentioned previously, tumor microenvironment also comprises of the ECM and the secreted ECM molecules that may act in paracrine or autocrine fashion in order to support tumor growth and development. It is this interaction between the cancer cell and the surrounding ECM that governs the tumor phenotype. This has been exemplified by a study in mice, wherein authors demonstrated the role of human tumor derived stromal fibroblasts in the development of human breast tumor xenografts (Kuperwasser et al. 2004). Stromal cells by themselves are not malignant in nature. However, they are induced by the surrounding cancer cells to create a microenvironment that drives tumor progression (Li et al. 2007). Further, since the tumor stroma is genetically intact as compared to the tumor cells that undergo a series of mutations, they could be potential targets in cancer therapeutics.

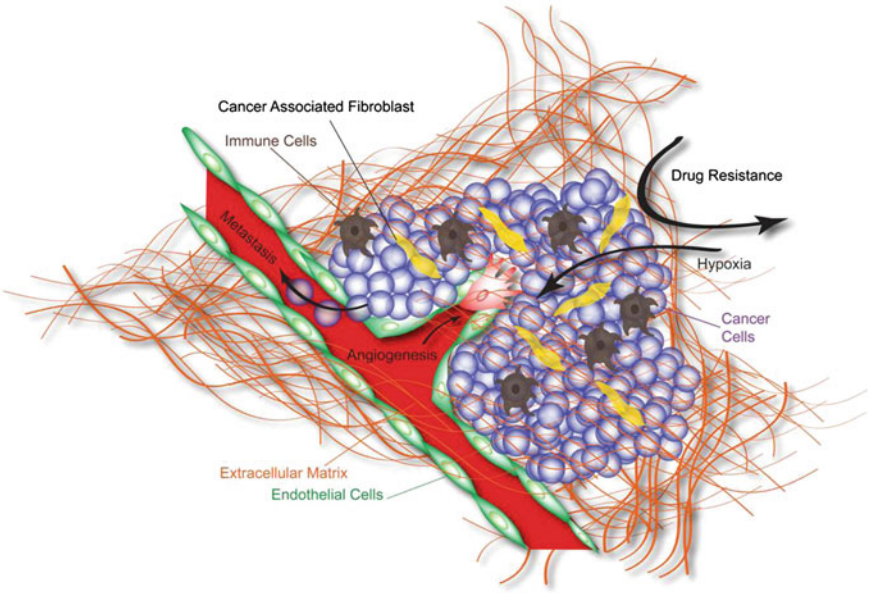

Fig. 1 Schematic demonstrating the in vivo tumor microenvironment. Tumor is embedded within a dense extracellular matrix and comprises of cancer cells as well as the non-neoplastic component (cancer associated fibroblasts (CAFs), immune cells and endothelial cells). Tumors in vivo are hypoxic in nature and the dense ECM can act as a diffusion barrier for anti-cancer drugs

2.1 Tumor-Stromal Cell Interaction

The role of tumor-stromal cell (mesenchyme) interaction in embryogenesis and cancer metastasis has been well established. Tumor cells secrete certain stroma-modulating growth factors (for example, basic fibroblast growth factor (bFGF), few members of vascular endothelial growth factor (VEGF) family, platelet-derived growth factor (PDGF), epidermal growth factor receptor (EGFR) ligands, various interleukins, colony-stimulating factors (CSFs) and transforming growth factor-β (TGFβ)) (Mueller and Fusenig 2004) that function in a paracrine fashion inducing angiogenesis (Bergers and Benjamin 2003) and inflammation (Coussens and Werb 2002) as a part of the stromal response. During this, other stromal cell types, for example, fibroblasts, smooth muscle cells (De Wever and Mareel 2003) as well as adipocytes (Manabe et al. 2003) are activated, which further induce the secretion of growth factors and proteolytic enzymes. Additionally, tumor cells also produce various proteolytic enzymes (Stetler-Stevenson and Yu 2001) that play an important role in ECM and basement membrane remodeling during metastasis. While the ECM degrades, it generates certain pro-migratory molecules/signals along with pro- and anti-angiogenic molecules. It is the matrix metalloproteases (MMPs) in the remodelled ECM which activate both the cell-surface and ECM bound growth factors and contribute to the cross-talk between the microenvironment and tumor cells. Further, the proteolytic enzymes secreted by tumor cells are mediated by the stromal environment. The next section will briefly discuss about the stromal cells within the tumor microenvironment.

2.1.1 Cancer Associated Fibroblasts

Fibroblasts are the most abundant type of cells in connective tissue and contribute to their structural framework via ECM secretion. During wound healing and fibrosis, quiescent fibroblasts are activated to myofibroblasts (MFs) (Gabbiani et al. 1971), which are characterized by the contractile stress fibers, expression of α-smooth muscle actin (α-SMA) and splice variants of fibronectin.

Tumor stroma, is also characterized by the presence of activated fibroblasts termed as peritumor fibroblasts, reactive stromal fibroblasts, CAFs or tumor associated fibroblasts (Mueller and Fusenig 2004; Kalluri and Zeisberg 2006) that are large spindle shaped mesenchymal cells and are present as a part of activated stroma of various cancers like breast (Chauhan et al. 2003), prostrate (Olumi et al. 1999) and skin (Skobe and Fusenig 1998) and have been demonstrated to affect tumor growth and progression. It has been shown previously that CAFs stimulate tumor progression in simian virus 40 (SV-40)—transformed normal prostate epithelial cells while normal fibroblasts did not induce any tumor formation (Olumi et al. 1999). Similarly, Skobe and Fusenig demonstrated the induction of tumorigenic behaviour in non-tumorigenic immortalized human keratinocytes (HaCaT) via activated stromal cells (Skobe and Fusenig 1998). Apart from tumor initiation, CAFs also play a role

in tumor progression. A previous study reported that co-injection of CAFs along with non-invasive cancer cells facilitate cancer cell invasion (Dimanche-Boitrel et al. 1994). In another study, it was shown that Ras-transformed MCF-7 cells generated tumors of bigger volume (indicative of tumor growth) when co-injected subcutaneously in immunodeficient nude mice with CAFs as compared to the ones injected with normal fibroblasts (Orimo et al. 2005). They also demonstrated greater angiogenesis in the former group and showed that the CAF-derived stromal-cell derived factor 1 (SDF1) is responsible for endothelial progenitor cell (EPC) recruitment, thereby playing a crucial role in tumor angiogenesis (Orimo et al. 2005).

CAFs share properties with smooth-muscle cells and fibroblasts, and stromal fibroblasts of solid tumors have been shown to express markers like α-SMA, vimentin, desmin and fibroblast activation protein (FAP) (Lazard et al. 1993). Further, CAFs are thought to originate from sources like fibroblasts, smooth muscle cells, pericytes or mesenchymal stem cells (MSCs) (Cirri and Chiarugi 2011; Lee et al. 2015). In this regard, tumor cells secrete growth factors like TGFβ, PDGF and bFGF that are responsible for activation of stromal cells (Elenbaas and A.Weinberg 2001). Once generated, they in turn activate tumor cells by secretion of pro-migratory molecules like tenasin (De Wever et al. 2004), upregulation of MMPs (Sato et al. 2004) and serine proteases, growth factors and cytokines (like insulin growth factor 1 (IGF1) which promotes tumor survival (Li et al. 2003) and hepatocyte growth factor (HGF) supports tumor cell migration and survival (De Wever et al. 2004; Lewis et al. 2004)). CAFs also promote a tumor progression environment as a result of VEGF expression that may stimulate angiogenesis (Orimo et al. 2001).

Given the essential contribution of CAFs in the stroma towards tumor progression, they may serve as crucial therapeutic targets and the therapeutics may be administered in combination with the conventional modes of cancer therapy. As an example, a cell-surface serine protease, FAP can be potentially used to target CAFs (Rettig 1993) since it is expressed by activated fibroblasts in the tumor stroma (Brennen et al. 2012; Julia et al. 2013). In this regard, a phase I dose escalation study was performed in patients with FAP positive cancer, wherein the patients were treated with sibrotuzumab, an antibody against FAP and was seen to be rapidly taken up by tumor tissue compared to normal cells. Although interesting, CAF targeting is still in its initial stages and needs further investigation.

2.1.2 Immune Cells

Tumors are usually infiltrated with immune cells like macrophages and T-lymphocytes that are responsible for cancer cell death. However, unlike the generation of a productive immune response against pathogens, immune cells like tumor associated macrophages (TAMs) within the tumor are impaired and incompetent (Kerkar and Restifo 2012). Over expression of inflammatory cytokines by tumor cells leads to recruitment of haematopoietic lymphocytes, macrophages as

well as neutrophils into the tumor environment (Coussens and Werb 2002; Pollard 2004). As an example, chemokine CC-motive ligand 2 (CCL2) is expressed by a variety of tumors namely, ovarian, cervical, bladder and breast tumors and is associated with poor prognosis in breast, cervical and bladder cancer (Pollard 2004). Further, colony stimulating factor 1 (CSF1) is one of the key growth factors responsible for growth and differentiation of mononuclear phagocytes (macrophages). It has also been shown to be widely expressed in tumors of ovary, breast, uterus as well as prostate and is also associated with poor prognosis (Smith et al. 1995; Kacinski 1997, 1995). Contribution of inflammatory cells in tumor progression was established by Lin et al. who performed experiments using CSF1-null mice and showed that the absence of CSF1 did not affect the incidence or the growth of primary tumors; however, its absence delayed the development of invasive carcinoma (Lin et al. 2001). In contrast, transient expression of CSF1 was associated with late staged carcinoma and enhanced infiltration of macrophages at the site of primary tumor indicating the role of CSF1 in promoting metastasis by macrophage infiltration at the tumor site.

Interestingly, haematopoietic growth factors like granulocyte colony stimulating factor (G-CSF) and granulocyte macrophage colony stimulating factor (GM-CSF) have been shown to contribute to tumor progression, especially in skin carcinoma, meningiomas and gliomas via the recruitment of inflammatory cells (Mueller and Fusenig 1999; Braun et al. 2004; Mueller et al. 1999). These growth factors also recruit EPCs for the induction of angiogenesis in the tumor (Obermueller et al. 2004). Macrophages also promote vascularization of the injected tumor cells via MMP-9 as well as VEGF (Amit-Cohen et al. 2013; Carmeliet and Jain 2000). In fact, a study by Coussens et al. demonstrated the role of tumor infiltrating mast cells in upregulation of angiogenesis (Coussens et al. 1999). In a transgenic mouse model of epithelial carcinogenesis (in which early region genes of human papilloma virus 16 (HPV16) were expressed in basal keratinocytes), mast cell infiltration led to the activation of MMP-9 and angiogenesis. Further, in mast cell deficient HPV16 transgenic mouse, premalignant angiogenesis was alleviated. MMP-9 null mice, on the other hand, demonstrated a decreased incidence of invasive tumor, however were indicative of greater keratinocyte differentiation. They were also high grade tumors and were more aggressive (Coussens et al. 2000). Additionally, the inflammatory cells express various angiogenic factors like VEGF, angiopoietin 1, bFGF, TGFβ, PDGF, tumor necrosis factor α (TNF-α) which induce and maintain tumor angiogenesis (Carmeliet and Jain 2000). It is through the release of the aforementioned factors that the stroma contributes to tumor progression.

2.1.3 Endothelial Cells

In order for a solid tumor to grow beyond 1–2 mm in diameter or to metastasize to distant locations, angiogenesis is a crucial phenomenon and takes care of the nutrient and oxygen requirements of the tumor. It was hypothesised in 1968 that tumors produce a ‘diffusible angiogenic substance’ (Ehrmann and Knoth 1968).

Further, it was proposed by Folkman in 1971 that tumor growth and metastasis was dependent on angiogenesis, thereby indicating the role of blocking angiogenesis in arresting tumor growth (Folkman 1971). Gullino further showed that a pre-cancerous tissue acquires property of angiogenesis while becoming cancerous, and this could be used as a therapy against cancer (Gullino 1978). 'Angiogenic switch' is a widely accepted model, wherein if the proangiogenic molecules are balanced by the anti-angiogenic molecules, it is turned off; however the switch is turned on when proangiogenic molecules favour angiogenesis (Hanahan and Weinberg 2000; Bouck et al. 1996). This is triggered by signals such as metabolic stress, immune stress, mechanical stress as well as genetic reasons.

Further, the leaky vasculature of solid tumor has been shown to promote tumor metastasis; high interstitial fluid pressure may facilitate efflux of cancer cells (Jain 2005). Leaky and haemorrhagic vasculature is contributed by the over expression of VEGF (also known as vascular permeability factor (VPF)). The phenomena of angiogenesis is regulated by endothelial cells; these cells residing in the tumor have an abnormal shape, ruffled margins, long cytoplasmic projections, high motility and possess leaky vasculature. In the early embryo, vasculogenesis takes place by recruitment of endothelial precursor cells from the bone marrow and their transport in the blood stream followed by incorporation into the growing blood vessel walls; this process has been adapted in adults and even tumors in some cases (Rafii et al. 2002).

Clinical trials for anti-angiogenic therapy are currently ongoing (Al-Husein et al. 2012) and are majorly based on interference with angiogenic ligands, upregulation of endogenous inhibitors or direct targeting of the tumor vasculature. However, they are associated with certain drawbacks; (a) pre-clinical studies were performed in subcutaneous tumors (b) tumor regression was considered as an end point for the treatment (c) few pre-clinical studies have focussed only on rapidly proliferating tumors. Additionally, as the tumors grow, they work through a wide variety of angiogenic molecules like VEGF, bFGF or interleukin-8 (IL-8). Therefore, blocking VEGF only would not be sufficient for anti-angiogenic therapy.

2.2 Tumor Hypoxia and Necrosis

Hypoxia was hypothesized by Thomlinson and Gray on the basis of necrotic regions (regions approximately 180 μm away from blood vessels) relative to blood vessels in human lung tumors (Thomlinson and Gray 1955). These are regions of low oxygen concentration as a result of disorganized and aberrant tumor vasculature with poor blood flow thereby resulting in decreased oxygen diffusion within the tissue. Hypoxia is toxic to both normal and cancerous cells, however cancerous cells adapt themselves to the hypoxic environment at the genetic level thereby allowing them to survive and proliferate in such an environment; this usually contributes to a malignant and aggressive tumor (Harris 2002).

Initial studies on hypoxia were done as tumor response to radiotherapy; radiotherapy works on the principle of free radicals generated from oxygen which lead to tumor cell destruction. However, since the cells in hypoxic regions were found to be radiation resistant, they continued to survive (Harris 2002). In another study, direct role of hypoxia was demonstrated by quantifying tumor oxygen supply with the help of oxygen electrodes (Höckel and Vaupel 2001; Höckel et al. 1999). The authors demonstrated that low oxygen tension in tumors is linked with increased metastasis in soft tissue sarcomas (Brizel et al. 1996).

In response to hypoxia, cells shift from aerobic to anaerobic metabolism and also induce the synthesis of new blood vessels. Cells respond to low oxygen levels through hypoxia-inducible transcription factor 1 (HIF-1), which further activates hypoxia-responsive genes like VEGF. Further, HIF-1α (which is a part of heterodimer HIF-1, the other part being HIF-1β) is associated with poor prognosis as well as therapeutic resistance to various types of cancers like head and neck, ovarian and oesophageal. Additionally, over-expression of HIF-1α has been reported in colon, breast, gastric, lung, skin, ovarian, pancreatic, prostate, and renal carcinomas (Zhong et al. 1999). Hypoxia inducible genes regulate various cell fate processes like proliferation, angiogenesis, metabolism, apoptosis, immortalization and migration; cancer cells have certain regulated mechanisms to take advantage of responses like angiogenesis and evade some of them like apoptosis. One of the most prominent regulation by HIF-1α is endothelial cell proliferation and blood vessel formation. Transcription of VEGF and its receptor (VEGF receptor 1- VEGFR/FLT-1), which are expressed by tumor and normal cells in response to hypoxia, is regulated by HIF-1.

Hypoxia targeted therapies include reduction of tissue hypoxia, administration of hypoxia activated pro-drugs and block HIF-1α itself or HIF-1α-interacting proteins.

2.3 Drug Resistance

As an anti-cancer drug encounters a solid tumor, its distribution is gradient oriented. Drug penetration in any tissue is governed by the phenomena of diffusion and convection. However, since the tumors usually lack a functional lymphatic system (Leu et al. 2000), there is high interstitial fluid pressure within the tumors (Jain 1996; Milosevic et al. 1998; Heldin et al. 2004), as a result of which convection is reduced leading to inhibition of drug/macromolecule distribution with the tumor. Tumor vasculature also influences the response to chemotherapy. On one hand, the anticancer drugs gain access to tumors via the blood supply, on the other hand, the leaky, disorganized, convoluted vasculature compromises delivery of anti-cancer drugs at the exact location.

The tumor ECM plays an important role in cancer cell survival by preventing drug penetration within the tumor (Tannock et al. 2002). Additionally, it also affects the sensitivity of cancer cells towards apoptosis (Croix and Kerbel 1997; Dalton 1999), primarily as a result of cancer cell interaction with each other within the

tumor (termed as cell-adhesion mediated drug resistance (CAM-DR) (Dalton 1999)) as well as with other components of tumor ECM. Further, the growth factors within the tumor ECM could also contribute to drug resistance. As an example, bone marrow stromal cells release interleukin-6 (IL-6) that not only influences myeloma cell survival and proliferation, but also contributes to anti-cancer drug resistance by preventing apoptosis (Jahangir et al. 2013; Chauhan et al. 1997; Lichtenstein et al. 1996). IL-6 prompts activation of pathways like JAK/STAT (Sansone and Bromberg 2012; Catlett-Falcone et al. 1999), MAPK (Ogata et al. 1997) and PI3-K/AKT (Wegiel et al. 2008; Hideshima et al. 2001; West et al. 2002), all of which regulate cell survival as well as apoptosis. Additionally, growth factors like IGF-1, epidermal growth factor (EGF) and bFGF play an important role in drug resistance through the activation of specific pathways (Denduluria et al. 2015; Guo et al. 1998; Miyake et al. 1998; Schmidt and Lichtner 2002).

ECM components also interact with cancer cell integrins and modulate anti-cancer drug resistance (Sethi et al. 1999; Hoyt et al. 1996; Kraus et al. 2002; Maubant et al. 2002). As an example, in small cell lung cancer (SCLC), ECM components like collagen IV, fibronectin and tenascin were found to be upregulated and were responsible for SCLC resistance against anti-cancer drugs (Sethi et al. 1999). This was mediated via integrin-ECM interaction as shown by blocking experiments using integrin β1 antibody/tyrosine kinase inhibitors that abrogated drug resistance. Apart from tumor-ECM interaction, ECM architecture also plays an important role in drug resistance. As an example, in breast cancer, basement membrane promoted polarised structures (as a result of basement membrane laminin and α6β4 interaction) that allowed protection against anti-cancer drugs (Weaver et al. 2002).

Further, tumor cells with stem-cell like properties have been described in a variety of solid tumors as well as haematopoietic malignancies and have been shown to confer drug resistance. These tumor cells are termed cancer stem cells (CSCs) and have been shown to represent a small sub-population of the tumor and have the capability of regenerating the entire tumor. CSCs have the ability to self-renew, differentiate or remain as a quiescent population. Drug resistance in CSCs is primarily due to over expression of specific ATP-binding cassette (ABC) transporters (like ABCB1, ABCG2, ABCC1 that represent three multidrug resistant genes (Gottesman et al. 2001; Dean et al. 2005; Dean 2009)), quiescent nature and their capacity for DNA repair. Another possibly contributing model is 'acquired resistance' wherein the CSCs expressing drug transporters survive, undergo mutation thereby leading to descendent cells with a drug-resistant property (Dean et al. 2005). Further, an 'intrinsic resistance' model suggests the presence of an inherently resistant phenotype of stem cells resulting in minimal effect following therapy. In this regard, clinical studies are currently being performed wherein combination chemotherapy of a drug transporter inhibitor (ABC transporter inhibitor) along with conventional anti-cancer agents are used. However, the aforementioned strategy with ABC transport inhibitors might be not useful since these inhibitors would also cause destruction of normal stem cells in vivo, thereby indicating the need to dwell more into CSCs-based therapies.

3 Gold Standard Techniques in Drug Testing

Conventional techniques used for drug testing and screening purposes include 2-D in vitro culture of cancer cells as well as small in vivo animal models (Cekanova 2014). However, they are associated with certain disadvantages (discussed in the following section) that have prompted the development of other reliable models. In this regard, 3-D models have been explored as potential bridging gaps between 2-D and in vivo models. 3-D models have demonstrated significant advantages compared to the aforementioned models and hence determine the state of the art of tumor models. The following section discusses about the advantages and disadvantages of 2-D and in vivo models and their comparison with intervening 3-D tumor models, Fig. 2 and Table 1.

3.1 Two-Dimensional Culture of Cancer Cells

Pharmaceutical industry and most laboratories perform routine 2-D culture of cancer cells for studying tumor biology and for drug screening assays. In these models, cancer cells are grown on a flat 2-D substratum as a monolayer allowing for easy culture as well as maintenance of cancer cells. 2-D flat culture of cancer cells has indeed added valuable information to the field of cancer biology. However, they fail to recapitulate the in vivo tumor microenvironment as they lack the cell-cell and cell-matrix interactions as well as signalling pathways involved in cell growth, metabolism and differentiation similar to in vivo (Smalley et al. 2006; Griffith and Swartz 2006; Yamada and Cukierman 2007). Further, 2-D monolayer culture lacks stroma, which forms an important part of breast cancer modelling as it accounts for a significant percentage of resting breast volume (Jo 1996). Absence of structural

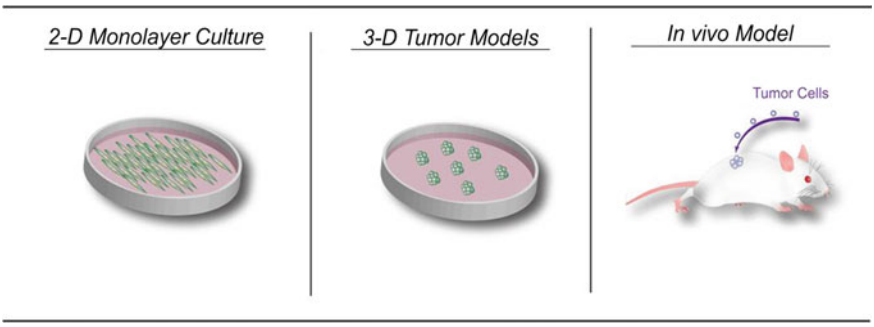

Fig. 2 Schematic demonstrating the models used for studying tumor biology and drug testing/screening application (*Left to Right* Two-dimensional (2-D) monolayer culture, Three-dimensional (3-D) tumor models and in vivo models)

Table 1 Advantages and disadvantages of tumor models

Type of model	Advantages	Disadvantages
2-D culture of cancer cells	• Simple, convenient • Cost effective • Allows easy monitoring of any change • Allows co-culture and downstream assays	• Lacks the right microenvironmental cues • Allows partial interaction of cells • Artificial cell polarization
3-D tumor models	• Simple, convenient • In vivo like cellular organization • In vivo like cell-ECM interaction • Allows co-culture and downstream assays	• Might require specialised equipments • Sometime difficult integration into high throughput screening process
In vivo models	• Representative of natural microenvironmental conditions • Genetically amendable models	• Increased time for experimentation • Expensive, ethical constraints, • Limited quantitation • No single animal model is true representative of multiple diseases

architecture in monolayer cultures also disables the property of transport limitation as observed in vivo, which is an important parameter for understanding drug resistance. Therefore, modeling of the 3-D environment through in vitro strategies is a potential alternative to overcome the disadvantages of 2-D monolayer culture.

As an example, human breast cancer cells, T4-2, derived from HMT-3522 (phenotypically normal cells), demonstrated differences in gene expression when cultured as 2-D monolayer as compared to 3-D basement model (Wang et al. 1998). When these cells were cultured as a 3-D basement model, they demonstrated concomitant down-regulation of β1-integrin as well as EGFR signalling, reversion of malignant behaviour of T4-2 cells to normal breast tissue morphogenesis and their subsequent growth arrest. This modulation was not observed in cells grown as 2-D monolayer culture. In another study, spheroids of breast cancer cell line (MCF-7) and its multidrug resistant variant (MDR-MCF-7) demonstrated decreased proliferation compared to their 2-D monolayer counterparts (Faute et al. 2002). Spheroid culture of MCF-7 further demonstrated reduced anti-cancer drug sensitivity in comparison to the 2-D culture, while the spheroid culture of MDR-MCF-7 demonstrated enhanced invasive properties compared to 2-D culture. In another interesting study, a non-small cell lung cancer (NSCLC) cell line, NCI-H460, when grown as 3-D cellular aggregates demonstrated enhanced expression of genes associated with metastasis, invasion and drug responsiveness as compared to cells grown on 2-D surfaces (Arya et al. 2012).

2-D culture are not only limited with respect to cell-cell and cell matrix interaction, but also with respect to other tumor properties like hypoxia. Hypoxic core is an important property of a solid tumor, wherein there is reduction in normal level of

oxygen tension within a tissue (Harris 2002). This property is present in a 3-D culture (Imamura et al. 2015), however, it cannot be mimicked by a 2-D monolayer culture wherein all the cells receive equal supply of oxygen as well as nutrients.

Therefore, the aforementioned limitations of a 2-D monolayer culture prompted the switch towards 3-D culture of tumor cells.

3.2 Animal Models

Modeling of human tumors in animal models has been widely used to study tumor biology as well as for drug screening purposes. Animal models are a better match to the human tumor microenvironment compared to 2-D monolayer culture since it has been reported that mouse models are predictive of chemotherapeutic drugs, when tested with clinically relevant doses (Kerbel 2003). Development of xenograft models of human tumors is most often performed by subcutaneous injection of cancer cells in immunodeficient or immunocompromised mice for a requisite incubation period for rapid assessment of tumor tissue (Richmond and Su 2008). However, due to the lack of immune system, these xenografts do not generate a response coherent to human tumors. Apart from such models, orthotopic mice models are also used, wherein cancer cells are implanted in respective tissues of interest in order to recapitulate the effect of microenvironment on tumor growth (Richmond and Su 2008). Additionally, metastatic and genetically engineered mouse models have also been developed and may contribute to drug testing/screening studies (Frese and Tuveson 2007). However, less than 8% of the results from animal models are successfully translated into clinical trials (Mak et al. 2014). Further, animal models are associated with disadvantages like high costs, increased incubation periods and ethical constraints which subsequently limit their potential. Therefore, the above mentioned limitations suggest the development of more refined 3-D models that have simple culturing practices and are able to recapitulate the body's response as well as potentially allow for temporal observation of the tumor development.

4 Intervention of Three-Dimensional Models

Due to the shortcomings associated with the gold standard 2-D monolayer culture and animal models, 3-D models have been developed as potential alternatives. These improved in vitro tumor models demonstrate simple culturing practices and also mimic in vivo cell-cell and cell-ECM interactions (Smalley et al. 2006). Spheroids (self-assembled aggregates/clusters of cells) generated using these models demonstrate a 3-D tissue architecture, cell arrangement as well as ECM deposition reminiscent of solid tumors in vivo. 3-D spheroids reflect some of the important properties of a solid tumor like tight junctions between epithelial cells

and metabolic (namely nutrients, oxygen and waste), proliferative as well as other macromolecular gradients (e.g. drugs) from exterior to the tumor core (Minchinton and Tannock 2006; Sutherland 1988). These steep gradients also result in formation of a necrotic core within the tumor center. These models are therefore advantageous since they provide an improved format to study kinetics of anti-cancer drug penetration within the spheroids (Minchinton and Tannock 2006). Additionally, spheroids hold the advantage to be cultured using two or more cell types along with CSCs (in ratios commensurating to in vivo) in order to understand the intercellular signalling and drug resistance as in vivo.

In the following sections, various types of 3-D in vitro models along with their advantages and limitations are discussed (Fig. 3 and Table 2).

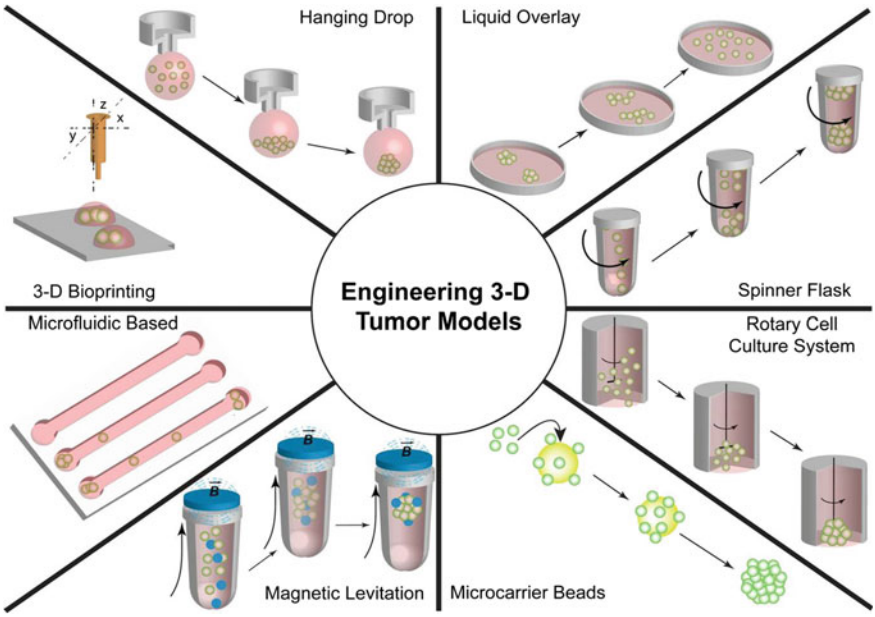

Fig. 3 Techniques for cancer cell aggregate/spheroid formation. *Clockwise* Hanging drop, liquid overlay, spinner flask, rotary cell culture system, microcarrier beads, magnetic levitation, microfluidic-based, 3-D bioprinting

Table 2 Advantages and disadvantages of 3D tumor models

Method type	Advantages	Disadvantages
Hanging drop	• Simple • Inexpensive when using standard 96 well plates • Easy spheroid harvesting • Uniform spheroid size	• Time consuming and labor intensive • Expensive with specialized plates • Medium exchange is difficult due to small volumes
Liquid overlay	• Simple and inexpensive • Allows for rapid and easy screening	• Spheroid heterogeneity in terms of size and number • Tedious medium exchange
Spinner flask spheroid culture	• Simple • Multicellular spheroid production on a large scale • Long term culture	• Requires specialized equipment • Shear forces may alter cell physiology • Requires bulk quantities of cell culture medium • Inconsistent spheroid size • No individual compartment for each sample
Rotary cell culture system	• Exerts minimal shear forces • Long term culture • Produces more differentiated epithelial like architecture • Mass production of spheroids	• Requires specialized equipment • May involve manual selection of uniform sized spheroids • No individual compartment for each sample
Microcarrier beads	• Allows for culture of cells that are difficult to grow or sensitive cells or attachment dependent cells • Allows for culturing of high proportion of cells in small volumes	• It is possible to generate pseudo-spheroids with large number of microcarrier beads
Magnetic levitation	• Non-invasive technique to pull cells together	• Magnetic particles might affect cell viability and functionality
Microfluidic 3-D tumor model	• Reduced reagent consumption and cost • Allows spatio-temporal control in micron sized channels • Flexibility of device design • Perfusion culture	• Complicated setup and device manufacturing • Smaller volumes might necessitate frequent medium change • Material compatibility with drug screening studies • Issue with long term culture • Issue with spheroid retrieval • Lack of isolated unit for each sample
3-D bioprinting of cancer cells	• Provides spatial and temporal control over cell seeding • Well organized constructs	• Reduced cell viability • Affect native phenotype/functional behavior of cancer cells
Scaffold-based	• Provides an external support (extracellular matrix mimic) for cell attachment and cell fate processes • Easy to set up • Long term culture • Compatible with multiwell plates	• Sample (Cell) retrieval might be difficult • Issues related to scaffold biocompatibility and biodegradability

4.1 Different Types of 3D Models

4.1.1 Hanging Drop Method

This is one of the easiest techniques to culture tumor cells in a 3-D format. Spontaneous aggregation into spheroids is a well characterized and established methodology due to its ability to generate reproducible spheroids and their similarity to near native tissue (Tung et al. 2011; Kunz-Schughart et al. 2004). This methodology of spheroid aggregation has been exploited by the technique of hanging drop. In this method, a small droplet of cell suspension (single cell or multiple cell can be used) is pipetted into wells (Fig. 3) of a multiwell plate that holds the droplet in place following its inversion by virtue of the surface tension. Density and type of cell suspension could be varied on the basis of desired spheroid size or type. Following pipetting and as a function of time, the cells within the droplet accumulate at its tip, self-aggregate at the liquid-air interface and eventually proliferate. During this technique, moisture/humidity within the plate is maintained in order to prevent drying of the droplet containing the cell suspension.

This technique has the advantage of being simple, inexpensive and reproducible in terms of generating a single spheroid per droplet and results in tightly packed spheroids of cells. As an example, Kelm reported patho-physiologically relevant 3-D spheroids of HepG2 and MCF7 cell lines that were described as tissue-like since they produced their own ECM (Kelm et al. 2003). In a study by Amann et al., lung cancer cells were co-cultured with lung fibroblasts in order to understand tumor-stroma interaction and development of a more in vivo like 3-D tumor model (Amann et al. 2014). Co-culture of lung cancer cells (A549) with lung fibroblasts led to enhanced vimentin and cytokeratin levels with a concomitant drop in Epithelial-cadherin (E-cad) levels compared to A549 only spheroids suggesting an epithelial to mesenchymal transition (EMT) in co-cultured spheroids. In another study, effect of loss of a gene function on spheroid formation and its maintenance was studied using a colorectal 3-D tumor model generated by hanging drop method (Horman et al. 2013). In this study, Horman et al. silenced specific integrin receptor and receptor tyrosine kinase (RTK) genes in order to study inhibition of spheroid formation (Horman et al. 2013) and demonstrated a new screening platform for potential therapeutic intervention. This technique has been widely used for the generation of cancer cell spheroids for application in drug screening (Tung et al. 2011).

Hanging drop technique has also been commercialized by companies like 3-D Biomatrix and InSphero. 3-D Biomatrix has developed 96 as well as 384 well plate format that support 3-D culture of cells on a larger scale since such platform allows for production of large number of spheroids in a single plate. The plate system developed by 3-D Biomatrix comprises of a hanging drop plate, a bottom tray and a lid. The hanging drop plate consists of access holes that act as regions for cell suspension to form a hanging drop and a plateau structure on the plate bottom helps in stabilization of the hanging drop. This plate then sits on the bottom tray that has a

reservoir around its periphery, usually filled with PBS in order to provide a humidified chamber and the entire system is covered with a lid. Hanging drop plates from 3-D Biomatrix has been utilized by a number of researchers (Tung et al. 2011; Hsiao et al. 2012; Wagner et al. 2013; Guzman et al. 2014; Lamichhane et al. 2016) and demonstrates potential to overcome the disadvantage of medium change and allows for easy spheroid development (96–384 spheroids at a time), handling and maintenance. However, the problem of medium volumes persists. Further, the hanging drop plate designed by Insphero (http://www.insphero.com/) is similar to the hanging drop plate by 3D Biomatrix in terms of cell seeding as well as medium exchange through the top port of the well plate. It consists of a 'Trap plate' that allows for easy harvesting of the spheroids. Further, the proprietary non-adhesive coating permits culturing over weeks while the micro tissue remains in suspension. This has also been used widely for development of 3-D tumor models (Anastasov et al. 2015; Falkenberg et al. 2016).

The technique of hanging drop utilizes the property of self-aggregation of cancer cells to each other and not any other external substrate, it makes sure that there is no effect of any external factors or their degradation products on the 3-D spheroids. However, hanging drop technique is associated with the difficulty of medium aspiration without causing any disturbance to the 3-D spheroid. Further, since hanging drop is based on manual pipetting, it is time consuming and labor intensive. Therefore, hanging drop method has been clubbed with bio-printing technology (Sect. 4.1.7) in recent studies which is reported to be simple, robust, rapid as well as generate spheroids of uniform size (Xu et al. 2011a).

4.1.2 Liquid Overlay Technique

In liquid overlay technique, the spheroids are formed due to stronger adhesive forces between cells compared to forces between cell and the underlying matrix. The spheroids are formed on a non-adhesive or attachment limiting substrate like agarose or non-adhesive petri dish and are usually present in a suspension (Yuhas et al. 1977), thereby promoting cell-cell attachment as compared to cell-substrate attachment. Liquid overlay technique involves two steps: the cells are grown over agar coated tissue culture plates, wherein the cells migrate towards each other resulting in cell-cell aggregation and spheroid formation. In the second stage, the cellular aggregates grow in size. Although there are other hydrophobic materials like poly (2-hydroxyethyl methacrylate) available for generation of non-adherent coating (Tong et al. 1992), agar remains the material of choice due to its low cost.

In a study by Mayer et al., a multicellular gastric cancer spheroid model was developed in vitro by liquid overlay method and was compared with xenografts in immunocompromised mice (Mayer et al. 2001). They demonstrated that out of 17 gastric cancer cell lines, 12 were able to recapitulate properties of parental gastric carcinoma when cultured as 3-D spheroids. In another interesting study, human prostate tumor cells were cultured as 3-D spheroids using liquid overlay technique and were compared to cells grown on 2-D substrates and as solid tumors in vivo

(Takagi et al. 2007). It was shown that the global gene expression profile under in vivo conditions was similar to 3-D tumor models, thereby demonstrating that the 3-D spheroids generated in vitro can be used as an alternative to xenografts as avascular in vitro models.

Although this technique is simple and inexpensive to set up in the laboratories, it is associated with disadvantages like heterogeneity in size and cell number. This could potentially be overcome by the generation of single spheroid within agar coated 96 well plate. The concave surface of agar would promote generation of single spheroid per well, of similar size and composition.

4.1.3 Spinner Flask Spheroid Culture

Spinner flask culture is one of the two agitation technique used for growing cells in suspension culture (Kim 2005; Lin and Chang 2008). The other technique is rotary cell culture system/bioreactor (RCCS) and is described in the next section (Sect. 4.1.4). Briefly, in agitation based cultures, cell suspension is placed in moving phase within a container (which is either gently stirred in case of spinner flask culture or rotated as in case of RCCS). Mobility prevents cell attachment to the wall of the container, and favours cell attachment to each other resulting in formation of 3-D spheroids.

Spinner flask bioreactors were developed by Sutherland et al. (1970) and were widely used for the generation of multicellular spheroids on a large scale. Also referred to as spinners, these bioreactors contain an impeller that maintains the cells in suspension or stirring mode. Dynamic motion may provide an advantage of nutrient as well as waste transport to and from the spheroids respectively. While the liquid overlay technique is suitable for cultivation and monitoring of single spheroids, spinner flask bioreactor is suitable for large scale culture of spheroids. Although spinner flask technique has been used for the generation of spheroids on a large scale, shear forces generated in this technique may alter the cell physiology (Lin and Chang 2008). Further, it also requires cell culture medium in bulk volumes and often results in inconsistent size of spheroids. This might require additional manual selection of similarly sized spheroids. In order to overcome the disadvantage of inconsistency in spheroid size, some researchers follow a two-step procedure, wherein the spheroids are initially formed on agarose coated plates (using liquid over technique) followed by their transfer to spinner flasks (Hirschhaeuser et al. 2009).

Hirschhaeuser et al. generated spheroids of FaDu (head and neck squamous cell carcinoma) by first culturing them on plates coated with 1.5% agarose followed by their transfer to spinner flasks when they reached diameter of around 700–800 μm (Hirschhaeuser et al. 2009). These spheroids were then co-cultured with peripheral blood mononuclear cells and the co-cultured spheroids were eventually evaluated for a therapeutic antibody for potential application in immune-cell mediated anti-cancer effects. In another study, Kim and Forbes utilized spheroids in understanding the effects of HIF-1α on the survival and intracellular metabolism of 3-D

spheroids (Kim and Forbes 2007). These spheroids were generated using single cell suspension of *ras*-transformed mouse embryonic fibroblasts (derived from mouse embryonic stem cells) in culture flasks coated with polyhydroxyethyl methacrylate (PHEMA), following which the spheroids were then transferred onto spinner flasks. As a next step, spheroids of two different dimensions were harvested and it was observed that larger spheroids comprised of a quiescent population demonstrating lower rates of energy metabolism and biosynthesis and high anaerobic to aerobic ratio (suggesting the effect of oxygen gradient on cellular metabolism) as compared to smaller spheroids. However, the ratio remained unchanged in wild-type and HIF-1α-null spheroids prompting that response to oxygen gradients is independent of this factor, suggesting its minimal role in metabolic microenvironment of 3-D spheroids. In another study, the effect of zinc sulfophthalocyanine ($ZnPcS_{mix}$) photosensitization on multicellular spheroids of varying sizes was studied (Manoto et al. 2015). These spheroids were cultured by growing A549 cells on agarose coated flasks followed by the transfer of cell aggregates to spinner flasks. Spheroids (500 and 250 μm) as well as monolayer culture were then exposed to photodynamic therapy (PDT) and it was demonstrated that the larger spheroids were less susceptible to PDT compared to smaller spheroids as well as monolayer culture, suggesting the importance of 3-D spheroids in PDT studies in vitro.

Further development of this technique as well as commercially available systems such as the Wheaton spinner flasks and the ones from Corning are expected to contribute to a broader dissemination of such technique for the large scale production of spheroids.

4.1.4 Rotary Cell Culture System

RCCS is similar to spinner flask bioreactor, except that the cell suspension is maintained via rotation of the suspension container itself. RCCS was introduced by NASA in 1992 wherein, it mimics microgravity and maintains cells in a suspension with the help of minimal hydrodynamic forces thereby exerting minimal shear force on the suspended cells (Goodwin et al. 1993). It comprises of a culture flask/vessel that rotates on its horizontal axis; constant rotation causes end to end mixing thereby preventing the cells from adhering to the chamber walls. Since the culture vessel is completely filled with culture medium, low fluid turbulence as well as low shear forces is a feature maintained in the culture chamber (Kim 2005). Additionally, hydrodynamic forces are also minimized since optimal aeration is provided through a semi-permeable membrane which eliminates air bubbles (Kim 2005). Low fluid turbulence provided in RCCS is an advantage, since agitation due to excessive stirring has been reported to cause cell damage (Goodwin et al. 1993). Further, low agitation rates provided by RCCS enhance aggregate formation by cellular bridging (Cherry and Papoutsakis 1988). Initially, rotational speed is maintained in a way that the culture medium as well as the cells demonstrate a synchronous rotation in lieu of low shear forces (Unsworth and Lelkes 1988). Once the aggregates are formed and

increase in size, rotational speed is enhanced to take care of the sedimentation rates of cells in the previous step (Unsworth and Lelkes 1988).

It has been demonstrated that RCCS allows generation of tissue constructs that are similar in their composition and other physical properties to the in vivo constructs (Unsworth and Lelkes 1988). Smith et al. performed thorough characterization of tumor spheroids of brain generated using RCCS. 3-D tumor model based on central nervous system (CNS) cancer cell lines was compared with cells grown on 2-D surfaces and it was observed that brain tumor aggregates generated by RCCS demonstrated morphology similar to brain tumors in vivo and depicted a proliferating rim, central necrotic region and oxygen gradient. Further, gene expression and metabolic profiles of RCCS aggregates demonstrated an intermediate phenotype between 2-D culture and in vivo tumors (Smith et al. 2012). Another interesting study by Laguinge et al. used a 3-D tumor model based on human colorectal carcinoma cells developed using RCCS and demonstrated the process of anoikis in these aggregates by virtue of fluid shear stress (Laguinge et al. 2004). They demonstrated that low fluid shear stress environment and 3-D growth of cancer cells increased levels of nitric oxide (NO) synthase compared to cells on 2-D surface, resulting in loss of microtubules thereby leading to anoikis. Results of this study indicate that increased intracellular NO (by using RCCS) could be a potential therapy to prevent metastasis.

Although the cells experience low shear stress in RCCS along with the possibility of long term culture, it requires specialized equipment and may involve manual selection of homogenous spheroids unless preceded by liquid overlay culture of spheroid formation using single cancer cell.

4.1.5 Microcarrier Beads

Microcarriers are spherical beads, of diameter around 500 μm and their enormous surface demonstrate potential to culture high density of cells in smaller volumes. Cell culture based on microcarrier beads is a convenient method for 3-D culture of cells and majorly supports aggregate formation of attachment dependent cells as well as cell lines that do not aggregate spontaneously (Kim 2005). These beads provide a platform for culturing sensitive cells or those that are difficult to grow, for example, endothelial cells (Davies 1981). Microcarrier beads could also be used for co-culture studies (Johns et al. 1995) and also find application in understanding cell-cell as well as cell-substrate interaction. In fact, these beads are often added to spinner flasks or RCCS in order to promote cell attachment on the bead thereby enabling spheroid formation.

Microcarrier beads can be either solid or porous in nature. Porous beads have an advantage of manipulating cellular response to gradients (both chemical and molecular) in 3-D similar to in vivo conditions (Barrila et al. 2010). Microbeads are adhesive spheres to which the cancer cells adhere. Adhesion is followed by cell growth and microbeads eventually degrade leading to the formation of a cellular

aggregate. Non-degradable beads can also be used, in which case the beads remain within the spheroid core. Currently available beads differ in their coating, for example, dextran cores coated with diethylaminoethyl (DEAE), trimethyl-2-hydroxyaminopropyl groups (Kim 2005). Microcarrier beads can also be coated with cell adhesion promoting materials like gelatin, collagen or laminin. One such commercially available microcarrier beads are from GE Healthcare that comprise of a thin layer of gelatin chemically coupled to cross-linked dextran matrix. It allows for easy microscopic examination of attached cells due to its transparent nature. Apart from this, Solohill Engineering and Global Cell solution provide animal-free coated microcarrier beads and a magnetic microcarrier with an alginate core coated with a thin gelatin layer (Global Eukaryotic Microcarriers—GEMs) respectively. The latter acts as a unique porous matrix that upregulates cell polarity and provides metabolic functions similar to in vivo. Presence of magnetic core allows greater control over sample while medium exchange or harvesting. Additional coatings such as basement membrane and laminin on GEMs have also been synthesised in order to allow for attachment of primary as well as stem cells. GEM is an optically clear and non-auto fluorescent platform that allows for easy visualization of cells and have also demonstrated application in absorbance and luminescence assays with cells still attached to them.

As mentioned previously in this section, microcarrier beads are usually combined with other techniques like spinner flask bioreactor or RCCS. To support this, Skardal et al. developed a microcarrier bead coated with a synthetic ECM (sECM) comprising of hyaluronan and gelatin hydrogel cross-linked through disulphide linkages and were applied for culturing human intestinal epithelial cells (Skardal et al. 2010). The sECM coating was designed in a way that it could be dissolved under mild conditions in order to release the cellular aggregates for further maturation in RCCS. The aggregates demonstrated >94% viability following recovery and were then successfully transferred to RCCS. Other studies demonstrated culturing of prostate and lung cancer cells (Rhee et al. 2001; Maurer et al. 1999). Microcarrier beads have also been applied for expansion of primary cells like chondrocytes (Malda et al. 2003) and mesenchymal stem cells (Yang et al. 2007).

Microcarrier beads are advantageous since they allow spheroid formation of attachment dependent cancer cells in high density. However, they require special coating on their surface for cell attachment. Further, the mechanical property of the microcarrier beads needs to be characterized since they might have an influence on fate of cancer cells.

4.1.6 Magnetic Levitation

Recently, magnetic techniques have been adopted for 3-D cell culture (Xu et al. 2011b; Gurkan et al. 2012; Tasoglu et al. 2014; Guven et al. 2015). In magnetic levitation, cells are labelled with magnetic materials (either paramagnetic or diamagnetic) and incubated in cell culture medium. The cells are then levitated on a

liquid-air interface using a magnetic force subsequently resulting in the formation of a 3-D cluster (Fig. 3).

This technique has been used for the generation of 3-D tumor spheroids that are reminiscent of tumors in vivo. As an example, Lee et al. demonstrated the application of iron oxide (Fe_3O_4)-encapsulated poly(lactic-co-glycolide) (PLGA) microparticles or poly(l-lactic acid)-*b*-poly(ethylene glycol)-folate [PLLA-*b*-PEG-folate] nanoparticles as substrates for magnetic levitation of human epidermoid tumor KB cells (Lee et al. 2011). In another study, the authors reported magnetic levitation of human glioblastoma cells in the presence of a hydrogel comprising of gold, magnetic iron oxide nanoparticles and filamentous bacteriophage (Souza et al. 2010). They demonstrated that the 3-D tumor model based on human glioblastoma cells exhibited gene expression profiles similar to the ones shown by human tumor xenografts. More specifically, Neural-cadherin (N-cad) showed a scattered expression in the cytoplasm and nucleus when grown on 2-D substrates; however, in 3-D levitated cells, N-cad expression was seen in the membrane, cytoplasm and cell junctions and was similar to the protein expression pattern in tumor xenografts. This system may find application in development of other complex tissues as well.

Apart from monoculture of cells using magnetic levitation method, it has also been used for co-culturing of breast cancer cells with fibroblasts in order to develop an improved in vitro tumor model, thereby allowing for homotypic and heterotypic cell-cell interaction (Jaganathan et al. 2014). The aforementioned model demonstrated histological similarity to in vivo tumors and also demonstrated enhanced fibronectin expression compared to 2-D co-culture. They were also able to control the density of the spheroid by controlling the initial seeding density of the cells used. Further, doxorubicin demonstrated a significant decline in viability in 2-D co-culture compared to 3-D tumor model thereby indicating that the 3-D structure developed using magnetic levitation method was indeed able to mimic physical barriers like stromal cell composition as well as cell density similar to in vivo tumors. Although magnetic levitation has been applied in the field of 3-D tumor models, it has also been utilized in adipose tissue engineering (Daquinag et al. 2013) as well as in the design of model for angiogenesis (Lin et al. 2008).

The aforementioned reports demonstrate the advantages of using magnetic levitation method. However, this technique utilizes magnetic nanoparticles that could potentially affect cell viability. Further, the use of magnetic nanoparticles has been approved by the FDA in applications like imaging agents. However, their use as 3-D spheroid models, in drug testing as well as tissue engineering requires further toxicological analysis (Laconte et al. 2005).

4.1.7 Microfluidic 3-D Tumor Models

3-D systems as potential tumor models described previously have overcome the limitations of traditional 2-D systems as well as in vivo models leading to new insights. However, the conventional 3-D tumor models do not capture sufficient

spatial organization, cell-cell interactions, lack vasculature and do not allow medium exchange in a continuous manner (van Duinen et al. 2015). Further, the sample volumes required in traditional 3-D tumor models make them inappropriate as models for high throughput screening applications. Therefore, scientists have introduced a potential alternative to the conventional 3-D systems, which function as improved in vitro models with reduced volumes and costs for high throughput screening applications with spatio-temporal control in micrometer-sized channels. Spatial control over cells in systems based on microfluidics provides an advantage of culturing multiple cell types that could potentially recapitulate cell and tissue organization in a more faithful manner. Further, microfluidics allow for precise control over gradients due to spatial control over fluids. Systems based on microfluidics have demonstrated application in cancer biology as well as drug screening/testing studies (Bischel et al. 2015; Bersini et al. 2014; Pavesi et al. 2016; Zervantonakis et al. 2012; Bruce et al. 2015; Chen et al. 2015).

As an example, Bischel et al. developed a microscale model of ductal carcinoma in situ (DCIS) that recapitulated crucial features of DCIS in order to understand why some types of DCIS become invasive (Bischel et al. 2015). In the first step, viscous finger patterning was used to line the lumen structures with ECM-based hydrogel (comprising of collagen I and Matrigel as the outer and inner layer respectively); following this, a DCIS model was generated by lining the lumens with a non-cancerous human mammary epithelial cell line, MCF10a followed by MCF10aDCIS cells. It was demonstrated that the 3-D model completely recapitulated the comedo-type DCIS in humans. In the next step, co-culture of human mammary fibroblasts (HMF) with DCIS lumen models induced invasion of DCIS, which was characterized by the sprouting of invasive lesions from the lumen filled with DCIS cells, loss of E-cad, and increased collagen I modification around the invasive lesion. The aforementioned results demonstrate the potential of viscous finger patterning method in the development of physiologically relevant tumor models.

In another interesting study, 3-D tumor-endothelial intravasation microfluidic-based assay was designed and it was observed that interaction with macrophages impaired the endothelial barrier and resulted in enhanced intravasation of breast cancer cells (Zervantonakis et al. 2012). Intravasation was also enhanced in the presence of soluble biochemical factors like TNF-α. Therefore, modelling of interactions between the invading cells and the endothelium in a microfluidic based 3-D environment may lead to new avenues for understanding endothelium barrier functions as well as trans-endothelial migration in other physiological processes as well. Bruce et al. developed a 3-D microfluidic cell culture platform to study acute lymphoblastic leukemia (Bruce et al. 2015). For this, they cultured biologically relevant population that constitute bone marrow microenvironment, namely, human bone marrow stromal cells, osteoblasts and human leukemic cells in a collagen matrix; the engineered triculture model imparted precise control over the mechanical properties as well as shear stress. Apart from demonstrating decreased cell spreading on the 3-D microfluidic platform, the triculture model also demonstrated decreased sensitivity to cytarabine (antimetabolite based chemotherapeutic) as compared to cells on 2-D surface.

Pavesi et al. developed an electrode embedded microfluidic device for alternating electric field therapy to cancer cell in a near physiological environment (3-D extracellular matrix) (Pavesi et al. 2016). Application of alternating electric field stimulation led to reduced viability in single cells (breast cancer) as well as lung cancer aggregates. Moreover, it led to selective cell death of breast cancer cells in a co-culture of breast cancer cells and endothelial cells thereby demonstrating a potential treatment protocol that could be combined with conventional therapeutics. Chen et al. on the other hand, developed a microfluidic sphere formation platform for demonstrating the efficacy of photodynamic therapy as an alternative treatment for cancer that is not affected significantly in cancer cells when they were co-cultured with CAFs (responsible for imparting resistance to conventional chemotherapy) (Chen et al. 2015).

Although microfluidic-based 3-D tumor models provide spatio-temporal control, reduced reagent consumption and involve perfusion culture, they are associated with certain disadvantages. They involve a complicated setup and there may be issues of material compatibility while screening hydrophobic drugs. Further, low cell numbers might not allow for downstream biochemical studies. Nevertheless, such systems demonstrate potential for advanced research in the area of 3-D tumor models.

4.1.8 3-D Bioprinting of Cancer Cells

This technique was first described by Charles W. Hull in the year 1986. The technique was initially called stereolithography, wherein thin layers of a material that could be cured using UV light were printed in a sequential manner in order to develop a 3-D structure (Hull 1986). It was then applied towards the formation of 3-D scaffolds using biological materials, for potential transplantation application and was further developed to work at the interface of cell biology and materials science as a part of TE domain (this term has been explained later, Sect. 5.1). 3-D bioprinting has found application in the area of stem cell technology, cell biopreservation as well as cancer research (Tasoglu and Demirci 2013; Xu et al. 2011a; Assal et al. 2014; Asghar et al. 2014; Gurkan et al. 2014; Visconti et al. 2015; Assal et al. 2015).

Briefly, 3-D bioprinting allows for generation of 3-D structures through layer-by-layer patterning of biomaterial, biochemical factors as well as the cells of choice with spatial and temporal control over the distribution and placement of functional components (Murphy and Atala 2014). It has been utilized for the generation of 3-D constructs with precise biological and mechanical properties for restoration and repair of organ functions. In 3-D printing, technologies utilized for the deposition and patterning of biological materials include inkjet bioprinting (Xu et al. 2005; Xu et al. 2013; Xiaofeng Cui et al. 2012a), microextrusion (Shor et al. 2009; Iwami et al. 2010; Cohen et al. 2006) and laser assisted printing (Guillemot et al. 2010; Guillotin et al. 2010; Barron et al. 2004).

Inkjet bioprinting is a common method used for biological as well as non-biological applications. Early conventional inkjet printers replaced the ink with a biological material and paper with an electronically controlled stage to modulate the *z* axis (Zohora et al. 2014); these methods are now custom-designed. Inkjet printers primarily uses either thermal (Xiaofeng Cui et al. 2012a) or acoustic forces (Demirci and Montesano 2007) for the generation of printed constructs. Thermal printers causes heating of the printer head to around 200–300 °C thereby releasing droplets from the nozzle. However, it is reported that short heating durations do not raise the temperature of printer head by more than 4–10 °C, hence localized high temperatures have not been reported to affect the stability of biological macromolecules, like nucleic acids (Murphy and Atala 2014) or cell viability (Xu et al. 2005, 2006). Although this technique demonstrates high speed of printing and low costs, it imposes critical challenges like increased exposure of living cells as well as biological macromolecules to thermal and mechanical stress, non-uniformity in droplet size, clogging of nozzle and difficulty in achieving droplet directionality (Murphy and Atala 2014). As an alternative to thermal inkject printers, printers based on acoustic waves were designed in order to allow for breakage of liquid droplets at regular intervals resulting in uniform droplet size. Acoustic waves can be generated using a piezoelectric material (Tekin et al. 2008) or an ultrasound field (Fang et al. 2012). Acoustic inkject printers are advantageous compared to their thermal counterparts since one can precisely control the droplet size, direction of ejected material as well as prevent exposure of live cells to high temperature and pressure.

In general, inkjet bioprinters have demonstrated low cost, high speed, compatibility with a large number of biomaterials. It has also been reported to generate gradients of cells as well as biological materials by alteration of droplet size or density (Campbell et al. 2005; Phillippi et al. 2008). However, it suffers from the limitation of using a material in liquid form in order to allow for droplet formation and its subsequent gelation or setting in a 3-D structure. It is also associated with decreased cell densities, cell viability and functionality.

Microextrusion is one of the most popular techniques as a non-biological 3-D printer. It extrudes the bioink (comprising of cell containing materials) with the help of pneumatic pressure (Kolesky et al. 2014; Lee et al. 2016a) or mechanical pressure like a piston (Visser et al. 2013). Dispensing systems based on mechanical pressure may provide a greater direct control over the material to be extruded since pneumatic systems are associated with a delay in compressed gas volume. With the help of the robotic movement of the printing head, the extruding stream is deposited on the fabrication plate in *x*, *y* and *z* directions. This is a faster process compared to inkjet or laser-assisted printing techniques. Further, microextrusion allows deposition of high cell densities and even multicellular spheroids which later on develop into a desired 3-D construct. However, viscous fluids cause the exposure of cells to high shear stress thereby leading to decreased cell viabilities as compared to inkjet printing.

Laser assisted bioprinting method relies on the ‘aim and shoot’ principle in order to deposit cell containing suspension using a laser beam (Jang et al. 2016;

Murphy and Atala 2014). This can be performed using laser-guided or laser-induced techniques. In laser guided technique, a laser beam is introduced into a cell suspension and the difference in refractive index of cells and the culture medium causes the laser beam to trap and direct the cells on the depositing substrate. Laser induced technique, on the other hand, starts with the production of cell containing droplets by focussing the laser beam on cell encapsulated hydrogel support (ribbon). Cell containing droplets are then transferred to the depositing/receiving substrate due to formation of laser-induced vapour pockets. Since this technique does not require a nozzle for formation of cell droplet; there are no clogging issues associated with the process unlike with the other bioprinting techniques. Further, this technique causes negligible effect on printed mammalian cells (Gruene et al. 2011; Hopp et al. 2005). However, due to the formation of ribbon cell coating, the process of cell deposition is a random process with inability to target and position the cells at precise locations (Guillotin and Guillemot 2011). Laser assisted printing causes the vaporization of laser absorbing metallic layer, subsequently resulting in presence of metallic residues in the final product (Guillotin and Guillemot 2011). Further, generation of single printed cell type or hydrogel type requires a single ribbon/vapour pocket. It is therefore time consuming, if one needs to co-deposit multiple cell or material types.

3-D bioprinting has been used for fabrication of tissues of skin (Skardal et al. 2012; Michael et al. 2013), and cartilage (Cui et al. 2012b), deposition of nano-hydroxyapatite in a mouse calvaria 3-D defect model (Keriquel et al. 2010) as well as medical devices that have been transplanted back into the patients (Zopf et al. 2013), few other tissues and tumor models (Duan et al. 2013; Norotte et al. 2009; Xu et al. 2011c).

As an example, Zhao et al. generated a cervical tumor model in vitro by 3-D printing of HeLa cells and hydrogels based on gelatin/alginate/fibrinogen (Zhao et al. 2014). A layer-by-layer construct was generated by forced extrusion which resulted in a spheroid morphology and tight cell-cell contact on day 5 as compared to cells grown on 2-D culture that demonstrated flat and elongated morphology. Cells in the 3-D printed model also demonstrated higher MMP-2 and MMP-9 expression compared to cells on 2D surface thereby demonstrating enhanced metastatic properties in former condition. They also showed enhanced chemoresistance in the 3-D printed model compared to cells on 2-D surface. Finally, the printing parameters led to more than 90% viability of HeLa cells demonstrating the potential of 3-D bioprinting in tumor model development.

In another interesting study, a co-culture model based on ovarian cancer was developed using a high throughput cell printing system (Xu et al. 2011c). In this, patterning of human ovarian cancer cells (OVCAR-5) and human fibroblasts (MRC-5) on Matrigel^{TM} was performed using a spatially controlled environment (pertaining to cell density and cell to cell distance). The environment also controlled the shear forces on the cells that were created during droplet formation, which in turn led to high cell viability post-cell ejection (more than 96%, 4 h post patterning). Micropatterned OVCAR-5 cells proliferated in Matrigel^{TM} and formed 3-D acinar structures, recapitulating micronodule property of ovarian cancer as in vivo

and may find potential in better understanding of ovarian cancer biology as well as therapeutics.

Next section will focus on the scaffold-based 3-D tumor models with a brief introduction on tissue engineering (TE) followed by the state of the art of TE in 3-D tumor models.

5 Role of Tissue Engineering in Development of 3-D Tumor Models

5.1 Tissue Engineering

Tissue engineering (TE) was developed with the aim to create organs which could solve the shortage of donor organs for transplantation purpose (Langer and Vacanti 1993). Towards this goal, various strategies have emerged that work at the interface of recent advances in field of developmental biology, biomaterials science and medicine. In that endeavor, materials that support the growth, organization and function of cells obtained from tissue biopsy were developed (Smeriglio et al. 2015). This led to landmark discoveries that helped in understanding interaction at the cell-biomaterial interface. Further, diverse experiments have demonstrated that the mechanical properties of the cell substrate play a major role in the cell organization, differentiation and migration (Reilly and Engler 2010; Discher et al. 2009). Likewise, the surface topography was demonstrated to impact the cell fate processes (Fisher et al. 2010). Progress in molecular biology further led to application of short cell-interacting peptides for decoration of synthetic materials thereby leading to introduction of targeted biological signaling into synthetic systems. These experiments have not only widened the knowledge in the area of cell biology, but have also led to advances in field of biomaterials science for the creation of biocompatible materials that reproduce the natural microenvironment of mammalian tissues.

Although, the current state of TE research will not be able to deliver synthetic organs anytime soon, learning and technologies developed can be used to create models that replicate disease behavior and help to better understand their progression while offering an accurate platform for testing of novel therapeutics (Kim 2005). Therefore, TE aims towards the fabrication of disease models that could be potentially used for understanding disease biology as well as for drug development and testing. Till date, skin tissue replicates are routinely used by cosmetics companies for the testing of product formulation, the first replicate tissue kidney model is now available for drug testing and a pre-eclampsia disease model was recently introduced for understanding of disease biology (Kuo et al. 2016). These models pave the way toward the broadening the role of in vitro tissue engineered disease models across research areas.

5.2 Scaffold-Based Three-Dimensional Models

In cancer biology, it was rapidly discovered that cancer cells cultured on 2-D substrates behave differently as compared to in vivo tumors (Bissell and Radisky 2001). In order to capture these differences, different in vitro models were utilized to reproduce the mechanical properties, growth factors, cell binding anchoring systems and appropriate cells that mimic the native tumor tissue microenvironment. In the previous sections, strategies and methods commonly used for spheroid formation were described; this section focuses on scaffold based 3-D models. These models aim to provide cancer cells with ECM mimics that will direct their organization into a potential in vivo-like tumor. This approach significantly distinguishes itself from the strategies utilized for spheroid formation as the ECM is not formed by the single cells during their course of aggregation into spheroids but is artificially provided before the cells organize themselves into tumor tissues. As the cells invade the scaffold and multiply, the ECM required to promote tumor development is then secreted by the seeded cells. In case of a biodegradable support material, the scaffold degrades as the cells proliferate within the artificial ECM. Additionally, while the spheroid approach works well for cellular aggregation, it failed to reconstruct the natural tumor progression, i.e., invasion of a healthy tissue by cancer cells and subsequent ECM remodeling to promote tumor growth and evolution. Furthermore, spheroid models do not understand the role played by the ECM in cancer invasion, progression and resistance to anticancer drugs. In order to recapitulate these critical steps to understand tumor biology and eventually apply these 3-D tumor models for drug testing studies, biomaterials of natural or synthetic origin have been utilized and are described in the following sections. While the synthetic materials offer the possibility to mimic the natural architecture as well as mechanical properties of the tumor and to study the impact of each of these specific features on the tumor progression and spreading, they lack key biological signals. This is because cell attachment to the material is solely dictated by its chemical composition. As an example, non-adherent materials, such as agarose will not offer the possibility for cancer cells to spread and will facilitate the aggregation of cells with each other (Liu et al. 2014). In contrast, materials such as poly(lactic acid) (PLA), provide cell adhesion through the deposition of proteins onto the material surface. However, these interactions are non-specific, as they do not target a specific cell receptor such as integrin binding receptor. In order to trigger a signaling cascade through dedicated cell receptors, signaling molecules need to be introduced onto the synthetic materials. This is possible through the attachment of cell-binding peptide sequences such as the arginine-glycine-aspartic acid (RGD) (Re'em et al. 2010), proteins such as fibronectin or coating of the synthetic materials with natural ECM molecules such as collagen (Gillette et al. 2008). In order to incorporate biological signals into in vitro ECM models, natural macromolecules such as collagen have also been directly utilized as a scaffold (Hartman et al. 2009).

Further, macromolecules can be used as such or modified and processed for the creation of a microenvironment which exhibits specific properties like porosity,

architecture and substrate stiffness; few examples are discussed in the subsequent sections (Sects. 5.2.1–5.2.4). The tissue mimics generated from natural and synthetic scaffolds can then be utilized for understanding tumor biology as well as for the testing of potent anti-cancer molecules. Comparison of scaffold based 3-D models to 2-D monolayer culture demonstrated modulated drug response by cells grown on 3-D substrates, mostly attributed to drug diffusion barriers and up regulation of drug resistance genes (Arya et al. 2012). This could greatly help to understand the drug kinetics and toxicology thereby offering a better way to mimic natural tumor tissues. Additionally, few of these models in comparison to small animal models could possibly offer an alternative to it in the future. In this regard, technologies developed by research laboratories need to consider specific requirements of the pharmaceutical industry such as: scalability of the technique, ease of production and incorporation of the model into industrial processes such as high throughput screening.

In the following sections, several techniques that have been used to engineer tumor microenvironments are presented: porous scaffolds, hydrogels, microparticles and polymeric fibers, Fig. 4. Each of them is illustrated by recent examples and their ability to mimic in vivo tumor features.

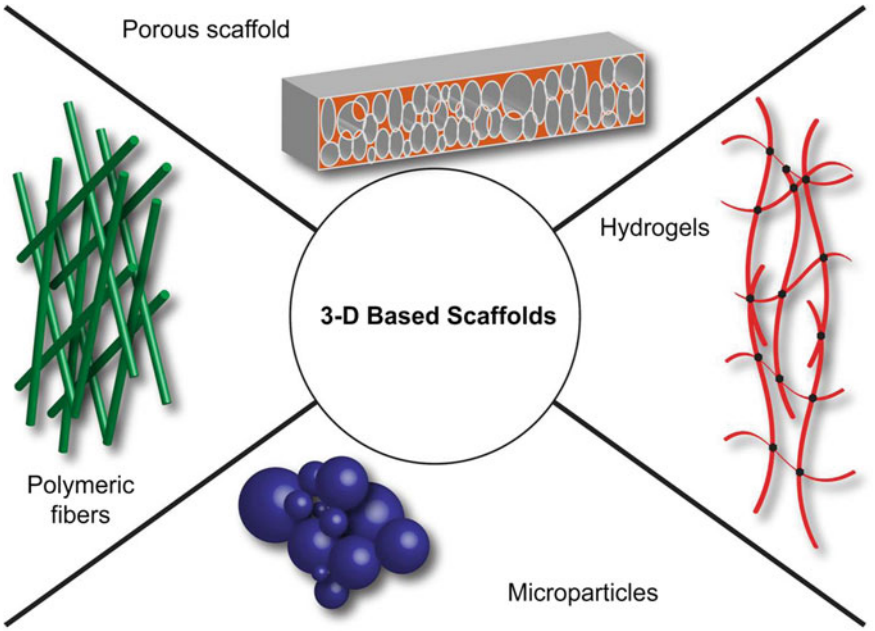

Fig. 4 Three-dimensional (3-D) biomaterials-based scaffolds developed for tissue engineering and adapted for 3-D culture of cancer cells and simulation of tumor ECM

5.2.1 Porous Scaffolds

Porous scaffolds are defined as matrices that have hollow pores at the micrometer scale. Different manufacturing techniques have been developed for their fabrication; most of them are based on a similar process: cross-linking of polymer chains dissolved previously in a solvent followed by solvent removal thereby resulting in a porous network (Lozinsky et al. 2003; Tripathi and Melo 2015). The porous scaffold could then utilized as an ECM mimic. In tumor models, this is of particular interest as scaffolds can reproduce the invasion and migration of cancer cells into a tissue and can also induce spheroid/cell aggregate formation. Techniques utilized for the manufacturing of porous scaffolds have been refined over the years and most of the systems can have a tunable pore size as well as mechanical property. These scaffolds have been utilized for the fundamental understanding of spheroid formation and cancer cell migration in a 3-D system.

Different crosslinking strategies have been defined in order to fabricate natural and synthetic based porous scaffolds. One of the most common system used for manufacturing of porous scaffolds is poly(vinyl alcohol) (PVA) cryogel (Lozinsky and Plieva 1998). PVA is a physical thermo-gelling polymer that forms cross-linking junctions between the polymer chains through hydrogen bonds. Briefly, the polymer is frozen in water and repeated freeze-thaw cycles allow for the generation of pores of different sizes (Lozinsky and Plieva 1998). For generation of chemically cross-linked scaffolds, the most common cross-linker is glutaraldehyde (GA), which has been extensively used to cross-link natural macromolecules. As an example, chitosan was crosslinked with GA for fabrication of porous scaffolds (Lai 2012). However, this cross-linker is cytotoxic and the resulting scaffolds need to be washed thoroughly prior to utilization. As an alternative, non-cytotoxic chemistries can also be used; genipin has been utilized to cross-link gelatin and chitosan (Arya et al. 2012). Other biocompatible chemistries such as the thiol–furan reaction have been reported towards the cross-linking of hyaluronic acid (HA) with polyethylene glycol (PEG); a solution of water and non-reactive monosaccharide was used as a porogen (Tam et al. 2016). This led to formation of transparent porous cryogels that are of special interest in 3-D culture imaging. Additionally, photo cross-linking has also been developed to cross-link modified natural polymers such as HA (Bian et al. 2013). This technique allows to control the site of cross-linking using a laser beam and can be used to create gradient of stiffness within the 3-D scaffolds (Zhou et al. 2011; Lin et al. 2011; Smeds et al. 2001).

The removal of the support solvent, so called porogen, can be achieved by different techniques. One of the most common methodologies for aqueous solvent removal is freeze drying, which is based on the sublimation of the water: frozen scaffold is subjected under vacuum wherein the frozen water sublimes leaving behind a porous network. Alternatively, the scaffold can also be dehydrated and water can be replaced by a volatile solvent such as ethanol, and a similar process used for mammalian tissue processing for histological examination is followed thereafter. Briefly, water in the scaffold is replaced with ethanol or other volatile water-miscible solvents by immersing the scaffold into successive gradients of

ethanol-water. Finally, the sample is left for drying; ethanol is removed thereby resulting in a porous scaffold. Porosity can also be generated through a foaming process; the cross-linking reaction generates a gas that form pores within the scaffold. This strategy avoids the recourse of solvents and allows for faster fabrication of porous scaffold. The precise control over the reaction stoichiometry and concentration of the reactants in the polymer solution enables a control over the reaction kinetics and gas generation, which in turns impacts the porosity of the scaffold. This technique was successfully utilized for the fabrication of PEG-caprolactone copolymer scaffolds (Ozcelik et al. 2014).

The aforementioned techniques can also be utilized for the fabrication of scaffolds with a defined elastic modulus by manipulating the biomaterials and the pore size and can be used to mimic tumor architecture under in vitro conditions. Such scaffolds have been used for the culture of prostate cancer cells (LNCaP) and offer a better tissue mimic than from comparative techniques such as hanging drop or 2-D monolayer culture (Göppert et al. 2016). Other cancer cells were also shown to behave differently on 3-D porous scaffolds in comparison to cells on 2-D monolayer culture (Arya et al. 2012; Talukdar et al. 2011). In an interesting example, breast cancer cells were seeded in a HA-PEG porous scaffold functionalized with cell binding peptide sequences. This study showed that the IKVAV peptide sequence, integrin binding sequence of laminin, induced the formation of T47D breast cancer cell spheroids while the RGD peptide sequence, integrin binding sequence of collagen, induced the formation of a monolayer (Tam et al. 2016). Similar porous systems have been also integrated into array chips suitable for the high throughput screening (HTS) assays to test the efficiency of anti-cancer drugs on cancer cells (Li et al. 2014a). A synthetic scaffold based on poly(lactide-co-glycolide) (PLG) (Fig. 5a) generated by gas foaming-particulate leaching was used to culture oral squamous cell carcinoma (OSSC-3) cells and the generated cancer model demonstrated hypoxic cores (Fig. 5b). It also led to production of pro-angiogenic factors like VEGF and IL-8 similar to in vivo tumors (Fischbach et al. 2007) (Fig. 5c). It was also observed that OSSC-3 as well as Lewis lung carcinoma cells cultured on 3-D PLG scaffolds and implanted into immunocompromised and immunocompetent mice respectively led to formation of bigger tumors as compared to those originating from same number of viable cancer cells previously cultured on 2-D monolayer substrates (Fig. 5d).

In another study, a natural biomaterial obtained from silkworm was used to fabricate a porous scaffold through freeze-drying technique. LNCaP prostate cancer cells cultured on these scaffolds were compared to Matrigel and 2-D monolayer culture. Characterization of the MMP-9 activity, glucose consumption and lactate production demonstrated that LNCaP cells on 3-D silk scaffold behaved similar to in vivo tumors (Talukdar et al. 2011). Other type of porous scaffolds based on chitosan-gelatin (CG) matrix demonstrated their relevance for the testing of anti-cancer drugs. For this, NCI-H460 cells (NSCLC cell line) were cultured on these 3-D porous scaffolds based on CG generated by freeze drying (Fig. 6a, b). CG scaffolds resulted in cancer cell aggregate formation (Fig. 6c(i), d); aggregates were not formed on CG films or 2-D tissue culture polystyrene (TCPS) surface (Fig. 6c (ii), (iii)). Further, the size of these aggregates increased as a function of time

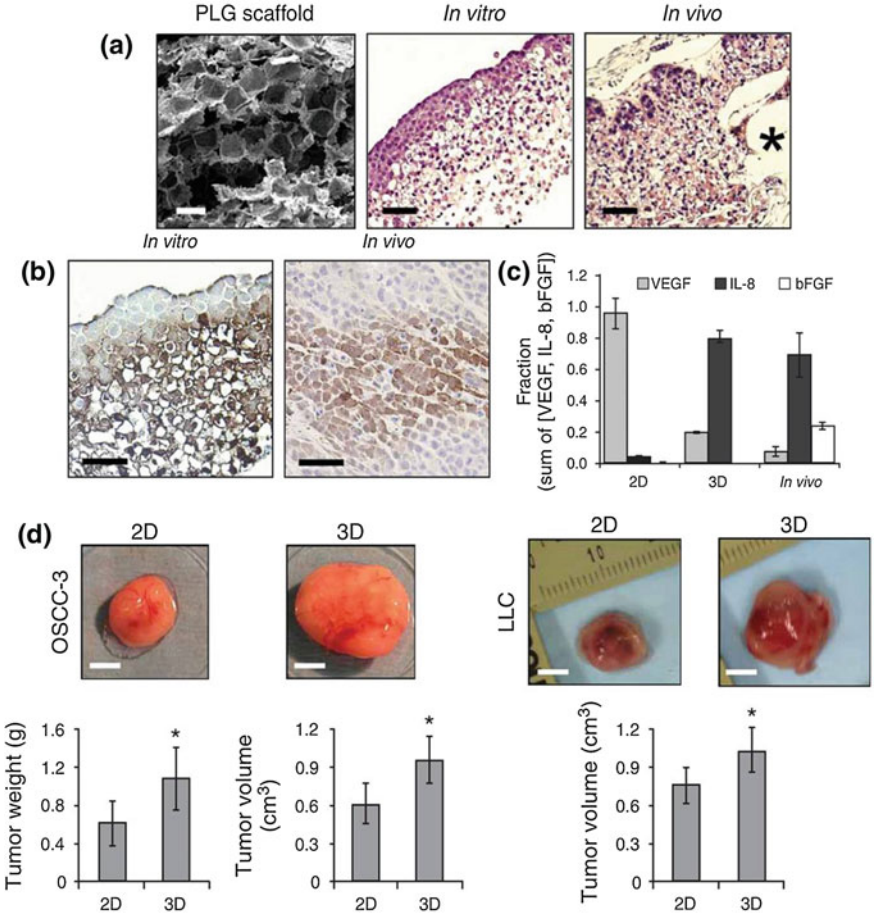

Fig. 5 Poly(lactide-co-glycolide) (PLG) scaffolds as potential in vitro tumor model for oral squamous cell carcinoma (OSSC-3) cells. **a** Scanning electron micrograph of OSCC-3 cells seeded PLG scaffold, H&E stained section of OSCC-3/PLG construct grown in vitro and in vivo. **b** Histological analysis of hypoxia OSCC-3/PLG construct grown in vitro and in vivo following staining with hypoxyprobe. **c** Comparison of pro-angiogenic factors (VEGF, IL-8 and bFGF secretion represented as a fraction of cumulative secretion of all the factors) after OSSC-3 culture on 2-D surface, 3-D scaffolds and as in vivo tumors **d** Comparison of tumor growth of OSCC-3 cells in SCID mice and mouse Lewis lung carcinoma (LLC) in C57BL/6J mice after pre-culture in 3-D PLG scaffolds or 2-D monolayer culture. (Adapted with permission from reference Fischbach et al. Nature Methods 2007)

(Fig. 6c(i)) and demonstrated enhanced reactive oxygen species compared to cells grown on 2-D surfaces (Fig. 6e). These aggregates also exhibited similar gene expression profiles as in vivo xenografts as well as enhanced survival in the presence of anti-cancer drugs compared to cells grown on 2-D substrates (Arya et al. 2012). In another study, utilization of natural biomaterials such as collagen,

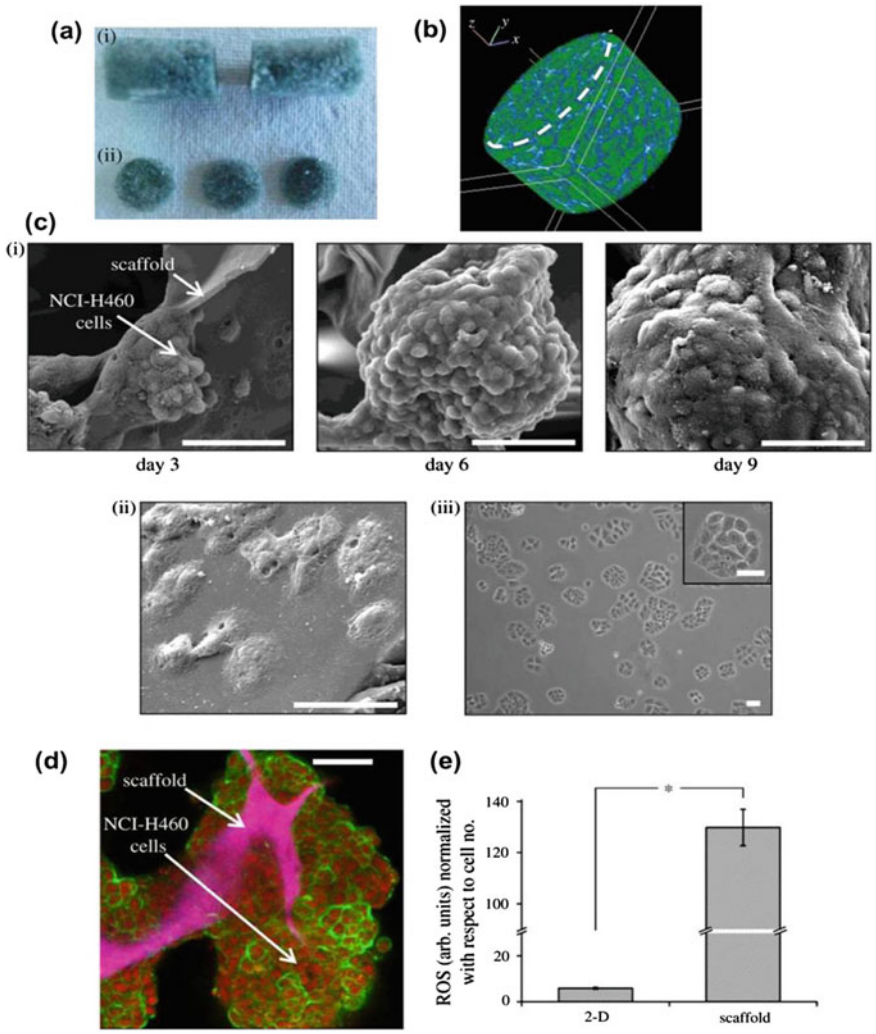

Fig. 6 Chitosan-gelatin (CG) 3-D porous scaffold as potential 3-D lung tumor model. **a** Digital photograph and **b** micro computed tomography demonstrating interconnected pores of CG scaffold fabricated by freeze drying technique **c** scanning electron micrographs of NCI-H460 cells on (*i*) 3-D CG scaffolds at the end of day 3, 6 and 9 (*ii*) CG films (*iii*) Phase contrast image of NCI-H460 cells on 2-D tissue culture polystyrene (TCPS) (Scale bar: 50 μm). **d** Confocal micrograph of NCI-H460 tumoroid on CG scaffold stained with phalloidin (actin) and propidium iodide (nucleus), Scale bar: 50 μm **e** Reactive oxygen species (a.u.) levels in NCI-H460 cells grown on 2-D TCPS and 3-D CG scaffolds normalized to cell number. (Adapted with permission from reference Arya et al. (2012), copyright 2012, Royal Society Publishing Group)

recapitulated natural features of the ECM such as enzymatic degradation. Gene profile demonstrated that MCF-7 cells (breast cancer cells) seeded onto 3-D collagen porous scaffolds expressed stem cell markers and further implantation of

the scaffold in an animal model formed larger tumors (Chen et al. 2012). One of the hallmarks of cancer is metastasis, i.e. migration of cell from its site of primary tumor to other sites resulting in secondary tumors. It is indeed interesting but a complex process to be recapitulated within 3-D in vitro models. While it is not known what triggers cell migration/metastasis, identification of these early parameters could help to develop an early diagnosis. Towards this goal, a synthetic porous scaffold made of poly(ε-caprolactone) (PCL) was utilized to generate a 3-D tumor model based on breast cancer with high metastatic potential. MDA-MB-231 cells cultured on these scaffolds showed increased invasiveness in vitro and lung metastasis in vivo (Balachander et al. 2015).

The previous section dealt with diverse techniques utilized for spheroids formation. Although spheroids can provide a 3-D geometry, they do not completely replicate the in vivo cell behavior. In contrast, seeding of the U251 (glioblastoma) spheroids within a porous 3D scaffold was shown to be a more appropriate model since the cells exhibited higher drug resistance compared to cells grown on 2-D substrates or spheroids on 2-D surface or single cells seeded onto the scaffolds. Additionally, spheroid seeded scaffolds demonstrated enhanced lactate production and higher expression of angiogenic factors as well (Ho et al. 2010). Such an in vitro tumor model takes advantage of the engineered scaffold along with the cell-cell interaction from the spheroid culture. Therefore, such systems can also be used to complement spheroid culture by providing a support structure to the tumor cells that the spheroid techniques do not provide. Taken together, due to the ease of use and scalable manufacturing, porous scaffolds demonstrate potential for the in vitro screening of novel anti-cancer molecules.

5.2.2 Hydrogels

Hydrogels are organized 3-D networks of macromolecular chains that connect together at cross-linking points. As the name indicates, hydrogels are able to retain large quantities of water similar to native tissue. Hydrogels can be also fabricated from natural or synthetic biomaterials similar to porous scaffolds. During their fabrication, density of the crosslinking points can be modulated by different processes according to their assembly mechanisms; covalent bonds for chemical hydrogels or physical interactions between the polymer chains for physical hydrogels.

Several hydrogel systems have been developed that promote the formation of tumor like spheroids from single cells. Hydrogels made of natural ECM-based macromolecules are one of the most utilized systems as they provide an environment comprising of mechanical properties as well as biological factors suitable for generating tumors in vitro. Matrices such as BD Matrigel® and Trevigne Cultrex® have been widely used across research laboratories for tissue engineering applications. These basement membrane extracts are routinely obtained from mouse sarcoma (Engelbreth-Holm-Swam, EHS) and can be used to culture various human

cancer cell lines (Kleinman and Martin 2005; Benton et al. 2014). They resemble the native tissue microenvironment and comprise of laminin, collagen and entactin as 60, 30 and 8% respectively. It also contains MMPs that play an important role in ECM remodeling (Kleinman and Martin 2005). Although experiments with basement membrane extracts work quite well (Webber et al. 1997; Shekhar et al. 2001), it is an animal product and does not completely recapitulate the human biology due to absence of large quantities of collagen-I and hyaluronan, suffers from batch to batch reproducibility and is not fully characterized in terms of soluble growth factors (Asghar et al. 2015).

Apart from Matrigel systems, natural materials made of a single ECM macromolecule have been used for the fabrication of hydrogels based 3-D cell culture. Such models are less complex than decellularized matrices and reconstitute a part of the ECM features. As an example, collagen hydrogels were used for the formation of tumor like environment with breast cancer cell lines, showing basal polarization of the cells dispersed within the hydrogel (Holliday et al. 2009). Other materials such as HA were chemically modified to form hydrogels and used as a 3-D support matrix for encapsulation and 3-D cluster formation of poorly adherent prostate cancer cells. HA hydrogel system was further utilized for testing the efficacy of anti-cancer drug like camptothecin, docetaxel, and rapamycin, alone and in combination (Gurski et al. 2009). In another study, bilayer HA hydrogels were formed wherein LNCaP prostate cancer cells embedded in the bottom layer received growth factors like heparin-binding epidermal growth factor-like growth factor (HB-EGF) from the top layer. Cells embedded in the HA scaffolds released significantly higher amounts of VEGF and IL-8 as compared to cells on 2-D surfaces thereby demonstrating the use of HA hydrogel model in studying tumor cell response to growth factors (Xu et al. 2012).

In order to decipher the impact of ECM features like mechanical properties, growth factors and cell-ECM signals, synthetic hydrogels have been developed. Such systems reproduce the 3-D microenvironment found in human cancer and helps in the identification of key features that enable early cancer diagnosis, understanding metastasis as well as for recapitulating tumors as in vivo for the testing of potent anti-cancer drugs. In the following section, synthetic hydrogel systems along with their potential for 3-D cellular aggregate formation for application in drug testing and understanding tumor biology are discussed. Different synthetic biocompatible polymers capable of hydrogels formation were developed previously for TE applications (Williams 2008). Following similar protocols, these materials have also been applied for 3-D tumor model development. Usually, cancer cells are dispersed within the hydrogel solution and upon mixing or use of external stimuli, the polymer chains cross-link and the cells are captured within the polymer network. The gelation process, i.e. cross-linking of the polymer chains, can occur through a chemical reaction (chemical cross-linking), or through the physical interactions between polymer chains domains (physical cross-linking) (Patel and Mequanint 2011).

Several techniques have been used to chemically cross-link synthetic and natural biopolymers in order to create hydrogels. Chemical reactions that occur under

physiological conditions enable cancer cell dispersion within a polymer solution before cross-linking. Amongst the various techniques, click chemistry has been the focus for a couple of decades with a promise to provide quantitative reaction with no side-products. As an example, the possibility to have an organism expressing amino acid bearing azide, which is of particular interest for in vivo protein labeling, is based on the Staudinger and 1, 3 Huisgen reactions. The Staudinger reaction is the reaction of an azide with a phosphine. Its modification enables its use under physiological conditions and is termed as Staudinger ligation (Saxon 2000; Saxon et al. 2000). The rather low stability of phosphine in air has led to the development of a new reaction: the 1,3 Huisgen cyclo-addition, which involves an alkyne and an azide to form a stable cycle with a copper catalyst (Nimmo and Shoichet 2011; DeForest et al. 2009). The introduction of activated cyclo-alkyne was a major step for the translation of this reaction to the biological field as it has removed the need of cytotoxic copper (Jewett et al. 2010). Other click reactions, Diels Alder addition and Michael S-addition have also been used for hydrogel cross-linking under physiological conditions (Koehler et al. 2013; Nimmo et al. 2011; Sui et al. 2010). Other strategies include the reaction of hydroxylamine with an aldehyde resulting in an oxime, which was successfully used for cross-linking of star PEG (Grover et al. 2013); the reaction of ketone with a primary amine giving rise to an imine (Kim et al. 2011), which has been used for the cross-linking of chitosan with a tri-block copolymer (PEO-PPO-PEO) (Ding et al. 2010); and the reaction of hydrazine with a ketone resulting in a hydrazone bond (Dahlmann et al. 2013). Natural proteins such as gelatin are modified with sulfated amino acids that are able to form disulfide bridges under physiological conditions. This reaction has been successfully used for the cross-linking of a modified HA with gelatin (Shu et al. 2002) or with HA and PEG (Choh et al. 2011). Further, boronic acid can quantitatively react with di-alcohol of specific geometry under physiological conditions. This strategy has been used with a modified PEG polymer to stabilize micelles and used as drug carrier by cross-linking the polymer chains (Li et al. 2012).

Polymer chains can interact with each other and form strong reversible cross-linking points. These interactions are governed by physical principles and directed by external stimuli such as pH, temperature and ionic strength. A modification of these parameters can impact the chain conformation of the polymer and create or destruct the 3-D hydrogel network. Reversible hydrogels can be obtained through ionic interaction wherein multiple valence cations can act as cross-linkers between two polyelectrolyte chains, such as in alginate polysaccharide (Rezende et al. 2007). This has been used in many biological applications such as for culturing of glioblastoma cells following immobilization of RGD peptide on the alginate backbone (Zustiak 2015). Alginate has also been reported for fabrication of 3-D cell culture systems for NSCLC-based spheroids followed by anti-cancer drug and nanoparticle uptake studies (Godugu et al. 2013). Similar to other studies, results demonstrated enhanced inhibition concentration 50 (IC50) values in alginate matrices as compared to the cells grown on 2-D surfaces. An alternative method for physical cross-linking is the aggregation of crystallization domains such as

α-helical domain that interacts with each other and forms cross-linking points that are temperature dependent. Among different polymers undergoing aforementioned network organization, agarose and the carrageenan family (possessing α-helical domains) form hydrogels by aggregation of these specific domains (Sanabria-DeLong et al. 2006; Arnott et al. 1974). Agarose has been used also as a 3-D substrate for cell culture, especially chondrocytes (Luo and Shoichet 2004; Emans et al. 2010). The non-adhesive property of agarose has also been utilized for the development of cancer models and formation of cancer cell spheroids (Xu et al. 2014; Zanoni et al. 2016). Weak interactions between the polymer chains can become strong with increase in their probability of occurrence. Based on this principle, it is possible to form strong interaction with polymers that exhibit hydrogen-bonding ability (Cantin et al. 2011; Kimura et al. 2004; Sekiguchi et al. 2003). One of the most commonly used natural and biocompatible polymer in biological application is cellulose that forms a β-sheet network through hydrogen-bond interaction (Bhattacharya et al. 2012; Granja et al. 2005). Synthetic polymers can also be engineered to form physical interaction by synthesis of block copolymer with blocks of polymers with different hydrophilic behavior (Artzner et al. 2007). As an example, poloxamer class exhibits such behavior wherein one block is hydrophilic and the other hydrophobic, such as pluronic (Higuchi et al. 2005). Physical hydrogels have recently attained much attention, as they can be utilized for 3-D printing and other extrusion methods. Dispersion of the cells within a hydrogel matrix form 'bioink' that can be used to precisely organize cells thereby reconstituting the complex natural organization of living tissues.

5.2.3 Microparticles

Particles of the order of nanoscale have been used in intracellular delivery of drugs and genes. Micro- and nano-particle manufacturing has been mainly developed with optimized parameters to achieve controlled release profile for delivery of bioactive agents. Based on these advances, techniques for fabrication of drug releasing particles can be applied to microparticles (MP) in tissue engineering applications. The conventional manufacturing protocols such as emulsion, electrospraying, hot melt and spray drying have been reported for the fabrication of microparticles (Oliveira and Mano 2011; Arya et al. 2009). However, the most common method is the emulsion process wherein the polymer is dispersed in an organic solvent and solution is subsequently added into the excess of a non-solvent for the polymer. The liquid is then mechanically stirred or homogenized by ultrasound waves. During this, the organic solvent evaporates forcing the polymer chains to aggregate and form particles. This technique typically produces spherical particles and is quite easy to implement and scale up (Lee et al. 2016b). While MPs usually act as cargoes in drug delivery applications, they may be manufactured as porous beads for TE purpose (Kang and Bae 2009). Such MPs are of particular interest in spheroid formation wherein the cells migrate within the porous MPs and result in spheroids of controlled diameter upon MP degradation. Using this technique, breast

cancer cells were successfully cultured on porous PLA-PVA MPs (Sahoo et al. 2005). Such MPs have also been used to study efficiency of anti-cancer drugs on MCF-7 breast cancer cell line-based 3-D tumor model (Horning et al. 2008). Likewise, natural polymers can also be processed into MPs. As an example, collagen-based MPs were manufactured through a microfluidic process, wherein collagen droplets were formed in a micro-channel, followed by droplet shrinkage and cross-linking of collagen molecules. Such collagen MPs exhibited similar composition as collagen hydrogels and allowed for generation of hepatocyte spheroids (Yamada et al. 2015). Similarly, gelatin-based MPs were used to promote the aggregation of pancreatic beta cells, MIN6 into spheroids for the formation of islet like structures (Bernard et al. 2014). This technique can also be translated to cancer cells for the formation of 3-D tumor like tissue. Further, MPs can fuse together to form bigger 3D structures, this process is called sintering and is of particular interest in regenerative medicine and could be also applied towards in vitro tumor models (Lee et al. 2008). Because they are injectable and allow diffusion during drug release studies, MPs have gained interest in the pharmaceutical industry. Further, due to their availability and popularity, MPs may also gain interest in the future for the generation of 3-D tumor models.

5.2.4 Polymeric Fibers

ECM of native tissues is composed of proteins such as collagen which exhibit a fibrous architecture (Wenger et al. 2007). Therefore, synthetic models that can reproduce such organization have been developed for TE applications (Bhardwaj and Kundu 2010). Nanofibers mimic the fiber organization of the collagen component in the ECM and they can be fabricated from synthetic or natural polymers resulting in fibers of different size, shape and length. Some of the fabrication processes include mechanical fiber extrusion and electrospinning (Kumar et al. 2012).

Fibers extrusion or spinning is a technique that originated from the textile industry. It consists of pushing/extruding a polymer solution or a polymer melt through a small needle or spinneret (Tuzlakoglu and Reis 2009). Natural and synthetic biocompatible materials have been successfully processed using this technique. As an example, chitosan was spun in an alcohol-based solution and fixed by exposure to hot air flow (Desorme et al. 2013) and in another study, collagen fibers were obtained through extrusion into a buffer which resulted in a fibrous organization (Enea et al. 2011). While this technique allows for the formation of fibers, which can be later woven and further processed into textile, it only achieves fibers at the micrometer scale.

More recently, mechanical extrusion has been combined with an electrostatic process. By creating a potential difference between the extrusion needle and the fiber target, fiber diameter at the micro as well as nanoscale can be achieved. This process called electrospinning, and is defined as the jetting of a polymer solution

from a needle under the influence of an electric field following which the charged solution jet evaporates resulting in deposition of randomly oriented microscale as well as nanoscale fibers on the collector surface (Huang et al. 2003; Arya et al. 2010). This technique has been successfully used for the fabrication of synthetic and natural fibers such as PCL (Sill and von Recum 2008), polysaccharide such as zein (Cai et al. 2013) or collagen fibers (Sell et al. 2009). Micro/nanofibers obtained through this technique exhibit a high surface area, inter-connected pores and mechanical properties that can be tuned in order to mimic the natural tissue environment. Therefore, electrospun scaffolds have found diverse application in the area of tissue engineering.

For 3-D tumor model application, electrospun collagen-based fibers were used for culturing of prostate cancer bone metastatic cell line, C4-2B. The testing of anticancer drugs, docetaxel and camptothecin on 3-D model demonstrated modulated drug responsiveness compared to cells grown on collagen coated TCPS which may be attributed to decreased drug diffusion in the 3-D colonies within the fibers (Hartman et al. 2009). Peptide hydrogel nanofiber used in regenerative medicine was also applied for the formation of 3-D tumor model based on ovarian cancer-based cell line and demonstrated higher anti-cancer drug resistance than 2-D monolayer culture (Yang and Zhao 2011). Synthetic polymers such as poly (3-hydroxybutyrate-co-3-hydroxyvalerate) electrospun nanofibers were used for the generation of gastric cancer–based 3-D model using MKN28 cancer cell line. Drug testing studies revealed that the concentrations required to inhibit the cell growth was found to be higher in cells grown on 3-D nanofibrous substrate than on 2-D monolayer culture (Kim et al. 2009). Alternative synthetic materials such as PLGA —PLA electrospun fibers were shown to induce EMT thereby reproducing one of the key characteristics of metastatic tumors as in vivo (Girard et al. 2013). Fibrous PCL, previously found application in engineering of bone environment, was also used to culture Ewing sarcoma (bone cancer) and exhibited morphology, growth kinetics and protein expression profile similar to human tumor (Fong et al. 2013). Therefore, similar to other scaffold-based models, electrospun fibers were found to be more representative of the natural 3-D environment as compared to 2-D monolayer culture. Such fibrous scaffolds could be then utilized in an HTS setup for screening of anti-cancer drugs.

5.3 ECM Remodeling

To date, most of the systems introduced for the fabrication of 3-D tumor models are passive (or inactive) materials that do not modulate themselves during cell culture. Although some systems like PLA and PEG degrade via hydrolysis, they do not reproduce the dynamic and natural evolution of the ECM. Indeed, ECM is a complex composite material that undergoes targeted degradation. It is well

documented that reorganization of the ECM in a tumor can impact cancer progression, angiogenesis and metastasis (Lu et al. 2012). It has also been reported that changes in the ECM impacts a cell's biology by providing variation in the cell binding and growth factor composition (Pickup et al. 2014). Further, changes in the ECM during cancer progression are not only biological but mechanical as well. As cancer cells proliferate, they secret an ECM of higher stiffness, mainly composed of collagen and glycosaminoglycan (GAG) with high content of sulfate groups (Cox and Erler 2011). Modulation in tumor ECM mainly originates from an unbalanced enzyme production between MMPs and tissue inhibitors of metalloproteinases (TIMPs) which are responsible for matrix degradation and its inhibition, respectively (Malik et al. 2015). Additionally, ECM also acts as a growth factor reservoir for molecules such as FGF or VEGF; changes in ECM constitution promotes release of the angiogenic factors (Bonnans et al. 2014). Reconstitution of the aforementioned events into synthetic systems will help to closely mimic the natural progression of cancer cells in vitro. In this regard, recapitulating events such as matrix reorganization into a synthetic scaffold requires degradable polymers that favor in vivo events in lieu of tumor growth and progression. Two types of degradation can occur: proteolytic degradation mediated by enzymes such as MMPs or cathepsins and hydrolysis of the macromolecules by oxidative species.

Proteolytic degradation is specifically directed to natural polymers like collagen or HA since synthetic ECM cannot promote such degradation. However, identification of degradable peptide sequences has made it possible to integrate these domains within synthetic polymers. Additionally, incorporation of cross-linkers undergoing degradation by MMPs or cathepsins has been successfully used to mimic the natural ECM degradation within the in vitro synthetic scaffolds. As an example, GPQGILGQ responsive sequence for MMP-2 and MMP-9 was incorporated within PEG cross-linked matrix resulted in a dynamic matrix (Zhu and Marchant 2011). Collagenase sensitive peptide sequence LGPA has also been used to detect the enzyme activity by binding a fluorescent molecule to PEG hydrogel (Lee et al. 2007). However, proteolytic degradation occurs only in small molecular weight polymer by a multistep process, which requires enzymatic diffusion (like hydrolases) into the bulk material (Azevedo and Reis 2005). Different peptide sequences have been identified that are specifically cleaved by diverse enzymes. Amongst them, DENPDIE laminin sequence can be cleaved by MMP-12 (Pirilä et al. 2003). Further, laminin can be cleaved by MMP-1 as well through the GPQGIWGQ (Patrick and Ulijn 2010), QLLADTPV (Tsubota et al. 2000), YSGDENP (Ogawa et al. 2004) and APGL peptide sequences, which have been tested in a cross-linked hydrogel system (West and Hubbell 1999). Plasmin degradation of fibrinogen macromolecule sequences such as YKNR, YKND and YKNRD have been demonstrated as minimal cleavable sites which can potentially be degraded by fibroblasts (Shikanov et al. 2011; Jo et al. 2010; Raeber et al. 2007). Elastase enzyme can also degrade specific sites such as AAAAAAAAAK (Mann et al. 2001), AAPVVRGMG and AAPVVRGGGK which have also been tested in cross-linked hydrogels, that demonstrated loss in mechanical properties following

enzymatic degradation (Aimetti et al. 2009). Proteoglycans can also undergo enzymatic degradation by MMP-13, which target PENFF (Salinas and Anseth 2008) and GPQGLA (Phelps et al. 2010) sequences. In order to simulate the proteolytic ECM degradation, invasive breast cancer cells (MDA-MB-231) and non-invasive cells (MCF-7) were used to study the phenomena in MMP cleavable HA hydrogels. Such platform could be used in the future to study the influence of matrix degradation and cross-linking in anti-cancer drug testing (Fisher et al. 2015).

Non-proteolytic degradation refers to non-specific degradation that occurs due to hydrolysis of the polymer or due to polymer solubilization under physiological conditions (Burkoth and Anseth 2000). Within a tumor, hydrolysis is mediated by the chemical environment such as reactive oxygen species or oxidative stress. Further, degradation kinetics is of great importance in tumor environment since ECM development requires space that can be made available through degradation of the support material. Degradation, which results in the loss of molecular weight, induces a loss of mechanical properties and this needs to be compensated by growth of the new tissue specific matrix. Degradation of synthetic polymers has been extensively studied and exhibits different degradation rates depending of their backbone composition (Reid et al. 2013; Lam et al. 2008). This can be used to design scaffolds that support the growth and organization of cancer cells into a solid tumor while the scaffold degrades during maturation of tumor mass.

5.4 Stiffness of the Tumor Environment

Tumor cells are capable of remodeling its ECM thereby resulting in modification of its mechanical properties; this remodeling supports tumor growth and progression (Levental et al. 2009; Paszek et al. 2005). It is now well documented that in a cancerous tissue, such as in breast tumors, the ECM undergoes drastic changes such as modulation of collagen density and results in formation of a stiffer ECM. Stiffness of the breast tumor microenvironment is around 4000 Pa as compared to healthy breast tissue which is around 200 Pa (Paszek et al. 2005). This change in tissue stiffness is detected as a palpable ‘stiffening’ of the tissue and can potentially be utilized as a diagnostic tool (Butcher et al. 2009). Scaffolds based on collagen have been used to understand the effect of matrix stiffness on cancer cell behavior (Paszek et al. 2005; Carey et al. 2012; Kraning-Rush and Reinhart-King 2012). In a study based on 3-D tumor model from reconstituted basement membrane (rBM) and collagen, the authors postulated whether increase in stiffness by virtue of collagen concentration would promote a malignant phenotype of the breast or its crosslinking would impede tumorigenesis. It was demonstrated that collagen cross-linking and ECM stiffening promoted breast tumorigenesis (Levental et al. 2009). Further, to delineate the effect of stiffness from changes in matrix composition and architecture, Chaudhuri et al. utilized rBM and alginate for modulation of ECM stiffness. They demonstrated that an increase in ECM stiffness could promote a malignant phenotype in normal mammary epithelial cells, which however was negated in the presence of

basement membrane ligands (Chaudhuri et al. 2014). Similar models based on natural polymers were utilized to decipher the role of matrix stiffness and cell adhesion. A study showed the organization of glioblastoma multiform with distinct morphological patterns as in vivo brain slices using hydrogels based on HA functionalized with short RGD peptides (Ananthanarayanan et al. 2011). In another study, a synthetic scaffold based on PEG modified with bioactive peptides was utilized to study the process of EMT in lung adeno-carcinoma and demonstrated that the bioactive scaffold recapitulated epithelial morphogenesis and was dependent on the substrate stiffness (Gill et al. 2012).

Wong and Kumar discussed about the role of ECM stiffness and its composition on cell migration which in turn could regulate tumor-initiating cells/CSCs driven metastasis (Wong and Kumar 2014). Therefore, cancer cell migration within a specific mechanical environment needs to be recapitulated in a 3-D in vitro model for understanding this mechanism (Mierke 2014; Keely and Nain 2015). In addition to in vitro and in vivo studies, in silico simulation can also help to identify key features of the ECM that impact cell migration. A computer simulation of cell movement proposed that cancer cell migration and invasiveness could be as a result of increased ECM stiffness as well as strong degree of ECM degradation (Li et al. 2014b). Such studies are building on in vitro 2-D experiments which demonstrated the role of stiffer cell substrate in promoting glioma cell migration and proliferation; similar studies on breast cancer cells have demonstrated corroborating results (Ulrich et al. 2009; Pickup et al. 2014). However, recent studies have contradicted the aforementioned results and demonstrated that across different glioblastoma cells lines that originated from different patients, migration of cancer cells in response to the substrate stiffness was patient dependent (Grundy et al. 2016). The interdependence of cancer cell migration and matrix stiffness is currently a conflictual research area that is still unsolved and requires further experimentation. Furthermore, towards a better understanding of the relation between stiffness and cancer cell behavior, CSCs originating from bone, breast, colorectal and gastric tissue were cultured on matrices of different stiffness. Similar to stem cells, which differentiate into functional cells depending on the substrate stiffness (Engler et al. 2006), CSCs also demonstrated marker expression while residing in a niche with optimum stiffness corroborating to their tissue of origin (Jabbari et al. 2015). These studies clearly demonstrate the relation between the stiffness of cell microenvironment and hallmarks of cancer. Recreation of the mechanical properties reminiscent of solid tumors in vivo would not only help to create 3-D systems that reproduce the cancer hallmarks in vitro but also demonstrate potential in identification of potent anti-cancer molecules with higher efficiency. In vitro studies performed on different 3-D cell culture models have already demonstrated that 3-D spheroids modulated cancer cells thereby making them less sensitive to anticancer drugs as compared to the cells grown on 2-D surface. One of the contributory reasons is decreased drug diffusion within the 3-D aggregates that is impaired by 3-D organization of cells; cells in the middle of the cluster receive less drugs than those at the periphery (Kim et al. 2009). The diffusion of molecules to the cells is further restrained as a function of ECM; dense ECM decreases the probability of

drug diffusion through it (Giussani et al. 2015). As the cells sense the ECM stiffness through cell binding receptor such as integrins, laminin receptor, syndecans and DDR1, intracellular signaling pathways are engaged which could also affect the tumor cell's response to anticancer drugs (Pickup et al. 2014). This was demonstrated in a 3-D alginate matrix with tethered RGD. An increase in substrate stiffness of the supporting matrix reduced the effect of toxins such as acrylamide and cadmium chloride; however tethered RGD undermined this effect in softer scaffolds (Zustiak et al. 2015). Hepatocellular carcinoma cells (HCC) embedded in alginate matrices of stiffness of the order of 105 kPa were also found to be more resistant to anti-cancer drug paclitaxel, 5-fluorouracil and cisplatin as compared to softer matrices (Liu et al. 2015). In another study, HCC cells pre-cultured in alginate-chitosan matrix showed higher blood vessel recruitment when implanted in animal models as compared to the cells pre-cultured on 2-D surfaces or Matrigel, thereby validating the in vitro tumor model. Cells cultured on alginate-chitosan matrix also demonstrated greater resistance to doxorubicin suggesting diffusional limitations as well as induction of drug resistance properties due to the 3-D microenvironment (Leung et al. 2010). Taken together, these findings have greatly contributed to the understanding of the relation between 3-D matrix properties such as stiffness, degradation and cell anchorage ability as well as cellular reprogramming (cell invasiveness, EMT and drug resistance) (Fig. 7).

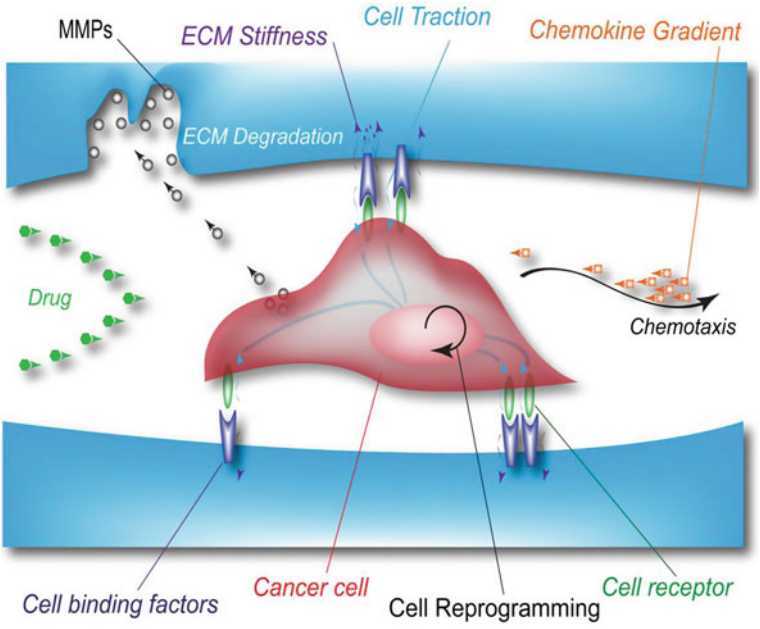

Fig. 7 Cancer cell in the tumor extracellular matrix. ECM stiffness, cell binding factors and enzyme cleavability can mediate the endothelial-mesenchymal transition of the cancer cell, control cell migration towards chemokine gradients as well as demonstrate drug resistance behavior

6 Future Perspective

3-D models recapitulate the tumor microenvironment to a great extent when compared to 2-D monolayer culture, thereby contributing towards understanding the role of individual microenvironmental parameters in modulating cancer progression. However, the tumor environment is exposed to a complex milieu of microenvironmental events and not individual parameters, hence making it even more crucial to develop complex 3-D tumor models in vitro. Therefore, co-culture of various cells in a single environment needs to be carefully planned due to different culture medium and growth factor requirements for each cell type under in vitro cell culture conditions and may require a complex design for potential co-culturing. Further, it is important to validate the effect of one cell type on the other for parameters like spheroid growth and invasion as well as various epigenetic changes that might occur as a by-product of co-culture.

Furthermore, there is a need to develop more standardized and automatic procedures for HTS applications. Although techniques like hanging drop method and 3-D bioprinting aim to generate spheroids on a large scale, there are protocols that need to be reviewed in order to obtain uniform sized spheroids that in turn would attribute towards uniform growth in each spheroid for reproducible in vitro drug screening studies.

Scaffolds, on the other hand, need to be carefully chosen in order to minimize the interaction between the potential molecules to be screened as anti-cancer drugs and the biomaterial surface used for scaffold synthesis. Few scaffolds, for example, limit the image analysis of cultured 3-D spheroids due to their self-limiting property of auto-fluorescence and opacity. Few others are further limited by the inability to gently recover cancer cells and their spheroids. In a recent study, 3-D scaffolds based on collagen and alginate, for prostate cancer cell-lymphocyte interaction in vitro, allowed cell harvesting via scaffold degradation in an ionic solution (Florczyk et al.2012). Similar scaffold degradation methodologies should be adapted for other polymers as well.

There is also a need to co-culture patient's own cells from the tumor microenvironment, including tumor cells, stromal cells and/or immune cells in order to perform anti-cancer drug testing towards the development of personalized treatment protocols. TE has developed an enormous collection of synthetic as well as natural biomaterial-based matrices in order to allow for precise and complex modulation of the tumor microenvironment. These matrices can be further modified for ligand patterning in order to generate bio-functional scaffolds. Modification can be performed using cell adhesion sequences like RGD (Park et al.2005) or with cell degradable peptide sequences (Salinas and Anseth2008). Further, based on tissue type, starting polymer and the polymerization conditions can be controlled in order to modulate pore size, architecture and scaffold stiffness (Sawhney1993), all of which will depend on the tumor type that needs to be recapitulated. One can also

design scaffolds with spatio-temporal localization of ligands with the matrices using photopolymerization (Zhu2010) and photo-assisted patterning (Nakajima et al.2007).

In this regard, various approaches have been developed to utilize decellularized matrices that possess preloaded biochemical and topographical features and have the ability to guide cells into functional organs. This could be extrapolated to the development of a decellularized tumor matrix (following removal of tumor cells) that would still retain the requisite mechanical, topographical and chemical cues. These matrices have found application in the area of tumor angiogenesis (Burns et al.2011). Although interesting, it suffers from the disadvantage of batch-to-batch variation since every tumor microenvironment is different.

TE has also led to the development of patterned natural and synthetic matrices with tunable properties. One such example is of stiffness patterning reported in hydrogels based on polyacrylamide and HA (Wong et al. 2003; Marklein and Burdick 2010). Another interesting study is based on spatially controlled immobilization of bioactive ligands by a technique called 'two-photon excitation', which allows spatial immobilization of ligands by virtue of a focussed laser beam via microscope objective lens. Wylie et al. reported the immobilization of two proteins, namely stem cell differentiation factors sonic hedgehog and ciliary neurotrophic factor in 3-D agarose gels by two-photon patterning, using orthogonal binding partners barnase–barstar and streptavidin–biotin, respectively (Wylie et al. 2011) (Fig. 8). This patterning led to precise localization of proteins/peptides resulting in physiologically relevant microenvironments. This model can also be extrapolated towards the generation of tissue specific 3-D tumor models.

Additionally, advancements in 3-D models based on microfluidic approach that recapitulates the physiology of human organs more than static 3-D models, can also act at the forefront of TE (Huh et al. 2012). A human-body-on-chip that encompasses organ-organ coupling would be useful for validation of lead drug molecules and could also be used for cancer immunotherapy, wherein multicellular interactions under so-called physiological conditions can be used to mount an immune response similar to in vivo (Bhatia and Ingber 2014). In another study, a microfluidic-based approach was designed by Xu et al. for screening different anti-cancer drugs (monotherapy and combination treatment) for development of individualised treatment for lung cancer (Xu et al. 2013). Approaches based on microfluidics will not only reduce the drug screening costs but also improve the efficiency of translational science in the area of 3-D tumor models.

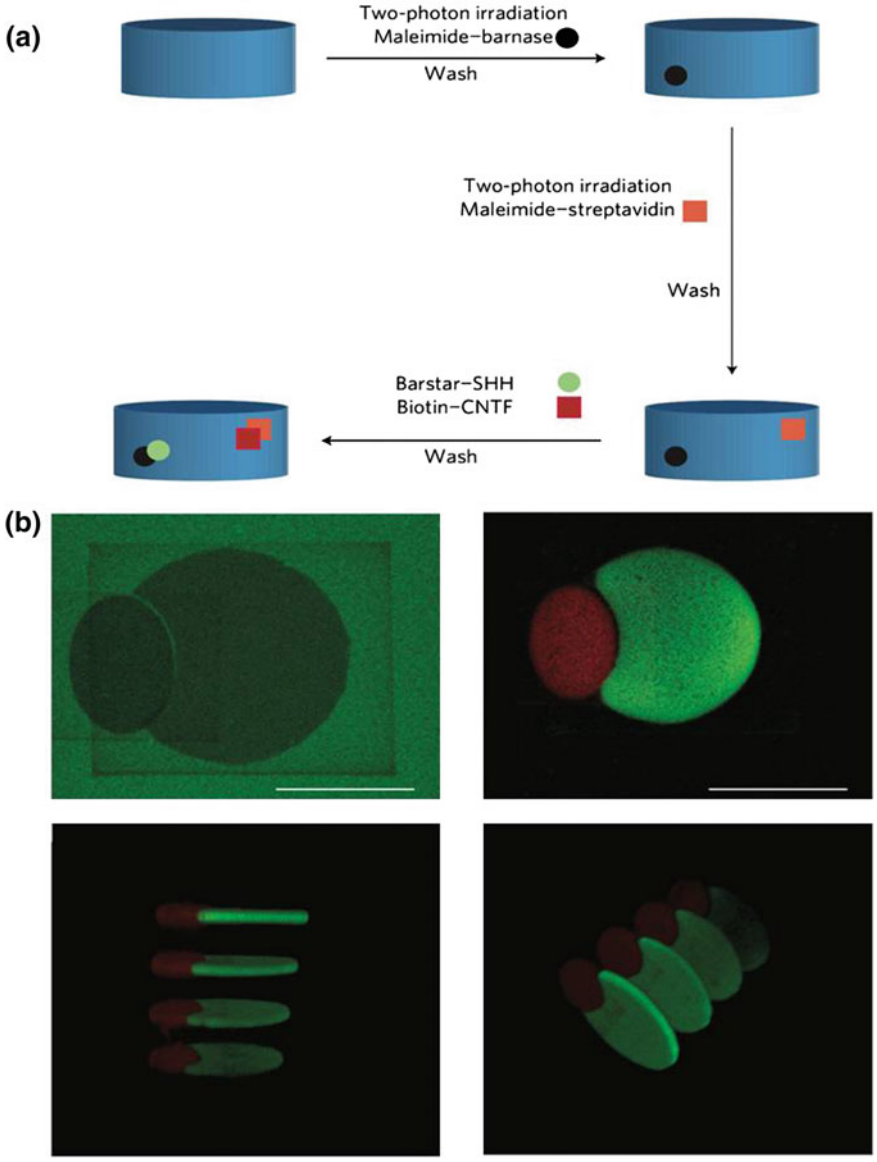

Fig. 8 Simultaneous patterning of multiple growth factors using two-photon chemistry in 3-D agarose gel. (**a**) Using two-photon chemistry, maleimide–barnase (*black circle*) is immobilized on the hydrogel, followed by washing and immobilization of maleimide–streptavidin (*orange square*) with another step of washing. This is followed by simultaneous attachment of barstar linked sonic hedgehog (SHH) and biotin linked ciliary neurotrophic factor (CNTF) to barnase and streptavidin respectively in the third dimension as shown by the confocal microscopy (**b**). (Adapted with permission from reference Wylie et al. Nature Materials 2011)

7 Conclusion

The tumor microenvironment is a complex arrangement of cell population as well as extracellular signals that mediate tumor growth, invasion, metastasis, angiogenesis as well as resistance to anticancer drugs. In vitro tumor models have therefore been utilized in order to reveal the contributions of various physical and chemical cues towards tumor progression and in drug screening studies. These models recapitulate tumor microenvironment similar to in vivo and have started replacing the conventional 2-D screening methodologies.

In particular, TE-based in vitro models have made tremendous progress in order to recreate defined tumor microenvironments and it is believed to greatly contribute to the area of cancer research and therapy. However, much work needs to be done in the direction of integrating various technologies of 3-D tumor model development (like TE-based and microfluidics or bioprinting) in order to generate the 'right' tumor microenvironment-recapitulating platforms for understanding tumor biology as well as for the development of personalized treatment protocols.

Acknowledgement NA would like to acknowledge the Department of Science and Technology, India for providing DST Inspire Faculty fellowship as well as All India Institute of Medical Sciences Bhopal, India as host institution. AF would like to acknowledge the University of South Australia as host institution.

References

Aimetti AA, Tibbitt MW, Anseth KS (2009) Human neutrophil elastase responsive delivery from poly(ethylene glycol) hydrogels. Biomacromolecules 10(6):1484–1489

Al-Husein B et al (2012) Antiangiogenic therapy for cancer: an update. Pharmacotherapy 32(12):1095–1111

Amann A et al (2014) Development of an innovative 3D cell culture system to study tumour—Stroma interactions in non-small cell lung cancer cells. PLoS ONE 9(3)

Amit-Cohen BC, Rahat MM, Rahat MA (2013) Tumor cell-macrophage interactions increase angiogenesis through secretion of EMMPRIN. Front Physiol 4:1–16

Ananthanarayanan B, Kim Y, Kumar S (2011) Elucidating the mechanobiology of malignant brain tumors using a brain matrix-mimetic hyaluronic acid hydrogel platform. Biomaterials 32(31):7913–7923

Anastasov N et al (2015) A 3D-microtissue-based phenotypic screening of radiation resistant tumor cells with synchronized chemotherapeutic treatment. BMC Cancer 15:466

Arnott S et al (1974) The agarose double helix and its function in agarose gel structure. J Mol Biol 90(2):269–284

Artzner F et al (2007) Interactions between Poloxamers in Aqueous Solutions: Micellization and Gelation Studied by Differential Scanning Calorimetry, Small angle scattering and rheology. Langmuir 26:5085–5092

Arya N et al (2009) Electrospraying: a facile technique for synthesis of chitosan-based micro/nanospheres for drug delivery applications. J Biomed Mater Res Part B: Appl Biomater 88(1):17–31

Arya N et al (2012) Recapitulating tumour microenvironment in chitosan-gelatin three-dimensional scaffolds: an improved in vitro tumour model. J R Soc Interface 9(77):3288–3302

Arya N, Sharma P, Katti DS (2010) Designing nanofibrous scaffolds for tissue engineering. In: Advanced biomaterials: fundamentals, processing, and applications. John Wiley & Sons, Inc., pp 435–497
Asghar W et al (2015) Engineering cancer microenvironments for in vitro 3-D tumor models. Mater Today 18(10):539–553
Asghar W et al (2014) Preserving human cells for regenerative, reproductive, and transfusion medicine 9(7):895–903
Assal R El et al (2014) Bio-inspired Cryo-ink preserves red blood cell phenotype and function during nanoliter vitrification. Adv Mater 26(33):5815–5822
Assal R El, Chen P, Demirci U (2015) Highlights from the latest articles in advanced biomanufacturing at micro- and nano-scale. Nanomed (Lond) 6(2):356–372
Azevedo H, Reis R (2005) Understanding the enzymatic degradation of biodegradable polymers and strategies to control their degradation rate. In: Reis RL, Román JS (eds) Biodegradable systems in tissue engineering and regenerative medicine, CRC Press, FL, pp 177–201
Balachander GM et al (2015) Enhanced metastatic potential in a 3D tissue scaffold toward a comprehensive in vitro model for breast cancer metastasis. ACS Appl Mater Interfaces 7 (50):27810–27822
Barrila J et al (2010) Organotypic 3D cell culture models: using the rotating wall vessel to study host-pathogen interactions. Nat Rev Microbiol 8(11):791–801
Barron JA et al (2004) Biological laser printing: a novel technique for creating heterogeneous 3-dimensional cell patterns. Biomed Microdevices 6(2):139–147
Benton G et al (2014) Matrigel: from discovery and ECM mimicry to assays and models for cancer research. Adv Drug Deliv Rev 79:3–18
Bergers G, Benjamin LE (2003) Tumorigenesis and the angiogenic switch 3:401–410
Bernard AB, Chapman RZ, Anseth KS (2014) Controlled local presentation of matrix proteins in microparticle-laden cell aggregates. Biotechnol Bioeng 111(5):1028–1037
Bersini S et al (2014) Biomaterials a micro fluidic 3D in vitro model for specificity of breast cancer metastasis to bone 35:2454–2461
Bhardwaj N, Kundu SC (2010) Electrospinning: a fascinating fiber fabrication technique. Biotechnol Adv 28(3):325–347
Bhatia SN, Ingber DE (2014) Microfluidic organs-on-chips. Nat Biotechnol 32(8):760–772
Bhattacharya M et al (2012) Nanofibrillar cellulose hydrogel promotes three-dimensional liver cell culture. J Control Release: Official J Control Release Soc 164(3):291–298
Bian L et al (2013) The influence of hyaluronic acid hydrogel crosslinking density and macromolecular diffusivity on human MSC chondrogenesis and hypertrophy. Biomaterials 34(2):413–421
Bischel LL, Beebe DJ, Sung KE (2015) Microfluidic model of ductal carcinoma in situ with 3D, organotypic structure. BMC Cancer 15(1):12
Bissell MJ, Radisky D (2001) Putting tumours in context. Nat Rev Cancer 1(1):46–54
Bonnans C, Chou J, Werb Z (2014) Remodelling the extracellular matrix in development and disease. Nat Rev Mol Cell Biol 15(12):786–801
Bouck N, Stellmach V, Hsu SC (1996) How tumors become angiogenic. Adv Cancer Res 69:135–174
Braun B et al (2004) Expression of G-CSF and GM-CSF in human meningiomas correlates with increased tumor proliferation and vascularization. J Neurooncol 68(2):131–140
Brennen WN, Isaacs JT, Denmeade SR (2012) Rationale behind targeting fibroblast activation protein–expressing carcinoma-associated fibroblasts as a novel chemotherapeutic strategy. Mol Cancer Ther 11(2):257–266
Brizel DM et al (1996) Tumor oxygenation predicts for the likelihood of distant metastases in human soft tissue sarcoma. Cancer Res 56(5):941–943
Bruce A et al (2015) Three-dimensional microfluidic tri-culture model of the bone marrow microenvironment for study of acute lymphoblastic leukemia. PLoS ONE 10(10):1–16
Burkoth AK, Anseth KS (2000) A review of photocrosslinked polyanhydrides: in situ forming degradable networks. Biomaterials 21(23):2395–2404

Burns JS et al (2011) Decellularized matrix from tumorigenic human mesenchymal stem cells promotes neovascularization with galectin-1 dependent endothelial interaction. PLoS ONE 6(7)
Butcher DT, Alliston T, Weaver VM (2009) A tense situation: forcing tumour progression. Nat Rev Cancer 9(2):108–122
Cai S et al (2013) Novel 3D electrospun scaffolds with fibers oriented randomly and evenly in three dimensions to closely mimic the unique architectures of extracellular matrices in soft tissues: Fabrication and mechanism study. Langmuir 29(7):2311–2318
Campbell PG et al (2005) Engineered spatial patterns of FGF-2 immobilized on fibrin direct cell organization. Biomaterials 26(33):6762–6770
Cantin K et al (2011) H-bonding-driven gel formation of a phenylacetylene macrocycle. Org Biomol Chem 9(12):4440–4443
Carey SP et al (2012) Biophysical control of invasive tumor cell behavior by extracellular matrix microarchitecture. Biomaterials 33(16):4157–4165
Carmeliet P, Jain RK (2000) Angiogenesis in cancer and other diseases. Nature 407:249–257
Catlett-Falcone R et al (1999) Constitutive activation of Stat 3 signaling confers resistance to apoptosis in human U266 myeloma cells. Immunity 10(1):105–115
Cekanova M (2014) Animal models and therapeutic molecular targets of cancer : utility and limitations 1911–1922
Chaudhuri O et al (2014) Extracellular matrix stiffness and composition jointly regulate the induction of malignant phenotypes in mammary epithelium. Nat Mater 13(June):1–35
Chauhan D et al (1997) Interleukin-6 inhibits Fas-induced apoptosis and stress-activated protein kinase activation in multiple myeloma cells. Blood 89:227–234
Chauhan H et al (2003) There is more than one kind of myofibroblast: analysis of CD34 expression in benign, in situ, and invasive breast lesions. J Clin Pathol 56(4):271–276
Chen L et al (2012) The enhancement of cancer stem cell properties of MCF-7 cells in 3D collagen scaffolds for modeling of cancer and anti-cancer drugs. Biomaterials 33(5):1437–1444
Chen Y-C et al (2015) High-throughput cancer cell sphere formation for characterizing the efficacy of photo dynamic therapy in 3D cell cultures. Sci Rep 5:12175
Cherry RS, Papoutsakis ET (1988) Physical mechanisms of cell damage in microcarrier cell culture bioreactors. Biotechnol Bioeng 32(8):1001–1014
Choh S, Cross D, Wang C (2011) Facile synthesis and characterization of disulfide-cross-linked hyaluronic acid hydrogels for protein delivery and cell encapsulation. Biomacromolecules 1126–1136
Cirri P, Chiarugi P (2011) Cancer associated fibroblasts: the dark side of the coin. Am J Cancer Res 1(4):482–497
Cohen DL et al (2006) Direct freeform fabrication of seeded hydrogels in arbitrary geometries. Tissue Eng 12(5):1325–1335
Coussens LM et al (1999) Inflammatory mast cells up-regulate angiogenesis during squamous epithelial carcinogenesis. Genes Dev 13(11):1382–1397
Coussens LM et al (2000) MMP-9 supplied by bone marrow-derived cells contributes to skin carcinogenesis. Cell 103(3):481–490
Coussens LM, Werb Z (2002) Inflammation and cancer 420:860–867
Cox TR, Erler JT (2011) Remodeling and homeostasis of the extracellular matrix: implications for fibrotic diseases and cancer. Dis Models Mech 4(2):165–178
Croix B St, Kerbel RS (1997) Cell adhesion and drug resistance in cancer. Curr Opin Oncol 9(6)
Cui X et al (2012a) Thermal inkjet printing in tissue engineering and regenerative medicine. Recent Pat Drug Deliv Formul 6(2):149–155
Cui X et al (2012b) Direct human cartilage repair using 3D bioprinting technology. Tissue Eng 18(11–12):1304–1312
Dahlmann J et al (2013) Fully defined in situ cross-linkable alginate and hyaluronic acid hydrogels for myocardial tissue engineering. Biomaterials 34(4):940–951
Dalton WS (1999) The tumor microenvironment as a determinant of drug response and resistance. Drug Resist. Updat. 2:285–288

Daquinag AC, Souza GR, Kolonin MG (2013) Adipose tissue engineering in three-dimensional levitation tissue culture system based on magnetic nanoparticles. Tissue Eng Part C Methods 19(5):336–344

Davies PF (1981) Microcarrier culture of vascular plastic on solid beads vascular endothelial cell culture is now firmly established as a valuable research approach to the pathophysiology of blood vessels

Dean M (2009) ABC transporters, drug resistance, and cancer stem cells. J Mammary Gland Biol Neoplasia 14(1):3–9

Dean M, Fojo T, Bates S (2005) Tumour stem cells and drug resistance. Nat Rev Cancer 5:275–284

DeForest CA, Polizzotti BD, Anseth KS (2009) Sequential click reactions for synthesizing and patterning three-dimensional cell microenvironments. Nat Mater 8(8):659–664

Demirci U, Montesano G (2007) Single cell epitaxy by acoustic picolitre droplets. Lab Chip 7(9):1139–1145

Denduluria SK et al (2015) Insulin-like growth factor (IGF) signaling in tumorigenesis and the development of cancer drug resistance. Genes Dis 2(2):13–25

Desorme M et al (2013) Spinning of hydroalcoholic chitosan solutions. Carbohydr Polym 98 (1):50–63

Dimanche-Boitrel MT et al (1994) In vivo and in vitro invasiveness of a rat colon-cancer cell line maintaining E-cadherin expression: an enhancing role of tumor-associated myofibroblasts. Int J Cancer. J Int du Cancer 56(4):512–521

Ding C et al (2010) Dually responsive injectable hydrogel prepared by in situ cross-linking of glycol chitosan and benzaldehyde-capped PEO-PPO-PEO. Biomacromolecules 11(4):1043–1051

Discher DE, Mooney DJ, Zandstra PW (2009) Growth factors, matrices, and forces combine and control stem cells. Sci (NY) 324(5935):1673–1677

Duan B et al (2013) 3D Bioprinting of heterogeneous aortic valve conduits with alginate/gelatin hydrogels. J Biomed Mater Res Part A 101 A(5):1255–1264

van Duinen V et al (2015) Microfluidic 3D cell culture: from tools to tissue models. Curr Opin Biotechnol 35:118–126

Ehrmann RL, Knoth M (1968) Choriocarcinoma. Trans filter stimulation of vasoproliferation in the hamster cheek pouch. Studied by light and electron microscopy. J Nat Cancer Inst 41(6):1329–1341

Elenbaas B, A.Weinberg R (2001) Heterotypic signaling between epithelial tumor cells and fibroblasts in carcinoma formation. Exp Cell Res 264:169–184

Emans PJ et al (2010) Autologous engineering of cartilage. Proc Natl Acad Sci USA 107(8):3418–3423

Enea D et al (2011) Extruded collagen fibres for tissue engineering applications: Effect of crosslinking method on mechanical and biological properties. J Mater Sci—Mater Med 22(6):1569–1578

Engler AJ et al (2006) Matrix elasticity directs stem cell lineage specification. Cell 126(4):677–689

Falkenberg N et al (2016) Three-dimensional microtissues essentially contribute to preclinical validations of therapeutic targets in breast cancer. Cancer Med 5(4):703–710

Fang Y et al (2012) Rapid generation of multiplexed cell cocultures using acoustic droplet ejection followed by aqueous two-phase exclusion patterning. Tissue Eng Part C: Methods 18(9):647–657

Faute MA dit et al (2002) Distinctive alterations of invasiveness, drug resistance and cell–cell organization in 3D-cultures of MCF-7, a human breast cancer cell line, and its multidrug resistant variant. Clinical Exp Metastasis 19(2):161–167

Fischbach C et al (2007) Engineering tumors with 3D scaffolds. Nat Methods 4(10):855–860

Fisher OZ et al (2010) Bioinspired materials for controlling stem cell fate. Acc Chem Res 43(3):419–428

Fisher SA et al (2015) Tuning the Microenvironment: Click-crosslinked hyaluronic acid-based hydrogels provide a platform for studying breast cancer cell invasion. Adv Funct Mater 25(46):7163–7172

Florczyk SJ et al (2012) 3D porous chitosan–alginate scaffolds: a new matrix for studying prostate cancer cell–lymphocyte interactions In Vitro. Adv Healthc Mater 1(5):590–599

Folkman J (1971) Tumor angiogenesis: therapeutic implications. The New Engl J Med 285:1182–1186
Fong ELS et al (2013) Modeling ewing sarcoma tumors in vitro with 3D scaffolds. Proc Natl Acad Sci USA 110(16):6500–6505
Frese KK, Tuveson DA (2007) Maximizing mouse cancer models. Nat Rev Cancer 7(9):654–658
Gabbiani G, Ryan GB, Majno G (1971) Presence of modified fibroblasts in granulation tissue and their possible role in wound contraction. Experientia 27(5):549–550
Gill BJ et al (2012) A synthetic matrix with independently tunable biochemistry and mechanical properties to study epithelial morphogenesis and EMT in a lung adenocarcinoma model. Cancer Res 72(22):6013–6023
Gillette BM et al (2008) In situ collagen assembly for integrating microfabricated three-dimensional cell-seeded matrices. Nat Mater 7(8):636–640
Girard YK et al (2013) A 3D fibrous scaffold inducing tumoroids: a platform for anticancer drug development. PLoS ONE 8(10)
Giussani M et al (2015) Tumor-extracellular matrix interactions: identification of tools associated with breast cancer progression. Semin Cancer Biol 35:3–10
Godugu C et al (2013) AlgiMatrix^{TM} based 3D cell culture system as an in-vitro tumor model for anticancer studies. PLoS ONE 8(1)
Goodwin TJ et al (1993) Reduced shear stress: a major component in the ability of mammalian tissues to form three-dimensional assemblies in simulated microgravity. J Cell Biochem 51(3):301–311
Göppert B et al (2016) Superporous Poly (ethylene glycol) Diacrylate Cryogel with a defined elastic modulus for prostate cancer cell research. Small 1–10
Gottesman MM, Fojo T, Bates SE (2001) Multidrug resistance in cancer: role of atp-dependent transporters, 2(January), pp 1–11
Granja P, Jéso B De, Bareille R (2005) Mineralization of regenerated cellulose hydrogels induced by human bone marrow stromal cells. Eur Cell … 31–39
Griffith LG, Swartz MA (2006) Capturing complex 3D tissue physiology in vitro. Nat Rev Mol Cell Biol 7(3):211–224
Grover GN, Braden RL, Christman KL (2013) Oxime cross-linked injectable Hydrogels for catheter delivery. Adv Mater 25(21):2937–2942
Gruene M et al (2011) Laser printing of stem cells for biofabrication of scaffold-free autologous grafts. Tissue Eng Part C: Methods 17(1):79–87
Grundy TJ et al (2016) Differential response of patient- derived primary glioblastoma cells to environmental stiffness. Nature Publishing Group, (Nov 2015), pp 4–13
Guillemot F et al (2010) High-throughput laser printing of cells and biomaterials for tissue engineering. Acta Biomater 6(7):2494–2500
Guillotin B et al (2010) Laser assisted bioprinting of engineered tissue with high cell density and microscale organization. Biomaterials 31(28):7250–7256
Guillotin B, Guillemot F (2011) Cell patterning technologies for organotypic tissue fabrication. Trends Biotechnol 29(4):183–190
Gullino PM (1978) Angiogenesis and oncogenesis. J Natl Cancer Inst 61(3):639
Guo Y-S et al (1998) Insulin-like growth factor-I promotes multidrug resistance in MCLM colon cancer cells. J Cell Physiol 175(2):141–148
Gurkan UA et al (2012) Emerging technologies for assembly of microscale hydrogels. Adv Healthc Mater 1(2):149–158
Gurkan UA et al (2014) Engineering anisotropic biomimetic fibrocartilage microenvironment by bioprinting mesenchymal stem cells in Nanoliter Gel Droplets. Mol Pharm 11:2151–2159
Gurski LA et al (2009) Hyaluronic acid-based hydrogels as 3D matrices for in vitro evaluation of chemotherapeutic drugs using poorly adherent prostate cancer cells. Biomaterials 30(30):6076–6085
Guven S et al (2015) Multiscale assembly for tissue engineering and regenerative medicine. Trends Biotechnol 33(5):37–54
Guzman A, Ziperstein MJ, Kaufman LJ (2014) The effect of fibrillar matrix architecture on tumor cell invasion of physically challenging environments. Biomaterials 35(25):6954–6963

Hanahan D, Weinberg RA (2000) The Hallmarks of Cancer Review University of California at San Francisco. Cell Press 100(7):57–70
Harris AL (2002) Hypoxia—a key regulatory factor in tumour growth. Nat Rev Cancer 2(1):38–47
Hartman O et al (2009) Microfabricated electrospun collagen membranes for 3-D cancer models and drug screening applications. Biomacromolecules 10(8):2019–2032
Heldin CH et al (2004) High interstitial fluid pressure—an obstacle in cancer therapy. Nat Rev Cancer 4(10):806–813
Hideshima T et al (2001) Biologic sequelae of interleukin-6 induced PI3-K/Akt signaling in multiple myeloma. Oncogene 20(42):5991–6000
Higuchi A et al (2005) Temperature-dependent cell detachment on Pluronic gels. Biomacromolecules 6(2):691–696
Hirschhaeuser F et al (2009) Test system for trifunctional antibodies in 3D MCTS culture. J Biomol Screen: Official J Soc Biomol Screen 14(8):980–990
Ho WJ et al (2010) Incorporation of multicellular spheroids into 3-D polymeric scaffolds provides an improved tumor model for screening anticancer drugs. Cancer Sci 101(12):2637–2643
Höckel M et al (1999) Hypoxic cervical cancers with low apoptotic index are highly aggressive. Cancer Res 59(18):4525–4528
Höckel M, Vaupel P (2001) Tumor hypoxia: definitions and current clinical, biologic, and molecular aspects. J Natl Cancer Inst 93(4):266–276
Holliday DL et al (2009) Novel multicellular organotypic models of normal and malignant breast: tools for dissecting the role of the microenvironment in breast cancer progression. Breast Cancer Res: BCR 11(1):R3
Hopp B et al (2005) Survival and proliferative ability of various living cell types after laser-induced forward transfer. Tissue Eng 11(11–12):1817–1823
Horman SR et al (2013) High-content analysis of three-dimensional tumor spheroids: investigating signaling pathways using small hairpin RNA. Nat Meth10(10)
Horning JL et al (2008) 3-D tumor model for in vitro evaluation of anticancer drugs. Mol Pharm 5 (5):849–862
Hoyt DG et al (1996) Integrin activation suppresses etoposide-induced DNA strand breakage in cultured murine tumor-derived endothelial cells. Cancer Res 56(18):4146–4149
Hsiao AY et al (2012) 384 hanging drop arrays give excellent Z-factors and allow versatile formation of co-culture spheroids. Biotechnol Bioeng 109(5):1293–1304
Huang ZM et al (2003) A review on polymer nanofibers by electrospinning and their applications in nanocomposites. Compos Sci Technol 63(15):2223–2253
Huh D et al (2012) A human disease model of drug toxicity—induced pulmonary edema in a lung-on-a-chip microdevice. Sci Trans Med 4(159):1–9
Hull CW (1986) Apparatus for production of three-dimensional objects by stereolithography
Hutmacher DW (2010) Biomaterials offer cancer research the third dimension. Nat Mater 9(2):90–93
Hutmacher DW et al (2010) Can tissue engineering concepts advance tumor biology research? Trends Biotechnol 28(3):125–133
Imamura Y et al (2015) Comparison of 2D- and 3D-culture models as drug-testing platforms in breast cancer. Oncol Rep 33(4):1837–1843
Iwami K et al (2010) Bio rapid prototyping by extruding/aspirating/refilling thermoreversible hydrogel. Biofabrication 2(1):014108
Jabbari E et al (2015) Optimum 3D matrix stiffness for maintenance of cancer stem cells is dependent on tissue origin of cancer cells. PLoS ONE 10(7):1–21
Jaganathan H et al (2014) Three-dimensional in vitro co-culture model of breast tumor using magnetic levitation. Sci Rep 4:6468
Jahangir A, Chen G, Chang H (2013) Drug resistance in multiple myeloma: latest findings and new concepts on molecular mechanisms. Oncotarget 4(12):2186–2207
Jain RK (1996) Delivery of molecular medicine to solid tumors. Sci (NY) 271(5252):1079–1080
Jain RK (2005) Normalization of tumor vasculature: an emerging concept in antiangiogenic therapy. Science 307(5706):58–62

Jang J, Yi H-G, Cho D-W (2016) 3D printed tissue models: present and future. ACS Biomater Sci Eng p.acsbiomaterials.6b00129

Jewett JC, Sletten EM, Bertozzi CR (2010) Rapid Cu-free click chemistry with readily synthesized biarylazacyclooctynones. J Am Chem Soc 132(11):3688–3690

Jo D (1996) Breast development in puberty. In: Angeli A DL, Bradlow HL (eds) Endocrinology of the breast: Basic and clinical aspects. Annals of the New York Academy of Sciences. The New York Academy of Sciences, New York, pp 58–66

Jo YS et al (2010) Biomimetic PEG hydrogels crosslinked with minimal plasmin-sensitive tri-amino acid peptides. J Biomed Mater Res, Part A 93(3):870–877

Johns RA et al (1995) Halothane and isoflurane inhibit endothelium-derived relaxing factor-dependent cyclic guanosine monophosphate accumulation in endothelial cell-vascular smooth muscle co-cultures independent of an effect on guanylyl cyclase activation. J Am Soc Anesthesiologists 83(4):823–834

Julia T et al (2013) Fibroblast activation protein expression by stromal cells and tumor-associated macrophages in human breast cancer. Hum Pathol 44(11):2549–2557

Kacinski BM (1997) CSF-1 and its receptor in breast carcinomas and neoplasms of the female reproductive tract. Mol Reprod Dev 46:71–74

Kacinski BM (1995) CSF-1 and its receptor in ovarian, endometrial and breast cancer. Ann Med 27(1):79–85

Kalluri R, Zeisberg M (2006) Fibroblasts in cancer. Nat Rev Cancer 6(5):392–401

Kang SW, Bae YH (2009) Cryopreservable and tumorigenic three-dimensional tumor culture in porous poly(lactic-co-glycolic acid) microsphere. Biomaterials 30(25):4227–4232

Keely P, Nain A (2015) Capturing relevant extracellular matrices for investigating cell migration. F1000 Res 4(May)

Kelm JM et al (2003) Method for generation of homogeneous multicellular tumor spheroids applicable to a wide variety of cell types. Biotechnol Bioeng 83(2):173–180

Kerbel RS (2003) Human tumor xenografts as predictive preclinical models for anticancer drug activity in humans: better than commonly perceived-but they can be improved. Cancer Biol Ther 2(4 Suppl 1)

Keriquel V et al (2010) In vivo bioprinting for computer- and robotic-assisted medical intervention: preliminary study in mice. Biofabrication 2(1):014101

Kerkar SP, Restifo NP (2012) Cellular constituents of immune escape within the tumor microenvironment. Cancer Res 72(13):3125–3130

Kim B, Forbes NS (2007) Flux analysis shows that hypoxia-inducible- factor-1-alpha minimally affects intracellular metabolism in tumor spheroids. Biotechnol Bioeng 96(6):1167–1182

Kim J et al (2011) NONOates–polyethylenimine hydrogel for controlled nitric oxide release and cell proliferation modulation. Bioconjug Chem 22(6):1031–1038

Kim J Bin (2005) Three-dimensional tissue culture models in cancer biology. Semin Cancer Biol 15(5):365–377

Kim YJ et al (2009) Three-dimensional gastric cancer cell culture using nanofiber scaffold for chemosensitivity test. Int J Biol Macromol 45(1):65–71

Kimura M et al (2004) Hydrogen-bonding-driven spontaneous gelation of water-soluble phospholipid polymers in aqueous medium. J Biomater Sci Polym Ed 15(5):631–644

Kleinman HK, Martin GR (2005) Matrigel: basement membrane matrix with biological activity. Semin Cancer Biol 15(5 SPEC. ISS.):378–386

Koehler KC, Anseth KS, Bowman CN (2013) Diels-Alder mediated controlled release from a poly (ethylene glycol) based hydrogel. Biomacromolecules 14(2):538–547

Kolesky DB et al (2014) 3D bioprinting of vascularized, heterogeneous cell-laden tissue constructs. Adv Mater 26(19):3124–3130

Kraning-Rush CM, Reinhart-King CA (2012) Controlling matrix stiffness and topography for the study of tumor cell migration. Cell Adhes Migr 6(3):274–279

Kraus AC et al (2002) In vitro chemo- and radio-resistance in small cell lung cancer correlates with cell adhesion and constitutive activation of AKT and MAP kinase pathways. Oncogene 21(57):8683–8695

Kumar PR et al (2012) Nanofibers: effective generation by electrospinning and their applications. J Nanosci Nanotechnol 12(1):1–25
Kunz-Schughart LA et al (2004) The Use of 3-D cultures for high-throughput screening. J Biomol Screen 9(4):273–285
Kuo CY et al (2016) Development of a 3D printed, bioengineered placenta model to evaluate the role of trophoblast migration in preeclampsia. ACS Biomater Sci Eng 2(10):1817–1826
Kuperwasser C et al (2004) Reconstruction of functionally normal and malignant human breast tissues in mice. Proc Nat Acad Sci USA 101(14):4966–4971
Laconte L, Nitin N, Bao G (2005) Magnetic nanoparticle probes. Mater Today 8(5):32–38
Laguinge LM et al (2004) Nitrosative stress in rotated three-dimensional colorectal carcinoma cell cultures induces microtubule depolymerization and apoptosis. Cancer Res 64(8):2643–2648
Lai J-Y (2012) Biocompatibility of genipin and glutaraldehyde cross-linked chitosan materials in the anterior chamber of the eye. Int J Mol Sci 13(9):10970–10985
Lam CX et al (2008) Dynamics of in vitro polymer degradation of polycaprolactone-based scaffolds: accelerated versus simulated physiological conditions. Biomed Mater 3(3):034108
Lamichhane SP et al (2016) Recapitulating epithelial tumor microenvironment in vitro using three dimensional tri-culture of human epithelial, endothelial, and mesenchymal cells. BMC cancer 16(1):581
Langer R, Vacanti JP (1993) Tissue engineering. Sci (NY) 260(5110):920–926
Lazard D et al (1993) Expression of smooth muscle-specific proteins in myoepithelium and stromal myofibroblasts of normal and malignant human breast tissue. Proc Nat Acad Sci USA 90(3):999–1003
Lee JW et al (2016a) Development of a 3D cell printed construct considering angiogenesis for liver tissue engineering. Biofabrication 8(1):15007
Lee BK, Yun Y, Park K (2016b) PLA micro- and nano-particles. Adv Drug Deliv Rev S0169–409X(16):30180–30186
Lee E et al (2015) Crosstalk between cancer cells and blood endothelial and lymphatic endothelial cells in tumour and organ microenvironment. Expert Rev Mol Med 17:e3
Lee S-H et al (2007) Poly(ethylene glycol) hydrogels conjugated with a collagenase-sensitive fluorogenic substrate to visualize collagenase activity during three-dimensional cell migration. Biomaterials 28(20):3163–3170
Lee SY et al (2008) A novel self-sintering microparticle-based system for regenerative medicine. Eur Cells Mater 16(3):71
Lee WR et al (2011) Magnetic levitating polymeric nano/microparticular substrates for three-dimensional tumor cell culture. Colloids Surf B 85(2):379–384
Leu AJ et al (2000) Absence of functional lymphatics within a murine sarcoma : a molecular and functional evaluation advances in brief absence of functional lymphatics within a murine sarcoma : a molecular and functional evaluation 1. Cancer Res 4324–4327
Leung M et al (2010) Chitosan-alginate scaffold culture system for hepatocellular carcinoma increases malignancy and drug resistance. Pharm Res 27(9):1939–1948
Levental KR et al (2009) Matrix crosslinking forces tumor progression by enhancing integrin signaling. Cell 139(5):891–906
Lewis MP et al (2004) Tumour-derived TGF-beta1 modulates myofibroblast differentiation and promotes HGF/SF-dependent invasion of squamous carcinoma cells. Br J Cancer 90(4):822–832
Li G et al (2003) Function and regulation of melanoma–stromal fibroblast interactions: when seeds meet soil. Oncogene 22(20):3162–3171
Li H, Fan X, Houghton J (2007) Tumor microenvironment: The role of the tumor stroma in cancer. J Cell Biochem 101(4):805–815
Li X et al (2014a) Micro-scaffold array chip for upgrading cell-based high-throughput drug testing to 3D using benchtop equipment. Lab Chip 14(3):471–481
Li Y et al (2014b) Effects of mechanical properties on tumor invasion: Insights from a cellular model. Conf Proc IEEE Eng Med Biol Soc 2014:6818–6821
Li Y et al (2012) Well-defined, reversible boronate crosslinked nanocarriers for targeted drug delivery in response to acidic pH values and cis -Diols. Angew Chem 124(12):2918–2923

Lichtenstein A et al (1996) Interleukin-6 inhibits apoptosis of malignant plasma cells. Cell Immunol 162(2):248–255
Lin EY et al (2001) Colony-stimulating factor 1 promotes progression of mammary tumors to malignancy. J Exp Med 193(6):727–740
Lin CC, Raza A, Shih H (2011) PEG hydrogels formed by thiol-ene photo-click chemistry and their effect on the formation and recovery of insulin-secreting cell spheroids. Biomaterials 32(36):9685–9695
Lin RZ, Chang HY (2008) Recent advances in three-dimensional multicellular spheroid culture for biomedical research. Biotechnol J 3(9–10):1172–1184
Lin RZ et al (2008) Magnetic reconstruction of three-dimensional tissues from multicellular spheroids. Tissue Eng Part C, Methods 14(3):197–205
Liu C et al (2015) Role of three-dimensional matrix stiffness in regulating the chemoresistance of hepatocellular carcinoma cells. Biotechnol Appl Biochem 62(4):556–562
Liu T et al (2014) Advanced micromachining of concave microwells for long term on-chip culture of multicellular tumor spheroids. ACS Appl Mater Interfaces 6(11):8090–8097
Lozinsky VI et al (2003) Polymeric cryogels as promising materials of biotechnological interest. Trends Biotechnol 21(10):445–451
Lozinsky VI, Plieva FM (1998) Poly(vinyl alcohol) cryogels employed as matrices for cell immobilization. 3. Overview of recent research and developments. Enzym Microb Technol 23(3–4):227–242
Lu P, Weaver VM, Werb Z (2012) The extracellular matrix: a dynamic niche in cancer progression. J Cell Biol 196(4):395–406
Luo Y, Shoichet MS (2004) Light-activated immobilization of biomolecules to agarose hydrogels for controlled cellular response. Biomacromolecules 5(6):2315–2323
Mak IW, Evaniew N, Ghert M (2014) Lost in translation: animal models and clinical trials in cancer treatment. Am J Transl Res 6(2):114–118
Malda J et al (2003) Expansion of bovine chondrocytes on microcarriers enhances redifferentiation. Tissue Eng 9(5):939–948
Malik R, Lelkes PI, Cukierman E (2015) Biomechanical and biochemical remodeling of stromal extracellular matrix in cancer. Trends Biotechnol 33(4):230–236
Manabe Y et al (2003) Mature adipocytes, but not preadipocytes, promote the growth of breast carcinoma cells in collagen gel matrix culture through cancer–stromal cell interactions. J Pathol 201(2):221–228
Mann BK et al (2001) Smooth muscle cell growth in photopolymerized hydrogels with cell adhesive and proteolytically degradable domains: synthetic ECM analogs for tissue engineering. Biomaterials 22(22):3045–3051
Manoto SL, Houreld NN, Abrahamse H (2015) Resistance of lung cancer cells grown as multicellular tumour spheroids to zinc sulfophthalocyanine photosensitization. 10185–10200
Marklein RA, Burdick JA (2010) Spatially controlled hydrogel mechanics to modulate stem cell interactions. Soft Matter 6(1):136–143
Maubant S et al (2002) Altered adhesion properties and alphav integrin expression in a cisplatin-resistant human ovarian carcinoma cell line. Int J Cancer 97(2):186–194
Maurer BJ et al (1999) Growth of human tumor cells in macroporous microcarriers results in p 53-independent, decreased cisplatin sensitivity relative to monolayers. Mol Pharmacol 55(5):938–947
Mayer B et al (2001) Multicellular gastric cancer spheroids recapitulate growth pattern and differentiation phenotype of human gastric carcinomas. Gastroenterology 121(4):839–852
Michael S et al (2013) Tissue engineered skin substitutes created by laser-assisted bioprinting form skin-like structures in the dorsal skin fold chamber in mice. PLoS ONE 8(3):e57741
Mierke CT (2014) The fundamental role of mechanical properties in the progression of cancer disease and inflammation. Rep Prog Phys 77(7):076602
Milosevic MF et al (1998) Interstitial fluid pressure in cervical carcinoma: within tumor heterogeneity, and relation to oxygen tension. Cancer 82:2418–2426
Minchinton AI, Tannock IF (2006) Drug penetration in solid tumours. Nat Rev Cancer 6(8):583–592

Miyake H et al (1998) Expression of basic fibroblast growth factor is associated with resistance to cisplatin in a human bladder cancer cell line. Cancer Lett 123(2):121–126
Mueller MM, Fusenig NE (1999) Constitutive expression of G-CSF and GM-CSF in human skin carcinoma cells with functional consequence for tumor progression. Int J Cancer 83(6):780–789
Mueller MM et al (1999) Autocrine growth regulation by granulocyte colony-stimulating factor and granulocyte macrophage colony-stimulating factor in human gliomas with tumor progression. Am J Pathol 155(5):1557–1567
Mueller MM, Fusenig NE (2004) Friends or foes—bipolar effects of the tumour stroma in cancer. Nat Rev Cancer 4(11):839–849
Murphy SV, Atala A (2014) 3D bioprinting of tissues and organs. Nat Biotechnol 32:773–785
Nakajima M et al (2007) Combinatorial protein display for the cell-based screening of biomaterials that direct neural stem cell differentiation. Biomaterials 28(6):1048–1060
Nimmo CM, Shoichet MS (2011) Regenerative biomaterials that "click": simple, aqueous-based protocols for hydrogel synthesis, surface immobilization, and 3D patterning. Bioconjug Chem 22(11):2199–2209
Nimmo CM, Owen SC, Shoichet MS (2011) Diels-Alder Click cross-linked hyaluronic acid hydrogels for tissue engineering. Biomacromolecules 12(3):824–830
Norotte C et al (2009) Scaffold-free vascular tissue engineering using bioprinting. Biomaterials 30 (30):5910–5917
Obermueller E et al (2004) Cooperative autocrine and paracrine functions of granulocyte colony-stimulating factor and granulocyte-macrophage colony-stimulating factor in the progression of skin carcinoma cells. Cancer Res 64(21):7801–7812
Ogata A et al (1997) IL-6 triggers cell growth via the Ras-dependent mitogen-activated protein kinase cascade. J Immunol (Baltimore, Md.: 1950) 159(Mm):2212–2221
Ogawa T et al (2004) Regulation of biological activity of laminin-5 by proteolytic processing of gamma2 chain. J Cell Biochem 92(4):701–714
Oliveira MB, Mano JF (2011) Polymer-based microparticles in tissue engineering and regenerative medicine. Biotechnol Prog 27(4):897–912
Olumi AF et al (1999) Carcinoma-associated fibroblasts direct tumor progression of initiated human prostatic epithelium carcinoma-associated fibroblasts direct tumor progression of initiated human. 59(19):5002–5011
Orimo A et al (2001) Cancer-associated myofibroblasts possess various factors to promote endometrial tumor progression. Clin Cancer Res 7(10):3097–3105
Orimo A et al (2005) Stromal fibroblasts present in invasive human breast carcinomas promote tumor growth and angiogenesis through elevated SDF-1/CXCL12 secretion. Cell 121(3):335–348
Ozcelik B et al (2014) Highly porous and mechanically robust polyester poly(ethylene glycol) sponges as implantable scaffolds. Acta Biomater 10(6):2769–2780
Paget S (1989) The distribution of secondary growths in cancer of the breast. 1889. Cancer Metastasis Rev 8(2):98
Park KH, Na K, Chung HM (2005) Enhancement of the adhesion of fibroblasts by peptide containing an Arg-Gly-Asp sequence with poly(ethylene glycol) into a thermo-reversible hydrogel as a synthetic extracellular matrix. Biotechnol Lett 27(4):227–231
Paszek MJ et al (2005) Tensional homeostasis and the malignant phenotype. Cancer Cell 8(3):241–254
Patel A, Mequanint K (2011) Hydrogels Biomaterials. www.intechopen.com
Patrick AG, Ulijn RV (2010) Hydrogels for the detection and management of protease levels. Macromol Biosci 10(10):1184–1193
Pavesi A et al (2016) Engineering a 3D microfluidic culture platform for tumor-treating field application. Sci Rep 6:1–10
Phelps EA et al (2010) Bioartificial matrices for therapeutic vascularization. Proc Natl Acad Sci USA 107(8):3323–3328
Phillippi JA et al (2008) Microenvironments engineered by inkjet bioprinting spatially direct adult stem cells toward muscle- and bone-like subpopulations. Stem Cells 26(1):127–134

Pickup MW, Mouw JK, Weaver VM (2014) The extracellular matrix modulates the hallmarks of cancer. EMBO Rep 15(12):1243–1253
Pirilä E et al (2003) Matrix metalloproteinases process the laminin-5 2-chain and regulate epithelial cell migration. Biochem Biophys Res Commun 303(4):1012–1017
Pollard JW (2004) Tumour-educated macrophages promote tumour progression and metastasis. Nat Rev Cancer 4:71–78
Raeber GP, Lutolf MP, Hubbell JA (2007) Mechanisms of 3-D migration and matrix remodeling of fibroblasts within artificial ECMs. Acta Biomater 3(5):615–629
Rafii S, Heissig B, Hattori K (2002) Efficient mobilization and recruitment of marrow-derrived endothelial and hematopoietic stem cells by adenoviral vectors expressing angiogenic factors. Gene Ther 9:631–641
Re'em T, Tsur-Gang O, Cohen S (2010) The effect of immobilized RGD peptide in macroporous alginate scaffolds on TGF??1-induced chondrogenesis of human mesenchymal stem cells. Biomaterials 31(26):6746–6755
Reid B et al (2013) PEG hydrogel degradation and the role of the surrounding tissue environment. J Tissue Eng Regenerative Med 9(3):315–318
Reilly GC, Engler AJ (2010) Intrinsic extracellular matrix properties regulate stem cell differentiation. J Biomech 43(1):55–62
Rettig WJ (1993) Regulation and heteromeric structure of the fibroblast activation protein in normal and transformed cells of mesenchymal and neuroectodermal origin. Cancer Res 53:3327–3335
Rezende R et al (2007) Experimental characterisation of the alginate gelation process for rapid prototyping. In: The eighth international conference on chemical & process engineering. vol 11. pp 509–514
Rhee HW et al (2001) Permanent phenotypic and genotypic changes of prostate cancer cells cultured in a three-dimensional rotating-wall vessel. In Vitro Cell Dev Biol Anim 37(3):127–140
Richmond A, Su Y (2008) Mouse xenograft models versus GEM models for human cancer therapeutics. Dis Models Mech 1(2–3):78–82
Sahoo SK, Panda AK, Labhasetwar V (2005) Characterization of porous PLGA/PLA microparticles as a scaffold for three dimensional growth of breast cancer cells. Biomacromolecules 6(2):1132–1139
Salinas CN, Anseth KS (2008) The enhancement of chondrogenic differentiation of human mesenchymal stem cells by enzymatically regulated RGD functionalities. Biomaterials 29(15):2370–2377
Sanabria-DeLong N et al (2006) Controlling hydrogel properties by crystallization of hydrophobic domains. Macromolecules 39(4):1308–1310
Sansone P, Bromberg J (2012) Targeting the interleukin-6/jak/stat pathway in human malignancies. J Clin Oncol 30(9):1005–1014
Sato T et al (2004) Tumor-stromal cell contact promotes invasion of human uterine cervical carcinoma cells by augmenting the expression and activation of stromal matrix metalloproteinases. Gynecol Oncol 92(1):47–56
Sawhney AS (1993) Bioerodible hydrogels based on Photopolymerized Poly(ethy1ene. Macromolecules 26:581–587
Saxon E (2000) Cell surface engineering by a modified staudinger reaction. Science 287 (5460):2007–2010
Saxon E, Armstrong JI, Bertozzi CR (2000) A "traceless" Staudinger ligation for the chemoselective synthesis of amide bonds. Org Lett 2(14):2141–2143
Schmidt M, Lichtner RB (2002) EGF receptor targeting in therapy-resistant human tumors. Drug Resist Updates 5(1):11–18
Sekiguchi Y, Sawatari C, Kondo T (2003) A gelation mechanism depending on hydrogen bond formation in regioselectively substituted O-methylcelluloses. Carbohydr Polym 53(2):145–153
Sell SA et al (2009) Electrospinning of collagen/biopolymers for regenerative medicine and cardiovascular tissue engineering. Adv Drug Deliv Rev 61(12):1007–1019

Sethi T et al (1999) Extracellular matrix proteins protect small cell lung cancer cells against apoptosis: a mechanism for small cell lung cancer growth and drug resistance in vivo. Nat Med 5(6):662–668
Shekhar MPV et al (2001) Breast stroma plays a dominant regulatory role in breast epithelial growth and differentiation: implications for tumor development and progression. Cancer Res 61(4):1320–1326
Shikanov A et al (2011) Hydrogel network design using multifunctional macromers to coordinate tissue maturation in ovarian follicle culture. Biomaterials 32(10):2524–2531
Shor L et al (2009) Precision extruding deposition (PED) fabrication of polycaprolactone (PCL) scaffolds for bone tissue engineering. Biofabrication 1(1):015003
Shu XZ et al (2002) Disulfide cross-linked hyaluronan hydrogels. Biomacromolecules 3(6):1304–1311
Siegel R, Miller K, Jemal A (2015) Cancer statistics, 2015. CA Cancer J Clin 65(1):5–29
Sill TJ, von Recum HA (2008) Electrospinning: applications in drug delivery and tissue engineering. Biomaterials 29(13):1989–2006
Skardal A et al (2012) Bioprinted amniotic fluid-derived stem cells accelerate healing of large skin wounds. Stem Cells Transl Med 1(11):792–802
Skardal A et al (2010) The generation of 3-D tissue models based on hyaluronan hydrogel-coated microcarriers within a rotating wall vessel bioreactor. Biomaterials 31(32):8426–8435
Skobe M, Fusenig NE (1998) Tumorigenic conversion of immortal human keratinocytes through stromal cell activation. Proc Nat Acad Sci USA 95(3):1050–1055
Smalley KSM, Lioni M, Herlyn M (2006) Life isn't flat: taking cancer biology to the next dimension. In vitro cellular & developmental biology. Animal 42(8–9):242–247
Smeds KA et al (2001) Photocrosslinkable polysaccharides for in situ hydrogel formation. J Biomed Mater Res 54(1):115–121
Smeriglio P et al (2015) 3D hydrogel scaffolds for articular chondrocyte culture and cartilage generation. J Visualized Exp 104:1–6
Smith HO et al (1995) The role of colony-stimulating factor 1 and its receptor in the etiopathogenesis of endometrial adenocarcinoma. Clin Cancer Res 1(3):313–325
Smith SJ et al (2012) Recapitulation of tumor heterogeneity and molecular signatures in a 3D brain cancer model with decreased sensitivity to histone deacetylase inhibition. PLoS ONE 7(12): e52335
Souza GR et al (2010) Three-dimensional tissue culture based on magnetic cell levitation. Nat Nanotechnol 5(4):291–296
Stetler-Stevenson WG, Yu AE (2001) Proteases in invasion: matrix metalloproteinases. Semin Cancer Biol 11(2):143–152
Sui X et al (2010) Preparation of a rapidly forming Poly(ferrocenylsilane)-Poly(ethylene glycol)-based hydrogel by a thiol-michael addition click reaction. Macromol Rapid Commun 31(23):2059–2063
Sutherland RM (1988) Microregions: the spheroid model. Science 240:177–240
Sutherland RM, Inch WR, McCredie JA (1970) A multi—component radiation survival curve using an in vitro tumour model Int J Rad Biol 18(5):491–495
Takagi A et al (2007) Three-dimensional cellular spheroid formation provides human prostate tumor cells with tissue-like features. Anticancer Res 27(1 A):45–54
Talukdar S et al (2011) Engineered silk fibroin protein 3D matrices for in vitro tumor model. Biomaterials 32(8):2149–2159
Tam RY et al (2016) Transparent porous polysaccharide cryogels provide biochemically defined, biomimetic matrices for tunable 3D cell culture. Chem Mater 28(11):3762–3770
Tannock IF et al (2002) Limited penetration of anticancer drugs through tumor tissue : a potential cause of resistance of solid tumors to chemotherapy limited penetration of anticancer drugs through tumor tissue : a potential cause of resistance of solid tumors to chemotherapy 1. Clin Cancer Res: Official J Am Assoc Cancer Res 8:878–884
Tasoglu S et al (2014) Guided and magnetic self-assembly of tunable magnetoceptive gels. Nat Commun 5:4702
Tasoglu S, Demirci U (2013) Bioprinting for stem cell research. Trends Biotechnol 6(2):149–155

Tekin E, Smith PJ, Schubert US (2008) Inkjet printing as a deposition and patterning tool for polymers and inorganic particles. Soft Matter 4(4):703–713
Thomlinson RH, Gray LH (1955) The histological structure of some human lung cancers and the possible implications for radiotherapy. Br J Cancer 9:539–549
Tong JZ et al (1992) Long-term culture of adult rat hepatocyte spheroids. Exp Cell Res 200(2):326–332
Tripathi A, Melo JS (2015) Preparation of sponge-like biocomposite agarose-chitosan scaffold with primary hepatocytes for establishing an in-vitro 3D liver tissue model. RSC Adv 5:30701–30710
Tsubota Y et al (2000) Isolation and activity of proteolytic fragment of laminin-5 alpha3 chain. Biochem Biophys Res Commun 278(3):614–620
Tung YC et al (2011) High-throughput 3D spheroid culture and drug testing using a 384 hanging drop array. Analyst 136(3):473–478
Tuzlakoglu K, Reis RL (2009) Biodegradable polymeric fiber structures in tissue engineering. Tissue Eng Part B, Rev 5(1):17–27
Ulrich TA, de Juan Pardo EM, Kumar S (2009) The mechanical rigidity of the extracellular matrix regulates the structure, motility, and proliferation of glioma cells. Cancer Res 69(10):4167–4174
Unsworth BR, Lelkes PI (1988) Growing Tissues Microgravity 4(8):901–907
Visconti RP et al (2015) Towards organ printing: engineering an intra-organ branched vascular tree 10(3):409–420
Visser J et al (2013) Biofabrication of multi-material anatomically shaped tissue constructs. Biofabrication 5(3):035007
Wagner I et al (2013) A dynamic multi-organ-chip for long-term cultivation and substance testing proven by 3D human liver and skin tissue co-culture. Lab Chip 13(18):3538–3547
Wang F, Weaver VM, Pete OW (1998) Reciprocal interactions between β1-integrin and epidermal growth factor receptor in three-dimensional basement membrane breast cultures: A different perspective in epithelial biology. Proc Natl Acad Sci USA 95:14821–14826
Weaver VM et al (2002) Beta 4 integrin-dependent formation of polarized three- dimensional architecture confers resistance to apoptosis in normal and malignant mammary epithelium. Cancer Cell 2:205–216
Webber MM et al (1997) Acinar differentiation by non-malignant immortalized human prostatic epithelial cells and its loss by malignant cells. Carcinogenesis 18(6):1225–1231
Wegiel B et al (2008) Interleukin-6 activates PI3K/Akt pathway and regulates cyclin A1 to promote prostate cancer cell survival. Int J Cancer 122(7):1521–1529
Wenger MPE et al (2007) Mechanical properties of collagen fibrils. Biophys J 93(4):1255–1263
West JL, Hubbell JA (1999) Polymeric biomaterials with degradation sites for proteases involved in cell migration. Macromolecules 32(1):241–244
West KA, Castillo SS, Dennis PA (2002) Activation of the PI3K/Akt pathway and chemotherapeutic resistance. Drug Resist Updates 5:234–248
De Wever O et al (2004) Tenascin-C and SF/HGF produced by myofibroblasts in vitro provide convergent pro-invasive signals to human colon cancer cells through RhoA and Rac. FASEB J 18(9):1016–1018
De Wever O, Mareel M (2003) Role of tissue stroma in cancer cell invasion. J Pathol 200(4):429–447
Williams DF (2008) On the mechanisms of biocompatibility. Biomaterials 29(20):2941–2953
Wong JY et al (2003) Directed movement of vascular smooth muscle cells on gradient-compliant hydrogels. Langmuir 19:1908–1913
Wong SY, Kumar S (2014) Matrix regulation of tumor-initiating cells. Prog Mol Biol Transl Sci 126:243–256
Wylie RG et al (2011) Spatially controlled simultaneous patterning of multiple growth factors in three-dimensional hydrogels. Nat Mater 10(10):799–806
Xu F, Sridharan B et al (2011a) Embryonic stem cell bioprinting for uniform and controlled size embryoid body formation. Biomicrofluidics 5(2):1–8
Xu F, Wu CAM et al (2011b) Three-dimensional magnetic assembly of microscale hydrogels. Adv Mater 23(37):4254–4260

Xu F, Celli J et al (2011c) A three-dimensional in vitro ovarian cancer coculture model using a high-throughput cell patterning platform. Biotechnol J 6(2):204–212
Xu G et al (2014) In vitro ovarian cancer model based on three-dimensional agarose hydrogel. J Tissue Eng 5:2041731413520438
Xu T et al (2013) Complex heterogeneous tissue constructs containing multiple cell types prepared by inkjet printing technology. Biomaterials 34(1):130–139
Xu T et al (2005) Inkjet printing of viable mammalian cells. Biomaterials 26(1):93–99
Xu T et al (2006) Viability and electrophysiology of neural cell structures generated by the inkjet printing method. Biomaterials 27(19):3580–3588
Xu X et al (2012) Recreating the tumor microenvironment in a bilayer, hyaluronic acid hydrogel construct for the growth of prostate cancer spheroids. Biomaterials 33(35):9049–9060
Xu Z et al (2013) Biomaterials Application of a micro fluidic chip-based 3D co-culture to test drug sensitivity for individualized treatment of lung cancer. Biomaterials 34(16):4109–4117
Yamada KM, Cukierman E (2007) Modeling tissue morphogenesis and cancer in 3D. Cell 130(4):601–610
Yamada M et al (2015) Cell-sized condensed collagen microparticles for preparing microengineered composite spheroids of primary hepatocytes. Lab Chip 15(19):3941–3951
Yang Y, Rossi FMV, Putnins EE (2007) Ex vivo expansion of rat bone marrow mesenchymal stromal cells on microcarrier beads in spin culture. Biomaterials 28(20):3110–3120
Yang Z, Zhao X (2011) A 3D model of ovarian cancer cell lines on peptide nanofiber scaffold to explore the cell-scaffold interaction and chemotherapeutic resistance of anticancer drugs. Int J Nanomed 6:303–310
Yuhas JM et al (1977) A simplified method for production and growth of multicellular tumor spheroids. Cancer Res 37:3639–3643
Zanoni M et al (2016) 3D tumor spheroid models for in vitro therapeutic screening: a systematic approach to enhance the biological relevance of data obtained. Sci Rep 6(August 2015), p. 19103
Zervantonakis IK et al (2012) Three-dimensional microfluidic model for tumor cell intravasation and endothelial barrier function. Proc Natl Acad Sci 109(34):13515–13520
Zhao Y et al (2014) Three-dimensional printing of Hela cells for cervical tumor model in vitro. Biofabrication 6(3):035001
Zhong H et al (1999) Overexpression of hypoxia-inducible factor 1α in common human cancers and their metastases. Cancer Res 59(22):5830–5835
Zhou Y et al (2011) Photopolymerized water-soluble chitosan-based hydrogel as potential use in tissue engineering. Int J Biol Macromol 48(3):408–413
Zhu J (2010) Bioactive modification of Poly(ethylenglykol) Hydrogels for tissue engineering. Biomaterials 31(17):4639–4656
Zhu J, Marchant RE (2011) Design properties of hydrogel tissue-engineering scaffolds. Expert Rev Med Devices 8(5):607–626
Zohora FT, Yousuf A, Anwarul M (2014) Inkjet printing: an emerging technology for 3D tissue or organ printing. Eur Sci J 10(30):339–352
Zopf DA et al (2013) Bioresorbable airway splint created with a three-dimensional printer. New Engl J Med 368(21):2042–2043
Zustiak SP (2015) The role of matrix compliance on cell responses to drugs and toxins: towards predictive drug screening platforms. Macromol Biosci 15(5):589–599
Zustiak SP et al (2015) Three-dimensional matrix stiffness and adhesive ligands affect cancer cell response to toxins. Biotechnol Bioeng 113(2):443–452

Magnetic Nanoparticles: Functionalization and Manufacturing of Pluripotent Stem Cells

Masanobu Horie, Anuj Tripathi, Akira Ito, Yoshinori Kawabe and Masamichi Kamihira

Abstract Regenerative medicine uses cell alone or in combination with carrier to deliver at the required site for restoring the normal functions of diseased or degenerated tissue. Various strategies to restore tissue functions involve specific cell types, scaffolds and delivery processes that are still in developmental stage. Obtaining sufficient quantity of cells by non-invasive approach for the application in regenerative medicine is still a challenge. Pluripotent stem cells (PSCs), including embryonic stem cells and induced pluripotent stem cells (iPSCs), possess the inherent ability of self-renewal and differentiation into many cell types. In particular, iPSCs are of a special interest because patient-derived iPSCs have the ability to reproduce patient-specific clinical conditions. The development of manufacturing systems for PSCs, including cell culture engineering, is a challenging research field for the clinical application of PSCs such as in regenerative medicine. One of these manufacturing systems uses magnetic nanoparticles which are well known for their application in magnetic resonance imaging and magnetic hyperthermia. Besides, this chapter is focused on the basics of magnetic nanoparticles, its functionalization and further applications of a magnetic force-based cell manufacturing system for pluripotent stem cells. Indeed, we have developed a procedure in which cells are labeled with magnetite cationic liposomes via electrostatic interaction between the positively charged liposomes and the target cells. The culture system may provide a useful tool for studying the behavior of PSCs and an efficient way of PSCs manufacturing for clinical applications.

M. Horie (✉)
Division of Biochemical Engineering, Radioisotope Research Centre,
Kyoto University, Yoshida Konoe-Cho, Sakyo-Ku, Kyoto 606-8501, Japan
e-mail: horie.masanobu.4z@kyoto-u.ac.jp

A. Tripathi
Nuclear Agriculture and Biotechnology Division, Bhabha Atomic Research Centre,
Mumbai 400085, India

A. Ito · Y. Kawabe · M. Kamihira
Department of Chemical Engineering, Faculty of Engineering, Kyushu University,
744 Motooka, Nishi-Ku, Fukuoka 819-0395, Japan

A. Tripathi and J.S. Melo (eds.), *Advances in Biomaterials for Biomedical Applications*, Advanced Structured Materials 66,
DOI 10.1007/978-981-10-3328-5_9

Keywords Regenerative medicine · Pluripotent stem cells · Feeder cells · Magnetic cell separation · Magnetite cationic liposomes

Abbreviations

3D	Three dimensional
PSC	Pluripotent stem cells
iPSCs	Induced pluripotent stem cells
ESCs	Embryonic stem cells
EBs	Embryoid bodies
mESCs	Mouse embryonic stem cells
mPSCs	Mouse pluripotent stem cells
Mag-TE	Magnetic force-based tissue engineering
MEFs	Mouse embryonic fibroblasts
MNPs	Magnetic nanoparticles
NPs	Nanoparticles
SPM	Superparamagnetic nanoparticles
CTAB	Cetyltrimethyl ammonium bromide
PLGA	Poly(lactic-coglycolic acid)
PVA	Polyvinyl alcohol
PEG	Polyethylene glycol
PAA	Polyacrylic acid
NIPAAM	N-isopropyl acrylamide
PEI	Polyethyleneamine
PVP	Polyvinyl pyrrolidone
MCLs	Magnetite cationic liposomes
MRI	Magnetic resonance imaging
TMAG	N-(α-trimethylammonioacetyl)-didodecyl-D- glutamate chloride
DLPC	Dilauroylphosphatidylcholine
DOPE	Dioleoylphosphati- dylethanolamine
LIF	Leukaemia inhibitory factor
BMP-4	Bone morphogenetic protein-4
TGF-β	Transforming growth factor-β
bFGF	Basic fibroblast growth factor
AP+	Alkaline phosphatase-positive

1 Introduction

One of the rapidly evolving interdisciplinary fields in biomedicine that replace or regenerate human cells, tissues or even the whole organ to restore its normal functions is dealt under the field of regenerative medicine. The current trend and impact of nano-technology in regenerative medicine is aiming to engineer a suitable non-invasive system for the manufacturing of cells that can provide reformative

strategies in clinical practices. Various nano-biomaterial systems have evolved in last few decades using metallic (like gold and magnetic nanoparticles) and non-metallic (natural and synthetic polymeric nanoparticles) precursors. The role of regenerative medicine would be reinforced and expanded in the future if it can provide a viable alternative to the conventional approaches of organ transplantation and implantation of mechanical support devices. In order to achieve this, novel technologies are required in regenerative medicine to manufacture biomimetic cellular three-dimensional (3D) tissue construct. Over two hundred products of regenerative medicine which includes implantable bio-mimetic devices, scaffolds, tissue-engineered constructs and cell-based therapies have been developed for the treatment of diabetes, immune and inflammatory diseases (Bokkelen 2013). However, only few products manage the onerous path for clinical applications, which has been challenged with scientific and engineering enquiries about manufacturing, packaging and delivery of stem cells or tissues, the understanding and control of cellular micro-environment and also the assessment of therapeutic potential (Healy et al. 2013; Martin et al. 2014; Weissman 2000).

Stem cells which encompass a large class of cell types like pluripotent stem cells (PSCs) including embryonic stem cells (ESCs) derived from embryos and induced pluripotent stem cells (iPSCs) derived from somatic cells (Takahashi and Yamanaka 2006; Thomson et al. 1998), are master cells from which all organs and tissues of the body can be generated. These PSCs derived from various kinds of mammals including mouse and humans are characterized by self-renewal and differentiation potentials. Thus, many researchers have focused on culturing of PSCs for the use as an infinite cell source in many areas of research and medicine. For example, the development of biologically active construct has the requirement of suitable cell types that do not show immunogenic behavior, can proliferate, are easy to harvest and have ability to differentiate in any cell type with respective cellular functions. iPSCs resemble biological similarities with ESCs like morphology, differentiation potential and molecular signature to generate different cell types which are organ specific and can be established from a patient's own somatic cells. These properties of iPSC surpass the limitation of ESCs and therefore it could be a suitable replacement of ESCs. The reprogramming of patient's own cells to generate iPSCs hold great promise for generating engineered tissues and other therapeutic applications by avoiding the ethical and histoincompatibility issues which are associated with the use of ESCs (Yamanaka 2012). Additionally, it excludes the invasive procedures to obtain pluripotent cells due to the huge availability of cell types that can be reprogrammed.

For biochemical engineers, the manufacturing of PSCs remains challenging. One of the processes that use magnetic nanoparticles and magnetic force has shown potential for efficient culturing of PSCs. In this process, cells are magnetically labeled through uptake of magnetic nanoparticles and the physical interaction between PSCs and feeder cells is enhanced by the magnetic force. Furthermore, this process allows a simple isolation of specific cell types from a co-culture system using magnetic separation. This technique also facilitates PSC manufacturing processes because target cells can be non-invasively manipulated using a magnetic

force. This novel methodology for tissue engineering using magnetic nanoparticles and magnetic force is designated as "magnetic force-based tissue engineering" (Mag-TE). Using Mag-TE techniques, an integrated manufacturing process from two-dimensional undifferentiated culture to three-dimensional tissue construction for PSCs culture was established. The contents of the chapter are arranged in the following manner; initially, the chapter introduces the basics of magnetic nanoparticles (MNPs). Later, the chapter discusses the toxicity and functionalization aspect of MNPs. Lastly, recent advancement in manufacturing of PSCs culture using magnetic nanoparticles and magnetic force are described in detail.

2 Magnetic Nanoparticles

Magnetic molecular clusters are commonly referred as "magnetic nanoparticles". However, narrow size distributed aggregates of nanoparticles are referred as nanoclusters, which are well-established nanomaterials in nanoscience. Emerging areas of nano-biotechnology utilize combined potential of both magnetic nanoparticles and biology, which provides understanding of nano-bio interface and helps in designing of more specific advanced biomaterials. Magnetic particles based on metals (such as iron (Fe), nickel (Ni), cobalt (Co)) and their metal oxides in the range of nanometer to micrometer scale have been studied in various biomedical applications. Magnetite (Fe_3O_4) is an abundant mineral on earth and it is present in all living systems from bacteria to human (Kirschvink et al. 1992; Blakemore 1975). Because of the unique magnetic feature of magnetite particles, they have been applied to many fields. Magnetic attraction to high magnetic flux density and large surface area for bio-chemical modification in accordance with target application are two important properties of MNPs used in various studies like magnetic resonance imaging, cell separation, targeted delivery and cancer therapy. Presently, various extensions in the forms of modified MNPs are being used by researchers for potential treatment of damaged tissue (Tiwari 2013). Studies have demonstrated a feasibility of magnetic force-assisted cell patterning and its potential applicability for the fabrication of functional three-dimensional tissue constructs for next-generation regenerative medicine.

2.1 Physical Properties

MNPs have several important properties like, it can be designed in various shapes (quasi-zero, quasi-one, quasi-two and quasi-three dimensional structures), and controlled size to mimic the size of biomolecules (gene, protein and virus), for remote controlling of cells, reducing risk of aggregation due to remnant magnetization after removing external magnetic field, for passive delivery of molecule by surface functionalization of MNPs, biocompatibility and high surface area. Efforts have been directed to the synthesis of magnetic nanomaterials and exploring its

properties which have helped in the development of magnetically assisted technologies. Over a period of time, techniques have been well-established for the preparation of magnetic nanomaterials of various sizes and structures. Both theoretical and experimental studies have revealed that magnetism of particles is not only due to the reduction of particle size, but also because of surface/interface effects and the interaction of particles. Future efforts are being focused on the improvement of magnetism of nanometer-sized particles through modeling. Although, theoretical modeling of nanoclusters consisting only a few to a few tens of atoms, is already well established. Experimentally, further improvement in the fabrication techniques is being carried out for the synthesis of particles more efficiently in order to achieve controllable size, uniform morphology, and easy methodology for studying individual particles. These experimental and theoretical exercise will provide the opportunity to identify an "identical" particles, which not only would enable closer scrutiny of size-dependent magnetic properties, but could also, through nano-manipulation, empower them to become building blocks of magnetic devices.

The basic structure of MNP is made up of magnetic domains which generally arrange in an ordered structure and are responsible for the degree of magnetic moment. The disturbance in the ordered magnetic domain is less in the small cluster or in the single domain particle compared to a bulk material and therefore magnetic property varies with reduction in size of magnetic particle. Superparamagnetic nanoparticles (SPM) have been extensively studied for potential applications in tissue regeneration (Tartaj et al. 2003). These SPM are having single-domain structure in the size-range of 15–150 nm and show advancement for nano-magnetic actuation. It is also observed that temperature can randomize the orientation of magnetic single-domain and thus it shows superparamagnetism and high magnetic resistance. For example, in case of single-domain of iron oxide particles (around 20 nm) superparamagnetism is exhibited at room temperature, but lose its magnetism below Curie temperature (Dobson 2008). In general, an aligned magnetic moment is presented by SPM in presence of electromagnetic field. However, it becomes zero in the absence of electromagnetic field at very high temperature. Therefore, absence of residual magnetism is observed after removing the external magnetic field which helps to maintain the colloidal stability and prevent agglomeration of nanoparticles. Ferrite based nanoparticles in their naive or functionalized forms are the most explored MNPs in the biomedical applications due to their biocompatibility and high chemical stability compared to other metallic nanoparticles.

2.2 Synthesis of Magnetic Nanoparticles

The synthesis of these MNPs is categorized under two approaches (Fig. 1). The first ap-proach is bottom-up approach, wherein the synthesis of nanoparticles is achieved by assembly of building blocks of molecules. These small molecules are

Fig. 1 Synthesis of nanoparticles; the '*Bottom-up*' method recruits atoms and molecules in the aggregated nanoparticle form. The '*Top-up*' method involves sculpting of bulk material which also generates high waste in comparison to *bottom-up* method

self-assembled in an aligned manner, which is dependent upon the competitive attractive or repulsive forces developed in a controlled manner during the synthesis of nanoparticles.

However, the second approach performs the sculpting of bulk material into its nanosize structures, which is called top-down approach. The precise control on the growth and maturation of nanoparticles without formation of waste in the bottom-up approach makes it more suitable for bulk synthesis of nanoparticles. The well-established methods for the hydrolytic and non-hydrolytic synthesis of magnetic nanoparticles are thermal decomposition, co-precipitation, microemulsion, polyols and flame spray/laser pyrolysis. Importantly, monodispersity of nanoparticles basically depends upon the nucleation and the growth of nanoparticle during the synthesis (Fig. 2). The control of separating these two steps during the synthesis

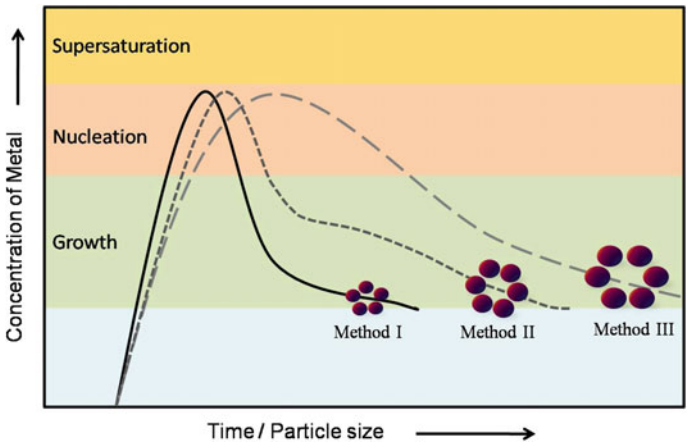

Fig. 2 Synthesis of monodisperse nanoparticles in different sizes. Method I shows the rapid nucleation and growth of metal salts which form small size nanoparticle. Method II shows the increased growth time period which cause aggregation of nanoparticle result in large nanoparticle. Method III suggest longer nucleation time period which cause multiple nucleation result in large aggregates of nanoparticle in the extended growth time period compare to Method I and II

gives precisely monodisperse nanoparticles. According to the LaMer theory, when concentration of constituent species increases in the medium up to the supersaturation stage, it causes a single and rapid burst nucleation. The nuclei formed by this process grow uniformly by the diffusion of solutes without further nuclei formation and results in a colloidal suspension of molecular clusters which can be defined as monodispersed nanoparticles (Murray et al. 2000; Lamer and Dinegar 1950). However, the size of particles can also be controlled by controlling the rate of velocity of thermal reaction and concentration of the solutes (iron salt) in the solution.

3 Functionalization of Magnetic Nanoparticles

The basic and necessary properties of any biomaterials are to provide suitable cellular compatibility and physiological stability. In order to achieve these properties, nanometers to sub-micron size of magnetic nanoparticles have been studied in an increasing number of biological and medical applications (Shinkai 2002). In particular, for any medical application, the non-toxicity of MNPs is the most important parameter. The bare iron oxide magnetic nanoparticles which are having a large surface area that is hydrophobic and induce their agglomeration under magnetic field result in the formation of large particle of iron oxide with reduced magnetic property due to random orientation of magnetic domains. Such large particles generally show ferromagnetic behavior. Moreover, two large particles can further interact and lead to a higher degree of aggregation (Veranth et al. 2007; Bulte et al. 2001). This agglomeration phenomenon can be overcome by lowering the surface energy of bare MNPs, which can be achieved by their surface functionalization. Additionally, surface functionalization of magnetic particles is advantageous for specific interaction, targeting and magnetic actuation to the specific tissue, cell or protein, only when they are used in stable nano-size form. The functionalized MNPs are fabricated by fusing their magnetic properties with functional biomolecules. This convergence enhances the stability of MNPs and its interaction at the interface of biological component. MNPs can be fabricated with hydrophobic and hydrophilic surfaces using various surface modulation processes. Based on this principle, number of studies is being carried out to achieve the precisely functionalized MNPs for biomedical applications (Ito et al. 2005d; Corchero and Villaverde 2009). The selection of appropriate capping material is ultimately dependent upon the surface chemistry of particle and its final application. However, the surface functionalization of MNPs causes relative size variation (Fig. 3). Preferably, the functionalized MNPs possessing hydrophilic surface property are stable in broad range of pH and high ionic strength and also provide option for the attachment of functional biomolecules.

The use of non-polymeric, polymeric and inorganic stabilizers for the functionalization of nanoparticle provides substrate-specific surface coating which increases its colloidal stability. The non-polymeric organic stabilizers like oleic

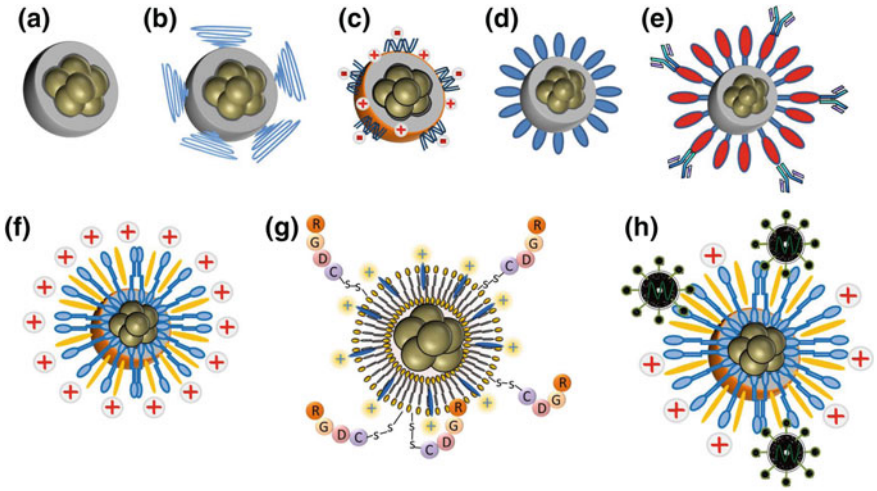

Fig. 3 Schematic illustration of different types of magnetic nanoparticles. A bare magnetic nanoparticle (**a**) can be functionalized by PEGylation for enhancing the biocompatibility and stabilizing the structure of MNPs (**b**). Some cationic stabilizers can also be used for ionic interaction of biomolecules like plasmid vector for gene delivery (**c**). The natural or synthetic polymer functionalized MNPs (**d**) can also be utilized for adjoining of kind of antibodies (Abs) for targeted application (**e**). Most commonly, passive cellular permeation of MNPs can be achieved by magnetic-cationic-liposomes (MCLs) for remotely controlled magnetic actuation of cells (**f**), which can be further functionalized for increased cellular interaction by integrating the RGD moieties on the surface of MCLs (**g**) and can be used for cell manipulation and delivery of bioactive molecules like phase-vector (**h**)

acid, cetyltrimethyl ammonium bromide (CTAB), alkanephosphonic acid, dodecylphosphonic acid, alkanesulphonic acid, hexadecylphosphonic acid and dihexadecylphosphonic acid, have been used for increasing the colloidal stability of MNPs (Sahoo et al. 2001; Yee et al. 1999). Some of the synthetic polymeric materials used for MNPs functionalization are poly(lactic-co-glycolic acid) (PLGA), polyvinyl alcohol (PVA), polyethylene glycol (PEG), polyacrylic acid (PAA), N-isopropyl acrylamide (NIPAAM), polyethyleneamine (PEI) and polyvinyl pyrrolidone (PVP) (Deng et al. 2003; Gupta and Gupta 2005; Lee et al. 1996). Among these, PEG is the most studied synthetic polymer for MNPs coating which provide resistance to protein, non-immunogenic and non-antigenic properties (Otsuka et al. 2003; Karakoti et al. 2011). Similarly, natural polymer including dextran, chitosan, alginate, starch, pullulan, agarose, aptamers, antibodies and even viral vectors have also been studied for functionalization of MNPs (Bhat et al. 2011; Chou et al. 2010; Tripathi and Kumar 2011; Yang et al. 2007). Inorganic materials like silica (Kim et al. 2008; Mahtab et al. 2011; Ruiz-Hernandez et al. 2011; Santra et al. 2001; Ulman 1996), gold (Carpenter 2001; Chen et al. 2003; Lu et al. 2010; Okada et al. 2011), gadolinium etc. have also been applied for the preparation of functional MNPs.

In contrast, incorporation of capping agents during the synthesis of magnetic particle may decrease the crystallinity of functionalized MNP and result in reduced superparamagnetic property. The reduction in magnetism can also occur during the post-synthesis functionalization probably due to the oxidation of iron oxide. The oxidation of iron oxide in the biological environment can also cause toxicity to cells. The concentration of MNPs above its critical acceptable limit (a variable factor that depends upon the application site and mode of action) can cause significant physical or molecular damage to the targeted cell or tissue. Homeostatic imbalance due to the high iron concentration in the tissue has a major concern which causes cellular toxicity including oxidative stress, nucleic acid damage, epigenetic consequences and other inflammatory responses (Ankamwar et al. 2010; Bulte et al. 2001; Hafeli et al. 2009; Veranth et al. 2007). Notably, high dose of MNPs could lead to profound DNA damage even if no cytotoxic events are visible. This may cause the initiation of carcinogenesis or adverse impact on next generations (Singh 2009). However, it is a debatable issue as to intake high concentration of iron as Fe_3O_4 and γ-Fe_2O_3, which are available naturally in the nano-sized crystal forms in the earth's crust is possible. Hence, lack of knowledge about the exact behavior and unrestrained side effects of any novel MNPs formulation requires appropriate evaluation before approval for its clinical use. However, cellular toxicity related issues are not diminishing the advantage of MNPs but providing insight to establish their improvised forms for the advancement of biomedical applications (Fig. 4).

Despite the toxicity concern, MNPs have shown their utility in cell sorting based on their ability to attract magnetically labeled cells using high magnetic flux density (Miltenyi et al. 1990; Moore et al. 1998; Radbruch et al. 1994). Magnetite cationic liposomes (MCLs) are cationic liposomes containing 10 nm magnetite nanoparticles (Fig. 3). They were developed, as functional magnetic nanoparticle, to mediate a better accumulation of magnetite nanoparticles in target cells through the electrostatic interaction between MCLs (positively charged) and cell membrane (negatively charged) (Shinkai et al. 1996). MCLs have been used as heat-generating mediators for hyperthermia (Ito et al. 2001; 2003 ; Shinkai et al. 1996), and as accessorial mediators to manipulate cells in artificial tissue construction (Ito et al. 2004c; Shimizu et al. 2007a; 2007b).

The target cells take up magnetite via endocytosis (Ito and Kamihira 2011) and the frequency of magnetic labeling of cell depends on the kind of cells. For example, when MCLs (100 pg magnetite/cell) were used for cell labeling; human hepatoblastoma HepG2 cells took up 49 pg magnetite/cell (Ito et al. 2007), human umbilical vein endothelial cells took up 34 pg magnetite/cells and primary human dermal fibroblast cells took up 14 pg magnetite/cell (Ino et al. 2007) after incubation for 24 h under specified culture conditions.

The toxicity of MCLs comprising of magnetite nanoparticles and cationic liposomes is an important issue for clinical application. Magnetite nanoparticles, as a core element of MCLs, have been clinically used as a contrast agent for magnetic resonance imaging (MRI). Also, the cationic liposomes consisting of three lipids, N-(α-trimethylammonioacetyl)-didodecyl-D-glutamate chloride (TMAG), dilauroylphosphatidylcholine

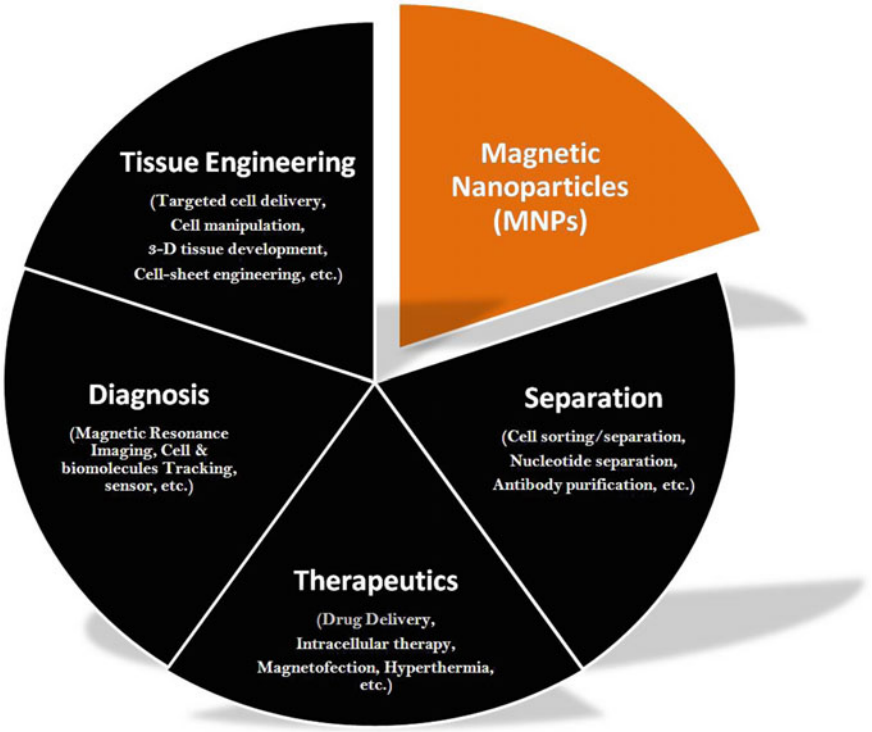

Fig. 4 Schematic illustration shows various biomedical applications of magnetic nanoparticles

(DLPC), and dioleoylphosphatidylethanolamine (DOPE), have been used as a liposomal vector for cancer gene therapy (Yoshida et al. 2004). We have previously reported that proliferation of MCL-labeled cells was not inhibited by magnetite in the concentration range tested [human keratinocytes, <50 pg/cell (Ito et al. 2004a); human mesenchymal stem cells, <100 pg/cell (Ito et al. 2004b); human aortic endothelial cells, <100 pg/cell (Ito et al. 2004c); human aortic smooth muscle cells, <100 pg/cell (Ito et al. 2005c); normal human dermal fibroblasts, <100 pg/cell (Ino et al. 2007); human umbilical vascular endothelial cells, <100 pg/cell (Ito et al. 2005c). Besides, human mesenchymal stem cells maintained differentiation ability into osteoblasts, adipocytes, or chondrocytes in magnetite concentrations below 100 pg/cell (Ito et al. 2004b; 2005b). Furthermore, we demonstrated that mouse ESCs also maintained an in vitro ability of proliferation and differentiation into three germ layers at magnetite concentration below 13 pg/cell (Horie et al. 2011). To investigate the toxicity of MCLs in vivo, we systematically administered MCLs to mice through intra-peritoneal injection of 90 mg dose, and none of the ten treated mice died after administration. Subsequently, we observed the liver and spleen of the treated mice to investigate substantial accumulation of MCLs. We found that MCLs were cleared from the circulation on day 10 after the administration probably by hepatic

Kupper cells and/or fixed macrophages in the spleen (Ito et al. 2003). Generally, upon clinical application, it is necessary to investigate the toxicity of MCLs for target cells and at the locally implanted site.

4 Magnetic Actuation of Cells

Actuation of cells from the distance is one of the major advantages associated with this magnetic force assisted engineering and has motivated researchers for applying it in various studies like mechanical conditioning bioreactor culture of mesenchymal stem cells (MSCs) (Dobson et al. 2006) and intermittent mechanical activation for long-term bone cells growth (Cartmell et al. 2002) using a wide range of magnetic particle size (130 nm–4 μm). The previous studies showed effective change in membrane potential, upregulation in the genes that are responsible for bone and cartilage formation and intracellular calcium deposition by MSCs. By the use of MNPs, magnetic manipulation in the biological systems can be achieved to target three major processes in the regenerative or therapeutic applications. First is 'magnetofection', the process involve magnetically assisted gene transfer for genetic alteration. Second is 'cell-patterning', an ordered arrangement of MNPs labeled cells using external magnetic force. Finally, third is 'magnetic-manufacturing', production of a 3D tissue in desired shape and size or production of the specific cell types. Type of stem cells like PSCs and iPSCs are considered as one of the potential cell source in regenerative therapy. Reprogramming of mouse and human cells into pluripotent stem cells was proposed by the group of Yamanaka (Takahashi and Yamanaka 2006) and Thomson (Yu et al. 2007). Because of ethical concern in using human embryo cells and increased complications of tissue rejection after transplantation, the pluripotent cells which are directly derived from the patient's own cells and referred as induced pluripotent cells (iPSCs) are a better alternative. The pluripotent stem cells provide a base to establish patient's specific disease model for drug discovery and development. In recent years, association of nanomaterials with PSCs has emerged as an advance field in cell based therapies. This section of the chapter will emphasize majorly on the 'magnetic-manufacturing' process of PSCs and subsequently discuss the recent advancements in this field.

4.1 Magnetic Culturing of PSCs

For PSC cultures, it is important to maintain the undifferentiated state during the self-renewal of PSCs. The undifferentiated state of mouse PSCs (mPSCs) is usually maintained by culturing on a feeder layer in the presence of anti-differentiation factors such as leukaemia inhibitory factor (LIF). Mouse embryonic fibroblasts (MEFs) isolated from mouse fetuses are often used as feeder cells for mPSCs, because they produce growth factors, including bone morphogenetic protein-4

(BMP-4), transforming growth factor-β (TGF-β), basic fibroblast growth factor (bFGF), Wnts and activin A (Lim and Bodnar 2002). MEFs are primary cells and can be cultured for several passages without a loss of function. On the other hand, mouse embryonic fibroblast cell line STO cells may present advantages over MEFs because they can proliferate infinitely and they do not require animal experiments to obtain them. However, the performance of STO cells as a feeder layer in mPSCs culture is inferior to MEFs. Previously, we reported the establishment of E-cadherin-expressing STO feeder cells that perform well as a feeder layer (Horie et al. 2010; 2013). E-cadherin is a member of the classic cadherin family and expressed in undifferentiated mPSCs (Larue et al. 1996; Takeichi 1991). It is presumed that an artificial cell-cell adhesion is constructed between mPSCs and E-cadherin-expressing feeder cells through E-cadherin. Furthermore, the expression of stem cell markers is comparable in mPSCs cultured on the E-cadherin-expressing STO feeder cells or MEFs and is much better than in mPSCs cultured on parental mouse STO cells. These results suggest that direct cell-cell interaction between mPSCs and feeder layer is crucial.

To enhance cell-cell interaction between mPSCs and feeder cells, we investigated two types of culture methods using MCLs and magnetic force. The first method consists in a magnetically labeled mPSCs system (Horie et al. 2014). Figure 5 illustrates the system in which MCL-labeled mPSCs are seeded into dishes in which mitotically inactivated feeder cells are cultured. A magnet is placed underneath the dish to attract mPSCs onto feeder cells by magnetic force. As a result, the MCL-labeled mPSCs were rapidly attracted to the magnet. After 3 day of culture, we measured alkaline phosphatase-positive (AP+) colony forming efficiency to quantitatively evaluate the undifferentiated state. Similar to the results using E-cadherin-expressing feeder cells, MCL-labeled mPSCs cultured on STO cells with applied magnetic force significantly improved the AP+ colony forming efficiency unlike without a magnet. These observations suggest that close contact between mPSCs and feeder cells is crucial to maintain the undifferentiated state of mPSCs.

The second culture method is a magnetically labeled feeder system, in which mPSCs are seeded with the MCL-labeled and mitotically inactivated feeder cells and then attracted to the culture surface by applying a magnetic force (Horie et al. 2014). Similar to the magnetically labeled mPSCs system, the AP+ colony forming efficiency was improved using this method compared with that without a magnet. In general, mitotically inactivated feeder cells are seeded on a few days before mPSCs passaging. This is a time-consuming and labor-intensive process when a large number of mPSCs are treated. In contrast, the magnetically labeled feeder system enables concurrent seeding of mPSCs and feeder cells which simplifies the whole process. Moreover, we demonstrated that the MCL-labeled feeder cells are magnetically removed from the co-cultures, resulting in mPSCs isolation (Horie et al. 2014; Ito et al. 2009). Generally, mPSCs are purified by pre-plating which is based on differential adhesion properties of mPSCs and feeder cells on a tissue culture surface. In our study, three cycles of re-plating were required to achieve 90% removal of feeder cells from co-culture with mESCs. Conversely, a single magnetic

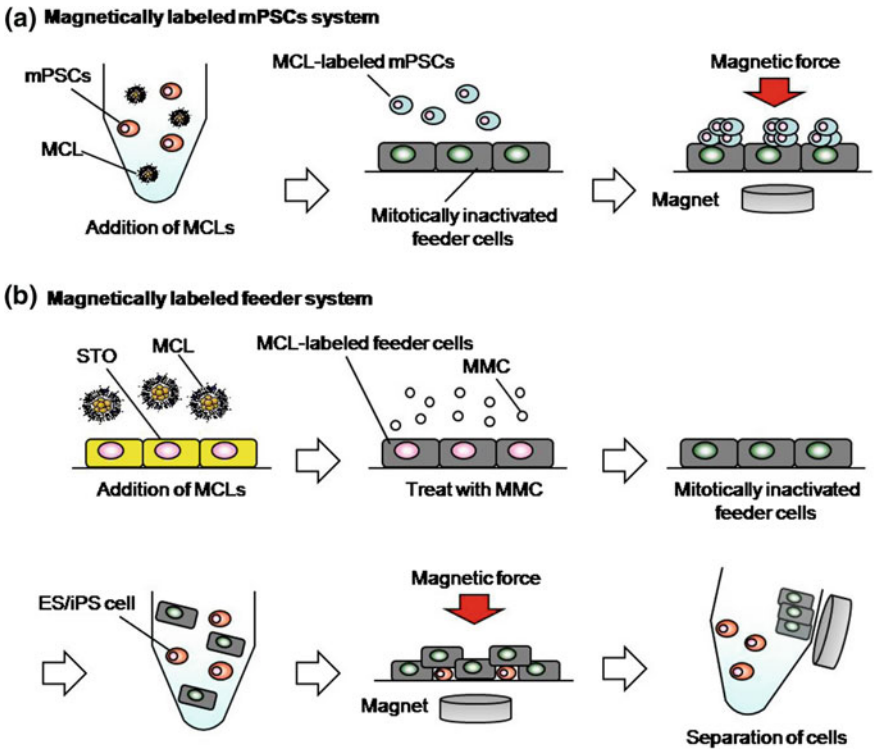

Fig. 5 Schematic illustration of magnetic culture systems. **a** Magnetically labeled mPSCs system. MCL-labeled mPSCs are co-cultured with mitotically inactivated feeder cells. mPSCs are attracted onto feeder cells by magnetic force through a magnet. **b** Magnetically labeled feeder system. mPSCs are co-cultured with the MCL-labeled feeder cells already mitotically inactivated by MMC. The magnetic force, through the magnet, is applied either to attract co-cultured cells to the culture surface or to separate them. *mPSC* mouse pluripotent stem cell, *MCL* magnetite cationic liposome, *STO* mouse embryonic fibroblast cell line, *MMC* mitomycin C

separation achieved more than 90% removal of feeder cells. These results indicate that the magnetically labeled feeder system represents a high-performance and a high-efficiency method for mPSC cultures. Taken together, these results demonstrate that the magnetic force-based mPSCs culture systems provide promising approaches for mPSCs manufacturing.

4.2 Magnetic Separation of PSCs

PSCs, possessing the inherence to differentiate into many cell types, have been reported to have a great potential for cell-based therapies in regenerative medicine (Murry and Keller 2008; Passier et al. 2008). Actually, many researchers succeeded

to induce various cell types from PSCs such as hematopoietic cells (Vanhee and Vandekerckhove 2016), cardiomyocytes (Laflamme and Murry 2011), dopamine neurons (Li et al. 2015), and immature pancreatic β cells (Pagliuca et al. 2014). The most commonly used method for PSCs differentiation is based on the formation of embryoid bodies (EBs) (Kurosawa 2007). Using this method, PSCs spontaneously form three-dimensional multicellular aggregates that include both differentiated and undifferentiated cells with various growth rates and similar to those in early-stage embryos. In order to characterize specific cell types, we developed a method to isolate cells from EBs using MCLs (Horie et al. 2011). Indeed, magnetic cell sorting is a simple method for cell isolation which is widely used in research and clinical applications. As the magnetite amount in MCL-labeled cells is diluted during culture due to cell proliferation, we hypothesized that a specific cell type could be isolated from developing EBs by magnetic separation according to magnetite amounts within the cells.

The scheme of magnetic cell separation using MCLs is illustrated in Fig. 6. First, we investigated whether magnetic cell capture rate of EBs got changed with EB growth. The magnetically captured cell number decreased with time during an

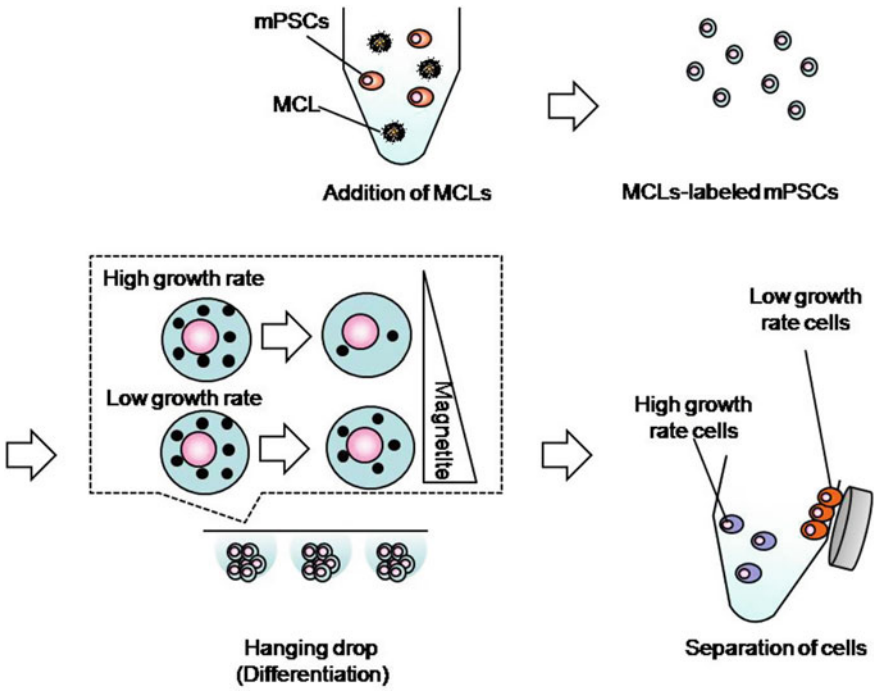

Fig. 6 Schematic illustration of the magnetic cell separation system. The magnetite (*black dots*) rate is diluted during mPSCs proliferation. In a co-culture, low growth rate cells are attracted by the magnetic force more efficiently than high growth rate cells. *mPSC* mouse pluripotent stem cell, *MCL* magnetite cationic liposome

8-day culture period, confirming that the magnetite within cells was diluted during cell proliferation. To examine the magnetically isolated cell types, they were analyzed by RT-PCR using primers for cell differentiation markers. On day 8, the magnetically captured cells only expressed the ectoderm marker (Nestin), whereas the magnetically non-captured cells expressed the markers of three germ lineages. Furthermore, we demonstrated that Mvh-positive cells, which are differentiated germ cells including primordial germ cells, were enriched in the fraction of magnetically captured cells. To investigate whether the magnetite particles co-localized with Mvh-positive cells, the cross-section of EBs were stained on day 8 with an anti-Mvh antibody and Berlin blue. It was observed that both Berlin blue-positive magnetite particles and Mvh-positive cells were mainly co-localized at the center of the EBs. These results indicate that the magnetic separation of cells from developing EBs based on their magnetite loading may provide an effective system for specific cell separation in PSCs manufacturing.

5 Challenges and Future Prospects

The remotely controlled magnetic actuation of magnetic nanoparticles has shown tremendous potential in cellular patterning, tissue regeneration and drug delivery (Ito and Kamihira 2011; Tripathi et al. 2013). Despite of several positive factors associated with MNPs for their biomedical applications, these nanoparticles also show some limitations. For example, high external magnetic force induced magnetic actuation of cells can pattern them in a highly dense three-dimensional tissue structure which can cause inability to transport sufficient oxygen and nutrients into the growing engineered tissue and thus ultimately affect cell viability and functionality. This is a critical issue particularly in magnetically engineered tissue constructs, although this approach shows potential in fabrication and replication of native tissue structures. Efforts have been made by researchers to overcome the associated complications, like use of gene therapy for modifying the existing Mag-TE procedure to promote vascularization for better exchange of gases, nutrients and waste (Luo and Saltzman 2000). A previous study demonstrated that the delivery of B-cell lymphoma-2 (Bcl-2) gene to artificial muscle tissue showed survival of cells in the tissue which was fabricated using Mag-TE technique (Li et al. 2007). Magnetic engineering of cells and tissues are promising approaches but have not yet materialized for the construction of native-like tissue recreation that can present its clinical application. MNPs have been approved and currently are being used in several clinical applications, however, it shows adverse effects in some applications probably due to high concentration, size and surface properties. Thus, application specific manufacturing of biocompatible MNPs and their assisted vascularized tissue fabrication is a future requirement to improve the existing magnetic actuation approaches. Interestingly, formation of protein coronas after the intra-venous injection of MNPs has shown different clinical properties depending upon their surface charge (Mahmoudi et al. 2015). Recent study suggest approximately 300 types of proteins are involved in this process (Tenzer et al. 2013).

Therefore, understanding the composition, functions and formation dynamics of protein coronas is essential for specific clinical applications. Designing of new integrated system of MNPs with micro and macro-systems could be a possible improvement in the performance and in the development of true biomaterials for regenerative medicine. For example, transplantation of cells into the patient's body can be killed by the immune system due to rejection by the body. The immunosuppressive drugs can be co-administered along with cells, but these drugs are commonly toxic to the cells and reduce the efficacy of treatments. Therefore, MNPs loaded hydrogels can be used to release the immunosuppressive drugs on demand using external magnetic field. Such integrated strategies not only reduce the drug side effects to the cells but also can be used for localization of implant by imaging. Iron oxide NPs (4–20 nm core size) are most commonly used contrasting agents in MRI for cell tracking. However, issue associated with MNPs for in vivo tracking of stem cells is the time-dependant weakening of the signals due to cell division and exocytosis. This affects the understanding of confined tracking, fate and biodistribution of stem cells for therapeutic applications. Therefore, fabrication of highly dense MNPs in biodegradable coatings and engineering of cells that can self-synthesize iron oxide NPs could be a possible approach to address this issue. We believe that future strategies may also combine the magnetically assisted biosensors application with regeneration systems for real-time monitoring. Such systems could also be supportive in triggering the release of specific signal/drug molecules if and when required and help the cells for regulatory growth. Overall, the current state-of-the-art of smart magnetic nanoparticles envisages its enormous potential in advanced biomedical applications in combination with pluripotent stem cells on demand at the specified site in the body. One day these next generation nanomaterials may be recruited as 'nano-robots', which can smartly travel throughout the body parts using external magnetic actuation and performing the job using host energy like ATP. This is our perception towards future of MNPs in biomedical applications.

6 Conclusion

This chapter highlights properties of magnetic nanoparticles followed by application in culture systems for PSCs that utilizes the advantage of magnetic cell manipulation. The PSCs are one of the attractive cell sources for tissue engineering and regenerative medicine. Combining the potential of PSCs and magnetic nanoparticles assisted remote controlling can provide a suitable microenvironment to support the culture and growth of PSCs for more specific purpose. Despite numerous technological advancements towards the derivation and application of PSCs, relatively little is known about their interaction with nano-microenvironment considering its importance in developing physiologically functional tissue and organ. The Mag-TE technique has been reported as a powerful tool for construction of 3D tissue like structures (Ito et al. 2004c; 2005c; 2005a), however, PSCs assisted Mag-TE is still in its infancy. Keeping this in mind, these magnetic manufacturing

processes should possess integrative studies that may involve the field of stem cell biology, regenerative medicine and ways to clinical implementation for successful regenerative medicine.

References

Ankamwar B, Lai TC, Huang JH, Liu RS, Hsiao M, Chen CH, Hwu YK (2010) Biocompatibility of Fe(3)O(4) nanoparticles evaluated by in vitro cytotoxicity assays using normal, glia and breast cancer cells. Nanotechnology 21(7):75102. doi:10.1088/0957-4484/21/7/075102

Bhat S, Tripathi A, Kumar A (2011) Supermacroprous chitosan-agarose-gelatin cryogels: in vitro characterization and in vivo assessment for cartilage tissue engineering. J Royal Society, Interface/Royal Society 8(57):540–554. doi:10.1098/rsif.2010.0455

Blakemore R (1975) Magnetotactic bacteria. Science (New York, NY) 190(4212):377–379

Bokkelen GV (2013) The application of regenerative medicine products and technologies toward areas of significant medical need—improving clinical outcomes and reducing costs. http://alliancerm.org/sites/default/files/ARM-Natl-Strat-Apr13.pdf

Bulte JW, Douglas T, Witwer B, Zhang SC, Strable E, Lewis BK, Zywicke H, Miller B, van Gelderen P, Moskowitz BM, Duncan ID, Frank JA (2001) Magnetodendrimers allow endosomal magnetic labeling and in vivo tracking of stem cells. Nat Biotechnol 19(12): 1141–1147. doi:10.1038/nbt1201-1141

Carpenter EE (2001) Iron nanoparticles as potential magnetic carriers. J Magn Magn Mater 225 (1–2):17–20. doi:10.1016/S0304-8853(00)01222-1

Cartmell SH, Dobson J, Verschueren SB, El Haj AJ (2002) Development of magnetic particle techniques for long-term culture of bone cells with intermittent mechanical activation. IEEE Trans Nanobiosci 1(2):92–97

Chen M, Yamamuro S, Farrell D, Majetich SA (2003) Gold-coated iron nanoparticles for biomedical applications. J Appl Phys 93(10):7551–7553. doi:10.1063/1.1555312

Chou SW, Shau YH, Wu PC, Yang YS, Shieh DB, Chen CC (2010) In vitro and in vivo studies of FePt nanoparticles for dual modal CT/MRI molecular imaging. J Am Chem Soc 132 (38):13270–13278. doi:10.1021/ja1035013

Corchero JL, Villaverde A (2009) Biomedical applications of distally controlled magnetic nanoparticles. Trends Biotechnol 27(8):468–476. doi:10.1016/j.tibtech.2009.04.003

Deng YH, Yang WL, Wang CC, Fu SK (2003) A novel approach for preparation of thermoresponsive polymer magnetic microspheres with core-shell structure. Adv Mater 15 (20):1729- + . doi:10.1002/adma.200305459

Dobson J (2008) Remote control of cellular behaviour with magnetic nanoparticles. Nat Nanotechnol 3(3):139–143. doi:10.1038/nnano.2008.39

Dobson J, Cartmell SH, Keramane A, El Haj AJ (2006) Principles and design of a novel magnetic force mechanical conditioning bioreactor for tissue engineering, stem cell conditioning, and dynamic in vitro screening. IEEE Trans Nanobiosci 5(3):173–177

Gupta AK, Gupta M (2005) Synthesis and surface engineering of iron oxide nanoparticles for biomedical applications. Biomaterials 26(18):3995–4021. doi:10.1016/j.biomaterials.2004.10.012

Hafeli UO, Riffle JS, Harris-Shekhawat L, Carmichael-Baranauskas A, Mark F, Dailey JP, Bardenstein D (2009) Cell uptake and in vitro toxicity of magnetic nanoparticles suitable for drug delivery. Mol Pharm 6(5):1417–1428. doi:10.1021/mp900083m

Healy KE, McDevitt TC, Murphy WL, Nerem RM (2013) Engineering the emergence of stem cell therapeutics. Sci Transl Med 5(207):207ed217. doi:10.1126/scitranslmed.3007609

Horie M, Ito A, Kiyohara T, Kawabe Y, Kamihira M (2010) E-cadherin gene-engineered feeder systems for supporting undifferentiated growth of mouse embryonic stem cells. J Biosci Bioeng 110(5):582–587. doi:10.1016/j.jbiosc.2010.06.002

Horie M, Ito A, Maki T, Kawabe Y, Kamihira M (2011) Magnetic separation of cells from developing embryoid bodies using magnetite cationic liposomes. J Biosci Bioeng 112(2):184–187. doi:10.1016/j.jbiosc.2011.04.011

Horie M, Ito A, Kawabe Y, Kamihira M (2013) A genetically engineered STO feeder system expressing E-cadherin and leukemia inhibitory factor for mouse pluripotent stem cell culture. J Bioprocess Biotechniques 03(01). doi:10.4172/2155-9821.s3-001

Horie M, Ito A, Maki T, Kawabe Y, Kamihira M (2014) Magnetically labeled feeder system for mouse pluripotent stem cell culture. J Biosci Bioeng. doi:10.1016/j.jbiosc.2014.10.020

Ino K, Ito A, Kumazawa H, Kagami H, Ueda M, Honda H (2007) Incorporation of capillary-like structures into dermal cell sheets constructed by magnetic force-based tissue engineering. J Chem Eng Jpn 40(1):51–58. doi:10.1252/Jcej.40.51

Ito A, Kamihira M (2011) Tissue engineering using magnetite nanoparticles. Prog Mol Biol Transl Sci 104:355–395. doi:10.1016/b978-0-12-416020-0.00009-7

Ito A, Shinkai M, Honda H, Kobayashi T (2001) Heat-inducible TNF-alpha gene therapy combined with hyperthermia using magnetic nanoparticles as a novel tumor-targeted therapy. Cancer Gene Ther 8(9):649–654. doi:10.1038/sj.cgt.7700357

Ito A, Nakahara Y, Tanaka K, Kuga Y, Honda H, Kobayashi T (2003) Time course of biodistribution and heat generation of magnetite cationic liposomes in mouse model. Jpn J Hyperthermic Oncol 19(3):151–159

Ito A, Hayashida M, Honda H, Hata K, Kagami H, Ueda M, Kobayashi T (2004a) Construction and harvest of multilayered keratinocyte sheets using magnetite nanoparticles and magnetic force. Tissue Eng 10(5–6):873–880. doi:10.1089/1076327041348446

Ito A, Hibino E, Honda H, K-i Hata, Kagami H, Ueda M, Kobayashi T (2004b) A new methodology of mesenchymal stem cell expansion using magnetic nanoparticles. Biochem Eng J 20(2–3):119–125. doi:10.1016/j.bej.2003.09.018

Ito A, Takizawa Y, Honda H, Hata K, Kagami H, Ueda M, Kobayashi T (2004c) Tissue engineering using magnetite nanoparticles and magnetic force: heterotypic layers of cocultured hepatocytes and endothelial cells. Tissue Eng 10(5–6):833–840. doi:10.1089/1076327041348301

Ito A, Hibino E, Kobayashi C, Terasaki H, Kagami H, Ueda M, Kobayashi T, Honda H (2005a) Construction and delivery of tissue-engineered human retinal pigment epithelial cell sheets, using magnetite nanoparticles and magnetic force. Tissue Eng 11(3–4):489–496. doi:10.1089/ten.2005.11.489

Ito A, Hibino E, Shimizu K, Kobayashi T, Yamada Y, Hibi H, Ueda M, Honda H (2005b) Magnetic force-based mesenchymal stem cell expansion using antibody-conjugated magnetoliposomes. J Biomed Mater Res B Appl Biomater 75(2):320–327. doi:10.1002/jbm.b.30304

Ito A, Ino K, Hayashida M, Kobayashi T, Matsunuma H, Kagami H, Ueda M, Honda H (2005c) Novel methodology for fabrication of tissue-engineered tubular constructs using magnetite nanoparticles and magnetic force. Tissue Eng 11(9–10):1553–1561. doi:10.1089/ten.2005.11.1553

Ito A, Shinkai M, Honda H, Kobayashi T (2005d) Medical application of functionalized magnetic nanoparticles. J Biosci Bioeng 100(1):1–11. doi:10.1263/jbb.100.1

Ito A, Jitsunobu H, Kawabe Y, Kamihira M (2007) Construction of heterotypic cell sheets by magnetic force-based 3-D coculture of HepG2 and NIH3T3 cells. J Biosci Bioeng 104(5):371–378. doi:10.1263/jbb.104.371

Ito A, Jitsunobu H, Kawabe Y, Ijima H, Kamihira M (2009) Magnetic separation of cells in coculture systems using magnetite cationic liposomes. Tissue Eng Part C, Methods 15(3):413–423. doi:10.1089/ten.tec.2008.0496

Karakoti AS, Das S, Thevuthasan S, Seal S (2011) PEGylated inorganic nanoparticles. Angew Chem Int Ed Engl 50(9):1980–1994. doi:10.1002/anie.201002969

Kim J, Kim HS, Lee N, Kim T, Kim H, Yu T, Song IC, Moon WK, Hyeon T (2008) Multifunctional uniform nanoparticles composed of a magnetite nanocrystal core and a mesoporous silica shell for magnetic resonance and fluorescence imaging and for drug delivery. Angew Chem Int Ed Engl 47(44):8438–8441. doi:10.1002/anie.200802469

Kirschvink JL, Kobayashi-Kirschvink A, Woodford BJ (1992) Magnetite biomineralization in the human brain. Proc Natl Acad Sci USA 89(16):7683–7687

Kurosawa H (2007) Methods for inducing embryoid body formation: in vitro differentiation system of embryonic stem cells. J Biosci Bioeng 103(5):389–398. doi:10.1263/jbb.103.389

Laflamme MA, Murry CE (2011) Heart regeneration. Nature 473(7347):326–335. doi:10.1038/nature10147

Lamer VK, Dinegar RH (1950) Theory, production and mechanism of formation of monodispersed hydrosols. J Am Chem Soc 72(11):4847–4854. doi:10.1021/Ja01167a001

Larue L, Antos C, Butz S, Huber O, Delmas V, Dominis M, Kemler R (1996) A role for cadherins in tissue formation. Development (Cambridge, England) 122(10):3185–3194

Lee J, Isobe T, Senna M (1996) Preparation of ultrafine Fe3O4 particles by precipitation in the presence of PVA at high pH. J Colloid Interf Sci 177(2):490–494. doi:10.1006/Jcis.1996.0062

Li W, Ma N, Ong LL, Nesselmann C, Klopsch C, Ladilov Y, Furlani D, Piechaczek C, Moebius JM, Lutzow K, Lendlein A, Stamm C, Li RK, Steinhoff G (2007) Bcl-2 engineered MSCs inhibited apoptosis and improved heart function. Stem Cells (Dayton, Ohio) 25(8):2118–2127. doi:10.1634/stemcells.2006-0771

Li W, Chen S, Li JY (2015) Human induced pluripotent stem cells in parkinson's disease: a novel cell source of cell therapy and disease modeling. Prog Neurobiol 134:161–177. doi:10.1016/j.pneurobio.2015.09.009

Lim JW, Bodnar A (2002) Proteome analysis of conditioned medium from mouse embryonic fibroblast feeder layers which support the growth of human embryonic stem cells. Proteomics 2(9):1187–1203. doi:10.1002/1615-9861(200209)2:9<1187:aid-prot1187>3.0.co;2-t

Lu Y, Shi C, Hu MJ, Xu YJ, Yu L, Wen LP, Zhao Y, Xu WP, Yu SH (2010) Magnetic alloy nanorings loaded with gold nanoparticles: synthesis and applications as multimodal imaging contrast agents. Adv Funct Mater 20(21):3701–3706. doi:10.1002/adfm.201001201

Luo D, Saltzman WM (2000) Enhancement of transfection by physical concentration of DNA at the cell surface. Nat Biotechnol 18(8):893–895. doi:10.1038/78523

Mahmoudi M, Sheibani S, Milani AS, Rezaee F, Gauberti M, Dinarvand R, Vali H (2015) Crucial role of the protein corona for the specific targeting of nanoparticles. Nanomedicine (London, England) 10(2):215–226. doi:10.2217/nnm.14.69

Mahtab F, Yu Y, Lam JWY, Liu JZ, Zhang B, Lu P, Zhang XX, Tang BZ (2011) Fabrication of silica nanoparticles with both efficient fluorescence and strong magnetization, and exploration of their biological applications. Adv Funct Mater 21(9):1733–1740. doi:10.1002/adfm.201002572

Martin I, Simmons PJ, Williams DF (2014) Manufacturing challenges in regenerative medicine. Sci Transl Med 6(232):232fs216. doi:10.1126/scitranslmed.3008558

Miltenyi S, Muller W, Weichel W, Radbruch A (1990) High gradient magnetic cell separation with MACS. Cytometry 11(2):231–238. doi:10.1002/cyto.990110203

Moore LR, Zborowski M, Sun L, Chalmers JJ (1998) Lymphocyte fractionation using immunomagnetic colloid and a dipole magnet flow cell sorter. J Biochem Biophys Methods 37(1–2):11–33

Murray CB, Kagan CR, Bawendi MG (2000) Synthesis and characterization of monodisperse nanocrystals and close-packed nanocrystal assemblies. Annu Rev Mater Sci 30:545–610. doi:10.1146/Annurev.Matsci.30.1.545

Murry CE, Keller G (2008) Differentiation of embryonic stem cells to clinically relevant populations: lessons from embryonic development. Cell 132(4):661–680. doi:10.1016/j.cell.2008.02.008

Okada Y, Takano TY, Kobayashi N, Hayashi A, Yonekura M, Nishiyama Y, Abe T, Yoshida T, Yamamoto TA, Seino S, Doi T (2011) New protein purification system using gold-magnetic beads and a novel peptide tag, "the Methionine Tag". Bioconjugate Chem 22(5):887–893. doi:10.1021/bc100429d

Otsuka H, Nagasaki Y, Kataoka K (2003) PEGylated nanoparticles for biological and pharmaceutical applications. Adv Drug Deliv Rev 55(3):403–419

Pagliuca FW, Millman JR, Gurtler M, Segel M, Van Dervort A, Ryu JH, Peterson QP, Greiner D, Melton DA (2014) Generation of functional human pancreatic beta cells in vitro. Cell 159 (2):428–439. doi:10.1016/j.cell.2014.09.040

Passier R, van Laake LW, Mummery CL (2008) Stem-cell-based therapy and lessons from the heart. Nature 453(7193):322–329. doi:10.1038/nature07040

Radbruch A, Mechtold B, Thiel A, Miltenyi S, Pfluger E (1994) High-gradient magnetic cell sorting. Methods Cell Biol 42 Pt B: 387–403

Ruiz-Hernandez E, Baeza A, Vallet-Regi M (2011) Smart drug delivery through DNA/magnetic nanoparticle gates. ACS Nano 5(2):1259–1266. doi:10.1021/nn1029229

Sahoo Y, Pizem H, Fried T, Golodnitsky D, Burstein L, Sukenik CN, Markovich G (2001) Alkyl phosphonate/phosphate coating on magnetite nanoparticles: a comparison with fatty acids. Langmuir 17(25):7907–7911. doi:10.1021/La010703+

Santra S, Tapec R, Theodoropoulou N, Dobson J, Hebard A, Tan WH (2001) Synthesis and characterization of silica-coated iron oxide nanoparticles in microemulsion: the effect of nonionic surfactants. Langmuir 17(10):2900–2906. doi:10.1021/La0008636

Shimizu K, Ito A, Lee JK, Yoshida T, Miwa K, Ishiguro H, Numaguchi Y, Murohara T, Kodama I, Honda H (2007a) Construction of multi-layered cardiomyocyte sheets using magnetite nanoparticles and magnetic force. Biotechnol Bioeng 96(4):803–809. doi:10.1002/bit.21094

Shimizu K, Ito A, Yoshida T, Yamada Y, Ueda M, Honda H (2007b) Bone tissue engineering with human mesenchymal stem cell sheets constructed using magnetite nanoparticles and magnetic force. J Biomed Mater Res B Appl Biomater 82(2):471–480. doi:10.1002/jbm.b.30752

Shinkai M (2002) Functional magnetic particles for medical application. J Biosci Bioeng 94 (6):606–613

Shinkai M, Yanase M, Honda H, Wakabayashi T, Yoshida J, Kobayashi T (1996) Intracellular hyperthermia for cancer using magnetite cationic liposomes: in vitro study. Jpn J Cancer Res: Gann 87(11):1179–1183

Singh N (2009) Conference scene—nanotoxicology: health and environmental impacts. Nanomedicine (London, England) 4(4):385–390. doi:10.2217/nnm.09.20

Takahashi K, Yamanaka S (2006) Induction of pluripotent stem cells from mouse embryonic and adult fibroblast cultures by defined factors. Cell 126(4):663–676. doi:10.1016/j.cell.2006.07.024

Takeichi M (1991) Cadherin cell adhesion receptors as a morphogenetic regulator. Science (New York, NY) 251(5000):1451–1455

Tartaj P, Morales Puerto M, Veintemillas-Verdaguer S, Gonzalez-Carreno T, Serna CJ (2003) The preparation of magnetic nanoparticles for applications in biomedicine. J Phys D Appl Phys 36: R182–197

Tenzer S, Docter D, Kuharev J, Musyanovych A, Fetz V, Hecht R, Schlenk F, Fischer D, Kiouptsi K, Reinhardt C, Landfester K, Schild H, Maskos M, Knauer SK, Stauber RH (2013) Rapid formation of plasma protein corona critically affects nanoparticle pathophysiology. Nat Nanotechnol 8(10):772–781. doi:10.1038/nnano.2013.181

Thomson JA, Itskovitz-Eldor J, Shapiro SS, Waknitz MA, Swiergiel JJ, Marshall VS, Jones JM (1998) Embryonic stem cell lines derived from human blastocysts. Science (New York, NY) 282(5391):1145–1147

Tiwari A (2013) Nanomaterials in drug delivery, imaging, and tissue engineering. In: Tripathi A, Melo JS, D'Souza, SF. (ed) Magnetic nanoparticles in tissue regeneration. WILEY-Scrivener, pp 443–492

Tripathi A, Kumar A (2011) Multi-featured macroporous agarose-alginate cryogel: synthesis and characterization for bioengineering applications. Macromol Biosci 11(1):22–35. doi:10.1002/mabi.201000286

Tripathi A, Melo JS, D'Souza SF (2013) Magnetic nanoparticles in tissue regeneration. In: Nanomaterials in drug delivery, imaging, and tissue engineering. doi:10.1002/9781118644591.ch14

Ulman A (1996) Formation and structure of self-assembled monolayers. Chem Rev 96(4): 1533–1554

Vanhee S, Vandekerckhove B (2016) Pluripotent stem cell based gene therapy for hematological diseases. Crit Rev Oncol/Hematol 97:238–246. doi:10.1016/j.critrevonc.2015.08.022

Veranth JM, Kaser EG, Veranth MM, Koch M, Yost GS (2007) Cytokine responses of human lung cells (BEAS-2B) treated with micron-sized and nanoparticles of metal oxides compared to soil dusts. Part Fibre Toxicol 4:2. doi:10.1186/1743-8977-4-2

Weissman IL (2000) Translating stem and progenitor cell biology to the clinic: barriers and opportunities. Science (New York, NY) 287(5457):1442–1446

Yamanaka S (2012) Induced pluripotent stem cells: past, present, and future. Cell Stem Cell 10 (6):678–684. doi:10.1016/j.stem.2012.05.005

Yang J, Lee CH, Park J, Seo S, Lim EK, Song YJ, Suh JS, Yoon HG, Huh YM, Haam S (2007) Antibody conjugated magnetic PLGA nanoparticles for diagnosis and treatment of breast cancer. J Mater Chem 17(26):2695–2699. doi:10.1039/b702538f

Yee C, Kataby G, Ulman A, Prozorov T, White H, King A, Rafailovich M, Sokolov J, Gedanken A (1999) Self-assembled monolayers of alkanesulfonic and -phosphonic acids on amorphous iron oxide nanoparticles. Langmuir 15(21):7111–7115. doi:10.1021/La990663y

Yoshida J, Mizuno M, Wakabayashi T (2004) Interferon-beta gene therapy for cancer: basic research to clinical application. Cancer Sci 95(11):858–865

Yu J, Vodyanik MA, Smuga-Otto K, Antosiewicz-Bourget J, Frane JL, Tian S, Nie J, Jonsdottir GA, Ruotti V, Stewart R, Slukvin II, Thomson JA (2007) Induced pluripotent stem cell lines derived from human somatic cells. Science (New York, NY) 318(5858):1917–1920. doi:10.1126/science.1151526

Fluorescent Gold Nanoclusters as a Powerful Tool for Sensing Applications in Cancer Management

Shiji R, Manu M. Joseph, Unnikrishnan BS, Preethi GU and Sreelekha TT

Abstract Fluorescent gold nanoclusters (AuNCs) comprising of several to tens of atoms with a dimension comparable to the Fermi wavelength of electrons have attracted greater attention in chemistry and medicine for the past decade due to their high fluorescence, good photostability, non-toxicity, excellent biocompatibility and water solubility. Green synthesis of AuNCs provides excellent possibilities to use them as biocompatible tools for fluorescent imaging, targeted therapy and have been extensively used in many fields of oncology. Biomolecules or functional molecules capped AuNCs could be further modified by conjugating targeting moieties and therapeutic molecules which allow active targeting, imaging and drug delivery at the tumor site. The current book chapter mainly focuses on the recent reports including mechanism of fluorescence, various synthesis strategies, bioconjugation and application of AuNCs for precise diagnosis and treatment of cancer.

Keywords Cancer · Nanoclusters · Bioconjugation · Imaging · Targeted therapy

Abbreviations

μg	Microgram
μM	Micromolar
A	Adenine
AgNCs	Silver nanoclusters
AML	Acute myeloid leukemia
Au DSNPs	Dendrimer stabilized AuNPs
AuNC@DHLA	Dihydrolipoic acid stabilized AuNCs
AuNCs	Gold nanoclusters
AuNCs@Tyr	L-Tyrosine capped AuNCs
AuNPs	Gold nanoparticles
AuNRs	Gold nanorodes

Shiji R · Manu M. Joseph · Unnikrishnan BS · Preethi GU · Sreelekha TT (✉)
Laboratory of Biopharmaceuticals and Nanomedicine, Division of Cancer Research, Regional Cancer Centre, Trivandrum 695011, Kerala, India
e-mail: ttsreelekha@gmail.com; ttsreelekha@rcc.gov.in

A. Tripathi and J.S. Melo (eds.), *Advances in Biomaterials for Biomedical Applications*, Advanced Structured Materials 66,
DOI 10.1007/978-981-10-3328-5_10

BGLA	(2-(4-(bis(4-(diethylamino)phenyl)(hydroxy)methyl)phenoxy) ethyl 5-(1,2-dithio-lan-3-yl)pentanoate)
BSA	Bovine serum albumin
C	Cytosine
CD	Cyclodextrin
CSC	Cancer stem cells
CT	Computed tomography
DFT	Density functional theory
DMF	Dimethylformamide
DNA	Deoxy ribonucleic acid
DOX	Doxorubicin
DPA	D-penicillamine
EDC	1-[(3-dimethylamino)-propyl]-3-ethylcarbodiimide hydrochloride
EDTA	Diamine tetra acetate
EGFR	Epithelial growth factor receptor
EPC	Endothelial progenitor cells
EPR	Enhanced permeation and retention
FA	Folic acid
FR	FA receptor
G	Guanine
G_4NH_2	Dendrimers with terminal amine group
G_4OH	Dendrimers with terminal hydroxyl group
HAEC	Human aortic endothelial cells
HDAC 1	Histone deacetylase 1
Her	Herceptin
HP-DNAs	Hairpin DNAs
HRP	Horseradish peroxidase
HRP-AuNCs	HRP functionalized AuNCs
ICG	Indocyanine green
Lf	Lactoferrin
LsGFC	Lysozyme-stabilized gold fluorescent clusters
MALDI-TOF MS	Matrix-assisted laser desorption ionization-time-of-flight mass spectrometry
MDR	Multidrug resistance
mg	Miliigram
ml	Milliliter
MPA	Mercaptopropionic acid
MPCs	Monolayer protected AuNCs
MRI	Magnetic resonance imaging
MTX	Methotrexate
NCAs	NP-based contrast agents
NIR	Near-infrared
nm	Nanometer

NPs	Nanoparticles
OCT	Optical coherence tomography
PA	Photoacoustic tomography
PDGF AA	Platelet-derived growth factor AA
PEG	Poly ethylene glycol
PEI	Polyethylenimine
PET	Positron emission tomography
pH	Potential of hydrogen
PKA	Protein kinase A
PTM	Post translational modification
QDs	Quantum dots
QY	Quantum yield
R	Rifampin
RNA	Ribonucleic acid
SERS	Surface-enhanced Raman scattering
SPR	Surface plasmon resonance
ss-DNAs	Single stranded DNAs
sulfo-NHS	Sulfo-N-hydroxysuccinimide
T	Thymine
TAT	Trans-activating transcriptional activator
TB	Tuberculosis
THPC	Tetrakis(hydroxymethyl)phosphonium chloride
TNF	Tumor necrosis factor
TPL	Two-photon luminescence
UV	Ultra violet

1 Introduction

Nanotechnology is a broad term which covers copious regions of science, technology and innovation. It works at atomic, sub-atomic and macromolecular scales wherein, quantum effects dominates and matter behaves differently. The rapid growth of biotechnology in sync with nanotechnology, commonly referred to as nanobiotechnology, is a rapidly flourishing arena that investigates biological systems for the fabrication of new biomaterials using nanoscale principles and techniques (Roco 2003), which could be useful tools for biosensing, cell labeling, molecular imaging, targeted therapy (Qu et al. 2015) and many more. This hybrid science has attained much higher imagination of fiction writers, engineers, scientists and every common individual interested in science. Today, it is estimated that there are more than 1,600 nanotechnology-based products and devices, with new ones entering the business sector at a quick pace. Nanoscale refers to size dimensions typically between approximately 1–100 nm. Even though particles above 100 nm

are also considered as nanoparticles, nanofabrication techniques are increasingly adapted to maintain the size below 100 nm, owing to the unique physicochemical parameters adapted under this range. Any type of a material that has one or more measurements in the nanoscale is considered to be as as nanomaterial (Sekhon 2014).

Cancer, a heterogeneous pathological condition is one among the most feared maladies in cutting edge social orders even though much progress was made in prevention, diagnosis and treatment. Cancer mortality could be abridged by implementing evidence-based strategies and assessment of the progress and suitability of therapies by rapid and non-invasive methods (Gao et al. 2014). Even though early detection had a large scope of cure, too many patients are diagnosed in late or too advanced stage where treatment response is in adequate (Weissleder 2002). Conventional therapies are the foundation of care in any disease conditions and also in cancer. Most people with cancer receive surgery, chemotherapy, radiation therapy, or immunotherapy therapies eventually amid treatment, and numerous will have a mix of these medications. Conventional therapies are constantly evolving and improving, with progresses in science and technology, to advance efficacy while fading destructive side effects. The field of nanotechnology has led to the development of many innovative strategies for effective detection and treatment of cancer by overcoming limitations associated with conventional cancer diagnosis and therapy (Srinivasan et al. 2015). Conventional chemotherapeutic compounds are non-targeting and act as cytotoxic agents which kills actively dividing cancer cells along with other healthy dividing normal cells, which creates significant side-effects on patient longevity and quality of life. Nanoparticles (NPs) have an excellent surface area/volume ratio which will enable them to adhere to tumor niche, moreover they could be surface decorated with cancer-specific molecules (drugs or ligands) which enable them to specifically bind to their targets on the cancer cell. Targeted delivery enables the distribution of drugs specific to the cancer cells, thereby decreasing the systemic toxicity in an accordable manner (Yu et al. 2012; Srinivasan et al. 2015). The difficulties in improving fabrication of nanoparticles custom-made to tumor specific signs still remain; however it can be assumed that nanoscale devices convey critical guarantee towards better approaches in every fields of oncology (Zamboni et al. 2012).

Precise and real time imaging of tumors using NP-based fluorescent probes (Wang et al. 2013) with long circulation times, excellent specificity and non-toxicity will be a boon in oncology. The clinical applications of contrast agents are severely limited due to their short half-lives, their ability to elicit an immune response and the difficulty that they experience with crossing biological membrane (Sivasubramanian et al. 2014). Carefully designed NP-based contrast agents (NCAs) could overcome biological barriers to reach tumors site either through active or passive targeting mechanisms (Ferrari 2005; Couvreur and Vauthier 2006; Peer et al. 2007) and simultaneously deliver both imaging agents and therapeutics. In passive targeting, the leaky vasculature of tumor enables NCA to accumulate via the enhanced permeation and retention (EPR) effect which allows for the extravasation of NPs from the circulation through abnormal fenestrations in tumor

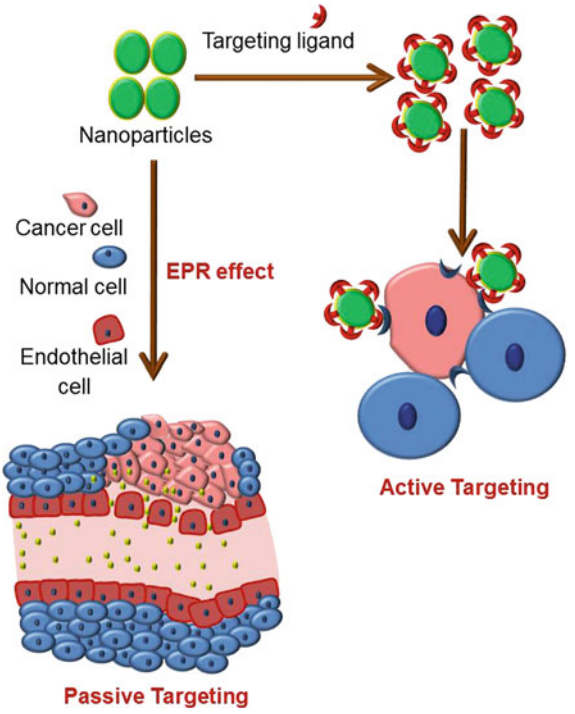

Fig. 1 Mechanism of passive and active targeting. In passive targeting, the leaky vasculature of tumor enables NCA to accumulate via the enhanced permeation and retention (EPR) effect. In active targeting involves the conjugation of targeting ligands or receptors to the surface of the NCA, enabling them to penetrate the cancer cells via receptor-mediated endocytosis

vasculature. Active targeting involves the conjugation of targeting ligands or receptors to the surface of the NCA, enabling them to penetrate the cancer cells via receptor-mediated endocytosis (Saravanakumar et al. 2009; Choi et al. 2010; McCarthy et al. 2010; Sivasubramanian et al. 2014) (Fig. 1). A fruitful, actively targeted NP system requires a sensitive balance of ligand volume and surface exposure which minimizes immunological response and clearance to give the NPs adequate course time to reach the target cells, while accomplishing suitable binding affinity to the surface receptors expressed on tumor cells. In this aspect the presence of multiple targeting agents per NP surface will yield a binding affinity stronger than for the single ligand, thus enhancing the ligand-receptor binding interaction for the nanoparticles (Zamboni et al. 2012).

Elemental gold (Au) is a dense, soft, malleable, and ductile metal; one ounce (28 g) of gold can be beaten out to 300 square feet. Gold is a good conductor of heat and electricity and is unaffected by air and most reagents. The contemporary use of gold-containing drugs focuses principally on rheumatoid arthritis, with some recent attention to other anti-inflammatory, new anticancer and antimicrobial uses (Pricker 1996). Since antiquated times gold has been considered as the "elixir of life". It was found with various applications in ancient and medieval era, and has a restorative history in both Eastern and Western conventions. Gold has been known to the Indians since antiquity and nano-formulation, called the '*Bhasma*' (ash) form of gold, has obtained immense therapeutic applications, especially in Sidha

medicine. Trace elements of metallic gold were used for rejuvenation in the Ayurvedic system of medicine, dating back to about 5000 years B.C. (Galib and Prajapati 2011).

Gold nanoparticle (AuNP) with excellent surface plasmon resonance (SPR) characteristics and superior biocompatibility found numerous applications in cancer diagnosis, therapy and many other biomedical fields (Shan and Tenhu 2007; Grzelczak et al. 2008; Sardar et al. 2009; Joseph and Sreelekha 2014). Fluorescent gold nanoclusters (AuNCs) are particular sort of gold nanomaterials with size

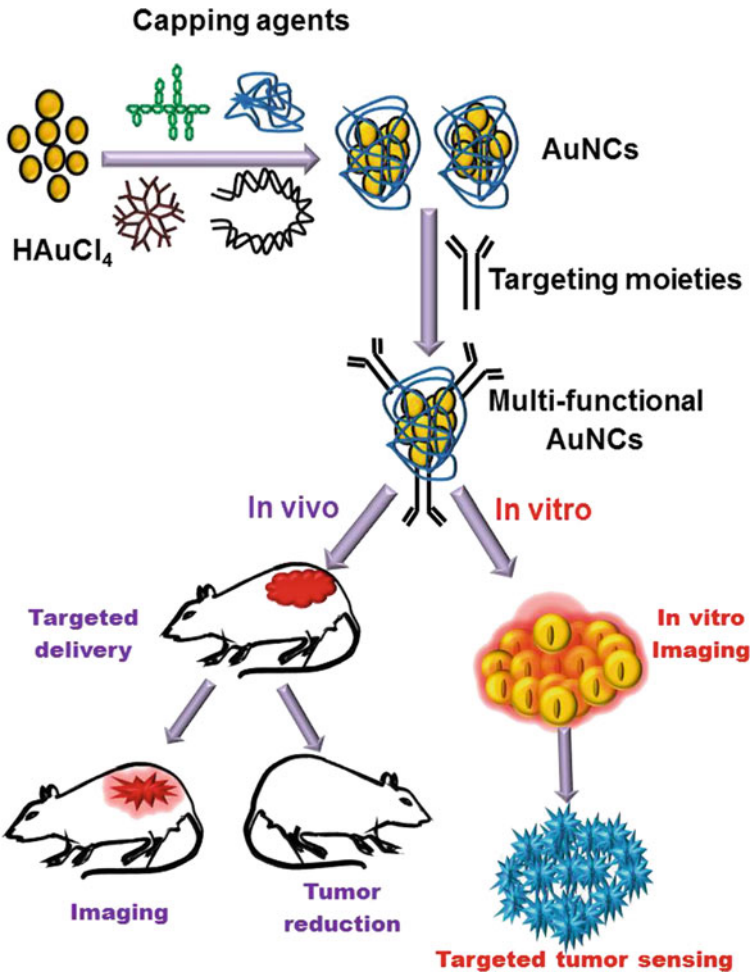

Scheme 1 Schematic representation of synthesis and biomedical application of AuNCs. Green synthesis of AuNCs utilizing different reducing and capping agents such as dendrimers, proteins, oligonucleotides and carbohydrates which can be used for biomedical applications such as targeted imaging and drug delivery for cancer

usually less than 3 nm. Not at all like the most prominent and widely understood spherical, large gold nanoparticles, AuNCs do not exhibit surface plasmon resonance (SPR) absorption in the visible region, but have fluorescence in the visible to near-infrared (NIR) region. With focal points of long lifetime, expansive Stokes movement, and biocompatibility, AuNCs have ended up fascinating detecting and imaging materials. AuNCs (Shichibu et al. 2007; Xie et al. 2009; Wei et al. 2011; Mayavan et al. 2011; Guevel et al. 2011; Garcia et al. 2013; Wen et al. 2011; Chen et al. 2013) comprising of several to tens of atoms have drawn greater attention in the recent decade owing to their high fluorescence, good photostability, non-toxicity, excellent biocompatibility and solubility in comparison with other organic fluorophores and semiconducting nanocrystals (Zheng et al. 2007; Lin et al. 2009a; Yang et al. 2011a, b; Shang et al. 2011a). AuNCs having a dimension comparable to the Fermi wavelength of electrons (Zhang and Wang 2014), which place them between single metal atoms and larger NPs (Zheng et al. 2004) enabled size-dependent fluorescence and other attractive features (Chen et al. 1998; Hicks et al. 1999, 2002; Quinn et al. 2003; Qu et al. 2015) making them ideal multifunctional imaging contrast agent. The present chapter mainly focuses on the synthesis strategies of fluorescent AuNCs along with their biomedical applications with special emphasis in oncology (Scheme 1).

2 Mechanisms Behind the Fluorescence of AuNCs

Gold is the most extensively studied inorganic material especially in bio-medical field due to its advisable physical, chemical properties and nontoxicity (Qu et al. 2015). Gold on bulk is highly stable; however nanoscale exhibit size-dependent optical and electronic properties. According to the number of metal atoms, nanoscale metals are roughly classified into three size domains: large NPs, small NPs and clusters, corresponding to three different characteristics length scales respectively (Zheng 2005). In bulk metal, the conduction band has no energy gap separating it from the valence band, so electrons do not suffer from a barrier and are free to move, where the scattering is determined by the electron mean free path. Mostly in case of large and small metal NPs, the size is comparable to or smaller than the electron mean free path, where the motion of electrons becomes limited by the size of the NP and interactions are expected to be mostly with the surface. This feature gives rise to SPR effects (Xu and Suslick 2010) and its optical and electronic behavior is explained by Gustav Mie in 1908 using Maxwell's equations (Mie 1908). In metal NCs, the size of metals is further reduced to around 2 nm or less, down to a few atoms, and the continuous band structure becomes discontinuous and broken up into discrete energy levels, which dramatically changes its optical, electronic and chemical properties compared with metal NPs. Moreover, due to quantum confinement effects of AuNPs with a dimension comparable to Fermi wavelength of electrons, they are too small to support SPR effect (Wu and Jin 2010). NCs are not conductive and plasmonic and cannot be explained using Mie

theory (Alvarez et al. 1997; Schaaff et al. 1997; Hostetler et al. 1998), but Rayleigh scattering principle solved the problem for the NCs because they are having a dimension which is smaller than wavelength of light.

Electronic transitions between the energy levels in fluorescent NCs leads to absorption and emission of light, which enables them to function as potential fluorescent probes in fluorescent bio-sensing and bio-imaging, like quantum dots (QDs) and fluorophores (Li et al. 2014). Although the detailed mechanism for the fluorescence of AuNCs is not completely deciphered yet, the generally accepted model is based on free electron theory. The free electrons on the NCs surface give rise to the polarization in an electronic field and the electron number determines the size dependent fluorescence optics (Haberland 1994; Barnes et al. 2003). Zheng suggested two possible mechanisms to explain the observed emission from this small metal NCs (Zheng 2005), one is due to intra-band (sp/conduction band) transition and the other is inter-band (d-sp) transition (Lin et al. 2009a; Apell et al. 1988) (Fig. 2). The observed fluorescence of AuNCs is determined by the numeric size of the energy level spacing (Eδ) (Haberland 1994; Kreibig and Vollumer 1995; Zheng 2007; Chen et al. 2014). When using the thermal energy (ET) as a criterion, AuNCs can emit only when Eδ is much larger than ET where a mobile electron hole can appear and current can flow when Eδ is much smaller than or comparable to ET. Hence AuNCs exhibit stronger fluorescence at low temperature than that at high temperature, mainly because the ET is smaller at a lower temperature. The relationship among the Eδ value of AuNCs and Au atom number (N) and the Fermi energy (Ef) is well predicted by the Jellium model, represented as:

$$E_\delta = E_f / N^{1/3}$$

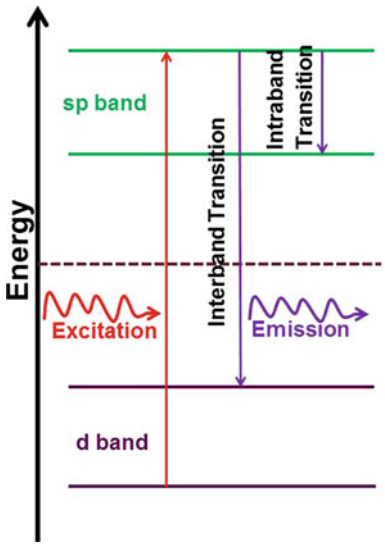

Fig. 2 Possible mechanism of fluorescence of AuNCs by intraband and interband transition. Excitation promotes an electron from the narrow d band to the empty sp band above the Fermi level. Intra-band (sp/conduction band) transition is due to emission above the Fermi level, that is within the conduction band and the inter-band (d-sp) transition is due to the emission probably one near or below the Fermi level

Unique electronic and fluorescent natures are prominent in this nanomaterial (Wilcoxon et al. 1998; Bigoni et al. 2000; Lee et al. 2004; Wang et al. 2005a; Zheng 2007; Bao et al. 2007), generating new horizons of opportunities in imaging.

3 Synthetic Strategies of AuNCs

Recent years witnessed a dramatic increment in publications involving various synthetic strategies adopted for fluorescent AuNCs (Shang et al. 2011a; Qu et al. 2015). AuNCs could be fabricated using different capping agents such as dendrimers, thiols, proteins, oligonucleotides, carbohydrates etc., with various fluorescence quantum yield (QY) (Table 1). Generally, during the synthesis of AuNCs, Au^{3+} is converted to Au^{+} and Au in the presence of reducing and capping agents and it entire process depends strongly on the concentration of $HAuCl_4$, pH, reaction conditions and many other parameters (Fig. 3). The following section will give a detailed account about the major reducing and capping agents used for the green synthesis of fluorescent AuNCs. Capping agents play a vital role in preventing the NCs from self-aggregation and dissociation. The stability of AuNCs depends mainly on the nature of capping agents used in the fabrication. Various natural and synthetic materials have been widely explored as efficient capping agents.

3.1 Dendrimers

Dendrimers are well-defined, multivalent, monodisperse artificial macromolecules which received continuous attention in recent years as promising candidates for myriad applications especially in cancer therapies and diagnostic imaging. In dendrimers, three dimensional polymers radiate from a central core and are built up by stepwise addition of monomers that contribute to each generation. Presence of internal cavities and high number of functional groups makes them attractive for biological and drug delivery applications.

Dendrimer templated AuNCs exhibited high fluorescence (>10% Quantum Yield) wherein the terminal groups on the dendrimer periphery could be tailored for the further conjugation with affinity ligands. Zheng et al. (2003, 2004) reported synthesis of water soluble, monodisperse, stable fluorescent Au_8NCs using fourth generation poly (amidoamine) (PAMAM) dendrimer and exhibit high QY of 42%. Stable, mono-dispersed and highly crystalline dendrimer-stabilized AuNPs (Au DSNPs) via hydrazine reduction chemistry and stabilized using primary amine-terminated poly (amidoamine) (PAMAM) dendrimers of different generations (generations 2–6) were synthesized with the same molar ratios of dendrimer terminal nitrogen ligands/gold atoms. The size of the synthesized Au DSNPs decreased with the increase of the number of dendrimer generations. These Au

Table 1 Capping agents used for the synthesis of AuNCs

Nature of capping agents	Capping agents	References
Dendrimers	Fourth generation poly(amidoamine) (PAMAM) dendrimer	Zheng et al. (2003, 2004)
	Primary amine-terminated poly(amidoamine) (PAMAM) dendrimers of 2–6 generations	Shi et al. (2006)
Proteins	Dendrimers with terminal amine (G4NH2) and hydroxyl (G4OH) groups	Jao et al. (2010)
	Bovine serum albumin(BSA)	Xie et al. (2009)
	Trypsin	Kawasaki et al. (2011b)
	Lysozyme	Wei et al. (2010), Lin and Tseng (2010), Chen and Tseng (2012)
	Transferrin-family proteins	Xavier et al. (2010), Le et al. (2011)
	Horseradish peroxidase (HRP)	Wen et al. (2011)
	DNase 1	West et al. (2014)
	RNase A	Kong et al. (2013)
	Isulin	Liu et al. (2011), Garcia et al. (2013)
	Pepsin	Kawasaki et al. (2011a)
Thiols	Substrate peptide 1, CCIHK (Ac), and substrate peptide 3, CCLRRASLG	Wen et al. (2013)
	Tiopronin thiolate	Huang and Murray (2001)
	Glutathione (-SG) and tetraphenyl-porphyrin (H_2TPPOASH)	Shibu et al. (2009)
	Multifunctional polymer ligand, containing thiol, thioether, and ester functional groups (PTMP-PVAc)	Huang et al. (2011b)
DNA	Glutathione (reduced)	Ghosh et al. (2012), Roy et al. (2015)
	Poly-cytosine and poly-adenine	Kennedy et al. (2012)
	Single stranded 50-GAGGCGCTGCCYCCACCATGAGC-30, Y = C, A, G, and T	Liu et al. (2012a)
	Hairpin DNAs (HP-DNAs) with a pristine stem segment and cytosine rich loop sequences	Liu et al. (2012b)
Carbohydrate	30 adenosine nucleotides (A_{30})	Li et al. (2015a)
	R-, β-, and γ-cyclodextrin (CD)	Shibu and Pradeep (2011)

(continued)

Table 1 (continued)

Nature of capping agents	Capping agents	References
Other molecules	Chitosan and mercaptopropionic acid (MPA)	Sahoo et al. (2014)
	Polyethylenimine (PEI) and $NaBH_2$ as reducing agent	Duan and Nie (2007)
	Dimethyl formaldehyde (DMF)	Kawasaki et al. (2010)
	Dihydrolipoic acid	Lin et al. (2009a)
	Amino-terminated poly(1,2-butadiene)	Yabu (2011)

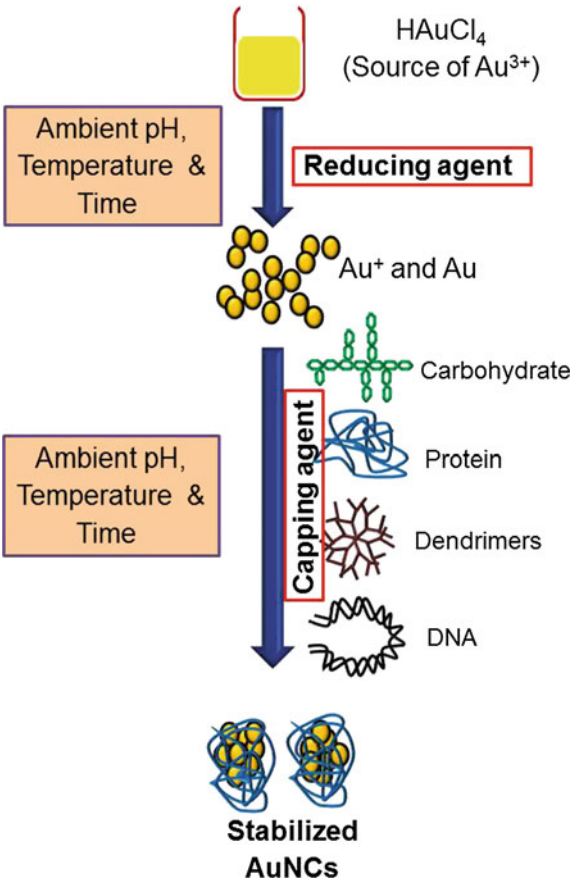

Fig. 3 Schematic representation of synthesis of AuNCs. During the synthesis of AuNCs, Au^{3+} in $HAuCl_4$ is converted to Au^{+} and Au in the presence of reducing and capping agents such as dendrimers, proteins, oligonucleotides, carbohydrates and it entire process depends strongly on the concentration of $HAuCl_4$, pH, temperature, reaction time etc

DSNPs are fluorescent and displayed strong blue emission intensity at 458 nm and could be further modified with various biological ligands for the application in biosensing and targeted cancer therapeutics (Shi et al. 2006). Jao et al. (2010)

employed a specific ion-pair approach using the dendrimers with terminal amine (G_4NH_2) and hydroxyl (G_4OH) groups for trapping gold salts. This facile strategy not only led to the polarity-dependent strong ion-pair association ($AuCl_4/G_4NH_2$ pair and $AuBr_4/G_4OH$ pair) but also significantly enhances the QY of gold nanodots from 20 to 62% after microwave irradiation.

3.2 Proteins

Bio-mineralization is a natural process in which biological organism's intake metal species to subsequently form mineral structures. Inspired by this process nanostructures could be formed by harnessing the biological organisms or macromolecules ability to naturally intake and arrange inorganic materials (Fendler 1997; Bhattacharya and Gupta 2005; Crookes-Goodson et al. 2008; Chen and Rosi 2010; Chevrier et al. 2012). Green chemistry approaches using biological materials was widely exploited in stabilizing gold atoms producing stable fluorescent AuNCs with excellent biocompatibility, which renders them suitable for biomedical applications. Proteins are the major bio-macromolecules exploited in green chemistry approach due to their numerous physical and chemical assets. Xie et al. (2009) developed highly fluorescent red emitting protein stabilized AuNCs by common protein bovine serum albumin (BSA) (Fig. 4A, B(a)). Besides being highly stable both in solutions (aqueous or buffer) and in the solid form, the light emitting AuNCs consist of 25 gold atoms (Au_{25}). Motivated with this promising approach, many other synthetic procedures were developed using other proteins such as trypsin (Kawasaki et al. 2011b), lysozyme (Wei et al. 2010; Lin and Tseng 2010; Chen and Tseng 2012), transferrin-family proteins (Xavier et al. 2010; Le et al. 2011), horseradish peroxidase (HRP) (Wen et al. 2011), DNase 1 (West et al. 2014), RNase A (Kong et al. 2013), insulin (Liu et al. 2011; Garcia et al. 2013) and much more.

Kawasaki et al. (2011a) reported the pH-dependent synthesis of pepsin-mediated AuNCs with fluorescent emissions of blue, green and red from Au_5 (Au_8), Au_{13}, and Au_{25}, respectively. The different charges on the pepsin molecule at different pH values could affect the structural nature and the strength of interaction between the pepsin chains and the gold surface or gold ions, leading to the formation of AuNCs with different sizes. Preparation of AuNCs for the detection of protein modifying enzymes and their inhibitors using peptides found widespread attention. Designed substrate peptides such as substrate peptide 1, CCIHK (Ac), and substrate peptide 3, CCLRRASLG were used for the synthesis of AuNCs and studied the effect of enzymatic modifications on their luminescence using two appropriate PTM enzymes, histone deacetylase 1 (HDAC 1) and protein kinase A (PKA) respectively. The study revealed that AuNCs fluorescence can be dynamically decreased with increasing concentration of enzymes, which offer label-free biosensor platform for the detection of PTM enzymes (Wen et al. 2013).

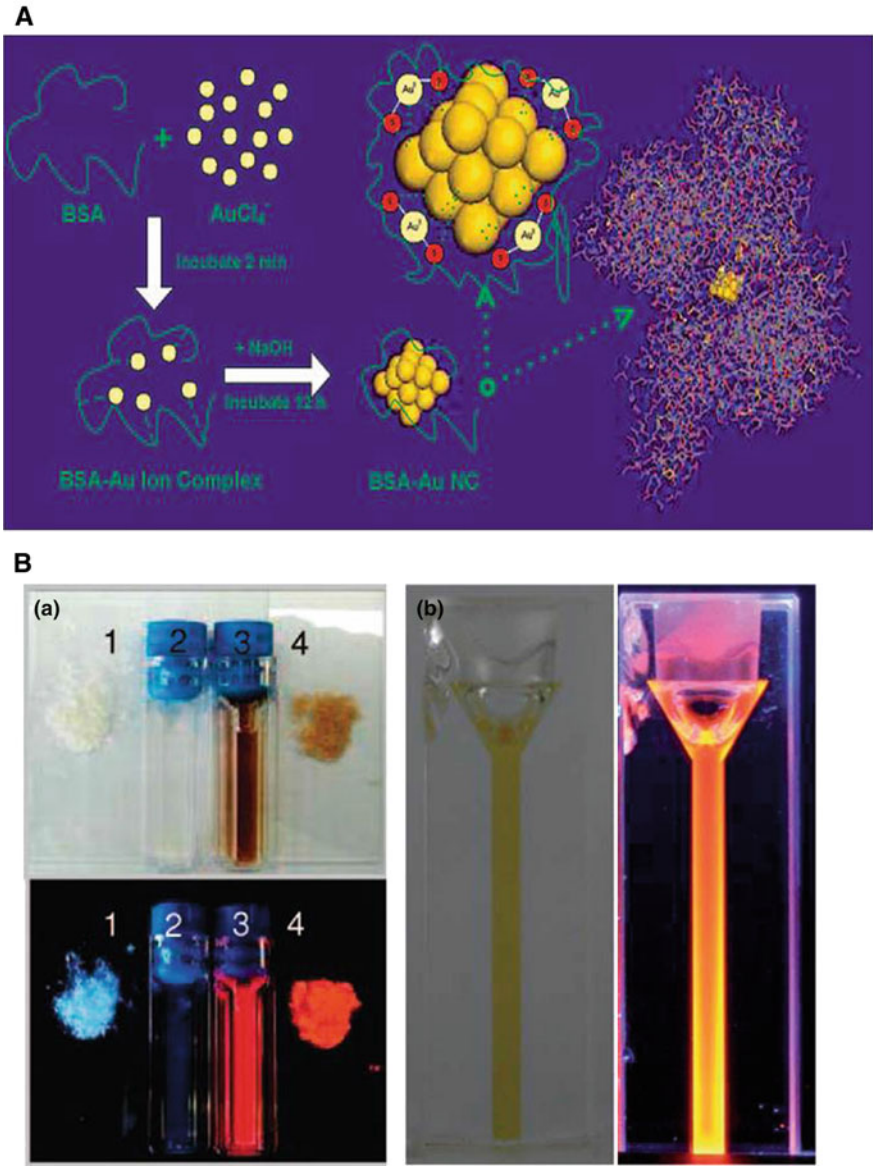

Fig. 4 **A** Schematic representation of the formation of AuNCs in BSA Solution. **B(a)** Photographs of BSA (*1*) powder and (*2*) aqueous solution, and BSA-AuNCs (*3*) aqueous solution and (*4*) powder under (*top*) visible and (*bottom*) UV light (Reprinted with permission from Xie et al. (2009) © 2009 American Chemical Society). **(b)** Photographs of aqueous solution of DPA–AuNCs in room light and under a UV light source with wavelength 365 nm respectively (Reproduced from Shang et al. (2011) with permission of The Royal Society of Chemistry)

Enzymes are widely employed as reducing and capping agent in preparation of AuNCs. The lysozyme-stabilized gold fluorescent clusters (LsGFC) with an average size of 1 nm and emission at 657 nm were effectively synthesized (Wei et al. 2010). Photo stable, trypsin-capped fluorescent AuNCs with an average size of 1 nm and a red emission at 645 nm were reported for the sensitive and selective detection of Hg^{2+} ions (Kawasaki et al. 2011b). Similarly construction of horseradish peroxidase (HRP) functionalized fluorescent AuNCs (HRP-AuNCs) via a bio-mineralization process at physiological conditions for the detection of hydrogen peroxide was also attempted. The fluorescence of HRP-AuNCs can be quenched quantitatively by adding H_2O_2, indicating that HRP enzyme remains active and enables catalytic reaction (Wen et al. 2011). The enzyme DNase 1 stabilized AuNCs (DNase 1: AuNCs) with core size consisting of either 8 or 25 atoms exhibited blue and red fluorescence respectively. In addition to the intense fluorescence emission, the synthesized DNase 1: AuNCs hybrid retained the native functionality of the protein, allowing simultaneous detection and digestion of DNA with a detection limit of 2 μg/ml, hence could be conveniently employed as efficient and fast sensors to augment the current time-consuming DNA contamination analysis techniques (West et al. 2014). Synthesis of AuNCs by core etching of AuNPs using appropriate ligands (Muhammed et al. 2008; Lin et al. 2009a; Qian et al. 2009) also attained scientific attention. Muhammed et al. (2010) employed synthesis of a luminescent AuNCs by core etching of mercaptosuccinic acid protected AuNPs using BSA(AuQC@BSA). The cluster core contains Au_{38} and exhibit QY of $\sim$4%. This AuQC@BSA is exploited as a "turn-off" sensor for Cu^{2+} ions and a "turn-on" sensor for glutathione detection.

Few of the amino acids play a key role in protein and peptide templated AuNCs synthesis due to their reducing and capping efficiency with gold (Brown et al. 2000; Naik et al. 2004). Tan et al. (2010) analyzed all the 20 amino acids alone and in combinations to determine their capability as a template in AuNCs preparation. Tryptophan was identified for being the strongest reducing agent and was therefore interdigitated into custom peptides for its reducing property. In a similar fashion; histidine was selected as the strongest metal binding amino acid and was also interdigitated into another set of peptides. From these preliminary peptide results, more diverse combinations with other amino acids were also investigated to determine the resultant shape and size of the AuNPs, along with tracking the periods of reaction initiation, growth, and termination (Chevrier et al. 2012). Tyrosine residues can reduce Au (III) or Ag (I) ions through their phenolic groups; their reduction capability can be greatly improved by adjusting the reaction pH above the pKa of Tyr ($\sim$10) (Xie et al. 2007). The AuNCs formed in the BSA solution could have been stabilized by a combination of Au-S bonding with the protein (via the 35 Cys residues in BSA), and the steric protection due to the bulkiness of the protein (Xie et al. 2009). Yang et al. (2011b) reported the synthesis of water-soluble, mono-dispersed and bluish green-emitting Au_{10}NCs through a simple reaction, in which histidine served as both reducing and protecting or capping ligand. The mechanism of this proposed reaction was explored and the

reducing ability of histidine was proved to be attained from its prominent imidazole group.

One-pot synthesis of fluorescent AuNCs templated with L-tyrosine which serves both as a reducing and capping agent (AuNCs@Tyr) were employed for investigating tyrosinase (TR) activity on the basis of aggregations of AuNCs@Tyr on its active sites during the catalysis reactions, thus leading to the fluorescence quenching of AuNCs@Tyr. The as prepared AuNCs@Tyr exhibited a fluorescence emission at 470 nm with a QY of approximately 2.5%. Significantly, TR has been considered as a critical marker for melanoma owing to its specific expression in melanoma cells. Therefore, this analytical method towards investigating TR activity may have broadened avenues for meaningful clinical applications (Yang et al. 2014).

3.3 Thiols

Thiols are the class of organic compounds that contain a sulfhydryl group (-SH), also known as a thiol group, that is composed of a sulfur atom and a hydrogen atom attached to a carbon atom (Prakash et al. 2009). Thiols containing small molecules are extensively used to stabilize AuNCs mainly because they can form strong Au-S bonding with Au atoms or ions (Link et al. 2002; Chen et al. 2014; Qu et al. 2015). Huang and Murray (2001) reported water soluble, monolayer protected gold clusters (MPCs) using tiopronin thiolate with an excitation and emission at 451 nm and 700-800 nm respectively. Fluorescent, Au_{22} clusters ($Au_{22}[(\text{-SG})_{15}(\text{-SAOPPTH}_2)_2]$) starting from Au_{25} clusters protected with glutathione (-SG) by a combined core reduction/ligand exchange protocol using tetraphenyl-porphyrin (H_2TPPOASH) were effectively prepared. The absence of a 672 nm intra-band transition of Au_{25} and the simultaneous emergence of new characteristic peaks at 520 and 635 nm in UV-visible spectrum indicated the formation of the Au_{22} core (Shibu et al. 2009).

Stable, blue fluorescent AuNCs of size and QY $\sim$ 1.2 nm and 24.3% respectively using a multifunctional polymer ligand, containing thiol, thio-ether, and ester functional groups (PTMP-PVAc) were fabricated by adjusting the molecular weight and concentration of the polymer ligand (Huang et al. 2011b). Similarly near-infrared (NIR) luminescent AuNPs (NIRL-AuNPs) by heat-assisted reduction of a gold(I)-thiol complex was prepared which exhibited strong emission with peak maximum at 810 nm, large stokes shifts (>400 nm) and stabilities towards photobleaching and chemical oxidation (Tu et al. 2011). Luminescent and water-soluble AuNCs (Au18SG14) were prepared using glutathione by a slow reduction process which emits red light in both aqueous and solid state under UV illumination but with a QY of only 0.053%. Although thiol protected AuNCs proved to be of great promise, the main problem behind them is the relatively low (0.001–0.1%) yield (Ghosh et al. 2012). Roy et al. (2015) successfully exploited the synthesis of blue, green, orange-red, red and NIR emitting AuNCs in aqueous media by using

a bioactive peptide glutathione (reduced) at physiological pH with excellent stability. Matrix-assisted laser desorption ionization-time-of-flight mass spectrometry (MALDI-TOF MS) analyses showed that the core structure size of the five different gold clusters are Au_7 (blue), Au_{16} (green), Au_{19} (orange-red), Au_{21} (red) and Au_{22} (NIR). The AuNCs demonstrated better cell internalization and non-toxicity on human lung adenocarcinoma A549 cells.

3.4 DNA

After water and oxygen, DNA is likely the most celebrated particle of life known to human race. This is not astounding, as we as a whole realize that an eye-catching, double helical particle of DNA conveys guidelines to produce and gather every one of the segments of a living being. The abundance of data encoded in a DNA molecule regularly eclipses its unique physical, chemical and biological properties (Maffeo et al. 2014). DNA has the unique capabilities to build complex nanostructures via self-assembly, which results from hydrogen-bonds formation between base pairs and hydrophilic-hydrophobic interactions (La Bean and Li 2007). The use of DNA as a template for metal NCs synthesis attained greater momentum due to the biocompatibility and extensive biomedical applications that the biomolecule holds. The mechanism of bonding between AuNPs and DNA and the factors which control its efficiency was well studied and documented (Kryachko and Remade 2005a, b; Shukla et al. 2009), which demonstrated the involvement of two major bonding factors: the anchoring, either of the Au-N or Au-O type, and the non-conventional N-H-Au hydrogen bonding. Shukla et al. (2009) revealed the interaction of AuNCs ($Au_{n,}$ Where n = 2, 4, 6, 8, 10, 12) with nucleic acid purine base guanine (G) and the Watson-Crick guanine-cytosine (GC) base pair through the major groove site (N7 site of guanine) of DNA by theoretical means (density functional theory (DFT)) and observed a greater interaction of AuNCs with the GC pair than with isolated guanine. Blue fluorescent AuNCs were prepared in the presence of poly-cytosine DNAs at low pH and poly-adenine at neutral pH using citrate as the reducing agent (Kennedy et al. 2012). Similarly stable, water-soluble and red-emitting AuNCs serving as promising nanoprobes in bio imaging and related fields were fabricated using single stranded DNA (50-GAGGCGCTGCCY CCACCATGAGC-30, Y = C, A, G, and T) and dimethylamine borane as a mild reductant in acidic solution (Liu et al. 2012a).

Liu et al. (2012b) compared sequence-dependent formation of fluorescent AuNCs using hairpin DNAs (HP-DNAs) with a pristine stem segment and varied loop sequences and observed that the emission behavior of the HP-DNA hosted AuNCs is dependent on the loop sequences. It was documented that the most efficient host to produce fluorescent AuNCs is the cytosine loop compared with other nucleotide's loops and the emission behavior of AuNCs hosted by the single-stranded DNAs (ss-DNAs) with an identical base composition to the corresponding HP-DNAs still exhibits a cytosine-rich dependence. A UV-light assisted

method for the synthesis of AuNCs using repeats of 30 adenosine nucleotides (A_{30}) was reported, which could be used for the detection of specific nucleic acid targets in human serum via the formulation of clusters along with the SYBR Green 1 that specifically binds to DNA sequence. The so formed AuNCs exhibited moderate fluorescence at 475 nm while on binding with perfectly matched nucleotide sequences, emit fluorescence at 525 nm that paved the way for the development of beneficial metal NCs in both research and medicine (Li et al. 2015b).

3.5 Carbohydrates

Carbohydrates are one of the most utilized classes of biological macromolecules for bio medical applications. They can differ significantly in size ranging from monosaccharides to polysaccharides consisting of many thousands of carbohydrate units. One of the most significant features of carbohydrates is their ability to form branched molecules, which stands in contrast to the linear nature of DNA, RNA, and proteins. Combined with the large heterogeneity of the monosaccharides, they exhibit a significantly higher structural diversity than other abundant macromolecules which makes them suitable candidates with ease of structural modification and manipulation in NP synthesis and modification (Frank and Schloissnig 2010). Carbohydrates have been widely used as both reducing and capping agents in the synthesis of AuNPs (Katti et al. 2009; Shervani and Yamaoto 2011; Thygesen and Jensen 2015) and attracted scientific attention due to its non-toxic and biocompatible nature. A simple and versatile methodology was adopted for tailoring sugar-functionalized fluorescent glyco-nanoparticles using biologically significant oligosaccharides as well as with differing carbohydrate density. The resultant nanoclusters are water soluble, stable and their highly polyvalent network can mimic glyco-sphingolipid clustering and interactions at the plasma membrane, providing a controlled system for glycobiological studies (Thygesen and Jensen 2015). Au_{15} quantum clusters anchored to R-, β-, and γ-cyclodextrin (CD) cavities was prepared, which are intensely luminescent in liquid as well as in solid state. Moreover, evaporation of the cluster solutions leads to luminescent gel like materials (Shibu and Pradeep 2011). Sahoo et al. (2014) synthesized AuNCs using chitosan and mercaptopropionic acid (MPA) and embedded as chitosan nanoparticles which exhibited simultaneous red, green, and blue emission on exposure to light of varying wavelength. The as formed AuNCs were conjugated to pCD-UPRT suicide gene that on targeting tumor cells caused apoptosis and helped in imaging.

3.6 Other Materials

Apart from the above mentioned molecules many other materials are also employed in the preparation of fluorescent AuNCs. A ligand-induced etching process was employed

in which hyper branched and multivalent coordinating polymers such as polyethylenimine (PEI) react with preformed gold nanocrystals to form atomic AuNCs which are soluble in water with an excitation and emission maxima located at 421 and 505 nm, respectively. These small atomic clusters consist of only 8 gold atoms (Au_8) and upon treatment by strong reducing agent such as $NaBH_4$, their excitation and emission peaks were shifted to 353 and 445 nm respectively (Duan and Nie 2007). Kawaski et al. (2010) reported the synthetic strategy for obtaining DMF protected AuNCs with high thermal stability ($\sim$150 °C) and dispersion stability in various solvents and having less than 20 gold atoms including Au_8 and Au_{13}. Water soluble dihydrolipoic acid stabilized AuNCs (AuNC@DHLA) were prepared which emits fluorescence upon ligand exchange with dihydrolipoic acid and also demonstrated tumor specific internalization in human hepatoma $HepG_2$ cells (Lin et al. 2009b). Blue light-emitting AuNCs were obtained by a simple one-pot process via reflux of Au ions with amino-terminated poly (1,2-butadiene) in toluene (Yabu 2011). A facile strategy for the preparation of water-soluble, fluorescent AuNCs using a mild reductant, tetrakis(hydroxymethyl)phosphonium chloride (THPC) and capped by zwitterionic functional ligand, D-penicillamine (DPA) was recently reported (Fig. 4B(b)). These DPA-AuNCs displayed excitation and emission bands at 400 and 610 nm, respectively with a fluorescence QY of 1.3% and demonstrated internalization in human cervical carcinoma HeLa cells (Shang et al. 2011b).

4 Bio-medical Applications of AuNCs

4.1 Bio Imaging and Targeted Therapy

Biomedical imaging techniques have accelerated the efficient early cancer detection and in treatment monitoring. Unfortunately, many of the conventional biomedical imaging techniques have lesser sensitivity to detect tumors when they are less than a centimeter in diameter. Efficient molecular imaging techniques with targeting moieties conjugated imaging agents can monitor biological processes at the cellular and subcellular levels with high sensitivity and specificity. NP-based molecular imaging agents can overcome biological barriers inside the body which leads to the development of multifunctional NPs for the simultaneous targeting, imaging and therapy of cancer (Sivasubramanian et al. 2014). Optical imaging techniques have wider applications due to its advantages such as low cost, low-energy radiation, high sensitivity, real-time monitoring and non-invasive or minimally invasive testing (Zheng et al. 2012). Multifunctional NPs based on AuNCs produced with green chemistry approaches are promising optical fluorescent probes for combined targeting, imaging and delivery of chemotherapeutics because of their biocompatibility, large stoke shift, long lifetime, photo and chemical stability and ease in conjugation (Fig. 5).

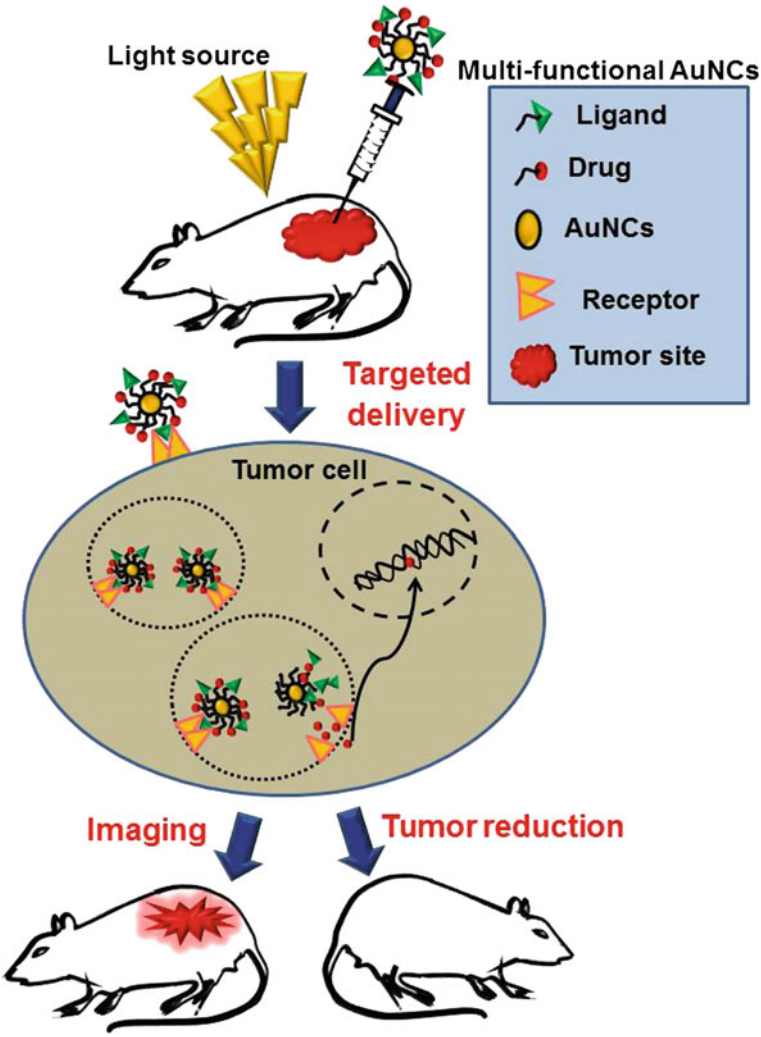

Fig. 5 Schematic diagram representing the mode of action of AuNCs in vivo. The ligand conjugated AuNCs with chemotherapeutics targeted specifically to the cancerous cell surface receptor after injection. This leads to internalization of Au NCs with drugs by receptor mediated endocytosis. Inside the tumor cells, the AuNCs release drugs and also help imaging. Chemotherapeutic drugs such as doxorubicin (Dox) and cisplatin enter the nucleus, resulting in cell death

Polavarapu et al. (2011) investigated one and two photon excitation and emission properties of water soluble glutathione monolayer protected AuNCs. The two-photon absorption cross section of these AuNCs was calculated through z-scan method using a mode-locked Ti:sapphire oscillator seeded regenerative amplifier and found to be 189,740 GM which is much higher compared with the values reported for

organic fluorescent dyes and quantum dots which make them a promising alternative for one- and two-photon bio-imaging and other nonlinear optical applications. Biological labeling and tumor targeted therapy could be achieved using AuNCs decorated with biomarker molecules on the surface (Huang et al. 2009, 2011a). The biomarkers could be tumor specific ligands such as small molecules, peptides, proteins, monoclonal antibodies and so forth which are specific for cell surface receptors over expressed on cancer cells as compared to normal cell (Table 2). Commonly used methods for bio-conjugation is through 1-[(3-dimethylamino)-propyl]-3-ethylcarbodiimide hydrochloride (EDC) and sulfo-N-hydroxysuccinimide (sulfo-NHS) activation in which NCs with functional groups such as primary amide or carboxylic acid can conjugate with other carboxylic or amino-terminal biomolecules. Avidin molecule containing NH_2 group can be conjugated to the carboxylic acid group containing capping agent of the AuNCs through EDC/NHS chemistry to synthesize AuNCs with high affinity to biotin overexpressed cancer cells. Likewise folic acid (FA) conjugated AuNCs can be internalized by certain cancerous cells, such as ovarian, oral, and breast which are rich in FA receptors (FR).

Wang et al. (2011a) investigated biocompatible AuNCs for in vitro and in vivo tracking of human aortic endothelial cells (HAEC) and endothelial progenitor cells (EPC) by delivering via the liposome complex and found no impaired angiogenesis by tube formation assay. In in vivo study using hind limb ischemic mice, intramuscular injection of AuNCs labeled human EPC showed that the cells preserved an angiogenic potential and exhibited traceable signals after 21 days which

Table 2 Ligands conjugated AuNCs and its targeting moieties

AuNCs	Ligand	Target	References
Glutathione thiolate capped Au25SG18	Streptavidin	Biotin	Muhammed et al. (2009)
Dihydrolipoic acid (DHLA) capped AuNCs (AuNC@DHLA)	Streptavidin	Biotin	Lin et al. (2009a)
BSA capped AuNCs	Folic acid	Folic acid receptor	Muhammed et al. (2010), Lin et al. (2013a)
Ovalbumin capped AuNCs	Folic acid	Folic acid receptor	Qiao et al. (2013)
Silica coated AuNCs (AuNCs@SiO2)	Folic acid	Folic acid receptor	Zhou et al. (2013)
BSA capped AuNCs	Monoclonal antibody against CD33	CD33	Retnakumari et al. (2011)
11-mercaptoundecanoic acid capped AuNCs	TAT-peptide	Nucleus	Vankayala et al. (2015)
BSA capped AuNCs	Herceptin	ErbB-2	Wang et al. (2011b)

highlighted the promising biocompatibility of this fluorescent probe. Physiological changes in cellular pH are better indicators of disease initiation or progression. Therefore, a pH-responsive material often serves as excellent tools in the fundamental understanding of cell biology or medicine for disease diagnosis and therapy. Negatively charged AuNCs synthesized using glutathione and cysteamine as surface ligands, exhibited high resistance to non-specific protein adsorption and strong pH-dependent adsorption in live cell membranes of HeLa cells within a biological pH range (5.3–7.4). Thus, metal NCs with pH-dependent membrane adsorption might find new applications in tumor diagnosis and therapy (Yu et al. 2011). Shang et al. (2011b) demonstrated the application of DPA–AuNCs as fluorescent nanoprobes in bioimaging of HeLa cells using zwitterionic functional ligand, D-penicillamine (DPA), as a capping agent (Fig. 6a). DPA-AuNCs was used for targeted biological imaging applications because the carboxylic and amino groups of DPA allow further functional molecules to be conjugated to the AuNCs for specific tagging. Established simple and spontaneous procedure for the synthesis of fluorescent AuNCs by cancerous cells such as HepG2 and K562 was developed in which the AuNCs is formed by Au(III) reduction inside the cellular cytoplasm and ultimately concentrate around their nucleoli, thus affording precise cell imaging and this does not occur in non-cancerous cells, as evidenced with L02 cells used as controls (Fig. 6b) (Wang et al. 2013).

Bright-red-emitting sub-nanocluster, Au_{23}, prepared by the core etching of glutathione thiolate capped Au25SG18 was used for imaging the hepatocellular carcinoma cell line HepG2 by employing the avidin–biotin interaction. Biotin is a water-soluble B-complex vitamin that is a cofactor in the metabolism of fatty acids and is present in large volume in these cancerous cells. For the specific labeling of the cells, Au_{23} clusters were functionalized with streptavidin following an EDC coupling reaction. Since biotin strongly binds with streptavidin, the cells can be imaged using the fluorescence of the clusters (Muhammed et al. 2009). In a similar study, dihydrolipoic acid (DHLA) capped AuNCs (AuNC@DHLA) particles with the quantum yield of around 13% were conjugated to biologically relevant molecules such as PEG, BSA, avidin and streptavidin by EDC chemistry separately to compare the cellular internalization in HepG2 cells. Streptavidin-conjugated AuNCs stained the biotin containing cells with high intensity which highlights the fact that streptavidin-conjugated AuNC@DHLA can specifically label endogeneous biotin (Lin et al. 2009b). BSA capped AuNCs (AuQC@BSA) functionalized with FA (folic acid) following EDC coupling of FA and BSA exhibited FR targeted cellular uptake in cancer cells. Cancerous cells are employed with increased FRs when compared to normal cells, and therefore FA-conjugated AuQC@BSA could be used for specific detection of cancer cells (Tan et al. 2010). Lin et al. (2013b) employed FR targeted internalization of BSA-Au-FA nanocomplex on human gastric carcinoma MGC803 cells. In a similar study ovalbumin protected AuNCs with FA as the targeting ligand linked by homopolymer N-acryloxysuccinimide has been investigated and its internalization was demonstrated on HeLa cells (Qiao et al. 2013).

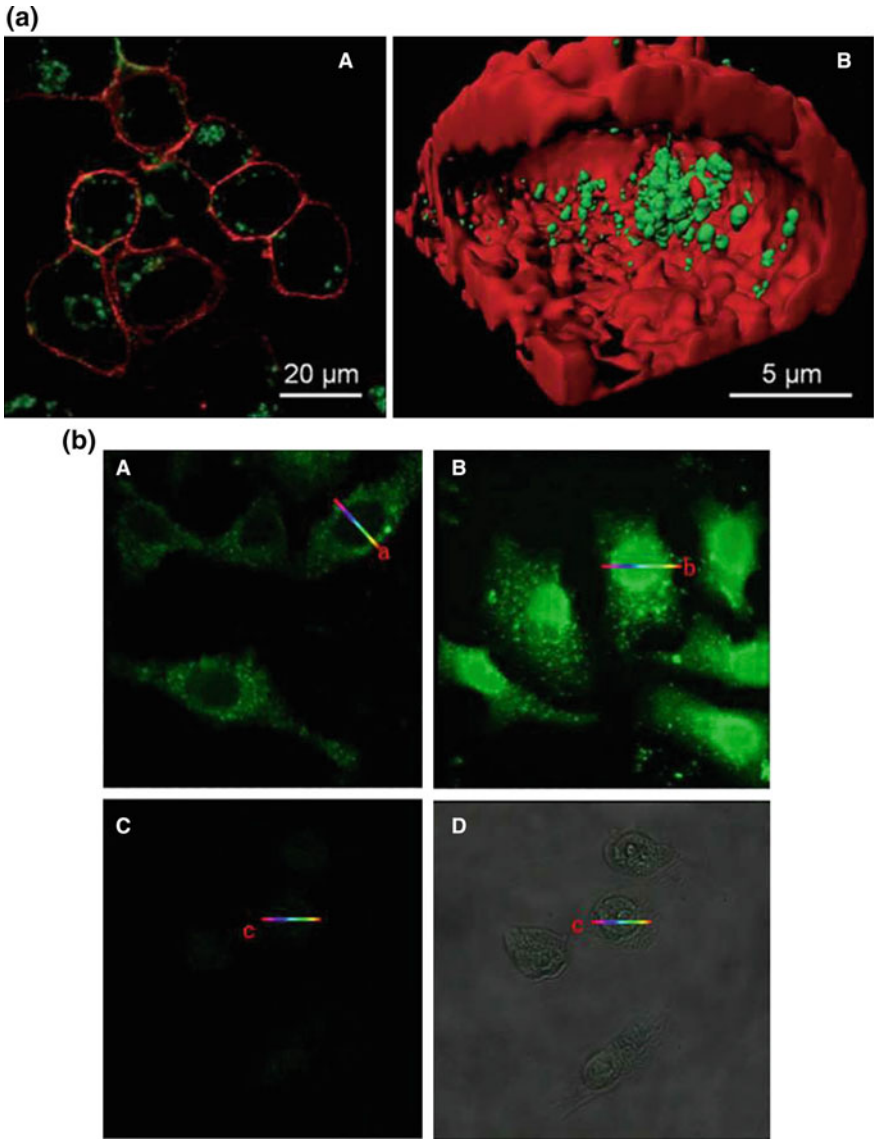

Fig. 6 **a** Internalization of DPA-AuNCs in HeLa cells. *A* Confocal image after 2 h incubation with DPA–AuNCs. *B* Cross-section of a 3D image reconstruction. Membranes were stained with the red dye DiD. Images were taken by 2-photon excitation at 810 nm. DPA– AuNCs (Reproduced from Shang et al. (2011b) with permission of The Royal Society of Chemistry). **b** Laser confocal fluorescence micrographs of HepG2 (*A* and *B*) and L02 control cells (*C* and *D*) incubated with identical 10 mmol/L $HAuCl_4$ solutions. *A* after 24 h incubation; *B*, *C* and *D* after 48 h incubation; *D* Overlay of the morphological and fluorescence image of **C**. Images were acquired at 400-fold magnification (Reprinted by permission from Macmillan Publishers Ltd: Scientific Reports (Wang et al. 2013), © 2013)

Molecular receptor (CD 33) targeted flow cytometry based detection and imaging of cancer cells was employed using monoclonal antibody conjugated BSA-AuNCs. The protein protected clusters were conjugated with monoclonal antibody against CD33 myeloid antigen, which is overexpressed in the primitive population of acute myeloid leukemia (AML) cells. The as prepared AuNC-CD33 conjugates having average size of ~ 12 nm retained bright fluorescence with excellent biocompatibility. Target specificity of the conjugates for detecting CD33 expressing AML cells in flow cytometry displayed specific staining of $\sim 95.4\%$ of leukemia cells within 1–2 h compared to a non-specific uptake of $\sim 8.2\%$ in normal human peripheral blood cells which was further confirmed with confocal imaging (Retnakumari et al. 2011). The possibility of using BSA capped ultra-small NIR emitting AuNCs as contrast imaging agents for tumor fluorescence imaging in vivo was explored and demonstrated by subcutaneous, intramuscular and intravenous injection in mice model (Fig. 7a). The fluorescence imaging signal of the tail vein administrated AuNCs in living organisms can spectrally be well distinguished from the background with maximum emission wavelength at about 710 nm, and the longer circulation time of AuNCs up to 5 h and clearance within 24 h promises continuous imaging in vivo. Moreover, the uptake of AuNCs by the reticulo-endothelial system is relatively low because of its ultra-small hydrodynamic size (~ 2.7 nm) and the body weights of mice injected with AuNCs had only changed slightly after 4 weeks compared with control mice, indicated that the ultrasmall NIR AuNCs had no potential toxicity to the animal model. The NCs also displayed tumor accumulation in MDA-MB-45 and HeLa tumor xenograft models due to the EPR effects which promotes its promising application as contrast imaging agents for in vivo fluorescence tumor imaging (Fig. 7b) (Wu et al. 2010).

Nucleus targeting using AuNCs was designed by conjugating nucleus targeting trans-activating transcriptional activator (TAT) peptide with AuNCs to perform simultaneous in vitro and in vivo fluorescence imaging, gene delivery and NIR light activated photodynamic therapy for effective cancer cell killing. The TAT peptide–Au NCs exhibit excellent photo-stabilities, and appreciable biocompatibility in HeLa cells as well as in vivo zebrafish model system. They demonstrated the co-localization and distribution in the cytoplasm with a significant fraction (>50%) entering into the nucleus of HeLa cells which could also serve as DNA delivery cargoes with ultrahigh cellular uptake (≈90%) and gene transfection efficiencies (≈ 80%) compared to commonly adopted LP2000 liposome gene carrier in HeLa cells. Moreover, the TAT peptide–AuNCs also sensitizes the formation of singlet oxygen upon long NIR light (850–1100 nm) excitation enabling effective photodynamic therapeutic effects on destruction of cancer cells via photo-induced DNA damages (Vankayala et al. 2015). Methionine was covalently linked to BSA stabilized AuNCs by EDC chemistry for tumor-selective optical imaging of methionine-dependent malignant cells. Hydrophilic indocyanine green (ICG) derivative MPA, a NIR fluorescent dye, was used to label methionine-modified AuNCs (Au-Met-MPA) for NIR tumor imaging which displayed non-toxicity and tumor specific bio-distribution pattern in different

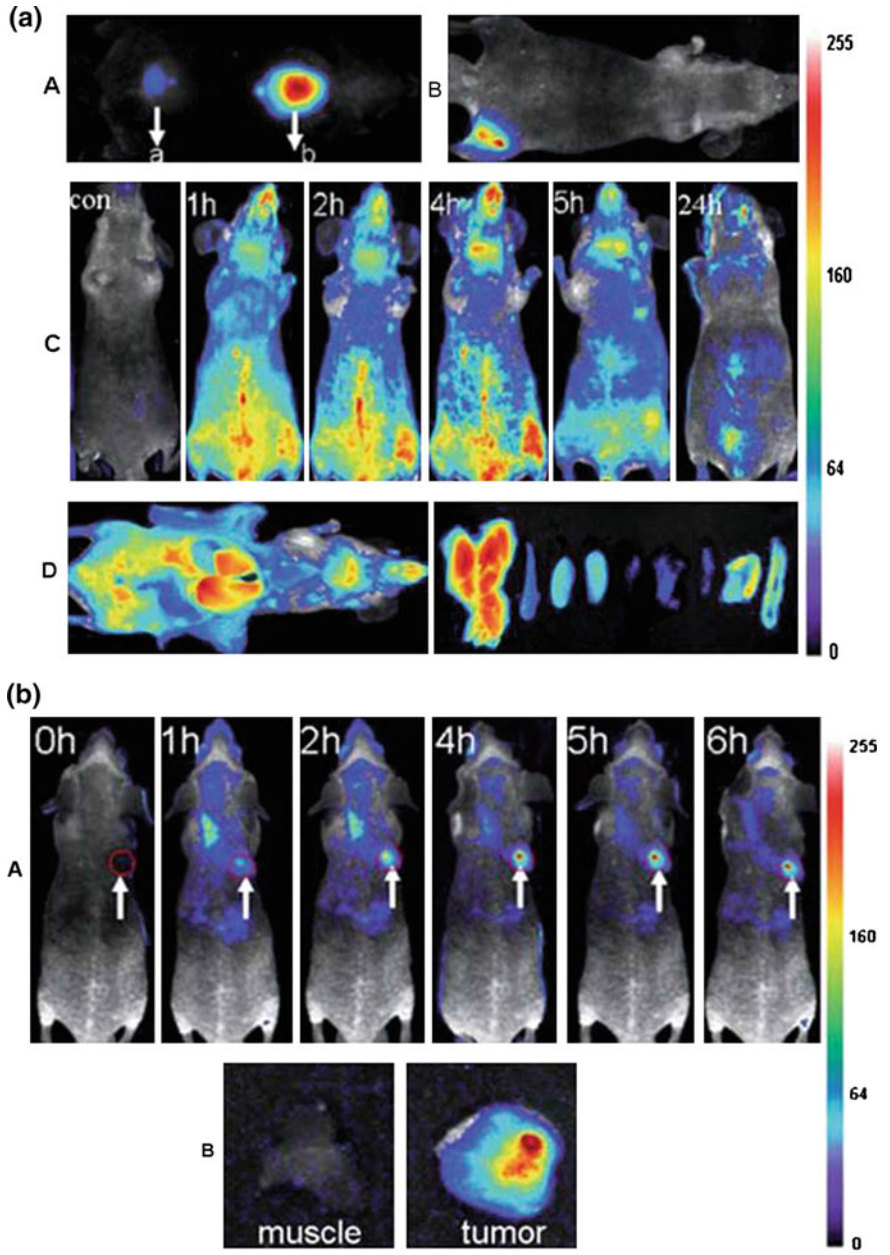

Fig. 7 **a** BSA-AuNCs as contrast imaging agents for tumor fluorescence imaging in vivo was demonstrated by subcutaneous *A*, intramuscular *B* and intravenous *C* injection in mice model at different time points of post injection. *D* Ex vivo optical imaging of anatomized mice and some dissected organs such as liver, spleen, left kidney, right kidney, heart, lung, muscle, skin and intestine from *left* to *right*. **b** Tumor accumulation BSA-AuNCs in MDA-MB-45 tumor xenograft models due to the EPR effects (Reproduced from Wu et al. (2010) with permission of The Royal Society of Chemistry)

tumor bearing mouse models. Doxorubicin (DOX), a widely used clinical anti-cancer drug, was immobilized on the methionine modified AuNCs to form a pro-drug, Au-Met-DOX. The enhanced tumor affinity and improved anti-tumor activity of this pro-drug were demonstrated on mouse sarcoma S180 tumor bearing mice. All the results in this study lead to tumor-targeted imaging and therapeutic efficacy of AuNCs as a core for the design of pro-drug in the field of cancer therapy (Chen et al. 2012). A fluorescence enzyme mimetic nanoprobe based on FR targeting AuNCs used for tumor tissues visualization was fabricated by one-step incubation method. The nanoprobes could distinguish efficiently cancerous cells from normal and could be a potential diagnostic tool for cancer imaging and prediction (Hu et al. 2014).

Recently, facile Au/Ce nanoclusters were synthesized by doping trivalent cerium ion into seed crystal growth process of gold and stabilized by glutathione which could be used as an excellent fluorescent probe for marking tumor cells due to their targeted absorption. These nanoclusters had no obvious cell cytotoxicity effect on HeLa, HepG2 and L02 cells and demonstrated in vivo imaging efficiency on a xenograft tumor model of cervical carcinoma (Ge et al. 2015). Since AuNCs can preferentially accumulate in tumor via the improved EPR effect due to its ultra-small size, they found profound applications as radio-sensitizers for cancer radiotherapy (Zhang et al. 2013). In an interesting study, fluorescent BSA-protected AuNCs conjugated with Herceptin (AuNCs-Her), for specific targeting and nuclear localization in ErbB-2 over-expressing breast cancer cells and tumor tissue for simultaneous imaging and cancer therapy was successfully prepared. These AuNCs-Her could escape the endo-lysosomal pathway and enter the nucleus of cancer cells and enhances the anticancer therapeutic efficacy of Herceptin by the induction of DNA damage which was evidenced in human breast cancer SK-BR3 cells (Wang et al. 2011b). In a separate work, folic acid conjugated silica coated AuNCs (AuNCs@SiO2) were developed for targeted dual-model fluorescent and X-ray computed tomography imaging (CT) of gastric cancer cells with over expression of FR. Tail vein injection of the AuNCs@SiO2-FA in MGC803 nude mice models exhibited excellent red emitting fluorescence optical property and X-ray absorbance for optical and CT dual-modality imaging (Zhou et al. 2013).

4.2 Sensing Applications

Fluorescent AuNCs found tremendous applications as sensors in the detection of metal ions, small molecules and biological macromolecules due to its quenching or enhancing effect when Au^{+} ions interacting with them. The impact of these AuNCs on resolving the headed issues in environment as well as medical sciences can provide greater tool for early detection of minuscule concentration of organic and inorganic molecules. In this context a discussion about the possible applications of as metal ion sensors, biosensors and so on need special attention.

4.2.1 Metal Ion Sensors

Presence of heavy metal ions such as Hg^{2+}, Cd^{2+}, Pb^{2+} and Cu^{2+} cause hazardous health issues because of their property of binding with vital organs or cellular components (Wei et al. 2010; Lin et al. 2010; Wang et al. 2014; Ding et al. 2014). Routine detection of mercuric ions (Hg^{2+}) is central to environmental monitoring in aquatic ecosystems. The first report in which the fluorescence of alkane thiols capped AuNCs (11-MUA-AuNPs) was quenched by the presence of mercury (II) (Hg (II)) due to Hg (II)-induced aggregation of AuNCs (Huang et al. 2007a) provide a ray of hope for enabling heavy metal detection using AuNCs. Similarly, Xie et al. (2010) developed a simple paper test strip system for the rapid routine monitoring of Hg^{2+} ions using AuNCs. Lysozyme type VI-stabilized gold nanoclusters (Lys VI-AuNCs) as a probe for the ultrasensitive detection of Hg^{2+} and CH_3Hg^+ in seawater based on fluorescence quenching due to the interaction between Hg^{2+}/CH_3Hg^+ and Au^+ on the Au surface could be further tapped (Lin and Tseng 2010). Although copper (Cu) is an integral part of a number of enzymes and involved in many vital biochemical processes, chronic Cu overload or exposure to excess Cu leads to abnormal Cu metabolism and fatal neurodegenerative changes (Gaetke and Chow 2003). Glutathione-protected AuNCs were used for the efficient detection of cupric ions (Cu^{2+}) based on aggregation-induced fluorescent quenching and it was recovered through the addition of a strong metal ion chelator, ethylene diamine tetra acetate (EDTA) (Chen et al. 2009). AuNCs stabilized by an iron binding transferrin family protein, lactoferrin (Lf) was also used for the effective and sensitive detection of Cu^{2+} (Xavier et al. 2010). Near-infrared luminescent AuNPs (NIRL-AuNPs) were synthesized by heat-assisted reduction of a gold (I)–thiol complex as a sensor for Cu^{2+} quantification (Tu et al. 2011).

Simultaneous detection of both $Hg^{2+}$and Cu^{2+} ions through fluorescence quenching was achieved through BSA-conjugated AuNCs. EDTA and sodium borohydride ($NaBH_2$) were used as masking reagents, in which EDTA complexed with Cu^{2+}, and borohydride reduced Hg^{2+} which eliminated quenching effect, thus detection of the other ion was achieved (Cao et al. 2013). Glutathione-capped Au/Ag nanoclusters (GS-Au/AgNCs) by microwave irradiation had an efficient sensing property to detect many analytes such as Cu^{2+}, sulfide, iodide, cysteine, and glutathione (Zhang et al. 2015). In a promising study, Annie et al. (2012) employed l-3,4-dihydroxyphenylalanine (L-DOPA) capped AuNCs for the sensitive detection of Fe^{3+} with a limit of detection of 3.5 μM which is much lower than the maximum level (0.3 mgL^{-1} equivalent to 5.4 μM) of Fe^{3+} permitted in drinking water by the U.S. Environmental Protection Agency. Screening of food materials for possible heavy metal contamination requires special consideration as a potent health issue, hence AuNC based sensing probes needs to be further explored to effectively handle the issues.

4.2.2 Biosensors

Carefully engineered AuNCs were observed to be capable for the efficient detection of various bio-macromolecules and other small molecules such as enzymes (Hu et al. 2012; Wen et al. 2013), folic acid (Hemmteenejad et al. 2014), proteins (Lin et al. 2013b; Selvaprakash and Chen 2014), dopamine (Tao et al. 2013; Aswathy and Sony 2014), cholesterol (Chen and Baker 2013) etc. The pioneering work in which AuNCs were used for detecting cellular proteins reported by Triulzi et al. (2006) used polyclonal, goat-derived anti-human IgG antibody conjugated PAMAM-AuNCs for the human IgG immunoassay. Huang et al. (2008) reported a new method using Platelet-derived growth factor AA (PDGF AA) modified fluorescent AuNCs (PDGF AA-L (AuND)) and PDGF binding aptamer modified AuNPs (Apt-Q (AuNP)) for the effective breast cancer specific protein detection. Fluorescence of PDGF AA-L(AuND) was quenched due to Apt-Q(AuNP) binding and addition of PDGFs, caused a decrease in interaction between Apt-Q(AuNP) and PDGF AA-L(AuND) which results in recovered fluorescence. Fluorescent mannose coated AuNCs were effectively used for the detection of Concanavalin A (Con A) and *Escherichia coli* (*E. coli*) wherein the fluorescence was increased after binding to corresponding proteins such as (Con A) and FimH of type 1 in *E. coli* (Huang et al. 2009). Serum glucose could be easily quantitated using cysteine stabilized AuNCs and the method is devoid of interference with other serum proteins (Hussain et al. 2011) and hence could be advantageous over the current colorimetric methods. Constant monitoring of rifampicin or rifampin (R), a common drug generally prescribed for long-term administration under regulated doses to treat inactive meningitis, cholestatic pruritus and tuberculosis (TB), is necessary to control the side effects and prevent overdose caused by chronic medication. Chatterjee et al. (2015) developed an efficient colorimetric assay for the detection of rifampicin in urine in which fluorescence of immobilized BSA-AuNCs on wax-printed papers was quenched by the increasing concentration of rifampicin.

5 Future Scopes of Fluorescent AuNCs

Many simple strategies have been formulated for the preparation of AuNCs from Au^{3+} in the presence of small biological molecules which acts as reducing and stabilizing agents. Despite the fact that the nature and concentration of the ligand, reaction temperature, time, solution pH, ionic strength and other parameters play significant roles in determining the formation of AuNCs with desirable physical, chemical and optical properties, they can be tuned for the fabrication of NCs for more sensitive fluorescence energy transfer based techniques. AuNCs have a few favourable circumstances as nanoprobes attributable to their great stability and mono-dispersion in the physiological environment which will lead to enhanced

sensitivity and increased tracking lifetime. Since AuNCs have the remarkable biocompatibility, it could be suited for in vitro and in vivo applications. AuNC-based platforms can be utilized to improve or empower a wide assortment of treatments including drug delivery, nucleic acid delivery, photothermal ablation, radiotherapy and real time fluorescent imaging. The capacity to tune the size, shape and thus the physical properties of NCs, alongside their low cytotoxicity, high biocompatibility, and scope of surface modulations, makes them promising contender for clinical use. It is sensible to trust that increasingly delicate and specific detection and imaging procedures utilizing Au based NCs will soon get to be brilliant measures for clinical applications.

In-depth molecular imaging and complete surgical resection of malignant tissue is still a challenging task in oncology (Kelderhouse et al. 2013; Nguyen and Tsien 2013). Even though semiconductor quantum dots (QDs) offered great assurance in early cancer detection and diagnosis due to its intense, stable fluorescence (Smith et al. 2006; Alivisatos et al. 2005; Michalet et al. 2005), its wide spread usage is heavily limited owing to the higher risk to human health as well as environment due to its heavy metal content (Hardmen 2006; Tsoi et al. 2013). Organic dyes used for imaging purpose are greatly liable to photo bleaching which makes them unsuitable for long term usage (Li et al. 2014; Jaiswal et al. 2003; Chen and Gerion 2004). AuNCs as an emerging fluorescent nanomaterial can overcome most of these disadvantages of quantum dots and organic dyes (Lin et al. 2009b; Qu et al. 2015) and have a greater potential for many applications in biomedical field (Lin et al. 2010). AuNCs synthesized by green-chemistry possessed greater water-solubility, high photostability, large Stokes shift, ultrasmall size, nontoxicity, and good biocompatibility and hence could be carefully tuned for diverse applications in biomedical field (Wang et al. 2011b; Qu et al. 2015; Muhammed et al. 2010). The surface modification of AuNCs using tumor specific ligands will offer targeted imaging and drug delivery (Huang et al. 2009; Huang et al. 2011a) thereby extending its promising role in personalized medicine. Functional molecules present as the capping agents in AuNCs will support conjugation of targeting molecules and chemotherapeutics for its efficient delivery at the tumor site (Shang et al. 2011b). Folic acid conjugated AuNCs (NCs-FA) highlighted the potential of AuNCs to become a diagnostic tool for cancer detection and imaging (Hu et al. 2014). Fluorescent AuNCs conjugated with diatrizoic acid and AS1411 aptamer (AS1411-DA-AuNPs) with nucleolin specific targeting function make NCs as a powerful tool in the field of fluorescence-guided surgery (Li et al. 2015a). Doxorubicin immobilized multifunctional AuNCs (Au-Met-DOX) and Herceptin conjugated AuNCs (AuNCs-Her) confirmed the promising future of AuNCs as a drug carrier with at most specificity and target ability (Chen et al. 2012; Wang et al. 2011b). Although marvelous transitions are undergoing in the study of AuNCs as promising multifunctional optical probes for molecular imaging and therapy, most studies are mainly concentrating on in vitro (Shang et al. 2011b; Muhammed et al. 2009; Qiao et al. 2013; Vankayala et al. 2015; Chen et al. 2012) applications than in vivo (Wu et al. 2010) real time uses. Further detailed in vivo and preclinical to clinical investigations are warranted to establish the full potential of AuNCs for myriad applications aiming in the betterment of human life.

6 Versatile Biomedical Applications of Other Gold Nanomaterials

Gold nanoparticles can be manufactured into a variety of forms, comprising of gold nanospheres, nanorods (AuNRs), nanoshells, nanobelts, nanocages, nanoprisms, nanotubes (Nandini et al. 2014, 2016a) nanoribbons (Nandini et al. 2016b) and nanostars (Fig. 8). Many processes have been developed to synthesize gold nanomaterials, including both chemical methods (e.g., chemical reduction, photochemical reduction, co-precipitation, thermal decomposition, hydrolysis, etc.) and physical methods (e.g., vapor deposition, laser ablation, grinding and many more).

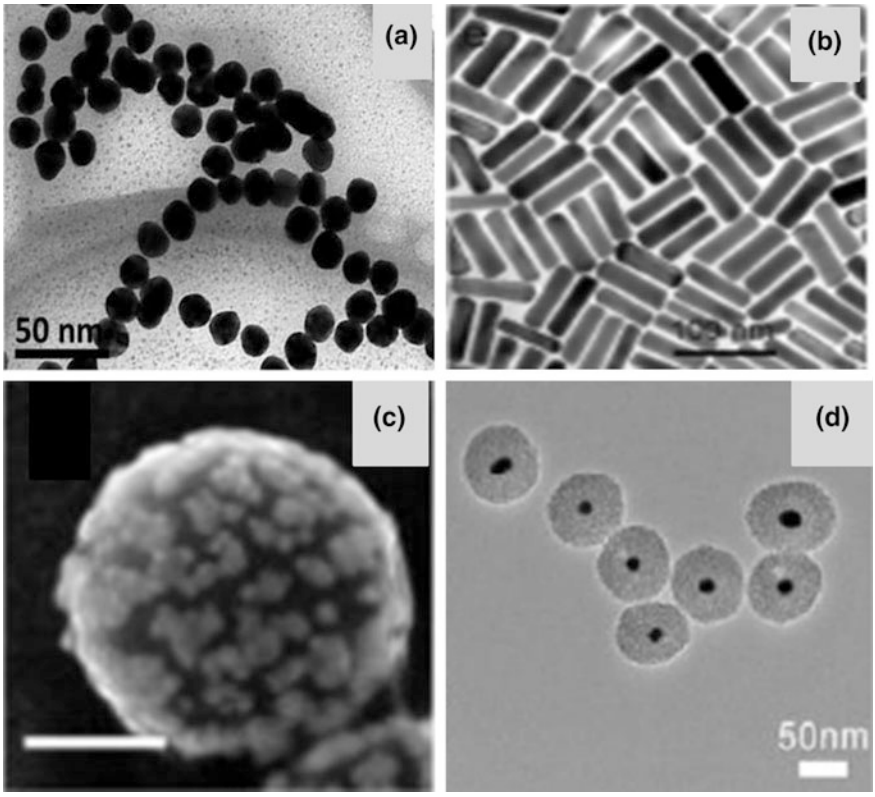

Fig. 8 **a** Electron microscopy of Au-citrate nanoparticles (Reprinted with permission from Plascencia-Villa et al. (2015) © 2015 American Chemical Society). **b** TEM images of silica-coated AuNRs. Scale bars correspond to 100 nm (Reprinted with permission from Jia et al. (2015) © 2015 American Chemical Society). **c** SEM image gold nanoshells on silica core particles. Scale bars correspond to 100 nm (Reprinted with permission from Sauerbeck et al. (2014) © 2014 American Chemical Society). **d** TEM image of gold nanospheres coated with mesoporous silica (Au@mSiO2-TTA) (Reprinted with permission from Song et al. (2015) © 2015 American Chemical Society)

The ultimate goal of every process is to obtain nanomaterials with a high level of homogeneity and provide fine control over size, shape and surface properties (Feldheim and Foss 2011). Such nanomaterials have attracted diverse role in biomedical field such as targeted imaging, drug delivery, photo dynamic and photo thermal therapy etc. These gold nanomaterials exhibit localized SPR effect because of it is much smaller in size than the light wavelength and its chemical, physical and optical properties depend on its size and shape which is different from bulk gold (Mie 1908). Gold nanomaterials of approximately 3–20 nm display light absorption but at 20–80 nm exhibit an increasing scattering/absorption ratio which gives great opportunity for biomedical imaging based on light scattering.

6.1 Contrast Agents

The plasmon absorption band varies on its shape and number from spherical to non-spherical NPs. Spherical AuNPs possesses only one plasmon absorption band. Different plasmon absorption bands of single NPs provides more information than a single visible band of spherical AuNPs (Liz Marzan 2006; Boisselier and Astruc 2009). AuNRs possess two plasmon bands, one in transverse and the other in longitudinal direction and its ratio is adjusted to shift the plasmon band to the NIR region which allows penetration into living tissues and avoid background fluorescence noise. Gold nanoshells are concentric spherical constructs consist of a thin outer gold shell and a silica core and its optical properties can be tuned by changing the core-shell ratio as well as the overall size and shape. Hence the absorption and scattering properties of AuNRs, gold nanospheres and gold nanoshell could be tuned to NIR region where blood and tissues are maximally transmissive. The specific tunable optical properties of these gold nanomaterials make it as ideal candidates for in vitro and in vivo imaging and photothermal therapy (Loo et al. 2005; Lin et al. 2006; Lal et al. 2008). It could also be used as contrast agents for optical coherence tomography (OCT) (Chen et al. 2005), photoacoustic tomography (PA) (Li et al. 2008; Yang et al. 2009; Kim et al. 2010), computed tomography (CT) (Hainfeld et al. 2006; Popovtzer et al. 2008; Maltzahn 2009), multi-photon microscopy, Surface-enhanced Raman spectroscopy (SERS), (Qian et al. 2008; Zavaleta et al. 2009) and Magnetic resonance imaging (MRI) (Lim et al. 2007; Eun et al. 2010). Optical imaging of epithelial growth factor receptor (EGFR) over expressed cervical epithelial cancer cells (SiHa cells) using monoclonal antibody conjugated AuNPs was achieved by Sokolov et al. (2003). In a similar work, immune-targeted AuNPs against EGFR was effectively utilized for imaging purpose in non-malignant epithelial cell line (HaCaT) and two malignant oral epithelial cell lines (HOC 313 clone 8 and HSC 3). Cancerous cells displayed a higher uptake of the NP which was colored in SPR scattering image with dark background using a white-light source from a conventional microscope (El-Sayed et al. 2005).

Gold is a new-age selective X-ray contrast agent which could be effectively exploited in early cancer diagnostics due to its greater X-ray attenuation ability

compared with iodine, which is currently used as a contrast agent (Hainfeld et al. 2006). Although X-ray based computed tomography (CT) is one of the most convenient imaging/diagnostic tools, it is not considered as molecular imaging tool since targeted and molecularly specific contrast agents for CT is not suitably established. Popovtzer et al. (2008) demonstrated a new CT imaging modality in head and neck cancer which enables, cancer detection at the cellular and molecular level with standard clinical CT using gold nano-probes that selectively target tumor specific antigen and inducing distinct contrast in CT imaging. Hybrid nanoparticles with superparamagnetic iron oxide embedded in AuNP shells displayed combined applications in MRI and optical imaging, photothermal therapy and targeted cancer therapy. Iron core of this NPs provides strong T2 (spin-spin relaxation time) contrast, while Au part act as optical contrast agent (Lim et al. 2007; Larson et al. 2007; Ji et al. 2007). The hybrid NPs targeted to the epidermal growth factor receptor (EGFR), demonstrated fascinating effects in MDA-MB-468 breast cancer cells (Larson et al. 2007).

Rayleigh scattering of AuNRs are excellent and hence could enhance SERS due to surface plasmon field overlap. Anti-epidermal growth factor receptor (anti-EGFR) antibodies conjugated AuNRs specifically bind to human oral cancer cells and gave enhanced Raman spectrum useful for diagnostic purpose (Huang et al. 2007b). Similarly, Lee et al. (2007) demonstrated the potential feasibility of SERS imaging in live human embryonic kidney cells HEK293 expressing PLCgamma1 using monoclonal antibody conjugated Au/Ag core-shell nanoparticles. Bi-functional poly ethylene glycol (PEG) coated AuNPs were covalently coupled to F19 monoclonal antibodies for the staining of resected human pancreatic adenocarcinoma cells and visualized by darkfield microscopy near the nanoparticle resonance scattering maximum (Eck et al. 2008). AuNRs functionalized with Herceptin (Her-PEG-GNRs) was used for in vivo targeting of breast cancer specific antigens. It demonstrated significant stability and targetability in vitro in the presence of blood and then in vivo in nude mice model for breast cancer. These observations could effectively translate AuNRs as a powerful molecular imaging agent (Eghtedari et al. 2009). Two-photon luminescence (TPL) intensity of AuNRs at 830 nm excitation on a far-field laser-scanning microscope was 58 times than that from a single rhodamine molecule and hence could be adopted for applications as TPL imaging agents. A simple colorimetric method was developed for the visual distinction between cancerous cells and normal ones using aptamer-conjugated AuNPs, in which cancer cells displayed a distinct color change compared with the normal cells (Medley et al. 2008).

6.2 Photothermal Therapy

Although chemotherapy holds the major share in cancer treatment regimen it is often accompanied with dramatic side effects; surgical removal of tumors limited to accessible sold tumors only and radiotherapy also affect healthy surrounding tissue

along the radiation path. Photothermal therapy is an emerging technique that uses optical sources to generate heat to destroy tumor cells. Among the gold nanomaterials; AuNRs, gold nanospheres and gold nanoshells absorb light in a broad spectrum range from near UV to NIR, but the NIR region is especially crucial in order to penetrate inside living tissues (Jain et al. 2007). Chemotherapeutic molecules conjugated photothermal agents can decipher better outcome because laser hypothermia induced drug release is possible at the tumor site (photo-chemotherapy).

PEG coated gold nanoshells with peak optical absorption in the NIR was effectively employed for the photothermal therapy in murine colon carcinoma (CT26WT) tumor bearing immune-competent mice, wherein tumors were illuminated with a diode laser for hyperthermia generation (O'Neal et al. 2004). Focused pulsed NIR laser irradiation of phosphatidylcholine-passivated gold nanorods (PC-NRs) achieved selective killing of single cells (Takahashi et al. 2006). Folate conjugated AuNRs renders the extensive blebbing of KB cells when irradiated with femto second Ti:sapphire laser (Huff et al. 2007). Anti-epidermal growth factor receptor (anti-EGFR) conjugated AuNPs and gold nanoshells were used for tumor targeted hyperthermia (El-Sayed et al. 2006; Huang et al. 2006). Similarly, prostate cancer ablation (PC-3 cell) in nude mice model were reported using 110 nm gold nanoshell, irradiated with 810 nm NIR laser at the spot site (Stern et al. 2008). NF-kappaB is a transcription factor critically involved in tumor formation and progression. Folate receptor conjugated gold nanospheres carrying siRNA recognizing NF-kappaB p65 subunit were synthesized for the successful down-regulation of NF-kappaB in cancer cells after NIR light irradiation (Lu et al. 2010). A dual-functional nanoparticle that mediates simultaneous photothermal cell killing and controllable drug release for complete reduction of tumor was devised, in which doxorubicin was loaded into hollow gold nanospheres (HAuNS) coated with PEG. The nano construct advertised superior anti-tumor activity than free DOX, NP3, or liposomal DOX in the in vitro and in vivo using human breast cancer MDA-MB-231 and ovarian cancer A2780 cells (You et al. 2010, 2012).

6.3 Drug Carriers

The increased surface to volume ratio of the nanoparticles allows the conjugation of targeting moieties with high drug loading which will ultimately enhance the therapeutic efficacy. Synthesis of gold nanomaterials using biological materials such as proteins, polysaccharides, microorganisms, plant extracts, cell extracts and many more predominate in biomedical applications because of its biocompatibility and non-toxicity (Joseph and Sreelekha 2014). NP based drug-delivery systems for cancer therapeutics are swiftly evolving to overcome the drug resistances of Cancer Stem Cells (CSC). Recently, NP-based strategies have illustrated promising therapeutic efficacy while reducing adverse effects, compared with those of conventional therapy (Joseph et al. 2016). Destruction of tumor mass by NPs targeting

both CSCs and cancer cells with possibly eliminate the tumor burden and also block any tumor relapse.

Gold nanomaterials have been well explored as a promising drug delivery vehicle for cancer in recent years. Multidrug resistance (MDR) is a major obstacle during chemotherapy of cancer in which drug efflux affects the therapy. AuNPs-doxorubicin (Au-PEG-SS-DOX) conjugates were developed to overcome MDR in cancer cells (Gu et al. 2011). Similarly, doxorubicin conjugated onto the surface of AuNPs with a PEG spacer via an SMCC linker also demonstrated highly efficient cellular entry and enhanced cytotoxicity in multidrug resistant HepG2-R cancer cells compared with free doxorubicin (Cheng et al. 2013). In another promising work, rifampicin (RF)which was known to reduce the MDR was conjugated to AuNPs to enhance the rate as well as efficiency of endocytosis of NPs in cancer cells which could lead to demand of decreased amount of AuNPs for cancer management (Ali et al. 2014). Anticancer and immuno-modulatory polysaccharide PST001 isolated from the seed kernels of *Tamarindus indica* acted both as reducing and capping agent for the preparation of PST-Gold nanoparticles (Joseph et al. 2013). The resultant nanoparticles showed high stability with no obvious aggregation for months and a broader range of pH tolerance. The nanoconjugate was effective against various human cancer cell lines and exhibited induction of apoptosis. Importantly, PST-Gold nanoparticles demonstrated significant increase in the life span of tumor-challenged mice models and displayed greater reduction in the tumor volume in both ascites and solid tumours (Joseph et al. 2014).

Methotrexate (MTX) conjugated AuNPs (MTX-AuNP) was found to be more effective than free drug in overcoming MDR (Chen et al. 2007). Similarly, Brown et al. (2010) synthesized oxaliplatin conjugated AuNPs which exhibited increased cytotoxicity, drug uptake, and localization in the A549 lung epithelial cancer cell lines and the colon cancer cell lines HCT116, HCT15, HT29 and RKO than free drug. In a more engineered fashion, DOX, tumor targeting ligand (cyclo (Arg-Gly-Asp-D-Phe-Cys) peptides, (cRGD)) and ^{64}Cu-chelators were conjugated to the PEGylated AuNRs via hydrazone bond for targeted anticancer drug delivery and positron emission tomography (PET) imaging of tumors. These multifunctional NPs triggers pH-sensitive controlled drug release and in vivo PET imaging (Xiao et al. 2012). In a similar way multifunctional theranostic nanoparticle was developed using amphiphilic AuNPs coated with a Raman reporter BGLA (2-(4-(bis(4-(diethylamino)phenyl)(hydroxy)methyl)phenoxy)ethyl 5-(1,2-dithio-lan-3-yl)pentanoate) for cancer targeted drug delivery. DOX was loaded on the as prepared nanoparticles and tagged with HER2 antibody as targeting moiety for specific tumor recognition. These nanoparticles trigger pH-sensitive drug release and SERS imaging (Song et al. 2012).

AuNPs was used as a vector for the targeted delivery of tumor necrosis factor (TNF) in MC-38 colon carcinoma tumors in mice and displayed superior tumor localization. It was found to be less toxic and more effective in reducing tumor burden than native TNF since maximal antitumor responses were achieved at lower doses of drug (Paciotti et al. 2004). PEGylated colloidal gold–TNFconstruct (CYT-6091) was tested in a phase I dose escalation clinical trial in advanced stage

cancer patients and found to be non-toxic compared to the doses of free recombinant human tumor necrosis factor alpha (rhTNF) (Libutti et al. 2010). In a similar study, PEG coated AuNPs incorporated with TNF-alpha payload and combined heating were studied in SCK mammary carcinomas grown A/J mice and found to decrease tumor growth (Visaria et al. 2006).

7 Conclusion

Gold based nanomaterials are one of the most widely studied molecules in the last decade, and are emerging as promising agents in cancer management in which fluorescent AuNCs holds a prominent position. Fluorescent AuNCs can be fabricated using many biological and organic materials as reducing and capping agents and the properties depends to the fabrication strategies adopted. AuNCs can overcome biological barriers and transport drugs to the tumor site and are potential alternatives to QDs and fluorophores which can enable early imaging, diagnosis and targeted therapy of cancer. Advances in genomics and proteomics provided accurate information about the expression of various receptors on cancers and hence different targeting moieties as well as chemotherapeutic agents could be conjugated to the surface of AuNCs for rapid and accurate tumor diagnosis and therapy. AuNCs could be used for combinatorial imaging with MRI, PET and CT for more potential tumor imaging. Although many reports suggest the biocompatible and non-toxic nature of AuNCs, detailed toxicity studies in suitable animal models are in infancy stage to make a stable conclusion about the safety in the wide spread use of this materials. Other forms of gold nanomaterials such as gold nanospheres, nanorods, nanoshells, nanobelts, nanocages, nanoprisms and nanostars also play much promising role in every aspect of human inference. In the pursuit of current knowledge, in the future of nanomedicine, AuNCs will be one of the innovative platforms for cancer diagnosis and treatment for improved patient survival outcome. Progresses in the fabrication of different useful nanomaterials and AuNCs might advantage for the advancement of more delicate fluorescence based strategies. It is our solid conviction that more sensitive and specific detecting and imaging systems utilizing Au based NCs will soon get to be brilliant principles for clinical applications.

References

Ali MRK, Panikkanvalappil SR, El-Sayed MA (2014) Enhancing the efficiency of gold nanoparticles treatment of cancer by increasing their rate of endocytosis and cell accumulation using rifampicin. J Am Chem Soc 136(12):4464–4467. doi:10.1021/ja4124412

Alivisatos A, Gu W, Larabell C (2005) Quantum dots as cellular probes. Annu Rev Biomed Eng 7:55–76

Alvarez MM, Khoury JT, Schaaff TG et al (1997) Optical absorption spectra of nanocrystal gold molecules. J Phys ChemB 101(19):3706–3712
Annie Ho JA, Chang HC, Su WT (2012) DOPA-mediated reduction allows the facile synthesis of fluorescent gold nanoclusters for use as sensing probes for ferric ions. Anal Chem 84(7):3246–3253
Apell P, Monreal R, Lundqvist S (1988) Photoluminescence of noble metals. Phys Scr 38(2):174–179
Aswathy B, Sony G (2014) Cu^{2+} modulated BSA-Au nanoclusters: a versatile fluorescence turn-on sensor for dopamine. Microchem J 116:151–156. doi:10.1016/j.microc.2014.04.016
Bao Y, Zhong C, Vu DM et al (2007) Nanoparticle-free synthesis of fluorescent gold nanoclusters at physiological temperature. J Phys Chem C 111(33):12194–12198
Barnes WL, Dereux A, Ebbesen TW (2003) Surface plasmon subwavelength optics. Nature 424 (6950):824–830
Bhattacharya D, Gupta RK (2005) Nanotechnology and potential of microorganisms. Crit Rev Biotechnol 25(4):199–204
Bigioni TP, Whetten RL, Dag O (2000) Near-infrared luminescence from small gold nanocrystals. J Phys Chem B 104(30):6983–6986
Boisselier E, Astruc D (2009) Gold nanoparticles in nanomedicine: preparations, imaging, diagnostics, therapies and toxicity. Chem Soc Rev 38:1759–1782. doi:10.1039/B806051G
Brown S, Sarikaya M, Johnson E (2000) A genetic analysis of crystal growth. J Mol Biol 299 (3):725–735
Brown SD, Nativo P, Smith JA et al (2010) Gold nanoparticles for the improved anticancer drug delivery of the active component of oxaliplatin. J Am Chem Soc 132(13):4678–4684
Cao D, Fan J, Qiu J et al (2013) Masking method for improving selectivity of gold nanoclusters in fluorescence determination of mercury and copper ions. Biosens Bioelectron 42C(1):47–50. doi:10.1016/j.bios.2012.10.084
Chatterjee K, Kuo CW, Chen A et al (2015) Detection of residual rifampicin in urine via fluorescence quenching of gold nanoclusters on paper. J Nanobiotechnol 13:46. doi:10.1186/s12951-015-0105-5
Chen X, Baker GA (2013) Cholesterol determination using protein-templated fluorescent gold nanocluster probes. Analyst 138(24):7299–7302
Chen FQ, Gerion D (2004) Fluorescent CdSe/ZnS nanocrystal-peptide conjugates for long-term, nontoxic imaging and nuclear targeting in living cells. Nano Lett 4:1827–1832
Chen CL, Rosi NL (2010) Peptide-based methods for the preparation of nanostructured inorganic materials. Angew Chem Int Ed 49(11):1924–1942
Chen TH, Tseng WL (2012) (Lysozyme type VI)-stabilized Au 8 clusters: synthesis mechanism and application for sensing of glutathione in a single drop of blood. Small 8(12):1912–1919
Chen SW, Ingram RS, Hostetler MJ et al (1998) Gold nano electrodes of varied size: transition to molecule-like charging. Science 28(5372):2098–2101
Chen J, Saeki F, Wiley BJ et al (2005) Gold nanocages: bioconjugation and their potential use as optical contrast agents. Nano Lett 5(3):473–477. doi:10.1021/nl047950t
Chen Y, Tsai C, Huang P et al (2007) Methotrexate conjugated to gold nanoparticles inhibits tumor growth in a syngeneic lung tumor model. Mol Pharm 4(5):713–722
Chen WB, Tu XJ, Guo XQ (2009) Fluorescent gold nanoparticles-based fluorescence sensor for Cu^{2+} ions. Chem Commun 13:1736–1738. doi:10.1039/B820145E
Chen H, Li B, Ren X et al (2012) Multifunctional near-infrared-emitting nano-conjugates based on gold clusters for tumor imaging and therapy. Biomaterials 33:8461–8476
Chen Y, Wang Y, Wang C et al (2013) Papain-directed synthesis of luminescent gold nanoclusters and the sensitive detection of Cu^{2+}. J Colloid Interface Sci 396:63–68. doi:10.1016/j.jcis.2013.01.031
Chen LY, Wang CW, Yuan Z et al (2014) Fluorescent gold nanoclusters: recent advances in sensing and imaging. Anal Chem 87(1):216–229
Cheng J, Gu YJ, Cheng SH et al (2013) Surface functionalized gold nanoparticles for drug delivery. J Biomed Nanotechnol 9(8):1362–1369

Chevrier DM, Chatt A, Zhang P (2012) Properties and applications of protein-stabilized fluorescent gold nanoclusters: short review. J Nanophoton 6:064504. doi:10.1117/1.JNP.6.064504

Choi YE, Kwak JW, Park JW (2010) Nanotechnology for early cancer detection. Sensors 10 (1):428–455

Couvreur P, Vauthier C (2006) Nanotechnology: intelligent design to treat complex disease. Pharm Res 23(7):1417–1450

Crookes-Goodson WJ, Slocik JM, Naik RR (2008) Bio-directed synthesis and assembly of nanomaterials. Chem Soc Rev 37(11):2403–2412

Ding H, Liang C, Sun K et al (2014) Dithiothreitol-capped fluorescent gold nanoclusters: An efficient probe for detection of copper (II) ions in aqueous solution. Biosens Bioelectron 59:216–220. doi:10.1016/j.bios.2014.03.045

Duan HW, Nie NM (2007) Etching colloidal gold nanocrystals with hyperbranched and multivalent polymers: a new route to fluorescent and water-soluble atomic clusters. J Am Chem Soc 129(9):2412–2413. doi:10.1021/ja067727t

Eck W, Craig G, Sigdel A et al (2008) PEGylated gold nanoparticles conjugated to monoclonal F19 antibodies as targeted labeling agents for human pancreatic carcinoma tissue. ACS Nano 2 (11):2263–2272

Eghtedari M, Liopo AV, Copland JA et al (2009) Engineering of hetero-functional gold nanorods for the in vivo molecular targeting of breast cancer cells. Nano Lett 9(1):287–291

El-Sayed IH, Huang XH, El-Sayed MA (2005) Surface plasmon resonance scattering and absorption of anti-EGFR antibody conjugated gold nanoparticles in cancer diagnostics: applications in oral cancer. Nano Lett 5:829–834

El-Sayed IH, Huang XH, El-Sayed MA et al (2006) Selective laser photo-thermal therapy of epithelial carcinoma using anti-EGFR antibody conjugated gold nanoparticles. Cancer Lett 239:129–135

Eun CC, Charles G, Jingyi C et al (2010) Inorganic nanoparticle-based contrast agents for molecular imaging. Trends Mol Med 16(12):561–573

Feldheim DL, Foss CA (2001) Metal nanoparticles synthesis, characterization, and applications. Marcel Dekker, New York

Fendler JH (1997) Biomineralization inspired preparation of nanoparticles and nanoparticulate films. Curr Opin Solid St M 2(3):365–369

Ferrari M (2005) Cancer nanotechnology: opportunities and challenges. Nat Rev Cancer 5(3): 161–171

Frank M, Schloissnig S (2010) Bioinformatics and molecular modeling in glycobiology. Cell Mol Life Sci 67(16):2749–2772. doi:10.1007/s00018-010-0352-4

Gaetke LM, Chow CK (2003) Copper toxicity, oxidative stress, and antioxidant nutrients. Toxicology 189(1–2):147–163

Galib Mayur B, Prajapati PK (2011) Therapeutic potentials of metals in ancient India: a review through Charaka Samhita. J Ayurveda Integr Med 2(2):55–63

Gao S, Chen D, Li Q et al (2014) Near-infrared fluorescence imaging of cancer cells and tumors through specific biosynthesis of silver nanoclusters. Sci Rep 4:4384. doi:10.1038/srep04384

Garcia AR, Rahn I, Johnson S et al (2013) Human insulin fibril-assisted synthesis of fluorescent gold nanoclusters in alkaline media under physiological temperature. Colloids Surf B 105:167–172. doi:10.1016/j.colsurfb.2012.12.052

Ge W, Zhang Y, Ye J et al (2015) Facile synthesis of fluorescent Au/Ce nanoclusters for high-sensitive bioimaging. J Nanobiotechnol 13:8. doi:10.1186/s12951-015-0071-y

Ghosh A, Udayabhaskararao T, Pradeep T (2012) One-step route to luminescent Au18SG14 in the condensed phase and its closed shell molecular ions in the gas phase. J Phys Chem Lett 3 (15):1997–2002. doi:10.1021/jz3007436

Grzelczak M, Perez-Juste J, Mulvaney P et al (2008) Shape control in gold nanoparticle synthesis. Chem Soc Rev 37:1783–1791. doi:10.1039/B711490G

Gu YJ, Cheng J, Man CWY et al (2011) Gold doxorubicin nanoconjugates for overcoming multidrug resistance. Nanomedicine 8(2):204–211

Guevel XL, Daum N, Schneider M (2011) Synthesis and characterization of human transferrin-stabilized gold nanoclusters. Nanotechnology 22(27):275103. doi:10.1088/0957-4484/22/27/275103

Haberland H (1994) Clusters of atoms and molecules: theory experiment, and clusters of atoms. Springer-Verlag, Berlin

Hainfeld JF, Slatkin D, Focella TM et al (2006) Gold nanoparticles: a new X-ray contrast agent. British J Radiol 79(939):248–253. doi:10.1259/bjr/13169882

Hardman R (2006) A toxicologic review of quantum dots: toxicity depends on physicochemical and environmental factors. Environ Health Perspect 114(2):165–172

Hemmateenejad B, Shakerizadeh-Shirazi F, Samari F (2014) BSA-modified gold nanoclusters for sensing of folic acid. Sensors Actuators B 199:42–46. doi:10.1016/j.snb.2014.03.075

Hicks JF, Templeton AC, Chen S et al (1999) The monolayer thickness dependence of quantized double-layer capacitances of monolayer-protected gold clusters. Anal Chem 71(17):3703–3711

Hicks JF, Miles DT, Murray RW (2002) Quantized double layer charging of highly monodisperse metal nanoparticles. J Am Chem Soc 124(44):13322–13328

Hostetler MJ, Wingate JE, Zhong CJ et al (1998) Alkanethiolate gold cluster molecules with core diameters from 1.5 to 5.2 nm: core and monolayer properties as a function of core size. Langmuir 14(1):17–30

Hu L, Han S, Parveen S et al (2012) Highly sensitive fluorescent detection of trypsin based on BSA stabilized gold nanoclusters. Biosens Bioelectron 32(1):297–299. doi:10.1016/j.bios.2011.12.007

Hu D, Sheng Z, Fang S et al (2014) Folate receptor-targeting gold nanoclusters as fluorescence enzyme mimetic nanoprobes for tumor molecular colocalization diagnosis. Theranostics 4(2):142–153

Huang T, Murray RW (2001) Visible luminescence of water-soluble monolayer-protected gold clusters. J Phys Chem B 105(50):12498–12502. doi:10.1021/jp0041151

Huang XH, Jain PK, El-Sayed IH et al (2006) Determination of the minimum temperature required for selective photothermal destruction of cancer cells with the use of immunotargeted gold nanoparticles. Photochem Photobiol 82(2):412–417

Huang CC, Yang Z, Lee KH et al (2007a) Synthesis of highly fluorescent gold nanoparticles for sensing mercury(II). Angew Chem Int Ed 46(36):6824–6828. doi:10.1002/anie.200700803

Huang XH, El-Sayed IH, Qian W et al (2007b) Cancer cells assemble and align gold nanorods conjugated to antibodies to produce highly enhanced, sharp, and polarized surface Raman spectra: a potential cancer diagnostic marker. Nano Lett 7(6):1591–1597

Huang CC, Chiang CK, Lin ZH et al (2008) Bioconjugated gold nanodots and nanoparticles for protein assays based on photoluminescence quenching. Anal Chem 80(5):1497–1504. doi:10.1021/ac701998f

Huang CC, Chen CT, Shiang YC et al (2009) Synthesis of fluorescent carbohydrate-protected Au nanodots for detection of Concanavalin A and *Escherichia coli*. Anal Chem 81(3):875–882. doi:10.1021/ac8010654

Huang P, Xu C, Lin J et al (2011a) Folic acid-conjugated graphene oxide loaded with photosensitizers for targeting photodynamic therapy. Theranostics 1:240–250. doi:10.7150/thno/v01p0240

Huang X, Li B, Li B et al (2011b) Facile preparation of highly blue fluorescent metal nanoclusters in organic media. J Phys Chem C 116(1):448–455. doi:10.1021/jp209662n

Huff TB, Tong L, Zhao Y et al (2007) Hyperthermic effects of gold nanorods on tumor cells. Nanomedicine 2(1):125–132. doi:10.2217/17435889.2.1.125

Hussain AM, Sarangi SN, Kesarwani JA et al (2011) Au-nanocluster emission based glucose sensing. Biosens Bioelectron 29(1):60–65. doi:10.1016/j.bios.2011.07.066

Jain P, El-Sayed IH, El-Sayed MA (2007) Au nanoparticles target cancer. Nanotoday 2(1):18–29

Jaiswal JK, Mattoussi H, Mauro JM et al (2003) Long-term multiple color imaging of live cells using quantum dot bioconjugates. Nat Biotechnol 21:47–51. doi:10.1038/nbt767

Jao YC, Chen MK, Lin SY (2010) Enhanced quantum yield of dendrimer-entrapped gold nanodots by a specific ion pair association and microwave irradiation for bioimaging. Chem Comm 46 (15):2626–2628

Ji X, Shao R, Elliott AM et al (2007) Bifunctional gold nanoshells with a superparamagnetic iron oxide-silica core suitable for both MR imaging and photothermal therapy. J Phys Chem C 111:6245–6251

Jia H, Fang C, Zhu XM et al (2015) Synthesis of absorption-dominant small gold nanorods and their plasmonic properties. Langmuir 31:7418–7426. doi:10.1021/acs.langmuir.5b01444

Joseph MM, Sreelekha TT (2014) Gold nanoparticles—synthesis and applications in cancer management. Recent Patents Mater Sci 7(1):8–25

Joseph MM, Aravind SR, Sheeja V et al (2013) PST-Gold nanoparticle as an effective anticancer agent with immunomodulatory properties. Colloids Surf B 104:32–39. doi:10.1016/j.colsurfb.2012.11.046

Joseph MM, Aravind SR, Sheeja V et al (2014) Antitumor activity of galactoxyloglucan-gold nanoparticles against murine ascites and solid carcinoma. Colloids Surf, B 116:219–227. doi:10.1016/j.colsurfb.2013.12.058

Joseph MM, George SK, Sreelekha TT (2016) Bridging 'Green' with nanoparticles: biosynthesis approaches for cancer management and targeting of cancer stem cells. Curr Nanosci 12(1): 47–62

Katti KK, Kattumuri V, Bhaskaran S et al (2009) Facile and general method for synthesis of sugar coated gold nanoparticles. Int J Green Nanotechnol Biomed 1(1):B53–B59. doi:10.1080/19430850902983848

Kawasaki H, Yamamoto H, Fujimori H et al (2010) Stability of the DMF-protected Au nanoclusters: photochemical, dispersion, and thermal properties. Langmuir 26(8):5926–5933. doi:10.1021/la9038842

Kawasaki H, Hamaguchi K, Osaka I et al (2011a) PH-dependent synthesis of pepsin-mediated gold nanoclusters with blue green and red fluorescent emission. Adv Funct Mater 21(18):3508–3515. doi:10.1002/adfm.201100886

Kawasaki H, Yoshimura K, Hamaguchi K et al (2011b) Trypsin-stabilized fluorescent gold nanocluster for sensitive and selective Hg_2+ detection. Anal Sci 27(6):591–596

Kelderhouse LE, Chelvam V, Wayua C et al (2013) Development of tumor-targeted near infrared probes for fluorescence guided surgery. Bioconjug Chem 24(6):1075–1080. doi:10.1021/bc400131a

Kennedy TAC, MacLean JL, Liu J et al (2012) Blue emitting gold nanoclusters templated by poly-cytosine DNA at low pH and poly-adenine DNA at neutral pH. Chem Commun 48 (54):6845–6847

Kim C, Cho EC, Chen J et al (2010) In vivo molecular photoacoustic tomography of melanomas targeted by bioconjugated gold nanocages. ACS Nano 4(8):4559–4564. doi:10.1021/nn100736c

Kong Y, Chen J, Gao F, Brydson R et al (2013) Near-infrared fluorescent ribonuclease-A-encapsulated gold nanoclusters: preparation, characterization, cancer targeting and imaging. Nanoscale 5(3):1009–1017. doi:10.1039/c2nr32760k

Kreibig U, Vollmer M (1995) Optical properties of metal clusters. Springer, Berlin

Kryachko ES, Remade F (2005a) Complexes of DNA bases and gold clusters Au3 and Au4 involving nonconventional N-H…Au hydrogen bonding. Nano Lett 5(4):735–739. doi:10.1021/nl050194m

Kryachko ES, Remade F (2005b) Complexes of DNA bases and Watson-Crick base pairs with small neutral gold clusters. J Phys Chem B 109(48):22746–22757

La Bean TH, Li HY et al (2007) Constructing novel materials with DNA. Nano Today 2(2):26–35. doi:10.1016/S1748-0132(07)70056-7

Lal S, Clarell SE, Halas NJ et al (2008) Nanoshell-enabled photothermal cancer therapy: impending clinical impact. Acc Chem Res 41(12):1842–1851. doi:10.1021/ar800150g

Larson TA, Bankson J, Aaron J et al (2007) Hybrid plasmonic magnetic nanoparticles as molecular specific agents for MRI/optical imaging and photothermal therapy of cancer cells. Nanotechnology 18(32):325101

Le GX, Daum N, Schneider (2011) Synthesis and characterization of human transferin-stabilized gold nanoclusters. Nanotechnology 22(27):275103. doi:10.1088/0957-4484/22/27/275103

Lee D, Donkers RL, Wang G et al (2004) Electrochemistry and optical absorbance and luminescence of molecule-like Au38 nanoparticles. J Am Chem Soc 126(19):6193–6199

Lee S, Kim S, Choo J et al (2007) Biological imaging of HEK293 cells expressing PLCgamma1 using surface-enhanced Raman microscopy. Anal Chem 79(3):916–922

Li PC, Wang CRC, Shieh DB et al (2008) In vivo photoacoustic molecular imaging with simultaneous multiple selective targeting using antibody-conjugated gold nanorods. Opt Express 16(23):18605–18615. doi:10.1364/OE.16.018605

Li J, Zhu J, Xu K (2014) Fluorescent metal nanoclusters: from synthesis to applications. Trends Anal Chem 58:90–98. doi:10.1016/j.trac.2014.02.011

Li CH, Kuo TR, Su HJ et al (2015a) Nanoparticles with computed tomography imaging accesses for in vivo tumor resection. Sci Rep 5:15675. doi:10.1038/srep15675

Li ZY, Wu YT, Tseng WL (2015b) UV-light-induced improvement of fluorescence quantum yield of DNA-templated gold nanoclusters: application to ratiometric fluorescent sensing of nucleic acids. ACS Appl Mater Interfaces 7(42):23708–23716. doi:10.1021/acsami.5b07766

Libutti SK, Paciotti GF, Byrnes AA et al (2010) Phase I and pharmacokinetic studies of CYT-6091, a novel PEGylated colloidal gold-rhTNF nanomedicine. Clin Cancer Res 16 (24):6139–6149

Lim YT, Cho MY, Kim JK et al (2007) Plasmonic magnetic nanostructure for bimodal imaging and photonic-based therapy of cancer cells. ChemBioChem 8(18):2204–2209. doi:10.1002/cbic.200700416

Lin YH, Tseng WL (2010) Ultrasensitive sensing of Hg^{2+} and CH_3Hg^+ based on the fluorescence quenching of lysozyme Type VI-stabilized gold nanoclusters. Anal Chem 82(22):9194–9200. doi:10.1021/ac101427y

Lin A, Lewinski N, Lee MH et al (2006) Reflectance spectroscopy of gold nanoshells: computational predictions and experimental measurements. J Nanoparticle Res 8(5):681–692

Lin CAJ, Lee CH, Hsieh JT et al (2009a) Synthesis of fluorescent metallic nanoclusters toward biomedical application: recent progress and present challenges. J Med Biol Eng 29(6):76–283

Lin CAJ, Yang TY, Lee CH et al (2009b) Synthesis, characterization, and bioconjugation of fluorescent gold nanoclusters toward biological labeling applications. ACS Nano 3(2): 395–401. doi:10.1021/nn800632j

Lin CAJ, Lee CH, Hsieh JT et al (2010) Synthesis and surface modification of highly fluorescent gold nanoclusters and their exploitation for cellular labeling. Proc SPIE 7575. doi:10.1117/12.841540

Lin H, Li L, Lei C et al (2013a) Immune-independent and label free fluorescent assay for Cystatin C detection based on protein stabilized Au nanoclusters. Biosens Bioelectron 41 (1):256–261

Lin J, Zhou Z, Li Z et al (2013b) Biomimetic one-pot synthesis of gold nanoclusters/nanoparticles for targeted tumor cellular dual-modality imaging. Nanoscale Res Lett 8(1):170. doi:10.1186/1556-276X-8-170

Link S, Beeby A, FitzGerald S et al (2002) Visible to infrared luminescence from a 28-atom gold cluster. J Phys Chem B 106(13):3410–3415. doi:10.1021/jp014259v

Liu CL, Wu HT, Hsiao YH et al (2011) Insulin-directed synthesis of fluorescent gold nanoclusters: preservation of insulin bioactivity and versatility in cell imaging. Angew Chem Int Ed 50 (31):7056–7060

Liu G, Shao Y, Ma K et al (2012a) Synthesis of DNA-templated fluorescent gold nanoclusters. Gold Bulletin 45(2):69–74. doi:10.1007/s13404-012-0049-6

Liu G, Shao Y, Wu F et al (2012b) DNA-hosted fluorescent gold nanoclusters: sequence-dependent formation. Nanotechnology 24(1):015503. doi:10.1088/0957-4484/24/1/015503

Loo C, Lowery A, Halas N et al (2005) Immunotargeted nanoshells for integrated cancer imaging and therapy. Nano Lett 5(4):709–711. doi:10.1021/nl050127s

Lu W, Zhang G, Zhang R et al (2010) Tumor site-specific silencing of NF-kappaB p65 by targeted hollow gold nanosphere-mediated photothermal transfection. Cancer Res 70:3177–3188. doi:10.1158/0008-5472

Maffeo C, Yoo J, Comer J et al (2014) Close encounters with DNA. J Phys Condense Matter 26 (41):413101. doi:10.1088/0953-8984/26/41/413101

Maltzahn GV et al (2009) Computationally guided photothermal tumor therapy using long-circulating gold nanorod antennas. Cancer Res 69:3892–3900

Marzan LML (2006) Tailoring surface plasmons through the morphology and assembly of metal nanoparticles. Langmuir 22(1):32–41. doi:10.1021/la0513353

Mayavan S, Dutta NK, Choudhury NR et al (2011) Self-organization, interfacial interaction and photophysical properties of gold nanoparticle complexes derived from resilin-mimetic fluorescent protein rec1-resilin. Biomaterials 32(11):2786–2796

McCarthy JR, Bhaumik J, Karver MR et al (2010) Targeted nanoagents for the detection of cancers. Mol Oncol 4(6):511–528

Medley CM, Smith JE, Tang Z et al (2008) Gold nanoparticle-based colorimetric assay for the direct detection of cancerous cells. Anal Chem 80:1067–1072

Michalet X, Pinaud FF, Bentolila LA et al (2005) Quantum dots for live cells, in vivo imaging and diagnostics. Science 307(5709):538–544. doi:10.1126/science.1104274

Mie G (1908) Beitra¨ge zur Optik tru¨ber Medien speziell kolloidaler Goldlo¨ sungen (contributions to the optics of diffuse media, especially colloid metal solutions). Ann Phys 25:377–445

Muhammed MAH, Ramesh S, Sinha SS et al (2008) Two distinct fluorescent quantum clusters of gold starting from metallic nanoparticles by pH-dependent ligand etching. Nano Res 1(4):333–340. doi:10.1007/s12274-008-8035-2

Muhammed MAH, Verma PK, Pal SK et al (2009) Bright, NIR-emitting Au23 from Au25: characterization and applications including biolabeling. Chem Eur J15:10110–10120. doi:10.1002/chem.200901425

Muhammed MAH, Verma PK, Pal SK et al (2010) Luminescent quantum clusters of gold in bulk by albumin-induced core etching of nanoparticles: metal ion sensing, metal-enhanced luminescence, and biolabeling. Chem Eur J 16(33):10103–10112. doi:10.1002/chem.201000841

Naik RR, Jones SE, Murray CJ et al (2004) Peptide templates for nanoparticle synthesis derived from polymerase chain reaction-driven phage display. Adv Funct Mater 14(1):25–30. doi:10.1002/adfm.200304501

Nandini S, Nalini S, Sanetuntikul J et al (2014) Development of a simple bioelectrode for the electrochemical detection of hydrogen peroxide using *Pichia pastoris* catalase immobilized on gold nanoparticle nanotubes and polythiophene hybrid. Analyst 139(22):5800–5812

Nandini S, Nalini S, Madhusudana Reddy MB et al (2016a) Synthesis of one-dimensional gold nanostructures and the electrochemical application of the nanohybrid containing functionalized graphene oxide for cholesterol biosensing. Bioelectrochem 110:79–90

Nandini S, Nalini S, Madhusudana Reddy MB et al (2016b) A novel bioassay based biosensor-credible to abet preclinical evaluation of anticancer properties developed by gold nanoribbons. RSC Adv 6:60693–60703. doi:10.1039/C6RA07501K

Nguyen QT, Tsien RY (2013) Fluorescence-guided surgery with live molecular navigation—a new cutting edge. Nat Rev Cancer 13:653–662. doi:10.1038/nrc3566

O'Neal DP, Hirsch LR, Halas NJ et al (2004) Photo-thermal tumor ablation in mice using near infrared-absorbing nanoparticles. Cancer Lett 209(2):171–176

Paciotti GF, Myer L, Weinreich D et al (2004) Colloidal gold: a novel nanoparticle vector for tumor directed drug delivery. Drug Deliv 11(3):169–183

Peer D, Karp JM, Hong S et al (2007) Nanocarriers as an emerging platform for cancer therapy. Nat Nanotechnol 2:751–760. doi:10.1038/nnano.2007.387

Plascencia-Villa G, Torrente D, Marucho M et al (2015) Biodirected synthesis and nanostructural characterization of anisotropic gold nanoparticles. Langmuir 31:3527–3536. doi:10.1021/acs.langmuir.5b00084

Polavarapu L, Manna M, Xu QH (2011) Biocompatible glutathione capped gold clusters as one- and two-photon excitation fluorescence contrast agents for live cells imaging. Nanoscale 3:429–434. doi:10.1039/C0NR00458H

Popovtzer R, Agrawal A, Kotov NA et al (2008) Targeted gold nanoparticles enable molecular CT imaging of cancer. Nano Lett 8:4593–4596. doi:10.1021/nl8029114

Prakash M, Shetty MS, Tilak P et al (2009) Total thiols: biomedical importance and their alteration in various disorders. Online J Health Allied Scs 8(2):2

Pricker SP (1996) Medical uses of gold compounds: past, present and future. Gold Bull 29(2): 53–60

Qian X, Peng XH, Ansari DO et al (2008) In vivo tumor targeting and spectroscopic detection with surface-enhanced Raman nanoparticle tags. Nature Biotechnol 26:83–90. doi:10.1038/nbt1377

Qian H, Zhu Y, Jin R (2009) Size-Focusing synthesis, optical and electrochemical properties of monodisperse Au38(SC2H4Ph)24 nanoclusters. ACS Nano 3(11):3795–3803. doi:10.1021/nn901137h

Qiao J, Mu X, Qi L et al (2013) Folic acid-functionalized fluorescent gold nanoclusters with polymers as linkers for cancer cell imaging. Chem Commun 49:8030–8032. doi:10.1039/C3CC44256J

Qu X, Li Y, Li L et al (2015) Fluorescent gold nanoclusters: synthesis and recent biological application. J Nanomater 2015:4. doi:10.1155/2015/784097

Quinn BM, Liljeroth P, Ruiz V et al (2003) Electro chemical resolution of 15 oxidation states for monolayer protected gold nanoparticles. J Am Chem Soc 125(22):6644–6645

Retnakumari R, Jayasimhan J, Chandran P et al (2011) CD33 monoclonal antibody conjugated Au cluster nano-bioprobe for targeted flow-cytometric detection of acute myeloid leukaemia. Nanotechnology 22(28):285102

Roco MC (2003) Nanotechnology: convergence with modern biology and medicine. Curr Opin Biotechnol 14(3):337–346

Roy S, Baral A, Bhattacharjee R et al (2015) Preparation of multi-coloured different sized fluorescent gold clusters from blue to NIR, structural analysis of the blue emitting Au7 cluster, and cell-imaging by the NIR gold cluster. Nanoscale 7:1912–1920. doi:10.1039/C4NR04338C

Sahoo AK, Banerjee S, Ghosh SS et al (2014) Simultaneous RGB emitting Au nanoclusters in chitosan nanoparticles for anticancer gene theranostics. ACS Appl Mater Interfaces 6(1):712–724. doi:10.1021/am4051266

Saravanakumar G, Kim K, Park JH et al (2009) Current status of nanoparticle-based imaging agents for early diagnosis of cancer and atherosclerosis. J Biomed Nanotechnol 5(1):20–35

Sardar R, Funston AM, Mulvaney P et al (2009) Gold nanoparticles: past, present, and future. Langmuir 25:13840–13851

Sauerbeck C, Haderlein M, Schurer B et al (2014) Shedding light on the growth of gold nanoshells. ACS Nano 8(3):3088–3096

Schaaff TG, Shafigullin MN, Khoury JT et al (1997) Isolation of smaller nanocrystal Au molecules: robust quantum effects in optical spectra. J Phys Chem B 101:7885–7891

Sekhon BS (2014) Nanotechnology in agri-food production: an overview. Nanotechnol Sci Appl 7:31–53. doi:10.2147/NSA.S39406

Selvaprakash K, Chen YC (2014) Using protein-encapsulated gold nanoclusters as photoluminescent sensing probes for biomolecules. Biosens Bioelectron 61:88–94. doi:10.1016/j.bios.2014.04.055

Shan J, Tenhu H (2007) Recent advances in polymer protected gold nanoparticles: synthesis, properties and applications. Chem Commun 44:4580–4598

Shang L, Dong SJ, Nienhaus GU (2011a) Ultra-small fluorescent metal nanoclusters: synthesis and biological applications. Nano Today 6(4):401–418

Shang L, Dörlich RM, Brandholt S et al (2011b) Facile preparation of water-soluble fluorescent gold nanoclusters for cellular imaging applications. Nanoscale 3(5):2009–2014. doi:10.1039/c0nr00947d

Shervani Z, Yamamoto Y (2011) Carbohydrate-directed synthesis of silver and gold nanoparticles: effect of the structure of carbohydrates and reducing agents on the size and morphology of the composites. Carbohydr Res 346(5):651–658. doi:10.1016/j.carres.2011.01.020

Shi X, Ganser TR, Sun K et al (2006) Characterization of crystalline dendrimer-stabilized gold nanoparticles. Nanotechnology 17:1072–1078. doi:10.1088/0957-4484/17/4/038

Shibu ES, Pradeep T (2011) Quantum clusters in cavities: trapped Au15 in cyclodextrins. Chem Mater 23(4):989–999. doi:10.1021/cm102743y

Shibu ES, Radha B, Verma PK et al (2009) Functionalized Au22 clusters: synthesis, characterization, and patterning. ACS Appl Mater Interfaces 1(10):2199–2210. doi:10.1021/am900350r

Shichibu Y, Negishi Y, Tsunoyama H et al (2007) Extremely high stability of glutathionate-protected Au 25 clusters against core etching. Small 3(5):835–839

Shukla MK, Dubey M, Zakar E et al (2009) DFT investigation of the interaction of gold nanoclusters with nucleic acid base guanine and the Watson-Crick guanine-cytosine base pair. J Phys Chem C 113(10):3960–3966

Sivasubramanian M, Hsia Y, Lo LW (2014) Nanoparticle-facilitated functional and molecular imaging for the early detection of cancer. Front Mol Biosci 1:15. doi:10.3389/fmolb.2014.00015

Smith AM, Dave S, Nie SM et al (2006) Multicolor quantum dots for molecular diagnostics of cancer. Expert Rev Mol Diagn 6(2):231–244

Sokolov K, Follen M, Aaron J et al (2003) Real-time vital optical imaging of precancer using anti-epidermal growth factor receptor antibodies conjugated to gold nanoparticles. Cancer Res 63:1999–2004

Song J, Zhou J, Duan H (2012) Self-assembled plasmonic vesicles of SERS-encoded amphiphilic gold nanoparticles for cancer cell targeting and traceable intracellular drug delivery. J Am Chem Soc 134(32):13458–13469

Song JT, Yang XQ, Zhang XS et al (2015) Facile synthesis of gold nanospheres modified by positively charged mesoporous silica, loaded with near-infrared fluorescent dye, for in vivo X-ray computed tomography and fluorescence dual mode imaging. ACS Appl Mater Interfaces 7:17287–17297. doi:10.1021/acsami.5b04359

Srinivasan M, Rajabi M, Mousa SA (2015) Multifunctional nanomaterials and their applications in drug delivery and cancer therapy. Nanomaterials 5(4):1690–1703

Stern JM, Stanfield J, Kabbani W et al (2008) Selective prostate cancer thermal ablation with laser activated gold nanoshells. J Urol 179(2):748–753

Takahashi H, Niidome T, Nariai A et al (2006) Gold nanorod-sensitized cell death: microscopic observation of single living cells irradiated by pulsed near-infrared laser light in the presence of gold nanorods. Chem Lett 35(5):500–501

Tan YN, Lee JY, Wang DIC (2010) Uncovering the design rules for peptide synthesis of metal nanoparticles. J Am Chem Soc 132(16):5677–5686. doi:10.1021/ja907454f

Tao Y, Lin Y, Ren J et al (2013) A dual fluorometric and colorimetric sensor for dopamine based on BSA-stabilized Au nanoclusters. Biosens Bioelectron 42(1):41–46

Thygesen MB, Jensen KJ (2015) Carbohydrate-modified gold nanoparticles. In: Stine KJ (ed) Carbohydrate nanotechnology. Wiley, Hoboken, NJ

Triulzi RC, Micic M, Giordani S et al (2006) Immunoassay based on the antibody-conjugated PAMAM-dendrimer-gold quantum dot complex. Chem Commun 48:5068–5070

Tsoi KM, Dai Q, Alman BA et al (2013) Are quantum dots toxic? Exploring the discrepancy between cell culture and animal studies. Acc Chem Res 46(3):662–671

Tu X, Chen W, Guo X (2011) Facile one-pot synthesis of near infrared luminescent gold nanoparticles for sensing copper (II). Nanotechnology 22(9):095701. doi:10.1088/0957-4484/22/9/095701

Vankayala R, Kuo CL, Nuthalapati K et al (2015) Nucleus-targeting gold nanoclusters for simultaneous in vivo fluorescence imaging, gene delivery, and NIR-light activated photodynamic therapy. Adv Funct Mater 25(37):5934–5945. doi:10.1002/adfm.201502650

Visaria R, Griffin R, Williams B et al (2006) Enhancement of tumor thermal therapy using gold nanoparticle assisted tumor necrosis factor-alpha delivery. Mol Cancer Ther 5(4):1014–1020

Wang G, Huang T, Murray RW et al (2005) Near-IR luminescence of monolayer-protected metal clusters. J Am Chem Soc 127(3):812–813

Wang HH, Lin CAJ, Lee CH et al (2011a) Fluorescent gold nanoclusters as a biocompatible marker for in vitro and in vivo tracking of endothelial cells. ACS Nano 5(6):4337–4344. doi:10.1021/nn102752a

Wang Y, Chen J, Irudayaraj J et al (2011b) Nuclear targeting dynamics of gold nanoclusters for enhanced therapy of HER2þ breast cancer. ACS Nano 5(12):9718–9725

Wang J, Zhang G, Li Q et al (2013) In vivo self-bio-imaging of tumors through in situ biosynthesized fluorescent gold nanoclusters. Sci Rep 3:1157. doi:10.1038/srep01157

Wang YQ, Zhao T, He XW et al (2014) A novel core-satellite CdTe/Silica/Au NCs hybrid sphere as dual-emission ratiometric fluorescent probe for Cu^{2+}. Biosens Bioelectron 51:40–46. doi:10.1016/j.bios.2013.07.028

Wei H, Wang Z, Yang L et al (2010) Lysozyme stabilized gold fluorescent cluster: synthesis and application as Hg2+ sensor. Analyst 135:1406–1410. doi:10.1039/C0AN00046A

Wei H, Wang Z, Zhang J et al (2011) Time dependent, protein-directed growth of gold nanoparticles within a single crystal of lysozyme. Nat Nanotechnol 6:93–97. doi:10.1038/nnano.2010.280

Weissleder R (2002) Scaling down imaging: molecular mapping of cancer in mice. Nat Rev Cancer 2(1):11–18

Wen F, Dong Y, Feng L et al (2011) Horseradish peroxidase functionalized fluorescent gold nanoclusters for hydrogen peroxide sensing. Anal Chem 83(4):1193–1196

Wen Q, Gu Y, Tang LJ et al (2013) Peptide-templated gold nanocluster beacon as a sensitive, label-free sensor for protein posttranslational modification enzymes. Anal Chem 85 (24):11681–11685. doi:10.1021/ac403308b

West AL, Griep MH, Cole DP et al (2014) DNase 1 retains endodeoxyribonuclease activity following gold nanocluster synthesis. Anal Chem 86(15):7377–7382. doi:10.1021/ac5005794

Wilcoxon JP, Martin JE, Parsapour F et al (1998) Photoluminescence from nano size gold clusters. J Chem Phys 108(21):9137–9143

Wu Z, Jin R (2010) On the ligand's role in the fluorescence of gold nanoclusters. Nano Lett 10 (7):2568–2573

Wu X, He X, Wang K et al (2010) Ultrasmall near-infrared gold nanoclusters for tumor fluorescence imaging in vivo. Nanoscale 2:2244–2249. doi:10.1039/C0NR00359J

Xavier PL, Chaudhari K, Verma PK et al (2010) Luminescent quantum clusters of gold in transferrin family protein, lactoferrin exhibiting FRET. Nanoscale 2(12):2769–2776. doi:10.1039/c0nr00377h

Xiao Y, Hong H, Javadi A et al (2012) Gold nanorods conjugated with doxorubicin and cRGD for combined anticancer drug delivery and PET imaging. Theranostics 2(8):757–768

Xie J, Lee JY, Wang DIC et al (2007) Silver nanoplates: from biological to biomimetic synthesis. ACS Nano 1(5):429–439

Xie J, Zheng Y, Ying JY (2009) Protein-directed synthesis of highly fluorescent gold nanoclusters. J Am Chem Soc 131(3):888–889

Xie J, Zheng Y, Ying JY (2010) Highly selective and ultrasensitive detection of Hg^{2+} based on fluorescence quenching of Au nanoclusters by Hg^{2+}–Au^{+} interactions. Chem Commun 46:961–963. doi:10.1039/B920748A

Xu HX, Suslick KS (2010) Water-soluble fluorescent silver nanoclusters. Adv Mater 22(10): 1078–1082

Yabu H (2011) One-pot synthesis of blue light-emitting Au nanoclusters and formation of photo-patternable composite films. Chem Commun 47(4):1196–1197. doi:10.1039/c0cc03539d

Yang X, Stein EW, Ashkenazi S et al (2009) Nanoparticles for photoacoustic imaging. WIREs Nanomed Nanobiotechnol 1:360–368. doi:10.1002/wnan.42

Yang QF, Liu JY, Chen HP et al (2011a) Preparation of noble metallic nanoclusters and its application in biological detection. Prog Chem 23(5):880–892

Yang X, Shi M, Zhou R et al (2011b) Blending of HAuCl4 and histidine in aqueous solution: a simple approach to the Au10 cluster. Nanoscale 3(6):2596–2601. doi:10.1039/c1nr10287g

Yang X, Luo Y, Zhuo Y et al (2014) Novel synthesis of gold nanoclusters templated with L-tyrosine for selective analyzing tyrosinase. Anal Chim Acta 840:87–92. doi:10.1016/j.aca.2014.05.050

You J, Zhang G, Li C (2010) Exceptionally high payload of doxorubicin in hollow gold nanospheres for near-infrared light-triggered drug release. ACS Nano 4(2):1033–1041

You J, Zhang R, Zhan G et al (2012) Photothermal-chemotherapy with doxorubicin-loaded hollow gold nanospheres: a platform for near-infrared light-trigged drug release. J Control Release 158 (2):319–328

Yu M, Zhou C, Liu J et al (2011) Luminescent gold nanoparticles with pH-dependent membrane adsorption. J Am Chem Soc 133(29):11014–11017. doi:10.1021/ja201930p

Yu MK, Park J, Jon S (2012) Targeting strategies for multifunctional nanoparticles in cancer imaging and therapy. Theranostics 2(1):3–44

Zamboni WC, Torchilin V, Patri A et al (2012) Best practices in cancer nanotechnology: perspective from NCI nanotechnology alliance. Clin Cancer Res 18(12):3229–3241. doi:10.1158/1078-0432.CCR-11-2938

Zavaleta CL, Smith BR, Walton I et al (2009) Multiplexed imaging of surface enhanced raman scattering nanotags in living mice using noninvasive raman spectroscopy. Proc Natl Acad Sci 106(32):13511–13516. doi:10.1073/pnas.0813327106

Zhang L, Wang E (2014) Metal nanoclusters: new fluorescent probes for sensors and bioimaging. Nano Today 9(1):132–157

Zhang XD, Chen J, Luo Z et al (2013) Enhanced tumor accumulation of sub-2 nm gold nanoclusters for cancer radiation therapy. Adv Healthcare Mater 3(1):133–141

Zhang J, Yuan Y, Wang Y et al (2015) Microwave-assisted synthesis of photoluminescent glutathione-capped Au/Ag nanoclusters: a unique sensor-on-a-nanoparticle for metal ions, anions, and small molecules. Nano Res 8(7):2329–2339. doi:10.1007/s12274-015-0743-9

Zheng J (2005) Fluorescent noble metal nanoclusters. Ph D Thesis, Georgia Institute of Technology, Atlanta

Zheng J, Petty JT, Dickson RM (2003) High quantum yield blue emission from water soluble Au_8 nanodots. J Am Chem Soc 125(26):7780–7781

Zheng J, Zhang CW, Dickson RM (2004) Highly fluorescent, water-soluble, size-tunable gold quantum dots. Phys Rev Lett 93(7):077402. doi:10.1103/PhysRevLett.93.077402

Zheng J, Nicovich PR, Dickson RM (2007) Highly fluorescent noble metal quantum dots. Annu Rev Phys Chem 58(1):409–431

Zheng CF, Zheng MB, Gong P et al (2012) Indocyanine green-loaded biodegradable tumor targeting nanoprobes for in vitro and in vivo imaging. Biomaterials 33(22):5603–5609

Zhou Z, Zhang C, Qian Q et al (2013) Folic acid-conjugated silica capped gold nanoclusters for targeted fluorescence/X-ray computed tomography imaging. J Nanobiotechnol 11:17. doi:10.1186/1477-3155-11-17

Graphene Metal Nanoclusters in Cutting-Edge Theranostics Nanomedicine Applications

Kasturi Muthoosamy, RenuGeetha Bai and Sivakumar Manickam

Abstract The major breakthrough of graphene in 2004 has paved the way for various approaches to synthesize graphene and its derivatives for biomedical applications. With the interest in graphene as a cargo in drug delivery, the exploration has slowly shifted to metal-graphene materials as fluorescent probes. Metals such as Cu, Au, Fe, Ce and etc., have been incorporated into graphene for various applications such as sensing and imaging. With the success of graphene—metal nanoparticles (NPs), its more recently discovered counterpart, graphene—metal nanoclusters (NCs) has gained much interest lately. Loosely defined, NCs are a cluster of NPs with sizes of 1–20 nm with a narrow size distribution, which endows it with unique electronic properties compared to metal NPs. NCs are size-dependent fluorescent materials with good photostability. They have been largely investigated in biosensing, diagnosis and therapy applications, a term coined as theranostics. In more recent applications, graphene metal NCs were stabilized with protein biomarkers for targeted sensing of cancer cells and diseases. Smart delivery system allows diagnosis, imaging and targeted therapy simultaneously. This chapter focusses on the synthesis and biomedical applications of graphene—metal NCs with a detailed discussion on their properties and applications in the biomedical field. A brief description on the toxicity is addressed as well, together with future considerations for possible applications of graphene—metal NCs clinically.

Keywords Graphene · Metal nanoclusters · Theranostics · Cancer · Diagnosis · Bioimaging

K. Muthoosamy · R. Bai · S. Manickam (✉)
Nanotechnology and Advanced Materials (NATAM),
Faculty of Engineering, University of Nottingham Malaysia
Campus (UNMC), 43500 Semenyih, Selangor, Malaysia
e-mail: Sivakumar.Manickam@nottingham.edu.my

A. Tripathi and J.S. Melo (eds.), *Advances in Biomaterials for Biomedical Applications*, Advanced Structured Materials 66,
DOI 10.1007/978-981-10-3328-5_11

Abbreviations

2D	Two dimensional
3D	Three-dimensional
Ag	Silver
Au	Gold
CT	Computed tomography
CTAB	Cetyltrimethylammonium bromide
CVD	Chemical vapour deposition
D	Diffusion coefficient
DFT	Density functional theory
DOS	Density of states
Dox	Doxorubicin
Gd	Gadolinium
GO	Graphene oxide
HREELS	High-resolution electron energy loss spectrometer
HRTEM	High-resolution transmission electron microscopy
IC_{50}	Half-inhibitory concentration
IONP	Iron oxide nanoparticles
LD_{50}	Lethal dose 50%
LDH	Lactate dehydrogenase
LEED	Low energy electron diffraction
MMP	Metalloproteinase-9
Mn	Manganese
MR	Magnetic resonance
MTT	(3-(4,5-dimethylthiazol-2-yl)-2,5-diphenyltetrazolium bromide)
MUA	Mercaptoundecanoic acid
NCs	Nanoclusters
NIR	Near Infrared
NOAEL	No observed adverse effect level
NPs	Nanoparticles
PET	Positron emission tomography
PMA	Phorbol myristate acetate
PM-IRAS	Polarization modulation infrared reflection absorption spectrometer
PVP	Polyvinyl-pyrrolidone
QUAMBO	Quasi-atom minimal basis orbitals
RGO	Reduced graphene oxide
ROS	Reactive oxygen species
RT	Room temperature
STM	Scanning tunneling microscopy

TEM	Transmission electron microscopy
TOAB	Tetraoctylammonium bromide
UHV	Ultrahigh vacuum
UV	Ultra-violet
XPS	X-ray photo-electron microscopy
XRD	X-ray diffraction

1 Introduction

Nanomaterials or nanoparticles (NPs) have been widely explored by researchers for biomedical applications. Their small size (>20 nm) and unique chemical properties pave the way to further explore even smaller particles or atomic aggregates called clusters. Nanoclusters (NCs) which are generally made of metals such as Au, Ag, Pt and others are less than 20 nm in size and consist of about few to 100 atoms. At this size regime, the metal NCs become a molecular species with sizes comparable to Fermi wavelength of electrons and bridges the gap between atomic and nanoparticle behaviour. Thus, NCs display many astounding properties with respect to their bulk crystalline such as strong photoluminescence (Peyser et al. 2001; Zheng and Dickson 2002; Häkkinen et al. 2003; Peyser et al. 2001), large Stokes shift and high emission rate, optical chirality (Gautier and Bürgi 2008; Román-Velázquez et al. 2003) as well as ferromagnetism (Crespo et al. 2004), which are of both scientific interest and technological importance. These amazing properties led to many biological applications such as single molecule photonics, biological labelling and biosensing (Liu et al. 2011a). Besides these applications, metal NCs have also shown advantages in heterogeneous catalysis, energy conversion and magnetic data storage devices (Meiwes and Karl 2012; Li and Somorjai 2010). It was reported that small metals like AuNCs and PtNCs have high chemical activity due to their highly reactive corner and edge atoms with low coordination number (Valden et al. 1998; Campbell 2004; Hvolbæk et al. 2007; Tian et al. 2007; Vajda et al. 2009).

When synthesizing NCs with particle size of less than 20 nm, one of the concerns is the production in controlled size and in a reproducible manner. Thus, a suitable substrate is necessary to serve as a template for metal deposition. In this connection, graphene, the strongest two dimensional (2D) materials known with a long-ranged ordered superstructure could serve for the above purpose. In addition, graphene has excellent mechanical strength, high surface area and exceptional heat transport as well as high electrical conductivity at room temperature (RT), which makes it a perfect candidate as a substrate for metal cluster deposition (Lee et al. 2008; Seol et al. 2010; Geim 2009; Guo et al. 2010; Yoo et al. 2009; Venkateswara Rao et al. 2011). Previous studies reported graphene as a perfect support substrate for a variety of metals such as Pt, Au, Ag, Ni, Cu, and Pd (Hamada and Otani 2010;

Varykhalov et al. 2010; Xu et al. 2008a), drugs (Muthoosamy et al. 2014; Geetha Bai et al. 2015) and fluorescent labels (Peng et al. 2010; Lin et al. 2016a; Kalluru et al. 2016). Graphene and its derivatives are also reported as biocompatible, thus safe for biomedical applications (Muthoosamy et al. 2015; Liu et al. 2011b; Wang et al. 2012; Zhao et al. 2014).

Added to these, appropriately stabilized metal NCs serve as an excellent biological labelling agent. Generally colorimetric cancer cell or disease detection are prepared by various methods such as enzyme-linked immunosorbent assay (Kjeldsen et al. 1992), activity-based labelling (Edgington et al. 2009), chemoluminescence (Richard et al. 2007) and fluorescent resonance energy transfer (FRET) (Hong et al. 2014; Rodems et al. 2002). In a FRET system, organic fluorophores are used as donors and acceptors; however, organic fluorophores suffer from major limitations such as pH susceptibility, narrow absorption band that overlaps with broad emission window and photodegradation (Nguyen et al. 2015; Rodems et al. 2002; Hong et al. 2014). Hence, NCs are emerging fluorescent material with excellent optical and physical properties (Zhang and Wang 2014; Cui et al. 2014; Zheng et al. 2007; Obliosca et al. 2013; Yuan et al. 2014) that avoids the limitations faced by common fluorophores.

Generally, the luminescence of metal NCs is due to the electronic transition between the highest occupied orbital and the lowest occupied orbital (HOMO-LUMO) as well as the electron transitions between the occupied "d" bands and states above the Fermi level, such as the sp bands (Fig. 1) (Lu and Chen 2012). Comparatively, bulk materials emit weak luminescence due to the absence of energy gap and nonradiative decay (Zheng et al. 2007), while in metal NPs, luminescent properties are highly dependent on surface plasmon resonance due to collective oscillation of conduction electrons when it interacts in the visible light (Díez and Ras 2011). However, in metal NCs, upon exposure to visible light, electron transition between energy levels takes place which results in strong absorption in the range of 400–1000 nm, shifting to longer wavelengths compared to NPs, hence inspiring further explorations for various biomedical applications (Zhang and Wang 2014; Zhu et al. 2008).

There are many excellent reviews reporting on the synthesis of metal NCs with a wide focus area (Wilcoxon and Abrams 2006; Fang et al. 2016; Choi et al. 2012; Latorre and Somoza 2012). In this chapter, an overview on the synthesis of metal NCs focusing on graphene based particles are provided. Although this is an emerging field, the fundamental concept and theory of metal NCs synthesis which dates back to decades ago are briefly discussed. Graphene-based metal NCs synthesis which are slowly gaining momentum in the application sector, especially for biosensing and theranostics applications are discussed extensively. Theranostics is a recent biomedical field that combines modalities of therapeutics and diagnostics (Modugno et al. 2015; Orecchioni et al. 2015; Mokdad et al. 2015; Ma et al. 2016; Tao et al. 2015). Toxicology concerns and future prospects of using graphene and its derivatives in the biomedical field conclude this chapter.

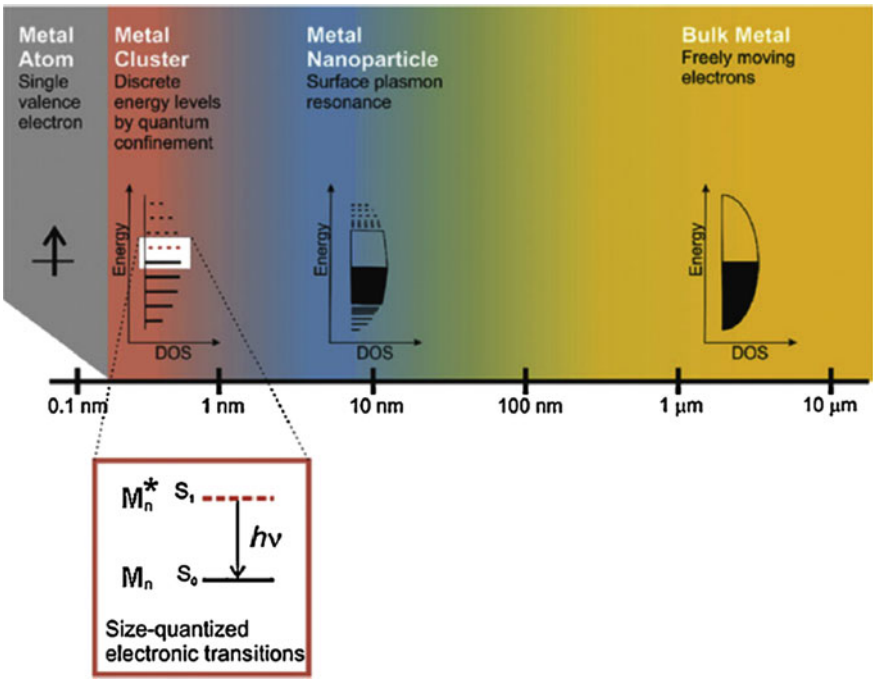

Fig. 1 Size related effects and the respective band energy in metals. Bulk metals have freely moving electrons whereas in metal NPs the band energy is dependent on surface plasmon resonance. In metal NCs, discrete energy levels exist, which allow interaction with light by electronic transitions between energy levels. Metal nanoclusters bridge the gap between single atoms and NPs. Reprinted with permission from Zhang and Wang (2014)

2 Introduction to Synthesis of Metal NCs

Generally, there are two design strategies to synthesize metal NCs, either by top-down approach or bottom-up approach. In a top-down approach, various lithographic methods are involved by working from macroscopic to nanoscopic levels. Whereas in the latter, self-assembly of metal atoms takes place on the surface of large structures. The bottom-up approach will allow fast processing time and scalable for mass production (Dupas and Lahmani 2007; Dupraz et al. 2003; Ndlovu et al. 2012).

One of the earlier methods for growing metal NCs on graphene is via the growth of NCs on a graphene/metal Moiré pattern. This type of fabrication would allow equally sized clusters to be arranged in a regular array on a flat large-scale substrate (N'Diaye et al. 2006). In addition, the graphene/metal Moiré superlattice was found to be versatile, whereby various transitional metals could be grown, did not suffer from uncovered substrate patches, was continuous and had high thermal stability (N'Diaye et al. 2009). These astounding properties are useful for coherent response

especially for applications warranting superior catalytic and magnetic properties (Weiss et al. 2005; Boyen et al. 2002; Talapin and Murray 2005).

The substrate or Moiré template is initially prepared by depositing graphene on a metal surface by thermal annealing a metal crystal such as Ru, Rh, Ir, Cu, etc. The reason for using a metal surface to grow the graphene is to overcome many shortcomings found in the initial researches: (1) graphene prepared by cleavage of highly oriented pyrolytic graphite (HOPG) suffers from uncontrollable size and spatial distribution of metal NCs (Clark and Kesmodel 1993; Whelan and Barnes 1997), and (2) graphene formed on SiC surface has structural defects (Pan et al. 2007a). Moreover, the graphene Moiré template was found to be thermally and chemically stable; homogeneous, thus forms well dispersed metal NCs and simplifies the determination of nucleation site; and unreactive, making determination of interaction between metal clusters and support much easier (Xu et al. 2011; Zhang et al. 2009a; Zhou et al. 2010).

In a typical Moiré structure, to attain periodicity and to form long–range and continuous pattern, moieties of C are either properly or improperly aligned with underlying metal atoms. Various transition metals such as Ir(111), Rh(111), Ru(0001) and Pt(111) have been exploited as the candidates for templated growth of metal nanoclusters. In this design, the C atoms which are bonded with the metal substrate become locally reactive and turn into a nucleation site for second deposited metal, thus forming NCs (Xu et al. 2011).

In this section, the fundamental theory behind the interaction of metals NCs and graphene is briefly discussed. Some of the experimental description is also provided for ease of understanding for subsequent sections. Due to the wide variety of synthesis approaches, preparation techniques are segmented based on the type of graphene Moiré templates used for metal NCs growth. Other conventional synthesis approaches are discussed as well such as using HOPG and SiC as substrate. More recent synthesis techniques are included based on simple chemical reduction of metal salts using both harsh and mild reducing agents.

3 Theory—Interaction Between Metal NCs and Graphene

Different metals (transitional metals, rare earth metals or noble metals) display unique growth morphology on graphene due to different bonding and interaction strength between the metal and graphene (Liu et al. 2013a). The interaction of metal NCs with the substrate should be weaker than in the epitaxial system. However, the interaction should be strong enough to maintain mechanical bonding required for surface analysis (Ndlovu et al. 2012). Density functional theory (DFT) has been extensively used to determine the first-principle calculations to study the adsorption properties of various metals and graphene (Ivanovskaya et al. 2010; Wehling et al. 2009; Wang et al. 2011b; Khomyakov et al. 2009). First-principle theory combined

with quasi-atom minimal basis orbitals (QUAMBO) scheme has been used to comprehend the growth behaviour of NCs on graphene (Chan et al. 2007; Qian et al. 2008; Yao et al. 2010). In addition, first-principle theory combined with Mulliken charge analysis has also been used to evaluate the electron transfer between graphene and metal NCs (Liu et al. 2010, 2011d, 2012a, 2012b; Binz et al. 2012; Hupalo et al. 2011a, b; Yao et al. 2010).

4 Experimental

4.1 Scanning Tunneling Microscopy (STM)

STM is often used in metal deposition studies to examine the growth morphology of the metals such as NC island shape, density (number of atoms) at various deposition rate (based on monolayer or ML values) and coverage. Commonly, surface coverage is given in ML, where 1 ML corresponds to surface atomic density of the metal such as Ru(0001). STM is also used to determine NC island dimensionality; either two-dimensional (2D) or three-dimensional (3D). In addition, the deposition temperature can also be determined by STM, which is imperative to evaluate the sintering effects of the metals. STM also allows direct imaging of the deposition, to gauge whether islands or films are grown at the various parameters as well as to determine whether the NC islands appear as crystalline or amorphous (Liu et al. 2013a).

4.2 Quantum Yield Measurement

Generally, the quantum yield (QY) of synthesized metal NCs are measured in reference to Rhodamine G6 in ethanol. Initially, a concentration series of Rhodamine G6 and test samples are prepared followed by determination of their absorption and fluorescence. The excitation wavelength is kept as 400 nm with optical density <0.1. QY is then determined using the following formula:

$$QY_s = I_s/I_r \times A_r/A_s \times n_s^2/n_r^2 \times QY_r$$

where s and r stand for sample and reference, respectively. I is the integral area under the fluorescence spectrum, A is the absorbance at a particular excitation wavelength, n is the refractive index of the solvent used and QY_r is fluorescence quantum yield of reference (0.95) (Nguyen et al. 2015; Dong et al. 2010).

5 Metals NCs Grown on Metal-Graphene Moiré Structure

5.1 Graphene Ir(111) Moiré Template

One of the pioneers in growing metal NCs on a graphene Moiré template dates back to 2006. N'Daiye and co-workers deposited Ir clusters by vapour phase deposition on graphene Moiré on Ir(111) lattice (N'Diaye et al. 2006). Briefly, ethylene was adsorbed on the Ir(111) surface at RT, forming a layer of ethylidyne (Zhang et al. 2009b). At elevated temperature ethylidyne was thermally decomposed in an ultrahigh vacuum (UHV) chamber, leaving behind only carbon atoms on the surface of the template. Upon annealing the surface at high temperature, large graphene flakes were formed on Ir(111) surface (Fig. 2). Graphene can also be grown on the Ir(111) substrate via chemical vapour deposition (CVD) technique. It was

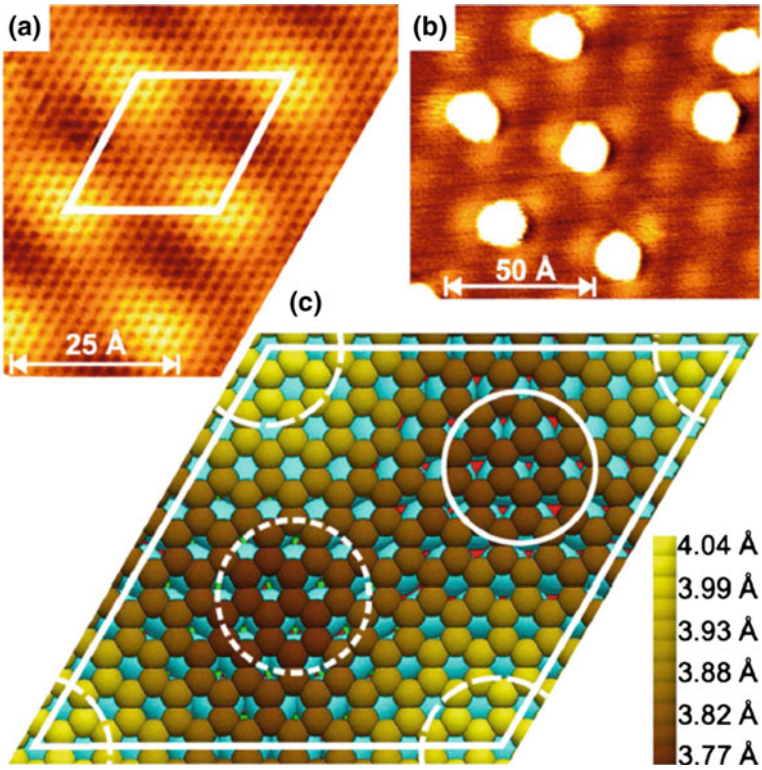

Fig. 2 **a** STM topograph of graphene on Ir(111) surface, which indicates a rhombic Moire' unit cell, **b** STM topography after deposition of 0.02 ML Ir on graphene at 350 K and **c** schematic illustration of the DFT optimized C(10 × 10)/Ir(9 × 9) unit cell. Shading of the C atoms corresponds to their heights as calculated by DFT. 1st, 2nd and 3rd layer Ir atoms are colored as *cyan*, *red* and *green*. Hcp-type region: *full circle*, fcc-type region: *short-dashed circle*, reprinted with permission (N'Diaye et al. 2006)

found that this method of deposition ensures full coverage of the substrate and avoids surface defect (Coraux et al. 2008, 2009).

Subsequently, Ir atoms were deposited by evaporation of Ir wire. The researchers found that Ir clusters have strong bonding to hcp- and fcc- regions of the graphene Moiré with average cluster size of 3.1 atomic layers with cluster height of 2.2 Å (N'Diaye et al. 2006). In addition, the Ir cluster superlattice showed high thermal stability of up to 600 K without sintering effects (N'Diaye et al. 2009). Feibelman (2008) investigated further on how the graphene displays strong attachment towards the Ir template. Local density approximation (LDA) measured by him showed that local rehybridization of C-C bonds from sp^2 to sp^3 takes place, resulting in binding of IrNCs to the graphene which simultaneously pins the graphene Moiré to the Ir substrate.

W forms a perfect NC superlattice with an average height of 6 Å on a graphene/Ir(111) surface. However, the cluster deviates from a perfect hexagonal superlattice, when compared with Pt and IrNCs (N'Diaye et al. 2009). As for Re, which has high cohesive energy of 8.03 eV, only partial order of cluster was obtained due to early coalescence and cluster rearrangements. On the other hand, for other metals such as Fe, Au and Ni, no defined shape or superlattice was formed which is mainly due to small cohesive energy: 4.28, 3.81 and 4.44 eV, respectively. In addition, these metals have low valence d-orbital radius, making binding of the metals to graphene weak and unable to stabilize the cluster growth (N'Diaye et al. 2009).

In a study by Cavallin and co-workers, Rh atoms were deposited on graphene/Ir (111) Moiré template at 90 K (Cavallin et al. 2012). Thermal annealing was investigated at 3 different temperatures: 170, 300 and 840 K. Regular and ordered single-atomic layer clusters were formed at 170 K, in contrast to preferential nucleation site observed by other researchers (Feibelman 2008; N'Diaye et al. 2008). In addition, large aggregates were found only at the step edges. At slightly higher temperature of 300 K, the clusters gained mobility and decreased cluster density was observed. Similar to Ir clusters on graphene/Ir(111) Moiré (Gerber et al. 2009), Rh cluster diffusion and coalescence were taking place at high temperature. At 840 K, the periodicity of the Moiré lattice was lost and larger clusters were formed with three-atomic layers (Cavallin et al. 2012).

PtNCs were also deposited at the hcp-site of a graphene/Ir(111) surface (Van Gastel et al. 2009). The effect of sintering upon CO gas adsorption on PtNCs arrays on graphene/Ir(111) Moiré template was investigated (Gerber et al. 2013). When sintering takes place, clusters are disrupted from their array arrangements and become a mobile metal reactant. This unfavourable effect decreases particle number in a cluster, thus increases the particle size, causes mass transport and ripening which consequently degrades their property as a catalyst (Sehested et al. 2004; Berko et al. 2004). The above groups found that upon CO exposure, small clusters (<10 atoms) detach from the graphene Moiré substrate and become mobile, whereas larger clusters remain intact and become more of 3D-like. Sintering was found to take place via Smoluchowski ripening that involve diffusion and coalescence of intact clusters as shown in Fig. 3, rather than Ostwald ripening, as was commonly reported (Gerber et al. 2013; Di Vece et al. 2008).

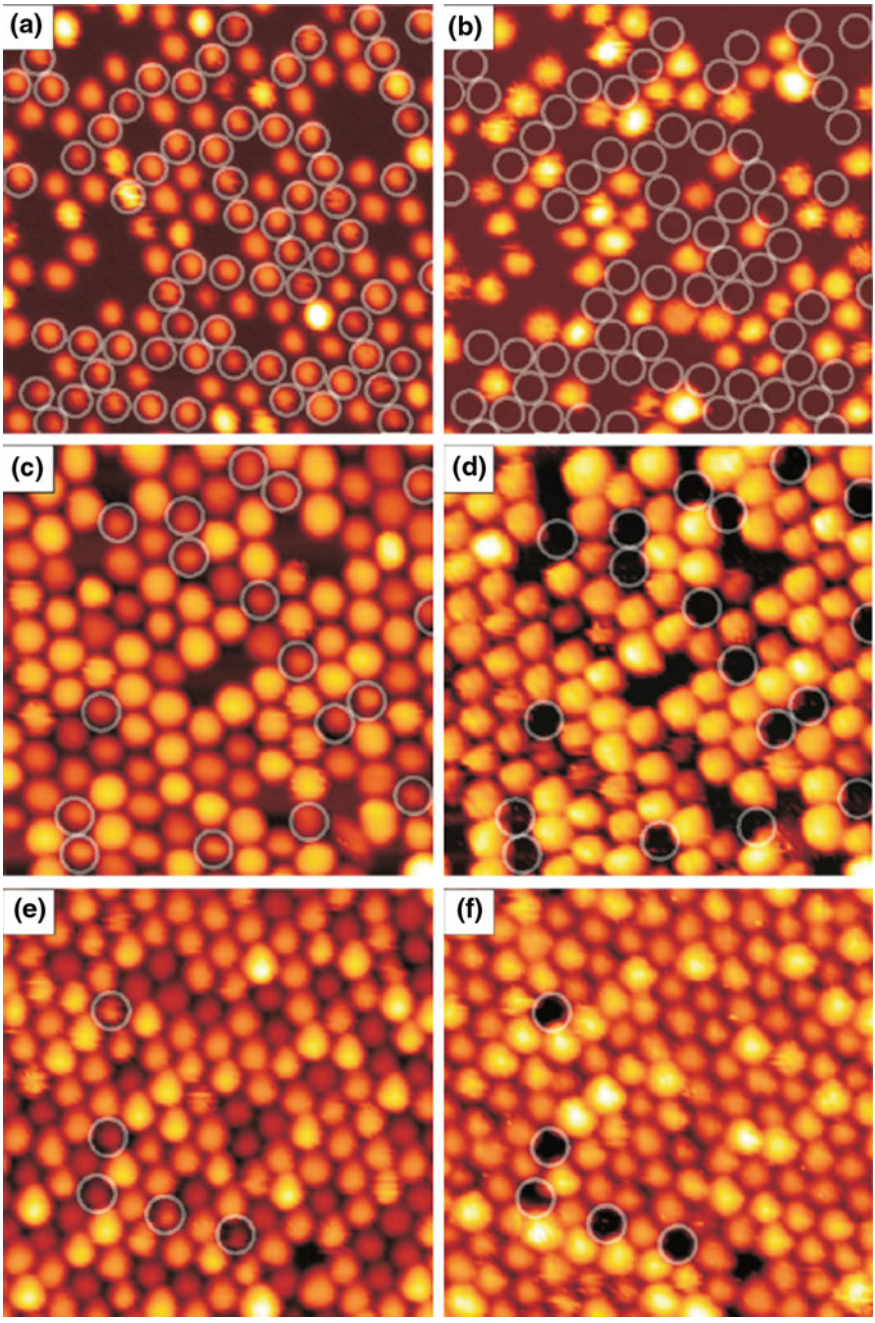

Fig. 3 STM images of PtNCs on graphene/Ir(111) after exposure to CO with **a** after 0.05 ML Pt deposition, **b** after exposure to 1.1 L CO to (**a**), **c** after 0.20 ML Pt deposition, **d** after 16 L CO exposure to (**c**), **e** after 0.44 ML Pt deposition and **f** after 20 L CO exposure to (**e**). Clusters which disappear during CO exposure and their former location are marked with circles in (**a**, **c**, **e**) and (**b**, **d**, **f**), respectively. Reprinted with permission from Gerber et al. (2013)

5.2 Graphene Ru(0001) Moiré Template

Since the graphene formed only on selective areas of the metal surface via vapour phase growth, Pan Yi and co-workers produced graphene monolayer on Ru(0001) surface by thermal annealing Ru crystals (Pan et al. 2007a). In this method, Ru (0001) crystal wafer was annealed in a UHV chamber, followed by cooling to RT and subsequently growing graphene on the Ru surface. A Moiré pattern was formed by superimposition of a monolayer of graphene on the Ru substrate forming continuous hexagonal superstructure. Generally, Moiré patterns which were discovered decades ago (Amidror and Hersch 1999) are formed by interference from rotation of two layers of any regular lattice and in this case the Moiré pattern is formed by overlapping two lattices with identical hexagonal patterns (Pong and Durkan 2005).

In another study, the same group produced a highly-ordered and continuous graphene monolayer (in the scale of millimetres) grown on Ru(0001) substrate as shown in Fig. 4 (Pan et al. 2009b). Superposition of the graphene and Ru lattice forms hexagonal Moiré pattern (Pong and Durkan 2005) with the ratio of graphene

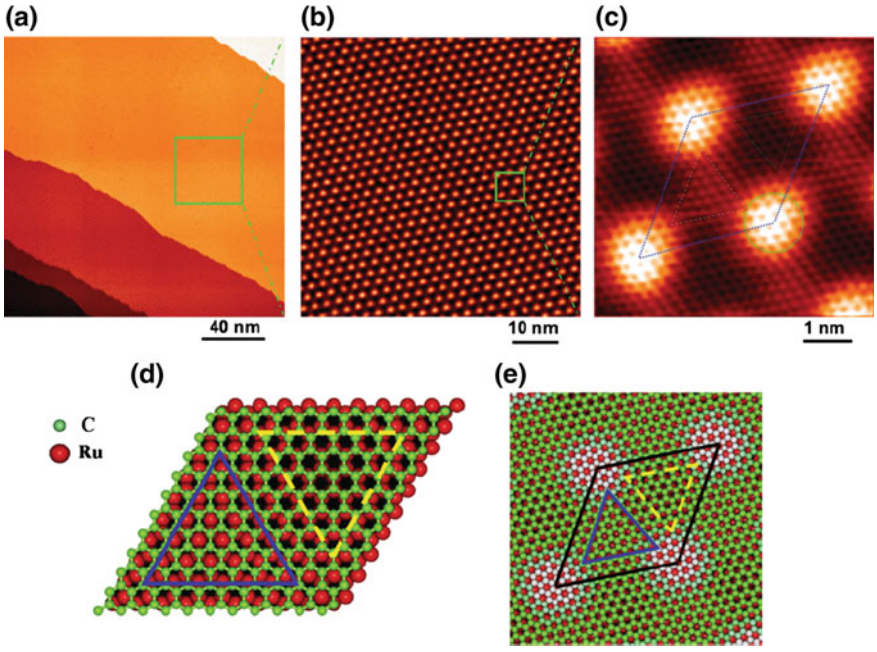

Fig. 4 **a** STM images of the atomically flat graphene layer on the Ru(0001) surface, **b** formation of the hexagonal Moire' pattern by superimposition of graphene and Ru substrate, **c** atomic resolution image of one unit cell of the Moire' pattern, **d** schematic illustration of one unit cell of the superlattice and **e** an enlarged perspective view of the graphene Moire' superlattice. Reprinted with permission from Pan et al. (2009b)

lattice constant to Ru about 12:11. Interestingly, the graphene layer formed was perfectly crystalline with no bond breakage or defects.

Similar to the technique used by N'Diaye et al. (2008), another research group fabricated PtNCs on a Ru(0001) graphene Moiré periodic template by vapour phase deposition (Zhang et al. 2009a). Briefly, single Ru(0001) crystal was pretreated by repeated Ar^+ sputtering and UHV annealing until no impurities were detected by X-ray photo-electron microscopy (XPS) and STM. Subsequently, graphene was grown on the Ru surface by using ethylene and coverage of PtNCs was controlled by the deposition time. Uniformly sized Pt clusters were produced with nucleation at fcc-sites of the graphene, compared to Ir clusters nucleating at the hcp-sites of the graphene/Ir(111) Moiré pattern (N'Diaye et al. 2006, 2008).

In another finding, PtNCs were grown on Ru(0001) graphene Moiré surface, whereby 1–4 atomic layer of clusters were formed at a unique region of the Moiré unit cell. Interestingly, the NCs remain monodispersed even with increasing Pt coverage of up to 0.36 ML. It is deduced that the Moiré pattern provides confinement to limit NCs growing laterally to preserve size uniformity without formation of islands via coalescence or coarsening (Pan et al. 2009a). In this report, the density of PtNCs deposited on graphene/Ru(0001) observed is lower than the previously reported IrNCs on graphene/Ir(111) (N'Diaye et al. 2006) due to the fact that the bond enthalpy of Ir-C is higher than the bond enthalpy of Pt-C. Thus, the diffusion coefficient (D) is larger in Pt than Ir which consequently contributed to smaller nucleation rate of PtNCs compared to IrNCs.

A similar finding was also observed by Zhou et al. (2010) whereby highly dispersed Pt clusters were formed on the fcc- site of a graphene/Ru(0001) template with a diameter of 2 nm. They also investigated on other metal clusters: Rh, Pd, Co and Au. Similar to Pt, Rh which has higher Rh-C bond dissociation energy or bond enthalpy formed highly dispersed clusters, whereas Pd and Co formed large 3D clusters with low density. Interestingly, small 2D Au clusters (0.4 nm) were formed, though the Au-C bond dissociation energy is lower than that of Rh-C. This could be due to the fact that the nearest neighbour distance of Au is 0.288 nm, which is too large to match the graphene lattice of 0.245 nm, thus making the Au to fit the underlying Ru support rather than the graphene (Van Gastel et al. 2009; N'Diaye et al. 2009).

Other uncommon metals were explored as well for cluster formation such as Ceria (CeO_2) NCs, which are known for their catalytic properties. However, the clusters grown at 330 K were found to be non-uniform as some regions were crowded, whereas others were denuded. The ceria islands display fractal-like shape in low density regions and the length dimension is generally larger (15 nm) than densely populated areas (3–6 nm). This finding is mainly due to the tendency for ceria to nucleate at the defect sites of the graphene Moiré surface (Novotny et al. 2016; Wang et al. 2016b).

In another study, Co metal was deposited on the graphene/Ru(0001) surface where hcp- and fcc- regions of the graphene Moiré have low potential energies and thus acted as nucleation centers (Liao et al. 2011). It was found that the Co clusters were loosely bound to the surface of graphene with random occupation of fcc- and

hcp-regions. This is in contrast with PtNCs grown on graphene/Ru(0001) template, whereby nucleation took place at the fcc-regions of the Moiré unit cell via self-assembly of PtNCs array. This finding is recorded due to stronger Pt–C bond compared to Co–C bond and smaller diffusion coefficient seen in Pt compared to Co (Brihuega et al. 2008). In addition, CoNCs did not form long-range ordered structures. This is similar to the findings of PtNCs deposited on the same Moiré template, where fewer and larger NCs were formed at temperature more than 190 K (Jakob et al. 1999). In addition, the CoNCs growth were in 3-D islands. In the case of Co growth was on the surface of Ru(0001) surface alone (without graphene), thick wetting layer was observed which was due to lower surface energy of Co (2.7 J cm^{-2}) compared to Ru(0001) 3.4 J cm^{-2} (Vitos et al. 1998). Besides, strain energy due to lattice mismatch between Co and Ru contributes to 3-D island growth rather than layer-by-layer growth upon further Co deposition (Ding et al. 2005).

Similarly, the surface energy of Co on graphene/Ru(0001) template is even smaller compared to Co, thus Co atoms possess mobility and thus 3D island clusters were formed (Kitakami et al. 1996; Wang et al. 2009). Added to this, the interlayer distance between graphene and Ru(0001) is around 0.145 nm, which is due to strong electronic interaction between Co and Ru (Sutter et al. 2008). As a consequence, this reduces the charge transfer from Co to graphene and thus the binding energy between graphene and Co overlayer is reduced, weakening the interaction between Co and graphene and forming small 3-D Co clusters (Yazyev and Pasquarello 2010). Interestingly, at higher temperatures, intercalation and lateral growth of Co atoms underneath graphene layer was observed (Liao et al. 2011). A similar observation was also found in Fe and NiNCs grown on graphene/Ni(111) surface, whereby the intercalation was due to intermediate destruction and subsequent reforming of graphene (Dedkov et al. 2008; Lahiri and Batzill 2010). However, in the case of Co, intercalation between graphene and Ru(0001) is suspected due to diffusion of Co atoms at defect areas such as steps and at dislocations.

Xu and co-workers used graphene/Ru(0001) Moiré structure as a template for the growth of gold (Au) NCs. Besides affecting the size of NCs formed, the choice of template affects stability, electronic properties, state of oxidation and geometric structure of Au (Xu et al. 2011). In order for better stabilization and dispersion of Au particles, strong interaction of Au with reactive oxide surfaces is necessary. However, chemically unreactive support such as carbon results in Au agglomeration (Chen and Goodman 2004, 2006b; Ketchie et al. 2007; Ma et al. 2007). Circumventing this, the researchers used graphene Moiré as a template for Au deposition. Low energy electron diffraction (LEED) pattern showed the formation of graphene overlayer on Ru(0001) as shown in Fig. 5 (Marchini et al. 2007). Based on DFT-optimized (12 × 12)-graphene/(11 × 11)-Ru(0001) model structure, the corresponding image shows bright, medium dark and dark regions, which are representative of mound-, fcc- and hcp- sites (Wang et al. 2008). The highest C atom was found at mound- region and the lowest at fcc- regions with the heights of 0.37 and 0.22 nm, respectively, which is in agreement with other previous reports (Martoccia et al. 2010; Pan et al. 2009b; Moritz et al. 2010; De Parga et al. 2008).

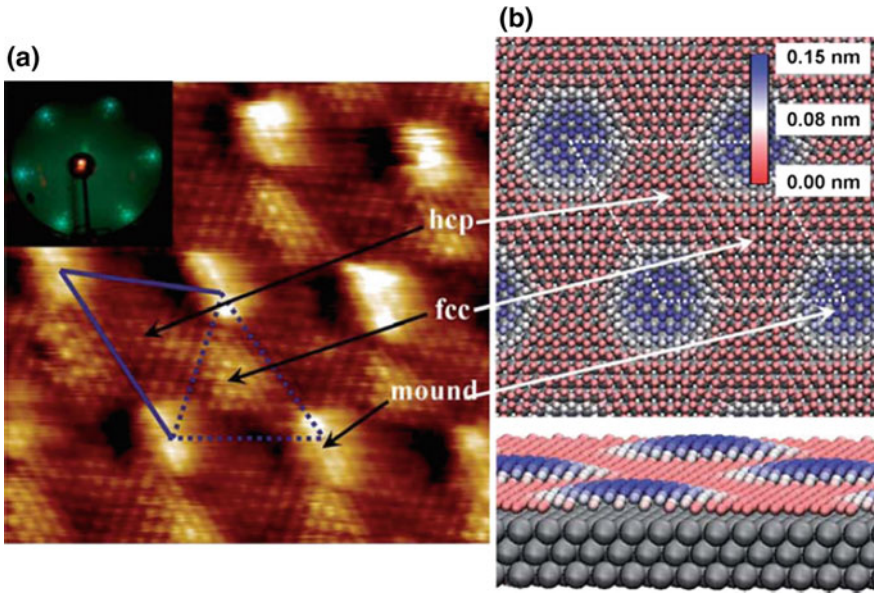

Fig. 5 **a** STM images of graphene Moiré structure on Ru(0001) and LEED pattern (*inset figure*) is displayed. **b** *Top* and *side view* of DFT-optimized (12 × 12)-graphene/(11 × 11)-Ru(0001) model structure. Hcp-, fcc- and mound-regions are indicated. Reprinted with permission from Xu et al. (2011)

Upon deposition of Au onto the graphene/Ru(0001) Moiré lattice, small 2D clusters were formed at RT, exclusively at fcc-sites. Upon further coverage, large 2D islands were formed and no intercalation between Ru and graphene layer was observed. With exposure of CO gas at 85 K, CO was found adsorbed onto the surface of AuNCs/graphene/Ru(0001), which can be titrated by O_2, showing the catalytic activity of AuNCs (Liu et al. 2011c). The same was not observed with bare graphene/Ru(0001), confirming the chemical inertness of the Moiré template. The catalytic activity was deduced due to enhanced reactant adsorption and activation by the under-coordinated Au atoms (Overbury et al. 2006; Williams et al. 2010; Lopez et al. 2004; Remediakis et al. 2005). Besides, the negative charge present on Au could also be another reason for the enhanced CO oxidation catalysis (Molina and Hammer 2005; Chen and Goodman 2006a).

A similar observation was also noted by Liu and co-workers (2011a, b, c). AuNCs are suspected to exist in a bilayer structure which is weakly adsorbed on the surface of graphene Moiré due to van der Waals energy between Au and graphene surface. However, when compared to graphene supported on SiO_2substrate, AuNCs form 3D clusters (Luo et al. 2010; Neto et al. 2009). In addition, 2D clusters were also observed in the graphene Moiré structure, which was postulated due to interactions between Au atoms and Ru(0001) through graphene (Liu et al. 2011c). The enhanced property of CO oxidation catalysis, as reported by Xu et al. (2011)

was further confirmed by the researchers using high resolution electron energy loss spectrometer (HREELS) and polarization modulation infrared reflection absorption spectrometer (PM-IRAS). Based on HREELS and PM-IRAS results, CO stretching was observed at 2095 cm^{-1} for graphene Moiré deposited with 0.5 ML Au. This suggests that the deposited Au atoms are electron rich and was supported further by DFT calculations, where electron transfer from graphene to Au was observed (Giovannetti et al. 2008; Khomyakov et al. 2009). The adsorbed CO was found reactive towards O_2 at 85 K and was due to strong adsorption of molecular oxygen. This was deduced due to the electron rich AuNCs, which can activate the O–O bond and form superoxo-like species via charge transfer from Au (Yoon et al. 2003; Liu et al. 2011c).

In another attempt, RuNCs were deposited on graphene/Ru(0001) surface with slight modifications, whereby graphene were grown on polycrystalline Ru films on SiO_2 (Sutter et al. 2012). Briefly, Ru film with the thickness of 50 nm was grown on SiO_2 substrate in a UHV system. The polycrystalline Ru films have nearly perfect (0001) surface orientation, with low roughness and average grain size of 0.5 μm. Graphene was then epitaxially grown on the surface of Ru film. RuNCs were then deposited on the graphene/Ru(0001)/SiO_2 by RF magnetron sputtering (Sutter et al. 2009a, b, 2010). Due to the growth of graphene on polycrystalline Ru, large scale single-crystalline graphene domain was produced, which covered many underlying Ru grains. In addition, different Moiré patterns with varying periodicities were formed due to misorientation of graphene and Ru lattice: 1.2, 1.7 and 2.5 nm Moiré patterns. When all 3 periodicities were compared, RuNCs deposited on 2.5 nm Moiré surface showed narrow size distribution in diameter and height. In comparison, NCs grown on 1.7 nm Moiré resulted in larger cluster sizes with no preferential nucleation site. A similar observation was also noted for 1.2 nm Moiré surface with large clusters. Graphene Moiré periodicity of 1.2 nm formed sparse ensembles of NCs, whereas in the 2.5 nm, specific nucleation site at low-fcc was observed, similar to previous findings (Sutter et al. 2011). Based on the density of states (DOS) findings, the Ru-Ru interaction energy is 2.1 eV (Wang and Bocquet 2011). For the 1.7 nm Moiré periodicity, the Ru-Ru interaction exceeds that of Ru-Graphene/Ru (−1.9 eV). Similarly, the Ru-Ru interaction equals to Ru-Graphene/Ru (−2.1 eV). Therefore, Ru adatoms tend to attach to the existing Ru islands and form large clusters. However, in a 2.5 nm Moiré pattern, the Ru-Graphene/Ru interaction (−2.5 eV) is larger than Ru-Ru interaction, and thus there is a preferential adsorption of Ru atoms to the vacant fcc- sites of the graphene domain, forming well-dispersed and small clusters (Sutter et al. 2012).

5.3 Graphene Pt(111) Moiré Template

In another study, instead of using ethylene as a source of carbon to produce graphene layer, Fujita and co-workers used benzene at elevated temperature (Fujita et al. 2005) on a Pt(111) surface. A much clearer hexagonal Moiré pattern was

observed as compared to growing graphene on Pt(111) via ethylene gas (Lang 1975). The group also observed that the graphene layer was continuous and grew beyond the step edges of Pt(111) surface, similar to those observed in Ni(111) (Rokuta et al. 1999).

5.4 *Graphene/Cu(111) Moiré Template*

With the success of graphene/Ir(111) and graphene/Ru(0001) synthesis, a group of researchers tried using Cu(111) surface as the template for the growth of graphene (Soy et al. 2015). The motive of employing Cu metal rather than the conventional but rare metals (Ir and Ru) is due to its low cost and practicality in catalyst applications. There were 4 types of different orientations produced in the Moiré superlattice: rotational angles of 7°, 3° and 12° with the heights of 2, 3 and 5.6 nm, respectively. Another rotational angle at 4° was in alignment with graphene with the height of 6.6 nm. These different types of Moiré structure are similar to previous reports (Süle et al. 2014; Gao et al. 2010) with an exception to the new rotation angle observed at 4°. The graphene domain on Cu(111) was determined as 100 nm, which is as large as noted in the previous reports (Gao et al. 2010; Martínez Galera et al. 2011). Moreover, when compared with other metal surfaces such as Ir(111) or Ru(0001), much larger graphene domain was observed in Cu(111). In addition, this graphene domain was found coherent over several terraces and step edges, which was not observed in Ir(111) (N'Diaye et al. 2008; Donner and Jakob 2009; Wintterlin and Bocquet 2009).

Pt and RhNCs were then deposited on the graphene/Cu(111) Moiré template via evaporation by a triple electron beam evaporator. From the STM topographic images, Pt was found to form brims and fingers at the Cu step edges, along with the formation of Pt-rich dendritic islands. It was deduced that intermixing of Pt and Cu takes place, forming the islands and multiple metastable states (Evans et al. 2006; Freire et al. 2014). The Pt clusters appear to grow layer-by-layer (2D), whereby the Pt atoms diffuse to certain sites of the graphene/Moiré lattice and attach to the edges of existing Pt islands. Upon reaching certain size, further addition of Pt atoms takes place on the top of the existing islands, forming 3D clusters (Brune 1998).

On the other hand, Rh diffuses to the step edges and form Rh-Cu alloy. Interestingly, it was found that Rh replace Cu below the graphene surface and the topmost layer consists mostly of Cu (Freire et al. 2014; Graham et al. 1990). An ordered array of RuNCs was observed only in graphene/Moiré pattern at 2.5 nm periodicity. This is because high projected density of the carbon atoms at the Fermi level was observed at the fcc- site. Thus, binding energy for Ru at the fcc- site was higher than Ru-Ru binding energy, which favoured nucleation at these sites. At 1.7 and 1.2 nm graphene/Moiré periodicity, however, the binding energy for Ru was not higher than Ru-Ru binding energies, and thus forming randomly distributed larger Ru clusters (Soy et al. 2015).

5.5 *Graphene/Rh(111) Moiré Template*

NiNCs are of specific interest due to their electronic and magnetic properties. Many substrates have been exploited for the growth of NiNCs such as h-BN nanomesh (Auwärter et al. 2002; Zhang et al. 2008), Au(111) surface (Repain et al. 2002; Weiss et al. 2005), reconstructed surfaces (Chen et al. 2004; Fonin et al. 2003) and alumina double layer on Ni_3Al (Degen et al. 2004; Schmid et al. 2007). In order to achieve regularly sized monodispersion, Sicot and co-workers deposited NiNCs on graphene/Rh(111) Moiré pattern (Sicot et al. 2010). NiNCs were deposited at low temperature (150 K) to suppress high mobility of small clusters and to induce ordered array formation on the graphene Moiré template. Selective nucleation was observed at fcc- site and deposition at higher temperature formed large epitaxial islands with the loss of ordered arrangement. Interestingly, at room temperature triangular-shaped islands were observed with large islands at the terraces. This could be due to the high mobility of Ni on graphene surface at RT as well as the weak bonding between Ni and graphene.

6 Intercalation of Metals at the Interface of Graphene and Ru(0001) Moiré Surface

As described earlier, a strong interaction exists between graphene and Ru(0001) which hybridizes the graphene's pi bond, which in turn could disrupt the unique electrical properties of the superlattice. To overcome this, several studies have been directed towards intercalating another layer of metals between the graphene and the Ru(0001) surface, such as Au, in order to retain graphene's linearly dispersed energy band (Varykhalov et al. 2008; Enderlein et al. 2010). With the same intention, Huang et al. (2011) intercalated metal islands: Pt, Pd, Ni, Co, Au, In and Ce at the interface of the epitaxially grown graphene and Ru(0001) surface. A symmetric honeycomb lattice was observed for graphene on the top of intercalated islands, as compared to a hexagonal lattice in the non-intercalated areas. Pt, Pd, Ni and Co did not show any difference in the height on the graphene Moiré surface. However, Au, In and Ce exhibited a different graphene Moiré pattern with obvious graphene nanomesh seen after the intercalation of rare earth metal, Ce (Huang et al. 2011).

7 Metal NCs Deposition on HOPG

Besides growing clusters on a metal graphene Moiré template, metal clusters can also be deposited on a HOPG surface. Pt clusters were deposited on HOPG with 1–3 atomic height via vapour phase deposition by heating Pt wire in a UHV

chamber (Kondo et al. 2009). The carbon atoms around the Pt clusters were found to possess Fermi level states, which were ascribed due to nonbonding pi electrons of graphite, formed by Pt-C hybridization. However, the Pt cluster deposition was found to be non-uniform. A similar finding was also observed in Fe and Pt metals, whereby the metals tend to nucleate at defect sites (Clark and Kesmodel 1993; Kholmanov et al. 2007). Thus, artificially made defects or nanopits have to be created to produce monodispersed metal NCs on the surface of HOPG (Kholmanov et al. 2007; Hövel et al. 1997).

Besides PtNCs, there is also specific interest in the production of AgNCs due to various applications such as catalysis, electronic devices and gas sensors (Henry 1998; Dupas and Lahmani 2007). Similar to the synthesis of PtNCs, AgNCs were deposited epitaxially on HOPG by Ndlovu et al. (2012). Many previous studies have been conducted on the nucleation of AgNCs on HOPG by taking advantage of the metallic properties of HOPG, which allows electron spectroscopy and microscopy to be conducted without surface charging problems (Patthey and Schneider 1995; Dietsche et al. 2008). Upon deposition of Ag on HOPG, random distribution of Ag atoms was observed with 15–18% coverage of HOPG's surface. Based on STM images, Ag exists as individual clusters, however, no signs of aggregation was seen. This could be due to the difference in lattice between silver and HOPG, consequently resulting in weak interaction between metal NCs and HOPG. Hence, this allows Ag clusters to be mobile and diffuse within the surface of HOPG. A similar observation was also noted (Dietsche et al. 2008; Goldby et al. 1996; Couillard et al. 2003). Upon further deposition of Ag, the cluster islands grow in 3D fashion via the Volmer-Weber growth mechanism. STM images revealed that the preferred site of nucleation is on the top of C atom and the AgNCs are predicted to be positively charged due to the charge transfer between the substrate, HOPG and the metal, AgNCs (Ndlovu et al. 2012).

8 Metal NCs Deposition on Graphene Grown on 6H-SiC(0001)

One of the advantages of using SiC substrate as a template for the growth of graphene is that the interaction between graphene and Si-C substrate is weak and thus the substrate does not play any role in controlling the growth morphology of the metal NCs. The growth of metal NCs is predominantly controlled by the interaction between graphene and the metal adatoms (Liu et al. 2013a). There has been much pervious work reporting on how the graphene on Si-C terminated substrate behaves differently from graphene grown on transition metals (Bartelt and McCarty 2012; Gierz et al. 2008; McChesney et al. 2010; Sandin et al. 2012). Briefly, graphene layers are grown on SiC substrate by thermal annealing. Due to the slow and controlled desorption of Si, the graphene layers formed are of high quality with domain extending up to micrometer range (Hupalo et al. 2009). Several

metals have been selected for the growth of NC on graphene/SiCsubstrate such as Gd, Dy, Eu, Fe and Pb. As for the first metal, fractal-like Gd islands in 3D were formed which were stable up to 800 K, however, crystalline shape was formed at higher annealing temperature (Liu et al. 2010, 2012a; Hupalo et al. 2011a). In comparison, larger well-shaped islands were formed by DyNCs with lower thermal stability, as annealing at 580 K formed multiple level islands and some were found to coalesce (Liu et al. 2010; Hupalo et al. 2011a). As for Eu, flat films of large terraces were formed and annealing at 365 K transformed the clusters to continuous film (Liu et al. 2010, 2012a). Interestingly, for Fe, number of atoms deposited continued to increase even at the maximum exposure of 2.3 ML, with half of the graphene/SiC surface covered with 3D islands and possibly beyond. Only a slight change in the density was observed even after annealing at 660 K (Hupalo et al. 2011a; Liu et al. 2013a). Fe showed similar thermal stability as Gd. Finally, for Pb deposited on graphene/SiC substrate, only two large Pb islands were formed with the height of 8 layers with regular fcc-shapes. This is mainly due to fast diffusion of Pb atoms on the graphene surface and thus these atoms have moved to islands (Hupalo and Tringides 2007; Liu et al. 2013a).

9 Other Synthesis Approaches

Aside from using graphene for the templated growth of NCs, a much simpler alternative is by noncovalent physisorption of metal NCs on the basal plane of graphene. There are many previous reports on the loading of polymer, aromatic molecules and metal NPs via either van der Waals interactions, pi-pi stacking or cation-pi interactions (Muthoosamy et al. 2014; Yang et al. 2011; Stankovich et al. 2006; Xu et al. 2008b).

One of the pioneering research was conducted by Wang et al. (2011a), whereby AuNCs were grown on reduced graphene oxide (RGO). AuNCs were prepared in organic phase by Brust-Schiffrin method (Brust et al. 1994). Briefly, an aqueous solution of $HAuCl_4 \cdot 4H_2O$ was mixed with tetraoctylammonium bromide (TOAB) in chloroform. $HAuCl_4$ was then transferred into organic phase followed by the addition of dodecanethiol. $NaHB_4$ was then added dropwise and the organic phase was evaporated using a rotary evaporator and the product was recovered in chloroform. Dodecanethiol-stabilized AuNCs were then purified in ethanol and then added to cetyltrimethylammonium bromide (CTAB) under vigorous stirring until no obvious phase boundary was seen. Finally, chloroform was removed by heating, thereby producing AuNCs (Wang et al. 2011a; Brust et al. 1994). In general, two processes take place, first, phase transfer of metal precursors (1) and second, the reduction of metal ions (2) as depicted below:

$$AuCl_4^-(aq) + N(C_8H_{17})_4^+(\text{Chloroform}) \rightarrow N(C_8H_{17})_4^+\ AuCl_4^-(\text{Chloroform}) \quad (1)$$

$$\begin{aligned} &mAuCl_4^-(\text{chloroform}) + nC_{12}H_{25}SH(\text{chloroform}) + 3me^- \\ &\rightarrow\ 4mCl^-(aq) + (Au_m)(C_{12}H_{25}SH)_n(\text{chloroform}) \end{aligned} \quad (2)$$

where m and n are the number of moles of metal precursors ($AuCI_4^-$) and the protecting ligand ($C_{12}H_{25}SH$), respectively (Brust et al. 1994; Lu and Chen 2012). The synthesis can also be done in a one-step using a polar solvent as reported elsewhere (Brust et al. 1995).

RGO was then mixed with dodecanethiol-CTAB-capped AuNCs followed by separation which produced water-soluble AuNCs-RGO. Generally, AuNPs exhibit a broad absorption peak in the UV/Vis at 520 nm, which represents surface Plasmon band. The absence of this characteristic peak in the AuNCs-RGO shows that the clusters formed were of less than 3 nm (Yang et al. 2011; Zhou et al. 2009). This is further confirmed using transmission electron microscopy (TEM) and high-resolution transmission electron microscopy (HRTEM) and the absence of deep-red colour that is usually observed in typical AuNPs.

Alternatively, AuNCs can also be grown by a simpler reduction process using peptide as a template. There are various templates used for the growth of AuNCs such as protein (Xiaofei et al. 2014), polymer (Zheng et al. 2003), DNA (Park and Park 2015) and peptide (Song et al. 2015). Peptides have gained major interest recently due to their simplicity and the following advantages: provide targeted site for cluster growth; amino acid sequence and length can be designed; provide multiple contact point with Au ions during synthesis (Gu et al. 2014). Nguyen and co-workers used a peptide that was designed for specific site for metalloproteinase-9 (MMP-9) cleavage, which is at Gly/Leu with a Cys residue at one of the terminal to facilitate interaction with gold ions. The interaction between the Cys from peptide and Au forms strong fluorescence due to the formation of Au(l)-thiol complex via various complex mechanisms. It was reported that the Au(l)-thiol complex is formed by ligand-to-metal nanoparticle core charge transfer (Koh et al. 2015), ligand-to-metal charge transfer (Hong et al. 2014; Wu and Jin 2010) as well as ligand-to-metal-metal charge transfer (Kennedy et al. 2012).

A one-step synthesis method was employed to prepare the peptide-AuNCs loaded onto graphene oxide (GO) (Fig. 6) to quench the AuNCs fluorescence and to obtain a turn-on biosensing system. Briefly, mercaptoundecanoic acid (MUA) was added to $AuCI_4$ salt and peptide, followed by mixing at RT in a dark room. MUA was used as an auxiliary ligand to stabilize the AuNCs (Xiaofei et al. 2014; Zheng et al. 2003). Cold $NaBH_4$ was then added followed by further incubation and purification. Peptide-AuNCs loaded GO (Peptide-AuNCs-GO) complex was then prepared by simply mixing the peptide-AuNCs solution and GO at RT followed by purification (Nguyen et al. 2015). HRTEM image revealed monodispersed AuNCs with an average diameter of 4 nm, which emitted intense red fluorescence at 365 nm in UV and light brown color in the visible light. Using Rhodamine 6G as reference, the quantum yield obtained was 4.35%.

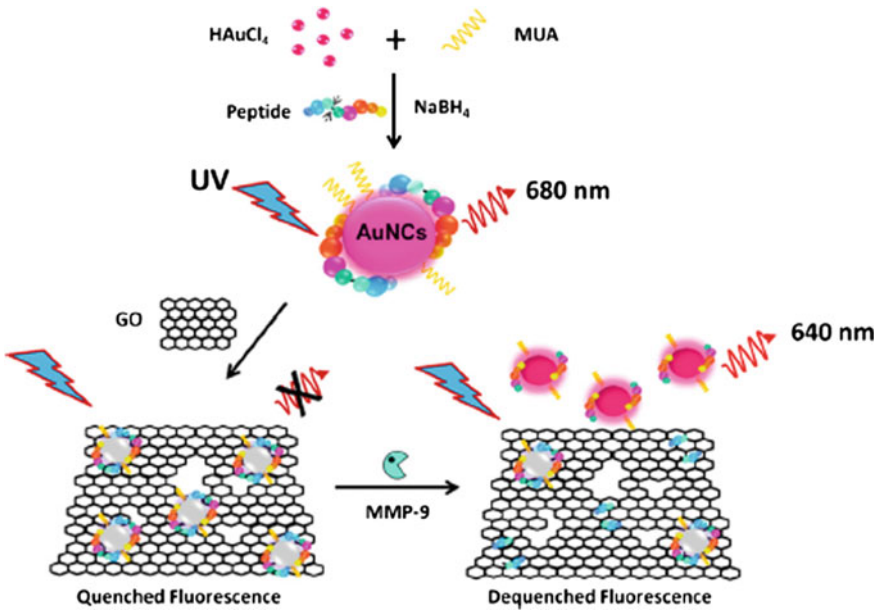

Fig. 6 Scheme explaining the synthesis and application of fluorescent peptide-stabilized-gold nanoclusters for the detection of proteins. Reprinted with permission from Nguyen et al. (2015)

In another study, Chang and co-workers used an even milder approach by using ascorbic acid or Vitamin C as a mild reducing agent for in situ reduction of GO and Pt salt (Chang et al. 2015). The group has also successfully used the same procedure to prepare PtNCs-RGO and applied in direct methanol fuel cell (Ji et al. 2012). In this design, graphite was initially converted to GO via Hummer's method (Hummers Jr and Offeman 1958). After which, K_2PtCl_4 salt and a polymer, polyvinyl-pyrrolidone (PVP) was added as a dispersing agent to obtain homogenous PtNCs. Finally, ascorbic acid was added and the reaction was left under stirring for 12 h at 85 °C. There have been many previous works carried on the synthesis of PtNPs loaded onto graphene, however, these reports lack selectivity and sensitivity (Bai et al. 2011; Kuila et al. 2011; Li et al. 2008). Based on the TEM images, the PtNCs-RGO synthesized by adding PVP resulted in small NCs which were well-dispersed on the basal plane and edges of RGO with an average particle size of 22 nm in diameter. Whereas, PtNCs synthesized without PVP appeared to agglomerate with average sizes in the range of 10–70 nm. PVP seems to have increased the dispersity of PtNCs and thus a homogeneous deposition was observed. This is due to strong interaction that exists between Pt precursors and C=O groups on PVP (Shen et al. 2008; Borodko et al. 2006, 2007). Upon close examination with HRTEM, interval between two lattice fringes was 0.224 nm, corresponding to (111) interplanar distance of fcc-, thus confirming the formation of Pt clusters (Chang et al. 2015; Shi et al. 2013). Further confirmation of the

deposition of Pt clusters on RGO was also seen by XPS analysis. Two peaks were observed at 71.8 and 75 eV in the XPS spectra which agrees to Pt $4f_{7/2}$ and $4f_{5/2}$ signals and confirms that the Pt clusters are in metallic form and not in ionic (Hsin et al. 2007; Wei et al. 2011). Another characterization technique to confirm the formation of PtNCs is the X-ray diffraction (XRD) analysis. Peaks of Pt's fcc-were observed at 39.9° and 46.5° which belong to the (111) and (200) crystal planes of Pt (Zhang et al. 2011).

In a nutshell, there are various techniques to grow metal NCs, however, a substrate or template is necessary to grow or deposit the metal NCs, in order to obtain homogeneous metal NCs. The fundamental synthesis which started from templated growth of metal NCs on a graphene/metal Moiré structure opens many possibilities for further exploration using much simpler approaches such as protein, polymer or peptide stabilized metal NCs. A more recent approach has avoided the use of harsh reducing agents and has opted for milder versions such as ascorbic acids. It is clear that the various synthesis techniques will produce metal clusters with different sizes as shown in Table 1.

Table 1 Various types of metal NCs grown on graphene template[a]

Metal NCs grown	Template/Moiré type	Size/height	Synthesis method	References
Ir	Graphene/Ir(111)	2.2 Å	Vapor phase deposition	N'Diaye et al. (2006)
Ir	Graphene/Ir(111)	2.05–2.15 Å	Vapor phase deposition	Feibelman (2008)
Ir	Graphene/Ir(111)	2.2 Å	Vapor phase deposition	N'Diaye et al. (2009)
–	Graphene/Ru(0001)	0.1 nm (height of graphene Moiré)	Thermal annealing	Pan et al. (2007a)
–	Graphene/Ru(0001)	0.4 Å (height of graphene Moiré)	Thermal annealing	Pan et al. (2009a)
–	Graphene/Pt(111)	–	Thermal annealing of benzene	Fujita et al. (2005)
–	Graphene/Cu(111)	2, 4, 5.6, 6.6 nm (height of graphene Moiré)	Thermal annealing	Soy et al. (2015)
Pt	HOPG	0.4 nm	Vapor phase deposition	Kondo et al. (2009)
Pt	Graphene/Ir(111)	2.3 Å	Vapor phase deposition	N'Diaye et al. (2009)
Pt	Graphene/Ir(111)	1.09 Å	Vapor phase deposition	Gerber et al. (2013)

(continued)

Table 1 (continued)

Metal NCs grown	Template/Moiré type	Size/height	Synthesis method	References
Pt	Graphene/Ru(0001)	3.06 nm	Vapor phase deposition	Zhang et al. (2009a)
Pt	Graphene/Ru(0001)	2–3 nm	Vapor phase deposition	Pan et al. (2009a)
Pt	Graphene/Ru(0001)	2 nm	Vapor phase deposition	Zhou et al. (2010)
Pt	RGO	22 nm (dia)	Reduction by ascorbic acid	Chang et al. (2015)
Pt[a]	Graphene/Ru(0001)	2.88 Å	Thermal annealing	Huang et al. (2011)
Pt	Graphene/Cu(111)	2.8 nm	Vapor phase deposition	Soy et al. (2015)
Rh	Graphene/Ru(0001)	0.3–1.2 nm	Vapor phase deposition	Zhou et al. (2010)
Rh	Graphene/Cu(111)	7 nm	Vapor phase deposition	Soy et al. (2015)
Rh	Graphene/Ir(111)	5 Å	Vapor phase deposition	Cavallin et al. (2012)
Pd	Graphene/Ru(0001)	8–14 nm	Vapor phase deposition	Zhou et al. (2010)
Pb	Graphene/SiC(0001)	–	Vapor phase deposition	Liu et al. (2013a)
Pd[a]	Graphene/Ru(0001)	2.70 Å	Thermal annealing	Huang et al. (2011)
Co	Graphene/Ru(0001)	10–12 nm	Vapor phase deposition	Zhou et al. (2010)
Co[a]	Graphene/Ru(0001)	3.00 Å	Thermal annealing	Huang et al. (2011)
Co	Graphene/Ru(0001)	0.225 nm	Vapor phase deposition	Liao et al. (2011)
Au	Graphene/Ru(0001)	0.4 nm	Vapor phase deposition	Zhou et al. (2010)
Au	Graphene/Ru(0001)	0.55 nm	Vapor phase deposition	Xu et al. (2011)
Au	Graphene/Ru(0001)	0.55 nm	Vapor phase deposition	Liu et al. (2011c)
Au	RGO	2.5 nm (dia)	Brust-Schiffrin and physisorption	Wang et al. (2011a)
Au	Peptide-templated and loaded onto GO	4 nm (dia)	Reduction using $NaBH_4$	Nguyen et al. (2015)

(continued)

Table 1 (continued)

Metal NCs grown	Template/Moiré type	Size/height	Synthesis method	References
Au	Graphene/Ir(111)	15 Å	Vapor phase deposition	N'Diaye et al. (2009)
Au[a]	Graphene/Ru(0001)	2.78 Å (different superlattice graphene Moiré pattern)	Thermal annealing	Huang et al. (2011)
Ag	HOPG	0.68 nm	Thermal evaporation	Ndlovu et al. (2012)
W	Graphene/Ir(111)	6 Å	Vapor phase deposition	N'Diaye et al. (2009)
Re	Graphene/Ir(111)	[a]partial cluster arrangement	Vapor phase deposition	N'Diaye et al. (2009)
Fe	Graphene/Ir(111)	23 Å	Vapor phase deposition	N'Diaye et al. (2009)
Fe	Graphene/SiC(0001)	–	Vapor phase deposition	Liu et al. (2013a)
Ni	Graphene/Ir(111)	Nil. no superlattice formed	Vapor phase deposition	N'Diaye et al. (2009)
Ni[a]	Graphene/Ru(0001)	2.50 Å	Thermal annealing	Huang et al. (2011)
Ni	Graphene/Rh(111)	0.85 nm	Vapor phase deposition	Sicot et al. (2010)
In[a]	Graphene/Ru(0001)	Nil. Different superlattice graphene Moiré pattern	Thermal annealing	Huang et al. (2011)
Ce[a]	Graphene/Ru(0001)	Nil. Graphene nanomesh formed	Thermal annealing	Huang et al. (2011)
Ce	Graphene/Ru(0001)	3.00 Å	Vapor phase deposition	Novotny et al. (2016)
Gd	Graphene/SiC(0001)	0.29–1.05 nm	Vapor phase deposition	Liu et al. (2013a)
Dy	Graphene/SiC(0001)	1.93 nm	Vapor phase deposition	Liu et al. (2013a)
Eu	Graphene/SiC(0001)	0.75 nm	Vapor phase deposition	Liu et al. (2013a)
Ru	Graphene/Ru(0001)/SiO_2	4.8 Å	Low-power RF magnetron sputtering	Sutter et al. (2012)

[a]Intercalation of metal islands at the interface of graphene and Ru(0001) Moiré structure

10 Applications of Graphene-Metal Nanocomposites

The tremendous acceptance and enormous interest of graphene–metal nanocomposites in the nano-therapeutics lead to their introduction to theranostic applications, where the diagnosis and therapy encourages on-time monitoring of the progression of treatment. The single atomic layer of carbon atoms exposing its wider surface area made graphene a great platform for the metal NPs to adsorb on the surface which encouraged the evolution of synergistic properties as a nanocomposite (Wintterlin and Bocquet 2009). Being very susceptible to conjugation, graphene and derivatives already performed as excellent carriers of drug and genes; where the combination of metal NPs encouraged the imaging platform through near Infrared (NIR) sensing, RAMAN spectroscopy, magnetic resonance (MR) imaging, computed tomography/positron emission tomography (CT/PET) scan etc. (Orecchioni et al. 2015; Yu et al. 2015; Swain et al. 2015; Yang et al. 2012). The combination of graphene derivatives with metal nanoparticles have been a popular topic of research in recent nanotheranostic applications.

Among noble metals, Au and Ag have been mostly involved in theranostic applications in combination with graphene due to their unique surface plasmon resonance (SPR), surface enhanced Raman scattering (SERS) and photothermal effects (Lin et al. 2016b). Hybrid plasmonic structures made of graphene-Au composition were used in the delivery of anticancer drugs in cancer cells with SERS imaging for chemo-phototherapy (Chen et al. 2016; Wang et al. 2014c; Xu et al. 2013a; Li et al. 2015b). In vitro evaluation of similar Au–graphene combinations lead to the development of highly sensitive SERS sensors for detecting breast cancer stem cells (BCSCs), which could be a future theranostic agent by introducing the photothermal interactions (Manikandan et al. 2014).

Likewise, the effectiveness of Au–graphene combinations in metastasis breast cancer were analysed by employing them on orthotopic 4T1 breast tumor-bearing nude mice for chemo-phototherapy, where effective tumor inhibition and growth suppression were observed. The superior anticancer effect was contributed mutually from the drug, Dox which caused apoptosis and hyperthermia-induced destruction of tumor tissue (Wang et al. 2016a). GO based systems with Au nanostars, Au nanorods and AuNPs have demonstrated both Raman imaging and photothermal therapy which promoted the theranostic applications for imaging and phototherapy (Nergiz et al. 2014; Dembereldorj et al. 2014; Zedan et al. 2012). Ag-Graphene combinations were also successfully utilized for chemo-photo therapies in DU145-human prostate cancer cell lines and HeLa-human cervical cancer cells. Here, photodynamic therapy is utilized where irradiation of light induced the generation of singlet oxygen by a multistate sensitization process and thus promoted the cancer cell death (Habiba et al. 2016). Pt based nanoGO systems also were verified in chemo-photo theranostic platform (Li et al. 2015a).

Gene delivery with imaging was another stepping stone in the theranostics. Au-Graphene combinations were also found successful in the gene delivery applications (Xu et al. 2013b; Zhi et al. 2013). The possibility of SERS imaging or

the drug conjugation to this Au-Graphene gene carrier could contribute as a perfect theranostic system based on efficient transfection results in gene therapy (Gehrig et al. 2014; Wang et al. 2013b). Utilizing this concept, in vitro and in vivo investigations of MiR-122-loaded graphene-Au composites were utilized for controlling the tumor cell apoptosis and growth (Yuan et al. 2015).

Multimodality imaging of the infection site along with drug delivery was performed when magnetic metals were utilized in combination with graphene materials. Photo-imaging in combination with MR, CT, NIR and fluorescence made multimodal imaging an inevitable possibility. Nanoparticles of iron oxide (IONP), gadolinium (Gd) and manganese (Mn) were utilized mostly in MR imaging arena (Huang et al. 2015; Lux et al. 2015; Le et al. 2016). When chemo-phototherapy were involved, AuNPs were used in combination with IONP for MR imaging studies (Chen et al. 2015). In addition, GO-metal based theranostic platforms were investigated for the MR imaging associated chemotherapeutic potential (Balcioglu et al. 2013; Zhang et al. 2013; Ma et al. 2012; Li et al. 2016). Being MR contrast agents, nanomaterials such as Fe, Gd, Mn, etc. enhance the signal strength of the images, which improves the real time monitoring of the infectious site, drug response and apoptosis effects. IONP–Mn decorated GO sheets were utilized in the triple stimuli responsive (pH responsive, reduction responsive and magnetic field responsive) imaging and hypothermia efficiency evaluation and monitoring of tumour location (Chen et al. 2014). Multiple theranostics were performed when multiple diagnoses combines with multiple therapies. Silica incorporated graphene based systems were employed for MR imaging, active–passive targeting and chemotherapy for the glioma cells, which is a perfect example of multiple theranostics (Wang et al. 2014b).

Similarly, chitosan functionalized magnetic graphene nanosystem involved in the gene–drug combo delivery and MR-fluorescence imaging of A549 lung cancer cells and C42b prostate cancer cells, show the future of multiple theranostic agents (Wang et al. 2013a). Another graphene nanosystem combined with IONPs showed the potential of dual-modality mapping guided photothermal therapy in pancreatic cancer (Wang et al. 2014a). Based on the performance of the proof-of-concept design, the graphene-metal based theranostic nanosystems can be considered as a novel approach for an efficient on-demand therapeutic system leading towards new generation of nanomedicines.

10.1 Graphene-Metal NCs for Theranostics Applications

Based on the exhaustive applications of graphene-metal nanocomposites for theranostics applications, the same has also been diligently explored for graphene-metal NCs. One of the earliest biological applications being explored for graphene NCs is as an imaging agent of cancer cells. When compared to quantum dots and organic dyes, graphene NCs do not contain toxic heavy metals nor functional groups for chemical reactivity (Lin et al. 2009; Retnakumari et al. 2009; Muhammed et al.

2009). Thus near-infrared range emission is made possible as it also avoids interference from biological molecules. Due to the simplicity, graphene NCs are ideal for bioimaging and superior compared to conventional fluorescent labels (Wang et al. 2011a; Pan et al. 2007b). The following sections describe briefly about the various applications of metals NCs loaded on graphene and its derivatives, by giving specific attention to multi-functionalities such as biosensing, imaging and in situ drug delivery.

NCs were reported to cause more cytotoxic effects than NPs in cancer cells. Thus, the cytotoxicity effects of AuNCs deposited on RGO were explored by loading an anti-cancer drug Doxorubicin (Dox) by pi-pi stacking (Wang et al. 2011a). The drug loading efficiency achieved was 91% with an encapsulation efficiency of 40%, which is high considering the aromatic groups on the graphene domain is also occupied by AuNCs. (3-(4,5-dimethylthiazol-2-yl)-2,5-diphenyltetrazolium bromide) MTT test on HepG2cells showed that AuNCs in the free form caused more cytotoxicity than AuNPs, which was also observed by Pan et al. (2007b). The highest growth inhibition was observed in Dox loaded AuNCs-RGO, which was even more potent than free Dox. It was deduced that the drugs are more efficiently transported to the cancer cells by the AuNCs-RGO compared to free Dox. Dox was seen well-distributed inside the cancer cells in the AuNCs-RGO system compared to poor drug distribution and agglomeration at the cell membrane. In addition, karyopyknosis was also observed in the AuNCs-RGO system, suggesting synergistic drug treatment might have taken place (Wang et al. 2011a).

AuNCs-RGO produced quantum yield, matching those of free AuNCs (Lin et al. 2009). At 490 nm excitation, two emission peaks were observed at 606 and 705 nm. Though loading of AuNCs on RGO would result in partial quenching due to electron transfer between AuNCs and RGO, however, it was found that AuNCs-RGO could be readily used for cellular imaging as moderate fluorescence intensity was observed. Clear imaging of HepG2 cells was observed including the cell edges as shown in Fig. 7 (Wang et al. 2011a).

PtNCs anchored on RGO were found to have excellent electrochemical properties in non-enzymatic glucose sensing (Chang et al. 2015). Conventionally, glucose sensing is carried out based on glucose oxidase immobilization on various substrates which have shown good selectivity and sensitivity (Wang 2001; Jia et al. 2007; Bo et al. 2010; Wu et al. 2013). Nevertheless, immobilization of enzyme on substrates are a tedious process as there are many factors to be considered in order to retain the enzyme's activity such as temperature, pH and denaturation due to long exposure time (Bo et al. 2010; Wu et al. 2013; Holt Hindle et al. 2008). To address these drawbacks, many attempts have been made to develop a non-enzymatic glucose sensor by catalytic oxidation of glucose on the surface of a substrate (Wang 2001, 2008; Chen et al. 2010). Pt particles was chosen as a perfect candidate for

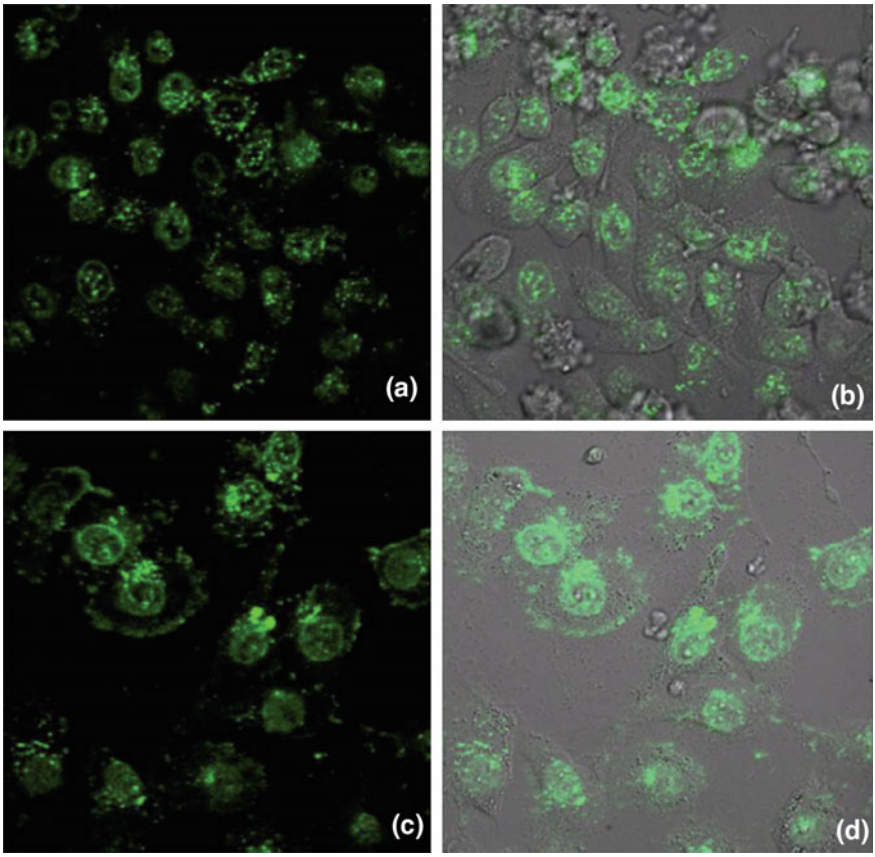

Fig. 7 Laser confocal microscopic images at 400X magnification with (**a**) and (**b**) HepG2 cells after Dox treatment. **c** and **d** AuNCs-RGO conjugated with Dox. **a** and **c** is the fluorescence micrographs images, whereas **b** and **d** is the overlay of morphological and fluorescence images. Reprinted with permission from Wang et al. (2011a)

glucose biosensing study as previous reports have shown excellent electro-oxidation of glucose (Chen and Holt Hindle 2010; Di Vece et al. 2008; Niu et al. 2012). However, PtNPs pose problems of agglomeration and well-dispersed particles are of great interest due to the limited supply of Pt for commercialization (Park et al. 2003; Di Vece et al. 2008; Qu et al. 2010; Zhang et al. 2011). Thus RGO which is chemically inert and has large surface area will be the best substrate to load these Pt particles to obtain homogenous clusters. The PtNCs-RGO displayed excellent catalytic activity towards glucose in neutral media and exhibited rapid response time (3 s) as shown in Fig. 8. The anodic peak at −0.35 V represents the electrochemical adsorption and desorption of hydrogen (Meng et al. 2009). The second anodic peak at 0.10 V is attributed to the oxidation of glucose molecules (Gao et al. 2011). Upon further increase in potential, lower current response was

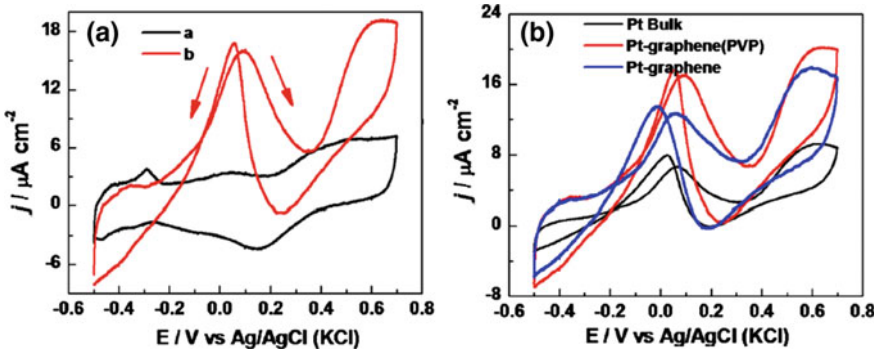

Fig. 8 **a** CV response of PtNCs/graphene in 0.1 M PBS (pH 7.4) with the scan rate of 5 mVs^{-1} in (*a*) the absence of glucose and (*b*) in the presence of 50 mM glucose. **b** CV response of Pt bulk electrode, PtNCs/graphene in 0.1 M PBS (pH 7.4) solution containing 50 mM glucose with a scan rate of 5 mVs^{-1}. Reprinted with permission from Chang et al. (2015)

observed due to the saturation of glucose on the surface of PtNCs-RGO and an inability for further oxidation. At 0.4 V, an increase in the current was observed due to further oxidation of glucose and glucose intermediates forming gluconolactone and gluconic acid (Meng et al. 2009; Wu et al. 2013; Gao et al. 2011). The PtNCs-RGO system also showed excelled stability and sensitivity with low detection limit of 1.21 $\mu Acm^{-2}mM^{-1}$. The system also exhibited excellent selectivity when tested against interfering molecules such as ascorbic acid, uric acid and 4-acetaminophen.

A turn-on detection of cancer cells was produced by immobilizing peptide-stabilized AuNCs on a GO (Nguyen et al. 2015). One of the recent applications was shown by Gu et al. (2014), whereby peptide templated AuNCs were used for the detection of elastase, a biomarker for tumor progression. In another study, the same template was used to prepare an enzyme-responsive fluorescent nanocluster beacon for the detection of post-transitional enzyme (Wen et al. 2013). Although they displayed high sensitivity, however, one of the major drawbacks is regarding its turn-off sensing system. In a turn-off system, many complex compounds in the sample can quench the fluorescence and thus results in false positive. In addition, the emissions are mostly located in the UV region which is undesirable due to interference from other biological compounds which limit its use in in vivo applications (Zhang et al. 2011; Geddes and Lakowicz 2009). Thus a turn-on biosensing system was necessitated.

In this turn-on biosensing system, the group loaded peptide stabilized AuNCs onto GO, a fluorescent quencher. Through self-assembly peptide-AuNCs-GO was formed with the fluorescence significantly quenched. However, upon detection of

MMP-9 proteins, peptide cleavage took place which simultaneously released the AuNCs from the GO's surface. This dequenched the AuNCs and thus a turn-on signal was produced (Nguyen et al. 2015). The quenching ability of GO was determined by adding an increasing amount of GO to the solution of AuNCs, where 81% quenching efficacy was achieved when 80 μg of GO was used. The quenching effect was deduced due to various interactions between GO and metal NCs such as electrostatic, pi-pi with aromatic amino acids in the peptide as well as hydrogen bonding (Xiaofei et al. 2014). The quenching effect is further confirmed by Stern-Volmer plot, whereby with an increase in the concentration of GO, a reduction in the fluorescence intensity was observed in a linear fashion with a quenching constant of 0.034 μg ml^{-1}, which is in agreement with the previous findings (Hidalgo 2012).

MMP-9 protein was chosen as a biomarker as it is the major constituent of cellular basement membrane and promotes cancer cell invasion (Wu et al. 2008). MMP-9 is also an important biomarker for an early detection of cancer metastasis as an increased amount of MMP-9 was detected in serum and plasma sample of humans with malignant tumors (Vasala and Turpeenniemi Hujanen 2007; Wu et al. 2008; Kang et al. 2015; Rucci et al. 2011). Upon addition of MMP-9 to the peptide-AuNCs-GO complex, the peptide was cleaved and as a consequence the quenched fluorescence was restored at 640 nm. When the concentration of enzyme increased, the recovery of fluorescence also increased linearly.

With the success of these findings the researchers then tested in live cancer cells by inducing MMP-9 secretion (Nguyen et al. 2015). Phorbolmyristate acetate (PMA) was used to stimulate MMP-9 secretion as it is well known to strongly stimulate cancer cell invasion by inducing overexpression of MMP-9 proteins (Rucci et al. 2011; Kang et al. 2015). Based on the immunofluorescent images, condensed distribution of F-actin (red) was observed after the treatment of cells with PMA (Fig. 9). This finding is in accordance with previous reports on over-expression of MMP-9 after the treatment with PMA (Chuang et al. 2014; Vargová et al. 2012). When the synthesized peptide-AuNCs-GO was added to the cells, a MMP-9 turn-on response was observed. The biosensor is selective as no turn-on response was observed in the absence of MMP-9. It was also highly sensitive with the limit of detection of 0.15 nM as compared to the previous reported findings (Son et al. 2013; Biela et al. 2015).

Besides a turn-on for cancer cell sensing, NCs can also be used for DNA sensing, specifically for hepatitis B virus gene (HBV), immunodeficiency virus gene (HIV) and syphilis (*Treponema pallidum*) gene detection (Liu et al. 2013b). Nucleic acid stabilized AgNCs were prepared and adsorbed onto the surface of GO for quenching effects (Fig. 10). Upon recognition by the target gene or aptamer sequence via DNA duplex structures or aptamer-substrate complexes, desorption of

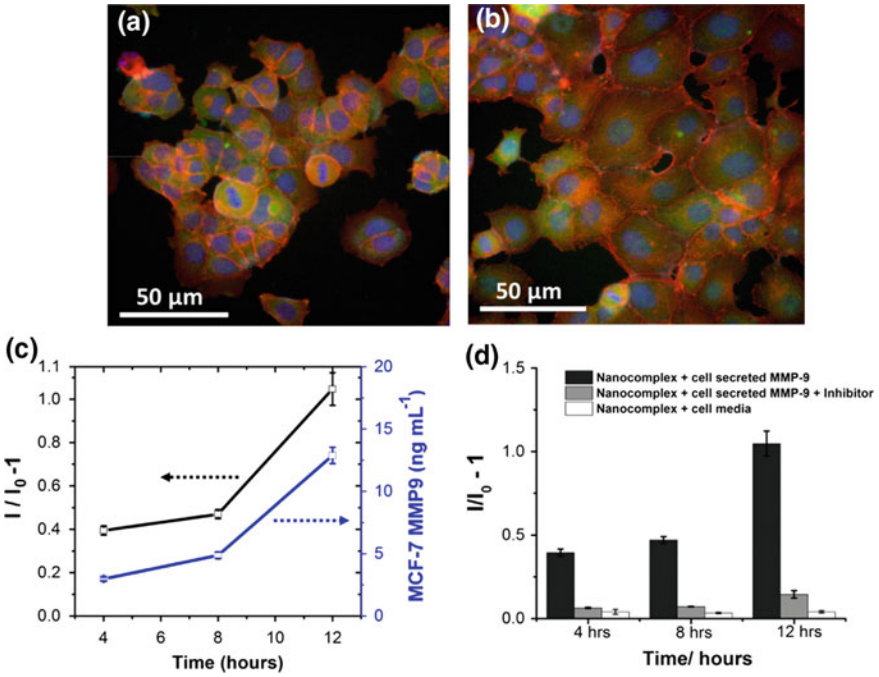

Fig. 9 **a** and **b** represent the immunofluorescent images (*red* F actin, *green* vinculin, *blue* nucleus) of MCF-7 cells after treatment with peptide-AuNCs-GO in **a** the absence of PMA, **b** in the presence of PMA, **c** fluorescence response of peptide-AuNCs-GO nanocomplex (*black line*) and ELISA (*blue line*) for in vitro detection of MMP-9 secreted from MCF-7 cells at different time (4, 8 and 12 h) and **d** *bar chart* of fluorescent response of peptide-inhibitor (*dark grey*), fluorescent response of peptide-AuNCs-GO nanocomplex to cell secreted MMP-9 in the presence of MMP-9 inhibitor (*light grey*), and fluorescent response of peptide-AuNCs-GO nanocomplex in cell media only (*white*). Reprinted with permission from Nguyen et al. (2015)

the nucleic acid-stabilized-AgNCs from GO takes place resulting in a turn-on fluorescence generation. Two types of nucleic acid stabilized AgNCs were used: red-emitting AgNCs (at 616 nm) and infrared-emitting AgNCs (775 nm). With the introduction of GO modified with nucleic acid-AgNCs probe to the HBV gene, red-emission was observed at 616 nm with the limit of detection for HBV gene of 0.5 nm. Using the near-infrared AgNCs for the HIV sensing, a limit of detection of 1 nm was achieved with emissions at 775 nm. The luminescent AgNCs were also used for ATP sensing by using anti-ATP-aptamer stabilized AgNCs as probe, which exhibited a detection limit of 2.5 µm.

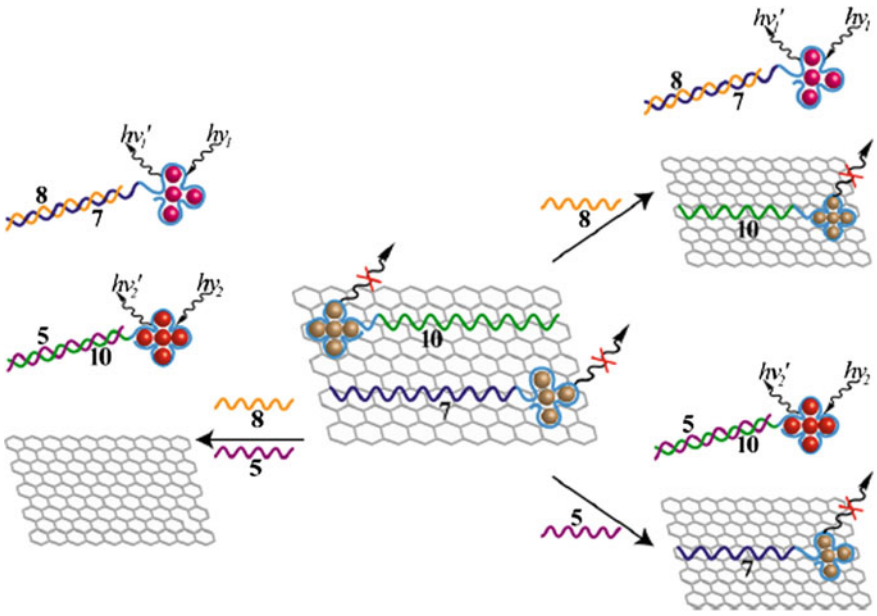

Fig. 10 Multiple analysis of genes using near-infrared and *red* emitting AgNCs probes. Gene HBV and HIV are labelled in the figure as 5 and 8 respectively. Reprinted with permission from Liu et al. (2013b)

11 Toxicity of Graphene-Metal Nanocomposites

Toxicity issues are the major concern limiting the application of any nanomaterials in therapeutics. Very few studies were involved in reporting the toxicity evaluation of the graphene family materials; where toxicity is often associated with dose, surface coatings, size, administration routes, etc. (Yang et al. 2013; Kiew et al. 2016; Yin et al. 2015). Most of the graphene theranostic platforms exhibited excellent solubility, biocompatibility and stability in the physiological pH and specific cytotoxicity towards the cancer cells (Chowdhury et al. 2013; Lu et al. 2014; Fiorillo et al. 2015). From the limited data available about graphene based toxicity, most of the cell viability issues are associated with size, dose or synthesis approach (Bianco 2013; Das et al. 2013; Kanakia et al. 2014; Chng and Pumera 2013).

Few reports on toxicity analysis of graphene in liver, lung, epithelial, brain cells and macrophages have exhibited dose dependant toxicity profiles. The cytotoxicity effects are associated with either apoptosis or necrosis, which are triggered by activation of caspases, intracellular reactive oxygen species (ROS) generation, mitochondrial stress, DNA damage and etc. (Chng and Pumera 2015; Vallabani et al. 2011). Size dependent genotoxicity effects in human stem cells were also reported for graphene materials (Akhavan et al. 2012, 2013). Above mentioned investigations of

cytotoxicity created an ambiguity in the selection of graphene for theranostic applications. However, preclinical investigations of graphene formulations on rodent and non-rodent model showed no significant toxicity towards respiratory, cardiovascular or haematological factors with a dose of <125 mg/kg. Graphene formulations caused minor changes in the heart, liver, lung, spleen, or kidney, and no changes in the brain. Moreover, the absence of accumulation or traces of the graphene formulation (after 30 days of injection) in major organs supports the effective clearance of graphene from body (Kanakia et al. 2014). Studies on in vivo and in vitro cytotoxicity analysis of metal NPs lead to the inflammogenic responses and immuno depression based on surface area and reactivity (Duffin et al. 2007; Danielsen et al. 2015; Giovanni et al. 2015; Petrarca et al. 2015). Metal NPs were investigated on their absorption, distribution, metabolism, excretion in cell lines and living model organisms and based on the oxidative, inflammatory and genotoxic responses, cytotoxicity profiles were evaluated. The uncertainties and the complexities in the cytotoxicity results depend on size, dose as well as mode of administration of different metal NPs (Johnston et al. 2010; Cho et al. 2012; Schrand et al. 2010; Park et al. 2007; Djurišić et al. 2015; Ivask et al. 2015).

To address the biocompatibility issues, graphene-metal hybrid materials were examined in theranostic applications and most of the studies revealed extended stability and good biocompatibility (Nergiz et al. 2014; Yang et al. 2015; Zhang et al. 2015). For instance, the RGO–Au nanosystem was utilized in the photoacoustic detection and thermal phototherapy, which were used in in vitro and in vivo analysis. No drop in body weight or any noticeable organ damage were observed for the subjected animal models, however, successful elimination of brain tumour cells and effective suppression of tumour recurrence was observed as a result of the treatment (Dembereldorj et al. 2014). Another core shell structure of GO-Au preparation was tested for chemo-phototherapy towards hepatoma with excellent biosafety towards untargeted cells (Xu et al. 2013a). In another study, Zhou et al. (2014) performed a quantitative analysis of intracellular interactions and cytotoxicity of Au-graphene and Ag-graphene materials in A549 cells and HepG2-liver hepatocellular carcinoma cells. From the observations, the graphene metal nanomaterials showed significant enhancement in the cellular uptake compared with the NPs alone. In detail, the GO conjugated AuNPs and AgNPs exhibited significantly higher toxicity than the corresponding bulk concentrations of metal nanoparticle alone. Observations on A549 cells resulted in high lactate dehydrogenase (LDH) release corresponding to the cell membrane damage, enhanced ROS levels and relative lower cell viability for the GO-metal complexes as compared with the metal NPs alone. In addition, Ag-GO nanocomposite showed the highest toxicity followed by AuNPs and AgNPs, GO and then Au-GO with the least toxicity effects. A similar observation was noticed in the case of HepG2 cells (Zhou et al. 2014).

Being the part of cell-mediated immune system, macrophage cells were also used for testing the biocompatibility of nanomaterials in a recent study. Nanocomposite made of GO and pristine Ag were tested against 2 macrophages—a tumoral lineage (J774) and peritoneal macrophages collected from Balb/c mouse. When tested along with GO and AgNPs, the GO-Ag nanocomposite materials

showed less cellular uptake by macrophages but induced a significant toxicity profile with higher oxidative stress. Additionally, the stability of the nanocomposite in terms of zeta potential values was drastically reduced in the cellular medium. The cytotoxicity analysis on peritoneal macrophages showed a dose and time dependent toxicity profile with half-inhibitory concentration (IC_{50}) of 2.9 μg/ml for Ag-GO nanocomposite, whereas the counterpart AgNPs and GO showed 3 and 24.7 μg/ml, respectively. But in the case of J774 macrophage, Ag showed the highest toxicity profile. The mechanism is explained by endocytosis of Ag–GO nanocomposite by the macrophage followed by nanocomposite degradation. Where, the Ag ions are released to the cytoplasm leading to the impairment of mitochondrial function thus generating toxic radicals and oxidative stress (Luna et al. 2016).

In another study, the microbial toxicity of RGO-Ag nanocomposite was evaluated qualitatively and quantitatively both in Gram positive and Gram negative bacterial cells. The results displayed enhanced cytotoxic effects of RGO-Ag as compared to RGO and Ag alone due to the synergistic antibacterial potential of RGO and AgNPs. The species specific cytotoxic response of RGO-Ag was comparable with standard antibiotic Chloramphenicol (Geetha Bai et al. 2016). Graphene nanoplatelets intercalated with Mn ions (10–500 μg/ml) were tested on NIH3T3 mouse fibroblasts and A498 human kidney epithelial cell for the analysis of biocompatibility, which resulted in dose and time dependant LDH release and dose dependent cytotoxicity. However, the therapeutic dosages introduced for its theranostic application involving CT and MR imaging was 5–10 times lower than the lethal dose 50% (LD_{50}) values which ensures the cytocompatibility, in vivo safety and efficacy of the graphene-Mn system (Lalwani et al. 2014).

Utilization of Pt incorporated GO with drug was also tested for the theranostic application in 4T1 breast cancer xenograft mouse models. From the investigations of biodistribution of the nanosystem in different organs, significant accumulation and apoptotic effects in tumour site were observed. No obvious weight loss or organ damage was found corresponding to the introduction of the nanosystem which confirmed the minimal systemic toxicity (Li et al. 2015a). In a separate study, graphene manganese ferrite system exhibited cytotoxicity towards bacterial model *E. coli* which showed 82% loss of viability after 2 h of treatment with 100 μg/ml, indicating its potential as an antimicrobial agent. The toxicity was contributed by membrane and oxidative stress (Chella et al. 2015). Another study focussed on the toxic potential of graphene-Cu nanocomposite performed on another model organism, Drosophila melanogaster larvae which displayed a dose and time dependent toxicity profile corresponding to higher dosage and longer incubation time. The dose dependent toxicity was correlated with the ROS generation, lipid peroxidation and apoptotic index, where, a concentration of 0.033 μg/μl was evaluated as the no observed adverse effect level (NOAEL) (Siddique et al. 2013). In a nutshell, there are very limited reports available on the graphene–metal based nanosystems, thus their biocompatibility and molecular interactions are not very clear. Further investigations are highly recommended for clarifying the fundamental mechanism of toxicity issues related with graphene metal nanotheranostic systems.

However, it is apparent that the cytotoxicity of the synthesized graphene-metal nanocomposite is highly dependent on the size, morphology of the nanocomposite as well as the synthesis of the graphene itself.

12 Conclusion

When the metal size is reduced to less than 20 nm and in cluster size, various amazing properties were observed including high catalytic activity, high magnetic potential as well strong luminescence which can be fabricated into a turn-on or turn-off biosensing system. As NCs tend to agglomerate or undergo coalescence, a substrate is required for homogeneous growth of the clusters. As reported in this chapter, graphene is an excellent platform or substrate for the growth of metal NCs as can be seen by the astounding single ML growth that can be achieved by depositing metal NCs on graphene. By changing the type of graphene/metal Moiré template, the nucleation site for the growth of NCs can be manipulated to either fcc-, hcp- or both depending on the type of metal substrate used. This property is highly advantageous for the development of magnetic devices. The graphene/metal Moiré template is also robust as it was thermally stable up to the tested temperature of 800 K. A much simpler approach for the synthesis of NCs loaded graphene in the form of GO or RGO was also explored. Metal NCs were either directly deposited on the graphene surface or was stabilized by inducing the growth of NCs in polymers, peptides or DNAs. Various applications are cited which range from drug delivery, to biosensing of glucose, cancer cells as well as specific genes. With the lucrative applications of NCs loaded graphene in theranostics, this raises the question of toxicity of the material for potential clinical applications. Based on the reports, it could be found that NCs are toxic, however, the toxicity is greatly subdued by the presence of graphene. It was also found that the cytotoxicity of graphene correlates well with the synthesis approaches towards its production. Thus, a more biocompatible graphene synthesis can be employed to produce metal NCs loaded graphene which are non-toxic to normal human cells. Although the practicality of utilizing comparatively new materials such as graphene and metal clusters in the biomedical field is still an ocean to be explored, however, with the fast growth of research in this sector and with recent huge focus for in vivo applications, metal NCs loaded graphene is not that far off for clinical applications.

Acknowledgements The authors would like to thank the University of Nottingham Malaysia Campus for the Internal Grant (UNR20007).

References

Akhavan O, Ghaderi E, Akhavan A (2012) Size-dependent genotoxicity of graphene nanoplatelets in human stem cells. Biomaterials 33:8017–8025

Akhavan O, Ghaderi E, Emamy H, Akhavan F (2013) Genotoxicity of graphene nanoribbons in human mesenchymal stem cells. Carbon 54:419–431

Amidror I, Hersch RD (1999). Methods and apparatus for authentication of documents by using the intensity profile of moiré patterns. Google Patents

Auwärter W, Muntwiler M, Greber T, Osterwalder J (2002) Co on h-BN/Ni (111): from island to island-chain formation and Co intercalation. Surf Sci 511:379–386

Bai H, Li C, Shi G (2011) Functional composite materials based on chemically converted graphene. Adv Mater 23:1089–1115

Balcioglu M, Rana M, Yigit MV (2013) Doxorubicin loading on graphene oxide, iron oxide and gold nanoparticle hybrid. J Mater Chem B 1:6187–6193

Bartelt N, McCarty K (2012) Graphene growth on metal surfaces. MRS Bull 37:1158–1165

Berko A, Szökő J, Solymosi F (2004) Effect of CO on the morphology of Pt nanoparticles supported on TiO_2 (110)-(1 × n). Surf Sci 566:337–342

Bianco A (2013) Graphene: Safe or toxic? The two faces of the medal. Angew Chem Int Ed 52:4986–4997

Biela A, Watkinson M, Meier UC, Baker D, Giovannoni G, Becer CR, Krause S (2015) Disposable MMP-9 sensor based on the degradation of peptide cross-linked hydrogel films using electrochemical impedance spectroscopy. Biosens Bioelectron 68:660–667

Binz SM, Hupalo M, Liu X, Wang CZ, Lu WC, Thiel PA, Ho KM, Conrad E, Tringides MC (2012) High island densities and long range repulsive interactions: Fe on epitaxial graphene. Phys Rev Lett 109:026103

Bo X, Ndamanisha JC, Bai J, Guo L (2010) Nonenzymatic amperometric sensor of hydrogen peroxide and glucose based on Pt nanoparticles/ordered mesoporous carbon nanocomposite. Talanta 82:85–91

Borodko Y, Habas SE, Koebel M, Yang P, Frei H, Somorjai GA (2006) Probing the interaction of poly (vinylpyrrolidone) with platinum nanocrystals by UV-Raman and FTIR. J Phys Chem B 110:23052–23059

Borodko Y, Humphrey SM, Tilley TD, Frei H, Somorjai GA (2007) Charge-transfer interaction of poly (vinylpyrrolidone) with platinum and rhodium nanoparticles. J Phys Chem C 111:6288–6295

Boyen HG, Kästle G, Weigl F, Koslowski B, Dietrich C, Ziemann P, Spatz J, Riethmüller S, Hartmann C, Möller M (2002) Oxidation-resistant gold-55 clusters. Science 297:1533–1536

Brihuega I, Michaelis CH, Zhang J, Bose S, Sessi V, Honolka J, Schneider MA, Enders A, Kern K (2008) Electronic decoupling and templating of Co nanocluster arrays on the boron nitride nanomesh. Surf Sci 602:L95–L99

Brune H (1998) Microscopic view of epitaxial metal growth: nucleation and aggregation. Surf Sci Rep 31:125–229

Brust M, Walker M, Bethell D, Schiffrin DJ, Whyman R (1994) Synthesis of thiol-derivatised gold nanoparticles in a two-phase Liquid-Liquid system. J Chem Soc Chem Commun 801–802

Brust M, Fink J, Bethell D, Schiffrin DJ, Kiely C (1995) Synthesis and reactions of functionalised gold nanoparticles. J Chem Soc Chem Commun 1655–1656

Campbell CT (2004) The active site in nanoparticle gold catalysis. Science 306:234–235

Cavallin A, Pozzo M, Africh C, Baraldi A, Vesselli E, Dri C, Comelli G, Larciprete R, Lacovig P, Lizzit S (2012) Local electronic structure and density of edge and facet atoms at Rh nanoclusters self-assembled on a graphene template. ACS Nano 6:3034–3043

Chan TL, Yao Y, Wang C, Lu W, Li J, Qian X, Yip S, Ho K (2007) Highly localized quasiatomic minimal basis orbitals for Mo from ab initio calculations. Physical Review B 76:205119

Chang G, Shu H, Huang Q, Oyama M, Ji K, Liu X, He Y (2015) Synthesis of highly dispersed Pt nanoclusters anchored graphene composites and their application for non-enzymatic glucose sensing. Electrochim Acta 157:149–157

Chella S, Kollu P, Komarala EVP, Doshi S, Saranya M, Felix S, Ramachandran R, Saravanan P, Koneru VL, Venugopal V (2015) Solvothermal synthesis of MnF_2O_4-graphene composite—investigation of its adsorption and antimicrobial properties. Appl Surf Sci 327:27–36

Chen M, Goodman D (2004) The structure of catalytically active gold on titania. Science 306:252–255

Chen M, Goodman D (2006a) Structure-activity relationships in supported Au catalysts. Catal Today 111:22–33

Chen M, Goodman DW (2006b) Catalytically active gold: from nanoparticles to ultrathin films. Acc Chem Res 39:739–746

Chen A, Holt Hindle P (2010) Platinum-based nanostructured materials: synthesis, properties, and applications. Chem Rev 110:3767–3804

Chen W, Loh KP, Xu H, Wee A (2004) Growth of monodispersed cobalt nanoparticles on 6H–SiC (0001) honeycomb template. Appl Phys Lett 84:281–283

Chen XM, Lin ZJ, Chen DJ, Jia TT, Cai ZM, Wang XR, Chen X, Chen GN, Oyama M (2010) Nonenzymatic amperometric sensing of glucose by using palladium nanoparticles supported on functional carbon nanotubes. Biosens Bioelectron 25:1803–1808

Chen Y, Xu P, Shu Z, Wu M, Wang L, Zhang S, Zheng Y, Chen H, Wang J, Li Y (2014) Multifunctional graphene oxidebased triple stimuliresponsive nanotheranostics. Adv Funct Mater 24:4386–4396

Chen H, Liu F, Lei Z, Ma L, Wang Z (2015) Fe_2O_3@ Au core@ shell nanoparticle–graphene nanocomposites as theranostic agents for bioimaging and chemo-photothermal synergistic therapy. RSC Adv 5:84980–84987

Chen H, Liu Z, Li S, Su C, Qiu X, Zhong H, Guo Z (2016) Fabrication of graphene and AuNP core polyaniline shell nanocomposites as multifunctional theranostic platforms for SERS real-time monitoring and chemo-photothermal therapy. Theranostics 6:1096

Chng ELK, Pumera M (2013) The toxicity of graphene oxides: dependence on the oxidative methods used. Chem-Eur J 19:8227–8235

Chng ELK, Pumera M (2015) Toxicity of graphene related materials and transition metal dichalcogenides. RSC Adv 5:3074–3080

Cho WS, Duffin R, Poland CA, Duschl A, Oostingh GJ, Macnee W, Bradley M, Megson IL, Donaldson K (2012) Differential pro-inflammatory effects of metal oxide nanoparticles and their soluble ions in vitro and in vivo; zinc and copper nanoparticles, but not their ions, recruit eosinophils to the lungs. Nanotoxicology 6:22–35

Choi S, Dickson RM, Yu J (2012) Developing luminescent silver nanodots for biological applications. Chem Soc Rev 41:1867–1891

Chowdhury SM, Lalwani G, Zhang K, Yang JY, Neville K, Sitharaman B (2013) Cell specific cytotoxicity and uptake of graphene nanoribbons. Biomaterials 34:283–293

Chuang MK, Lin SW, Chen FC, Chu CW, Hsu CS (2014) Gold nanoparticle-decorated graphene oxides for plasmonic-enhanced polymer photovoltaic devices. Nanoscale 6:1573–1579

Clark G, Kesmodel L (1993) Ultrahigh vacuum scanning tunneling microscopy studies of platinum on graphite. J Vac Sci Technol, B 11:131–136

Coraux J, N'Diaye AT, Busse C, Michely T (2008) Structural coherency of graphene on Ir (111). Nano Lett 8:565–570

Coraux J, Engler M, Busse C, Wall D, Buckanie N, Zu Heringdorf FJ. M., Van Gastel, R., Poelsema, B. & Michely, T. 2009. Growth of graphene on Ir (111). *New Journal of Physics,* 11, 023006

Couillard M, Pratontep S, Palmer R (2003) Metastable ordered arrays of size-selected Ag clusters on graphite. Appl Phys Lett 82:2595

Crespo P, Litrán R, Rojas T, Multigner M, de la Fuente J, Sánchez-López J, García M, Hernando A, Penadés S, Fernández A (2004) Permanent magnetism, magnetic anisotropy, and hysteresis of thiol-capped gold nanoparticles. Phys Rev Lett 93:087204

Cui M, Zhao Y, Song Q (2014) Synthesis, optical properties and applications of ultra-small luminescent gold nanoclusters. TrAC Trends Anal Chem 57:73–82

Danielsen PH, Cao Y, Roursgaard M, Møller P, Loft S (2015) Endothelial cell activation, oxidative stress and inflammation induced by a panel of metal-based nanomaterials. Nanotoxicology 9:813–824

Das S, Singh S, Singh V, Joung D, Dowding JM, Reid D, Anderson J, Zhai L, Khondaker SI, Self WT (2013) Oxygenated functional group density on graphene oxide: its effect on cell toxicity. Part Part Syst Charact 30:148–157

De Parga AV, Calleja F, Borca B, Passeggi Jr M, Hinarejos J, Guinea F, Miranda R (2008) Periodically rippled graphene: growth and spatially resolved electronic structure. Phys Rev Lett 100:056807

Dedkov YS, Fonin M, Rüdiger U, Laubschat C (2008) Graphene-protected iron layer on Ni (111). Appl Phys Lett 93:022509

Degen S, Becker C, Wandelt K (2004) Thin alumina films on Ni 3 Al (111): a template for nanostructured Pd cluster growth. Faraday Discuss 125:343–356

Dembereldorj U, Choi SY, Ganbold EO, Song NW, Kim D, Choo J, Lee SY, Kim S, Joo SW (2014) Gold nanorod assembled PEGylated graphene oxide nanocomposites for photothermal cancer therapy. Photochem Photobiol 90:659–666

di Vece M, Grandjean D, van Bael M, Romero C, Wang X, Decoster S, Vantomme A, Lievens P (2008) Hydrogen-induced ostwald ripening at room temperature in a Pd nanocluster film. Phys Rev Lett 100:236105

Dietsche R, Lim DC, Bubek M, Lopez Salido I, Ganteför G, Kim YD (2008) Comparison of electronic structures of mass-selected Ag clusters and thermally grown Ag islands on sputter-damaged graphite surfaces. Appl Phys A 90:395–398

Díez I, Ras RH (2011) Fluorescent silver nanoclusters. Nanoscale 3:1963–1970

Ding H, Schmid A, Keavney D, Li D, Cheng R, Pearson J, Fradin F, Bader S (2005) Selective growth of Co nanoislands on an oxygen-patterned Ru (0001) surface. Phys Rev B 72:035413

Djurišić AB, Leung YH, Ng A, Xu XY, Lee PK, Degger N (2015) Toxicity of metal oxide nanoparticles: mechanisms, characterization, and avoiding experimental artefacts. Small 11:26–44

Dong H, Gao W, Yan F, Ji H, Ju H (2010) Fluorescence resonance energy transfer between quantum dots and graphene oxide for sensing biomolecules. Anal Chem 82:5511–5517

Donner K, Jakob P (2009) Structural properties and site specific interactions of Pt with the graphene/Ru (0001) moiré overlayer. J Chem Phys 131:164701

Duffin R, Tran L, Brown D, Stone V, Donaldson K (2007) Proinflammogenic effects of low-toxicity and metal nanoparticles in vivo and in vitro: highlighting the role of particle surface area and surface reactivity. Inhalation Toxicol 19:849–856

Dupas C, Lahmani M (2007) Nanoscience: nanotechnologies and nanophysics, Springer Science & Business Media

Dupraz CJF, Nickels P, Beierlein U, Huynh WU, Simmel FC (2003) Towards molecular-scale electronics and biomolecular self-assembly. Superlattices Microstruct 33:369–379

Edgington LE, Berger AB, Blum G, Albrow VE, Paulick MG, Lineberry N, Bogyo M (2009) Noninvasive optical imaging of apoptosis by caspase-targeted activity-based probes. Nat Med 15:967–973

Enderlein C, Kim Y, Bostwick A, Rotenberg E, Horn K (2010) The formation of an energy gap in graphene on ruthenium by controlling the interface. New J Phys 12:033014

Evans J, Thiel P, Bartelt MC (2006) Morphological evolution during epitaxial thin film growth: Formation of 2D islands and 3D mounds. Surf Sci Rep 61:1–128

Fang J, Zhang B, Yao Q, Yang Y, Xie J, Yan N (2016) Recent advances in the synthesis and catalytic applications of ligand-protected, atomically precise metal nanoclusters. Coord Chem Rev 322:1–29

Feibelman PJ (2008) Pinning of graphene to Ir (111) by flat Ir dots. Phys Rev B 77:165419

Fiorillo M, Verre AF, Iliut M, Peiris Pagés M, Ozsvari B, Gandara R, Cappello AR, Sotgia F, Vijayaraghavan A, Lisanti MP (2015) Graphene oxide selectively targets cancer stem cells,

across multiple tumor types: implications for non-toxic cancer treatment, via "differentiation-based nano-therapy". Oncotarget 6:3553–3562
Fonin M, Dedkov YS, Rüdiger U, Güntherodt G (2003) Growth and structure of Mn on Au (111) at room temperature. Surf Sci 529:L275–L280
Freire RL, Kiejna A, da Silva JL (2014) Adsorption of Rh, Pd, Ir, and Pt on the Au (111) and Cu (111) surfaces: A density functional theory investigation. J Phys Chem C 118:19051–19061
Fujita T, Kobayashi W, Oshima C (2005) Novel structures of carbon layers on a Pt (111) surface. Surf Interface Anal 37:120–123
Gao L, Guest JR, Guisinger NP (2010) Epitaxial graphene on Cu (111). Nano Lett 10:3512–3516
Gao H, Xiao F, Ching CB, Duan H (2011) One-step electrochemical synthesis of PtNi nanoparticle-graphene nanocomposites for nonenzymatic amperometric glucose detection. ACS App Mater Interfaces 3:3049–3057
Gautier C, Bürgi T (2008) Chiral inversion of gold nanoparticles. J Am Chem Soc 130:7077–7084
Geddes CD, Lakowicz JR (2009) Reviews in fluorescence 2007. Springer
Geetha Bai R, Kasturi M, Sivakumar M (2015) Nanotechnology applications for tissue engineering. In: Thomas S, Grohens Y, Ninan N (eds) Nanomedicine in theranostics. Elsevier, Netherlands, pp 195–213
Geetha Bai R, Muthoosamy K, Shipton FN, Pandikumar A, Rameshkumar P, Huang NM, Manickam S (2016) The biogenic synthesis of a reduced graphene oxide–silver (RGO–Ag) nanocomposite and its dual applications as an antibacterial agent and cancer biomarker sensor. RSC Adv 6:36576–36587
Gehrig S, Sami H, Ogris M (2014) Gene therapy and imaging in preclinical and clinical oncology: recent developments in therapy and theranostics. Ther Deliv 5:1275–1296
Geim AK (2009) Graphene: status and prospects. Science 324:1530–1534
Gerber T, Busse C, Mysliveček J, Coraux J, Michely T (2009) A versatile fabrication method for cluster superlattices. New J Phys 11:103045
Gerber T, Knudsen J, Feibelman PJ, Granas E, Stratmann P, Schulte K, Andersen JN, Michely T (2013) CO-induced Smoluchowski ripening of Pt cluster arrays on the graphene/Ir (111) Moiré. ACS Nano 7:2020–2031
Gierz I, Riedl C, Starke U, Ast CR, Kern K (2008) Atomic hole doping of graphene. Nano Lett 8:4603–4607
Giovannetti G, Khomyakov P, Brocks G, Karpan VV, van den Brink J, Kelly P (2008) Doping graphene with metal contacts. Phys Rev Lett 101:026803
Giovanni M, Yue J, Zhang L, Xie J, Ong CN, Leong DT (2015) Pro-inflammatory responses of RAW264. 7 macrophages when treated with ultralow concentrations of silver, titanium dioxide, and zinc oxide nanoparticles. J Hazard Mater 297:146–152
Goldby I, Kuipers L, von Issendorff B, Palmer R (1996) Diffusion and aggregation of sizeselected silver clusters on a graphite surface. Appl Phys Lett 69:2819–2821
Graham G, Schmitz P, Thiel PA (1990) Growth of Rh, Pd, and Pt films on Cu (100). Phys Rev B 41:3353
Gu Y, Wen Q, Kuang Y, Tang L, Jiang J (2014) Peptide-templated gold nanoclusters as a novel label-free biosensor for the detection of protease activity. RSC Advances 4:13753–13756
Guo S, Wen D, Zhai Y, Dong S, Wang E (2010) Platinum nanoparticle ensemble-on-graphene hybrid nanosheet: one-pot, rapid synthesis, and used as new electrode material for electrochemical sensing. ACS Nano 4:3959–3968
Habiba K, Encarnacion Rosado J, Garcia-Pabon K., Villalobos Santos JC, Makarov VI, Avalos JA, Weiner BR, Morell G (2016) Improving cytotoxicity against cancer cells by chemo-photodynamic combined modalities using silver-graphene quantum dots nanocomposites. Int J Nanomed 11:107
Häkkinen H, Abbet S, Sanchez A, Heiz U, Landman U (2003) Structural, electronic, and impuritydoping effects in nanoscale chemistry: supported gold nanoclusters. Angew Chem Int Ed 42:1297–1300
Hamada I, Otani M (2010) Comparative van der Waals density-functional study of graphene on metal surfaces. Phys Rev B 82:153412

Henry CR (1998) Surface studies of supported model catalysts. Surf Sci Rep 31:231–325
Hidalgo C (2012) Physical properties of biological membranes and their functional implications, Springer Science & Business Media
Holt Hindle P, Nigro S, Asmussen M, Chen A (2008) Amperometric glucose sensor based on platinum–iridium nanomaterials. Electrochem Commun 10:1438–1441
Hong Y, Ku M, Heo D, Hwang S, Lee E, Park J, Choi J, Lee HJ, Seo M, Lee EJ (2014) Molecular recognition of proteolytic activity in metastatic cancer cells using fluorogenic gold nanoprobes. Biosens Bioelectron 57:171–178
Hövel H, Becker T, Bettac A, Reihl B, Tschudy M, Williams E (1997) Controlled cluster condensation into preformed nanometer-sized pits. J Appl Phys 81:154–158
Hsin YL, Hwang KC, Yeh CT (2007) Poly (vinylpyrrolidone)-modified graphite carbon nanofibers as promising supports for PtRu catalysts in direct methanol fuel cells. J Am Chem Soc 129:9999–10010
Huang L, Pan Y, Pan L, Gao M, Xu W, Que Y, Zhou H, Wang Y, Du S, Gao HJ (2011) Intercalation of metal islands and films at the interface of epitaxially grown graphene and Ru (0001) surfaces. Appl Phys Lett 99:163107
Huang CC, Chang PY, Liu CL, Xu JP, Wu SP, Kuo WC (2015) New insight on optical and magnetic Fe_3O_4 nanoclusters promising for near infrared theranostic applications. Nanoscale 7:12689–12697
Hummers Jr WS, Offeman RE (1958) Preparation of graphitic oxide. J Am Chem Soc 80:1339–1339
Hupalo M, Tringides M (2007) Ultrafast kinetics in Pb/Si (111) from the collective spreading of the wetting layer. Phys Rev B 75:235443
Hupalo M, Conrad E, Tringides M (2009) Growth mechanism for epitaxial graphene on vicinal 6 H-SiC (0001) surfaces: a scanning tunneling microscopy study. Phys Rev B 80:041401
Hupalo M, Binz S, Tringides M (2011a) Strong metal adatom–substrate interaction of Gd and Fe with graphene. J Phys: Condens Matter 23:045005
Hupalo M, Liu X, Wang CZ, Lu WC, Yao YX, Ho KM, Tringides MC (2011b) Metal nanostructure formation on graphene: weak versus strong bonding. Adv Mater 23:2082–2087
Hvolbæk B, Janssens TV, Clausen BS, Falsig H, Christensen CH, Nørskov JK (2007) Catalytic activity of Au nanoparticles. Nano Today 2:14–18
Ivanovskaya V, Zobelli A, Teillet Billy D, Rougeau N, Sidis V, Briddon P (2010) Hydrogen adsorption on graphene: a first principles study. Eur Phys J B 76:481–486
Ivask A, Titma T, Visnapuu M, Vija H, Kakinen A, Sihtmae M, Pokhrel S, Madler L, Heinlaan M, Kisand V (2015) Toxicity of 11 metal oxide nanoparticles to three mammalian cell types in vitro. Curr Top Med Chem 15:1914–1929
Jakob P, Gsell M, Menzel D (1999) Directional preference in particle motion: Self-trapping of vacancies in an ordered adsorbate layer. Phys Rev B 59:13285
Ji K, Chang G, Oyama M, Shang X, Liu X, He Y (2012) Efficient and clean synthesis of graphene supported platinum nanoclusters and its application in direct methanol fuel cell. Electrochim Acta 85:84–89
Jia WZ, Wang K, Zhu ZJ, Song HT, Xia XH (2007) One-step immobilization of glucose oxidase in a silica matrix on a Pt electrode by an electrochemically induced sol-gel process. Langmuir 23:11896–11900
Johnston HJ, Hutchison G, Christensen FM, Peters S, Hankin S, Stone V (2010) A review of the in vivo and in vitro toxicity of silver and gold particulates: particle attributes and biological mechanisms responsible for the observed toxicity. Crit Rev Toxicol 40:328–346
Kalluru P, Vankayala R, Chiang C-S, Hwang KC (2016) Nano-graphene oxide-mediated In vivo fluorescence imaging and bimodal photodynamic and photothermal destruction of tumors. Biomaterials 95:1–10
Kanakia S, Toussaint JD, Chowdhury SM, Tembulkar T, Lee S, Jiang YP, Lin RZ, Shroyer KR, Moore W, Sitharaman B (2014) Dose ranging, expanded acute toxicity and safety pharmacology studies for intravenously administered functionalized graphene nanoparticle formulations. Biomaterials 35:7022–7031

Kang H, Jang SW, Pak JH, Shim S (2015) Glaucine inhibits breast cancer cell migration and invasion by inhibiting MMP-9 gene expression through the suppression of NF-κB activation. Mol Cell Biochem 403:85–94

Kennedy TAC, Maclean JL, Liu J (2012) Blue emitting gold nanoclusters templated by poly-cytosine DNA at low pH and poly-adenine DNA at neutral pH. Chem Commun 48:6845–6847

Ketchie WC, Murayama M, Davis RJ (2007) Promotional effect of hydroxyl on the aqueous phase oxidation of carbon monoxide and glycerol over supported Au catalysts. Top Catal 44:307–317

Kholmanov I, Gavioli L, Fanetti M, Casella M, Cepek C, Mattevi C, Sancrotti M (2007) Effect of substrate surface defects on the morphology of Fe film deposited on graphite. Surf Sci 601:188–192

Khomyakov P, Giovannetti G, Rusu P, Brocks GV, van den Brink J, Kelly P (2009) First-principles study of the interaction and charge transfer between graphene and metals. Physical Review B 79:195425

Kiew SF, Kiew LV, Lee HB, Imae T, Chung LY (2016) Assessing biocompatibility of graphene oxide-based nanocarriers: a review. J Controlled Release 226:217–228

Kitakami O, Okamoto S, Shimada Y (1996) Effect of surface free energy of underlayer materials on crystal growth of Co polycrystalline films. J Appl Phys 79:6880–6883

Kjeldsen L, Bjerrum OW, Hovgaard D, Johnsen AH, Sehested M, Borregaard N (1992) Human neutrophil gelatinase: a marker for circulating blood neutrophils. Purification and quantitation by enzyme linked immunosorbent assay. Eur J Haematol 49:180–191

Koh TW, Hiszpanski AM, Sezen M, Naim A, Galfsky T, Trivedi A, Loo YL, Menon V, Rand BP (2015) Metal nanocluster light-emitting devices with suppressed parasitic emission and improved efficiency: Exploring the impact of photophysical properties. Nanoscale 7:9140–9146

Kondo T, Iwasaki Y, Honma Y, Takagi Y, Okada S, Nakamura J (2009) Formation of nonbonding π electronic states of graphite due to Pt-C hybridization. Phys Rev B 80:233408

Kuila T, Bose S, Khanra P, Mishra AK, Kim NH, Lee JH (2011) Recent advances in graphene-based biosensors. Biosens Bioelectron 26:4637–4648

Lahiri J, Batzill M (2010) Graphene destruction by metal-carbide formation: An approach for patterning of metal-supported graphene. Appl Phys Lett 97:023102

Lalwani G, Sundararaj JL, Schaefer K, Button T, Sitharaman B (2014) Synthesis, characterization, in vitro phantom imaging, and cytotoxicity of a novel graphene-based multimodal magnetic resonance imaging-X-ray computed tomography contrast agent. J Mater Chem B 2:3519–3530

Lang B (1975) A LEED study of the deposition of carbon on platinum crystal surfaces. Surf Sci 53:317–329

Latorre A, Somoza Á (2012) DNA mediated silver nanoclusters: synthesis, properties and applications. ChemBioChem 13:951–958

Le AT, Giang CD, Tuan TQ, Phan VN, Alonso J, Devkota J, Garaio E, García JÁ, Martín Rodríguez R, Fdez Gubieda ML (2016) Enhanced magnetic anisotropy and heating efficiency in multi-functional manganese ferrite/graphene oxide nanostructures. Nanotechnology 27:155707

Lee C, Wei X, Kysar JW, Hone J (2008) Measurement of the elastic properties and intrinsic strength of monolayer graphene. Science 321:385–388

Li Y, Somorjai GA (2010) Nanoscale advances in catalysis and energy applications. Nano Lett 10:2289–2295

Li D, Mueller MB, Gilje S, Kaner RB, Wallace GG (2008) Processable aqueous dispersions of graphene nanosheets. Nat Nanotechnol 3:101–105

Li J, Lyv Z, Li Y, Liu H, Wang J, Zhan W, Chen H, Chen H, Li X (2015a) A theranostic prodrug delivery system based on Pt (IV) conjugated nano-graphene oxide with synergistic effect to enhance the therapeutic efficacy of Pt drug. Biomaterials 51:12–21

Li X, Zhang Y, Wu Y, Duan Y, Luan X, Zhang Q, An Q (2015b) Combined photothermal and surface-enhanced Raman spectroscopy effect from spiky noble metal nanoparticles wrapped

within graphene-polymer layers: using layer-by-layer modified reduced graphene oxide as reactive precursors. ACS Appl Mater Interfaces 7:19353–19361
Li Z, Ke H, Wang J, Miao Z, Yue X (2016) Graphene oxide and gadolinium-chelate functionalized poly (lactic acid) nanocapsules encapsulating perfluorooctylbromide for ultrasound/magnetic resonance bimodal imaging guided photothermal ablation of cancer. J Nanosci Nanotechnol 16:2201–2209
Liao Q, Zhang H, Wu K, Li H, Bao S, He P (2011) Nucleation and growth of monodispersed cobalt nanoclusters on graphene moiré on Ru (0001). Nanotechnology 22:125303
Lin CAJ, Yang TY, Lee CH, Huang SH, Sperling RA, Zanella M, Li JK, Shen JL, Wang HH, Yeh HI (2009) Synthesis, characterization, and bioconjugation of fluorescent gold nanoclusters toward biological labeling applications. ACS Nano 3:395–401
Lin J, Chen X, Huang P (2016a) Graphene-based nanomaterials for bioimaging. Adv Drug Delivery Rev
Lin J, Wang X, Shen G, Cui D (2016b) 3D plasmonic ensembles of graphene oxide and nobel metal nanoparticles with ultrahigh SERS activity and sensitivity. J Nanomaterials
Liu X, Wang C, Hupalo M, Yao Y, Tringides M, Lu W, Ho K (2010) Adsorption and growth morphology of rare-earth metals on graphene studied by ab initio calculations and scanning tunneling microscopy. Phys Rev B 82:245408
Liu CL, Wu HT, Hsiao YH, Lai CW, Shih CW, Peng YK, Tang KC, Chang HW, Chien YC, Hsiao JK (2011a) Insulindirected synthesis of fluorescent gold nanoclusters: preservation of insulin bioactivity and versatility in cell imaging. Angew Chem Int Ed 50:7056–7060
Liu K, Zhang J-J, Cheng F-F, Zheng T-T, Wang C, Zhu J-J (2011b) Green and facile synthesis of highly biocompatible graphene nanosheets and its application for cellular imaging and drug delivery. J Mater Chem 21:12034–12040
Liu L, Zhou Z, Guo Q, Yan Z, Yao Y, Goodman DW (2011c) The 2-D growth of gold on single-layer graphene/Ru(0001): Enhancement of CO adsorption. Surf Sci 605:L47–L50
Liu X, Wang CZ, Hupalo M, Lu WC, Thiel PA, Ho KM, Tringides MC (2011d) Fe-Fe adatom interaction and growth morphology on graphene. Phys Rev B 84:235446
Liu X, Hupalo M, Wang CZ, Lu WC, Thiel PA, Ho KM, Tringides MC (2012a) Growth morphology and thermal stability of metal islands on graphene. Phys Rev B 86:081414
Liu X, Wang CZ, Hupalo M, Lu W, Tringides MC, Yao Y, Ho K-M (2012b) Metals on graphene: Correlation between adatom adsorption behavior and growth morphology. Phys Chem Chem Phys 14:9157–9166
Liu X, Wang CZ, Hupalo M, Lin HQ, Ho K-M, Tringides MC (2013a) Metals on graphene: interactions, growth morphology, and thermal stability. Crystals 3:79–111
Liu X, Wang F, Aizen R, Yehezkeli O, Willner I (2013b) Graphene oxide/nucleic-acid-stabilized silver nanoclusters: functional hybrid materials for optical aptamer sensing and multiplexed analysis of pathogenic DNAs. J Am Chem Soc 135:11832–11839
Lopez N, Janssens T, Clausen B, Xu Y, Mavrikakis M, Bligaard T, Nørskov JK (2004) On the origin of the catalytic activity of gold nanoparticles for low-temperature CO oxidation. J Catal 223:232–235
Lu Y, Chen W (2012) Sub-nanometre sized metal clusters: from synthetic challenges to the unique property discoveries. Chem Soc Rev 41:3594–3623
Lu Y, Wu P, Yin Y, Zhang H, Cai C (2014) Aptamer-functionalized graphene oxide for highly efficient loading and cancer cell-specific delivery of antitumor drug. J Mater Chem B 2:3849–3859
Luna LAV, Moraes ACM, Consonni SR, Pereira CD, Cadore S, Giorgio S, Alves OL (2016) Comparative in vitro toxicity of a graphene oxide-silver nanocomposite and the pristine counterparts toward macrophages. J Nanobiotechnol 14:1
Luo Z, Somers LA, Dan Y, Ly T, Kybert NJ, Mele E, Johnson AC (2010) Size-selective nanoparticle growth on few-layer graphene films. Nano Lett 10:777–781
Lux F, Sancey L, Bianchi A, Crémillieux Y, Roux S, Tillement O (2015) Gadolinium-based nanoparticles for theranostic MRI-radiosensitization. Nanomedicine 10:1801–1815

Ma Z, Liang C, Overbury SH, Dai S (2007) Gold nanoparticles on electroless-deposition-derived MnO x/C: synthesis, characterization, and catalytic CO oxidation. J Catal 252:119–126

Ma X, Tao H, Yang K, Feng L, Cheng L, Shi X, Li Y, Guo L, Liu Z (2012) A functionalized graphene oxide-iron oxide nanocomposite for magnetically targeted drug delivery, photothermal therapy, and magnetic resonance imaging. Nano Research 5:199–212

Ma Y, Huang J, Song S, Chen H, Zhang Z (2016) Cancertargeted nanotheranostics: Recent advances and perspectives. Small

Manikandan M, Abdelhamid HN, Talib A, Wu HF (2014) Facile synthesis of gold nanohexagons on graphene templates in Raman spectroscopy for biosensing cancer and cancer stem cells. Biosens Bioelectron 55:180–186

Marchini S, Günther S, Wintterlin J (2007) Scanning tunneling microscopy of graphene on Ru (0001). Phys Rev B 76:075429

Martínez Galera AJ, Brihuega I, Gómez Rodríguez JM (2011) Ethylene irradiation: a new route to grow graphene on low reactivity metals. Nano Lett 11:3576–3580

Martoccia D, Björck M, Schlepütz C, Brugger T, Pauli S, Patterson B, Greber T, Willmott P (2010) Graphene on Ru (0001): a corrugated and chiral structure. New J Phys 12:043028

McChesney JL, Bostwick A, Ohta T, Seyller T, Horn K, González J, Rotenberg E (2010) Extended van Hove singularity and superconducting instability in doped graphene. Phys Rev Lett 104:136803

Meiwes B, Karl H (2012) Metal clusters at surfaces: structure, quantum properties, physical chemistry, Springer Science & Business Media

Meng L, Jin J, Yang G, Lu T, Zhang H, Cai C (2009) Nonenzymatic electrochemical detection of glucose based on palladium—single-walled carbon nanotube hybrid nanostructures. Anal Chem 81:7271–7280

Modugno G, Ménard Moyon C, Prato M, Bianco A (2015) Carbon nanomaterials combined with metal nanoparticles for theranostic applications. Br J Pharmacol 172:975–991

Mokdad A, Dimos K, Zoppellaro G, Tucek J, Perman JA, Malina O, Andersson KK, Datta KKR, Froning JP, Zboril R (2015) The non-innocent nature of graphene oxide as a theranostic platform for biomedical applications and its reactivity towards metal-based anticancer drugs. RSC Adv 5:76556–76566

Molina L, Hammer B (2005) Some recent theoretical advances in the understanding of the catalytic activity of Au. Appl Catal A 291:21–31

Moritz W, Wang B, Bocquet ML, Brugger T, Greber T, Wintterlin J, Günther S (2010) Structure determination of the coincidence phase of graphene on Ru (0001). Phys Rev Lett 104:136102

Muhammed MAH, Verma PK, Pal SK, Kumar R, Paul S, Omkumar RV, Pradeep T (2009) Bright, NIRemitting Au23 from Au25: characterization and applications including biolabeling. Chem Eur J 15:10110–10120

Muthoosamy K, Bai RG, Manickam S (2014) Graphene and graphene oxide as a docking station for modern drug delivery system. Curr Drug Deliv 11:701–718

Muthoosamy K, Geetha Bai R, Abubakar IB, Sudheer SM, Lim HN, Loh H-S, Huang NM, Chia CH, Manickam S (2015) Exceedingly biocompatible and thin-layered reduced graphene oxide nanosheets using an eco-friendly mushroom extract strategy. Int J Nanomed 10:1505

N'Diaye A, Bleikamp S, Feibelman PJ, Michely T (2006) Two dimensional Ir-cluster lattices on Moiré of graphene with Ir (111). Phys Rev Lett 97:215501–215504

N'Diaye AT, Johann C, Tim NP, Carsten B, Thomas M (2008) Structure of epitaxial graphene on Ir (111). New J Phys 10:043033

N'diaye AT, Gerber T, Busse C, Myslivecek J, Coraux J, Michely T (2009) A versatile fabrication method for cluster superlattices. New J Phys 11

Ndlovu GF, Roos WD, Wang ZM, Asante JK, Mashapa MG, Jafta CJ, Mwakikunga BW, Hillie KT (2012) Epitaxial deposition of silver ultra-fine nano-clusters on defect-free surfaces of HOPG-derived few-layer graphene in a UHV multi-chamber by in situ STM, ex situ XPS, and ab initio calculations. Nanoscale Res Lett 7:1–8

Nergiz SZ, Gandra N, Tadepalli S, Singamaneni S (2014) Multifunctional hybrid nanopatches of graphene oxide and gold nanostars for ultraefficient photothermal cancer therapy. ACS Applied Materials & Interfaces 6:16395–16402

Neto AC, Guinea F, Peres NM, Novoselov KS, Geim AK (2009) The electronic properties of graphene. Rev Mod Phys 81:109

Nguyen PD, Cong VT, Baek C, Min J (2015) Fabrication of peptide stabilized fluorescent gold nanocluster/graphene oxide nanocomplex and its application in turn-on detection of metalloproteinase-9. Biosens Bioelectron (In Press)

Niu X, Lan M, Chen C, Zhao H (2012) Nonenzymatic electrochemical glucose sensor based on novel Pt–Pd nanoflakes. Talanta 99:1062–1067

Novotny Z, Netzer F, Dohnalek Z (2016) Ceria nanoclusters on graphene/Ru (0001): a new model catalyst system. Surf Sci 652:230–237

Obliosca JM, Liu C, Yeh H-C (2013) Fluorescent silver nanoclusters as DNA probes. Nanoscale 5:8443–8461

Orecchioni M, Cabizza R, Bianco A, Delogu LG (2015) Graphene as cancer theranostic tool: progress and future challenges. Theranostics 5:710

Overbury SH, Schwartz V, Mullins DR, Yan W, Dai S (2006) Evaluation of the Au size effect: CO oxidation catalyzed by Au/TiO2. J Catal 241:56–65

Pan Y, Dong Xia S, Hong Jun G (2007a) Formation of graphene on Ru (0001) surface. Chin Phys 16:3151

Pan Y, Neuss S, Leifert A, Fischler M, Wen F, Simon U, Schmid G, Brandau W, Jahnen Dechent W (2007b) Sizedependent cytotoxicity of gold nanoparticles. Small 3:1941–1949

Pan Y, Gao M, Huang L, Liu F, Gao HJ (2009a) Directed self-assembly of monodispersed platinum nanoclusters on graphene moiré template. Appl Phys Lett 95:093106

Pan Y, Zhang H, Shi D, Sun J, Du S, Liu F, Gao HJ (2009b) Highly ordered, millimeter-scale, continuous, singlecrystalline graphene monolayer formed on Ru (0001). Adv Mater 21:2777–2780

Park KS, Park HG (2015) A DNA-templated silver nanocluster probe for label-free, turn-on fluorescence-based screening of homo-adenine binding molecules. Biosens Bioelectron 64:618–624

Park S, Chung TD, Kim HC (2003) Nonenzymatic glucose detection using mesoporous platinum. Anal Chem 75:3046–3049

Park S, Lee YK, Jung M, Kim KH, Chung N, Ahn EK, Lim Y, Lee K-H (2007) Cellular toxicity of various inhalable metal nanoparticles on human alveolar epithelial cells. Inhalation Toxicol 19:59–65

Patthey F, Schneider WD (1995) Layer-by-layer resolved surface states of ultrathin silver islands on graphite: a photoemission study. Surf Sci 334:L715–L718

Peng C, Hu W, Zhou Y, Fan C, Huang Q (2010) Intracellular imaging with a graphene based fluorescent probe. Small 6:1686–1692

Petrarca C, Clemente E, Amato V, Pedata P, Sabbioni E, Bernardini G, Iavicoli I, Cortese S, Niu Q, Otsuki T (2015) Engineered metal based nanoparticles and innate immunity. Clin Mol Allergy 13:1

Peyser LA, Vinson AE, Bartko AP, Dickson RM (2001) Photoactivated fluorescence from individual silver nanoclusters. Science 291:103–106

Pong WT, Durkan C (2005) A review and outlook for an anomaly of scanning tunnelling microscopy (STM): Superlattices on graphite. J Phys D Appl Phys 38:R329

Qian X, Li J, Qi L, Wang CZ, Chan TL, Yao YX, Ho KM, Yip S (2008) Quasiatomic orbitals for ab initio tight-binding analysis. Phys Rev B 78:245112

Qu L, Liu Y, Baek J-B, Dai L (2010) Nitrogen-doped graphene as efficient metal-free electrocatalyst for oxygen reduction in fuel cells. ACS Nano 4:1321–1326

Remediakis IN, Lopez N, Nørskov JK (2005) CO oxidation on rutile-supported Au nanoparticles. Angew Chem Int Ed 117:1858–1860

Repain V, Baudot G, Ellmer H, Rousset S (2002) Two-dimensional long-range–ordered growth of uniform cobalt nanostructures on a Au (111) vicinal template. Europhys Lett 58:730

Retnakumari A, Setua S, Menon D, Ravindran P, Muhammed H, Pradeep T, Nair S, Koyakutty M (2009) Molecular-receptor-specific, non-toxic, near-infrared-emitting Au cluster-protein nanoconjugates for targeted cancer imaging. Nanotechnology 21:055103

Richard JA, Jean L, Romieu A, Massonneau M, Noack Fraissignes P, Renard PY (2007) Chemiluminescent probe for the in vitro detection of protease activity. Org Lett 9:4853–4855

Rodems SM, Hamman BD, Lin C, Zhao J, Shah S, Heidary D, Makings L, Stack JH, Pollok BA (2002) A FRET-based assay platform for ultra-high density drug screening of protein kinases and phosphatases. Assay Drug Dev Technol 1:9–19

Rokuta E, Hasegawa Y, Itoh A, Yamashita K, Tanaka T, Otani S, Oshima C (1999) Vibrational spectra of the monolayer films of hexagonal boron nitride and graphite on faceted Ni(755). Surf Sci 427–428:97–101

Román-Velázquez CE, Noguez C, Garzón IL (2003) Circular dichroism simulated spectra of chiral gold nanoclusters: a dipole approximation. J Phys Chem B 107:12035–12038

Rucci N, Sanita P, Angelucci A (2011) Roles of metalloproteases in metastatic niche. Curr Mol Med 11:609–622

Sandin A, Jayasekera T, Rowe J, Kim KW, Nardelli MB, Dougherty DB (2012) Multiple coexisting intercalation structures of sodium in epitaxial graphene-SiC interfaces. Phys Rev B 85:125410

Schmid M, Kresse G, Buchsbaum A, Napetschnig E, Gritschneder S, Reichling M, Varga P (2007) Nanotemplate with holes: ultrathin alumina on Ni 3 Al (111). Phys Rev Lett 99:196104

Schrand AM, Rahman MF, Hussain SM, Schlager JJ, Smith DA, Syed AF (2010) Metal-based nanoparticles and their toxicity assessment. Wiley Interdisc Rev: Nanomed Nanobiotechnol 2:544–568

Sehested J, Gelten JA, Remediakis IN, Bengaard H, Nørskov JK (2004) Sintering of nickel steam-reforming catalysts: effects of temperature and steam and hydrogen pressures. J Catal 223:432–443

Seol JH, Jo I, Moore AL, Lindsay L, Aitken ZH, Pettes MT, Li X, Yao Z, Huang R, Broido D (2010) Two-dimensional phonon transport in supported graphene. Science 328:213–216

Shen Q, Jiang L, Zhang H, Min Q, Hou W, Zhu J-J (2008) Three-dimensional dendritic Pt nanostructures: Sonoelectrochemical synthesis and electrochemical applications. J Phys Chem C 112:16385–16392

Shi J, Nie R, Chen P, Hou Z (2013) Selective hydrogenation of cinnamaldehyde over reduced graphene oxide supported Pt catalyst. Catal Commun 41:101–105

Sicot M, Bouvron S, Zander O, Rüdiger U, Dedkov YS, Fonin M (2010) Nucleation and growth of nickel nanoclusters on graphene Moiré on Rh (111). Appl Phys Lett 96:093115

Siddique YH, Fatima A, Jyoti S, Naz F, Khan W, Singh BR, Naqvi AH (2013) Evaluation of the toxic potential of graphene copper nanocomposite (GCNC) in the third instar larvae of transgenic Drosophila melanogaster (hsp70-lacZ) Bg 9. PLoS ONE 8:e80944

Son KJ, Shin DS, Kwa T, Gao Y, Revzin A (2013) Micropatterned sensing hydrogels integrated with reconfigurable microfluidics for detecting protease release from cells. Anal Chem 85:11893–11901

Song W, Wang Y, Liang R-P, Zhang L, Qiu J-D (2015) Label-free fluorescence assay for protein kinase based on peptide biomineralized gold nanoclusters as signal sensing probe. Biosens Bioelectron 64:234–240

Soy E, Liang Z, Trenary M (2015) Formation of Pt and Rh nanoclusters on a graphene Moiré pattern on Cu (111). J Phys Chem C 119:24796–24803

Stankovich S, Piner RD, Chen X, Wu N, Nguyen ST, Ruoff RS (2006) Stable aqueous dispersions of graphitic nanoplatelets via the reduction of exfoliated graphite oxide in the presence of poly (sodium 4-styrenesulfonate). J Mater Chem 16:155–158

Süle P, Szendrő M, Hwang C, Tapasztó L (2014) Rotation misorientated graphene moiré superlattices on Cu (1 1 1): classical molecular dynamics simulations and scanning tunneling microscopy studies. Carbon 77:1082–1089

Sutter PW, Flege JI, Sutter EA (2008) Epitaxial graphene on ruthenium. Nat Mater 7:406–411

Sutter E, Albrecht P, Sutter P (2009a) Graphene growth on polycrystalline Ru thin films. Appl Phys Lett 95:133109

Sutter P, Hybertsen M, Sadowski J, Sutter E (2009b) Electronic structure of few-layer epitaxial graphene on Ru (0001). Nano Lett 9:2654–2660

Sutter E, Albrecht P, Camino FE, Sutter P (2010) Monolayer graphene as ultimate chemical passivation layer for arbitrarily shaped metal surfaces. Carbon 48:4414–4420

Sutter E, Albrecht P, Wang B, Bocquet M-L, Wu L, Zhu Y, Sutter P (2011) Arrays of Ru nanoclusters with narrow size distribution templated by monolayer graphene on Ru. Surf Sci 605:1676–1684

Sutter E, Wang B, Albrecht P, Lahiri J, Bocquet ML, Sutter P (2012) Templating of arrays of Ru nanoclusters by monolayer graphene/Ru Moirés with different periodicities. J Phys: Condens Matter 24:314201

Swain AK, Pradhan L, Bahadur D (2015) Polymer stabilized Fe_3O_4-graphene as an amphiphilic drug carrier for thermo-chemotherapy of cancer. ACS Appl Mater Interfaces 7:8013–8022

Talapin DV, Murray CB (2005) PbSe nanocrystal solids for n-and p-channel thin film field-effect transistors. Science 310:86–89

Tao Y, Li M, Ren J, Qu X (2015) Metal nanoclusters: novel probes for diagnostic and therapeutic applications. Chem Soc Rev 44:8636–8663

Tian N, Zhou ZY, Sun SG, Ding Y, Wang ZL (2007) Synthesis of tetrahexahedral platinum nanocrystals with high-index facets and high electro-oxidation activity. Science 316:732–735

Vajda S, Pellin MJ, Greeley JP, Marshall CL, Curtiss LA, Ballentine GA, Elam JW, Catillon Mucherie S, Redfern PC, Mehmood F (2009) Subnanometre platinum clusters as highly active and selective catalysts for the oxidative dehydrogenation of propane. Nat Mater 8:213–216

Valden M, Lai X, Goodman DW (1998) Onset of catalytic activity of gold clusters on titania with the appearance of nonmetallic properties. Science 281:1647–1650

Vallabani N, Mittal S, Shukla RK, Pandey AK, Dhakate SR, Pasricha R, Dhawan A (2011) Toxicity of graphene in normal human lung cells (BEAS-2B). J Biomed Nanotechnol 7:106–107

Van Gastel R, Martínez Galera AJ, Coraux J, Hattab H, Wall D, Zu Heringdorf F-JM, Horn Von Hoegen M, Gómez Rodríguez JM, Poelsema B, Busse C (2009) In situ observation of stress relaxation in epitaxial graphene. New J Phys 11:113056

Vargová V, Pytliak M, Mechírová V (2012) Matrix metalloproteinases. Springer, Matrix Metalloproteinase Inhibitors

Varykhalov A, Sánchez Barriga J, Shikin A, Biswas C, Vescovo E, Rybkin A, Marchenko D, Rader O (2008) Electronic and magnetic properties of quasifreestanding graphene on Ni. Phys Rev Lett 101:157601

Varykhalov A, Scholz MR, Kim TK, Rader O (2010) Effect of noble-metal contacts on doping and band gap of graphene. Phys Rev B 82:121101

Vasala K, Turpeenniemi Hujanen T (2007) Serum tissue inhibitor of metalloproteinase-2 (TIMP-2) and matrix metalloproteinase-2 in complex with the inhibitor (MMP-2:TIMP-2) as prognostic markers in bladder cancer. Clin Biochem 40:640–644

Venkateswara Rao C, Cabrera CR, Ishikawa Y (2011) Graphene-supported Pt–Au alloy nanoparticles: a highly efficient anode for direct formic acid fuel cells. J Phys Chem C 115:21963–21970

Vitos L, Ruban A, Skriver HL, Kollar J (1998) The surface energy of metals. Surf Sci 411:186–202

Wang J (2001) Glucose biosensors: 40 years of advances and challenges. Electroanalysis 13:983

Wang J (2008) Electrochemical glucose biosensors. Chem Rev 108:814–825

Wang B, Bocquet ML (2011) Monolayer graphene and h-BN on metal substrates as versatile templates for metallic nanoclusters. J Phys Chem Lett 2:2341–2345

Wang B, Bocquet ML, Marchini S, Gunther S, Wintterlin J (2008) Chemical origin of a graphene moire overlayer on Ru(0001). Phys Chem Chem Phys 10:3530–3534

Wang S, Zhang Y, Abidi N, Cabrales L (2009) Wettability and surface free energy of graphene films. Langmuir 25:11078–11081

Wang C, Li J, Amatore C, Chen Y, Jiang H, Wang XM (2011a) Gold nanoclusters and graphene nanocomposites for drug delivery and imaging of cancer cells. Angew Chem Int Ed 50:11644–11648

Wang W, Liang S, Yu T, Li D, Li Y, Han X (2011b) The study of interaction between graphene and metals by Raman spectroscopy. J Appl Phys 109:07C501

Wang Y, Zhang P, Liu CF, Zhan L, Li YF, Huang CZ (2012) Green and easy synthesis of biocompatible graphene for use as an anticoagulant. RSC Adv 2:2322–2328

Wang C, Ravi S, Garapati US, Das M, Howell M, Mallela J, Alwarappan S, Mohapatra SS, Mohapatra S (2013a) Multifunctional chitosan magnetic-graphene (CMG) nanoparticles: a theranostic platform for tumor-targeted co-delivery of drugs, genes and MRI contrast agents. J Mater Chem B 1:4396–4405

Wang Y, Wang K, Zhao J, Liu X, Bu J, Yan X, Huang R (2013b) Multifunctional mesoporous silica-coated graphene nanosheet used for chemo-photothermal synergistic targeted therapy of glioma. J Am Chem Soc 135:4799–4804

Wang S, Zhang Q, Luo XF, Li J, He H, Yang F, Di Y, Jin C, Jiang XG, Shen S (2014a) Magnetic graphene-based nanotheranostic agent for dual-modality mapping guided photothermal therapy in regional lymph nodal metastasis of pancreatic cancer. Biomaterials 35:9473–9483

Wang Y, Huang R, Liang G, Zhang Z, Zhang P, Yu S, Kong J (2014b) MRI-visualized, dualtargeting, combined tumor therapy using magnetic graphenebased mesoporous silica. Small 10:109–116

Wang Y, Polavarapu L, Liz Marzán LM (2014c) Reduced graphene oxide-supported gold nanostars for improved SERS sensing and drug delivery. ACS Appl Mater Interfaces 6:21798–21805

Wang F, Sun Q, Feng B, Xu Z, Zhang J, Xu J, Lu L, Yu H, Wang M, Li Y (2016a) Polydopaminefunctionalized graphene oxide loaded with gold nanostars and doxorubicin for combined photothermal and chemotherapy of metastatic breast cancer. Adv Healthc Mater

Wang Y, Deng R, Xie X, Huang L, Liu X (2016b) Nonlinear spectral and lifetime management in upconversion nanoparticles by controlling energy distribution. Nanoscale 8:6666–6673

Wehling T, Katsnelson M, Lichtenstein A (2009) Impurities on graphene: midgap states and migration barriers. Phys Rev B 80:085428

Wei G, Xu F, Li Z, Jandt KD (2011) Protein-promoted synthesis of Pt nanoparticles on carbon nanotubes for electrocatalytic nanohybrids with enhanced glucose sensing. J Phys Chem C 115:11453–11460

Weiss N, Cren T, Epple M, Rusponi S, Baudot G, Rohart S, Tejeda A, Repain V, Rousset S, Ohresser P (2005) Uniform magnetic properties for an ultrahigh-density lattice of noninteracting Co nanostructures. Phys Rev Lett 95:157204

Wen Q, Gu Y, Tang LJ, Yu R-Q, Jiang JH (2013) Peptide-templated gold nanocluster beacon as a sensitive, label-free sensor for protein post-translational modification enzymes. Anal Chem 85:11681–11685

Whelan C, Barnes C (1997) An STM study of structural transitions during the nucleation and growth of Pd and Cu cluster catalysts on HOPG. Appl Surf Sci 119:288–300

Wilcoxon J, Abrams B (2006) Synthesis, structure and properties of metal nanoclusters. Chem Soc Rev 35:1162–1194

Williams WD, Shekhar M, Lee WS, Kispersky V, Delgass WN, Ribeiro FH, Kim SM, Stach EA, Miller JT, Allard LF (2010) Metallic corner atoms in gold clusters supported on rutile are the dominant active site during water—gas shift catalysis. J Am Chem Soc 132:14018–14020

Wintterlin J, Bocquet ML (2009) Graphene on metal surfaces. Surf Sci 603:1841–1852

Wu Z, Jin R (2010) On the ligand's role in the fluorescence of gold nanoclusters. Nano Lett 10:2568–2573

Wu ZS, Wu Q, Yang JH, Wang HQ, Ding XD, Yang F, Xu XC (2008) Prognostic significance of MMP-9 and TIMP-1 serum and tissue expression in breast cancer. Int J Cancer 122:2050–2056

Wu GH, Song XH, Wu YF, Chen XM, Luo F, Chen X (2013) Non-enzymatic electrochemical glucose sensor based on platinum nanoflowers supported on graphene oxide. Talanta 105:379–385

Xiaofei W, Ruiyi L, Zaijun L, Junkang L, Guangli W, Zhiguo G (2014) Synthesis of double gold nanoclusters/graphene oxide and its application as a new fluorescence probe for Hg^{2+} detection with greatly enhanced sensitivity and rapidity. RSC Adv 4:24978–24985

Xu C, Wang X, Zhu J (2008a) Graphene–metal particle nanocomposites. J Phys Chem C 112:19841–19845

Xu Y, Bai H, Lu G, Li C, Shi G (2008b) Flexible graphene films via the filtration of water-soluble noncovalent functionalized graphene sheets. J Am Chem Soc 130:5856–5857

Xu Y, Semidey Flecha L, Liu L, Zhou Z, Goodman DW (2011) Exploring the structure and chemical activity of 2-D gold islands on graphene moiré/Ru (0001). Faraday Discuss 152:267–276

Xu C, Yang D, Mei L, Li Q, Zhu H, Wang T (2013a) Targeting chemophotothermal therapy of hepatoma by gold nanorods/graphene oxide core/shell nanocomposites. ACS Appl Mater Interfaces 5:12911–12920

Xu C, Yang D, Mei L, Lu B, Chen L, Li Q, Zhu H, Wang T (2013b) Encapsulating gold nanoparticles or nanorods in graphene oxide shells as a novel gene vector. ACS Appl Mater Interfaces 5:2715–2724

Yang X, Xu M, Qiu W, Chen X, Deng M, Zhang J, Iwai H, Watanabe E, Chen H (2011) Graphene uniformly decorated with gold nanodots: in situ synthesis, enhanced dispersibility and applications. J Mater Chem 21:8096–8103

Yang K, Hu L, Ma X, Ye S, Cheng L, Shi X, Li C, Li Y, Liu Z (2012) Multimodal imaging guided photothermal therapy using functionalized graphene nanosheets anchored with magnetic nanoparticles. Adv Mater 24:1868–1872

Yang K, Gong H, Shi X, Wan J, Zhang Y, Liu Z (2013) In vivo biodistribution and toxicology of functionalized nano-graphene oxide in mice after oral and intraperitoneal administration. Biomaterials 34:2787–2795

Yang L, Tseng YT, Suo G, Chen L, Yu J, Chiu WJ, Huang CC, Lin CH (2015) Photothermal therapeutic response of cancer cells to aptamer–gold nanoparticle-hybridized graphene oxide under nir illumination. ACS Appl Mater Interfaces 7:5097–5106

Yao Y, Wang C, Ho K (2010) Chemical bonding analysis for solid-state systems using intrinsic oriented quasiatomic minimal-basis-set orbitals. Phys Rev B 81:235119

Yazyev OV, Pasquarello A (2010) Metal adatoms on graphene and hexagonal boron nitride: Towards rational design of self-assembly templates. Phys Rev B 82:045407

Yin PT, Shah S, Chhowalla M, Lee KB (2015) Design, synthesis, and characterization of graphene–nanoparticle hybrid materials for bioapplications. Chem Rev 115:2483–2531

Yoo E, Okata T, Akita T, Kohyama M, Nakamura J, Honma I (2009) Enhanced electrocatalytic activity of Pt subnanoclusters on graphene nanosheet surface. Nano Lett 9:2255–2259

Yoon B, Häkkinen H, Landman U (2003) Interaction of O_2 with gold clusters: molecular and dissociative adsorption. J Phys Chem A 107:4066–4071

Yu J, Yin W, Zheng X, Tian G, Zhang X, Bao T, Dong X, Wang Z, Gu Z, Ma X (2015) Smart MoS_2/Fe_3O_4 nanotheranostic for magnetically targeted photothermal therapy guided by magnetic resonance/photoacoustic imaging. Theranostics 5:931

Yuan Z, Chen YC, Li HW, Chang HT (2014) Fluorescent silver nanoclusters stabilized by DNA scaffolds. Chem Commun 50:9800–9815

Yuan Y, Zhang Y, Liu B, Wu H, Kang Y, Li M, Zeng X, He N, Zhang G (2015) The effects of multifunctional MiR-122-loaded graphene-gold composites on drug-resistant liver cancer. J Nanobiotechnol 13:1

Zedan AF, Moussa S, Terner J, Atkinson G, el Shall MS (2012) Ultrasmall gold nanoparticles anchored to graphene and enhanced photothermal effects by laser irradiation of gold nanostructures in graphene oxide solutions. ACS Nano 7:627–636

Zhang L, Wang E (2014) Metal nanoclusters: New fluorescent probes for sensors and bioimaging. Nano Today 9:132–157

Zhang J, Sessi V, Michaelis C, Brihuega I, Honolka J, Kern K, Skomski R, Chen X, Rojas G, Enders A (2008) Ordered layers of Co clusters on BN template layers. Phys Rev B 78:165430

Zhang H, Fu Q, Cui Y, Tan D, Bao X (2009a) Fabrication of metal nanoclusters on graphene grown on Ru (0001). Chin Sci Bull 54:2446–2450

Zhang H, Fu Q, Cui Y, Tan D, Bao X (2009b) Growth mechanism of graphene on Ru (0001) and O_2 adsorption on the graphene/Ru (0001) surface. J Phys Chem C 113:8296–8301

Zhang Y, Gu YE, Lin S, Wei J, Wang Z, Wang C, Du Y, Ye W (2011) One-step synthesis of PtPdAu ternary alloy nanoparticles on graphene with superior methanol electrooxidation activity. Electrochim Acta 56:8746–8751

Zhang M, Cao Y, Chong Y, Ma Y, Zhang H, Deng Z, Hu C, Zhang Z (2013) Graphene oxide based theranostic platform for T 1-weighted magnetic resonance imaging and drug delivery. ACS Appl Mater Interfaces 5:13325–13332

Zhang H, Wu H, Wang J, Yang Y, Wu D, Zhang Y, Zhang Y, Zhou Z, Yang S (2015) Graphene oxide-BaGdF5 nanocomposites for multi-modal imaging and photothermal therapy. Biomaterials 42:66–77

Zhao X, Liu L, Li X, Zeng J, Jia X, Liu P (2014) Biocompatible graphene oxide nanoparticle-based drug delivery platform for tumor microenvironment-responsive triggered release of doxorubicin. Langmuir 30:10419–10429

Zheng J, Dickson RM (2002) Individual water-soluble dendrimer-encapsulated silver nanodot fluorescence. J Am Chem Soc 124:13982–13983

Zheng J, Petty JT, Dickson RM (2003) High quantum yield blue emission from water-soluble Au8 nanodots. J Am Chem Soc 125:7780–7781

Zheng J, Nicovich PR, Dickson RM (2007) Highly fluorescent noble metal quantum dots. Annu Rev Phys Chem 58:409

Zhi F, Dong H, Jia X, Guo W, Lu H, Yang Y, Ju H, Zhang X, Hu Y (2013) Functionalized graphene oxide mediated adriamycin delivery and miR-21 gene silencing to overcome tumor multidrug resistance in vitro. PLoS ONE 8:e60034

Zhou R, Shi M, Chen X, Wang M, Chen H (2009) Atomically monodispersed and fluorescent sub-nanometer gold clusters created by biomoleculeassisted etching of nanometersized gold particles and rods. Chem—Eur J 15:4944–4951

Zhou Z, Gao F, Goodman DW (2010) Deposition of metal clusters on single-layer graphene/Ru (0001): factors that govern cluster growth. Surf Sci 604:L31–L38

Zhou X, Dorn M, Vogt J, Spemann D, Yu W, Mao Z, Estrela Lopis I, Donath E, Gao C (2014) A quantitative study of the intracellular concentration of graphene/noble metal nanoparticle composites and their cytotoxicity. Nanoscale 6:8535–8542

Zhu M, Aikens CM, Hollander FJ, Schatz GC, Jin R (2008) Correlating the crystal structure of a thiol-protected Au25 cluster and optical properties. J Am Chem Soc 130:5883–5885

Development of Nano-antimicrobial Biomaterials for Biomedical Applications

Shekhar Agnihotri and Navneet Kaur Dhiman

Abstract Around the globe, there is a great concern about controlling growth of pathogenic microorganisms for the prevention of infectious diseases. Moreover, the greater incidences of cross contamination and overuse of drugs has contributed towards the development of drug resistant microbial strains making conditions even worse. Hospital acquired infections pose one of the leading complications associated with implantation of any biomaterial after surgery and critical care. In this regard, developing non-conventional antimicrobial agents which would prevent the aforementioned causes is under the quest. The rapid development in nanoscience and nanotechnology has shown promising potential for developing novel biocidal agents that would integrate with a biomaterial to prevent bacterial colonization and biofilm formation. Metals with inherent antimicrobial properties such as silver, copper, zinc at nano scale constitute a special class of antimicrobials which have broad spectrum antimicrobial nature and pose minimum toxicity to humans. Hence, novel biomaterials that inhibit microbial growth would be of great significance to eliminate medical device/instruments associated infections. This chapter comprises the state-of-art advancements in the development of nano-antimicrobial biomaterials for biomedical applications. Several strategies have been targeted to satisfy few important concern such as enhanced long term antimicrobial activity and stability, minimize leaching of antimicrobial material and promote reuse. The proposed strategies to develop new hybrid antimicrobial biomaterials would offer a potent antibacterial solution in healthcare sector such as wound healing applications, tissue scaffolds, medical implants, surgical devices and instruments.

Keywords Antimicrobial biomaterial · Immobilization · Nanocomposites · Silver nanoparticles · Metal nanoparticles · Biomedical coatings · Surface modification · Hydrogel · Cytotoxicity · Carbon nanotubes · Implant · Wound healing · Tissue scaffold

S. Agnihotri (✉) · N.K. Dhiman
Department of Biotechnology, Thapar University, Patiala 147004, Punjab, India
e-mail: shekharagnihotri@gmail.com; shekhar.agnihotri@thapar.edu

A. Tripathi and J.S. Melo (eds.), *Advances in Biomaterials for Biomedical Applications*, Advanced Structured Materials 66,
DOI 10.1007/978-981-10-3328-5_12

List of Abbreviations

2D	Two dimensional
3D	Three dimensional
A549	Human lung adenocarcinoma epithelial cell line
AB	Anti bacterial
AF	Antifungal
AgNP	Silver nanoparticles
AV	Antiviral
BAI	Biomaterial assisted infection
BEAS2B	Human normal bronchial epithelial cells
CACC	Calcium alginate-cotton cellulose
CFU	Colony forming units
CMC	Carboxymethyl chitosan
CNS	Carbon nanoscrolls
CNTs	Carbon nanotubes
CSNPs	Chitosan nanoparticles
CuNPs	Copper nanoparticles
CuO NPs	Copper oxide nanoparticles
DD	Degree of deacetylation
GNPs	Gold nanoparticles
GO	Graphene oxide
HA	Hydroxyapatite
HaCaT	Human keratinocyte
HAIs	Hospital acquired infections
HepG2	Human hepatoma cells
HNC	Hybrid nanocomposite
HNTs	Halloysite nanotubes
IPN	Inter-penetrating network
LBL	Layer-by-layer
MBC	Minimum bactericidal concentration
MDR	Multiple drug resistance
MIC	Minimum inhibitory concentration
MWCNTs	Multiple-walled carbon nanotubes
NCs	Nanocomposites
ND	Not Determined
NIR	Near-Infrared
NSP	Nanosilicate platelets
PTFE	Polytetrafluorethylene
QCS NPs	Quaternary ammonium chitosan derivative nanoparticles
rGO	Reduced grapheme oxide
ROS	Reactive oxygen species
SWCNTs	Single-walled carbon nanotubes
TEM	Transmission electron microscopy
USEPA	US environmental protection agency

VRE	Vancomycin resistant *Enterococci*
ZnO	Zinc oxide
ZoI	Zone of inhibition

1 Introduction

The recent progresses in health care sector have witnessed the use of biomaterials for improving life quality of critically ill patients. Biomaterials have revolutionized a few emerging areas such as biomedical engineering and tissue engineering by facilitating less-invasive techniques for continuous monitoring, improving drug administrating and enhanced mobility by either restoring or replacing organ functions (Hench and Polak 2002; Place et al. 2009; Hubbell 1995). As compared to the conventional technologies, biomaterials with improved functionality and durability have been utilized in form of vascular grafts, biocompatible coatings, medical implants, stents tissue scaffolds which might remain functional even for several months (Place et al. 2009; Ratner et al. 2004). Despite considerable success of biomaterials in ageing society, only a few biomaterials can prove their safety concerns under practically relevant conditions. Regardless of implant composition and applications, i.e., from prosthetic joints, artificial heart and dental implants to vascular valves and intraocular lenses, virtually all biomaterials behave as a "niche" to pathogenic microorganisms (Zaat et al. 2010; Busscher et al. 2012; Stewart and Costerton 2001). Under in vivo conditions, the microbes get attracted and subsequently lead to biofilm formation on biomaterial surface, leading to one of the major clinical complications often referred as biomaterial-associated infections (BAIs) (Percival et al. 2015; Campoccia et al. 2013a; Zaat et al. 2010; Busscher et al. 2012; Stewart and Costerton 2001). The greater incidences of biomaterial-associated infections thus compromise with the intended use of any implant or device and add risk to humans in terms of high morbidity and even mortality (Parsek and Singh 2003; Hall-Stoodley and Stoodley 2009). Moreover, it marks an adverse impact on economy since the existing treatment strategies to cure infection could cost even more than the initial biomaterial implantation. In a broad sense, a biomaterial faces two major challenges when implanted within the body i.e., to make suitable integration with native tissue while preventing colonization of microbes on its surface. In 1987, an orthopedic surgeon Anthony Gristina introduced a phrase "the race for the surface" referring that there exists a stern competition between tissue integration and bacterial attachment on biomaterial surface (Gristina 1987). A successful implantation of biomaterial without any infection would thus be a 'winning' situation for its intended use, though it is not the case with few of them.

Biomaterial-associated infections are most commonly caused by *Staphylococcus epidermidis*, *Staphylococcus aureus*, *Staphylococcus haemolyticus*, *Staphylococcus capitis*, *Staphylococcus saprophyticus, Staphylococcus warneri*, *Staphylococcus*

cohnii, *Staphylococcus xylosus, Staphylococcus chromogenes, Staphylococcus schleiferi, Staphylococcus lugdunensis, Escherichia coli*, *Pseudomonas aeruginosa*, *Proteus mirabilis*, *Proteus vulgaris, Candida albicans, Propionibacterium acnes* including a few other bacterial strains having low virulence potential on healthy individuals but resides within skin and mucous membranes (Jukes et al. 2010; Mack et al. 2013). The cascade for pathogenesis of BAIs follows a series of common events (Costerton et al. 1999; Parsek and Singh 2003; Busscher et al. 2012; Stewart and Costerton 2001). First step involves an initial attachment of microbial cells to biomaterial surface while the attached cells start accumulating in multiple layers leading to the formation of biofilm as a second step. Subsequently, the maturation of microbial biofilm takes place and finally, microbial consortium is detached for spreading to other parts of biomaterial surface. The implants are thus susceptible to many infections, as direct contamination to biomaterial surface during surgery starts even after few hours of implantation i.e., preoperative contamination (Maathuis et al. 2005; Campoccia et al. 2013b). The site of implant can also be accessed to microbes during hospitalization, known as hospital-acquired infections. The spreading of microbes occur due to microbial contamination on several locations other than the implant site through blood stream i.e., post-operative infections and is inevitable (Siegel et al. 2007; Campoccia et al. 2013b). As a result, the durability and functionality of biomaterial implants is severely affected which is manifested by severe complications that arise during patient's recovery.

The accumulation of microbial biofilm leads to the secretion of extracellular polymeric substance (EPS), which tends to hide microbes within its polymeric mesh and make them inaccessible to host immune system and antimicrobial therapies (Costerton et al. 1999; Hall-Stoodley et al. 2004; Hall-Stoodley and Stoodley 2009; Stewart and Costerton 2001). Sessile and adherent bacteria are thus intrinsically more resistant towards host clearance and require nearly 500–5,000 times higher concentration of common clinical antibiotics than planktonic or non-biofilm forming pathogens (Boucher et al. 2009; Donlan and Costerton 2002; Subbiahdoss et al. 2013). The therapeutic and prophylactic use of antibiotics for curing post operative infections has even contributed towards the development of microbial strains with high resistance against those drugs making conditions unmanageable. Ultimately, the removal of an infected implant would be the only possible solution followed by weeks of antibiotic treatment to remove infection before implantation of new device (Maathuis et al. 2005; Campoccia et al. 2013b; Busscher et al. 2012; Ratner et al. 2004). For these reasons, local or topical administration of antibacterial agents is preferred over routine systemic approaches which would minimize an initial attachment of bacteria on implant surfaces. Accordingly, a promising strategy for reducing the occurrence of BAIs is to prevent an initial attachment of bacteria to implant and device surfaces (Bazaka et al. 2012; Salwiczek et al. 2014; Monteiro et al. 2009). This has spurred research efforts on developing antimicrobial surfaces and coatings that can be applied to biomedical devices so as to confer resistance against bacterial colonization. To achieve this, the antibacterial biomaterial surface should reflect non-cytotoxic characteristics against mammalian cells and it should not pose any adverse effects on healthier tissues and body fluids of patients

(Harding and Reynolds 2014; Norowski and Bumgardner 2009). Moreover, therapeutic approaches to inhibit bacterial colonization yet retaining the intended properties of biomaterials is always advisable, such as the visual clarity of contact lenses or the flexibility of vascular grafts would not be compromised.

In last few years, nanotechnology has provided immense opportunities to manipulate substances at nano scale altering their physicochemical properties and transform them into potential antimicrobial agents. Owing to its small size, nanomaterials have high surface area to volume ratio which makes them more effective even at relatively lower dose concentration than their bulk form (Mauter and Elimelech 2008; Sharma et al. 2009; Rai et al. 2009; Singh et al. 2008). Moreover, the mechanism of antimicrobial action of nanomaterials can be mediated through several pathways, i.e., disruption of bacterial membrane, formation of holes and pits on cell wall, generation of ROS, binding to sulfhydryl groups of metabolic enzymes of the bacterial electron transport chain to inhibit respiratory activity, and integration with DNA (Kumar et al. 2008; Morones et al. 2005; Rai et al. 2009; Hill 2009; Zhang et al. 2012a; Panáček et al. 2006; Sharma et al. 2009; Chopra 2007). This provides inability of microorganism to develop resistance against them. Recently few reports have elucidated a more efficient, direct contact killing action of silver nanoparticles to the bacterial cell wall, which do not even require the internalization of nanoparticles into the cells and thus would be more efficient than antibiotics to inhibit bacterial resistance. As a result, nanomaterials are particularly very effective to kill the multiple drug resistant microbial strains. In particular, the inherent antimicrobial properties of coinage metals i.e., silver, gold and copper were known to us from ancient times, these metallic nanoparticles have been utilized by researchers as potential disinfectants in biomedical and water purification applications (Atiyeh et al. 2007; Russell et al. 1994). They are being introduced as one of the important component in our daily life style. Imagine an odorless textiles (antibacterial T shirts) to public hygiene (deodorants, toothbrushes, washing machines) to water purifier to processed foods packing material, to antibacterial bandages, sunscreen lotions, and cosmetics that you would certainly feel the existence of nanomaterials. More recently, silver nanoparticles are used in the coating of medical equipments such as catheters, infusion systems and dental composites. In addition, there is increasing interest in utilization of 'nanoparticulate' forms of metal, metal oxides like copper/copper oxides, zinc oxides (ZnO) and biopolymers which exhibit remarkable antimicrobial properties.

Despite this, materials at nano scale pose certain challenges which limit their development as an efficient antimicrobial agent. In the absence of any support material, the nanoparticles tend to aggregate due to their high surface reactivity such that their actual antimicrobial efficacy is severely inhibited (Gupta and Silver 1998; Li and Lenhart 2012; Morones et al. 2005; Agnihotri et al. 2012, 2013, 2015). Moreover, colloidal nanomaterials cannot be used repeatedly and thus seem to be uneconomical under practically relevant conditions. Over past few years, tremendous research activities have been focused to minimize these limitation by either immobilizing or incorporating nanoparticles onto solid support with an aim to enhance their antibacterial activities and promote their reusability

(Agnihotri et al. 2015, 2012, 2013; Zhou et al. 2014; Bakare et al. 2016; Cao et al. 2010; Lin et al. 2013; Ifuku et al. 2015; Zheng et al. 2016; Chernousova and Epple 2013). In general, various immobilization approaches fall in one of three categories; (1) incorporation and entrapment of segregated nanoparticles inside a porous matrix, (2) simultaneous in situ generation and immobilization of nanoparticles on to a support matrix and (3) immobilization of nanoparticles on a surface functionalized solid support. Among all approaches, one common procedure that would facilitate a stable association between nanoparticles and the support matrix is the selection of appropriate surface modification methods. However, the choice of the method to be employed for immobilization would certainly depend on many other factors such as type of solid support used, size/shape, morphology, surface functionalization and stability of nanoparticles, and the kind of application for which it is used. For example, a low-moderate level of immobilization may give the desired signals for optical/biosensor applications (Johnsson et al. 1991) while, a relatively higher level of immobilization would always be desired for the long term antibacterial effects. Moreover, in order to develop a antimicrobial biomaterial, the physical behavior of a biomaterial during nanomaterials integration must be in compliance with clinical requirements (Stickler 2000). For example, the mechanical specifications of antimicrobial biomaterial would be desirable for a very high load as in case with hip and knee implants. On the other hand, a biomaterial should either have high transmittance for designing intraocular/contact lenses or should be highly elastic while fabricating artificial blood vessels. In many cases, haemocompatibility and cytocompatibility of a biomaterial is compromised while introducing the nano-antimicrobial component, which ultimately would lead to immunological rejection of implant. A thorough understanding of the interaction of nano antimicrobial moiety with the biological environment like proteins, cells and tissue, is therefore crucial in order to be able to improve the functionality of nano-biomaterial interfaces.

The current chapter summarizes the recent progress and state-of-art facts on developing novel hybrid nanomaterials based systems as antimicrobial agents for various biomedical applications. The fabrication of nano-antimicrobial biomaterials would be explained on the basis of various mechanism through which a nanomaterial is bound to a biomaterial surface such as by (i) covalent immobilization (ii) impregnation (iii) sustained release of antimicrobial component (iv) synergistic action due to inherent antimicrobial action of support material. The aforementioned strategies aim for one common objective i.e., to provide an effective, stable and long term antibacterial efficacy to the biomaterial, promoting their reuse without causing any cytotoxicity responses against normal cells. The role of silver, gold, copper/copper oxide, zinc oxide, chitosan and their hybrid nanocomposites will be considered while designing new nano-antimicrobials for much needed applications in wound healing, tissue scaffolds, medical implants, coating surgical devices and instruments.

2 Unsupported Nano-Silver as Antimicrobial Agent

Silver and its compounds have been recognized for its antimicrobial efficacy since antiquity. Greeks and Romans used silver coins and vessels to disinfect potable water and keeping the milk fresh (Hill 2009). However, silver based antimicrobial therapy was first documented by Ravelin in 1889 which demonstrated that silver when used in ultra low concentration, proved to be highly germicidal (Zhang et al. 2012a). In late eighteenth century, eye drops constituting of 2% silver nitrate solution were also used to thwart the ocular infections in newborns which lead to blindness and against the treatment of typhoid and anthrax. In 1920s, the US Food and Drug Administration (FDA) agency has recognized colloidal silver as an effective agent to manage wound healing (Chopra 2007). Silver was then continued as a promising strategy for controlling infections during burns till World War II, which outraged its role with huge demands and development of new antibiotics (Dunn and Edwards-Jones 2004). However, such a heavy use of antibiotics lead to the development of drug resistant microbial strains which propelled the researchers to find novel remedies based on silver. In concurrence with growing interest in exploiting materials at nano level, nano silver has shown the highest level of commercialization (Agnihotri et al. 2014). Silver nanoparticles constitute an important component in nearly 57% (435 out of 762 products) of nano enabled consumer products (health care and fitness sector) available in market (Vance et al. 2015). As a result, AgNPs have emerged as the most exploited antimicrobial nanomaterial in diverse applications such as cosmetics, textiles and fabrics, dietary supplements, food packaging, surgical coatings, silver dressings, water sanitation and disinfection (Rai et al. 2009; Chen and Schluesener 2008; Dunn and Edwards-Jones 2004; Raghupathi et al. 2011; Dorobantu et al. 2015; Gajbhiye and Sakharwade 2016).

It is widely accepted that smaller the size of nanoparticles, higher would be its antimicrobial action. These results might be possible due to higher penetration rates of small sized nanoparticle owing to their high surface to volume ratios (Chen and Schluesener 2008; Rai et al. 2009). The antimicrobial property of AgNPs is governed by several other factors such as shape, aggregation state, stability, dispersion medium, types of capping agents, and methods of surface functionalization of nanoparticles. Even similar sized nanoparticles show variation in antimicrobial action against two different strains of same microbial species, known as strain-specific biocidal killing (Agnihotri et al. 2014; Mukherji et al. 2012; Ruparelia et al. 2008). Regarding shape, the truncated AgNPs appear to be more potent than spherical AgNPs in terms of their antimicrobial efficacies (Pal et al. 2007). However, spherical AgNPs are usually preferred over other shapes due to their ease in synthesis, control on particle size, handling and recovery for use either as colloidal state, or immobilized form (Agnihotri et al. 2013, 2014).

Regarding in vitro evaluation of the antibacterial activity of AgNPs, the potency is quantified either by using disk diffusion tests in solid media or by serially diluting the antibacterial material in liquid culture (Agnihotri et al. 2014; Ruparelia et al.

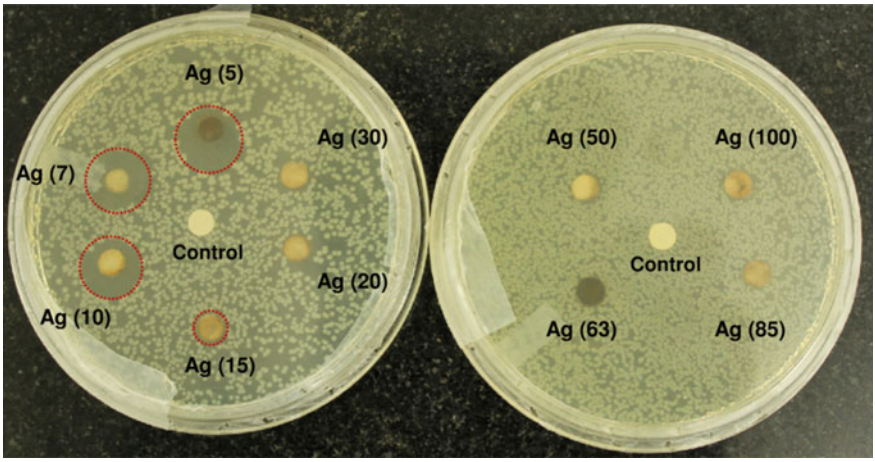

Fig. 1 Disk diffusion tests for different sized (5–100 nm) silver nanoparticles against the *E. coli*. The zone of inhibition (ZoI) is highlighted with a dashed circle indicating a noticeable antibacterial effect. The number in parentheses indicates the average size of silver nanoparticles in nanometer (Reproduced from Agnihotri et al. (2014), Royal Society of Chemistry)

2008). In disk diffusion studies, the sensitivity of a microbe is tested by calculating the diameter of zone of inhibition (ZoI) created by nanoparticles-laden disc by inhibiting the microbial growth surrounding that disc. Thus, a higher value of ZoI would indicate a more sensitive microbial strain and a more effective antimicrobial nanomaterial (Fig. 1). On the other hand, the liquid broth assay is used to quantify the minimum inhibitory concentration (MIC) and minimum bactericidal concentration (MBC) of nanoparticles as shown in Table 1. The minimum inhibitory concentration (MIC) is defined as the minimum concentration of antimicrobial

Table 1 (a) Minimum inhibitory concentration (MIC, μg ml^{-1}) and (b) minimum bactericidal concentration (MBC, μg ml^{-1}) values for silver nanoparticles of varying size[a]. (Reproduced (Agnihotri et al. 2014), Royal Society of Chemistry)

Bacterial strain	Different sized silver nanoparticles (nm)									
	(5)	(7)	(10)	(15)	(20)	(30)	(50)	(63)	(85)	(100)
(a)										
E. coli MTCC 443	20	20	30	30	40	50	80	90	90	110
E. coli MTCC 739	60	90	90	90	100	100	120	140	160	160
B. subtilis MTCC 441	30	40	40	50	50	60	80	90	110	120
S. aureus NCIM 5021	70	70	80	100	90	100	130	160	180	200
(b)										
E. coli MTCC 443	30	30	40	50	50	80	100	110	130	140
E. coli MTCC 739	90	100	100	110	120	120	140	170	170	180
B. subtilis MTCC 441	40	50	50	60	70	80	100	120	130	140
S. aureus NCIM 5021	80	90	100	110	100	120	160	200	>200	>200

[a]Studies were done at 10^5–10^6 CFU ml^{-1} initial bacterial concentrations

agent that inhibits the visible growth of microbes whereas, the lowest concentration of biocidal agent that kills 99.9% of microbial population is termed as minimum bactericidal concentration (Ruparelia et al. 2008).

The antimicrobial property of silver nanoparticles strongly depends on synthesis routes by which they were produced. Out of several methods (physical, chemical and biological) explored for producing silver nanoparticles, biological methods are gaining enormous interest due to its eco-friendly, non-toxic nature and often synthesize AgNPs with higher antimicrobial properties than that of produced by any other means (Panáček et al. 2006; Sharma et al. 2009). For instance Nanda and Saravanan (2009) investigated the antibacterial activity of biogenic AgNPs (160–180 nm) using S. *aureus* and found that these NPs showed excellent biocidal efficacy against clinically pathogenic multidrug resistant *Staphylococcus aureus* (*MRSA*), multidrug resistant *Staphylococcus epidermis (MRSE), and S. pyogenes.* Similarly, Ingle et al. (2008) reported the extracellular synthesis of AgNPs using *Fusarium accuminatum*, isolated from infected ginger and demonstrated nearly 2–3 times higher biocidal activity of AgNPs than bulk silver (Ag^+) against highly pathogenic bacterial strains i.e., MRSA, *Salmonella typhi*, *S. epidermidis*, and *Escherichia coli*. Results revealed that the antimicrobial activity of silver nanoparticles is 2.4–2.9 times that of silver ions. In a recent study, AgNPs (average size, 19–54 nm) synthesized using whole plant extract and callus extract of *Linum usitatissimum* demonstrated good efficacy against pathogenic strains *E. coli, Klebsiella pneumoniae and S. aureus* (Anjum and Abbasi 2016). Similarly, Shanthi et al. (2016) used cell free extract of *Bacillus licheniformis* to produce 18–64 nm AgNPs which exhibited strong antibacterial and antibiofilm properties against *Vibrio parahaemolyticus* Dav1. Silver nanoparticles synthesized through green route have also demonstrated good antimycotic activity against various fungal species viz, *Candida albicans, Dermatophyte Trichophyton* and *Mentagrophytes* (Panáček et al. 2009; Rodrigues et al. 2013). These strains are among few of the most common pathogens that cause hospital-acquired sepsis in immunocompromised patients with nearly 40% mortality rate (Panáček et al. 2009).

Silver nanoparticles can prove to be effective to prevent infectious diseases mediated through viruses. Rogers et al. (2008) demonstrated that AgNPs (10 nm) with biocompatible coating would significantly inhibit Monkey pox virus infection under laboratory conditions. Speshock et al. (2010) elucidated that AgNPs are capable of inhibiting viral infection by significantly reducing the production of viral RNA and release of progeny viruses. The authors however claimed that AgNPs treatment would be effective only if administered within initial 2–4 h of replication stage. A recent study showed antibacterial, antifungal and antiviral activity against variety of microorganisms *E. coli, K. pneumoniae, S. sonnei, P. aeruginosa, S. epidermidis, MRSA, S. bovis, A. flavus, C. albicans,* and Bean Yellow Mosaic Virus (BYMV) by AgNPs produced from micro organisms (Elbeshehy et al. 2015). Similarly, Lu et al. (2008) elucidated antiviral activity of AgNPs against Hepatitis B virus. Another study reported the potential antiviral activity of biogenic AgNPs (size range, 20–46 nm) against human parainfluenza virus type 3, Herpes Simplex Virus 1, and Herpes Simplex Virus 2 (Gaikwad et al. 2013).

3 Silver Based Hybrid Nanocomposites

Considering several limitations associated with using conventional antibiotics and rising demands for better hygiene has motivated researchers to develop effective yet affordable antimicrobial nanomaterials. Antimicrobial activities of metals like silver, gold, copper, zinc etc. can be enhanced by incorporating them into a material matrix thus obtaining a composite material. Nanocomposites are defined as composites in which at least one of the phases shows dimensions in the order of nanometre range. On the basis of types of matrix material, silver based nanocomposites fall into four major categories, silver-polymeric, silver-inorganic, silver-organic, and hybrid metal nanocomposites each with distinct properties that can be utilized in several biomedical applications.

3.1 Silver-Polymeric Nanocomposites

The use of polymers in medical sector continues to grow, thanks to some of its interesting properties like its resistance towards heat, irradiation and chemicals, inert nature, clarity, durability and flexibility to be molded into various sizes and/or shapes (Sastri 2013). Admittedly, the growing concerns for single usage disposable items that have succeeded in reducing the chances of infection in hospitals are made up of polymeric materials. However, the major drawback associated using polymers is that they also provide the necessary surface for microbial contamination, colonization, migration and somehow mimic the conditions require for their subsequent biofilm formation (Hall-Stoodley et al. 2004; Hall-Stoodley and Stoodley 2009). As a result, a large portion of hospital acquired infections (HAIs) are spread through surface contacts with disposable syringes, blood sachets, bottles, pipings, hospitals furniture/wardrobes, which are mostly based on polymeric (polypropylene and polyethylene) materials. It was estimated that roughly 80% of hospital-acquired urinary tract infections originate from urinary catheters, which are of polyvinyl chloride (PVC) origin (Curtis 2008).

Polymer-silver nanocomposites (NCs) are gaining importance as a new generation broad spectrum antimicrobial material in biomedical applications due to their ease in modifications, haemocompatibility, biodegradable nature, and enhanced activity of incorporated AgNPs within the polymeric network. Moreover, the presence of AgNPs would impart an additional biocidal feature to polymer without compromising its properties desired for a particular application. For the preparation of polymer/metal nanocomposites, metals can be incorporated via two approaches; (1) ex situ, in which pre synthesized nanoparticles are incorporated into the surface modified polymeric matrix and (2) in situ, in which polymeric matrix acts both as a nano reactor for synthesizing nanoparticles as well as a template for their subsequent immobilization. The immobilization is achieved through surface modification that allows favorable interaction between the nanoparticles and the support matrix.

Although the current discussion is limited to the incorporation of AgNPs on to polymeric template, similar methods can also be employed for immobilization copper, gold, ZnO nanoparticles in later sections.

AgNPs are quite commonly used as antimicrobial filler in polymeric nanocomposites (Muñoz-Bonilla and Fernández-García 2012) with diverse biomedical applications ranging from wound dressings, coating medical implants and devices, to tissue scaffolds. The polymeric support can be fabricated into various structures such as nanofibers, thin films, solid support and porous gel that act as a template for immobilizing silver nanoparticles (Mukherji et al. 2012). Among various structures, nanofibers have emerged as the most promising biomaterial scaffolds owing to its nano scale architecture similar to natural human tissue along with microporous morphology which facilitates adhesion, proliferation, and differentiation of cells for tissue engineering application (Dahlin et al. 2011). Nanofibers posses a high surface area to volume ratio while its characteristics such as composition, biodegradation, and mechanical strength can be manipulated to the intended role, which is beneficial for other biomedical applications as well (Peng et al. 2016). For example, Almajhdi et al. (2014) incorporated AgNPs (1–7 wt%, 5–10 nm diameter) on polylactic-co-glycolic acid (PLGA) nanofibers through electrospinning process (Fig. 2) and the antibacterial activities were tested against

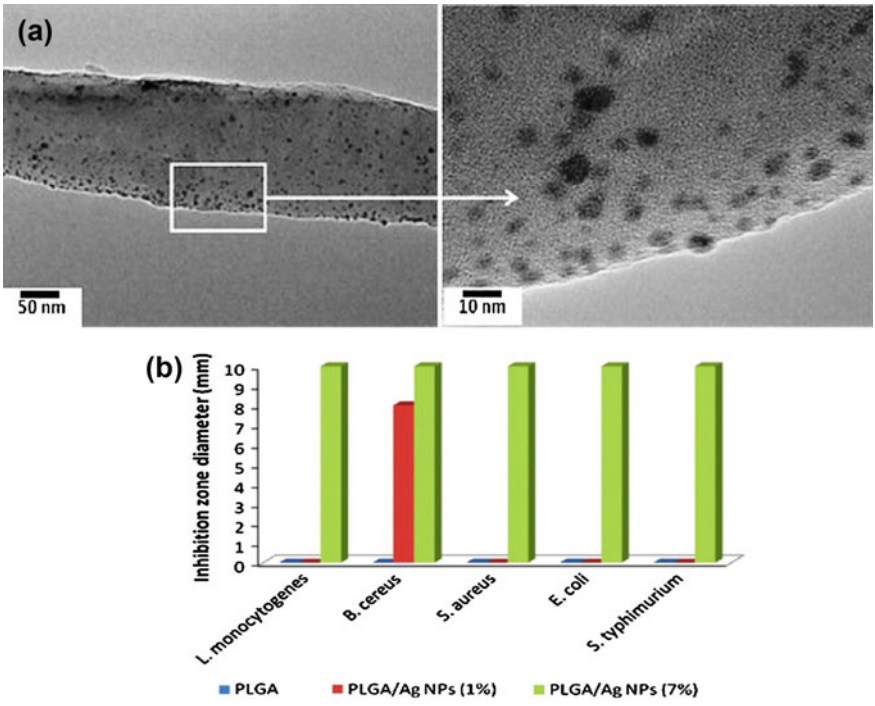

Fig. 2 **a** A highly dense incorporation of silver nanoparticles on the surface of PLGA nanofibers as shown through transmission electron microscopy (TEM). **b** Variation in the sensitivity of microbial pathogens against silver/polymer nanocomposite as marked by difference in their zone of inhibition. (Reproduce with permission from Almajhdi et al. (2014), Springer)

five pathogenic strains *E. coli* o157:H7, *S. aureus* ATCC 13565, *Bacillus cereus* EMCC 1080, *Listeria monocytogenes* EMCC 1875 and *S. typhimurium* ATCC25566 using disc diffusion method. PLGA nanofibers with 7 wt% AgNP demonstrated the best antimicrobial action displaying the highest ZoI (10 mm) against all tested strains. PLGA/Ag nanofibers were found to be suitable for therapeutic applications since they enhanced the anticancer activity along with the biocidal nature without posing any cytotoxicity effects to normal cells.

In another study, Raghavendra et al. (2013) synthesized polymer/Ag nanocomposite fibers based on cellulose for antibacterial skin scaffolds using gum acacia and gaur gum (0.3–0.7 wt%) as biogenic reductants. The incorporation of AgNPs improved mechanical strength and thermal stability of resulting nanocomposite than pristine cellulose fibers along with promising antibacterial activity against pathogenic strains of *E. coli*. Kim et al. (2009) successfully prepared a biodegradable electrospun poly(ethylene oxide)/AgNP NC which showed efficient biocidal control against *S. aureus* and *K. pneumoniae* pathogens. Similar to previous study, they also reported that incorporating AgNPs on to polymeric nanofibers enhanced their mechanical strength without any significant decline in antimicrobial efficacy of AgNPs. Regarding biocompatibility and biodegradability, electrospun nanofibers made from PLGA, polylactic acid (PLA), polycaprolactam (PCL) polymers have been used in many biomedical applications such as fabricating sutures, scaffolds, guided conduits for nerve tissue regeneration wherein the antimicrobial effect to fibers is bestowed due to the presence of AgNPs (Vargas-Villagran et al. 2014).

Currently, the use of natural polymers in tissue scaffolds, drug delivery systems, layer by layer (LBL) assembled films, and as a cargo for bioactive compounds has increased the demand for investigation in biomedical fields. Polymers of natural origin like cellulose, chitosan, dextran, hyaluronan, collagen, alginate have been traditionally used as sources of wound dressings, suture threads, vaccines, and as bioactive compounds (anti-ageing, anti-coagulants and antibacterial agents) in their natural or modified forms (Travan et al. 2009; Ahamed et al. 2015; Anna et al. 2013; Azizi et al. 2014; Lavorgna et al. 2014; Pinto et al. 2009; Raghavendra et al. 2013; Zahran et al. 2014). Interestingly, polymers from natural sources offer many advantages over synthetic ones which make them suitable as biomaterials in regenerative medicine and therapeutics (Allen et al. 2015). Being natural, they are inherently biocompatible, biodegradable, renewable, nontoxic and are relatively cheaper (Dang and Leong 2006). Moreover, natural polymers are easy for chemical modifications thereby improving the structural and functional properties required for the biomaterials (Allen et al. 2015). With this approach, several biocidal agents including AgNPs have been incorporated on natural polymers after surface functionalization in order to enhance their utility as nano-antimicrobials in biomedical applications.

In order to design an efficient and greener polymeric nanocomposites, Pinto et al. (2009) reported in situ synthesis of AgNPs on the surface of cellulosic fibers for biomedical applications. Authors demonstrated that positively charged Ag^+ ions can form stable electrostatic interactions with functional moieties available at the surface

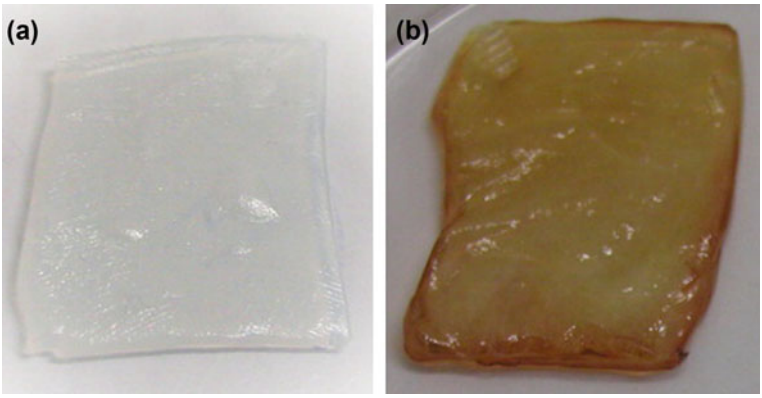

Fig. 3 Photographic images of **a** pristine cellulose membrane and **b** Ag-cellulose nanocomposite membrane fabricated by in-situ synthesis of AgNPs. (Reproduced with permission from Pinto et al. (2009), Elsevier)

of cellulose, and subsequently can be reduced to nanoscale under UV irradiation. The successful immobilization of AgNPs was evidenced by observing a visual change in the color of nanocomposites after immobilization (Fig. 3). Electron microscopy analyses confirmed a highly dense and homogenous distribution of AgNPs over the nanocomposite. The nanocomposite with high Ag content (0.57–4.4 wt%) exhibited strong antibacterial activity toward *S. aureus, K. pneumoniae and B. subtilis* strains. A modified form of cellulose i.e., carboxymethylcellulose has also been utilized as a template for incorporating copper, silver and even iron oxide nanoparticles with an aim to fabricate antimicrobial and antifungal coatings as novel therapeutics (Nadagouda and Varma 2007).

Azizi et al. (2014) synthesized poly(vinyl alcohol)/chitosan (PVA/CS) based nanocomposites using different proportions of zinc oxide and silver nanoparticles as multifunctional nano fillers. As compared to pristine PVA/Cs, presence of nano ZnO and AgNPs increased the mechanical strength (from 0.055 to 0.205 GPa), demonstrated good visibility and UV-shielding effects along with excellent antimicrobial properties against *Salmonella choleraesuis* and *S. aureus* strains. Recently, a cellulose-chitosan hybrid nanocomposites containing a unique blend of AgNPs and antibiotic gentamicin was prepared for wound dressing applications (Ahamed et al. 2015). For preliminary experiments performed on rats, the physicochemical and biochemical studies revealed faster healing pattern in wounds while the presence of AgNPs ruled out the chances for contamination. The authors claim this nanocomposite as an eco-friendly wound dressing material for humans after being successfully implemented on other animals. Zahran et al. (2014) described an eco-friendly approach for synthesizing Ag/alginate nanocomposite using a one step in situ reduction of Ag^+ ions in alginate solution, which acted as both reducing and stabilizing agent. The resulting nanocomposite was applied on cotton fabrics so as to testify its antimicrobial potential on clinical isolates. The

modified cotton fabrics showed excellent antibacterial activity towards *E. coli, S. aureus and P. aeruginosa* strains. A slight reduction in the antibacterial efficacy of modified fabrics was observed when used repeatedly for 20 washing cycles, however 90% bacterial killing was still achievable with such high number of washing steps. Authors claimed this NC as a promising approach for fabricating antibacterial finishing for wound healing purposes. Similarly, Ag/collagen based hybrid nanocomposites have been exploited as tissue scaffold for promoting biocidal response against *E. coli, P. mirabilis, B. cereus, and S. aureus* pathogens (Mandal et al. 2012). Due to their good mechanical strength, biological functionalities and potential to immobilize metallic nanoparticles, collagen based scaffolds can successfully be utilized in fabricating prosthetic heart valves. Polymers isolated from non-primate sources such as crustaceans (chitosan, chitin), *Bombyx mori* (silk fibroin) has also been employed as a bio-template for in situ production of AgNPs besides acting both as a reducing agent and stabilizer to prevent their aggregation (Fei et al. 2013; Lavorgna et al. 2014). The resulting nanocomposites have demonstrated efficient killing of MRSA, *S. epidermidis*, and *K. pneumoniae* with disruption of biofilm formation afterwards. Nevertheless, the scientific advancements prompted towards establishing polymers-silver nanocomposites as an ideal antimicrobial biomaterial are still poised with several challenges such as broadening their applicability while combating against virulent pathogens.

3.2 Silver-Inorganic Nanocomposites

In past two decades, the application of inorganic nanomaterials in biomedical fields has drawn attention among the researchers. Inorganic nanocomposites consisting of micro and mesoporous silica, glass (silicon dioxide), silicates and zeolites have particularly been exploited for potential antimicrobial actions. Other than being inert, inorganic nanomaterials can easily be engineered into desired morphology while its porous architecture contributes toward dense immobilization of AgNPs (Agnihotri et al. 2013). Moreover, inorganic nanocomposite are inherently hydrophilic due to the presence of several functional groups such as hydroxyl, carboxyl,–SH and act as cargo vehicle for delivering drugs, bioactive molecules and even antimicrobial agent owing to its high surface area.

For instance, Song et al. (2013) reported synthesis of silver/polyrhodanine nanocomposites on silica nanoparticles as potential antimicrobial therapeutics. In this study, metal binding affinity of thiol-functionalized silica NPs was exploited for loading Ag^+ ions on its surface followed by treatment with rhodanine monomer solution. The polymerization of rhodanine was then carried at the silica surface, where silver ions were subsequently reduced to silver nanoparticles (average size, 7 nm) forming stable silver-polyrhodanine complex (Fig. 4). The antibacterial potential of Ag/PRh–SiO_2 nanocomposite was evaluated toward *E. coli* and *S. aureus* strains which showed MIC values of 1.5 and 2.5 mg ml^{-1} at an initial bacterial concentration of $10^5 - 10^6$ CFU ml^{-1}. The enhanced antimicrobial

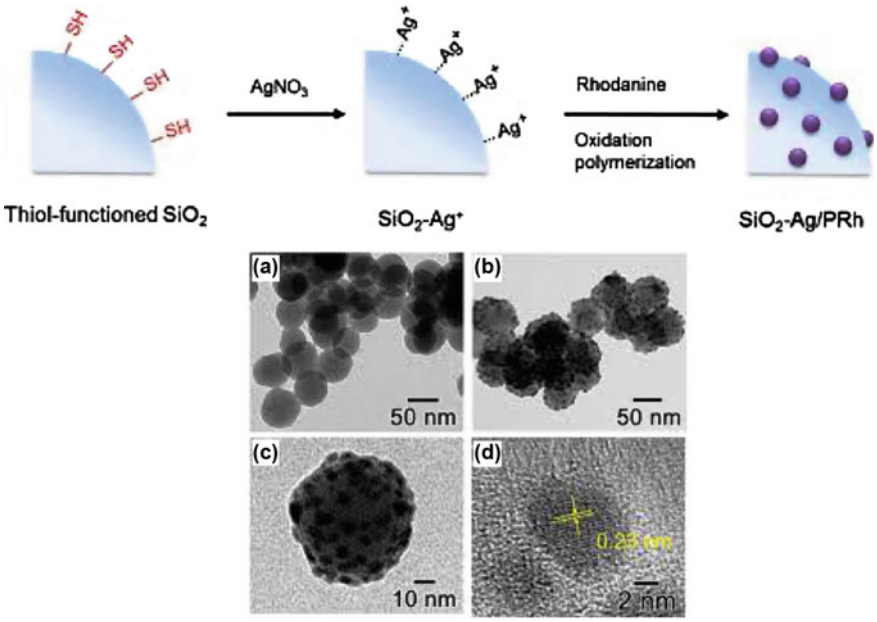

Fig. 4 Schematic representation for the synthetic protocol of Ag/PRh-SiO_2 nanocomposite. TEM images of **a** thiol-modified silica nanoparticles and **b**, **c** Ag/PRh-SiO_2 nanoparticles at lower and higher magnifications, respectively. **d** High resolution TEM image of Ag/PRh-SiO_2 nanocomposite. (Reproduced with permission from Song et al. (2013), American Chemical Society)

activity of silver/polyrhodanine-silica nanocomposite was attributed to the dual role of microbial killing through release of silver ions as well as direct contact with polyrhodamine.

In another study, fully exfoliated clay, i.e., nanosilicate platelets (NSP) were used as a dispersing agent and immobilizing matrix for depositing AgNPs and the Ag/NSP/Poly(ether)urethane (PEU) hybrid nanocomposites were evaluated for its biocompatibility, immunological response, and antimicrobial activities against few clinical isolates (Lin et al. 2013). Owing to its immobilization, AgNPs could not enter inside cells thereby lowering the risk associated with cellular uptake of AgNPs. The Ag/NSP composite having 20 ppm AgNP concentration were translated into an effective biocompatible material by further mixing with PEU which showed no cytotoxic responses to mouse skin fibroblasts (L929 cells) and human hepatoma cells (HepG2), yet exhibiting complete bacterial killing (99.9%) of *E. coli* cells (Fig. 5). The amount of leachable silver in form of either free Ag^+ or AgNPs was found to be 170 and 270 ppb, respectively, whereas the supernatant of silver nanohybrids did not show antibacterial activity after aging for 6 months. Authors thus claimed that this antimicrobial biomaterial can effectively be employed in biomedical application considering the biosafety associated with minimizing the excessive discharge of silver.

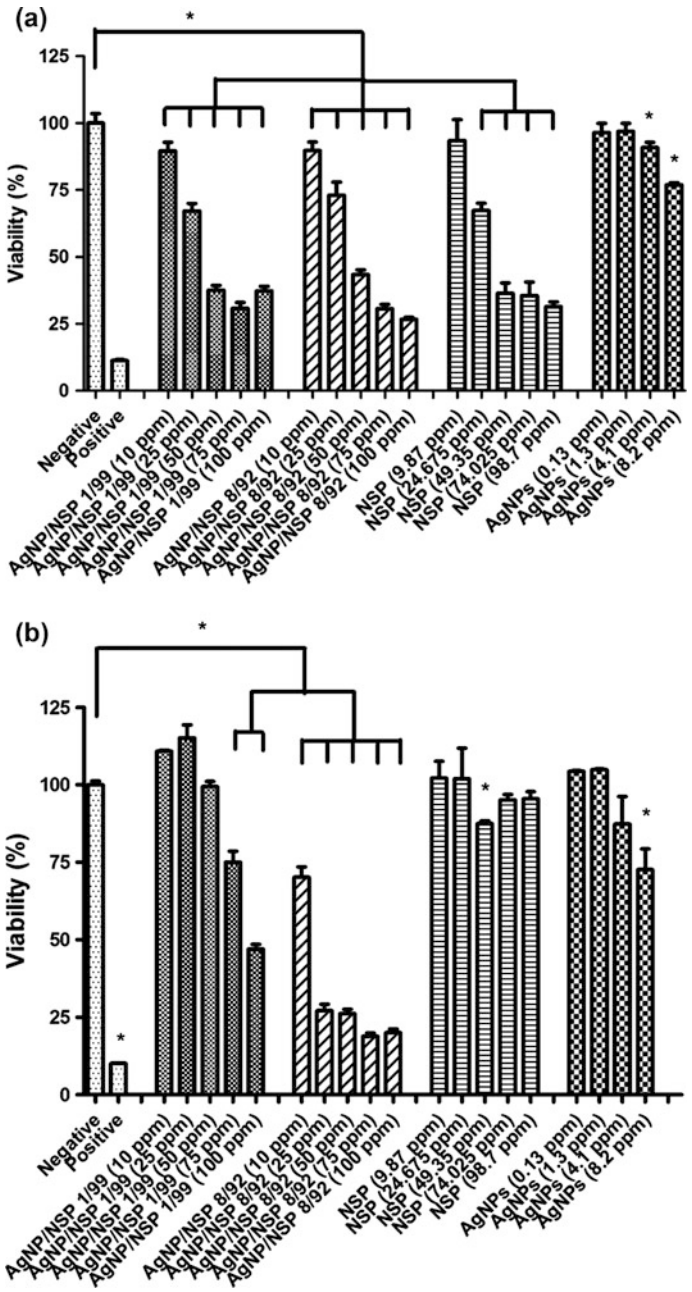

Fig. 5 Cytotoxic effects of AgNP/NSP (silver-nanosilicate platelets), NSP, and AgNPs on **a** L929 cells and **b** HepG2 cells. The concentration of NSP or AgNPs corresponded to the content of each component within the AgNP/NSP hybrid. The concentration was based on the total weight, e.g., AgNP/NSP 1/99 10 ppm contains 9.87 ppm NSP and 0.13 ppm AgNPs. * indicates a statistical difference from the control, $p < 0.05$. (Reproduced with permission from Lin et al. (2013), American Chemical Society)

It is a matter of immense discussion whether the mode of antibacterial action of AgNPs is mediated solely on the basis of either release of silver ions or nanoparticles-specific, or may be both (Li et al. 2006; Hoop et al. 2015; Wang et al. 2013). Another study hypothesizing the dual role of antibacterial action of Ag/SiO_2 based nanocomposites was given by (Agnihotri et al. 2013) where a high localized immobilization of AgNPs (8.6 nm, average size) was achieved on an amine-functionalized silica substrate using 3-(2-aminoethylaminopropyl) trimethoxysilane as a cross linker molecule. The bactericidal potential of AgNP–glass nanocomposite was tested against two *E. coli* strains, MTCC 443 and MTCC 739, and one *Bacillus subtilis* strain, MTCC 441, in both deionized water and phosphate buffer medium. The antibacterial tests were performed independently at two different initial bacterial concentrations i.e., 10^3 and 10^5 CFU ml^{-1}, where bacterial counts were reduced to zero within 120 min under all the test conditions. It was concluded that contact killing is the predominant bactericidal mechanism and surface immobilized nanoparticles showed greater efficacy than other sources of silver (free AgNPs, bulk Ag and bulk AgCl) and released even less than 25 ppb of silver in solution (Fig. 6). Interestingly, AgNP–SiO_2 substrate was reused 11 times

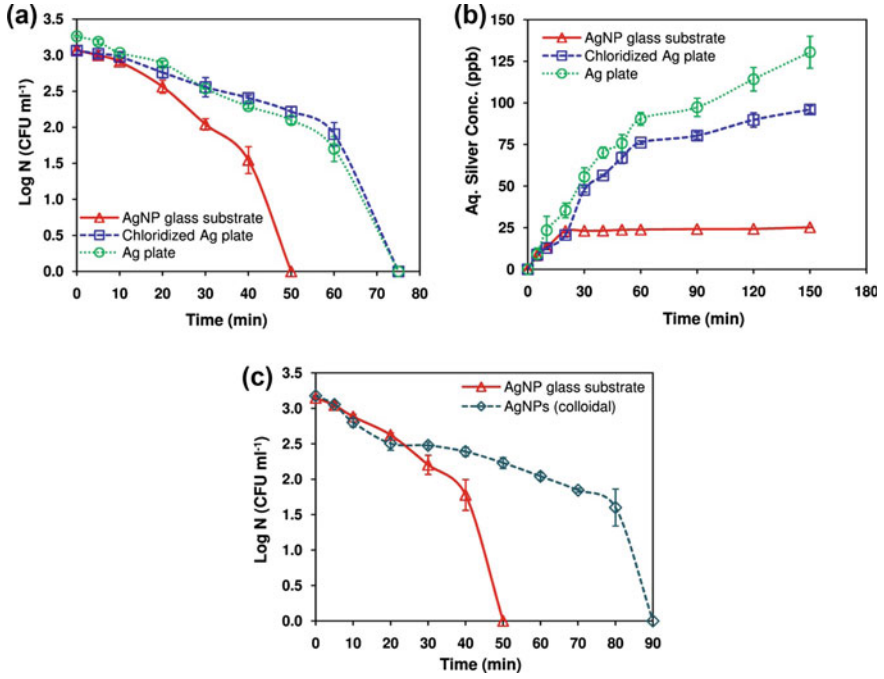

Fig. 6 Comparative effect of various Ag sources, i.e., pure silver, AgCl and AgNP–glass substrate, all with same dimensions on **a** disinfection and **b** silver release profile is presented. **c** Comparative bactericidal potential of AgNP–glass substrate and AgNP colloidal suspension (average size 8.6 nm) against the *E. coli* MTCC 443 strain having a similar content of silver. (Reproduced with permission from Agnihotri et al. (2013), Royal Society of Chemistry)

without losing its bactericidal efficacy. This indicates that the proposed immobilization protocol could prove to be effective while minimizing the toxicity issues associated with excess release of AgNPs into solution as required in case with antimicrobial coatings, especially for surgical devices and synthetic implants.

A research group lead by Prof. Alexander Seifalian at University College London (UK) has developed a novel nanocomposite biomaterial based on polyhedral oligomeric silsesquioxane-poly(carbonate-urea)urethane (POSS-PCU) having required mechanical properties and histo-compatibility for cardiovascular applications (Ghanbari et al. 2016; Kannan et al. 2006; Raghunath et al. 2009). This polymer has been successfully implanted in humans in form of vascular bypass graft, a lachrymal duct, and tracheal implants. However, the biomaterial suffers from graft infection involving MRSA, *S. epidermidis* which prevails with serious consequences including bacteremia, systemic sepsis, higher incidences of amputation, and even death. With an aim to impart biocidal component to this polymer, pre synthesized silver nanoparticles (average diameter, 15 nm) were mixed with POSS-PCU at different concentrations (16, 32, 64, 128 mg) and its effect on the platelets was evaluated (de Mel et al. 2012).

Platelet adhesion on test surfaces was quantified using the Alamar blue assay, which is a direct measurement of metabolic activity of platelets and is proportionate to the color intensity. Authors demonstrated that POSS-PCU up to 64 mg AgNPs marked no significant variation in platelet adhesion as compared to POSS-PCU without AgNPs. However, for higher conc. of AgNPs (i.e., 128 mg), POSS-PCU-demonstrated a 50% reduction in platelet adhesion as with pristine POSS-PCU. While comparing the morphology of the platelets, the positive controls (Collagen and PTFE) showed the existence of platelets in a highly aggregated state with extended pseudopodia. In contrast to this, the platelets treated with Ag incorporated POSS-PCU showed a very few platelets with a rounded appearance at their initial state of adhesion. Comparing other results, it was evidenced that the incorporation of AgNP not only enhanced the anti-thrombogenic properties of POSS-PCU, it also provided an additional benefits in terms of its biocidal nature, and thus potentially can be used in fabrication of cardiovascular implants.

Shameli et al. (2011) developed a new method for in situ synthesis and immobilization of AgNPs within interlayer space of montmorillonite (MMT), a modified silicate clay. To this composite, chitosan polymer was intercalated through cationic exchange and hydrogen bonding processes so as to convey some important properties like biocompatibility, biodegradability, non toxicity, and bioactivity in the resulting nanocomposites for potential biomedical applications. The modified clay (MMT/chitosan) not only acted as a stabilizing agent preventing the AgNPs from being aggregated, it also assisted in reducing silver ions to AgNPs under room temperature conditions. The antibacterial activity of Ag/MMT/chitosan bio-nanocomposite was examined against *S. aureus*, MRSA *E. coli* O157:H7, and *P. aeruginosa* by disc diffusion method having different sizes (6.2–9.8 nm) of AgNPs. Results indicated that bio-nanocomposite was found to be highly bactericidal against all pathogenic strains where the range of ZoI varied from 7.6 to 11.9 mm showing its strain specific sensitivity. Authors claimed that the

Ag/MMT/chitosan nanocomposites can successfully be applied as biocompatible antimicrobial coating in surgical devices and as drug delivery vehicles. In a different study, Ag/MMT/chitosan nanocomposites have also been evaluated for topical treatment of chronic skin lesions during the treatment of skin ulcers (Sandri et al. 2014). The antimicrobial properties were examined against four bacterial strains, *S. aureus, S. pyogenes, E. coli,* and *P. aeruginosa* which often complicate skin lesions during wound healing.

3.3 Silver-Carbon Nanocomposites

Several attempts have been made to incorporate silver on various carbon based nanostructures like single-walled carbon nanotubes (SWCNTs), multi-walled carbon nanotubes (MWCNTs), graphene, graphene oxide and carbon aerogels for antibacterial applications. The size (diameter) of nanotubes is considered to be an important factor for assessing the bactericidal potential of CNTs since SWCNTs are more lethal to microbes than MWCNTs (Kang et al. 2008). Through gene expression data, it was evidenced that *E. coli* expressed a higher levels of stress-related gene products when treated with SWCNTs as compared to MWCNTs. The enhanced toxicity of SWCNTs is attributed to their sharp edges which acted as nanosyringes for inducing a direct contact to microbes thereby causing damage to cell membrane (Afzal et al. 2013). In addition to this, the presence of carbon nanotubes in Ag-CNTs nanocomposite serves many purposes. First, CNTs act as an immobilizing template for dense localization of silver nanoparticles owing to its high surface area. Secondly, CNTs may undergo simple surface functionalization procedures and the modified CNTs can offer the required nucleation sites for in situ synthesis of AgNP via forming stable silver-CNTs complexes (Wildgoose et al. 2006). Most importantly, Ag-CNTs often mediate synergistic antibacterial effect due to the inherent bactericidal action of CNTs and thus strengthen their antimicrobial performance in addition to being acted as an immobilizing substrate material (Akhavan et al. 2011; Yu et al. 2014; Seo et al. 2014; Rangari et al. 2010).

Exploring the above possibilities, Mohan et al. (2011) described a wet chemical approach to immobilize AgNPs onto carbon nanotubes following surface functionalization procedure. In this study, silver ions were initially grafted over acid functionalized surface (–COOH) forming stable silver-MWCNTs complexes, which acted as the template for AgNP growth. After exposing it to reducing agent, AgNPs were decorated onto MWCNTs in a highly ordered fashion with dense packing. The antibacterial experiments performed against *E. coli* strain had shown that while Ag-MWCNT contributed toward 97% bacterial killing, the acid functionalized MWCNTs (without AgNPs) killed only 20% of bacterial population. Authors suggested their role as antibacterial coatings in biomedical devices and antibacterial controlling system.

In order to construct an orthopedic implant biomaterial, Afzal et al. (2013) described Ag-reinforced composite material containing hydroxyapatite (HA) and

MWCNTs, where the presence of silver landed an antimicrobial character to the biomaterial without compromising their inherent mechanical, physiochemical and biological properties. In this study, HA-CNT composites were mixed with 5% Ag powder (particle size < 100 nm) while the samples were sintered in vacuum under uniaxial pressure of 30 MPa at 950 °C for 5 min. The antibacterial tests performed using *E. coli* and *S. epidermidis* showed a significant decrease (65–86%) in the number of bacteria adhered to Ag/HA/MWCNT composites. The density of *E. coli* on HA, Ag/HA, only CNT, and Ag/CNT was found as 330, 70, 1320, and 430 cells/mm^2, respectively. Similarly, the density of *S. epidermidis* on the corresponding substrates was estimated to be 370, 130, 350, and 50 cells/mm^2, respectively. This indicates that bacteria were proliferating more over the surface of pure HA and CNTs whereas the addition of Ag particles resulted in the inhibition of bacterial growth and bacterial proliferation was retarded. Later, the same group reported synthesis of ceramic biomaterial based on Ag/HA/CNTs for minimizing bacterial infections for bone replacement prosthesis (Herkendell et al. 2014). Introducing small amounts of silver (2–5 wt%) demonstrated a profound antibacterial effects as the bacterial adhesion was reduced to 60% in contrast to pure-CNTs and pure-HA who promoted bacterial growth on their surface by 8.5%. Several other approaches have also been applied to synthesize Ag/CNTs nanocomposites employing biocompatible, environmental benign molecules such as dendrimers (Murugan and Vimala 2011), PMMA (Rusen et al. 2014), and liposomes (Barbinta-Patrascu et al. 2014) which demonstrated excellent antibacterial activity against various pathogens strains *B. subtilis*, *S. aureus*, *E. coli*, and *E. faecalis*.

The development of toxic free biomaterials has become a great challenge in recent times. The chemical procedure for synthesizing Ag-carbon nano hybrids mainly involves the use of either sodium borohydride or hydrazine hydrate as reducing agents. These chemicals are inflammable, toxic and potentially hazardous, and their left over residues persists in the system despite several washing steps. As a result, they elicit cytotoxic effects both under in vitro and in vivo conditions and limit the applicability of synthesized biomaterial for long term use. Synthesis of nanocomposites by green method using some biocompatible reducing agents can potentially eliminate this problem. Recently, Yallappa et al. (2015) proposed a green method for synthesizing Ag-MWCNTs composite using *Terminalia arjuna* bark extracts under microwave irradiation. In this study, $AgNO_3$ precursor was introduced in aqueous dispersion containing MWCNTs and the biological extract. The phytochemicals present in the extract acted as reducing and stabilizing agent such that AgNPs were synthesized in situ and subsequently grown on the surface of MWCNTs. The hybrid nanocomposite was found to be very effective against bacterial and fungal strains, which are the causative agents for hospital-acquired infections. The antimicrobial activity was evaluated on the basis of disc diffusion studies, where the zone of inhibition (ZoI) was calculated in the range from 10–16 mm for bacterial strains and 7–8 mm for fungal strains. While comparing the antibacterial results with pristine MWCNTs, the order of bactericidal and antifungal potential of Ag/MWCNTs was observed as *E. coli* > *S. typhi* > *S. aureus* > *P. aeruginosa* and *C. albicans* > *T.*

rubrum ≈ *C. indicum*, respectively. Authors explained this enhanced antimicrobial activity of nanobiohybrids as a combined effect of CNTs, AgNPs, and the presence of phytochemicals from plant extract in the dispersing media. These results suggest that the biohybrid nanomaterials can compete with commercial antimicrobial agents.

Graphene i.e., a monolayer array of carbon atoms linked together in a 2D hexagonal lattice constitutes another class of nanomaterials that exhibits broad spectrum antimicrobial activity. The potential for using graphene based nanocomposites in films and coatings applications has been rapidly expanded over the past decade. Graphene is considered as a biocompatible material towards mammalian cells and osteoblasts while graphene oxide has been utilized as a carrier matrix to deliver bioactive agents and drugs into the cells. Hu et al. (2010) described a novel route for synthesizing graphene-based antibacterial paper via introducing several functional groups (hydroxyl, epoxy, and carboxyl) over graphene sheets enabling it to be water dispersible. The antibacterial activity of graphene paper was validated by observing a significant reduction (up to 70%) in metabolic activity of *E. coli* DH5α cells and suppressing bacterial growth up to 98.5% in presence of GO nanosheets. In another study, Wang et al. (2015) investigated the antibacterial potential of reduced graphene oxide/magnetic NPs/polyethylenimine nanocomposite onto which AgNPs were grown through in situ approach. The resulting biomaterial exhibited excellent antibacterial performance against model strain, *E. coli* O157:H7 with 99.9% killing rate (initial bacterial count, 10^7 CFU ml^{-1}) using a dosage of 0.1 μg ml^{-1} followed by a photothermal treatment (5 min) under a near-Infrared (NIR) laser irradiation. Moreover, a MBC value of 0.1 μg ml^{-1} could be achieved under near infrared (NIR) laser irradiation for 10 min, while no colony of *E. coli* O157:H7 was found in solid agar plate. The strong absorbance characteristics of graphene in NIR has been exploited in another study (Tian et al. 2014), where AgNP/GO/iron oxide nanocomposite showed synergistic antibacterial effect against *E. coli* and *S. aureus* strain. Moreover, due to the presence of iron oxide nanoparticles, the antibacterial composite were recoverable and hence can be used repeatedly.

Recently, a sandwich-like antibacterial nanomaterial was constructed by introducing halloysite nanotubes (HNTs) to Ag/graphene nanosheets combining the adhesive potential of 3, 4-dihydroxyphenylalanine (DOPA) after self polymerization (Yu et al. 2014). It was a single-step synthesis protocol and was performed under mild atmosphere without involving any hazardous chemicals or specific process conditions. Electron microscopy studies indicated that the presence of DOPA not only facilitated the intercalation of HNTs within GO sheets, it also caused reduction of silver ions to AgNPs and their subsequent attachment to both HNTs and graphene oxide (GO) nanosheets (Fig. 7). Synthesized AgNPs were found to be in a range between 5–15 nm through TEM micrographs. The antibacterial experiments indicated a very high bactericidal potential of Ag/HNTs/rGO (reduced graphene oxide) towards *E. coli* and *S. aureus* having MIC value of 2 μg/ml as compared to their control groups, i.e., Ag/GO (16 μg ml^{-1}), Ag/HNTs (32 μg ml^{-1}), colloidal Ag (64 μg ml^{-1}) and GO nanosheets (1064 μg ml^{-1}). Authors also demonstrated that Ag/HNTs/rGO nanocomposite can be fabricated into a paper-like antibacterial film

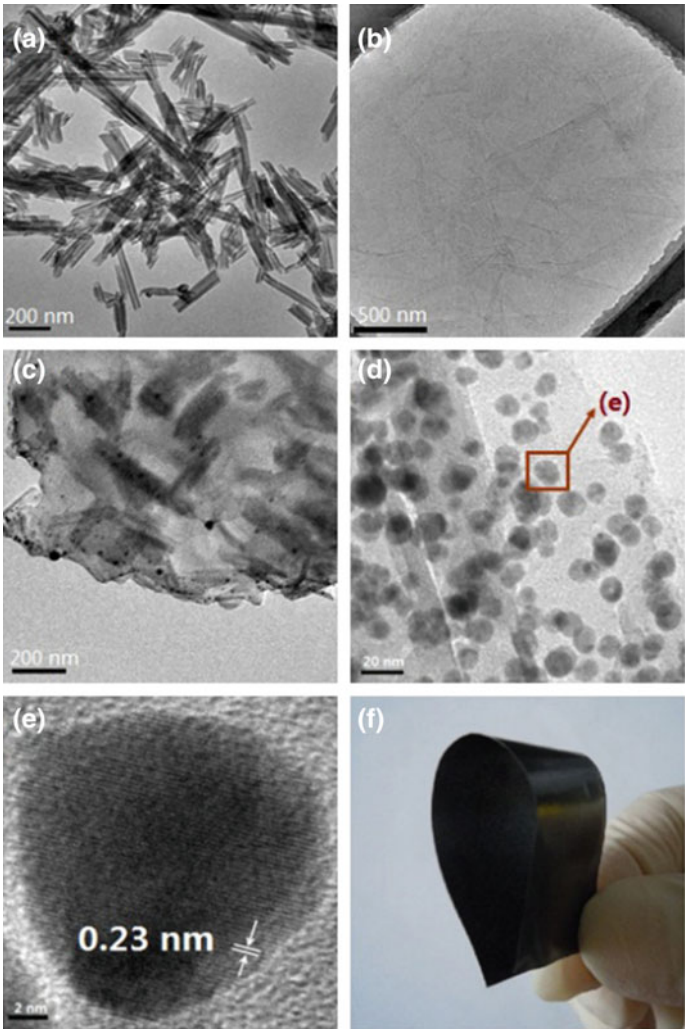

Fig. 7 TEM images of **a** HNTs, **b** GO nanosheets and **c**, **d**, sandwich-like nanomaterials at different magnifications. **e** HRTEM image of single entity silver nanoparticles with fringe spacing. **f** Photograph of antibacterial film prepared from Ag/HNTs/reduced GO. (Reproduced with permission from Yu et al. (2014), Nature publishing group)

by introducing a small proportion of polyethersulfone which showed excellent flexibility and can be used for biomedical purposes as antimicrobial coatings.

As evident from literature review, most of the studies involving use of Ag-graphene nanocomposites as antimicrobial biomaterial have targeted to exploit their efficacy either in terms of their ability to preventing bacterial colonization and/or inhibiting bacterial growth on the biomaterial surface. However, the clinical

relevance of these nanocomposites is not limited to their antibacterial nature since a few studies have specifically evaluated their antifungal effects as well. For examples, Li et al. (2013) explained a method for synthesizing carbon nanoscrolls (CNS) filled with AgNPs and was tested against *Candida albicans* (ATCC 90029) and *Candida tropical* fungal strains, isolated from a patient suffering from urethritis at a local hospital. The synthetic process involved in situ reduction of silver ions followed by their anchoring on the surface functionalized GO resulting in the formation of Ag–GO nanocomposite. Moreover, the composite was sonicated for next 6 h so that most of the exfoliated GO could be curled into scroll while wrapping most of AgNPs into it, called as carbon nanoscrolls.

At first, the antifungal activity of GO, Ag–GO and CNS–AgNPs were evaluated by modified agar disk diffusion method. Results indicate while no inhibition zone was observed for pure GO samples during 24 h of incubation, both GO–AgNPs and CNS–AgNPs showed a clear zone of inhibition (ZoI) even after an incubation period of 8 h. However, as the incubation time was increased to 12, 20, and 24 h, the no. of viable colonies were much lesser in CNS–AgNPs treated samples as compared to GO–AgNPs for same strains under similar test conditions. The antifungal activity of GO, GO-AgNPs and CNS–AgNPs also was evaluated by liquid culture assay broth micro dilution method. The MIC values of CNS–AgNPs against *C. albicans* and *C. tropical* strains were calculated as 0.25 and 0.125 mg mL^{-1}, respectively. On the contrary, GO–AgNPs demonstrated a higher MIC value of 0.5 mg mL^{-1} against both fungal strains. In order to elucidate the enhanced

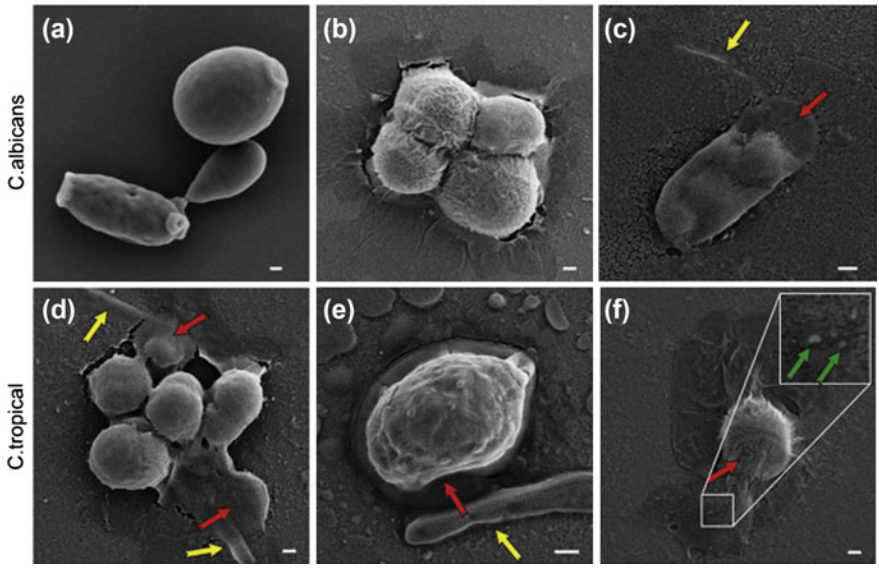

Fig. 8 Scanning electron micrographs (SEM) of **a** native *C. albicans* cells, **b** *C. albicans* cells treated with pure GO and **c** CNS–AgNPs for 24 h. **d** and **e** *C. tropical* cells treated with CNS–AgNPs. **f** *C. tropical* cells treated with GO–AgNPs for 24 h. *Red*, *green* and *yellow arrows* indicate breakage of yeast cells, CNS–AgNPs and AgNPs on GO surface, respectively. (Reproduced with permission from Li et al. (2013), Elsevier)

Table 2 Silver nanocomposites based antimicrobial biomaterials and their biomedical applications

Silver based nanocomposites (NCs)	Size of AgNP	Activity	Microbes tested	Evaluation parameters	Biomedical applications	References
Ag/Polyurethane (PU)	5 nm	AB	*B. subtilis, E. coli*	ND	Antibacterial catheter	Hsu et al. (2010)
Ag/Polystyrene NCs	8 nm	AB	*P. fluorescens, E. coli, B. circulens, S. aureus*	ZoI: 2–27 mm	Antibacterial coatings	Kamrupi et al. 2011)
Ag/TiO_2 nanocomposite films	10–30 nm	AB	*E. coli*	ZoI: 7 mm	Antibacterial coatings, Antibiofilm material	Yu et al. (2011)
Ag/Calcium phosphate		AB	*S. aureus, S. epidermidis*	85–98% inhibition	Antibacterial scaffold	Ewald et al. (2011)
Ag/PLA thin films	3–4 nm	AB	*E. coli, S. aureus, V. parahaemolyticus*	ZoI: 9–15 mm	Antibacterial scaffold, Biomedical coatings	Shameli et al. (2010)
Ag/Carbon/platinum NC	3–5 nm	AB	*Staphylococcus, P. aeruginosa*	ND	Antibiofilm coatings	Narayan et al. (2005)
Ag/Calcium phosphate NC	2.7 nm	AB	*S. mutan,* S. *sobrinus*	75% inhibition	Antibiofilm plaques	Cheng et al. (2012)
Ag/PU/PCL/PMMA	20–27 nm	AB	*E. coli*	10^6 fold reduction	Antibiofilm implants	Sawant et al. (2013)
Ag/Bioactive glass/chitosan	<50 nm	AB	*S. aureus*	ZoI:16 mm	Antimicrobial coatings	Pishbin et al. (2013)
Ag/pCBMA NC	ND	AB	*E. coli*	99.8% inhibition	Antimicrobial coatings, Anti adhesive biomaterial	Hu et al. (2013)
Ag/Nylon-6/CNT hybrid NCs	5–10 nm	AB	*S. aureus, S. pyogenes, E. coli, Salmonella enterica*	ZoI: 19–28 mm	Antimicrobial coatings, Disinfectant filters	Rangari et al. (2010)
Ag/Polyamide-6 NC	<100 nm	AB	*E. coli*	100% inhibition	Antimicrobial material	Damm et al. (2007)

(continued)

Table 2 (continued)

Silver based nanocomposites (NCs)	Size of AgNP	Activity	Microbes tested	Evaluation parameters	Biomedical applications	References
Ag/hydroxyapatite NC	20–30 nm	AB	*E. coli*	100% inhibition	Bone substitute material, Implant coatings	Liu et al. (2013)
Ag/Graphene hydrogel	10 nm	AB	*E. coli, S. aureus*	ZoI: 9.7–11.8 nm	Burns wound healing	Fan et al. (2014)
Ag/Montmorillonite/chitosan NC	2–3 nm	AB	*E. coli, S. aureus, MRSA*	ZoI: 8–9.5 mm	Coating surgical devices, Delivery system	Ahmad et al. (2009)
Ag/PES/SPES film	40–50 nm	AB	*S. aureus, S. albus, E. coli*	ZoI: 1–2.5 mm	Coatings medical devices	Cao et al. (2010)
Ag/collagen scaffold	30–60 nm	AB	*E. coli, P. mirabilis, B. cereus, S. aureus*	ND	Tissue scaffold	Mandal et al. (2012)
Ag/collagen/PHBV film	ND	AB	*E. coli, S. aureus, P. aeruginosa*	100% inhibition	Tissue scaffold	Bakare et al. (2016)
Ag/PLGA electrospun nanofibers	5–10 nm	AB	ND	ND	Tissue scaffolds Wound dressing	Khalil et al. (2013)
Ag/chitosan/PEG film		AB	*E. coli*	88% inhibition	Wound dressing	Rao et al. (2012)
Ag/Cellulose	5–11 nm	AB	*E. coli, S. aureus*	ZoI: 2–3.5 nm	Wound dressing	Maneerung et al. (2008)
Ag/gelatin electrospun pads	11–20 nm	AB	*P. aeroginosa, E. coli, MRSA, S. aureus*	ZoI: 1.9–2.4 mm	Wound dressing	Rujitanaroj et al. (2008)
AgNP/chitosan	–	AB	*S. aureus, B. subtilis, E. coli, S. choleraesuis*	MIC: 0.03–0.06 mg/ml	Wound dressing	Chen et al. (2014)
Ag/Cellulose acetate nanofibres	21 nm	AB	*S. aureus, E. coli, K. pneumoniae, P. aeruginosa*	99.9% inhibition	Wound dressing Tissue scaffolds	Son et al. (2006)
AgNP/Cu-loaded mullite NC		AB	*E. coli, S. aureus*	MIC: 1.6 mg/ml	Wound dressings, Antimicrobial coatings	Kar et al. (2014)

(continued)

Table 2 (continued)

Silver based nanocomposites (NCs)	Size of AgNP	Activity	Microbes tested	Evaluation parameters	Biomedical applications	References
Ag/silica polystyrene	1–10 nm	AB, AF	*S. aureus, C. albicans, K. pneumonia, E. coli, P. fluorescens, A. niger Salmonella enterica*	MIC: 62.5 µg/ml	Antimicrobial coatings	Egger et al. (2009)
AgNPs/rice-paper plant	<100 nm	AB, AF	*E. coli, C. albicans*	MIC: 14–28 mg/l	Wound dressing	Zeng et al. (2007)
AgNPs/CMC/PEO nanofibers	12–18 nm	AB, AF	*S. aureus, E. coli, P. aeruginosa, C. albicans*	ZoI: 12–20 mm	Wound dressing	Fouda et al. (2013)
AgNP/Chitosan nanofibers	10 nm	AF	*Alternaria sps., Bipolaris oryzae, B. cinerea, P. digitatum, C. higginsianum, Fusarium oxysporum*	40–90% reduction in spore germination	Antifungal therapies	Ifuku et al. (2015)
Ag/Graphene oxide NC	30–50 nm	AF	*C. albicans,C. tropical*	ZoI: 15 mm MIC: 0.125 µg/ml	Nosocomial infections, Local antifungal therapy	Li et al. (2013)
Ag/Carbon supported matrix	20 nm	AB, AV	*E. coli, B. subtilis,* Bacteriophage M13	60–80% inhibition in bacterial and fungal counts,	Antibacterial material Antiviral infection control	Vijayakumar and Prasad (2009)
AgNP/Chitosan NCs	3.5–13 nm	AV	H1N1 influenza A	60–85% inhibition in viral replication	Antiviral infection control	Mori et al. (2013)
AgNP/Graphene NC film	5–25 nm	AV	feline coronavirus, infectious bursal disease virus	25% inhibition in viral replication	Antiviral infection control	Chen et al. (2016)

AB Antibacterial; *AF* Antifungal, *AV* Antiviral, *ND* Not Determined

antifungal activity of CNS-AgNPs over GO, scanning electron microscopy was employed (Fig. 8). The SEM micrographs indicated that no significant morphological change was observed in *C. albicans* and *C. tropical* cells treated with pure GO. However, both fungal strains treated with CNS-AgNPs demonstrated a distinct damage to cytoplasmic membrane such that their intracellular contents were leaked completely. Moreover, release of silver ions from CNS-AgNPs also caused a more severe effect such that a clear concave zone was observed in the cell membrane. Similarly, a hydrogel based contact lens has recently been tested as antimicrobial biomaterial comprising of quaternized chitosan, AgNPs and graphene oxide (Huang et al. 2016). Contact lenses loaded with AgNP and GO demonstrated good mechanical properties and excellent antifungal efficacy under both in vitro and in vivo conditions. Authors indicated its therapeutic use as drug delivery vehicle for the treatment of fungal keratitis, a severe ocular disease in developing countries which often leads to blindness and ocular morbidity. Analogous antimicrobial performance of various silver based nanocomposites and their biomedical applications has been summarized in Table 2.

3.4 Nano Silver Based Antimicrobial Hydrogels

Hydrogel is a porous 3D semi interpenetrating polymeric network which has high water holding capacity than its own weight without getting dissolved into it (Mukherji et al. 2012; Agnihotri et al. 2012). Due to their soft architectures and ability to mimic the microenvironment of native tissue, they can be engineered to a myriad of applications such as in drug delivery, tissue engineering, stem cell engineering, immunomodulation, molecular therapies and even in cancer research (Lee and Mooney 2001; Drury and Mooney 2003). Another expanding area where hydrogels have gained enormous attention is in wound dressings and coating surgical devices to prevent nosocomial infections. Other than being non-toxic, hydrophilic, biocompatible and biodegradable, hydrogel exhibits several other remarkable properties such as oxygen permeability, good adhesion and easy handling, which make them an ideal candidate for biomedical applications (Peppas et al. 2006; Hoffman 2012; Zhu and Marchant 2011; Jones and Milton 2000). Especially for wound healing purposes, the water holding ability of hydrogel keeps the wound hydrated and prevents scar formation, which is inevitable several times. Moreover, their low abrasion characteristics and ability to supply nutrients in a controlled manner accelerates healing process and alleviate pain. Some commercial hydrogel based products like Hydrofiber® and Aquagel® are already in the market which allow to keep a moist environment around the wound site and promotes wound healing (Jones et al. 2006).

Despite several advantages associated with hydrogels, their utilization had been limited for two main reasons. First, hydrogels suffer with poor mechanical durability which restrict their applications in several domains such as tissue engineering and corneal implants where tough and flexible properties are specifically needed

(Zhu and Marchant 2011). Secondly, with few exceptions, hydrogels are generally more susceptible to get infected and their applications at the infected site may elevate the risk of spreading infection to surrounding tissues (Jones and Milton 2000). Integration of nanotechnological advances to hydrogel thus have succeeded to minimize these limitations and extended its accepted applications beyond treating sloughy and necrotic wounds. Reinforcing hydrogel with nanomaterials such as silica nanoparticles, graphene oxide, carbon nanotubes, clay nanosheets as nano-fillers have tremendously improved their mechanical strength. On the other side, introduction of nano-antimicrobials to hydrogel is becoming an utmost concern for its clinical relevance in much needed areas such as prostheses, ocular surgery, biodegradable sutures, and coating surgical implants and devices.

There exists a plethora of techniques for making nanocomposites hydrogels for diverse applications (Fig. 9). However, the development of nano antimicrobial hydrogels involves two classical approaches. In one approach, a wide range of nanomaterials with antimicrobial characteristics such as metallic nanoparticles (Ag, Au, Cu), carbon based (nanotubes, graphene, graphene oxide), polymeric, and inorganic materials (SiO_2, TiO_2) can be incorporated within the hydrogel structure so as to obtain nanocomposites with tailored functionalities. Secondly, polymeric materials which can form hydrogels and also contain innate antibacterial properties can be used with nanomaterials to demonstrate their synergistic effects. As compared to synthetic polymers, polymers having natural origin (cellulose, starch, chitosan, alginate, etc.) are increasingly utilized for biomedical applications due to their biocompatible, biodegradable and low cost attributes.

For example, Sacco et al. (2015) demonstrated the use of AgNP impregnated tripolyphosphate-chitosan hydrogels for the treatment of non-healing wounds. They investigated that there exist a synergism between AgNPs and chitosan, responsible for the enhanced antibacterial action of hydrogel against *S. aureus*, *E. coli*, *S. epidermidis*, and *P. aeruginosa* strains. Moreover, the hybrid gel contributed toward inhibiting the maturation of their biofilms whereas no harmful effects on the viability of keratinocytes and fibroblasts cells were observed through the biocompatibility tests. Another natural polymer isolated from microbial strain *Acetobacter xylinum* TISTR 975 i.e., bacterial cellulose was tested as an immobilizing template for AgNPs (Maneerung et al. 2008). Silver nanoparticles were synthesized in situ within bacterial cellulose by introducing polymeric material into $AgNO_3$ solution followed by the borohydride mediated reduction. The resulting hydrogel exhibited good physicochemical properties and a strong bactericidal performance against *E. coli* and *S. aureus* strains. Panacek et al. (2014) synthesized sodium polyacrylate stabilized AgNPs (size 10 nm) and incorporated into methylcellulose to form a hydrogel based nanocomposite which could be used as a potential topical antimicrobial formulation for treatment of burns and wounds. The hybrid nanocomposite showed excellent antibacterial and antifungal efficacy against infective pathogens *S. aureus, C. albicans, E. coli, P. auregenosa, S. epidermis* with MIC values of 25 mg L^{-1}. As claimed by the authors, this material could act as a barrier preventing the attack of microorganisms causing infections at wound site.

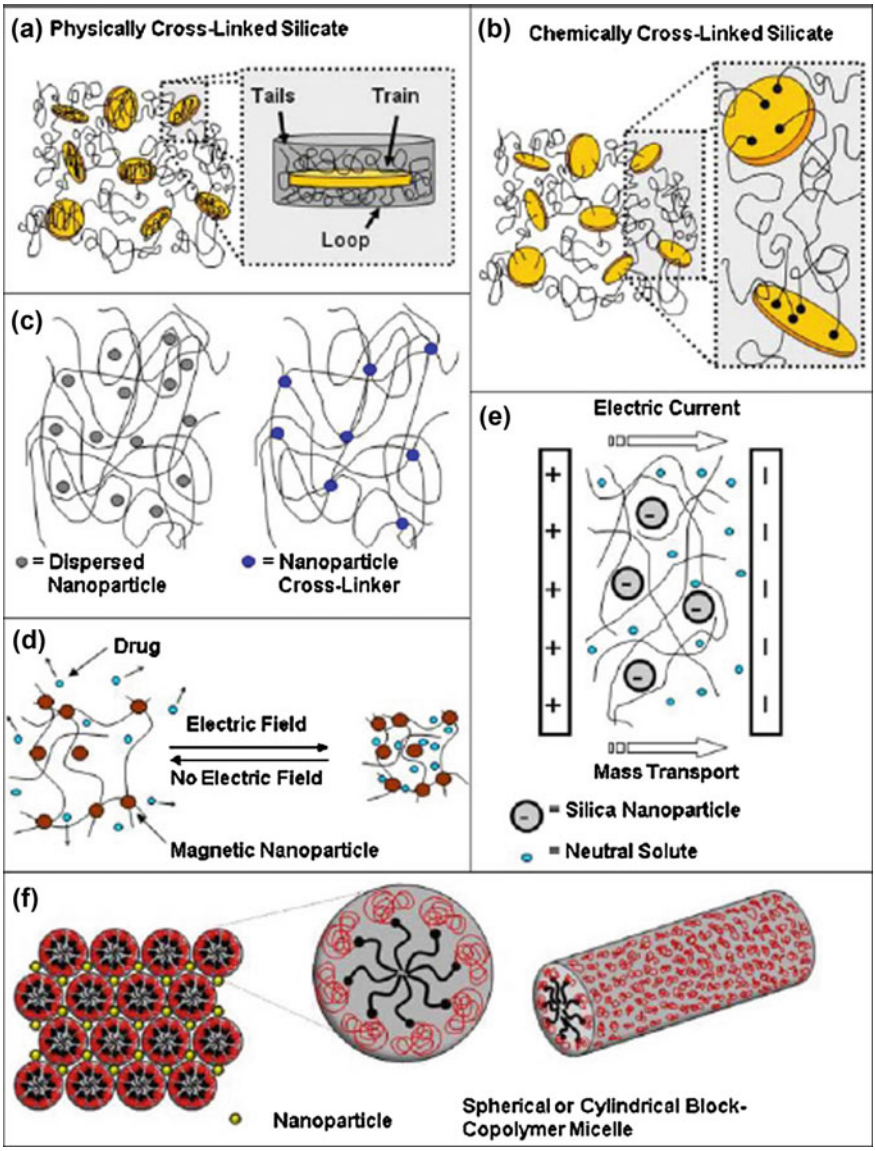

Fig. 9 Various techniques for synthesizing nanocomposite hydrogels. **a** Physical, but unstable interactions between polymeric chains and nanoparticles. **b** Nanoparticles are chemically bonded to polymers, often during radical polymerization processes. **c** Nanoparticles are chemically crosslinked within semi interpenetrating polymeric chains so as to enhance its antimicrobial properties. **d** Polymer–magnetic nanocomposites, with NPs dispersed within and/or crosslinking polymer chains for drug delivery applications. **e** Electro-osmotic flow of NPs embedded within polymeric matrix for the mass transport of drugs, proteins, and bioactive molecules. **f** Template block-copolymer gel with nanoparticles residing in the interstitial space between neighboring micelles. (Reproduced with permission from Schexnailder and Schmidt (2009), Springer)

Similarly, Vimala et al. (2011) incorporated an additional agent, curcumin obtained from *Curcuma longa* which has intrinsic wound healing, antibacterial, anti-inflammatory and anti-cancer properties into chitosan-PVA/Ag nanocomposite hydrogel. Antimicrobial assays yielded a noteworthy antibacterial and antifungal activity against *E. coli, Staphylococcus, Micrococcus, C. albicans, P. aeruginosa* with the diameter of ZoI ranging from 1 to 2.1 mm whereas, pristine hydrogel could not contributed towards forming a distinct zone of inhibition. In addition to that, the hydrogel nanocomposites exhibited satisfactory mechanical properties in order to employ them for wound dressings in treating/preventing infections. Agnihotri et al. (2012) also exploited chitosan–PVA-based hydrogel with dual functionalities

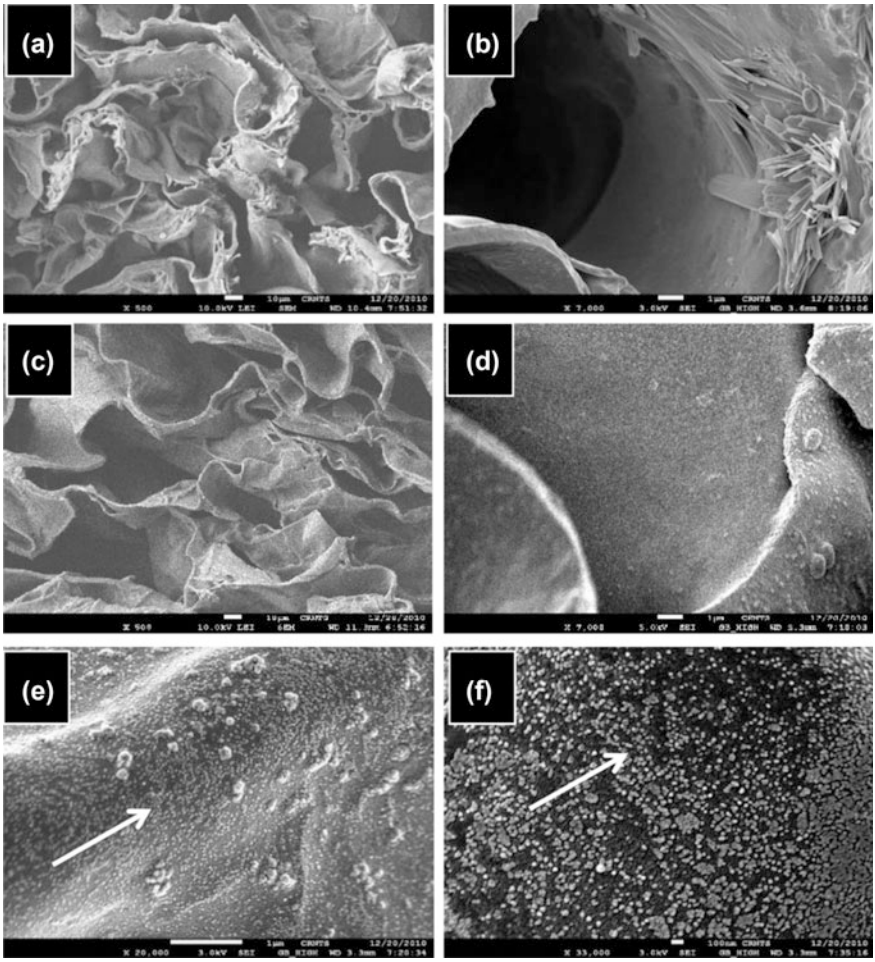

Fig. 10 FEG-SEM images of pure chitosan–PVA hydrogel (CP-50) at **a** 9500, and **b** 97,000 magnification. **c–f** demonstrated Ag-loaded chitosan–PVA hydrogel at different magnifications: **c** 9500, **d** 97,000, **e** 920,000, **f** 933,000. (Reproduced with permission from Agnihotri et al. (2012), Springer)

serving as a nano reactor in addition to its role for AgNP immobilization. SEM analyses indicated that semi-interpenetrating network of hydrogel not only facilitated a controlled and uniform distribution of AgNPs (Average size, 13 nm), it also precluded the requirement of adding any stabilizer to keep AgNPs in segregated state (Fig. 10). Swelling studies confirmed that the incorporation of silver incorporation enhanced the porosity and chain entanglement of the polymeric species of the hydrogel. The AgNP-hydrogel exhibited good antibacterial activity and was found to cause significant reduction in growth of *E. coli* in 12 h while such activity was not observed for the hydrogel without AgNPs.

A series of antibacterial superabsorbent hydrogels have been successfully prepared using polyacrylamide for biomedical applications. For example, Varaprasad et al. (2010) synthesized a semi-IPN Ag/poyacryalamide nanocomposite through free radical polymerization of acrylamide monomer in aqueous suspension containing desired amount of ammonia persulfate (as a cross linker), polyvinyl acetate, and ionic silver. The polymerization process was continued up to 8 h at 35 °C where silver ions were anchored at the surface of hydrogel through electrostatic interactions. To this polymeric mixture, sodium borohydride was introduced as to convert silver ions into AgNPs yielding hydrogel–silver nanocomposites. The antibacterial tests performed in solid agar demonstrated a significant and distinct ZoI while good antibacterial activity was observed against *E. coli* strains using liquid broth assays. Murthy et al. (2008) demonstrated the use of polyacrylamide/polyvinyl pyrrolidone semi-IPN hydrogel with AgNPs (size 3–5 nm) as excellent antibacterial biomaterials with 100% reduction in growth rate of *E. coli* under in vitro conditions. On a similar concept, Aggor et al. (2010) incorporated AgNPs (average size range, 1–12 nm) into polyacrylamide-co-acrylic acid hydrogel network and found that the hydrogel nanocomposite exhibits strong antibacterial and antifungal activity against *E. coli, S. aureus, B. subtilis,* and *C. albicans* strains. While increasing the dose of silver in hydrogel from 0.01 to 0.04 g/g of monomer mixture, there was a significant rise in antimicrobial study as manifested through a rise in the zone of inhibition (ZoI) from 10 to 20 mm. Moreover, the extraordinary swellable characteristics of hydrogel nanocomposite established its suitability as antimicrobial coatings for diverse biomedical applications.

A novel approach combining the antimicrobial therapy with nano-dressings has recently been cited for controlling foot infection in diabetic patients (El-Naggar et al. 2016). The nano-formula describes the fabrication of starch-chitosan/AgNP based dressing membranes through the conventional in situ synthesis of AgNPs within porous chitosan networks. The antibacterial experiments were tested against clinical pathogens isolated from the patients suffering from diabetic ulcers which mainly include *S. aureus, P. aeruginosa, K. pneumoniae*, *Proteus mirabilis* and *S. pyogenes*. Results indicated that chitosan-AgNP hydrogels always mediated higher antibacterial performance than pure chitosan under relevant conditions, regardless of the bacterial species tested. Specifically, the diameter of ZoI was calculated as 14.67 and 15.67 mm for the chitosan-AgNP against *S. aureus* and *P. aeruginosa* strains which was reduced to 11.88 and 14.11 mm when tested with pure chitosan

against respective strains. Interestingly, The MIC values of all bacterial isolates treated with pure amikacin (antibiotic) were lowered from 48 to 2 μg ml^{-1} after combining amikacin with chitosan-based silver nanoparticles, indicating their synergistic role. The proposed nano-formulation having 4 μg ml^{-1} amikacin with chitosan-AgNP hydrogel (5 ppm Ag in 6.9 mg ml^{-1} chitosan) was recommended for the treatment of MRSA and *P. aeruginosa* chronic wound infection without emergence of any nephrocytotoxicity or liver biochemical functions.

Another study hypothesized the concept of multifunctional biomaterial as a synthetic bone draft by encapsulating AgNPs (60–80 nm) within porous methacrylate hydrogels containing Na_2HPO_4 and $CaCl_2$ micro particles (Gonzalez-Sanchez et al. 2015). The antimicrobial efficacy of AgNP-hydrogel composites were determined on the basis of variation in the apparent lag phase and growth rate of *S. aureus* and *S. epidermidis* cells. Results indicate that hydrogel with 0.1 mM AgNP concentration demonstrated a better antibacterial activity than hydrogel having lower (0.5 mM) AgNP content. The maximum antibacterial effect of AgNP-hydrogel was achieved in 48 h while a further increase in contact time marked no increment in its antibacterial activity. Moreover, the presence of AgNPs did not pose either any cytotoxic effects on osteoblast cells or rheological characteristics of hydrogel. With both osteoconductive and antibacterial features, such hybrid gel could effectively be used in biomedical and dentistry applications as bone graft material.

In recent years, catheters with hydrogel coatings loaded with antimicrobial agents have been used to reduce the burden of catheters related infections. In a recent article, Loo et al. (2014) demonstrated the importance of AgNP-PVA hydrogels as antimicrobial coating on commercial endotracheal tubes. The antibacterial potential of hydrogel nanocomposite was evaluated on the basis of their degree of colonization on its surface after desired durations. Results showed that the density of *P. aeruginosa* colonization on pure PVA hydrogels was estimated to be in the range of 2.2–5.5 $\times$ 10^3 CFU cm^{-2} after 6 h of incubation whereas, no adherent bacterial colony was found on AgNP loaded PVA hydrogel for initial 6 h. After 18h, the bacterial colonization in pure PVA was increased up to 2.0–3.0 $\times$ 10^5 CFU cm^{-2} however AgNP-PVA hydrogel severely inhibited biofilm formation with density of colonization ranging from 1.2–9.0 $\times$ 10^4 CFU cm^{-2}. Similar trend was observed in case of *S. aureus* strains attachment to the hydrogels surface. Moreover, exposing hydrogel to human normal bronchial epithelial (BEAS2B) cells showed no cytotoxicity consequences. In another perspective, incorporating AgNPs into PVA matrix enhanced Young's modulus and ultimate tensile strength whereas its elongation at break was decreased than pristine PVA hydrogel. The mechanical property of hydrogel was found to comparable with commercially available endotracheal tubes and hence their utilization as antibacterial coatings for preventing nosocomial infections was envisaged by the authors. The details of other silver-based hydrogel nanocomposites and their potential biomedical applications have been summarized in Table 3.

Table 3 Silver nanoparticles hydrogel nanocomposites and their biomedical applications

AgNP based hydrogel nanocomposites	AgNP Size (nm)	Activity	Organisms tested	Evaluation parameter	Potential biomedical application	References
Ag/methacrylamide	<20	AB	*E. coli, S. aureus, P. auregenosa*	ZoI: 129–157% increase in diameters	Antimicrobial wound dressing	GhavamiNejad et al. (2016)
AgNPs/Dextran	20–30	AB	*Bacillus cereus*	ND	Antimicrobial material	Ma et al. (2009)
Ag/Polyacrylamide/PVP	3–5	AB	*E. coli*	100% reduction rate	Antimicrobial material	Murthy et al. (2008)
Ag/cellulose acetate aerogel	2.8	AB	ND	ND	Antimicrobial membranes	Luong et al. (2008)
Ag/carboxymethyl cellulose	8–14	AB	*E. coli, K. pneumoniae, P. aeruginosa, P. vulgaris, S. aureus, P. mirabilis*	ZoI: 14.8–16.2 mm	Antimicrobials against UTI infections	Alshehri et al. (2016)
Ag/Chitosan-PVA	13.3	AB	*E. coli*	83.5% inhibition rate	Disinfectants	Agnihotri et al. (2012)
Ag/Nap-FFC peptide	15	AB	*MRSA, Acinetobacter baumannii*	MIC: 40 μg/ml	Wound dressings	Simon et al. (2016)
Ag/hyaluronan/PVA	20–50	AB	*E. coli*	70–95% inhibition rate	Wound dressings	Zhang et al. (2012b)
Ag/Chitosan–Chitlac-blend	20	AB	*S. aureus, E. coli, S. epidermidis, P. aeruginosa*	3 Log reduction in bacterial counts	Wound dressings	Sacco et al. (2015)
Ag/Polyacrylamide-co-acrylic acid	1–12	AB, AF	*E. coli, S. aureus, B. subtilis, C. albicans*	Maximum ZOI: 20 mm	Antimicrobial material	Aggor et al. (2010)
Ag/Chitosan-PVA	16.5	AB, AF	*E. coli, P. aeruginosa, C. albicans, Micrococcus, Staphylococcus*	Maximum ZOI: 2.1 mm	Wound dressing	Vimala et al. (2011)

(continued)

Table 3 (continued)

AgNP based hydrogel nanocomposites	AgNP Size (nm)	Activity	Organisms tested	Evaluation parameter	Potential biomedical application	References
Ag/PHEMA/IA)/PVP hybrid hydrogels	ND	AB, AF	*S. aureus, C. albicans, E. coli*	70–95% inhibition rate	Tissue scaffold	Jovašević et al. (2011)
Ag/methylcellulose	10	AB, AF	*S. aureus, C. albicans, E. coli, P. auregenosa, S. epidermis*	MIC: 25 mg/L	Topical burns, Wounds healing	Panacek et al. (2014)

AB Antibacterial; *AF* Antifungal, *ND* Not Determined

4 Nanomaterials Based on Chitosan/Chitin

After cellulose, chitin is the most abundant mucopolysaccharide on earth. Chemically, it is a long chain polymer of poly (β-(1-4)-N-acetyl-d-glucosamine) virtually present in the exoskeleton of crustaceans/invertebrates as internal supporting structure and in the cell walls of fungus and yeasts (Jayakumar et al. 2010). Chitosan is a deacetylated form of chitin derivative which is a linear copolymer of N-acetyl glucosamine and glucosamine. Owing to its poor solubility in both aqueous and organic solvents, chitin polymer limits its practical applications and was widely accepted in the form of chitosan, which provided ample opportunities for further development (Dash et al. 2011). Moreover, chitosan offers some extraordinary properties such as innate biocompatibility, biodegradability, intrinsic antimicrobial efficacy, bone forming capability, and wound healing knack difficult to achieve with any other natural or synthetic polymer, making it a promising biomaterial to be used in various biomedical applications (Dash et al. 2011). With the shift of dimension from macro to nano, chitosan nanomaterials have also been shown to have expansive antibacterial, antiviral, and antifungal activity (Rabea et al. 2003), which depend upon several factors, including pH, degree of deacetylation, and the type of solvent (Tavaria et al. 2013; Chung et al. 2003). Moreover, the average molecular weight is also an important parameter that signifies the solubility of chitosan in various solvents.

In past two decades, chitosan has been proved to be a safer carrier for drug formulations (Felt et al. 1998). A number of delivery vehicles based on colloidal chitosan have been recently cited for delivering drugs, peptides, proteins, vaccines, DNA and siRNA (Almeida and Souto 2007; Mao et al. 2010). Due to its excellent mucoadhesive nature to a variety of hard and soft tissues, chitosan based hybrid materials may serve as a temporary skeleton in bone tissue engineering (Cañas et al. 2016). Fortunately, most of the chitosan based formulations has not been reported to provoke either inflammatory responses or allergic consequence within human body which has established its wide acceptability and utilization as biocompatible implants, injection, oral ingestions, topical applications for diverse biomedical purposes. Chitosan films/membranes has been tested as an efficient biomaterial for wound healing applications (skins, burns) and coating implants, thanks to its innate antimicrobial nature which inhibits biofilm formation yet promoting cell (e.g., fibroblasts, keratinocytes) proliferation for epidermal regeneration (Blažević et al. 2016). For example, Qi et al. (2004) synthesized chitosan and copper loaded chitosan nanoparticles (CSNPs) based on ionic gelation interaction between positively charged chitosan and negatively charged tripolyphosphate molecules. The processing was operated at room temperature and copper ions were absorbed on to CSNPs via ion exchange resins and/or surface chelation respectively. The average size of pure CSNPs and Cu-loaded CSNPs was calculated as 40 and 257 nm, respectively through AFM. These NPs showed effective antibacterial activity than their pristine counterparts against *E. coli*, *S. choleraesuis*, *S. typhimurium*, and *S. aureus* with MIC values ranging between 0.01 and 0.13 μg ml^{-1}. AFM analyses

revealed that CSNPs severely killed *S. choleraesuis* cells via membrane disruption such that membrane permeability was severely damaged resulting in the leakage of intracellular components. In another study, a synergistic antibacterial activity of Cu loaded CSNPs was observed against *E. coli* K88 strain with MIC (9 μg ml^{-1}) and MBC values 21–42 folds lower than the individual antibacterial entities i.e., copper ions and chitosan nanoparticles (Du et al. 2008). Therefore, it is anticipated that CSNPs often integrated with metallic nanoparticles can be used as potential antibacterial agents in biomedicine.

Anitha et al. (2009) synthesized CSNPs (average size, 40–50 nm) and their water soluble derivatives i.e., O-carboxymethyl chitosan (O-CMC, 90–100 nm) and N,O-carboxymethyl chitosan (N,O-CMC, 80–85 nm) nanoparticles, to compare their antibacterial efficacy against *S. aureus*. They found that among modified NPs; N,O-CMC NPs showed maximum antibacterial efficiency than O-CMC and CSNPs, with 100% inhibition rate at a maximum concentration of 1 mg ml^{-1}. The greater antibacterial effect of N,O-CMC NPs was attributed to their relatively higher degree of substitution of carboxymethyl groups on chitosan than unmodified chitosan, (Sun et al. 2006). Earlier, It was hypothesized that the introduction of carboxymethyl groups strengthen the overall positive charge on chitosan molecules, resulting in greater interaction with negatively charged components (lipopolysaccharides, proteins) present in the bacterial membrane, thereby causing membrane disruption and release of major content of intracellular material outside cells (Sudarshan et al. 1992).

Yien et al. (2012) evaluated the antifungal activity of CSNPs prepared from both low and high molecular weight chitosan against *Candida albicans, Fusarium solani* and *Aspergillus niger* species. Results showed a significant antimycotic activity with MIC values ranging from 0.6–1.0 and 0.5–1.2 mg ml^{-1} against *C. albicans* while 0.25–0.86 and 0.86–1.2 mg ml^{-1} against *F. solani* for high mol. wt. and low mol. wt. CSNPs, respectively. Among all the tested strains, *A. niger* appeared as the most resistant strain since there was an increase in MIC values by ten times (2–3 mg ml^{-1}). Therefore, these types of NPs could be incorporated into biomaterials for natural antifungal effect.

Biofilm formation due to the growth of *Streptococcus mutans* bacterial colonies in oral cavities is a major concern because it can cause diseases like caries, gum inflammation (gingivitis), and dilapidation of periodontal tissues i.e., periodontitis (Marsh 2004, 2005). In order to combat this problem nanoscale systems with antibacterial properties are being developed as a biological carrier materials to inhibit biofilms formation, maturation and growth. For the above mentioned reasons endodontic irrigants like sodium hypochlorite have been used for successful elimination of biofilms but these irrigants when retained in higher amounts for longer period of time may even cause more structural damage into the dentin (Zhang et al. 2010). Also, they leave smear layers because of incomplete elimination of bacteria and hence there is a need of chelating agents used as final irrigant to get rid of smear layers from the root canals (Çalt and Serper 2002). However the chelates may cause additional damage by compromising the mechanical integrity and amplified bacterial adherence on collagen (Kishen et al. 2008). Inspired by this approach, de Paz et al.

(2011) tested the antibacterial efficiency of chitosan nanoparticles prepared from chitosan (high and low mol. wt.) against *Streptococcus mutans* biofilms. Confocal scanning laser microscopy (CSLM) image analysis showed high antibacterial potency of low MW CSNPs with more than 95% destruction rate of bacterial cells as compared to 25% killing rate for high MW CSNPs. In line to this, a recent study has demonstrated the chelating and antibacterial effect of CSNPs to remove the smear layer and inhibit bacterial colonization on bovine dentin (del Carpio-Perochena et al. 2011). Results showed noteworthy chelation and antibacterial potency of NaOCl-EDTA, NaOCl-EDTA-CNPs and NaOCl-CNPs in comparison with that of the control and NaOCl groups, with 73% of live cells in case of NaOCl-EDTA-CNPs compared to 92% of control. This establishes the fact that CSNPs can be used as anti-biofilm and chelating agent in dental applications, however, further work on the above issues is needed.

Degradation of root canal system and the periradicular spot by bacterial infection and its toxin release can cause apical periodontitis and tissue demolition. These defects can be treated with guided tissue regeneration (GTR) method using collagen membrane barriers which prevents the apical migration of gingival epithelial into the bereaved root surface with improved healing and bone closure (Stoecklin-Wasmer et al. 2013) however, bacterial colonization still persists. Therefore, Barreras et al. (2016) used chitosan nanoparticles with chlorhexidine to demonstrate its antibacterial activity against *E. faecalis* in infected collagen membrane. Results show that CSNPs displayed significant antibacterial efficacy on conjugating with chlorhexidine since no bacterial growth was observed even at its lowest concentration, i.e., 0.08%. Thus, CSNPs/chlorhexidine nanosystems can be applied into membrane barriers to prevent periodontal infections.

Regarding fabrication of a drug delivery vehicle, Lee et al. (2016a) developed a method to load two drugs, tetracycline and lovastatin into PLGA/CSNPs (Average size, 107.8 nm) for fighting against bacterial infection concurrently with minimizing bone material loss. Preliminary studies conducted in dogs for potential antibacterial, bone formation/regeneration ability showed promising results against *A. actinomycetemcomitans* and *P. nigrescens* pathogens with a distinct ZoI appearing in PLGA/CSNPs/lovastatin-tetracycline (0.3%). Histopathological examination of tissue treated with prepared nanocomposite showed no sign of inflammation, though new deposits of cementum on the root surface and active plasmacytoid osteogenic activity were observed than in the control group. Therefore this material can be applied for controlled release of tetracycline and lovastatin into the periodontic defect for antibacterial and osteogenic activity.

Joint replacement procedures are being done now with high success rate however microbial colonization on artificial biomaterial still remains a problem causing serious implant rejections. Poly(methyl methacrylate) (PMMA) has been being used as bone cement for joint replacements however due to no intrinsic antibacterial activity, it is susceptible to infections due to biofilm formation over its surface (Hendriks et al. 2004). The addition of antibacterial agent in bone cement can really help to solve the persisting problem. Therefore, doping of CSNPs into PMMA and quaternary ammonium chitosan derivative nanoparticles (QCS NPs) has been done

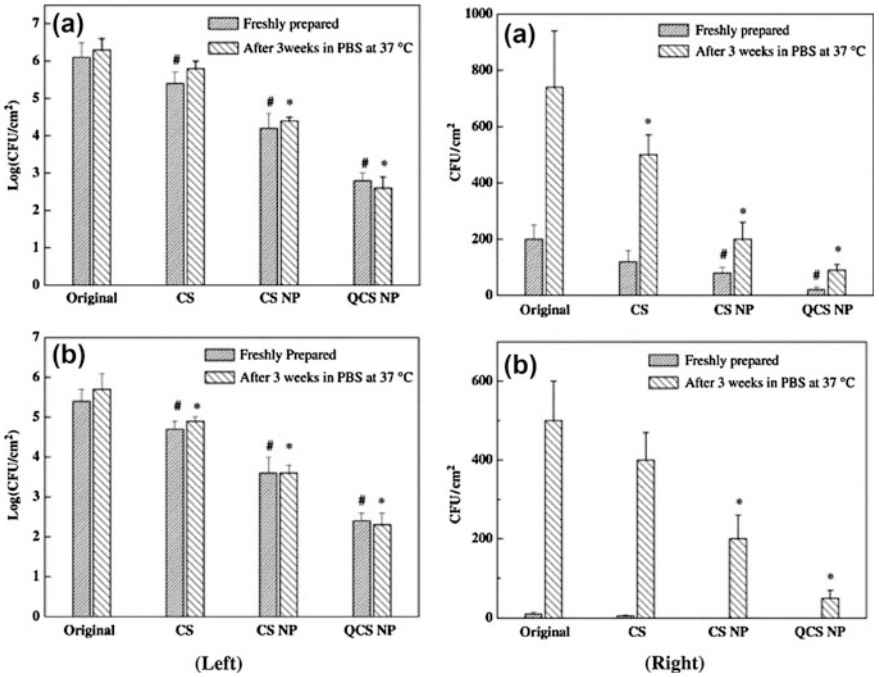

Fig. 11 Number of viable adherent *S. aureus* (**a**) and *S. epidermidis* (**b**) cells on the different substrates based on Smart set bone cement without (*Left*) and with gentamicin (*Right*). (Reproduced with permission from Shi et al. (2006), Elsevier)

to check their potential use as bactericidal agents (Shi et al. 2006). CSNPs & QCS NPs embedded cements showed decrease in viability of *S. aureus* and *S. epidermidis* with two and three orders of magnitude, respectively (Fig. 11). Moreover, the cytotoxicity assays of CSNPs and QCSNP-loaded bone cements showed no adverse effects on 3T3 mouse fibroblasts compared to pure PMMA cement.

Regarding the development of antibacterial coatings for medical devices and wound healing applications, a few reports have been published in recent times. For example, Romainor et al. (2014) demonstrated the potential of CSNPs (216 nm) doped cellulose films as an antibacterial wound dressing material. Disk diffusion assays revealed that while pure cellulose film could not exhibit any inhibitory effects on bacterial growth, no colonies were able to grown on the surface in contact with either chitosan-doped or chitosan nanoparticles-doped cellulose films. It was hypothesized that being polar in nature, both chitosan and CSNPs were able to diffuse slowly from films to agar plate, facilitating a direct contact killing action. The polar nature of film was further increased after cross linking with citric acid, which demonstrated a larger diameter of zone of inhibition i.e., an enhanced bactericidal potency of CSNP-doped cellulose films, validating the above hypothesis. The antibacterial assays showed the highest activity against *E. coli* with 85% and

81% inhibition rate in bacterial growth at 5% and 10% doping concentration of CSNPs and chitosan in cellulosic films, respectively. The value MIC and MBC values of CSNPs/cellulose films were determined as 10 and 13 μg ml^{-1} respectively, which was significantly lower than the bulk chitosan/cellulose films (MIC: 16.37 μg ml^{-1}; MBC: 19.70 μg ml^{-1}). Similarly, Jamil et al. (2016) developed cefazolin loaded chitosan nanoparticles (CSNPs) and tested their antimicrobial activity against *K. pneumoniae*, *P. aeroginosa* and extended spectrum beta lactamase (ESBL) positive *E. coli*. Antibiotic loaded CSNPs showed ZoI ranging from 15 to 22 mm with increasing concentration of drug from 200 to 2000 μg ml^{-1}. It indicates that CSNPs can be used to fabricate antibacterial agent for effective therapeutic solutions against MDR bacteria and can be employed in antimicrobial coatings on medical devices.

5 Other Nano-Antimicrobials

Despite the highest antibacterial potency manifested by silver, an overwhelming demand of nano-based products in biomedical and healthcare sector has obliged researchers to explore a few other materials, such as gold, copper/copper oxide, ZnO due to their inherent antibacterial properties. A number of publications describing antimicrobial applications of these nanomaterials for targeted drug delivery, antimicrobial coatings, biocidal medical devices and wound dressings have risen exponentially. While most research focused on claiming antimicrobial potential of these nanomaterials have employed either the colloidal state or often conjugated with antibiotics/drugs, the hypotheses of using them as next generation antimicrobial agents has limited clinical relevance. It is worth mentioning that for treating biomaterial associated infections, it is an important concern that a biocidal agent would not only kill the invaded microbes, but it should also prevent further bacterial adhesion and colonization on biomaterial surface. At the same time, antimicrobial agent must also encourage tissue integration at the implant site (Subbiahdoss et al. 2013). The incorporation of nanomaterials on to some support materials would thus be the most promising approach for developing novel nano-antimicrobial surfaces with multiple functionalities, durability with an enhanced biocidal response against clinical pathogens. In this section, only those studies are included where the antimicrobial potency of gold, copper oxide, and zinc oxide nanomaterials were explicitly assessed for specific biomedical applications.

5.1 Gold Based Antimicrobial Nanomaterials

Gold in bulk form is generally considered as an inert metal with feeble antimicrobial properties. However, it can be modified to introduce antimicrobial

properties when synthesized as nano sized particles. Similar to nano silver, a variety of biological synthesis approaches for gold nanoparticles (GNPs) has been published in recent times. For example, MubarakAli et al. (2011) used *Mentha piperita* plant extract to synthesize GNPs (150 nm) which were found to be active against clinically isolated human *E. coli* pathogen. Similarly, Ramamurthy et al. (2013) reported a simple and economical approach for synthesizing gold nanoparticles using aqueous extract of *Solanum torvum* fruit for treating several oxidative stress diseases and controlling human and veterinary infections. Gold nanoparticles demonstrated a noticeable zone of inhibition against *E. coli*, *Pseudomonas* and *Bacillus* while serving as a strong hydroxyl, superoxide, nitric oxide radical scavengers. Some recent reports employing fungal and bacterial mediated routes have shown the existence of phytochemicals in biological extracts, which might play a major role in improving the antibacterial efficacy of biogenic GNPs than conventional antibiotics (Prema et al. 2016; Balakumaran et al. 2016).

Another promising aspects of using GNPs in nanomedicine as carrier of antimicrobial agents and antibiotics is currently under investigation (Dykman and Khlebtsov 2012). GNPs are appropriate to deliver drugs to cellular addresses due to their ease in fabrication, functionalization, biocompatibility and their ability to cross cellular barriers while interacting with cell surface lipids (Huang et al. 2009). On the other hand, antibacterial efficacies of GNPs can be increased by adding antibiotics (Grace and Pandian 2007; Rai et al. 2010) whereas on conjugating with target-specific biomolecules, GNPs can be used as powerful therapeutics to destroy even cancerous cells. Gu et al. (2003) synthesized vancomycin-conjugated GNPs exploiting the strong binding affinity of gold to thiol (–SH) groups such that the antimicrobial activity of vancomycin was significantly improved on coating with gold nanoparticles (5 nm) against vancomycin resistant *Enterococci* (VRE) well as *E. coli*. These gold NP conjugates were more effective than vancomycin itself against various bacterial strains. Similar findings were presented in another study (Huang et al. 2007) where polygonal shaped GNPs after immobilizing vancomycin were used as an effective photothermal agents for the selective killing of VRE, MRSA, and other potentially drug-resistant microorganisms. Authors revealed that the dual functionalities of GNPs (to absorb near-infrared radiations) and vancomycin (binding with the terminal D-Ala-D-Ala moieties of the peptide units of bacterial cell wall) contributed towards its photothermal destruction with high efficiency without eliciting any toxic effects on human cells.

Rosemary et al. (2006) also demonstrated that ciprofloxacin-encapsulated gold-silica nanoshells mediated enhanced antibacterial activity as compared to free ciprofloxacin against *E. coli* DH5. The ability of Cefaclor, a second-generation antibiotic for synthesizing GNPs showed potent antimicrobial activities on both Gram positive *S. aureus* and Gram-negative bacteria *E. coli* strains (Rai et al. 2010). As compared to individual components, GNPs-antibiotic conjugate facilitated more severe perforations in bacterial cell wall followed by disrupting the bacterial DNA leading to cell death. Demurtas and Perry (2014) created a proficient drug delivery/carrier system by conjugating stable GNPs with antibiotic amoxicillin (a member of the penicillin family) which also reduced the chloroauric acid to form

nanoparticles (30–40 nm) and simultaneously coated them to afford the functionalized nanomaterial. Figure 12 shows the comparative antibacterial performances of pure amoxicillin, pure GNPs and amox-GNPs conjugates with various proportions over duration of 4 h. Results indicate that amoxicillin-conjugated GNPs showed an enhancement in antibacterial potency against *E. coli* as compared to the antibiotics and GNPs alone. The conjugated form exhibited 100% inhibition of *E. coli* growth in minimum time (2 h) with an MIC value of 300 μg ml^{-1}. Authors claimed that these GNPs conjugates can be used to coat a wide variety of biomaterial surfaces for instance implants, fabrics for treatment of wounds and glass surfaces to maintain hygienic conditions in the home, in hospitals and other infected prone areas (Das et al. 2009).

In a recent article, Naveena and Prakash (2013) evaluated ciprofloxacin-conjugated GNPs for its antibacterial activity against *S. aureus, E. faecalis, E. aerogenes* and *E. coli* pathogenic bacteria and demonstrated the highest ZoI in case of antibiotic conjugated GNPs with *E. coli* (24 mm) and *E. aerogenes* (21 mm), and *S. aureus* (19 mm) bacteria whereas a reasonable activity was observed against *E. faecalis* (14 mm). The combined antibacterial and antifungal activities of GNPs on conjugating with 5-fluorouracil (5-FU, anti-cancer drug) was also testified against *Micrococcus luteus*, *S. aureus*, *P. aeruginosa*, *E. coli, Aspergillus fumigatus* and *Aspergillus niger* (Selvaraj and Alagar 2007). 5-FU conjugated GNPs were

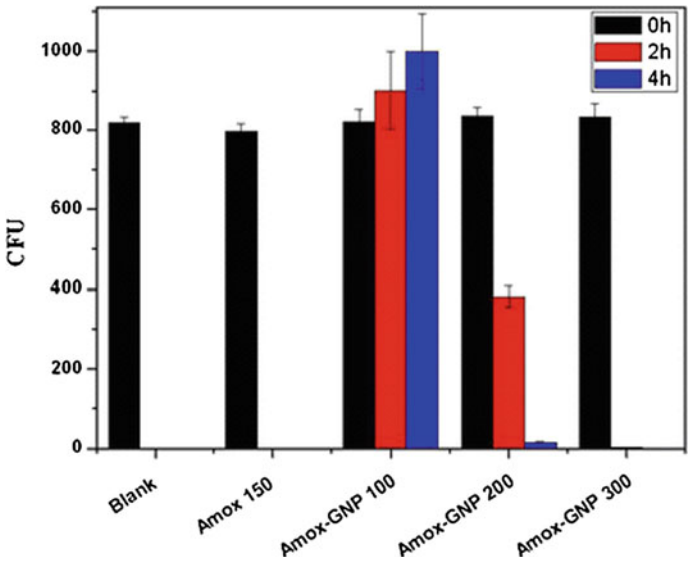

Fig. 12 Histogram plot showing antimicrobial activity of pure amoxicillin (Amox), pure gold nanoparticles (GNP) and amoxicillin-conjugated GNPs against *E. coli* after different incubation times (0, 2, and 4 h). All concentrations are in units of μg ml^{-1}. The 'blank' without addition of amoxicillin or amoxicillin-conjugated gold nanoparticles is shown for $t = 0$ only where it was possible to measure the colony forming units. (Reproduced with permission from Demurtas and Perry (2014), Springer)

found to be more effective on Gram negative bacteria than Gram positive due to their easier permeability into the cells. Additionally, they showed antifungal activity on *A. fumigates* and *A. niger*.

Apart from nano colloids, gold based nanocomposites have also been employed in biomedical applications as they prove to be a promising multifunctional platform, combining various diagnostic, therapeutic and antimicrobial modalities. For example, Chen et al. (2010) synthesized lysozyme-protected gold nano clusters combining the individual antibacterial properties of lysozyme and gold nanoclusters which inhibited the growth of antibiotic-resistant bacteria, such as *Acinetobacter baumannii* and vancomycin-resistant *E. faecalis* (VRE). Zaporojtchenko et al. (2006) produced an antibacterial metal/polymer nanocomposite coating system employing Ag/Au together with polytetrafluorethylene (PTFE) film having thickness between 100 and 300 nm. Higher antimicrobial effect of Ag–Au/PTFE nanocomposite coatings was estimated as compared to either individual Ag/PTFE or Au/PTFE as manifested by evaluating the extent of inhibition of *S. aureus* and *S. epidermidis* model bacterial strains. Marsich et al. (2011) prepared a nanocomposite hydrogel based on natural polysaccharides alginate and chitlac with incorporated GNPs (Average size, <20 nm). A good antimicrobial efficacy of these hydrogels was tested against *S. aureus* and *P. aeruginosa* though the GNPs containing nanocomposites showed some cytotoxic effects towards eukaryotic cell lines HepG2 and MG63. Recently, a novel biodegradable hydrogels based on gold nanocomposites was synthesized using acrylamide and wheat protein isolate through an environmentally benign route (Jayaramudu et al. 2013). GNPs were synthesized by reducing $HAuCl_4$ using neem leaf extract (*Azadirachta indica)* within the hydrogels network with an average size of 10 nm. The gold-nanocomposite hydrogel showed potential applications for wound/burns dressings as it exhibited a strong antibacterial activity against *S. pyogenes* and *E. coli* with ZoI 0.9 cm and 1 cm respectively, however it was entirely absent for hydrogel without GNPs. Zhou et al. (2014) synthesized cellulose nanofiber mats by alternatively depositing negatively charged GNPs (Average size 18.7 nm) and positively charged lysozyme through layer-by-layer (LBL) self-assembly technique. Multiple functional moieties present in lysozyme provided the necessary electrostatic interactions required for binding GNPs and lysozyme to the supporting substrate. The resulting GNPs/lys/cellulose LBL multilayer assembly was found to be highly stable while exposing them under dilute acid, alkali and surfactant solutions. These film coated mats were tested against *E. coli* and *S. aureus* which showed good antimicrobial potency for food packing, tissue engineering, wound dressings applications. The fabrication process for GNPs coated cellulose mats is shown in Fig. 13.

In a more recent study, Regiel-Futyra et al. (2015) have developed chitosan-gold nanocomposite (CS-GNPs) films, where biodegradable chitosan polymer was used both as reducing and stabilizing agent for GNPs. Three different grades of chitosan with low, medium, high average molecular weight & having different degrees of deacetylation (DD) were used for nanoparticles synthesis. Films based on chitosan with medium molecular weight and the highest DD exhibited the highest antibacterial activity against multi-drug resistant pathogens *S. aureus* and *P. aeruginosa*.

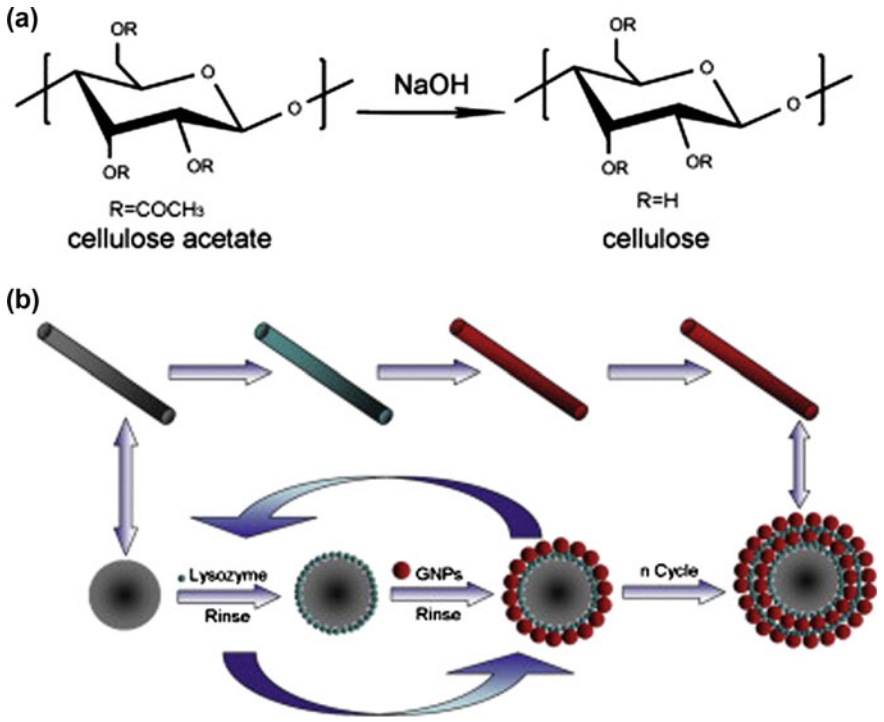

Fig. 13 **a** Hydrolysis scheme of cellulose acetate and **b** Schematic diagram illustrating the fabrication process of the layer by layer film of GNP/lysozyme coated cellulose mats (**b**). (Reproduced with permission from Zhou et al. (2014), Elsevier)

Moreover, small sized GNPs (16 nm) did not pose any cytotoxic effects on A549 (human lung adenocarcinoma epithelial cell line) and HaCaT (human keratinocyte) cell lines thereby these nanocomposites can be used for wound dressings as an adhesive bandages, or as antimicrobial coatings.

5.2 Copper/Copper-Oxide Based Antimicrobial Nanomaterials

The antimicrobial properties of copper have been known to us since ancient times contemporary with silver (Longano et al. 2012b). Later, the use of copper for treating sores and skin infections was well accepted by Greeks and Americans while a similar approach is still functional in many parts of Africa and Asia (Dollwet and Sorenson 1988). Copper materials combined with metals like cadmium and lead have been considered for sanitary and hygienic purposes since 1980s because of its biocidal activity against a varieties of microbes (Domek et al.

1984; Gould et al. 2009). CuNPs are currently gaining enormous interests due its low cost, availability and are considered to be practically more safe for humans (Grass et al. 2011; Longano et al. 2012b). In addition to this, CuNPs exhibit excellent antimicrobial activity against a varieties of clinically relevant pathogens including bacteria, fungi, and algae while a recent few reports have demonstrated their antimicrobial and catalytic efficacies similar to other metallic nanoparticles, i.e., silver and gold (Wei et al. 2010; Usman 2013) with intrinsic antimicrobial activities. Nano copper is considered as a potential candidate for new generation of antimicrobials since in trace amounts it is necessary for the execution of several metabolic processes in organisms (Krupanidhi et al. 2008) and at the same time it shows bactericidal activity at a relatively higher dose due to membrane disruption, nucleic acid and protein damage (Gant et al. 2007) and ROS production (Pelgrift and Friedman 2013; Longano et al. 2012b).

As compared to other popular antimicrobial nanoparticles of silver, a few studies in accordance with antimicrobial property of copper and CuO NPs have been reported. This is because of the fact that the antimicrobial potency of CuNPs is inferior as compared to silver or ZnO and hence, a higher concentration of CuNPs would be required to show similar biocidal effect as of other potential NPs (Ren et al. 2009). Nevertheless, being more economical than silver, CuO NPs are useful in combating against nosocomial infections and after immobilizing on to some support matrix, they can be utilized effectively with enhanced antibacterial properties (Xu et al. 1999; Longano et al. 2012b).

Nicola Cioffi and coworkers have done pioneer research for exploiting the nano copper based nanocomposites for antimicrobial applications (Longano et al. 2012a, b; Cioffi et al. 2004, 2005a, b). In 2005, they first reported the synthesis of bioactive coatings made from polymeric thin films loaded with copper nanoparticles for antibacterial and antifungal applications (Cioffi et al. 2005b). Copper nanoparticles (average size, 3.2 nm) were synthesized employing a novel electrochemical method under an inert and stabilizing environment. The synthesized CuNP were embedded in polymer matrices of polyvinylmethyl ketone (PVMK), poly(vinyl chloride) (PVC), and polyvinylidene fluoride (PVDF) followed by spin casting the resulting solution on to some substrate in order to get Cu-polymeric mixture in form of films with an average thickness of 400–500 nm. The bioactivity of three nanocomposites was screened against *S. cerevisiae* (yeast), *E. coli*, *S. aureus*, *Lysteria monocytogenes*, and molds, where CuNPs-PVMK films exhibited the strongest biostatic effect with more than 99.9 and 95% inhibition of bacterial and molds colonies, respectively. The higher antimicrobial activity of Cu nanocomposites was attributed to their higher release kinetics of Cu into the solution which was in turn linearly correlated with CuNPs loading. CuNPs-PVDF nanocomposites showed minimum antibacterial activity since the amount of Cu loading among all three coatings followed order as PVMK > PVC > PVDF. Authors envisaged the application of these CuNP based nanomaterials for the preparation of antibacterial coatings in household, biomedical and hospital, which are prone to receive infections. In another study, (Cioffi et al. 2005a), same research group investigated the electrochemical synthesis of copper and silver core-shell nanoparticles (range, 1.7–

6.3 nm) using tetraoctylammonium (TOA) salts as both base electrolyte and stabilizing agents to NPs. The nanocoatings formed after incorporating them onto PVMK polymer showed an extraordinary inhibitory effect on both eukaryotes and prokaryotes microbes, thanks to the synergistic action of nanoparticles and tetraoctylammonium as potential disinfectants. The enhanced physicochemical properties with good stability of Cu nanocoatings thus prompted the authors to find applications in antifouling paint and coating formulations. In a different study, CuNPs synthesized using laser ablation method were deposited on to polylactic acid after drop casting so as to make a self assembled antimicrobial film. The resulting nanocomposite showed good bioactivity against *Pseudomonas* spp. which is the most causative pathogen in food processing (Longano et al. 2012a).

A few other researchers have exploited the antimicrobial potential of CuNPs after incorporating onto some support material. For example, Grace et al. (2009) embedded CuNPs (37.5 nm) on alginate-cotton Cellulose (CACC) fibers for fabricating an antimicrobial package for wound dressing applications. The hybrid nanofibers demonstrated a noticeable antibacterial activity against *E. coli* with a MIC value of 5 CFU cm^2 when composites were loaded with 4% wt. of copper had. In addition to this, the presence of cellulose provided the required mechanical strength to alginate nanofibers for holding CuNPs for intended applications. In another study, polyurethane nanofibrous scaffold (Fig. 14) was used as a template for incorporating CuNPs (5–10 nm) for making antimicrobial wound dressing material (Sheikh et al. 2011). Ahmad et al. (2012) synthesized a CuO NPs doped polyurethane coatings by infusing CuO NPs (50 nm) into polyurethane (PU) elastomer and showed 90% reduction in growth of methicillin resistant *S. aureus* after an incubation period of 4 h with CuO (10% w/w)as a dopant. Owing to its good mechanical stability and excellent biocompatible properties, the prospects of CuO-PU nanocomposite in designing new antibacterial dental fillers, coatings, and tissue engineering constructs was discussed.

Similarly, Cady et al. (2011) synthesized CuNPs/cellulose nanofibrous composites as wound care materials exhibiting strong antibacterial activity against a multi-drug resistant pathogen, *A. baumannii.* The nanocomposite was fabricated by an alternative deposition of copper ions onto functionalized (negatively charged) cotton nanofibers followed by its reduction resulting in the synthesis of copper nanoparticles (Average size, 5 nm) onto cellulose substrate as a self assembled multilayer coatings. The antibacterial properties of CuNPs coated cotton substrates were assessed in solid media using zone of inhibition assay and growth inhibition assay in liquid broth. ZoI results indicated while Acticoat^{TM} (a commercial silver dressings) exhibited the largest zone of inhibition, which is an indicative of high Ag^+ ions release from sample into the solid agar medium, CuNP-cotton nanocomposite did not shown any distinct ZoI, thanks to non-leachable CuNPs that were bound firmly to the functionalized cotton surface. Contrary to this, CuNP-cotton caused a 8 log reduction in growth of *A. baumannii* in liquid assay within 10 min of incubation as compared to merely 1 log reduction for bacterial cells treated with AgNP-cotton samples. Moreover, CuNPs coated cotton exhibited

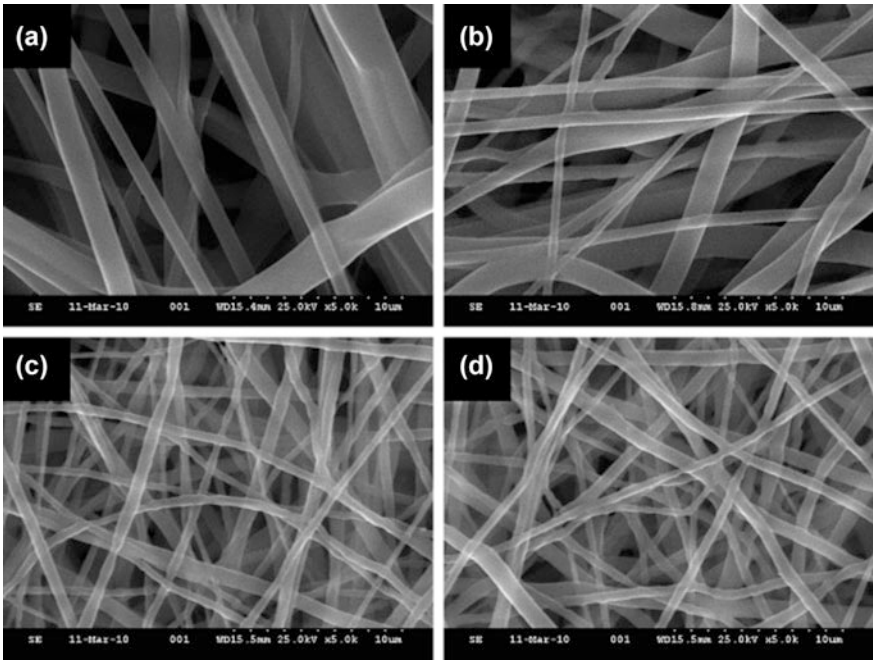

Fig. 14 SEM images for nanofibers that contain different amounts of Cu: **a** 0%, **b** 5%, **c** 7% and **d** 10%. (Reproduced with permission from Sheikh et al. (2011), Elsevier)

more effective bacterial killing than Acticoat^{TM} despite having approximately 90% less metal cm^{-2}. Authors envisaged the enhanced bactericidal killing of Cu-coated cotton samples to be predominantly contact killing activity, a similar mechanism of action proposed by (Agnihotri et al. 2013) in a different study related to immobilized silver nanoparticles. Several examples of Cu/CuO nanoparticles based nanocomposites and their biomedical applications are summarized in Table 4.

5.3 Zinc/Zinc-Oxide Based Antimicrobial Nanomaterials

Zinc oxide is a wurtzite-type semiconductor material with unparalleled physical and chemical properties such as piezoelectric behavior, high chemical stability, capability to absorb broad range radiations and photocatalytic activity. In recent years, It is being widely accepted in a variety of applications related to sensors, UV-light shielding, semiconductors, piezoelectric devices, field emission displays, pharmaceuticals, agriculture, photocatalytic degradation of pollutants, and as antimicrobial agents (Kołodziejczak-Radzimska and Jesionowski 2014; Wang 2004). Owing to its innate broad range antimicrobial features, ZnO nanoparticles represent another class of antimicrobial biomaterial which are considered to be safe, biocompatible,

Table 4 Copper/Copper oxide based nanocomposite and their biomedical applications

Cu/CuO based nanocomposites	CuNP size (nm)	Activity	Organisms tested	Evaluation parameter	Potential biomedical application(s)	References
CuNPs/Alginate-Cotton Cellulose fibers	37.5	AB	*E. coli*	5 CFU cm^{-2} at 4 wt% CuNPs	Antimicrobial dressing materials	Grace et al. (2009)
Cu/polypropylene & CuO/polypropylene	10–40	AB	*E. coli*	99.9% reduction in 4 h	Antimicrobial filler	Delgado et al. (2011)
CuNPs/polyurethane	5–10	AB	*E. coli, B. subtilis*	ND	Wound dressings	Sheikh et al. (2011)
CuNPs/cellulose	5	AB	*A. baumannii*	8 log reduction in 4 h	Antimicrobial dressing materials	Cady et al. (2011)
Cu doped diamond-like carbon films	10	AB	*E. coli*	99.9% reduction rate	Surface coatings in cardiovascular applications.	Chan et al. (2011)
CuNPs/polyurethane	50	AB	*MRSA*	90% reduction rate at 10% w/w CuO	Antibacterial dental fillers, Tissue engg. constructs, coatings,	Ahmad et al. (2012)
CuNPs/Soda lime glass/Ceramic coating	ND	AB, AF	*E. coli, Micrococcus luteus, Issatchenkia orientalis* (yeast)	MIC: 10–15 $\mu g/cm^2$	Biocide coatings on medical devices	Esteban-Tejeda et al. (2012)
CuO/TiO_2 nanorods	100	AB	*E. coli, S. aureus*	Reduction in viable counts	Antibacterial bone and dental implants	Hassan et al. (2013)
CuNPs/montmorillonite/epoxy nanocomposites	10–20	AB	*K. pneumonia, E. coli*	ZOI: 23–26 mm	Antimicrobial coating	Das et al. (2014)

(continued)

Table 4 (continued)

Cu/CuO based nanocomposites	CuNP size (nm)	Activity	Organisms tested	Evaluation parameter	Potential biomedical application(s)	References
CuO/Carboxymethyl cellulose hydrogels	40–75	AB	*E. coli, S. aureus*	ZOI: *E. coli* - 14 mm *S. aureus*-19 mm	Antibacterial material	Yadollahi et al. (2015)
Copper/bioactive glass/eggshell membrane	40–50	AB	*E. coli*	90% reduction rate	Wound dressing	Li et al. (2016)
Sn, Cu, Hg, and Ag composite nanopowders	<100	AB	*Streptococcus mutans, L. acidophilus*	MIC-12 mg/ml ZoI: 6, 13 mm	Disinfectant in dental filling materials	Lee et al. (2016b)
CuO/Chitosan hydrogel	10–25	AB	*E. coli, S. aureus*	ZOI: 8–11 mm	Antibacterial dressings	Farhoudian et al. (2016)

AB Antibacterial; *AF* Antifungal; *ND* Not determined

economically viable and have been used in our daily products such as cosmetics, delivery vehicles, and even as nanofillers in medical implants. Furthermore, ZnO posses some remarkable features such as low toxicity, biocompatibility and biodegradability which makes it a multifunctional material of interest for biomedical applications (Stoimenov et al. 2002).

ZnO NPs tend to have an extensive range of antimicrobial activity against various microorganisms which in turn dependent on concentration, size, shape, surface charge, porosity, surface functionalization and ligand binding ability of ZnO NPs (Yamamoto 2001). For instance, Narayanan et al. (2012) synthesized ZnO NPs of size ranging between 41–167 nm by precipitation method using zinc nitrate and NaOH. The antimicrobial activity was tested against common human pathogens such as *S. aureus, E. coli, K. pneumoniae, E. faecalis*, and *P. aeruginosa* with an average ZoI of nearly 21, 17, 13, 16, and 30 mm for respective strains at 100 μg concentration of ZnO NPs. In addition to this, the biogenic synthesis of nanoparticles can alleviate various limitations associated with the involvement of toxic chemicals and reagents through chemical approaches. For example, the antimicrobial efficacies of ZnO nanoparticles synthesized using green (average size, 40 nm) and chemical (average size, 25 nm) approaches were tested against various bacterial and fungal pathogens viz. *S. aureus, Serratia marcescens*, *Proteus mirabilis, Citrobacter freundii,* and fungal strains *Aspergillus flavus, Aspergillus nidulans, Trichoderma harzianum*, and *Rhizopus stolonifer* (Gunalan et al. 2012). Amongst the various tested bacterial strains, ZnO NPs showed the highest antimicrobial activity against *S. aureus* as demonstrated through a larger ZoI (26 mm) than *P. mirabilis* (27 mm), *S. marcescens* (24 mm) and *C. freundii* (19 mm). Among fungal pathogens, the order of antifungal effect was noticed as *R. stolonifer* > *A. flavus* > *A. nidulans* > *T. harzianum*. Interestingly, ZnO NPs synthesized through green route exhibited enhanced antibacterial & antifungal activity than chemical ones, despite having larger nanoparticle size. Several other studies have also reported the improved antimicrobial potency of ZnO NPs synthesized through green routes over chemical approaches (Gnanasangeetha and Thambavani 2013; Salem et al. 2015; Sharma et al. 2010).

In order to design antimicrobial coatings based on ZnO NPs, surface functionalization or immobilization to a support material would be utmost concern for facilitating their ease in handling, utilization and applicability. Antimicrobial activity and stability of ZnO nanoparticles can be improved by incorporating them into some carrier matrix. Moreover, ZnO in the form of nanorods can even act as an immobilizing template for other nano-antimicrobials like AgNPs and may contribute towards an unprecedented antimicrobial performance. For instance, Agnihotri et al. (2015) described a facile approach for dense immobilization of silver nanoparticles (AgNPs) on ZnO nanorods using arginine molecule as an eco-friendly cross linker. Various characterization studies indicated that arginine molecules provided numerous nucleation sites on ZnO nanorods forming stable silver-arginine complexes, which was subsequently reduced into silver nanoparticles (Fig. 15). The resulting Ag/ZnO hybrid nanocomposite (HNC) demonstrated an extraordinary antibacterial activity against *E. coli* and *B. subtilis* strains under the

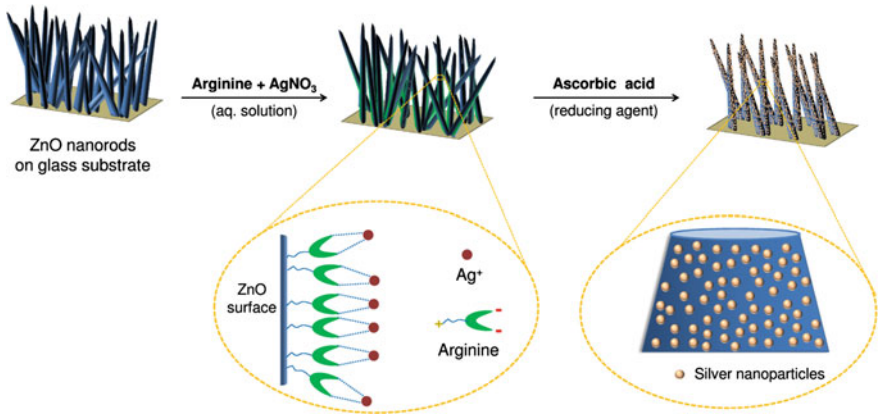

Fig. 15 Schematic representation shows in situ synthesis and immobilization of silver nanoparticles on ZnO nanorods using arginine as a linker. (Reproduced with permission from Agnihotri et al. (2015), Royal Society of Chemistry)

given test conditions. A dual mode of bactericidal action of HNCs, i.e., mediated through direct-contact as well as release of silver ions was hypothesized. Ag/ZnO HNCs showed no significant reduction in antibacterial efficacy even after being recycled multiple times. A good extent of immobilization was confirmed by measuring the amount of Ag and Zn release in potable water which was found to be well below the USEPA recommended standard. Interestingly, the Ag/ZnO HNC did not show any cytotoxic effects on the human hepatocarcinoma cell line (HepG2) and no significant generation of ROS was observed by the treated cells after an exposure of 24 h. The immobilized substrate thus showed good biocompatibility and sustained bactericidal activity and has good potential as a nano-antimicrobial biomaterial.

A hybrid nanocomposite based on ZnO & soluble starch (stabilizer) for coating onto cotton fabrics in order to make antimicrobial textiles was described earlier (Vigneshwaran et al. 2006). Incorporation of 1% ZnO NPs (average size, 38 nm) exhibited good antibacterial activity against *S. aureus* and *K. pneumonia* strains and inhibited biofilm formation by 99.9% along with preventing damage of cotton fabrics under UV illumination. In another study, dental composites made from polymer resin and ZnO NPs (as nanofillers) were employed to inhibit dental plaque (biofilm) formation that contribute to dental caries and often leads to degradation of resin composite (Aydin Sevinç and Hanley 2010). The plaque inhibition potency of polymer/ZnO nanocomposites were examined against various strains *Streptococcus sobrinus*, which is known to cause dental caries and possesses a superior adherence on tooth surfaces as compared to other *Streptococcus* species. The MIC and MBC values of ZnO NPs against *S. sobrinus* were found to be 50 and 150 μg ml^{-1}, respectively while the incorporation of 10% ZnO-NPs in polymeric resin reduced biofilm growth by 80% as compared to polymeric resin without ZnO NPs. Moreover, the adherence of *S. sobrinus* cells was found to be significantly higher on

pristine polymer resin as compared to 10% ZnO/polymer nanocomposites. On a similar account, higher biofilm coverage was observed on pure polymer resin after 3 days of incubation whereas, 10% ZnO/polymer nanocomposite showed significantly less colonies of *S. sobrinus* attached on its surface which discouraged the formation of a continuous biofilm layer.

Shalumon et al. (2011) synthesized an electrospun hybrid nanofibrous scaffold from sodium alginate/polyvinyl alcohol co-polymeric mixture containing dispersed ZnO NPs. Three nanocomposites were designed with varying amount (0.5, 1, 2 and 5%) of nano ZnO (average size, 160 nm) incorporated inside the polymeric nanofibers. The addition of ZnO NPs leads to increase in diameter of electrospun magnifiers from 190–240 to 220–360 nm. The evaluation of antibacterial activity on the basis of disc diffusion assays revealed that a larger ZoI was obtained for nanocomposites with higher ZnO concentration. Among the two strains, *S. aureus* appeared to be more sensitive to nanofibrous composite where the diameter of ZoI was calculated in the range of 15–16 mm as compared to 14–15 mm in case with *E. coli*. For assessing cytocompatibility, the nanofibrous scaffolds with low concentrations of ZnO (up to 0.5%) showed good adherence and spreading of L929 cells up to 96 h while a further increase in ZnO concentrations, the cell spreading is severely affected (Fig. 16). Moreover, a significant change in cell morphology was also observed and the existence of more rounded cells was attributed to cytotoxic consequences of ZnO NPs. Thus, nanofibrous composite with 5% ZnO was considered as a suitable material for wound dressing applications by providing good antibacterial activities yet remaining non cytotoxic.

Similarly, Ul-Islam et al. (2014) synthesized a potential wound dressing/healing nanocomposite films using bacterial cellulose with different concentrations of ZnO NPs (size range, 70–90 nm). The antimicrobial efficacies of nanostructured films were tested against *E. coli* where an introduction of 1 and 2% ZnO to cellulosic

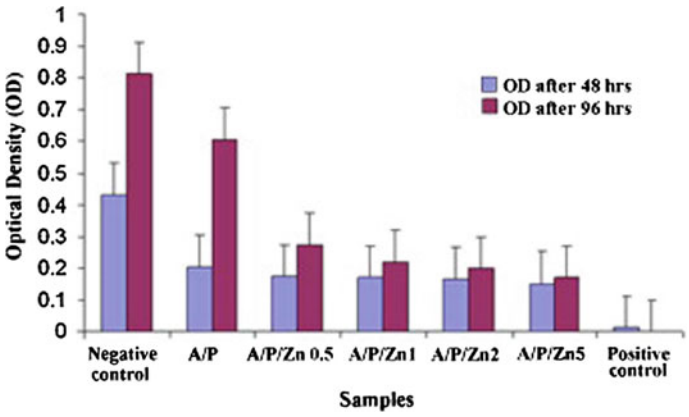

Fig. 16 Cytotoxicity studies on sodium alginate/PVA/ZnO mats using L929 at 48 and 96 h of attachment. A, P and Zn respectively represents alginate, PVA and ZnO. (Reproduce with permission from Shalumon et al. (2011), Elsevier)

Table 5 Zinc oxide based nanocomposites and their biomedical applications

ZnO based nanocomposites	NPs size (nm)	Activity	Organisms tested	Evaluation parameter	Potential biomedical applications	References
ZnO/sodium alginate/PVA nanofibers	160	AB	*S. aureus, E. coli*	ZoI: 15–16 mm	Wound dressings	Shalumon et al. (2011)
ZnO/Chitosan/PEG/Ag	25–65	AB	*E. coli, S. aureus, P. aeruginosa, B. subtilis*	ZoI: 11.9- 17.2 mm	Wounds/burns dressings	Liu and Kim (2012)
ZnO/parylene-glass	15	AB	*E. coli, S. aureus,*	Reduction rate: 100% (*E. coli*) & 76% (*S. aureus*)	Biomedical coatings Disinfectants	Applerot et al. (2010)
ZnO/TiO_2 coatings	20–80	AB	*E. coli, S. aureus,*	Reduction rate: 100% (*E. coli*) & 99.8% (*S. aureus*)	Antibacterial orthopedic and dental implants.	Hu et al. (2012)
ZnO/Polyvinylchloride	20	AB	*S. aureus*	Reduction rate: 100% at 30% ZnO conc.	Antibacterial endotracheal tube	Geilich and Webster (2013)
ZnO/Polyurethane membranes	<100	AF	*Aspergillus*	ND	Antibacterial scaffold	Vlad et al. (2012)
ZnO/Polycaprolactone	60	AB	*E. coli, S. aureus,*	ZoI: 9.8- 10. 2 mm	Antibacterial scaffold for tissue engineering	Augustine et al. (2014)
ZnO/Poly(D,L-lactide) nanofiber mats	8–20	AB	*E. coli, S. aureus*	Reduction rate: 35% (*E. coli*) & 95% (*S. aureus*)	Antimicrobial wound dressings.	Rodríguez-Tobías et al. (2014)
ZnO/Polypyrrole/chitosan	ND	AB	*E. coli, S. aureus, B. cereus, P. aeruginosa*	ZoI: 17.7- 29.6 mm	Surgical devices, biosensor and drug-delivery vehicles	Ebrahimiasl et al. (2015)

AB Antibacterial; *AF* Antifungal; *ND* Not determined

depicted a ZoI of 34 and 41 mm, respectively. Also, there was a significant up gradation in thermal, mechanical and biological properties of composites with addition of ZnO NPs. The resulting nanocomposites were also found to be non toxic and biocompatible to be used in biomedical applications. In a similar sense, several other polymeric and inorganic nanocomposites have been translated as an effective antimicrobial coating material for medical implants, devices after incorporating ZnO NPs which remain active for months without posing any cytotoxicity to human cells (Sudheesh Kumar et al. 2012; Applerot et al. 2010; Schwartz et al. 2012). A summary of various ZnO based nanocomposite and their biomedical applications are shown in Table 5.

6 Conclusions

The demands for high living standards and hygienic disciplines call new challenges for exploring some advanced, reliable but effective antimicrobial agents that should be environmentally benign and extremely safe for human use. Moreover, there is a daunting concern about the reoccurrence of drug-resistant microorganisms in infection prone areas such as hospitals, where the development of new antimicrobial materials for therapeutics, antisepsis or disinfection purposes are anticipating new strategies for employing them under clinically relevant conditions. In this context, nanotechnology is playing major role in some high priorities areas such as biomedical implants, surgical devices, catheters, stents, and antimicrobial coatings where the application of nano-antimicrobials based on metallic nanoparticles (silver, gold, copper/copper oxide), zinc oxide, chitosan nanoparticles along with their hybrid nanocomposites have been evaluated at various parameters such as their broad spectrum antimicrobial nature, efficacy, reusability and potential cytotoxicity towards mammalian cells. Each nanomaterial has shown its advantages and limitations therefore, accepting an ideal strategy or procedure for developing the antimicrobial biomaterials is not feasible. However, in future the involvement of "translational research" for making nano-antimicrobial biomaterials needs to be urgently constructed so as to implement the actual transformation of laboratory research for the realization of product for commercial applications.

References

Afzal MA, Kalmodia S, Kesarwani P, Basu B, Balani K (2013) Bactericidal effect of silver-reinforced carbon nanotube and hydroxyapatite composites. J Biomater Appl 27 (8):967–978. doi:10.1177/0885328211431856

Aggor FS, Ahmed EM, El-Aref A, Asem M (2010) Synthesis and characterization of poly (Acrylamide-co-Acrylic acid) hydrogel containing silver nanoparticles for antimicrobial applications. J Am Sci 12:6

Agnihotri S, Bajaj G, Mukherji S, Mukherji S (2015) Arginine-assisted immobilization of silver nanoparticles on ZnO nanorods: an enhanced and reusable antibacterial substrate without human cell cytotoxicity. Nanoscale 7(16):7415–7429

Agnihotri S, Mukherji S, Mukherji S (2012) Antimicrobial chitosan–PVA hydrogel as a nanoreactor and immobilizing matrix for silver nanoparticles. Appl Nanosci 2(3):179–188

Agnihotri S, Mukherji S, Mukherji S (2013) Immobilized silver nanoparticles enhance contact killing and show highest efficacy: elucidation of the mechanism of bactericidal action of silver. Nanoscale 5(16):7328–7340. doi:10.1039/C3nr00024a

Agnihotri S, Mukherji S, Mukherji S (2014) Size-controlled silver nanoparticles synthesized over the range 5–100 nm using the same protocol and their antibacterial efficacy. RSC Adv 4 (8):3974–3983

Ahamed MI, Sankar S, Kashif PM, Basha SK, Sastry TP (2015) Evaluation of biomaterial containing regenerated cellulose and chitosan incorporated with silver nanoparticles. Int J Biol Macromol 72:680–686. doi:10.1016/j.ijbiomac.2014.08.055

Ahmad MB, Shameli K, Darroudi M, Yunus W, Ibrahim NA, Hamid AA, Zargar M (2009) Antibacterial activity of silver/clay/chitosan bionanocomposites. Res J Biol Sci 4(11):1156–1161

Ahmad Z, Vargas-Reus MA, Bakhshi R, Ryan F, Ren GG, Oktar F, Allaker RP (2012) Antimicrobial properties of electrically formed elastomeric polyurethane-copper oxide nanocomposites for medical and dental applications. Methods Enzymol 509:87–99. doi:10.1016/b978-0-12-391858-1.00005-8

Akhavan O, Abdolahad M, Abdi Y, Mohajerzadeh S (2011) Silver nanoparticles within vertically aligned multi-wall carbon nanotubes with open tips for antibacterial purposes. J Mater Chem 21(2):387–393

Allen AB, Priddy LB, Li MT, Guldberg RE (2015) Functional augmentation of naturally-derived materials for tissue regeneration. Ann Biomed Eng 43(3):555–567. doi:10.1007/s10439-014-1192-4

Almajhdi FN, Fouad H, Khalil KA, Awad HM, Mohamed SH, Elsarnagawy T, Albarrag AM, Al-Jassir FF, Abdo HS (2014) In-vitro anticancer and antimicrobial activities of PLGA/silver nanofiber composites prepared by electrospinning. J Mater Sci Mater Med 25(4):1045–1053

Almeida AJ, Souto E (2007) Solid lipid nanoparticles as a drug delivery system for peptides and proteins. Adv Drug Del Rev 59(6):478–490

Alshehri SM, Aldalbahi A, Al-hajji AB, Chaudhary AA, in het Panhuis M, Alhokbany N, Ahamad T (2016) Development of carboxymethyl cellulose-based hydrogel and nanosilver composite as antimicrobial agents for UTI pathogens. Carbohydr Polym 138:229–236

Anitha A, Rani VD, Krishna R, Sreeja V, Selvamurugan N, Nair S, Tamura H, Jayakumar R (2009) Synthesis, characterization, cytotoxicity and antibacterial studies of chitosan, O-carboxymethyl and N, O-carboxymethyl chitosan nanoparticles. Carbohydr Polym 78 (4):672–677

Anjum S, Abbasi BH (2016) Thidiazuron-enhanced biosynthesis and antimicrobial efficacy of silver nanoparticles via improving phytochemical reducing potential in callus culture of *Linum usitatissimum* L. Int J Nanomedicine 11:715

Anna R, Silvia I, Agnieszka K, Manuel A, Jesus S (2013) Preparation and characterization of chitosan–silver nanocomposite films and their antibacterial activity against *Staphylococcus aureus*. Nanotechnology 24(1):015101

Applerot G, Abu-Mukh R, Irzh A, Charmet J, Keppner H, Laux E, Guibert G, Gedanken A (2010) Decorating parylene-coated glass with ZnO nanoparticles for antibacterial applications: a comparative study of sonochemical, microwave, and microwave-plasma coating routes. ACS Appl Mater Interfaces 2(4):1052–1059

Atiyeh BS, Costagliola M, Hayek SN, Dibo SA (2007) Effect of silver on burn wound infection control and healing: review of the literature. Burns 33(2):139–148

Augustine R, Malik HN, Singhal DK, Mukherjee A, Malakar D, Kalarikkal N, Thomas S (2014) Electrospun polycaprolactone/ZnO nanocomposite membranes as biomaterials with antibacterial and cell adhesion properties. J Polym Res 21(3):1–17

Aydin Sevinç B, Hanley L (2010) Antibacterial activity of dental composites containing zinc oxide nanoparticles. J Biomed Mater Res Part B Appl Biomater 94(1):22–31

Azizi S, Ahmad MB, Hussein MZ, Ibrahim NA, Namvar F (2014) Preparation and properties of poly(vinyl alcohol)/chitosan blend bionanocomposites reinforced with cellulose nanocrystals/ZnO–Ag multifunctional nanosized filler. Int J Nanomed 9:1909–1917. doi:10.2147/ijn.s60274

Bakare R, Hawthrone S, Vails C, Gugssa A, Karim A, Stubbs J 3rd, Raghavan D (2016) Antimicrobial and cell viability measurement of bovine serum albumin capped silver nanoparticles (Ag/BSA) loaded collagen immobilized poly(3-hydroxybutyrate-co-3-hydroxyvalerate) (PHBV) film. J Colloid Interface Sci 465:140–148. doi:10.1016/j.jcis.2015.11.041

Balakumaran M, Ramachandran R, Balashanmugam P, Mukeshkumar D, Kalaichelvan P (2016) Mycosynthesis of silver and gold nanoparticles: Optimization, characterization and antimicrobial activity against human pathogens. Microbiol Res 182:8–20

Barbinta-Patrascu ME, Ungureanu C, Iordache SM, Iordache AM, Bunghez IR, Ghiurea M, Badea N, Fierascu RC, Stamatin I (2014) Eco-designed biohybrids based on liposomes, mint-nanosilver and carbon nanotubes for antioxidant and antimicrobial coating. Mater Sci Eng C Mater Biol Appl 39:177–185. doi:10.1016/j.msec.2014.02.038

Barreras US, Méndez FT, Martínez REM, Valencia CS, Rodríguez PRM, Rodríguez JPL (2016) Chitosan nanoparticles enhance the antibacterial activity of chlorhexidine in collagen membranes used for periapical guided tissue regeneration. Mater Sci Eng C Mater Biol Appl 58:1182–1187

Bazaka K, Jacob MV, Crawford RJ, Ivanova EP (2012) Efficient surface modification of biomaterial to prevent biofilm formation and the attachment of microorganisms. Appl Microbiol Biotechnol 95(2):299–311

Blažević F, Milekić T, Romić MD, Juretić M, Pepić I, Filipović-Grčić J, Lovrić J, Hafner A (2016) Nanoparticle-mediated interplay of chitosan and melatonin for improved wound epithelialisation. Carbohydr Polym 146:445–454

Boucher HW, Talbot GH, Bradley JS, Edwards JE, Gilbert D, Rice LB, Scheld M, Spellberg B, Bartlett J (2009) Bad bugs, no drugs: no ESKAPE! An update from the infectious diseases society of America. Clin Infect Dis 48(1):1–12

Busscher HJ, Van Der Mei HC, Subbiahdoss G, Jutte PC, Van Den Dungen JJ, Zaat SA, Schultz MJ, Grainger DW (2012) Biomaterial-associated infection: locating the finish line in the race for the surface. Sci Transl Med 4 (153):153rv110–153rv110

Cady NC, Behnke JL, Strickland AD (2011) Copper-based nanostructured coatings on natural cellulose: Nanocomposites exhibiting rapid and efficient inhibition of a Multi-Drug Resistant wound pathogen, A. baumannii, and mammalian cell biocompatibility in vitro. Adv Funct Mater 21(13):2506–2514

Çalt S, Serper A (2002) Time-dependent effects of EDTA on dentin structures. J Endod 28(1):17–19

Campoccia D, Montanaro L, Arciola CR (2013a) A review of the biomaterials technologies for infection-resistant surfaces. Biomaterials 34(34):8533–8554

Campoccia D, Montanaro L, Arciola CR (2013b) A review of the clinical implications of anti-infective biomaterials and infection-resistant surfaces. Biomaterials 34(33):8018–8029

Cañas AI, Delgado JP, Gartner C (2016) Biocompatible scaffolds composed of chemically crosslinked chitosan and gelatin for tissue engineering. J Appl Polym Sci 133 (33)

Cao X, Tang M, Liu F, Nie Y, Zhao C (2010) Immobilization of silver nanoparticles onto sulfonated polyethersulfone membranes as antibacterial materials. Colloids Surf B Biointerfaces 81(2):555–562. doi:10.1016/j.colsurfb.2010.07.057

Chan Y-H, Huang C-F, Ou K-L, Peng P-W (2011) Mechanical properties and antibacterial activity of copper doped diamond-like carbon films. Surf Coat Technol 206(6):1037–1040

Chen Q, Jiang H, Ye H, Li J, Huang J (2014) Preparation, antibacterial, and antioxidant activities of silver/chitosan composites. J Carbohydr Chem 33(6):298–312

Chen WY, Lin JY, Chen WJ, Luo L, Wei-Guang Diau E, Chen YC (2010) Functional gold nanoclusters as antimicrobial agents for antibiotic-resistant bacteria. Nanomed (Lond) 5 (5):755–764. doi:10.2217/nnm.10.43

Chen X, Schluesener H (2008) Nanosilver: a nanoproduct in medical application. Toxicol Lett 176 (1):1–12

Chen YN, Hsueh YH, Hsieh CT, Tzou DY, Chang PL (2016) Antiviral activity of Graphene-silver nanocomposites against non-enveloped and enveloped viruses. Int J Environ Res Public Health 13(4). doi:10.3390/ijerph13040430

Cheng L, Weir MD, Xu HH, Antonucci JM, Kraigsley AM, Lin NJ, Lin-Gibson S, Zhou X (2012) Antibacterial amorphous calcium phosphate nanocomposites with a quaternary ammonium dimethacrylate and silver nanoparticles. Dent Mater 28(5):561–572. doi:10.1016/j.dental.2012.01.005

Chernousova S, Epple M (2013) Silver as antibacterial agent: ion, nanoparticle, and metal. Angew Chem Int Ed 52(6):1636–1653

Chopra I (2007) The increasing use of silver-based products as antimicrobial agents: a useful development or a cause for concern? J Antimicrob Chemother 59(4):587–590

Chung Y-C, Wang H-L, Chen Y-M, Li S-L (2003) Effect of abiotic factors on the antibacterial activity of chitosan against waterborne pathogens. Bioresour Technol 88(3):179–184

Cioffi N, Ditaranto N, Torsi L, Picca RA, De Giglio E, Sabbatini L, Novello L, Tantillo G, Bleve-Zacheo T, Zambonin PG (2005a) Synthesis, analytical characterization and bioactivity of Ag and Cu nanoparticles embedded in poly-vinyl-methyl-ketone films. Anal Bioanal Chem 382(8):1912–1918. doi:10.1007/s00216-005-3334-x

Cioffi N, Torsi L, Ditaranto N, Sabbatini L, Zambonin PG, Tantillo G, Ghibelli L, D'Alessio M, Bleve-Zacheo T, Traversa E (2004) Antifungal activity of polymer-based copper nanocomposite coatings. Appl Phys Lett 85(12):2417–2419

Cioffi N, Torsi L, Ditaranto N, Tantillo G, Ghibelli L, Sabbatini L, Bleve-Zacheo T, D'Alessio M, Zambonin PG, Traversa E (2005b) Copper nanoparticle/polymer composites with antifungal and bacteriostatic properties. Chem Mater 17(21):5255–5262

Costerton JW, Stewart PS, Greenberg E (1999) Bacterial biofilms: a common cause of persistent infections. Science 284(5418):1318–1322

Curtis L (2008) Prevention of hospital-acquired infections: review of non-pharmacological interventions. J Hosp Infect 69(3):204–219

Dahlin RL, Kasper FK, Mikos AG (2011) Polymeric nanofibers in tissue engineering. Tissue Eng Part B Rev 17(5):349–364

Damm C, Münstedt H, Rösch A (2007) Long-term antimicrobial polyamide 6/silver-nanocomposites. J Mater Sci 42(15):6067–6073

Dang JM, Leong KW (2006) Natural polymers for gene delivery and tissue engineering. Adv Drug Deliv Rev 58(4):487–499. doi:10.1016/j.addr.2006.03.001

Das G, Kalita RD, Gogoi P, Buragohain AK, Karak N (2014) Antibacterial activities of copper nanoparticle-decorated organically modified montmorillonite/epoxy nanocomposites. Appl Clay Sci 90:18–26

Das SK, Das AR, Guha AK (2009) Gold nanoparticles: microbial synthesis and application in water hygiene management. Langmuir 25(14):8192–8199. doi:10.1021/la900585p

Dash M, Chiellini F, Ottenbrite R, Chiellini E (2011) Chitosan—A versatile semi-synthetic polymer in biomedical applications. Prog Polym Sci 36(8):981–1014

de Mel A, Chaloupka K, Malam Y, Darbyshire A, Cousins B, Seifalian AM (2012) A silver nanocomposite biomaterial for blood-contacting implants. J Biomed Mater Res A 100 (9):2348–2357. doi:10.1002/jbm.a.34177

de Paz LEC, Resin A, Howard KA, Sutherland DS, Wejse PL (2011) Antimicrobial effect of chitosan nanoparticles on Streptococcus mutans biofilms. Appl Environ Microbiol 77 (11):3892–3895

del Carpio-Perochena AE, Bramante CM, Duarte MA, Cavenago BC, Villas-Boas MH, Graeff MS, Bernardineli N, de Andrade FB, Ordinola-Zapata R (2011) Biofilm dissolution

and cleaning ability of different irrigant solutions on intraorally infected dentin. J Endod 37 (8):1134–1138
Delgado K, Quijada R, Palma R, Palza H (2011) Polypropylene with embedded copper metal or copper oxide nanoparticles as a novel plastic antimicrobial agent. Lett Appl Microbiol 53 (1):50–54. doi:10.1111/j.1472-765X.2011.03069.x
Demurtas M, Perry CC (2014) Facile one-pot synthesis of amoxicillin-coated gold nanoparticles and their antimicrobial activity. Gold Bulletin 47(1–2):103–107
Dollwet H, Sorenson J (1988) Roles of copper in bone maintenance and healing. Biol Trace Elem Res 18(1):39–48
Domek MJ, Lechevallier MW, Cameron SC, McFeters GA (1984) Evidence for the role of copper in the injury process of coliform bacteria in drinking water. Appl Environ Microbiol 48 (2):289–293
Donlan RM, Costerton JW (2002) Biofilms: survival mechanisms of clinically relevant microorganisms. Clin Microbiol Rev 15(2):167–193
Dorobantu LS, Goss GG, Burrell RE (2015) Effect of light on physicochemical and biological properties of nanocrystalline silver dressings. RSC Adv 5(19):14294–14304
Drury JL, Mooney DJ (2003) Hydrogels for tissue engineering: scaffold design variables and applications. Biomaterials 24(24):4337–4351
Du WL, Xu YL, Xu ZR, Fan CL (2008) Preparation, characterization and antibacterial properties against *E. coli* K(88) of chitosan nanoparticle loaded copper ions. Nanotechnology 19 (8):085707. doi:10.1088/0957-4484/19/8/085707
Dunn K, Edwards-Jones V (2004) The role of Acticoat™ with nanocrystalline silver in the management of burns. Burns 30:S1–S9
Dykman L, Khlebtsov N (2012) Gold nanoparticles in biomedical applications: recent advances and perspectives. Chem Soc Rev 41(6):2256–2282
Ebrahimiasl S, Zakaria A, Kassim A, Basri SN (2015) Novel conductive polypyrrole/zinc oxide/chitosan bionanocomposite: synthesis, characterization, antioxidant, and antibacterial activities. Int J Nanomed 10:217
Egger S, Lehmann RP, Height MJ, Loessner MJ, Schuppler M (2009) Antimicrobial properties of a novel silver-silica nanocomposite material. Appl Environ Microbiol 75(9):2973–2976. doi:10.1128/aem.01658-08
El-Naggar MY, Gohar YM, Sorour MA, Waheeb MG (2016) Hydrogel dressing with a nano-Formula against methicillin-resistant *Staphylococcus aureus* and *Pseudomonas aeruginosa* diabetic foot bacteria. J Microbiol Biotechnol 26(2):408–420. doi:10.4014/jmb.1506.06048
Elbeshehy EK, Elazzazy AM, Aggelis G (2015) Silver nanoparticles synthesis mediated by new isolates of Bacillus spp., nanoparticle characterization and their activity against Bean Yellow Mosaic Virus and human pathogens. Front Microbiol 6
Esteban-Tejeda L, Malpartida F, Díaz LA, Torrecillas R, Rojo F, Moya JS (2012) Glass-(nAg, nCu) biocide coatings on ceramic oxide substrates. PLoS ONE 7(3):e33135
Ewald A, Hosel D, Patel S, Grover LM, Barralet JE, Gbureck U (2011) Silver-doped calcium phosphate cements with antimicrobial activity. Acta Biomater 7(11):4064–4070. doi:10.1016/j.actbio.2011.06.049
Fan Z, Liu B, Wang J, Zhang S, Lin Q, Gong P, Ma L, Yang S (2014) A novel wound dressing based on Ag/graphene polymer hydrogel: effectively kill bacteria and accelerate wound healing. Adv Funct Mater 24(25):3933–3943
Farhoudian S, Yadollahi M, Namazi H (2016) Facile synthesis of antibacterial chitosan/CuO bio-nanocomposite hydrogel beads. Int J Biol Macromol 82:837–843
Fei X, Jia M, Du X, Yang Y, Zhang R, Shao Z, Zhao X, Chen X (2013) Green synthesis of silk fibroin-silver nanoparticle composites with effective antibacterial and biofilm-disrupting properties. Biomacromolecules 14(12):4483–4488. doi:10.1021/bm4014149
Felt O, Buri P, Gurny R (1998) Chitosan: a unique polysaccharide for drug delivery. Drug Dev Ind Pharm 24(11):979–993. doi:10.3109/03639049809089942

Fouda MM, El-Aassar MR, Al-Deyab SS (2013) Antimicrobial activity of carboxymethyl chitosan/polyethylene oxide nanofibers embedded silver nanoparticles. Carbohydr Polym 92 (2):1012–1017. doi:10.1016/j.carbpol.2012.10.047

Gaikwad S, Ingle A, Gade A, Rai M, Falanga A, Incoronato N, Russo L, Galdiero S, Galdiero M (2013) Antiviral activity of mycosynthesized silver nanoparticles against herpes simplex virus and human parainfluenza virus type 3. Int J Nanomed 8:4303

Gajbhiye S, Sakharwade S (2016) Silver nanoparticles in cosmetics. J Cosmet Dermatol Sci Appl 6(01):48

Gant VA, Wren MW, Rollins MS, Jeanes A, Hickok SS, Hall TJ (2007) Three novel highly charged copper-based biocides: safety and efficacy against healthcare-associated organisms. J Antimicrob Chemother 60(2):294–299

Geilich BM, Webster TJ (2013) Reduced adhesion of Staphylococcus aureus to ZnO/PVC nanocomposites. In: Bioengineering Conference (NEBEC), 2013 39th Annual Northeast, 2013. IEEE, pp 7–8

Ghanbari H, Radenkovic D, Marashi SM, Parsno S, Roohpour N, Burriesci G, Seifalian AM (2016) Novel heart valve prosthesis with self-endothelialization potential made of modified polyhedral oligomeric silsesquioxane-nanocomposite material. Biointerphases 11(2):029801. doi:10.1116/1.4939036

GhavamiNejad A, Park CH, Kim CS (2016) In situ synthesis of antimicrobial silver nanoparticles within antifouling zwitterionic hydrogels by catecholic redox chemistry for wound healing application. Biomacromolecules 17(3):1213–1223

Gnanasangeetha D, Thambavani DS (2013) Biogenic production of zinc oxide nanoparticles using *Acalypha Indica*. J Chem Bio Phys Sci 4(1):238

Gonzalez-Sanchez MI, Perni S, Tommasi G, Morris NG, Hawkins K, Lopez-Cabarcos E, Prokopovich P (2015) Silver nanoparticle based antibacterial methacrylate hydrogels potential for bone graft applications. Mater Sci Eng C Mater Biol Appl 50:332–340. doi:10.1016/j.msec.2015.02.002

Gould SW, Fielder MD, Kelly AF, Morgan M, Kenny J, Naughton DP (2009) The antimicrobial properties of copper surfaces against a range of important nosocomial pathogens. Ann Microbiol 59(1):151–156

Grace AN, Pandian K (2007) Antibacterial efficacy of aminoglycosidic antibiotics protected gold nanoparticles—A brief study. Colloids Surf Physicochem Eng Aspects 297(1):63–70

Grace M, Chand N, Bajpai SK (2009) Copper alginate-cotton cellulose (CACC) fibers with excellent antibacterial properties. J Eng Fiber Fabr 4(3):1–14

Grass G, Rensing C, Solioz M (2011) Metallic copper as an antimicrobial surface. Appl Environ Microbiol 77(5):1541–1547

Gristina AG (1987) Biomaterial-centered infection: microbial adhesion versus tissue integration. Science 237(4822):1588–1595

Gu H, Ho PL, Tong E, Wang L, Xu B (2003) Presenting vancomycin on nanoparticles to enhance antimicrobial activities. Nano Lett 3(9):1261–1263. doi:10.1021/nl034396z

Gunalan S, Sivaraj R, Rajendran V (2012) Green synthesized ZnO nanoparticles against bacterial and fungal pathogens. Prog Nat Sci Mater Int 22(6):693–700

Gupta A, Silver S (1998) Molecular genetics: silver as a biocide: will resistance become a problem? Nat Biotechnol 16(10):888

Hall-Stoodley L, Costerton JW, Stoodley P (2004) Bacterial biofilms: from the natural environment to infectious diseases. Nat Rev Microbiol 2(2):95–108

Hall-Stoodley L, Stoodley P (2009) Evolving concepts in biofilm infections. Cell Microbiol 11(7):1034–1043

Harding JL, Reynolds MM (2014) Combating medical device fouling. Trends Biotechnol 32(3):140–146

Hassan MS, Amna T, Kim HY, Khil M-S (2013) Enhanced bactericidal effect of novel CuO/TiO_2 composite nanorods and a mechanism thereof. Compos B Eng 45(1):904–910

Hench LL, Polak JM (2002) Third-generation biomedical materials. Science 295(5557): 1014–1017

Hendriks J, Van Horn J, Van Der Mei H, Busscher H (2004) Backgrounds of antibiotic-loaded bone cement and prosthesis-related infection. Biomaterials 25(3):545–556

Herkendell K, Shukla VR, Patel AK, Balani K (2014) Domination of volumetric toughening by silver nanoparticles over interfacial strengthening of carbon nanotubes in bactericidal hydroxyapatite biocomposite. Mater Sci Eng C Mater Biol Appl 34:455–467. doi:10.1016/j.msec.2013.09.034

Hill JW (2009) Colloidal silver: medical uses, toxicology and manufacture. Clear Springs Press

Hoffman AS (2012) Hydrogels for biomedical applications. Adv Drug Del Rev 64:18–23

Hoop M, Shen Y, Chen XZ, Mushtaq F, Iuliano LM, Sakar MS, Petruska A, Loessner MJ, Nelson BJ, Pané S (2015) Magnetically driven silver-coated nanocoils for efficient bacterial contact killing. Adv Funct Mater 26(7):1063–1069. doi:10.1002/adfm.201504463

Hsu SH, Tseng HJ, Lin YC (2010) The biocompatibility and antibacterial properties of waterborne polyurethane-silver nanocomposites. Biomaterials 31(26):6796–6808. doi:10.1016/j.biomaterials.2010.05.015

Hu H, Zhang W, Qiao Y, Jiang X, Liu X, Ding C (2012) Antibacterial activity and increased bone marrow stem cell functions of Zn-incorporated TiO_2 coatings on titanium. Acta Biomater 8(2):904–915

Hu R, Li G, Jiang Y, Zhang Y, Zou JJ, Wang L, Zhang X (2013) Silver-zwitterion organic-inorganic nanocomposite with antimicrobial and antiadhesive capabilities. Langmuir 29(11):3773–3779. doi:10.1021/la304708b

Hu W, Peng C, Luo W, Lv M, Li X, Li D, Huang Q, Fan C (2010) Graphene-based antibacterial paper. ACS Nano 4(7):4317–4323. doi:10.1021/nn101097v

Huang JF, Zhong J, Chen GP, Lin ZT, Deng Y, Liu YL, Cao PY, Wang B, Wei Y, Wu T, Yuan J, Jiang GB (2016) A hydrogel-based hybrid theranostic contact lens for fungal keratitis. ACS Nano. doi:10.1021/acsnano.6b00601

Huang WC, Tsai PJ, Chen YC (2007) Functional gold nanoparticles as photothermal agents for selective-killing of pathogenic bacteria. Nanomed (Lond) 2(6):777–787. doi:10.2217/17435889.2.6.777

Huang X, Neretina S, El-Sayed MA (2009) Gold nanorods: from synthesis and properties to biological and biomedical applications. Adv Mater 21(48):4880–4910

Hubbell JA (1995) Biomaterials in tissue engineering. Biotechnol (N Y) 13(6):565–576

Ifuku S, Tsukiyama Y, Yukawa T, Egusa M, Kaminaka H, Izawa H, Morimoto M, Saimoto H (2015) Facile preparation of silver nanoparticles immobilized on chitin nanofiber surfaces to endow antifungal activities. Carbohydr Polym 117:813–817. doi:10.1016/j.carbpol.2014.10.042

Ingle A, Gade A, Pierrat S, Sonnichsen C, Rai M (2008) Mycosynthesis of silver nanoparticles using the fungus Fusarium acuminatum and its activity against some human pathogenic bacteria. Curr Nanosci 4(2):141–144

Jamil B, Habib H, Abbasi S, Nasir H, Rahman A, Rehman A, Bokhari H, Imran M (2016) Cefazolin loaded chitosan nanoparticles to cure multi drug resistant Gram-negative pathogens. Carbohydr Polym 136:682–691

Jayakumar R, Menon D, Manzoor K, Nair S, Tamura H (2010) Biomedical applications of chitin and chitosan based nanomaterials—A short review. Carbohydr Polym 82(2):227–232

Jayaramudu T, Raghavendra GM, Varaprasad K, Sadiku R, Raju KM (2013) Development of novel biodegradable Au nanocomposite hydrogels based on wheat: for inactivation of bacteria. Carbohydr Polym 92(2):2193–2200

Johnsson B, Lofas S, Lindquist G (1991) Immobilization of proteins to a carboxymethyldextran-modified gold surface for biospecific interaction analysis in surface plasmon resonance sensors. Anal Biochem 198(2):268–277

Jones V, Grey JE, Harding KG (2006) Wound dressings. BMJ 332(7544):777–780. doi:10.1136/bmj.332.7544.777

Jones V, Milton T (2000) When and how to use hydrogels. Nurs Times 96(23):3–4

Jovašević J, Dimitrijević S, Filipović J, Tomić SLj MM (2011) Swelling, mechanical and antimicrobial studies of Ag/P (HEMA/IA)/PVP semi-IPN hybrid hydrogels. Acta Phys Pol A 2:279–283

Jukes L, Mikhail J, Bome-Mannathoko N, Hadfield SJ, Harris LG, El-Bouri K, Davies AP, Mack D (2010) Rapid differentiation of *Staphylococcus aureus*, *Staphylococcus epidermidis* and other coagulase-negative staphylococci and methicillin susceptibility testing directly from growth-positive blood cultures by multiplex real-time PCR. J Med Microbiol 59(12):1456–1461

Kamrupi I, Phukon P, Konwer B, Dolui S (2011) Synthesis of silver–polystyrene nanocomposite particles using water in supercritical carbon dioxide medium and its antimicrobial activity. J Supercrit Fluids 55(3):1089–1094

Kang S, Herzberg M, Rodrigues DF, Elimelech M (2008) Antibacterial effects of carbon nanotubes: size does matter! Langmuir 24(13):6409–6413. doi:10.1021/la800951v

Kannan RY, Salacinski HJ, De Groot J, Clatworthy I, Bozec L, Horton M, Butler PE, Seifalian AM (2006) The antithrombogenic potential of a polyhedral oligomeric silsesquioxane (POSS) nanocomposite. Biomacromolecules 7(1):215–223. doi:10.1021/bm050590z

Kar S, Bagchi B, Kundu B, Bhandary S, Basu R, Nandy P, Das S (2014) Synthesis and characterization of Cu/Ag nanoparticle loaded mullite nanocomposite system: A potential candidate for antimicrobial and therapeutic applications. Biochimica et Biophysica Acta (BBA)-General Subjects 1840(11):3264–3276

Khalil KA, Fouad H, Elsarnagawy T, Almajhdi FN (2013) Preparation and characterization of electrospun PLGA/silver composite nanofibers for biomedical applications. Int J Electrochem Sci 8:3483–3493

Kim J, Lee J, Kwon S, Jeong S (2009) Preparation of biodegradable polymer/silver nanoparticles composite and its antibacterial efficacy. J Nanosci Nanotechnol 9(2):1098–1102

Kishen A, Sum C-P, Mathew S, Lim C-T (2008) Influence of irrigation regimens on the adherence of *Enterococcus faecalis* to root canal dentin. J Endod 34(7):850–854

Kołodziejczak-Radzimska A, Jesionowski T (2014) Zinc oxide—from synthesis to application: a review. Materials 7(4):2833–2881

Krupanidhi S, Sreekumar A, Sanjeevi C (2008) Copper & biological health. Indian J Med Res 128 (4):448

Kumar A, Vemula PK, Ajayan PM, John G (2008) Silver-nanoparticle-embedded antimicrobial paints based on vegetable oil. Nat Mater 7(3):236–241

Lavorgna M, Attianese I, Buonocore GG, Conte A, Del Nobile MA, Tescione F, Amendola E (2014) MMT-supported Ag nanoparticles for chitosan nanocomposites: structural properties and antibacterial activity. Carbohydr Polym 102:385–392. doi:10.1016/j.carbpol.2013.11.026

Lee B-S, Lee C-C, Wang Y-P, Chen H-J, Lai C-H, Hsieh W-L, Chen Y-W (2016a) Controlled-release of tetracycline and lovastatin by poly (d, l-lactide-co-glycolide acid)-chitosan nanoparticles enhances periodontal regeneration in dogs. Int J Nanomed 11:285

Lee J-H, Velmurugan P, Park J-H, Lee K-J, Jin J-S, Park Y-J, Bang K-S, Oh B-T (2016b) In vitro fabrication of dental filling nanopowder by green route and its antibacterial activity against dental pathogens. J Photochem Photobiol B: Biol 159:229–236

Lee KY, Mooney DJ (2001) Hydrogels for tissue engineering. Chem Rev 101(7):1869–1880

Li C, Wang X, Chen F, Zhang C, Zhi X, Wang K, Cui D (2013) The antifungal activity of graphene oxide-silver nanocomposites. Biomaterials 34(15):3882–3890. doi:10.1016/j.biomaterials.2013.02.001

Li J, Zhai D, Lv F, Yu Q, Ma H, Yin J, Yi Z, Liu M, Chang J, Wu C (2016) Preparation of copper-containing bioactive glass/eggshell membrane nanocomposites for improving angiogenesis, antibacterial activity and wound healing. Acta Biomater 36:254–266

Li X, Lenhart JJ (2012) Aggregation and dissolution of silver nanoparticles in natural surface water. Environ Sci Technol 46(10):5378–5386

Li Z, Lee D, Sheng X, Cohen RE, Rubner MF (2006) Two-level antibacterial coating with both release-killing and contact-killing capabilities. Langmuir 22(24):9820–9823. doi:10.1021/la0622166

Lin JJ, Lin WC, Li SD, Lin CY, Hsu SH (2013) Evaluation of the antibacterial activity and biocompatibility for silver nanoparticles immobilized on nano silicate platelets. ACS Appl Mater Interfaces 5(2):433–443. doi:10.1021/am302534k

Liu X, Mou Y, Wu S, Man H (2013) Synthesis of silver-incorporated hydroxyapatite nanocomposites for antimicrobial implant coatings. Appl Surf Sci 273:748–757

Liu Y, Kim H-I (2012) Characterization and antibacterial properties of genipin-crosslinked chitosan/poly (ethylene glycol)/ZnO/Ag nanocomposites. Carbohydr Polym 89(1):111–116

Longano D, Ditaranto N, Cioffi N, Di Niso F, Sibillano T, Ancona A, Conte A, Del Nobile M, Sabbatini L, Torsi L (2012a) Analytical characterization of laser-generated copper nanoparticles for antibacterial composite food packaging. Anal Bioanal Chem 403(4):1179–1186

Longano D, Ditaranto N, Sabbatini L, Torsi L, Cioffi N (2012b) Synthesis and antimicrobial activity of copper nanomaterials. In: Cioffi N, Rai M (eds) Nano-antimicrobials: progress and prospects. Springer, Berlin, Heidelberg, pp 85–117. doi:10.1007/978-3-642-24428-5_3

Loo CY, Young PM, Lee WH, Cavaliere R, Whitchurch CB, Rohanizadeh R (2014) Non-cytotoxic silver nanoparticle-polyvinyl alcohol hydrogels with anti-biofilm activity: designed as coatings for endotracheal tube materials. Biofouling 30(7):773–788. doi:10.1080/08927014.2014.926475

Lu L, Sun R, Chen R, Hui C-K, Ho C-M, Luk JM, Lau G, Che C-M (2008) Silver nanoparticles inhibit hepatitis B virus replication. Antiviral Ther 13(2):253

Luong ND, Lee Y, Nam J-D (2008) Highly-loaded silver nanoparticles in ultrafine cellulose acetate nanofibrillar aerogel. Eur Polym J 44(10):3116–3121

Ma Y-Q, Yi J-Z, Zhang L-M (2009) A facile approach to incorporate silver nanoparticles into dextran-based hydrogels for antibacterial and catalytical application. J Macromol Sci, Pure Appl Chem 46(6):643–648

Maathuis PG, Neut D, Busscher HJ, van der Mei HC, van Horn JR (2005) Perioperative contamination in primary total hip arthroplasty. Clin Orthop Relat Res 433:136–139

Mack D, Davies AP, Harris LG, Jeeves R, Pascoe B, Knobloch JK-M, Rohde H, Wilkinson TS (2013) *Staphylococcus epidermidis* in biomaterial-associated infections. In: Moriarty FT, Sebastian ZAJ, Busscher HJ (eds) Biomaterials associated infection: Immunological aspects and antimicrobial strategies. Springer, New York, pp 25–56. doi:10.1007/978-1-4614-1031-7

Mandal A, Meda V, Zhang WJ, Farhan KM, Gnanamani A (2012) Synthesis, characterization and comparison of antimicrobial activity of PEG/TritonX-100 capped silver nanoparticles on collagen scaffold. Colloids Surf B Biointerfaces 90:191–196. doi:10.1016/j.colsurfb.2011.10.021

Maneerung T, Tokura S, Rujiravanit R (2008) Impregnation of silver nanoparticles into bacterial cellulose for antimicrobial wound dressing. Carbohydr Polym 72(1):43–51

Mao S, Sun W, Kissel T (2010) Chitosan-based formulations for delivery of DNA and siRNA. Adv Drug Del Rev 62(1):12–27

Marsh P (2004) Dental plaque as a microbial biofilm. Caries Res 38(3):204–211

Marsh P (2005) Dental plaque: biological significance of a biofilm and community life-style. J Clin Periodontol 32(s6):7–15

Marsich E, Travan A, Donati I, Di Luca A, Benincasa M, Crosera M, Paoletti S (2011) Biological response of hydrogels embedding gold nanoparticles. Colloids Surf B Biointerfaces 83(2):331–339

Mauter MS, Elimelech M (2008) Environmental applications of carbon-based nanomaterials. Environ Sci Technol 42(16):5843–5859

Mohan R, Shanmugharaj AM, Sung Hun R (2011) An efficient growth of silver and copper nanoparticles on multiwalled carbon nanotube with enhanced antimicrobial activity. J Biomed Mater Res B Appl Biomater 96(1):119–126. doi:10.1002/jbm.b.31747

Monteiro DR, Gorup LF, Takamiya AS, Ruvollo-Filho AC, de Camargo ER, Barbosa DB (2009) The growing importance of materials that prevent microbial adhesion: antimicrobial effect of medical devices containing silver. Int J Antimicrob Agents 34(2):103–110

Mori Y, Ono T, Miyahira Y, Nguyen VQ, Matsui T, Ishihara M (2013) Antiviral activity of silver nanoparticle/chitosan composites against H1N1 influenza A virus. Nanoscale Res Lett 8(1):93. doi:10.1186/1556-276x-8-93

Morones JR, Elechiguerra JL, Camacho A, Holt K, Kouri JB, Ramírez JT, Yacaman MJ (2005) The bactericidal effect of silver nanoparticles. Nanotechnology 16(10):2346

MubarakAli D, Thajuddin N, Jeganathan K, Gunasekaran M (2011) Plant extract mediated synthesis of silver and gold nanoparticles and its antibacterial activity against clinically isolated pathogens. Colloids Surf B Biointerfaces 85(2):360–365

Mukherji S, Ruparelia J, Agnihotri S (2012) Antimicrobial activity of silver and copper nanoparticles: variation in sensitivity across various strains of bacteria and fungi. In: Cioffi N, Rai M (eds) Nano-Antimicrobials: Progress and Prospects. Springer, Berlin, Heidelberg, pp 225–251

Muñoz-Bonilla A, Fernández-García M (2012) Polymeric materials with antimicrobial activity. Prog Polym Sci 37(2):281–339. doi:10.1016/j.progpolymsci.2011.08.005

Murthy PK, Mohan YM, Varaprasad K, Sreedhar B, Raju KM (2008) First successful design of semi-IPN hydrogel–silver nanocomposites: a facile approach for antibacterial application. J Colloid Interface Sci 318(2):217–224

Murugan E, Vimala G (2011) Effective functionalization of multiwalled carbon nanotube with amphiphilic poly(propyleneimine) dendrimer carrying silver nanoparticles for better dispersability and antimicrobial activity. J Colloid Interface Sci 357(2):354–365. doi:10.1016/j.jcis.2011.02.009

Nadagouda MN, Varma RS (2007) Synthesis of thermally stable carboxymethyl cellulose/metal biodegradable nanocomposites for potential biological applications. Biomacromolecules 8(9):2762–2767. doi:10.1021/bm700446p

Nanda A, Saravanan M (2009) Biosynthesis of silver nanoparticles from Staphylococcus aureus and its antimicrobial activity against MRSA and MRSE. Nanomed Nanotechnol Biol Med 5(4):452–456

Narayan R, Abernathy H, Riester L, Berry C, Brigmon R (2005) Antimicrobial properties of diamond-like carbon-silver-platinum nanocomposite thin films. J Mater Eng Perform 14(4):435–440

Narayanan P, Wilson WS, Abraham AT, Sevanan M (2012) Synthesis, characterization, and antimicrobial activity of zinc oxide nanoparticles against human pathogens. BioNanoScience 2(4):329–335

Naveena BE, Prakash S (2013) Biological synthesis of gold nanoparticles using marine algae *Gracilaria corticata* and its application as a potent antimicrobial and antioxidant agent. Asian J Pharm Clin Res 6:179–182

Norowski PA, Bumgardner JD (2009) Biomaterial and antibiotic strategies for peri-implantitis: A review. J Biomed Mater Res Part B Appl Biomater 88(2):530–543

Pal S, Tak YK, Song JM (2007) Does the antibacterial activity of silver nanoparticles depend on the shape of the nanoparticle? A study of the gram-negative bacterium Escherichia coli. Appl Environ Microbiol 73(6):1712–1720

Panacek A, Kilianova M, Prucek R, Husickova V, Vecerova R, Kolar M, Kvitek L, Zboril R (2014) Preparation and in vitro bactericidal and fungicidal efficiency of nanosilver/methylcellulose hydrogel. Int J Chem Mol Nucl Mater Metall Eng 8(6):493–498

Panáček A, Kolář M, Večeřová R, Prucek R, Soukupová J, Kryštof V, Hamal P, Zbořil R, Kvítek L (2009) Antifungal activity of silver nanoparticles against *Candida* spp. Biomaterials 30(31):6333–6340. doi:10.1016/j.biomaterials.2009.07.065

Panáček A, Kvitek L, Prucek R, Kolar M, Vecerova R, Pizurova N, Sharma VK, Tj Nevečná, Zboril R (2006) Silver colloid nanoparticles: synthesis, characterization, and their antibacterial activity. J Phys Chem B 110(33):16248–16253

Parsek MR, Singh PK (2003) Bacterial biofilms: an emerging link to disease pathogenesis. Ann Rev Microbiol 57(1):677–701

Pelgrift RY, Friedman AJ (2013) Nanotechnology as a therapeutic tool to combat microbial resistance. Adv Drug Del Rev 65(13):1803–1815

Peng S, Jin G, Li L, Li K, Srinivasan M, Ramakrishna S, Chen J (2016) Multi-functional electrospun nanofibers for advances in tissue regeneration, energy conversion & storage, and water treatment. Chem Soc Rev

Peppas NA, Hilt JZ, Khademhosseini A, Langer R (2006) Hydrogels in biology and medicine: from molecular principles to bionanotechnology. Adv Mater 18(11):1345–1360

Percival SL, Suleman L, Vuotto C, Donelli G (2015) Healthcare-associated infections, medical devices and biofilms: risk, tolerance and control. J Med Microbiol 64(4):323–334

Pinto RJ, Marques PA, Neto CP, Trindade T, Daina S, Sadocco P (2009) Antibacterial activity of nanocomposites of silver and bacterial or vegetable cellulosic fibers. Acta Biomater 5(6):2279–2289. doi:10.1016/j.actbio.2009.02.003

Pishbin F, Mourino V, Gilchrist JB, McComb DW, Kreppel S, Salih V, Ryan MP, Boccaccini AR (2013) Single-step electrochemical deposition of antimicrobial orthopaedic coatings based on a bioactive glass/chitosan/nano-silver composite system. Acta Biomater 9(7):7469–7479. doi:10.1016/j.actbio.2013.03.006

Place ES, Evans ND, Stevens MM (2009) Complexity in biomaterials for tissue engineering. Nat Mater 8(6):457–470

Prema P, Iniya P, Immanuel G (2016) Microbial mediated synthesis, characterization, antibacterial and synergistic effect of gold nanoparticles using *Klebsiella pneumoniae* (MTCC-4030). RSC Adv 6(6):4601–4607

Qi L, Xu Z, Jiang X, Hu C, Zou X (2004) Preparation and antibacterial activity of chitosan nanoparticles. Carbohydr Res 339(16):2693–2700

Rabea EI, Badawy ME-T, Stevens CV, Smagghe G, Steurbaut W (2003) Chitosan as antimicrobial agent: applications and mode of action. Biomacromolecules 4(6):1457–1465

Raghavendra GM, Jayaramudu T, Varaprasad K, Sadiku R, Ray SS, Raju KM (2013) Cellulose–polymer–Ag nanocomposite fibers for antibacterial fabrics/skin scaffolds. Carbohydr Polym 93(2):553–560

Raghunath J, Zhang H, Edirisinghe MJ, Darbyshire A, Butler PE, Seifalian AM (2009) A new biodegradable nanocomposite based on polyhedral oligomeric silsesquioxane nanocages: cytocompatibility and investigation into electrohydrodynamic jet fabrication techniques for tissue-engineered scaffolds. Biotechnol Appl Biochem 52(1):1–8. doi:10.1042/ba20070256

Raghupathi KR, Koodali RT, Manna AC (2011) Size-dependent bacterial growth inhibition and mechanism of antibacterial activity of zinc oxide nanoparticles. Langmuir 27(7):4020–4028

Rai A, Prabhune A, Perry CC (2010) Antibiotic mediated synthesis of gold nanoparticles with potent antimicrobial activity and their application in antimicrobial coatings. J Mater Chem 20(32):6789–6798

Rai M, Yadav A, Gade A (2009) Silver nanoparticles as a new generation of antimicrobials. Biotechnol Adv 27(1):76–83

Ramamurthy C, Padma M, Mareeswaran R, Suyavaran A, Kumar MS, Premkumar K, Thirunavukkarasu C (2013) The extra cellular synthesis of gold and silver nanoparticles and their free radical scavenging and antibacterial properties. Colloids Surf B Biointerfaces 102:808–815

Rangari VK, Mohammad GM, Jeelani S, Hundley A, Vig K, Singh SR, Pillai S (2010) Synthesis of Ag/CNT hybrid nanoparticles and fabrication of their nylon-6 polymer nanocomposite fibers for antimicrobial applications. Nanotechnology 21(9):095102. doi:10.1088/0957-4484/21/9/095102

Rao KK, Reddy PR, Lee Y-I, Kim C (2012) Synthesis and characterization of chitosan–PEG–Ag nanocomposites for antimicrobial application. Carbohydr Polym 87(1):920–925

Ratner BD, Hoffman AS, Schoen FJ, Lemons JE (2004) Biomaterials science: an introduction to materials in medicine. Academic Press, Cambridge

Regiel-Futyra A, Kus-Liskiewicz M, Sebastian V, Irusta S, Arruebo M, Stochel G, Kyziol A (2015) Development of noncytotoxic chitosan-gold nanocomposites as efficient antibacterial materials. ACS Appl Mater Interfaces 7(2):1087–1099. doi:10.1021/am508094e

Ren G, Hu D, Cheng EW, Vargas-Reus MA, Reip P, Allaker RP (2009) Characterisation of copper oxide nanoparticles for antimicrobial applications. Int J Antimicrob Agents 33(6):587–590

Rodrigues AG, Ping LY, Marcato PD, Alves OL, Silva MC, Ruiz RC, Melo IS, Tasic L, De Souza AO (2013) Biogenic antimicrobial silver nanoparticles produced by fungi. Appl Microbiol Biotechnol 97(2):775–782

Rodríguez-Tobías H, Morales G, Ledezma A, Romero J, Grande D (2014) Novel antibacterial electrospun mats based on poly (D, L-lactide) nanofibers and zinc oxide nanoparticles. J Mater Sci 49(24):8373–8385

Rogers JV, Parkinson CV, Choi YW, Speshock JL, Hussain SM (2008) A preliminary assessment of silver nanoparticle inhibition of monkeypox virus plaque formation. Nanoscale Res Lett 3(4):129–133

Romainor ANB, Chin SF, Pang SC, Bilung LM (2014) Preparation and characterization of chitosan nanoparticles-doped cellulose films with antimicrobial property. J Nanomater 2014:130

Rosemary MJ, MacLaren I, Pradeep T (2006) Investigations of the antibacterial properties of ciprofloxacin@SiO_2. Langmuir 22(24):10125–10129. doi:10.1021/la061411h

Rujitanaroj P-O, Pimpha N, Supaphol P (2008) Wound-dressing materials with antibacterial activity from electrospun gelatin fiber mats containing silver nanoparticles. Polymer 49(21):4723–4732

Ruparelia JP, Chatterjee AK, Duttagupta SP, Mukherji S (2008) Strain specificity in antimicrobial activity of silver and copper nanoparticles. Acta Biomater 4(3):707–716

Rusen E, Mocanu A, Nistor LC, Dinescu A, Calinescu I, Mustatea G, Voicu SI, Andronescu C, Diacon A (2014) Design of antimicrobial membrane based on polymer colloids/multiwall carbon nanotubes hybrid material with silver nanoparticles. ACS Appl Mater Interfaces 6(20):17384–17393. doi:10.1021/am505024p

Russell A, Path F, Sl FP, Hugo W (1994) Antimicrobial activity and action of silver. Prog Med Chem 31:351

Sacco P, Travan A, Borgogna M, Paoletti S, Marsich E (2015) Silver-containing antimicrobial membrane based on chitosan-TPP hydrogel for the treatment of wounds. J Mater Sci Mater Med 26(3):128. doi:10.1007/s10856-015-5474-7

Salem W, Leitner DR, Zingl FG, Schratter G, Prassl R, Goessler W, Reidl J, Schild S (2015) Antibacterial activity of silver and zinc nanoparticles against *Vibrio cholerae* and enterotoxic *Escherichia coli*. Int J Med Microbiol 305(1):85–95

Salwiczek M, Qu Y, Gardiner J, Strugnell RA, Lithgow T, McLean KM, Thissen H (2014) Emerging rules for effective antimicrobial coatings. Trends Biotechnol 32(2):82–90

Sandri G, Bonferoni MC, Ferrari F, Rossi S, Aguzzi C, Mori M, Grisoli P, Cerezo P, Tenci M, Viseras C, Caramella C (2014) Montmorillonite-chitosan-silver sulfadiazine nanocomposites for topical treatment of chronic skin lesions: in vitro biocompatibility, antibacterial efficacy and gap closure cell motility properties. Carbohydr Polym 102:970–977. doi:10.1016/j.carbpol.2013.10.029

Sastri VR (2013) Materials used in medical devices. In: Sastri V R (eds), Plastics in medical devices: properties, requirements, and applications. William Andrew Publishing, Oxford, pp 19–31. doi:10.1016/B978-1-4557-3201-2.00003-3

Sawant SN, Selvaraj V, Prabhawathi V, Doble M (2013) Antibiofilm properties of silver and gold incorporated PU, PCLm, PC and PMMA nanocomposites under two shear conditions. PLoS ONE 8(5):e63311. doi:10.1371/journal.pone.0063311

Schexnailder P, Schmidt G (2009) Nanocomposite polymer hydrogels. Colloid Polym Sci 287 (1):1–11

Schwartz VB, Thétiot F, Ritz S, Pütz S, Choritz L, Lappas A, Förch R, Landfester K, Jonas U (2012) Antibacterial surface coatings from zinc oxide nanoparticles embedded in poly (n-isopropylacrylamide) hydrogel surface layers. Adv Funct Mater 22(11):2376–2386

Selvaraj V, Alagar M (2007) Analytical detection and biological assay of antileukemic drug 5-fluorouracil using gold nanoparticles as probe. Int J Pharm 337(1–2):275–281. doi:10.1016/j.ijpharm.2006.12.027

Seo Y, Hwang J, Kim J, Jeong Y, Hwang MP, Choi J (2014) Antibacterial activity and cytotoxicity of multi-walled carbon nanotubes decorated with silver nanoparticles. Int J Nanomed 9:4621–4629. doi:10.2147/ijn.s69561

Shalumon K, Anulekha K, Nair SV, Nair S, Chennazhi K, Jayakumar R (2011) Sodium alginate/poly (vinyl alcohol)/nano ZnO composite nanofibers for antibacterial wound dressings. Int J Biol Macromol 49(3):247–254

Shameli K, Ahmad MB, Yunus WM, Ibrahim NA, Rahman RA, Jokar M, Darroudi M (2010) Silver/poly (lactic acid) nanocomposites: preparation, characterization, and antibacterial activity. Int J Nanomed 5:573–579

Shameli K, Bin Ahmad M, Zargar M, Yunus WM, Ibrahim NA, Shabanzadeh P, Moghaddam MG (2011) Synthesis and characterization of silver/montmorillonite/chitosan bionanocomposites by chemical reduction method and their antibacterial activity. Int J Nanomed 6:271–284. doi:10.2147/ijn.s16043

Shanthi S, Jayaseelan BD, Velusamy P, Vijayakumar S, Chih CT, Vaseeharan B (2016) Biosynthesis of silver nanoparticles using a probiotic Bacillus licheniformis Dahb1 and their antibiofilm activity and toxicity effects in *Ceriodaphnia cornuta*. Microb Pathog

Sharma D, Rajput J, Kaith B, Kaur M, Sharma S (2010) Synthesis of ZnO nanoparticles and study of their antibacterial and antifungal properties. Thin Solid Films 519(3):1224–1229

Sharma VK, Yngard RA, Lin Y (2009) Silver nanoparticles: green synthesis and their antimicrobial activities. Adv Colloid Interf 145(1):83–96

Sheikh FA, Kanjwal MA, Saran S, Chung W-J, Kim H (2011) Polyurethane nanofibers containing copper nanoparticles as future materials. Appl Surf Sci 257(7):3020–3026

Shi Z, Neoh K, Kang E, Wang W (2006) Antibacterial and mechanical properties of bone cement impregnated with chitosan nanoparticles. Biomaterials 27(11):2440–2449

Siegel JD, Rhinehart E, Jackson M, Chiarello L (2007) 2007 guideline for isolation precautions: preventing transmission of infectious agents in health care settings. Am J Infect Control 35(10): S65–S164

Simon T, Wu C-S, Liang J-C, Cheng C, Ko F-H (2016) Facile synthesis of a biocompatible silver nanoparticle derived tripeptide supramolecular hydrogel for antibacterial wound dressings. New J Chem

Singh M, Singh S, Prasad S, Gambhir I (2008) Nanotechnology in medicine and antibacterial effect of silver nanoparticles. Dig J Nanomater Biostruct 3(3):115–122

Son WK, Youk JH, Park WH (2006) Antimicrobial cellulose acetate nanofibers containing silver nanoparticles. Carbohydr Polym 65(4):430–434

Song J, Kim H, Jang Y, Jang J (2013) Enhanced antibacterial activity of silver/polyrhodanine-composite-decorated silica nanoparticles. ACS Appl Mater Interfaces 5 (22):11563–11568. doi:10.1021/am402310u

Speshock JL, Murdock RC, Braydich-Stolle LK, Schrand AM, Hussain SM (2010) Interaction of silver nanoparticles with Tacaribe virus. J Nanobiotechnol 8(1):19

Stewart PS, Costerton JW (2001) Antibiotic resistance of bacteria in biofilms. Lancet 358 (9276):135–138

Stickler DJ (2000) Biomaterials to prevent nosocomial infections: is silver the gold standard? Curr Opin Infect Dis 13(4):389–393

Stoecklin-Wasmer C, Rutjes A, Da Costa B, Salvi G, Jüni P, Sculean A (2013) Absorbable collagen membranes for periodontal regeneration: A systematic review. J Dent Res 92(9):773–781

Stoimenov PK, Klinger RL, Marchin GL, Klabunde KJ (2002) Metal oxide nanoparticles as bactericidal agents. Langmuir 18(17):6679–6686

Subbiahdoss G, da Silva Domingues JF, Kuijer R, van der Mei HC, Busscher HJ (2013) Bridging the gap between in vitro and in vivo evaluation of biomaterial-associated infections. Springer

Sudarshan N, Hoover D, Knorr D (1992) Antibacterial action of chitosan. Food Biotechnol 6 (3):257–272

Sudheesh Kumar P, Lakshmanan V-K, Anilkumar T, Ramya C, Reshmi P, Unnikrishnan A, Nair SV, Jayakumar R (2012) Flexible and microporous chitosan hydrogel/nano ZnO

composite bandages for wound dressing: in vitro and in vivo evaluation. ACS Appl Mater Interfaces 4(5):2618–2629

Sun L, Du Y, Fan L, Chen X, Yang J (2006) Preparation, characterization and antimicrobial activity of quaternized carboxymethyl chitosan and application as pulp-cap. Polymer 47 (6):1796–1804

Tavaria FK, Costa EM, Gens EJ, Malcata FX, Pintado ME (2013) Influence of abiotic factors on the antimicrobial activity of chitosan. J Dermatol 40(12):1014–1019

Tian T, Shi X, Cheng L, Luo Y, Dong Z, Gong H, Xu L, Zhong Z, Peng R, Liu Z (2014) Graphene-based nanocomposite as an effective, multifunctional, and recyclable antibacterial agent. ACS Appl Mater Interfaces 6(11):8542–8548. doi:10.1021/am5022914

Travan A, Pelillo C, Donati I, Marsich E, Benincasa M, Scarpa T, Semeraro S, Turco G, Gennaro R, Paoletti S (2009) Non-cytotoxic silver nanoparticle-polysaccharide nanocomposites with antimicrobial activity. Biomacromolecules 10(6):1429–1435. doi:10.1021/bm900039x

Ul-Islam M, Khattak WA, Ullah MW, Khan S, Park JK (2014) Synthesis of regenerated bacterial cellulose-zinc oxide nanocomposite films for biomedical applications. Cellulose 21(1):433–447

Usman SM (2013) Synthesis, characterization, and antimicrobial properties of copper nanoparticles. Int J Nanomedicine 8:4467–4479

Vance ME, Kuiken T, Vejerano EP, McGinnis SP, Hochella MF, Rejeski D, Hull MS (2015) Nanotechnology in the real world: Redeveloping the nanomaterial consumer products inventory. Beilstein J Nanotechnol 6:1769–1780. doi:10.3762/bjnano.6.181

Varaprasad K, Mohan YM, Ravindra S, Reddy NN, Vimala K, Monika K, Sreedhar B, Raju KM (2010) Hydrogel–silver nanoparticle composites: A new generation of antimicrobials. J Appl Polym Sci 115(2):1199–1207

Vargas-Villagran H, Romo-Uribe A, Teran-Salgado E, Dominguez-Diaz M, Flores A (2014) Electrospun polylactic acid non-woven mats incorporating silver nanoparticles. Polym Bull 71 (9):2437–2452. doi:10.1007/s00289-014-1200-8

Vigneshwaran N, Kumar S, Kathe A, Varadarajan P, Prasad V (2006) Functional finishing of cotton fabrics using zinc oxide–soluble starch nanocomposites. Nanotechnology 17(20):5087

Vijayakumar PS, Prasad BL (2009) Intracellular biogenic silver nanoparticles for the generation of carbon supported antiviral and sustained bactericidal agents. Langmuir 25(19):11741–11747. doi:10.1021/la901024p

Vimala K, Yallapu MM, Varaprasad K, Reddy NN, Ravindra S, Naidu NS, Raju KM (2011) Fabrication of curcumin encapsulated chitosan-PVA silver nanocomposite films for improved antimicrobial activity. J Biomater Nanobiotechnol 2(01):55

Vlad S, Tanase C, Macocinschi D, Ciobanu C, Balaes T, Filip D, Gostin I, Gradinaru L (2012) Antifungal behaviour of polyurethane membranes with zinc oxide nanoparticles. Dig J Nanomater Bios 7:51–58

Wang N, Hu B, Chen ML, Wang JH (2015) Polyethylenimine mediated silver nanoparticle-decorated magnetic graphene as a promising photothermal antibacterial agent. Nanotechnology 26(19):195703. doi:10.1088/0957-4484/26/19/195703

Wang Z, Liu S, Ma J, Qu G, Wang X, Yu S, He J, Liu J, Xia T, Jiang GB (2013) Silver nanoparticles induced RNA polymerase-silver binding and RNA transcription inhibition in erythroid progenitor cells. ACS Nano 7(5):4171–4186. doi:10.1021/nn400594s

Wang ZL (2004) Zinc oxide nanostructures: growth, properties and applications. J Phys: Condens Matter 16(25):R829

Wei Y, Chen S, Kowalczyk B, Huda S, Gray TP, Grzybowski BA (2010) Synthesis of stable, low-dispersity copper nanoparticles and nanorods and their antifungal and catalytic properties. J Phys Chem C 114(37):15612–15616

Wildgoose GG, Banks CE, Compton RG (2006) Metal nanoparticles and related materials supported on carbon nanotubes: methods and applications. Small 2(2):182–193

Xu J, Ji W, Shen Z, Tang S, Ye X, Jia D, Xin X (1999) Preparation and characterization of CuO nanocrystals. J Solid State Chem 147(2):516–519

Yadollahi M, Gholamali I, Namazi H, Aghazadeh M (2015) Synthesis and characterization of antibacterial carboxymethylcellulose/CuO bio-nanocomposite hydrogels. Int J Biol Macromol 73:109–114

Yallappa S, Manjanna J, Dhananjaya B, Vishwanatha U, Ravishankar B, Gururaj H, Niranjana P, Hungund B (2015) Phytochemically functionalized Cu and Ag nanoparticles embedded in MWCNTs for enhanced antimicrobial and anticancer properties. Nano-Micro Lett 1–11

Yamamoto O (2001) Influence of particle size on the antibacterial activity of zinc oxide. Int J Inorg Mater 3(7):643–646

Yien L, Zin NM, Sarwar A, Katas H (2012) Antifungal activity of chitosan nanoparticles and correlation with their physical properties. Int J Biomater

Yu B, Leung KM, Guo Q, Lau WM, Yang J (2011) Synthesis of Ag–TiO_2 composite nano thin film for antimicrobial application. Nanotechnology 22(11):115603

Yu L, Zhang Y, Zhang B, Liu J (2014) Enhanced antibacterial activity of silver nanoparticles/halloysite nanotubes/graphene nanocomposites with sandwich-like structure. Sci Rep 4:4551. doi:10.1038/srep04551

Zaat S, Broekhuizen C, Riool M (2010) Host tissue as a niche for biomaterial-associated infection. Future Microbiol 5(8):1149–1151

Zahran MK, Ahmed HB, El-Rafie MH (2014) Surface modification of cotton fabrics for antibacterial application by coating with AgNPs-alginate composite. Carbohydr Polym 108:145–152. doi:10.1016/j.carbpol.2014.03.005

Zaporojtchenko V, Podschun R, Schürmann U, Kulkarni A, Faupel F (2006) Physico-chemical and antimicrobial properties of co-sputtered Ag–Au/PTFE nanocomposite coatings. Nanotechnology 17(19):4904

Zeng F, Hou C, Wu S, Liu X, Tong Z, Yu S (2007) Silver nanoparticles directly formed on natural macroporous matrix and their anti-microbial activities. Nanotechnology 18(5):055605

Zhang H, Wu M, Sen A (2012a) Silver nanoparticle antimicrobials and related materials. In: Cioffi N, Rai M (eds) Nano-antimicrobials: progress and prospects. Springer, Berlin, Heidelberg, pp 3–45. doi:10.1007/978-3-642-24428-5

Zhang K, Kim YK, Cadenaro M, Bryan TE, Sidow SJ, Loushine RJ, J-q Ling, Pashley DH, Tay FR (2010) Effects of different exposure times and concentrations of sodium hypochlorite/ethylenediaminetetraacetic acid on the structural integrity of mineralized dentin. J Endod 36(1):105–109

Zhang R, Xue M, Yang J, Tan T (2012b) A novel injectable and in situ crosslinked hydrogel based on hyaluronic acid and α, β-polyaspartylhydrazide. J Appl Polym Sci 125(2):1116–1126

Zheng Y, Cai C, Zhang F, Monty J, Linhardt RJ, Simmons TJ (2016) Can natural fibers be a silver bullet? Antibacterial cellulose fibers through the covalent bonding of silver nanoparticles to electrospun fibers. Nanotechnology 27(5):055102

Zhou B, Li Y, Deng H, Hu Y, Li B (2014) Antibacterial multilayer films fabricated by layer-by-layer immobilizing lysozyme and gold nanoparticles on nanofibers. Colloids Surf B Biointerfaces 116:432–438. doi:10.1016/j.colsurfb.2014.01.016

Zhu J, Marchant RE (2011) Design properties of hydrogel tissue-engineering scaffolds. Expert Rev Med Devices 8(5):607–626